MODELLING GEOMECHANICS OF RESIDUAL SOILS WITH DMT TESTS

Nuno Bravo de Faria Cruz

Supervised by:

Prof. António Viana da Fonseca (Dr. Eng. Civil, Prof. Associado com Agregação, FEUP, Univ. Porto)

Co-supervised by:

Prof. Fernando Joaquim Tavares Rocha (Prof. Catedrático, Geociencias, Univ. Aveiro)

Prof. Carlos Manuel Gonçalves Rodrigues (Prof. Adjunto, Instituto Politécnico da Guarda)

Abstract

The work presented herein integrates a long term research activity under the subject of residual soils characterization, performed by the author since 1995 within his professional activity in Laboratório de Geotecnia e Materiais de Construção (LGMC of CICCOPN) and MOTA-ENGIL, in very fruitful partnership with FEUP. The aim of that research has been the establishment of a model for characterizing residual soils using Marchetti´s Dilatometer test (DMT), on its own or combined with other tests.

In the last decade this partnership developed several studies to improve the knowledge and measurement of granitic residual soils mechanical behaviour, using the last generation technologies of testing equipments. In this context, several scientific papers were produced, where some conclusions were outlined and some local correlations were established, namely for cohesion interception, shear strength angle corrections and deformability moduli. As a consequence of this work, it became fundamental to develop experimental work in controlled environment to calibrate the field experimental data.

To do so a special apparatus was created to work with large artificially cemented samples, aiming the evaluation of static penetration influence in the loss of cementation strength, and the overall effects over the stiffness response, to produce adequate correlations for deriving design parameters. The experience was based in the development of artificially cemented samples tested both in triaxial cell and in a special large dimension measurement apparatus (CemSoil Box), where blades could be installed and/or pushed. Water level, suction and seismic wave velocities were monitored during the whole experience.

The research work will be described with emphasis in: the theoretical background of residual soils and brief overview of in-situ testing (Part A – Background), the available rich and abundant data of Portuguese granitic residual soils, including the one obtained by DMT (Part B – The Residual Ground), the calibration work (Part C – The Experience) and the proposed model for residual soil characterization (Part D – The Model)

Resumo

O trabalho de dissertação apresentado no presente documento integra um percurso de investigação de longo curso que tem vindo a ser realizado pelo autor desde 1995. Esse trabalho evoluiu no decurso da sua actividade profissional no LGMC do CICCOPN e na empresa MOTA-ENGIL, Engenharia e Construção, assentando igualmente numa profícua parceria com a Faculdade de Engenharia da Universidade do Porto (FEUP). O objectivo principal dessa investigação consiste no estabelecimento de um modelo para caracterização mecânica de solos residuais graníticos, baseado no ensaio com Dilatómetro de Marchetti (DMT), combinado, ou não, com outros ensaios in-situ.

Na última década esta parceria com a FEUP permitiu o desenvolvimento de vários trabalhos destinados a aprofundar o conhecimento sobre o comportamento mecânico dos solos residuais graníticos portugueses, bem como contribuir para um incremento da qualidade dos parâmetros geotécnicos obtidos por ensaios laboratoriais e in-situ. Neste contexto, um número significativo de comunicações foi apresentado em congressos e revistas da especialidade, apresentando correlações específicas para dedução do estado de tensão em repouso, coesão efectiva, ângulo de resistência ao corte e módulos de deformabilidade. Em consequência, tornou-se fundamental o desenvolvimento de uma experiência específica em ambiente controlado, para calibração da extensa e variada base de informação geotécnica obtida através de ensaios in-situ e laboratoriais.

Para o efeito, foi desenvolvido um dispositivo específico para trabalhar com amostras de grande dimensão, procurando avaliar a influência da penetração na perda de resistência e rigidez, sobretudo devida à destruição parcial da estrutura de cimentação. O trabalho experimental consistiu na preparação de amostras cimentadas artificialmente, as quais foram ensaiadas em câmara triaxial e numa célula de grandes dimensões (CemSoil Box) onde foi possível instalar e cravar lâminas DMT, a par com outros equipamentos de medição de níveis de água, sucção e velocidades de ondas sísmicas.

Na dissertação dá-se enfoque a: estado de arte relacionado com o comportamento dos solos residuais bem como um resumo sobre a actualidade dos ensaios in-situ (Part A – Background), informação (rica e variada) sobre o comportamento mecânico dos materiais graníticos portugueses, incluindo aquela obtida através de ensaios DMT

(Part B – The Residual Ground), experiência de calibração em ambiente controlado (Part C – The Experience) e proposta de um modelo para caracterização mecânica de solos residuais (Part D – The Model).

Résumé

Le travail de recherche présenté dans ce document intègre un parcourt d'investigation de longue durée qui a été menée par l'auteur depuis 1995. Ce travail a évolué au cours de son activité professionnelle dans le LGMC du CICCOPN et dans l'entreprise MOTA-ENGIL, Engenharia e Construção, en fabuleux partenariat avec la Faculté d'Ingénierie de l'Université du Porto (FEUP). L'objectif principal de cette investigation consiste dans l'établissement d'un modèle pour la caractérisation mécanique des sols granitiques résiduels, basée sur l'essaie du dilatomètre de Marchetti (DMT), combinés ou non avec d'autres essais in-situ.

Dans la dernière décennie le partenariat avec la FEUP a permis le développement de plusieurs travails visant approfondir les connaissances sur le comportement mécanique des sols granitiques résiduels portugais, ainsi comme contribuer à l'amélioration de la qualité des paramètres géotechniques obtenus par des essais en laboratoire et in-situ. Dans ce contexte, un nombre significatif de communications a été présenté à des conférences et à des revues de la spécialité, présentant des corrélations spécifiques pour déduire l'état de tension au repos, la cohésion effectif, l'angle de résistance au cisaillement et les modules de déformabilité. Par conséquent, il est devenu fondamental développer une expérience spécifique dans un environnement contrôlé, pour la calibration de l'étendue et variée base d'informations géotechniques obtenues par des essais in-situ et en laboratoire.

À cette fin, il y a été développé un dispositif spécifique pour travailler avec des échantillons de grande taille, essayant d'évaluer l'influence de la pénétration dans la perte de la résistance et de la rigidité, principalement en raison de la destruction partielle de la structure de cimentation. Le travail expérimental a consisté en la préparation des échantillons artificiellement cimenté, lesquelles ont été testés dans une chambre triaxiale et sur une cellule de grande dimension (CemSoil Box) où il était possible d'installer et poussé des lames DMT, avec d'autres équipements pour mesurer les niveaux d'eau, las succion et les vitesses des ondes sismiques.

Dans ce travail de recherche, nous nous concentrant sûr: le contexte théorique lié à la fois au comportement des sols résiduels et aussi sur le domaine des essais in-situ (Part A – Background), l'information (riche et varié) sur le comportement mécanique des matériaux granitiques portugais, y compris celle obtenue avec des essais DMT (Part B – The Residual Ground), l'expérience de calibration dans un environnement

contrôlé (Part C – The Experience) et la proposition d'un modèle pour la caractérisation mécanique des sols résiduels (Part D – The Model).

Acknowledgments

This work became possible only because there was always someone ready to walk along with me, to point out horizons to look into, to fill my soul with hope and joy and to always make me smile with my "stumbles and falls".

A big smile, a big kiss& big hug to the team mates that directly and greatly contribute to this work.

This work is the work we were able to do together.
OUR work.

By order of appearance: José Manuel Carvalho, Fernando Gomes, Antonio Viana da Fonseca, Sonia Figueiredo, Eduardo Neves, Jorge Saraiva Cruz, Jorge Ribeiro, Cárin Mateus, Ricardo Rocha, João Branco, Patrícia Vieira, Mike Lopes, David Felizardo, my Bro. Manuel Cruz, Carlos Rodrigues,Manuel Gairrão, Fernando Almeida and the "rookies" Luis Machado and Sofia Vaz.

Also, i would like to express my deepest thanks …

…to Silvia, Migo, Kika e Licas, for letting me be as i am and for the amazing family that we are. ***You'll never walk alone****.*
I hope you can feel proud of me

to my father, who put Tibet and freedom in my soul, a long time ago,
my mother for teaching me the word "Love", my brothers for the brotherhood and the incredible and immense Bravos family to whom i´m proud to belong

to my uncle Duarte for the ideals and the balance i have learnt from him.

to my supervisors…
António Viana da Fonseca, a long cruise partner in Science & Travelling,
since the first hour,
for the fantastic adventures we have lived together,

Fernando Rocha, for his belief in all this,

and Carlos Rodrigues with whom i have learnt so many things,
so impossible to describe, the huge friendship this work has offered me
A miracle, to have you and Manuel on the same side of the road.
I´d love to climb another Volcano with you, my friend.

To Silvano Marchetti, who invented a fantastic tool

to my "Guru" Almeida e Sousa and to Manuel Alves Ribeiro
for teaching me how to think like an engineer
and for the kick-off of this Dream

to my "twin" Jorge Cruz that always made possible the dream to go on,
bearing the same bearing I had to bear,
and even making my mistakes useful
Great partnership, my friend, let´s make it last

to my sweet and courageous Cárin, that stood up for me and covered my weaknesses
and also to the smiley Patrícia by the light she brought in

To my bright geophysical partner, Fernando Almeida

to my dearest "Cluster" by their love, permanent support and a lot of things more that cannot be expressed by words. You bring balance to my life: Cristina, João, Claudia e Vitor (Cunhas Gomes), Silvio Marroquin, Vitor Az, Vitor Drejo, Angel Oramas, Raquel Pina.

to João Bustorff, for feeding my dreams
to "Giros" and "Costas", for a life time friendship

to Silvano and Diego Marchetti and the precious Paola Monaco,
to my Brazilian brothers Fernando Schnaid, Roberto Coutinho, Eduardo Marques,
to the Gang of 4, John Powell, Marcelo Devincenzi, Tom Lunne,
to the Geomusicians Paul Mayne, Martin Fahey, John Mitchell with whom i had the pleasure of mixing Science & Art,
to Roger Failzmeger and Mike Long,
to all the "Knights of the Blade",
for your friendship and confidence in my skills
I sincerely hope i haven't disappointed

to Fernando Gonçalves, for believing in my engineering efficiency since the early beginning,
to Vieira Simões by opening a decisive door in a dead end,
and to Pedro Januario by the friendship and respect offered me in the dark.

To my mates from Aveiro, Coimbra and Porto Universities, where i have learnt teaching and taught learning:
Fernando Rocha, Fernando Almeida, Jorge Medina, Eduardo Silva, Luis Lemos, Paulo Pinto, Jorge Almeida e Sousa, Sara Rios, António Topa Gomes, Cristiana Ferreira,

To Sandra Andrade, Maria José, Miguel Meireles, Francisco Silva, Fernando Paiva, Denise Silva, Leonel Conde, Maria do Carmo Pinto, Luís Póvoas and the whole drilling team,
for their permanent and indestructible support
in CICCOPN and in MOTA-ENGIL.

To all those that walked with me in"A PhD on the Road", transforming a huge task in a fantastic adventure

Tibetan say…There is no way to happiness
Happiness is the way

YOU all have made happy my way

Thanks so much.

INDEX

1. Introduction 3

1.1. Brief history of Marchetti´s Dilatometer (DMT) use in Portugal 3

1.2. Objectives 9

1.3. Thesis Lay-out 10

2. Weathering processes and soil genesis 17

2.1. Weathering and its influence 17

2.2. Weathering and its influence factors 20

2.3. Weathering indexes 24

2.4. Residual and transported soils 26

2.5. Classification for engineering purposes 28

2.5.1. Overview 28

2.5.2. Wesley Classification 30

3. Mechanical Evolution with Weathering 37

3.1. Unweathered to medium weathered rock massifs 38

3.1.1. Massif controlled by rock matrix 40

3.1.2. Massif controlled by discontinuities 42

3.1.3. Massif controlled by rock matrix and discontinuities 45

3.1.4. Stiffness 47

3.2. Intermediate Geomaterials (IGM) and residual soils 49

3.2.1. Background 49

3.2.1.1. General Characteristics 49

3.2.1.2. Microfabric and sampling influences 52
3.2.2. Strength behaviour 54
3.2.3. Critical or steady states 61
3.2.4. Stiffness 65
3.2.5. The role of suction 75
4. Geotechnical parameters from in-situ characterization 85
4.1. Overview 85
4.2. Sampling 87
4.3. In-situ testing 91
4.3.1. Cone Penetration Tests (SCPTu) 100
4.3.1.1. Classification and Stratigraphy 104
4.3.1.2. Unit weight 108
4.3.1.3. Shear Strength 110
4.3.1.4. Stiffness 115
5. Marchetti Dilatometer Test 121
5.1. Introduction 121
5.2. Basic Pressures 124
5.3. Material Index, I_D 126
5.4. Horizontal stress index, K_D 129
5.4.1. Fine grained soils 130
5.4.1.1. State Characteristics 130
5.4.1.2. Undrained shear strength 135
5.4.2. Coarse-grained soils 139

5.4.2.1. State Properties 139
5.4.2.2. Drained Strength 140
5.5. Dilatometer modulus, E_D 145
5.6. Pore Pressure Index, U_D 164
5.7. Unit Weight (combining E_D and I_D) 166
5.8. Summary 168
6. Geotechincal Caracterization of Porto and Guarda Granitic Formations 175
6.1. Introduction 175
6.2. Geology 178
6.3. Sampling disturbance and quality control 187
6.4. Identification and classification 190
6.5. Physical Properties 193
6.6. Strength and stiffness 196
6.6.1. Laboratory testing 197
6.6.2. In-situ testing 201
6.7. Proposal for a modified Wesley Classification 207
6.8. Geotechnical parameters deduced from in-situ and laboratory tests 210
6.9. Other available geotechnical test parameters 216
6.10. Summary 217
7. Residual Soil In Situ Characterization 223
7.1. Introduction 223
7.2. Basic Test parameters, P_0 and P_1 (DMT) and q_c and f_s (CPTu) 227
7.3. Stratigraphy and unit weight 228

7.4. Strength evaluation 229
7.4.1. Virtual overconsolidation ratio, vOCR 230
7.4.2. Coefficient of earth pressure at rest, K_0 233
7.4.3. Cohesion Intercept, c' 235
7.4.4. Angle of shearing resistance, ϕ' 239
7.5. Deformability 240
7.5.1. Constrained modulus, M 241
7.5.2. Maximum shear modulus 242
7.6. A case study – Casa da Música Metro Station 248
7.6.1. Geological and geotechnical site conditions 249
7.6.2. In-situ tests correlations 250
7.6.2.1. Soil classification and unit weight 250
7.6.2.2. Stress state at rest and vOCR 252
7.6.2.3. Shear strength 253
7.6.2.4. Stress-strain relations 256
7.7. Summary 259
8. Accuracy of Results 263
8.1. Influence of blade geometry 263
8.2. Influence of penetration modes 265
8.2.1. Basic considerations 265
8.2.2. Typical Profiles 267
8.2.3. Basic parameters 268
8.2.4. Intermediate Parameters 270

8.2.5. Geomechanical Parameters 272
8.3. Influence of measurement devices 275
9. Laboratorial Testing Program 287
9.1. Sample Preparation 291
9.1.1. Soils 291
9.1.2. Cements 294
9.2. Triaxial testing 308
9.2.1. Equipments and methodologies 308
9.2.2. Presentation and Discussion of Strength Results 312
9.2.3. Presentation and discussion of stiffness results 330
9.2.4. Naturally and artificially cemented soil behaviours 345
10. Cemsoil Box Experimental Program 351
10.1. Introduction 351
10.2. Matrix suction measurements 359
10.3. Seismic wave velocities 364
10.4. DMT Testing 372
10.4.1. Introduction 372
10.4.2. Basic Parameters 375
10.4.3. Intermediate parameters 386
10.5. Deriving geotechnical parameters 391
10.5.1. Strength 391
10.5.2. Stiffness parameters 399
10.5.2.1. Deriving geotechnical parameters 399

10.5.2.2. Calibration of correlations using triaxial data 400

10.5.2.3. Calibration of stiffness correlations using seismic wave data..... 409

11. The Characterization Model..... 419

11.1. Introduction..... 419

11.2. In-situ Test Selection 420

11.3. Procedure..... 421

11.3.1. Loose to Compact Soils 421

11.3.2. (W_5 to W_4) IGM and rock materials..... 422

11.4. Deriving Geotechnical Data 423

12. Final Considerations..... 429

IMAGES INDEX

Figure 1.1 - Marchetti Dilatometer Test, DMT. 3

Figure 2.1 - Lithologic Cycle (after Hunt S.L., 2001) 18

Figure 2.2 - Sedimentary Cycle 19

Figure 2.3 - Tectonic Cycle (after José F. Vigil. USGS, 2000). 19

Figure 2.4 - Water Cycle (Press et al., 1997) 20

Figure 2.5 - Precipitation, temperature and evaporation as function of climatic zones. 22

Figure 2.6 - Goldich/Bowen Series 23

Figure 2.7 - Erosion and transport modes 27

Figure 2.8 - Schematic diagram of typical residual soil profile (after Little 1969) 29

Figure 3.1 - Mechanical evolution through weathering (after Wesley, 1988). 38

Figure 3.2 - Strength control as function of scale effects (after Hoek & Brown, 1980).39

Figure 3.3 - JRC profiles. Strength control as function of scale effects (after Hoek & Brown, 1980). 43

Figure 3.4 - Strength variation within a four joint set massif (after Valejo et al., 2002). 45

Figure 3.5 - Rock Mass Rating, RMR_{84} (after Branco, 2008). 47

Figure 3.6 - Idealized behaviour of residual soils (after Coop, 2000) 57

Figure 3.7 - Stress – void ratio possibilities in residual soils (after Anon, 1995). 59

Figure 3.8 - Idealized behaviour of residual soils (Rios da Silva, 2007). 60

Figure 3.9 - Critical state point determination (after Toll et al., 2006) 63

Figure 3.10 - Yield point determination (after Cuccovillo & Coop, 1997) 67

Figure 3.11 - Typical yield sequence purposed by Malandraki & Toll (1994, 2000). 68

Figure 3.12 - Modulus reduction (adapted from Mayne, 2001). 72

Figure 3.13 - Variation of shear modulus (G_0) with strain level (ε). 74

Figure 3.14 - Yield surfaces for volumetric compression (σ_1 = vertical stress, σ_3= horizontal stress) – a) Viana da Fonseca et al. (1997a); b) Limit state curve for saturated condition (Futai et al. 2006) (After Viana & Coutinho, 2008) 75

Figure 3.15 - Soil-water retention curve (after Futai et al. 2007). 79

Figure 3.16 - Cohesion intercept and angle of shearing resistance versus suction (after Viana da Fonseca & Coutinho, 2008). 80

Figure 3.17 - Yield curves under constant suction (after Viana da Fonseca & Coutinho, 2008) 80

Figure 3.18 - Three-dimensional view of the yield stresses in q:p:s space. 82

Figure 4.1 - Typical stress path associated to sampling (after Ladd & Lambe, 1963) 87

Figure 4.2 - Sampler geometric parameters (after Clayton et al, 1998). 89

Figure 4.3 - Details on SCPTu testing devices 101

Figure 4.4 - Different configurations of SCPTu cones (after Mayne, 2001). 102

Figure 4.5 - Typical SCPTu data presentation (courtesy of Mota-Engil). 103

Figure 4.6 - CPTu Classification (Douglas & Olsen, 1981) 105

Figure 4.7 - CPTu Classification (Robertson et al. 1986) 106

Figure 4.8 - CPTu Classification (Robertson et al. 1986) 107

Figure 4.9 - Unit weight based in side friction (Mayne, 2007) 109

Figure 4.10 - Unit weight evaluation based in v_s and depth (Mayne, 2007) 109

Figure 4.11 - Angle of shearing resistance based on q_c/σ'_{V0} (Robertson & Campanella, 1983). 114

Figure 4.12 - Angle of shearing resistance based on qc/σ'_{V0} (Marchetti, 1988). 114

Figure 4.13 - P and S wave propagation 116

Figure 4.14 - Wave generation: a) P waves; b) S waves (after Saraiva Cruz, 2008) 117

Figure 4.15 - Wave generation apparatus: a) P waves; b) S waves 117

Figure 5.1 - DMT test lay-out 122

Figure 5.2 - a) DMT test equipment; b) acquisition unit; c) blade details. 122

Figure 5.3 - DMT presentation data sheet (Courtesy of MOTA-ENGIL) 123

Figure 5.4 - A, B, C measurements (after Marchetti, 1997). 125

Figure 5.5 - Projection of sedimentary considered data in CPTu classification chart (Robertson, 1990). 128

Figure 5.6 - Typical K_D profiles (after Marchetti, 1980). 130

Figure 5.7 - K_0 comparisons 133

Figure 5.8 - OCR results in Mondego's alluvial deposits. 134

Figure 5.9 - OCR results in Vouga's alluvial deposits. 134

Figure 5.10 - Undrained shear strength, S_u (DMT) for organic and non-organic soils, compared with FVT. 137

Figure 5.11 - Results from Marchetti's correlation, compared with triaxial testing 137

Figure 5.12 - Results from Marchetti's and Roque's correlation, compared with FVT 138

Figure 5.13 - Ratios S_u (DMT) / S_u (FVT) versus of OCR. 138

Figure 5.14 - Re-adapted Durgonuglu & Mithcell diagram (Robertson & Campanella, 1991) 143

Figure 5.15 – Angle shearing resistence, ϕ, from K_D 144

Figure 5.16 - Marchetti lower bound determination of ϕ' compared with CPTu results (Portugal and Spain) 145

Figure 5.17 - Comparison between M_{DMT} and E_{oed} (after Marchetti, 1980) 147

Figure 5.18 - Comparison between M_{DMT} and E_{oed} 148

Figure 5.19 - M/qt correlations 148

Figure 5.20 - Ratios G_0/E_D and G_0/M_{DMT} 150

Figure 5.21 - Comparison between reference G_0 and E_D 150

Figure 5.22 - G_0/E_D ratio versus I_D in Portuguese soils (Cruz et al., 2006a) 151

Figure 5.23 - G_0/E_D ratio versus I_D (Marchetti & Cruz data) 151

Figure 5.24 - Comparison between G_0/E_D and I_D (global data) 151

Figure 5.25 - Global data in 3D plot 152

Figure 5.26 - G_0/E_D ratios as function of K_D (after Monaco et al., 2009) 153

Figure 5.27 - G_0/M_{DMT} ratios as function of K_D (after Monaco et al. (2009) 153

Figure 5.28 - Factors a and b variation with I_D 154

Figure 5.29 - Portuguese sedimentary data plotted against Marchetti's (2008) correlations. 154

Figure 5.30 -3D representation of function F_1 156

Figure 5.31 -3D representation of function F_2 157

Figure 5.32 -3D representation of function F_3 158

Figure 5.33 -3D representation of function F_4 159

Figure 5.34 - Experimental results comparing with Hryciw's determination 161

Figure 5.35 - Seismic Dilatometer, SDMT 161

Figure 5.36 - Adjustment of time arrivals obtained in a two-geophone device (after Marchetti, 2006). 162

Figure 5.37 - Decay ratio G_{DMT}/G_0 vs. K_D for various soil types (after Monaco et al., 2009). 163

Figure 5.38 - Monotonic cyclic degradation response with logarithm of shear strain(after Mayne et al., 1999). 163

Figure 5.39 - P_2 (DMT) - u_2 (CPTU) comparing results 165

Figure 5.40 - Variation P_2 / u_2 with I_D in fine grained soils. 165

Figure 5.41 - Variation of U_D with I_D 166

Figure 5.42 - Soil unit weight after Marchetti & Crapps (1981) 167

Figure 5.43 - Unit Weight comparisons 168

Figure 6.1 - Partial views of the studied area: a) from south; b) from west. 179

Figure 6.2 - Geologic Map of Portugal (1:1.000.000) 180

Figure 6.3 - Geologic Map of Porto (1:25.000). 180

Figure 6.4 - Microstructure characterization by degree of decomposition (Viana da Fonseca, 2003). 182

Figure 6.5 - Typical residual medium compacted to compacted residual soils from granite 182

Figure 6.6 - Typical decomposed to highly weathered granite 183

Figure 6.7 - Typical medium weathered granite 183

Figure 6.8 - Typical cross section of Porto Granitic Formation showing different weathering degrees 184

Figure 6.9 -Sequence of geologic evolution of Estrela massif (after Rodrigues, 2003): a) Diagenesis and Metamorphism; b) Installation of granites; c) Erosion and uplift of granitic masses; d) Formation of the mountain complex; e) Glaciation 185

Figure 6.10 -3D schematic diagram of Serra da estrela Geologic complex (Ferreira e Vieira, 1999) 186

Figure 6.11 - Microstructure characterization by degree of decomposition (after Rodrigues, 2003). 186

Figure 6.12 - Typical cross-section of Guarda residual soils (after Rodrigues, 2003) 187

Figure 6.13 - Normalized shear wave velocities CICCOPN specimens (after Ferreira, 2009) 189

Figure 6.14 - Normalized shear wave velocities CEFEUP specimens (after Ferreira, 2009) 189

Figure 6.15 - Grain size distribution 190

Figure 6.16 - Plasticity Index, IP 191

Figure 6.17 - Representation of consistency limits in Casagrande Chart 191

Figure 6.18 - Representative unit weights in Porto and Guarda Granite Formations 193

Figure 6.19 - Representative void ratios in Porto and Guarda Granite Formations 194

Figure 6.20 - Representative porosities in Porto Granite Formation 194

Figure 6.21 - Representative permeability coefficients in Porto Granite Formation. 195

Figure 6.22 - PGM (COBA, 2003) in-situ permeability in Porto Granite Formation. 195

Figure 6.23 - Representative uniaxial compressive strength in Porto Granite Formation 197

Figure 6.24 - Evolution of uniaxial deformability modulus in Porto Granite Formation 198

Figure 6.25 - Representative uniaxial compressive strength obtained from uniaxial compression, point load and Schmidt hammer tests, in Porto Granite Formation 198

Figure 6.26 - Evolution of uniaxial compressive strength, tensile strength in Porto Granite Formation 199

Figure 6.27 - Evolution of effective cohesion in Porto Granite Formation 200

Figure 6.28 - Angles of shearing resistance of rock matrix in Porto Granite Formation 200

Figure 6.29 - Evolution of angle of shearing resistance of joint in Porto Granite Formation 200

Figure 6.30 - Evolution of N_{SPT} in Porto and Guarda Granite Formations 202

Figure 6.31 - Evolution of dynamic point resistance, q_d, in Porto and Guarda Granite Formations 202

Figure 6.32 - Correlation between N_{SPT} and q_d in granitic residual soils 202

Figure 6.33 - Evolution of static point resistance, q_c, in Porto and Guarda Granite Formations 204

Figure 6.34 - Correlation between q_t and q_d in granitic residual soils 204

Figure 6.35 - Evolution of PMT yield pressure, P_Y, in Porto and Guarda Granite Formations 205

Figure 6.36 - Evolution of PMT limit pressure, P_l, in Porto and Guarda Granite Formations 205

Figure 6.37 - Evolution of PMT parameters in Porto and Guarda Granite Formations 205

Figure 6.38 - Correlation between E_{PMT} and N_b (CME)) 206

Figure 6.39 - Correlation between P_y/ P_l and N_b (CME) 206

Figure 6.40 - Seismic wave velocities in Porto and Guarda Granite Formations 207

Figure 6.41 - Angles of shearing resistance from in-situ tests: a) Peck et al., 1953; b) (Decourt, 1989); c) Hatanaka & Uchida (1996); d) Baguelin et al., 1978 211

Figure 6.42 - Comparisons of angle of shearing resistance deduced from in-situ and laboratorial test results. 213

Figure 6.43 - Deformability modulus deduced from in-situ (PMT) and laboratorial (uniaxial) test results 215

Figure 6.44 - Retention curves of Salgueiros Metro Station (after Topa Gomes, 2009). 217

Figure 7.1 - Typical P_0 and P_1 profiles related to q_c 228

Figure 7.2 - Porto granitic residual soils after Robertson (1990) classification: a) Cruz et al. (2006); b) CEFEUP and Casa da Música (after Viana da Fonseca et al., 2006) 229

Figure 7.3 - Representative K_D, vOCR, and M/q_c profiles 232

Figure 7.4 - Representative K_D, vOCR, and M/q_t profiles 232

Figure 7.5 - K_0 results derived from sedimentary and residual correlations. 234

Figure 7.6 - c' vs K_D and c'/σ'_{vo} (*100) vs K_D correlations 237

Figure 7.7 - c' vs vOCR and c'/σ'_{vo} (*100) vs vOCR correlations 237

Figure 7.8 - c' vs M/q_t and c'/σ'_{vo} (*100) vs M/q_t correlations 238

Figure 7.9 - Relation between c' and σ'_p 238

Figure 7.10 - Comparison between ϕ_{DMT} and ϕ_{CPTU} 239

Figure 7.11 - Trends between (ϕ_{DMT}-ϕ'_{triax}) and c', 100* c'/σ'_{vo} 240

Figure 7.12 - Relation between M derived through DMT and CPTu tests 241

Figure 7.13 - Relations between G_0 and N_{60} for structured soils (after Viana da Fonseca et al., 2007) 243

Figure 7.14 - Relations between G_0 and q_c for structured soils (after Viana da Fonseca et al., 2007) 244

Figure 7.15 - Relations between G_0/E_D vs I_D 244

Figure 7.16 -3D plot of G_0 as function of E_D and I_D 245

Figure 7.17 -3D Representation of best fitting surfaces. 246

Figure 7.18 - Global G_0 deduced by Hricyw correlation compared with reference values 248

Figure 7.19 - G_0 deduced by Hricyw correlation, for each experimental site 248

Figure 7.20 - Granulometric curves of the soil at two different depths 250

Figure 7.21 - Estimation of the coefficient of earth pressure, K_0 (adapted from Viana da Fonseca et al., 2007, 2009). 252

Figure 7.22 - vOCR profile estimated from DMT parameters (adapted from Viana da Fonseca et al., 2007) 253

Figure 7.23 - Angle of shearing resistance obtained with various correlations (adapted from Viana da Fonseca et al., 2007, 2009) 254

Figure 7.24 - Relations between q_c/σ'_{vo} e K_D (after Viana da Fonseca et al., 2007, 2009) 255

Figure 7.25 - Angle of shearing resistance from CPT data (adapted from Viana da Fonseca et al., 2007, 2009) 255

Figure 7.26 - Cohesive intercept derived from Cruz et al. (2006). Profile in cross-section 2 (adapted from Viana da Fonseca et al., 2007, 2009) 256

Figure 7.27 - Comparison between G_0 (CH) and correlated G_0 (after Viana da Fonseca et al., 2007, 2009) 257

Figure 7.28 - Comparison between Cross-Hole G_0, Hryriw G_0 and corrected G_0 (adapted from Viana da Fonseca et al., 2007, 2009) 258

Figure 7.29 - Relations between G_0/E_D and p_{0N} (after Viana da Fonseca et al., 2009) 259

Figure 8.1 - Distortions caused by CPT and DMT (Baligh & Scott, 1975) 264

Figure 8.2 - Ratios N_{20} (DMT) versus N(60) and N_{20} (DPSH) 267

Figure 8.3 - Evolution of static/dynamic basic parameters 270

Figure 8.4 - K_D - OCR and E_D-M relations. 274

Figure 9.1 - IPG local facilities for the assembly of CemSoil box. 289

Figure 9.2 - Experimented soils in its natural ground. 292

Figure 9.3 - Mineralogical composition obtained by X-ray diffraction (Rodrigues, 2003) 292

Figure 9.4 - Grain Size Distribution 293

Figure 9.5 - Compaction test results 294

Figure 9.6 - Indicative values of uniaxial strength of concrete produced with 350 kg/m^3 of CIM I 52.5R (adapted from Secil catalogue) 295

Figure 9.7 - Sample preparation process 296

Figure 9.8 - Chamber used for curing of artificially cemented samples. 296

Figure 9.9 - Uniaxial compression test apparatus. 297

Figure 9.10 - Diametral compression test apparatus 298

Figure 9.11 - Compression test results of 2, 4 and 6 % of CIM I 52.5R at 7 and 21 days 300

Figure 9.12 - Tensile strength results of 2, 4 and 6 % of CIM I 52,5R at 7 and 21 days 300

Figure 9.13 - Mean values of compressive strength produced with 350 kg/m^3 of CEM II/B-L 32.5N. 301

Figure 9.14 - Uniaxial compressive strength of soil mixtures 302

Figure 9.15 - Tensile strength of soil mixtures 303

Figure 9.16 - Strength evolution of samples mixed with the two different cements 305

Figure 9.17 - Uniaxial compression strength in saturated and non saturated samples. 306

Figure 9.18 - Global results of compression tests in saturated and unsaturated samples 308

Figure 9.19 - lPG triaxial apparatus 309

Figure 9.20 - Triaxial control system 310

Figure 9.21 - Remolding conditions: 1st row - Static compaction; 2nd and 3rd rows – Mounting the cell; 4th row – Placing LVDT's 311

Figure 9.22 - Stress and strain curves for 25 kPa of confining stress 312

Figure 9.23 - Stress and strain curves for 50 kPa of confining stress 313

Figure 9.24 - Stress and strain curves for 75 kPa of confining stress 313

Figure 9.25 - Stress and strain curves for 300 kPa of confining stress 313

Figure 9.26 - Peak strength and maximum dilatancy for 25 kPa of confining stress 318

Figure 9.27 - Peak strength and maximum dilatancy for 300 kPa of confining stress319

Figure 9.28 - Evolution of strain for maximum dilatancy with normalized deviatoric stress 320

Figure 9.29 - Evolution of volume change related to maximum dilatancy with normalized deviatoric stress 320

Figure 9.30 - Strength envelopes in q-p' stress space (artificial samples) 321

Figure 9.31 - Strength envelopes in q-p' stress space (natural samples – Rodrigues, 2003) 321

Figure 9.32 - Correlations between cohesion and compressive and tensile stresses. 322

Figure 9.33 - Peak deviatoric stresses versus uniaxial compressive stress. 323

Figure 9.34 - Peak deviatoric stresses versus uniaxial compressive stress: actual data represented by full lines and Schnaid et al (2001) data represented by dashed lines. 324

Figure 9.35 - Peak deviatoric stresses versus tensile strength. 324

Figure 9.36 - Critical State Line (CSL) of: a) non-cemented; b) For1; c) Fra2; d) Fra3; e) For2 325

Figure 9.37 - Critical State Line (CSL) representation. 326

Figure 9.38 - Failure envelopes of destructured samples (present work and Rodrigues, 2003) 327

Figure 9.39 - Critical State Line of destructured samples (present work and Rodrigues, 2003). 327

Figure 9.40 - Naturally and artificially cemented samples behaviour as approaching Critical State 328

Figure 9.41 - Final look of naturally and artificially cemented samples after failure 329

Figure 9.42 - Normalized deviatoric stress against maximum dilatancy of naturally and artificially cemented samples. 330

Figure 9.43 - Secant modulus obtained for confining stresses of 25 kPa. 331

Figure 9.44 - Secant modulus obtained for confining stresses of 50 kPa 331

Figure 9.45 - Secant modulus obtained for confining stresses of 75 kPa. 332

Figure 9.46 - Secant modulus obtained for confining stresses of 300 kPa. 332

Figure 9.47 - Representation of first yield in q-p' space. 334

Figure 9.48 - Representation of second yield partial surface in q-p' space 334

Figure 9.49 - Normalized E_i moduli plotted against initial mean effective stress. 336

Figure 9.50 - Normalized $E_{s0.1\%}$ moduli plotted against initial mean effective stress. 336

Figure 9.51 - Normalized E_{s50} moduli plotted against initial mean effective stress. 337

Figure 9.52 - Reference Ei moduli plotted against normalized deviatoric stresses. 338

Figure 9.53 - Reference $Es_{0.1\%}$ moduli plotted against normalized deviatoric stresses. 338

Figure 9.54 - Reference Es_{50} moduli plotted against normalized deviatoric stresses 338

Figure 9.55 - Reference moduli plotted against normalized deviatoric stresses. 340

Figure 9.56 - Reference moduli plotted as function of tensile strength: a) E_i; b) $E_{s0,1\%}$; c) $E_{s50.}$ 341

Figure 9.57 - Modulus reduction as function of normalized deviatoric stress, ordered by cementation level. 343

Figure 9.58 - Modulus reduction as function of normalized deviatoric stress, ordered by confining stress 344

Figure 9.59 - Naturally and artificially cemented soil strength behaviours. 346

Figure 9.60 - Naturally and artificially cemented soils stiffness behaviours. 347

Figure 10.1 - CemSoil box: General view of CemSoil box (upper row); location of central beam (mid row); placing the central beam (lower row) 353

Figure 10.2 - Fixation details of the interior of CemSoil box 354

Figure 10.3 - Details of the interior of CemSoil box 355

Figure 10.4 - Shear strains due to penetration (Whittle & Aubeny, 1992) 356

Figure 10.5 - Plant and Cross section of Cemsoil instrumentation 357

Figure 10.6 - CemSoil sample preparation; a) preparing the mixtures; b) filling the CemSoil; c) compaction of mixtures. 358

Figure 10.7 - Device installation: a) first blade; b) second blade; c) detail of open piezometric tubes; d) installation of piezometers. 359

Figure 10.8 - Suction measurements: a) reading device; b) tensiometer; c) tensiometer installation 360

Figure 10.9 - Suction measurements. 362

Figure 10.10 - Suction results: a) retention curve (no cemented) b) suction at testing times. 363

Figure 10.11 - Seismic devices installation. 364

Figure 10.12 - Schematic representation of seismic wave apparatus 364

Figure 10.13 - Details of seismic wave measurement apparatus. 365

Figure 10.14 - Wave registration 366

Figure 10.15 - Example of seismic wave velocity statistical analysis 367

Figure 10.16 - Frequency of events 368

Figure 10.17 - S wavess versus P wave velocities variation. 368

Figure 10.18 -3D representation of shear / compressive waves and Poisson's ratio. 369

Figure 10.19 - Shear wave velocities obtained before saturation. 370

Figure 10.20 - Shear wave velocities obtained after saturation. 370

Figure 10.21 - Compression wave velocities obtained before saturation. 371

Figure 10.22 - Compression wave velocities obtained after saturation. 371

Figure 10.23 - Compression and shear wave comparisons. 372

Figure 10.24 - Final aspect of the instrumented block sample. 373

Figure 10.25 - Final aspect of a CemSoil sample (Fra2). 373

Figure 10.26 - DMT testing conditions: penetrometer rig (upper row), partial views from lower and upper stages (mid row) and penetration test conditions (lower row). 374

Figure 10.27 - Basic pressures obtained after static pushing in-situ and in CemSoil 377

Figure 10.28 - Basic pressures obtained in pre-installed and static pushed-in conditions (no cemented). 378

Figure 10.29 - Basic pressures obtained in pre-installed and static pushed-in conditions (For1). 378

Figure 10.30 - Basic pressures obtained in pre-installed and static pushed-in conditions (Fra2). 379

Figure 10.31 - Evolution of basic pressures and readings with cementation level 381

Figure 10.32 - Global A-readings 382

Figure 10.33 - Global B-readings. 382

Figure 10.34 - Evolution of P_0 corrected parameter related to different penetration and saturation conditions.. 383

Figure 10.35 - Evolution of P_1 corrected parameter related to different penetration and saturation conditions. 383

Figure 10.36 - Evolution of basic pressure ratios with cementation level: a) P_1/ P_0; b) $P_1- P_0$ 384

Figure 10.37 - P_1* normalized parameter obtained in pushed-in conditions. 385

Figure 10.38 - I_D parameter obtained in installed and pushed conditions. 386

Figure 10.39 - K_D parameter obtained in installed and pushed-in conditions. 387

Figure 10.40 - K_D comparison in installed and pushed conditions 387

Figure 10.41 - E_D parameter obtained in installed and pushed-in conditions. 388

Figure 10.42 - Intermediate parameters obtained in pushed conditions. 389

Figure 10.43 - I_D*, K_D* and E_D* normalized parameters obtained in pushed conditions. 390

Figure 10.44 - Normalized parameters as function of tensile strength. 391

Figure 10.45 - Angle of shearing resistance results. 392

Figure 10.46 - c' deduced by DMT: a) CemSoil; b) normalized c'*. 393

Figure 10.47 - Correlation of global cohesion intercept (c'_g) as function of OCR for no cemented and cemented mixtures. 395

Figure 10.48 - Correlations of global cohesion intercept (c'_g) as function of vOCR. 395

Figure 10.49 - Upper and lower expected bounds for overall cohesive intercept (c'_g) correlation. 396

Figure 10.50 - Overall cohesive intercept (c'_g) results in: a) Cemsoil; b) In-situ. 397

Figure 10.51 - Evolution of uniaxial compression, triaxial deviatoric and tensile strength with P_1 pressure. 398

Figure 10.52 - Correlation to correct angle of shearing resistance. 398

Figure 10.53 - Triaxial and deduced angle of shearing resistance results in: a) Cemsoil; b) In-situ. 399

Figure 10.54 - Comparison of E_D and triaxial reference moduli. 401

Figure 10.55 - Comparison of E_D and normalized triaxial reference moduli. 402

Figure 10.56 - Comparison of initial tangent and secant deformability moduli and E_D 402

Figure 10.57 - Variation of ratio E_i/E_D as function of P_{0N} normalized parameter. 403

Figure 10.58 - Variation of ratio E/E_D as function of P_{0N} normalized parameter. 403

Figure 10.59 - Constrained Modulus: a) CemSoil and Guarda in-situ results; b) Normalized parameter, M* 404

Figure 10.60 - E_D location in E_{sec} vs. axial strain (pre-installed conditions. 405

Figure 10.61 - E_D location in E_{sec} vs. axial strain (pushed-in conditions). 406

Figure 10.62 - E_{DMT} location in E_{sec} vs. axial strain (pre-installed conditions). 407

Figure 10.63 - E_{DMT} location in E_{sec} vs. axial strain (pushed-in conditions). 408

Figure 10.64 - G_0 deduced from DMT (Cruz & Viana da Fonseca, 2006a) and from Cross-hole tests, in Guarda Residual soils. 410

Figure 10.65 - G_0 deduced from DMT tests performed in CemSoil box (Cruz & Viana da Fonseca, 2006a). 410

Figure 10.66 - G_0 deduced from seismic measurements within CemSoil box. 411

Figure 10.67 - Results of G_0 – DMT correlations in sedimentary and residual soils. 412

Figure 10.68 - Results of G_0 (DMT) correlations in sedimentary and residual soils, plotted in a log – log scale: a) 2D Plot; b) 3D plot 413

Figure 10.69 - Residual and sedimentary sand data in G_0/M_{DMT} vs. K_D space. 414

Figure 10.70 - Upper and lower bounds for residual and sedimentary sandy soils, in G_0/M_{DMT} vs. K_D plot. 414

Figure 11.1 Example of a characterization model for residual soils 422

TABLES INDEX

Table 1.1 - DMT history in Portugal. 8

Table 2.1 - Compositions of some typical residual soils 23

Table 2.2 - Weathering petrographic indexes. 25

Table 2.3 - Weathering chemical indexes. 25

Table 3.1 - Failure criteria for typified situations (Valejo et al., 2002). 40

Table 3.2 - m_i parameter for the common rock types (Hoek & Brown, 1997). 41

Table 3.3 - Basic friction angle, $\phi_{b,}$ for the common rock types (Hoek & Brown, 1997). 44

Table 3.4 - Empirical correlations for massif modulus determination, $E_{m.}$ 48

Table 3.5 - Typical soil and rock index parameters ranges 49

Table 3.6 - Residual versus transported soil responses. 50

Table 3.7 - Reference works in bonded soil strength (after Viana da Fonseca & Coutinho, 2008). 58

Table 3.8 - Stiffness vs stress state parameters for residual soil (Viana & Coutinho, 2008) 70

Table 3.9 - Values of a and b (adapted from Barros, 1997). 71

Table 3.10 - Suction devices (adapted from Ridley & Wray, 1995 and Guan, 1996). 78

Table 4.1 - Sampling disturbance (adapted from Clayton et al., 1995). 88

Table 4.2 - Characteristics of in-situ tests 96

Table 4.3 - In-situ tests fields of applications 97

Table 4.4 - Quality of deduced parameters. 97

Table 4.5 - Possible test combinations 100

Table 4.6 - Correlation between graphical and numerical methods (Saraiva Cruz, 2008). 107

Table 4.7 - Unit weight by Robertson, 1986 108

Table 4.8 - Unit weight (Saraiva Cruz, 2008) 110

Table 4.9 - Cone Factor N_k typical values 111

Table 4.10 - Cone Factor N_{kt} typical values 112

Table 4.11 - Cone Factor N_{ke} typical values 112

Table 4.12 - Cone Factor $N_{\Delta u}$ typical values 112

Table 5.1 - Base functions considered in MatLab® analysis. 155

Table 5.2 - Statistical parameters and constants related the four designated functions 156

Table 6.1 – Adopted class designations in the present work 177

Table 6.2 - Classification for sampling quality and sample condition (Ferreira, 2009) 188

Table 6.3 - Typical ranges of granitic physical properties (Viana da Fonseca et al., 1994) 194

Table 6.4 - Trend values of permeability by classes of weathering of Porto Granite (after Viana da Fonseca & Coutinho, 2008) 196

Table 6.5 - Some local strength parameters 201

Table 6.6 - Index parameters for Modified Wesley Classification 209

Table 6.7 - Values of α to derive deformability modulus (Amar *et al*., 1991) 214

Table 6.8 - Summary of some strength parameters in residual soils 217

Table 6.9 - Summary of geotechnical parameters global ranges (laboratorial) 219

Table 6.10 - Summary of geotechnical parameters global ranges (in-situ) 220

Table 7.1 - In-situ efficiency in residual soil characterization 226

Table 7.2 - CPTu and DMT ranges obtained in Porto Formation 227

Table 7.3 - DMT and CPTu reference values of studied sites 235

Table 7.4 - Triaxial reference values of studied sites 236

Table 7.5 - Function parameters and statistics. 246

Table 7.6 - In-situ test parameters at Casa da Música Metro Station (Rios Silva, 2007; Viana da Fonseca ehav., 2007, 2009) 249

Table 7.7 - DMT parameters at Casa da Música Metro Station (Viana da Fonseca ehav., 2007, 2009) 249

Table 7.8 - Unit weight determinations (Cross section 1) 251

Table 7.9 - Unit weight determinations (Cross section 2) 251

Table 7.10 - Correlations for granitic residual soils from Porto and Guarda 260

Table 8.1 - Mechanical characterization of the sites 266

Table 8.2 - Basic and intermediate DMT parameters obtained after static and dynamic penetration of the blade 268

Table 8.3 - Statistics on P_0 (S)/P_0 (D) 269

Table 8.4 - Statistics on P_1 (S)/P_1 (D) 269

Table 8.5 - Statistics on I_D (S) / I_D (D 271

Table 8.6 - Statistics on K_D (S) / K_D (D) 271

Table 8.7 - Statistics on E_D (S) / E_D (D) 271

Table 8.8 - Statistics on γ (S)/γ (D) 272

Table 8.9 - Statistics on ϕ' (S)/ϕ' (D) 272

Table 8.10 - Statistics on M (S)/M (D) 273

Table 8.11 - Statistics on OCR (S) / OCR (D) 273

Table 8.12 - Summary of measurements distributions (global values). 276

Table 8.13 - Maximum absolute errors of DMT devices 277

Table 8.14 - Maximum absolute errors of current used devices 277

Table 8.15 - Relative error range of basic parameters (%). 278

Table 8.16 - Relative error range of intermediary parameters (%). 278

Table 8.17 - Relative error range of geotechnical parameters (%). 279

Table 8.18 - In-situ test error propagation (Mateus et al., 2010) 281

Table 9.1 - Identification and physical properties of natural soil used in the main experiment (after Rodrigues, 2003) 293

Table 9.2 - Identification and physical properties of the soil used in the main experiment 293

Table 9.3 - Soil-cement sample constitution 295

Table 9.4 - Physical characterization of samples used in compression strength (CIM I 52.5R, 7 e 21 days). 298

Table 9.5 - Maximum uniaxial compression strength (CIM I 52.5R, 7 e 21 days) 299

Table 9.6 - Physical characterization of samples used in diametral compression strength (CIM I 52.5R, 7 and 21 days) 299

Table 9.7 - Maximum diametral compression strength (CIM I 52.5R, 7 and 21 days) 300

Table 9.8 - Cement compositions for CEM II/B-L 32.5N. 302

Table 9.9 - Physical characterization of samples used in compression strength 303

Table 9.10 - Uniaxial compression test results 304

Table 9.11 - Physical characterization of samples used in diametral compression strength 304

Table 9.12 - Diametral compression test results 304

Table 9.13 - Compressive strength test results under different saturation conditions 307

Table 9.14 - Characteristics of devices used in triaxial testing 310

Table 9.15 - Global laboratory testing results 315

Table 9.16 - Reference strength parameters. 316

Table 9.17 - Determined and deduced tensile strengths 323

Table 9.18 - Reference Moduli and Janbu parameters 333

Table 9.19 - Moduli correlation parameters and factors 337

Table 9.20 - Moduli correlation parameters and factors 339

Table 9.21 - *f* and *g* hyperbolic distortion parameters 342

Table 10.1 - Results obtained in pre-installed conditions 375

Table 10.2 - Results obtained in pushed-in conditions. 376

Table 10.3 - Summary of axial strains related to E_D and $E_{DMT.}$ 406

Table 11.1 – Correlations for deriving geotechnical parameters in Porto Granite Formation 426

Latin Alphabet

A – area

– Skempton pore pressure parameter;

– DMT reading;

AR – sampler area ratio;

A_c – CPT tip cross section;

A_f – Skempton pore pressure parameter at failure;

A_s – CPT side friction area;

A_t – clay activity;

a_v – compression coefficient;

B – Skempton pore pressure parameter;

– DMT reading;

B_q – normalized pore pressure ratio (CPTu);

c' – cohesive intercept in Mohr-Coulomb criteria;

c'_g – cohesive intercept in Mohr-Coulomb criteria due to cementation and suction;

C – constant depending on the shape and nature of grains;

– DMT reading;

CF ratio – clay/fine ratio

C_C – coefficient of curvature;

C_c – compressibility index

CH – *cross-hole*; seismic test

CID – triaxial test with isotropic consolidation;

CIU – isotropically consolidated undrained triaxial testing;

CK_0D – triaxial test with consolidation "K_0";

C_N – effective overburden stress correction for N_{SPT};

CPT – static cone penetrometer;

CPTu – piezocone;

CSL – critical state line*;*

c_u (S_u) – undrained cohesion (undrained strength);

C_u – grain size uniformity coefficient;

c_v – consolidation coefficient;

C_α – área ratio;

D_c – inside cutting edge diameter of samplers;

D_e – outside cutting edge diameter of sampler;

D_i – internal diameter of samplers;

DMT – Marchetti´s flat dilatometer;

DP – dynamic probing;

DPH – dynamic probing heavy;

DPL – dynamic probing light;

DPM – dynamic probing medium;

DPSH – dynamic probing super-heavy;

D_r – relative density;

e – void ratio;

E – deformability modulus;

– Young modulus;

E_0 – initial deformability modulus;

e_0 – in-situ void ratio;

e_{cv} – critical state void ratio;

E_{PMT} – pressiometric modulus (PMT)

E_D/ E_D* – dilatometer modulus (DMT) / dilatometer modulus ratio (unsaturated/saturated)

E_i – deformability modulus of intact rock

– initial tangent modulus;

E_m massif deformability modulus rock E_m

E_s – secant deformability modulus;

E_{s50} – secant modulus at 50% of maximum deviatoric stress

$E_{s(n\%)}$ – secant deformability modulus (at n% of strain level);

E_t – tangent deformability modulus;

F – load;

$F(e)$ – void ratio function

F_r – normalized friction ratio (CPT);

f_s – side friction (CPT);

G – shear modulus

G8A – compact residual soil unit in Porto Geotechnical Map;

G4 – medium compact residual soil unit in Porto Geotechnical Map;

G4K – kaolinized unit in Porto Geotechnical Map;

G_0 – small strain shear modulus;

GSI – Geological Stress Index

G_s – solids density;

H – altura de queda da massa M num ensaio de penetração dinâmico;

h – height;

ICR – sampler inside clearance ratio;

I_c – classification index for CPTu

I_D/ I_D* – DMT material index ; DMT material index ratio (unsaturated/saturated)

IL – liquidity index;

I_p – plasticity index;

JCS – joint compression strength

JRC – joint roughness coefficient

k – coefficient of permeability;

K – bulk modulus;

K_0 – at rest pressure coefficient;

K_D/ K_D* – horizontal stress index (DMT); horizontal stress index ratio (unsaturated/saturated)

k_n – discontinuity ratio

$K_{0(NC)}$ – at rest pressure coefficient of normally consolidated soil;

$K_{0(OC)}$ – at rest pressure coefficient of overconsolidated soil;

L – length;

LC – loading-collapse yield curves

LCI – linha de compressibilidade intrínseca;

LL – liquid limit;

LP – plasticity limit;

M – constrained modulus (DMT);

m – parameter of Hoek & Brown failure model

M_0 – initial constrained modulus;

m_i – rock type factor

m_v – volumetric compression coefficient;

$(N_1)_{60}$ – normalized N_{60} to the reference vertical stress;

N_{60} – N_{SPT} corrected for the reference energy of SPT tests (60 % of theoretical energy);

N_k, N_{kt}, N_{ke}, $N_{\Delta u}$ – cone factors for deducing s_u from CPTu tests;

N_c – cone factor for deducing s_u from DMT tests;

NC – normally consolidated soil;

NCL – normal compression line;

N.F. – water level;

$N_{20\ DPSH}$ –number of blows to penetrate 20cm with DPSH cone tip;

$N_{20\ DMT}$ –number of blows to penetrate 20cm with DMT blade;

N_{SPT} – número de pancadas da segunda fase do ensaio SPT;

OC – overconsolidated soil;

OCR – overconsolidation ratio;

p – mean total stress, $[(\sigma_1+\sigma_2+\sigma_3)/3]$;

p_y^* – differential creep pressure of PMT;

p_l^* – differential limit pressure of PMT;

p' – mean effective stress, $[(\sigma'_1+\sigma'_2+\sigma'_3)/3]$;

p'_{cs} – mean effective stress at critical state;

P_0 – PMT lift-off pressure;
– DMT lift-off pressure

P_{0N} – normalized DMT lift-off pressure

P_1/ P_1* – DMT pressure/ DMT pressure ratio (unsaturated/saturated)

P_2 – DMT pressure;

p_a – atmospheric pressure (101,3 kPa);

p_y – PMT creep pressure;

P_l – PMT limit pressure;

PLT – plate load test;

PMT – Ménard pressuremeter test;

q – deviator stress $(\sigma_1-\sigma_3)$;

q_c – cone tip resistance (CPT/CPTu);

q_d – dynamic cone resistance obtained in dynamic probing, DP;

q_f – deviator stress at failure;

Q_T – normalized cone resistance (CPT);

q_t – corrected cone resistance (CPTU);
– diametral compression strength

q_{t1} – q_t corrected for the effect of effective stress (CPTU);

q_u – uniaxial compression strength*;*

q_{ult} – ultimate bearing capacity

R – rebound of schimdt hammer test on a unweathered surface;

r – rebound of schimdt hammer test on a weathered joint surface;

R^2 – correlation coefficient;

R_d – dynamic point resistence DP;

R_f – friction ratio of CPT (q_c/f_s);

RMR – Rock Mas Rating

s – settlement;
– parameter of Hoek & Brown failure model
– suction

S – saturation degree;
– cross-section;
– surface;
– the spacing of the joint family

SBPT – self-boring pressuremeter;

SCPTu – seismic piezocone;

SDMT – seismic dilatometer;

SI – suction-increase yield curves

SP – screw-plate test;

SPT – standard penetration test;

SSL – steady state line

t – thickness;
– time;

U_D/U_D^* –pore pressure index (DMT); pore pressure index ratio (unsaturated/saturated)

u_2 – CPTu measured pore pressure;

u, u_w – pore water pressure;

u_0 – at rest pore water pressure;

u_a –pore air pressure;

vOCR/AOCR – virtual OCR/apparent OCR

v_P – compressional wave velocity;

v_S – shear wave velocity;

v_s^* – shear wave velocity normalized by the void ratio;

w – water content;

W_1 – unweathered;

W_2 – slightly weathered;

W_3 – medium weathered;

W_4 – highly weathered;

W_5 – decomposed;

W_6 – residual soil;

w_{nat} – in-situ water content;

X_d – decomposition degree;

Y1 – first yield, limit of linear elastic behaviour according to Jardine model

Y2 – second yield, limit of of recoverable behaviour according to Jardine model

Y3 – third yield, represents complete destruction of any structure according to Jardine model

z_M – pressure gauge at atmospheric pressure;

z – depth;

Greek alphabet

$\varnothing$ – diameter;

Δ – finite increment;

ΔA – DMT calibration parameter;

ΔB – DMT calibration parameter;

Δu – pore water change;

ΔV – volume change;

Γ – specific volume in the critical state line related with p' = 1;

α – inclination angle at which the relative movement of a discontinuity starts;

– parameter of failure Hoek & Brown model;

– outside cutting edge angle of samplers;

– q_c / N_{60} correlation factor;

– E_{PMT} / E correlation factor;

β – lexiviation index;

– inside cutting edge angle of samplers

δ – displacement;

ε – strain;

ε_a – axial strain;

ε_r – radial strain;

ε_v – vertical strain;

– volumetric strain;

ϕ – angle of shearing resistance;

ϕ' – effective angle of shearing resistance;

ϕ_b – basic friction angle of joints;

ϕ^b – suction angle of shearing resistance;

ϕ'_{cv} – angle of shearing resistance at critical state;

ϕ'_p – peak angle of shearing resistance;

ϕ'_r – residual angle of shearing resistance;

ϕ_{ps} – plane strain angle of shearing resistance;

γ – distortion;

– unit weight;

γ_h – hyperbolic shear strain;

γ_r – reference shear strain;

γ_{nat} – in-situ unit weight;

γ_d – dry unit weight;

γ_s – solids unit weight;

γ_{sat} – saturated unit weight;

γ_w – water unit weight;

λ – slope of virgin compression line in ν-lnp' plot;

λ_{ss} – slope of steady state points projection on e-logp' plane

ν – Poisson coefficient;

– specific volume (1+e);

σ – stress;

σ_1 – principal maximum stress

σ_3 – principal minimum stress

σ' – effective stress;

σ'_c – consolidation effective stress;

σ_h – horizontal stress;

σ_{h0} – in-situ horizontal stress;

σ'_{h0} – in-situ effective horizontal stress;

σ'_p – pre-consolidation stress;

σ'_{pv} – virtual pre-consolidation stress;

σ_{v0} – in-situ vertical stress;

σ'_{v0} – in-situ effective stress;

σ_0, σ_i – initial stress;

σ_a – axial stress;

σ_r – radial stress;

σ_v – vertical stress;

τ – shear stress;

τ_{max} – maximum shear stress;

τ_f – shear stress at failure;

ψ – angle of dilatancy;

Abreviations

ASCE – American Society of Civil Engineers;

ASTM – American Society for Testing and Materials;

BS – British Standard;

CICCOPN – Centro de Formação Profissional da Indústria da Construção Civil e Obras Públicas do Norte;

DIN – Deutsches Institut für Normung;

FCTUC – Faculdade de Ciências e Tecnologia da Universidade de Coimbra;

IPG – Instituto Politécnico da Guarda;

ISSMGE – International Society for Soil Mechanics and Geotechnical Engineering;

LNEC – Laboratório Nacional de Engenharia Civil;

LVDT – Linear variable differential transformer;

NF – Norme Française;

PGM – Porto Geotechnical Map

Chapter 1. Introduction

1. INTRODUCTION

1.1. Brief history of Marchetti´s Dilatometer (DMT) use in Portugal

Marchetti dilatometer test or flat dilatometer (Figure 1.1), commonly designated by DMT, was developed by Silvano Marchetti (1980) and is one of the most versatile tools for soil characterization, namely loose to medium compacted granular soils and soft to medium clays, or even stiffer if a good reaction system is provided. The main reasons for its usefulness deriving geotechnical parameters are related to the simplicity and the speed of execution generating continuous data profiles of high accuracy and reproducibility. The test equipment exhibits high accuracy, and yet is very friendly and easy to use, robust to face the work in the field, and very easy to repair for most of common problems.

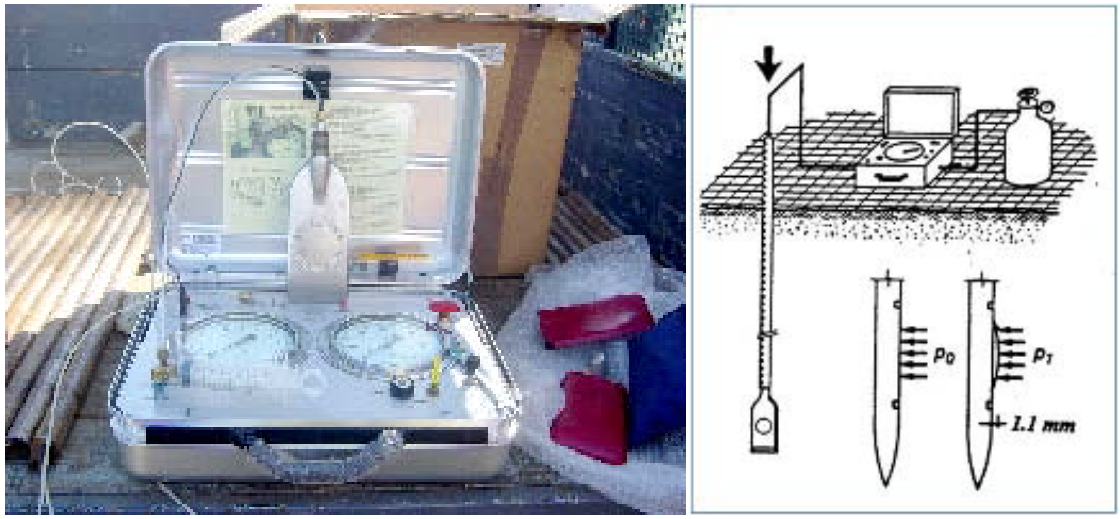


Figure 1.1 - Marchetti Dilatometer Test, DMT.

It was running the year of 1994 when the author first met DMT, in the entrance hall of Industrial de Sondeos (ISSA) in Madrid, which really impressed by its simplicity and parameter versatility. As a consequence, one DMT unit was bought (the first in Portugal) by *Laboratorio de Geotecnia e Materiais de Construção* (LGMC) of *Centro de Formação Profissional da Industria da Construção Civil e Obras Públicas do Norte* (CICCOPN), a quality certified laboratory (by Portuguese Institute for Quality, IPQ) of mechanical testing, where the author was working at the time, launching a long run after its applicability in residual soils. One year later, the first DMT paper dealing with sedimentary Portuguese soils was published in the Portuguese geotechnical

conference (Cruz, 1995a), followed by the first MSc dissertation on DMT in Portuguese soils (Cruz, 1995b), which included three sedimentary and two residual experimental sites. Working in a quality certified laboratory (at the time were rare in Portugal), allowed collecting an important quality controlled data set. Efficient procedures for data treatment and storing generated a high quality and trustable database, providing important possibilities for cross-checking with information coming from a wide range of testing equipments, such as the laboratorial triaxial and consolidation tests, or the in-situ field vane (FVT), piezocone (CPTu), plate load (PLT) and screw-plate (SP) tests. The possibilities arising from this testing interaction become immense, suggesting that a multi-test technique (*MT technique*) was a very promising methodology to deal with the extra variables of residual soils. At the end of the century, characterization campaigns combining DMT and CPTu tests were the common base proposed to its customers by LGMC, both in sedimentary and residual environments (Saraiva Cruz, 2003, 2008; Cruz et al; 2004a, 2004b, Cruz & Viana da Fonseca 2006a).

The first approach to evaluate DMT test applicability was established to check the adequacy of response in sedimentary soils and compare it with international references, to serve as a launching base for residual soils since test applications to residual soils were not available in 1994 when the equipment was acquired. Three of the main portuguese river alluvial deposits (Vouga, Mondego and Tejo) were selected, settling combined campaigns to derive strength and stiffness properties of soft soils by DMT, cross-checked with triaxial, oedometer, FVT and CPTu tests (Cruz, 1995a, 1995b; Cruz et al., 1997b, Cruz et al. 2006a). The results confirmed the global recognition in sedimentary soil characterization reported by DMT users and researchers, not only deriving strength and stiffness both in fine and coarse grained soils, but also in stress history and state of stress of fine grained soils. The work performed by that time marked the first step of data collection from where the research programs in sedimentary, residual soils and also in earthfill quality control were launched.

In sedimentary framework, the research led to an extensive work published in the DMT conference held in Washington (Cruz et al, 2006a), which included 20 experimental sites of varying geology and grain size distributions, from fine to coarse grained soils, bringing answers and confirmations about DMT data quality and versatility in geotechnical characterization. Drained and undrained strength and stiffness were checked and confirmed and a new correlation to reduce shear modulus in sedimentary soils was proposed (Cruz et al., 2006a). State of stress and stress history of fine soils

were also checked ant confirmed, while pore water pressure evaluation (P_2 or U_D) revealed itself quite accurate when compared to CPTu (u_2).

Meanwhile, residual soil data analysis had started from ground zero, collecting information to create a statistically significative data set, which allowed for the further established trends and specific correlations development adequate for these non-text book materials. This generated a specific framework related with DMT applications in residual soils. The first experience with DMT in residual soils was performed in CICCOPN facilities in Maia within the author MSc thesis (Cruz, 1995b), followed by a campaign performed in Hospital de Matosinhos experimental site, which at the time was being studied in a PhD framework on foundation in residual soils (Viana da Fonseca, 1996). These two well characterized sites gave rise to the early attempts to correlate DMT test parameters with cohesive intercept (Cruz, 1995; Cruz & Viana da Fonseca, 1997a; Cruz et al., 1997b) and horizontal stresses (Viana da Fonseca, 1996; Cruz et al., 1997), being the kick-off for the work produced ever since.

Taking advantage of a well equipped certified laboratory (LGMC) located in the facilities, CICCOPN experimental site have been extensively used since then (Cruz et al., 2000, 2004a, 2004b, 2004c; 2006a; Cruz & Viana da Fonseca, 2006a) becoming an important reference base for deducing DMT correlations in residual soils, also used by FEUP (Viana da Fonseca et al., 2001; Vieira, 2001; Ferreira, 2009) in its residual soil research framework. The previous confirmation of DMT adequacy characterizing Portuguese sedimentary soils together with the important research carried out by FEUP (Faculty of Engineering of University of Porto) in residual soils (Viana da Fonseca, 1988, 1996, 1998, Viana et al, 2001) provided a properly calibrated experimental data set, from where the studies of application of DMT to residual soils was developed. Although LGMC and FEUP had followed their own specific ways and objectives, the interaction between both institutions became regular generating very important cross contributions and leading to an increasingly sustainable understanding of the test possibilities in these non-text book materials, reflected by significant published data on subject (Cruz, 1995; Viana da Fonseca, 1996; Cruz et al., 1997a, 2000; Viana da Fonseca et al., 2001, Cruz et al., 2004b and 2004c; Cruz & Viana da Fonseca, 2006a). In addition, the intensive interaction between CICCOPN and other research institutions led to the participation both in the characterization of IPG experimental site (Rodrigues et al., 2002) and ISC2 Pile Prediction Event (Viana da Fonseca et al., 2004), providing important and extensive high quality DMT data in

granitic residual soils. This experimental site lasted beyond ISC'2 event, being later renamed *CEFEUP* experimental site, the latter being the designation adopted herein.

A specific framework on the evaluation of cementation effects in strength and stiffness was held since the beginning, leading to a first important interpretation model created based upon comparisons with triaxial testing performed on high quality samples (Cruz et al., 2004b, 2006b), which was successfully applied in some referenced works such as Casa da Música Metro station integrated in Porto network (Viana da Fonseca et al., 2007, 2009), that will be presented in the course of this work.

Following another point of view, the specific nature of residual soil typical (erratic) profiles usually creates some difficulties in DMT or CPT installation, due to the presence of stiff bodies within the residual mass. Being so, a another framework was established to evaluate the disturbance of dynamic insertion of the blade, since this methodology opened a possibility of overcoming these rigid layers and thus, providing more complete profiles (Cruz & Viana da Fonseca, 2006b). Naturally, the possibility of dynamic insertion opened new opportunities in stiff material characterization and thus earthfill characterization became another interesting research direction. Special attention was paid to the earthworks composed by granitic residual soils, once they constitute an important reference (destrucutred materials) for the main research work (Cruz et al., 2006b, 2008a).

On the other hand, these research goals somehow created the necessity of evaluating and comparing the final results quality with other in-situ tests. In this context, although measurement device accuracy and precision are adequately studied and considered by the quality control management commonly followed in construction industry, it should be recognized that accuracy of measurement devices might have quite different consequences in the wide range of parameters or other calculations obtained from the direct test measurements. Thus, departing from the accuracy of the commercially measurement devices included in test equipments, another research path was established, aiming to the evaluation of the errors propagation on final calculation of either sedimentary or residual geotechnical parameters (Mateus, 2008, Cruz et al., 2008b, 2009b), not only for DMT but also for other commonly used testing equipments, such as PMT and SCPTu (Vieira, 2009, Mateus et al, 2010). This research line was developed within an important partnership with Mathematical Department of Instituto Politécnico do Porto (IPP), which brought in some important and decisive new tools for data analysis.

Apart the PhD thesis presented herein, fully dedicated to DMT test in residual soils, the described global research work gave rise to more than twenty publications, six final engineering degree works (Figueiredo, 2002; Saraiva Cruz, 2003; Ribeiro, 2004; Vaz, 2006; Branco, 2008, Felizardo, 2008), four MSc thesis (Cruz, 1995; Mateus, 2008; Saraiva Cruz, 2008; Vieira, 2009), apart from the already referred PhD thesis on foundation analysis (Viana da Fonseca, 1996) that included DMT test characterization. All those contributions allowed deducing correlations for in-situ state of stress (Viana da Fonseca, 1996; Cruz et al., 1997), cohesion intercept (Cruz et al., 2004c; Cruz & Viana da Fonseca, 2006a), angle of shearing resistances (Cruz & Viana da Fonseca, 2006a) and laboratorial stiffness moduli (Viana da Fonseca, 1996), as well as the mentioned studies on dynamic versus static pushing disturbance (Cruz & Viana da Fonseca, 2006b), control of compaction (Cruz et al., 2008a) and propagation error analysis (Mateus, 2008; Cruz et al, 2008b, 2009b). In Table 1.1, a summary of this historic evolution is presented, following the main important dates, achieved goals and respective references. Of course, far beyond one man's work, this has been produced by a fantastic and enthusiastic group of operators, trainees, MSc students and professional engineers that worked together with the author as team mates in LGMC of CICCOPN, MOTA-ENGIL geotechnical department (to where the author has moved in 2003) and in Aveiro University (UNAVE). All of them have given decisive contributions to the actual knowledge on the subject and thus, to the experience presented herein.

Table 1.1 - DMT history in Portugal.

Type of material	Subject	Date	References
All kinds	Date of DMT acquisition	1994	---
	Training of the first Portuguese DMT operators	1994	J. Carvalho and F. Gomes
	Organizing calculation and data storing	1995-1998	---
Sedimentary Soils	First experimental sedimentary sites (Alluvial deposits of Vouga, Mondego and Tagus rivers)	1995	Cruz, 1995a; Cruz, 1995b (MSc); Cruz et al 1997
	First global portuguese data analysis	1998	Figueiredo, 2002; Cruz et al, 2006a
	Specific correlations for small strain shear modulus	2005	Rocha, 2005; Cruz et al., 2006
Residual soils	CICCOPN and Hospital de Matosinhos experimental sites data collection and interpretation, which became the kick-off of DMT experiences in residual soils from Porto granites.	1994, 1995	Cruz, 1995b (MSc); Viana da Fonseca, 1996 (PhD)
	In-situ state of stress correlation adapted from sedimentary approach; earlier correlations of cementation influence in strength and stiffness.	1995, 1996	Viana da Fonseca, 1996; Cruz et al., 1997a, 1997b, 2000
	CICCOPN experimental site intensively used to study DMT in residual soils. Introduction of combined DMT+CPTU in regular campaigns. First global portuguese data collection and analysis. Participation of LGMC in IPG residual soil characterization experimental site	1998-2003	Figueiredo, 1998; Rodrigues et al., 2002; Cruz et al, 2004a; Cruz & Viana da Fonseca, 2006a; Saraiva Cruz, 2003, 2008;
	Definition of sustainable correlations to derive cohesion intercept and angle of shearing resistance, based on DMT and DMT+CPTU testing. Participation in ISC2 Pile Prediction Event characterization	2003	Cruz et al., 2004b; VIana da Fonseca e tal., 2004; Cruz & Viana da Fonseca, 2006a;
	Pushing versus driven installation. Small strain shear modulus correlation based in DMT intermediate parameters	2004-2005	Cruz & Viana da Fonseca, 2006b; Cruz et al, 2006b
	First PhD thesis on DMT in residual soils	2007-2010	Cruz (2010)
Earthfills	Compaction and grain size control in earth works. Definition of compaction layers thickness	2005-2007	Cruz et al., 2006b; Cruz et al., 2008a
Error Propagation	Advanced mathematics applied to data analysis. DMT, PMT and CPTu Error Propagation.	2006-2009	Mateus, 2008 (MSc); Vieira, 2009 (MSc); Cruz et al, 2008b, 2009b; Mateus et al., 2010

1.2. Objectives

The research work mentioned in the previous section had to deal with many uncertainties, being the more important the one related with sampling. As it as been widely recognized, one of the main characteristics of residual soils is related to the presence of a bonding structure, which generates the presence of a cohesive intercept in Mohr-Coulomb failure criterion and the development of more than one yield stress locus. The main problem in residual soil characterization is related with sampling and test equipment installation, which can drastically damage bonding structure. Since triaxial testing was the base for correlation establishment, it became important to calibrate the global work with a specific experiment performed under controlled conditions, which will be the base of the research work presented and discussed in this dissertation.

Residual soil strength evaluation through in-situ testing using sedimentary approaches, usually relies on one single parameter determination, namely angle of shearing resistance in granular soils and undrained shear strength in fine soils, which may in fact be point out as a similar limitation to the most common cavity-expansion theories These approaches, however, are not adequate since it makes very complex to distinguish cohesive and friction components. In fact, when the sedimentary procedures are applied to residual environments, it has been verified that available correlations overestimate angles of shear resistance, as a result of the bonding structure influence in final determination. This is also true in other tests, such as CPT, PMT or SBPT, as demonstrated by the works of Viana da Fonseca (1996) and Viana da Fonseca et al (1997, 1998). To properly separate both cohesive and friction contributions, multi-parameter tests and/or combined tests (Multi-Test Technique) are needed, due to the generated possibility of combining more test parameters and thus assess differentiated strength contributions.

The research work presented herein aimed the establishment of a specific model for residual soil characterization based on DMT tests, performed alone or in combination with other in-situ tests (such as SCPTu and PMT), as well as the development of respective correlations to deduce strength and stiffness properties. Moreover, the evaluation of the error propagation and its effects on final results, arising from the basic measurement devices is also under scope.

1.3. Thesis Lay-out

Apart from this introductory chapter, the present document is divided in 4 parts (A, B, C and D), respectively designated by Background, The Residual Ground, The Experience and The Model. **Part A – Background** is a perspective of soil and rock mechanical evolution throughout weathering, described along chapters 2, 3, 4 and 5. In Chapter 2 a general overview of geologic processes involved in residual and transported soil genesis is presented, emphasizing weathering influence factors, main indexes and available classifications for engineering purposes. In this latter context, special emphasis will be given to Wesley Classification, since it represents the best suited system to index basic engineering properties of intermediate geomaterials. Chapter 3 is an insight in the mechanical behaviour evolution throughout weathering from the strongest rock to the weakest soil. Departing from rock massifs, a general description of the mechanical properties and the respective degradation as weathering proceeds is presented, with special emphasis to residual soils, the essence of this work. Once the general behaviour and material genesis is understood, a quick glance of in-situ available techniques to characterize residual soil behaviours is provided in Chapter 4. Since the literature about in-situ testing is abundant, this chapter doesn't need to be exhaustive, but just present the main issues related with the subject and giving some detailed attention to SCPTu test, since it is one privileged DMT test partner in residual soil characterization. Finally, Chapter 5 closes Part A with a detailed discussion on Marcheti's Dilatometer Test (DMT), with special emphasis in available correlations to derive geotechnical parameters in sedimentary soils, which will be used as a reference base to define a specific model for residual soil characterization. Whenever it is possible, this discussion will be illustrated with the DMT results obtained in Portuguese sedimentary soils in campaigns performed and controlled by the author, which includes the alluvial deposits of three main Portuguese rivers, namely Vouga, Mondego and Tagus. This information can be described as a very extensive data base collected in more than 10 years, representing all types of soils from clays to sands, organic to non-organic, stable to sensitive and corresponds to 57 DMT, 50 FVT, 23 CPTu, 4 PMT, 4 SCPTu, 5 cross-hole, 9 triaxial and 37 oedometer tests (plus identification and physical index tests).

Part B – The Residual Ground, is divided in Chapters 6, 7 and 8 and aims a detailed characterization and discussion on the general characteristics of portuguese granitic materials, based in abundant available data on Porto and Guarda granites were the whole experience with DMT has been settled. In this context, Chapter 6 presents a

detailed analysis of the available geotechnical information on granitic formations of Porto and Guarda, namely Porto Geotechnical Map (PGM) and CICCOPN, IPG and CEFEUP/ISC2 reference experimental sites, aiming representative typical patterns and parameter ranges of the different units usually found within these portuguese granitic formations. At the end of this chapter, a proposal to improve Wesley Classification is presented, designated as *Modified Wesley Classification*. In sequence, in Chapter 7 the results of the work integrated in 20 geotechnical campaigns performed and controlled by the author in CICCOPN and MOTA-ENGIL are presented, followed by a detailed discussion based in comparisons with other in-situ and laboratorial tests that led to the development of specific correlations for deriving strength and stiffness properties of residual soils. The respective data base was built from data collected in residual masses of the granites located between Porto and Braga, including the experimental site (CICCOPN) created by the author in the course of the present framework, globally representing a total of 40 drillings with SPT tests, 36 DMT tests, 22 CPT(U) tests, 4 PMT tests, 5 DPSH tests, 6 Cross-Hole tests and 10 triaxial tests. Calibration "bridges" will also be launched with other three important referred experimental sites, namely IPG, CEFEUP/ISC2 and Casa da Música (Metro do Porto network), where DMT tests were also performed and controlled by the author. Part B will then be finalized, in Chapter 8, with a discussion on the disturbance effects and efficiency of DMT results, related with the influences of blade geometry, penetration modes and efficiency in measurement, with the last two supported by experimental data within the present research work.

Part C – The Experiment, is composed by Chapters 9 and 10, where a specific laboratory controlled experiment (executed in IPG facilities) established to calibrate and/or correct the correlations resulting from the work described in Part B is presented and discussed. The experience was based in the development of artificially cemented samples tested both in triaxial cell and in a special large dimension measurement apparatus (CemSoil Box), where blades could be installed and/or pushed. Water level, suction and seismic wave velocities were monitored during the whole experience. In Chapter 9, the mechanical behaviour of reconstituted soil-cement mixtures is evaluated through the results obtained in tensile and uniaxial compressive tests, as well as isotropically consolidated drained (CID) triaxial testing, and compared with the global recognized behaviours described in the literature. On its turn, in Chapter 10 the specific experimental apparatus used in the experience is presented, the respective measurement devices as well as definitions and experimental procedures followed in the course of the main calibration experience. Obtained results are discussed and

compared both with the laboratory reference testing (Chapter 9), and the global data presented in Part B, aiming to the establishment of reliable correlations between DMT and residual soil strength and stiffness parameters.

Part D – The Model, is related to a proposal of a specific characterization model adapted to residual soils, which arises from the conclusions of the experimental work, thus motivating a simultaneous presentation and discussion. Suggestions and orientations for further research will also be provided in this part.

Only what we dream means what we really are,
since everything we achieve,
belongs to the world and to everybody.

Álvaro de Campos (free translation)

PART A – BACKGROUND

Chapter 2.
Weathering process and soil genesis

2. WEATHERING PROCESSES AND SOIL GENESIS

2.1. Weathering and its influence

The complete genesis of a soil is a complex and long process, starting with the weathering acting at the earth's surface to decompose and breakdown rocks by mechanical, chemical and biological actions, followed by wind, water and glacial transportation until a final deposition. These deposits are then buried by consecutive depositions, generating a sort of compaction and cementation processes (diagenesis) that will move towards a new sedimentary rock formation, with varying microfabric as function of the formation conditions. For instance, a deposition with precipitation will generate an open void cemented soil vulnerable to collapse, while a deposition where cementation develops only after significative compaction have occurred, will generate a soil where density is the major feature. Further on, deeper burials cause deformations, metamorphism and melting, feeding magmas in depth, which will move up and crystallize, becoming again vulnerable to weathering and so starting a new cycle. This complete path is designated as Lithologic Cycle (Figure 2.1) and together with the Water and Tectonic Cycles composes the global Geologic Cycle.

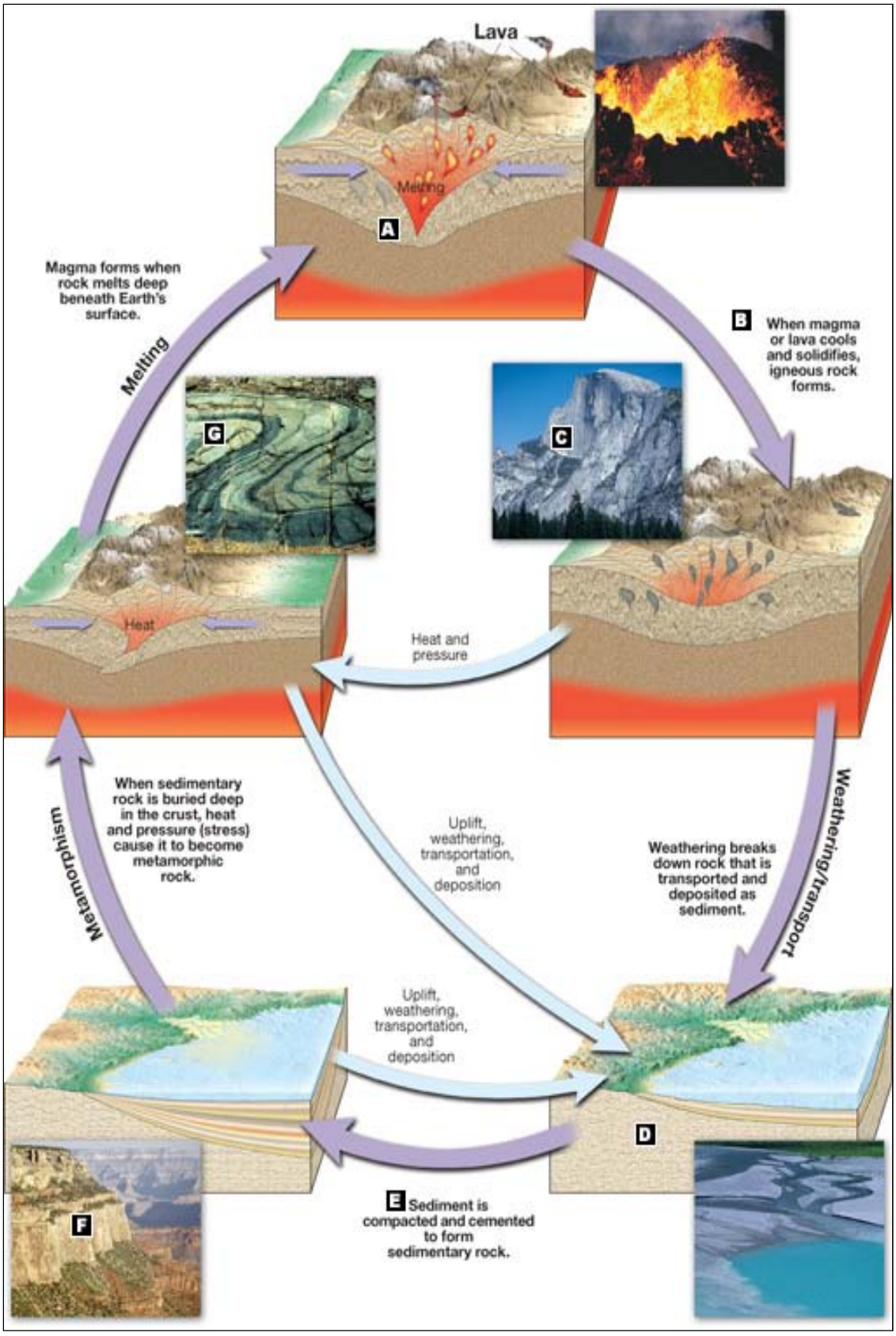


Figure 2.1 - Lithologic Cycle (after Hunt S.L., 2001)

Soil formation and respective evolution are within the first half of lithologic cycle, and is a (sedimentary) sub cycle of the earlier, as illustrated in Figure 2.2.



Figure 2.2 - Sedimentary Cycle

The different process sequences related to the genesis of all magmatic, metamorphic or sedimentary rocks generate important temperature and pressure variations that are responsible for more or less intensive fracturing of the massifs. Furthermore, after its formation the massifs are stressed by tectonic forces (tectonic cycle) related to crust movements created by earth internal energy arising from a very dense iron-niquel nucleus, which gives rise to an extra-level of fracturing (Figure 2.3).

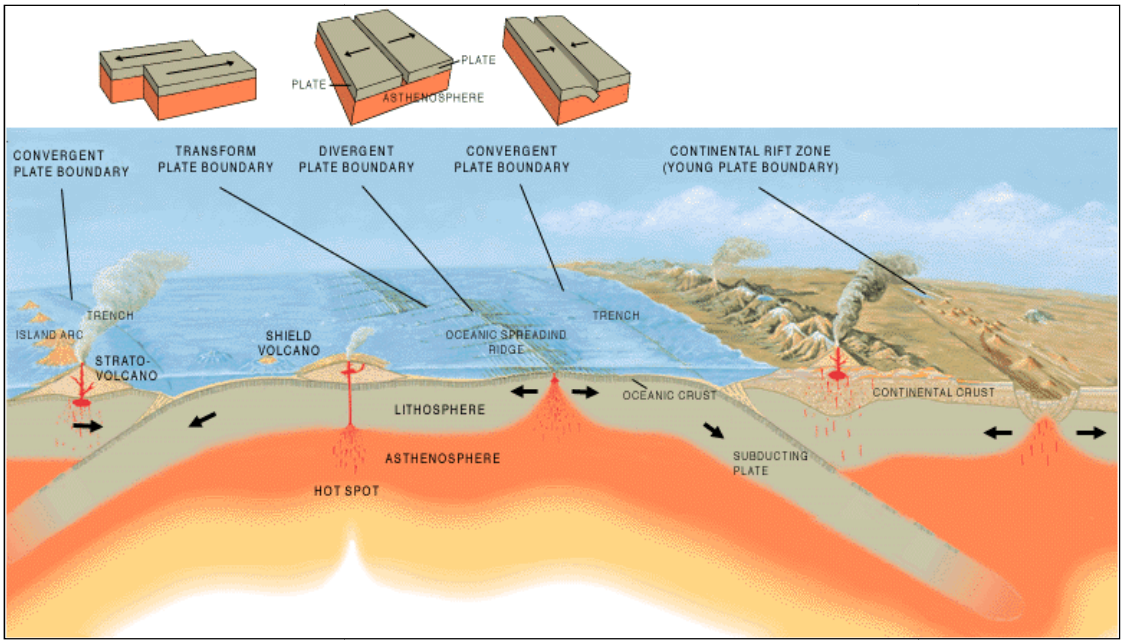


Figure 2.3 - Tectonic Cycle (after José F. Vigil. USGS, 2000).

As stated, weathering is the first stage of sedimentary cycle and can be defined as the physical, chemical and biological reactions that decompose a rock massif in increasingly smaller grains with lesser attractions forces between them. The respective evolution is closely linked to another important geologic cycle: the Water Cycle (Figure 2.4), described as a sequence of surface water evaporation (from oceans, rivers, lakes)

due to sun incidence, which generates a moving water steam that will precipitate in the face of earth, as rain or snow. As soon it touches the ground, water moves by gravity towards the lowest possible topographic levels, eventually reaching the ocean. In this sense, water is considered the most powerful and versatile active agent in weathering, sediment transportation and relief modeling, with the respective presence or absence being decisive in all the processes related to soil genesis and respective evolution.

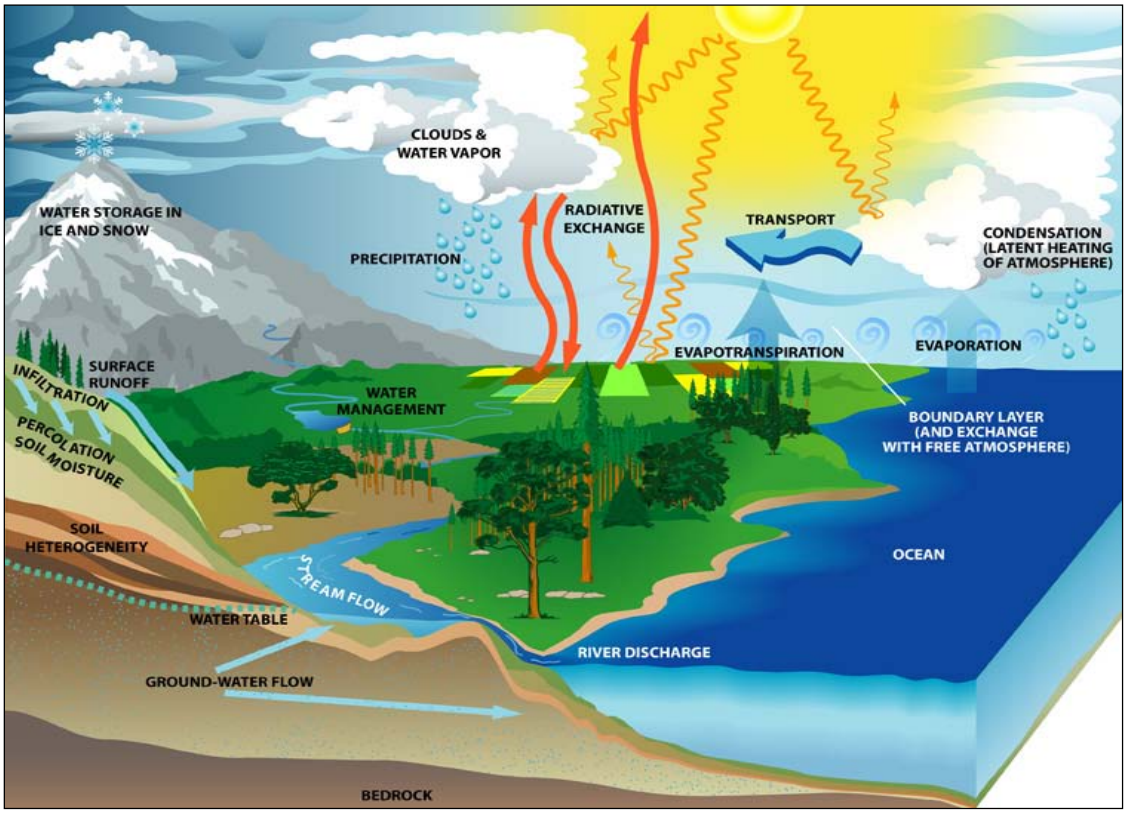


Figure 2.4 - Water Cycle (Press et al., 1997)

2.2. Weathering and its influence factors

At the massif macro level, the departing point for weathering processes is the joint systems developed by both formation processes and tectonic cycles, as a result of temperature and pressure changes as well as by internal tectonic stressing. These fracturation systems are mostly composed by sets of parallel fractures (or joints) crossing the rock matrix, which may globally vary from two to six joint sets. These sets are characterized by a strike and a plunge and also by the average spacing between joints, its width, roughness, infilling and access for water flow into each joint set. Depending on these characteristics, physical weathering take place on fractures separating blocks and breaking down grain particles by application of a series of cyclic stresses such as those resulting freeze-thaw, wetting-drying, heating-cooling, erosion

stress release, plant roots growing or crystallization processes (Fookes et al, 1988). These actions reduce the main particle size and increase micro-fracturing. On the other hand, rock materials are poor heat conductors, which can lead to thermal gradients between surfaces heated by insolation and inner parts of the massif. Furthermore, polymineralic rocks can also develop stresses along grain contacts due to different coefficients of thermal expansion, which will result in microfracturing and, ultimately, disintegration. The referred actions enlarge the old fractures and separate closed grains, dismantling the massif without mineralogical changes, thus increasing the permeability and conditions for an effective chemical attack, greatly controlled by water. In fact, chemical reactions like hydrolysis, cation exchange and oxidation, promoted by water, alter the original mineralogy into more stable or metastable secondary mineral products, mostly clay minerals. Other chemical reactions such as leaching, hydration and reactions with organic matter play important role in the chemical weathering, also altering rock minerals into clay minerals. Loughnan, quoted by Fookes et al (1988), pointed out three simultaneous processes involved in chemical weathering, acting for long periods of time:

a) The breakdown of the parent structure with release of ionic or molecular constituents;
b) Removal in solution of some of those released material;
c) Reconstitution of residuum with other components to generate new minerals; in stable or metastable equilibrium with the neoformation.

Furthermore, biological actions contribute to both physical, by means of roots growing inside the fractures, and chemical weathering by bacteriological oxidation, chelation (liquens promoting the rate of hydrolysis) and reduction of iron and sulphur compounds.

Besides the mineralogy and micro and macrofabric of the original rock, the possibilities for weathering evolution is strongly related to four important macro-environmental factors: hydrosphere, climate, topography and its vegetal covering layers.

The influence of hydrosphere in weathering processes is obvious since it has a fundamental role in physical and chemical weathering, as well as in transportation of eroded grains, as mentioned above. Climate has a major influence on the type of weathering, since moisture content and local temperature strongly influence its degree and extent (Blight, 1997). In fact, climate influences precipitation, evaporation and temperature variations within the local environment, as well as the intensity, frequency

and duration of precipitation along with season. Temperature amplitudes also play a major role in the type of weathering to occur. Generally it could be said that physical weathering prevails in dry climates and chemical in humid conditions (Figure 2.5). In moderate climates, as it is the case of Portugal, the percolation and the seasonal gradients of the water levels are the main factors for the existence of differently weathered soil, and residual masses are usually of saprolitic type.

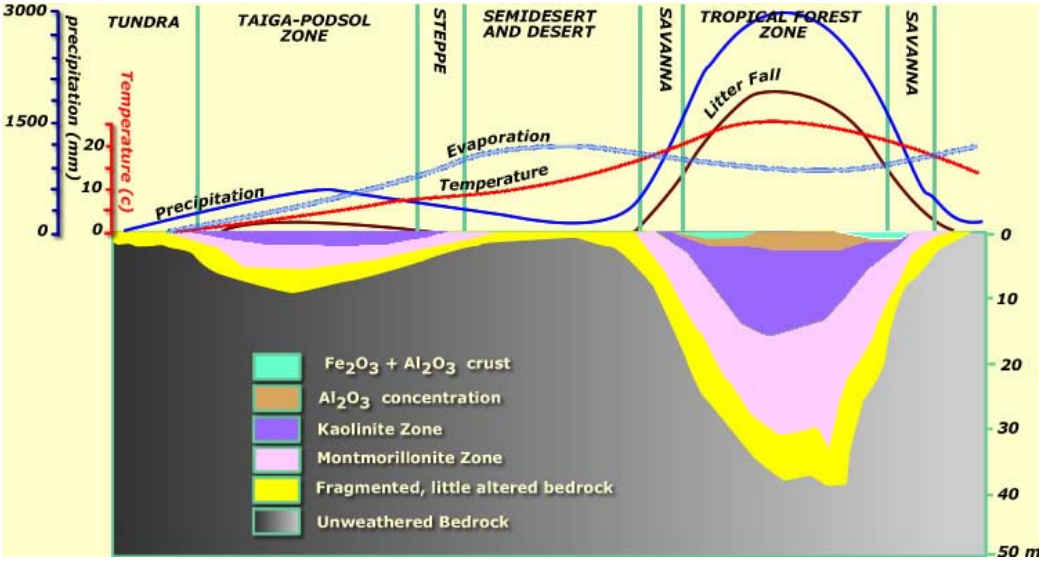


Figure 2.5 - Precipitation, temperature and evaporation as function of climatic zones.

Climate also has influence in the development of suction forces so typical of unsaturated soils, which happens to be very common in residual soils. The effects of unsaturation, desiccation and seasonal or long term re-wetting, have a major importance in the geotechnical behaviour of the respective massifs. These distinctive behaviours can be roughly estimated by Weinert index, N (1964), which reflects a relationship between potential evaporation during warmest month (E_w) and the mean annual measured precipitation (P_a). The value of five is pointed out as a frontier for physical and chemical process domination:

$$N = 12\, E_w/P_a \qquad (2.1)$$

On the other hand, climate can also interact with topography in different manners generating distinctive residual profiles. To produce a deep residual profile the rate of removal weathering products has to be lower than the advancing weathering, which is mainly dependent on the topography. In fact, the local relief determines the amount of available water and the rate at which it moves through the weathering zone, namely run-off and infiltration rates. Thus, deeper residual profiles will mostly be found in valleys and smooth slopes rather than on high ground or steep slopes. Furthermore,

vegetal cover also gives an important contribution to the weathering rate, by promoting water catchment, keeping moisture content in the upper zones and freeing organic acids that react with the present mineralogy.

On the other side of these discussed issues, the intrinsic characteristics of the original rock massif composed by a rock matrix and the systematic joint systems have natural direct influence in weathering potential. In that context, mineralogy of rock matrix will influence type and rate of chemical weathering due to the different mineral susceptibilities. Regarding silicates, which are the most abundant in earth surface, the weathering strength can be represented by the so-called Bowen/Goldich series, presented in Figure 2.6, showing the higher susceptibility for those with a higher fusion temperature (iron, magnesium and calcium minerals). Quartz is the one with lower susceptibility, which explains its usual presence in igneous, sedimentary and metamorphic rocks. Distinctive types of soil arise from this different susceptibility, as indicated in Table 2.1 (Chiossi, 1979).

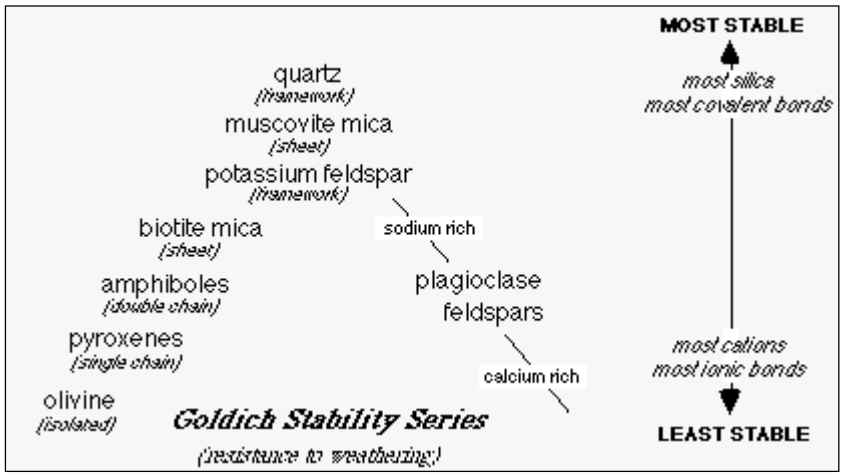


Figure 2.6 - Goldich/Bowen Series

Table 2.1 - Compositions of some typical residual soils

Rock type	Mineralogy	Residual soil type	Composition
Basalt	Plagioclase, pyroxene	Clayey	Fe, Mg clay
Quartzite	quartz	Sandy	Quartz
Schist	Sericite	Clayey	Clay
Granite	Quartz, feldspars, mica	Clayey or silty sands	Quartz and clay
Limestone	Calcite	Clayey	Clay

On its turn, micro and macrofabric control the rate of penetration and the flow of water through the weathered masses. Because the weathering proceeds from the surface down and inwards from joint surfaces and other percolation paths, the intensity of weathering generally reduces with increasing spacing of joints and with the decrease of void ratios. Since weathering develops itself around the fractures and there is a large variation in the mineralogy and properties of decomposed materials, massifs experiment different stress magnitudes with varying local levels of fracturing, which lead to the development of very erratic residual profiles, not only vertically but also laterally,. Furthermore, individual particles are often constituted by amalgams of smaller particles, and larger particles may be weakened by the presence of micro-fractures, which will lead to particle breakage during loading, thus increasing the compressibility of the soil. Bonding in these soils can result either from the parent rock or from crystallization of minerals during weathering (Lee & Coop, 1995).

Finally, it can be concluded that formation processes of a residual profile are extremely complex, difficult to understand and generalize, as a result of a wide range of influencing factors and, apart from a few valid generalizations, it is difficult to relate the properties of a residual soil directly to its parent rock. Each situation requires individual consideration and it is rarely extrapolated from experience in one area to predict conditions in another, even if the underlying hard rock geology is similar (Blight, 1997).

2.3. Weathering indexes

Once weathering is an evolutive process with significative impact in soil and rock behaviour, it is important to settle some classification indexes to relate them with a particular stage of weathering. In spite of the existence of various approaches based both in petrographic (Table 2.2) and chemical (Table 2.3) indexes, the truth is that they can be applied only for geological differentiation, being useless for geotechnical classification. A possible exception may be represented by petrographic X_d index (Lumb, 1962), showing some potential for a sustainable indexation of a general mechanical behaviour when plotted against void ratios (Baynes & Dearman, 1978). In fact, chemical indexes allow the evaluation of chemical weathering but don´t represent any information in material macro and microfabric, while petrographic ones give information on the mineralogical and fabric evolution but can not represent inter-particle bond strength. Thus, mechanical properties are only indirectly estimated through a probable behaviour (Baynes & Dearman, 1978).

Table 2.2 - Weathering petrographic indexes.

Petrographic index	Designation / Variables	Reference
$\chi_d = \frac{N_q - N_{q0}}{1 - N_{q0}}$	X_d – Feldspars decomposition index weathered rock N_q – Weight rate (Qz/Qz+Felds) unweathered rock N_{q0} – Weight rate (Qz/Qz+Felds) Qz – quartz; Felds – feldspars	Lumb (1962)
$IP = \frac{\%\ \text{unweathered grains}}{\%\ \text{weathered grains}}$	IP - micropetrographic index Unweathered - primary order minerals Weathered - secondary+voids+microjoints	Irfan & Dearman (1978)
$R_{sm} = \sum[(P,M)]TR$	Rs_m – Proportion of secondary minerals P – % of secondary minerals M – Stability of mineral TR – Fabric proportion	Cole & Sandy (1980)
$SMC = \frac{S}{M} \times 100$	SMC – Rate of secondary minerals S – Rate of secondary+voids+microjoints M – total of minerals (primary and secondary)	County Roads Board (1982)

Table 2.3 - Weathering chemical indexes.

Chemichal Index	Designation	Reference
$WPI = \frac{(Na_2O + K_2O + MgO + CaO + H_2O)}{(SiO_2 + Al_2O_3 + FeO + MgO + Na_2O + CaO + K_2O + TiO_2)} \times 100$	Weathering potential index	Reiche (1943)
$PI = \frac{100 moles(SiO_2)}{moles(SiO_2 + Al_2O_3 + Fe_2O_3 + FeO + TiO_2)} \times 100$	Potential index	Reiche (1943)
Parker = [Na/0.35+Mg/0.9+K/0.25+Ca/0.7]×100	Parker Index	Parker (1970)
$\beta = \frac{\eta\ \text{of weathered rock}}{\eta\ \text{of the fresh rock}}$; with $\eta = \frac{K_2O + Na_2O}{Al_2O_3}$	Leachate index	Rocha Filho *et al.* (1985)
$I_{mob} = \left(\frac{Mob_f - Mob_w}{Mob_f}\right) mole$ Mob_f, Mob_w = (K_2O+Na_2O+CaO); unweathered, weathered	Mobility index	Irfan (1996)

2.4. Residual and transported soils

Altogether, the actions and influence factors generate a global breakdown in the parent rock and rock minerals, releasing internal energy and forming more stable substances, thus reducing the contact forces between minerals until the ancient rock massif becomes a soil-mass. If the resulting grains remain in the same place of origin, the soil mass is designated by *residual soil*. Globally, residual soils can be seen as young (saprolitic) or mature (lateritic), characterized by the preservation of parent rock original structure (young) or by the complete disintegration of original structure and development of new inter-particle bonds by leaching or other chemical reactions (mature). Lateralization usually occurs in residual soils, but ancient transported soils may also have been lateralized. Desai (1985) proposes a definition of the degree of lateralization in terms of silica-aluminum ratio, with unlaterized soils characterized by SiO_2/Al_2O_3 greater than 2, transition lateritic soils between 1.3 and 2 and true lateritic less than 1.3.

The loose grains of the massif are now fragile to erosion and transporting agents, namely gravity, glacial, water and wind, which erode them from its birth place, transport them down (Figure 2.7) and, when the energy to transport is no longer available, a gentle settling of mineral grains takes place. In this situation, the resulting soil-mass is called *transported soil* or simply *sedimentary soil*. From this moment on, there will be a progressive densification of the lower levels due to subsequent depositions, expelling the water and reducing voids, followed by precipitation of chemical cement from trapped or circulating waters (cementation) and finalized by recrystallization in response to new equilibrium conditions. Compaction, cementation and recrystallization together compose the process called *Diagenesis*.

As it can be inferred by the above lines, transported soils depart from the loosest state going stronger with time. In clays, the subsequent properties depend greatly on its stress history, while granular soils can be deposited with a wide range of initial structures and porosities that will govern its mechanical behaviour. In opposition, residual soils arise from a gradual weakening by weathering of a strong body that will modify soil properties independently of stress history. Soil structure is modified (from the one existing in the parent rock) by chemical alteration and leaching or precipitation of soluble material. This will lead to a weakening of the rock involving an increase of mass, while strength, stiffness and porosity reduce. Furthermore, if weathering produces swelling clay minerals, it is possible to observe a volume increase at constant effective stress. Finally, if weathering has occurred at high pore water suctions,

collapse on wetting may be developed, depending on the magnitude of the mentioned suctions.

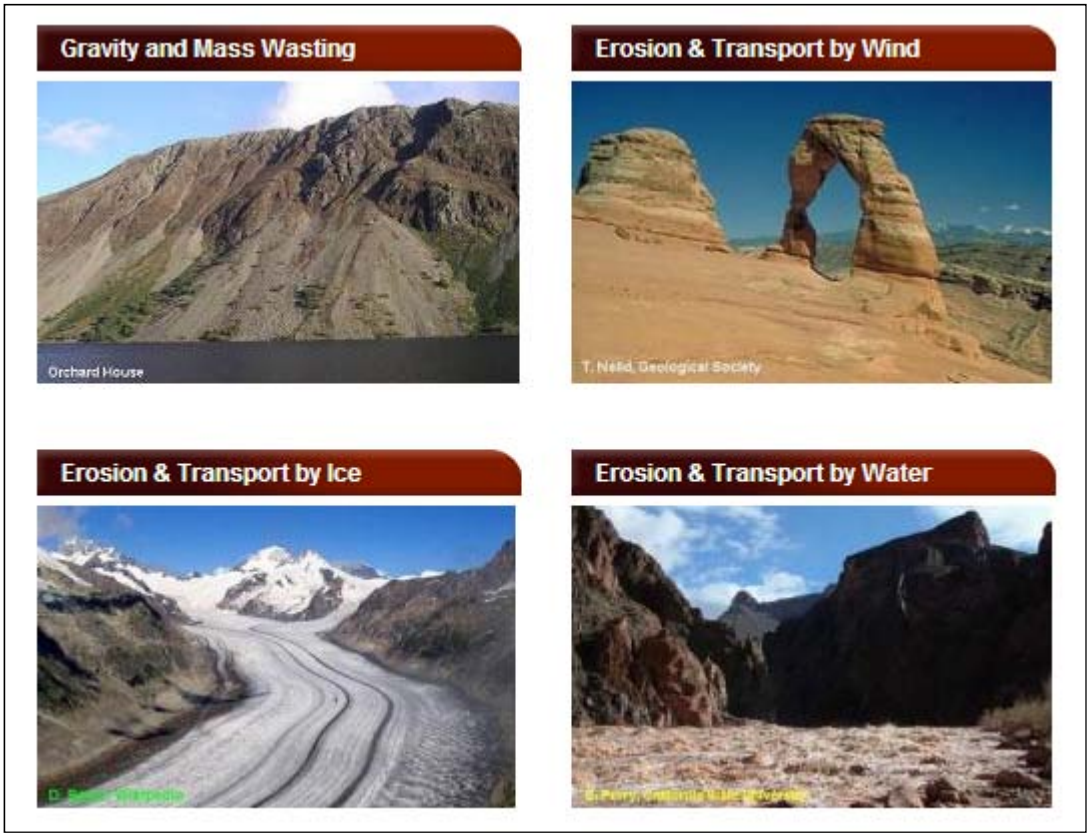


Figure 2.7 - Erosion and transport modes

Globally, the differences between residual and transported soils can be presented as follows (Vaughan, 1988). In transported soils the particles are generated elsewhere, delivered by some transporting agent and deposited in a certain way. After deposition, the soil is loaded and/or unloaded by subsequent depositions or removals, with particles remaining stable within time. The stress history reflects the modification of porosity and fabric by the plastic strains occurring due to loading and/or unloading in geological time. Residual soils develop in-place without transportation. Particles and their arrangements evolve progressively as a consequence of weathering, with widely varying mineralogy, grain size distribution and void ratio, and are not dependent of stress history. As a consequence the mechanical behaviour of both types of soil is quite different, and Classical Soil Mechanics applied to transported soils is not suitable for modeling residual soils behaviour.

2.5. Classification for engineering purposes

2.5.1. Overview

The weathering degree and respective extension is difficult to preview, but some typical arrangements can be identified (Ruxton & Berry, 1957, Little, 1969, Blight, 1997): an upper horizon with highly weathered material, followed by an intermediate less weathered horizon composed by boulders within highly weathered material and a lower horizon represented by the sound rock massif.

Several proposals for the classification of weathering profiles are available in the literature (e.g. Little, 1969; Deere & Patton, 1971; Vargas, 1985; Wesley, 1997). The first known classification for engineering purposes was settled by Moye (1955) for a granitic massif where a dam construction would take place. The massif was divided in six classes, where the first three were considered sound rock and then there was an abrupt break of strength with the last three being classified as a soil. Ruxton & Berry (1957), working on Hong Kong granites, followed Moye descriptions and set the basis for actual classifications. Finally, Little (1969) divided the typical profile of residual soil into six classes, as illustrated in Figure 2.8, which would become a stable base for further developments.

Later, London Geological Society (1970, 1972, and 1977) synthesized previous works and developed some systematic classification maintaining the 6 classes, differentiated by some basic descriptions, such as color, fabric and discontinuity conditions, from where weathering degree should be identified. In 1981, International Association of Engineering Geology (IAEG) set a similar classification improving the description details, now based in color, physical disaggregation and chemical decomposition and its effects on physical and mechanical properties. This was a particularly active year, with important contributions published by International Society of Rock Mechanics (ISRM) and the first attempt of normalization by British Standards (BS 5930).

Fifteen years later, Geological Society of London (1995) presents a reviewed classification with several approaches which allows distinguishing some typical features associated to different types of rock massifs (karstic, sedimentary, metamorphic, magmatic, etc) and, for the first time, incorporates the level of an estimated strength. Finally, in the new millennium, the International Organization for Standardization (2003) approved an international standard designated “Geotechnical Engineering – Identification and Description of Rock” (ISO/CEN 14689-1).

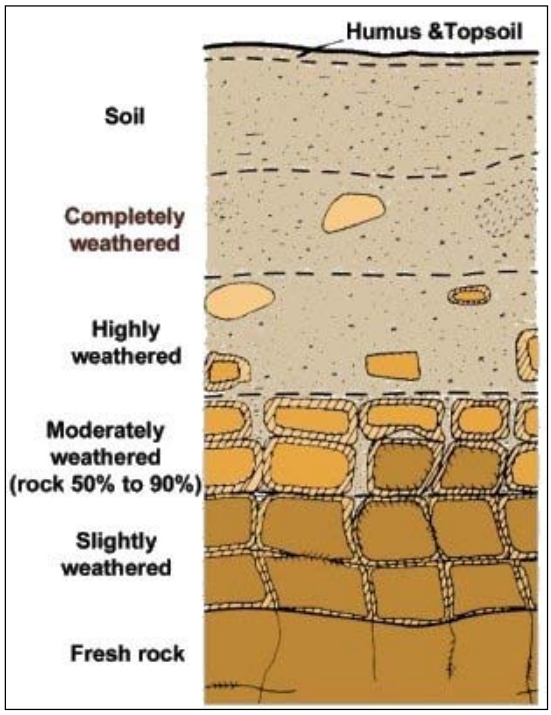


Figure 2.8 - Schematic diagram of typical residual soil profile (after Little 1969)

Generally, all these classifications agree in dividing profiles in six classes, based in visual descriptions of some important factors, such as color of rock matrix and discontinuities, preservation of original fabric, disintegration, chemical decomposition and strength offered by rock samples when solicited by common tools (fingers, spoon, hammer, etc). The most widely used classification in Portugal is the one proposed by ISRM, although it is expected that in the near future ISO/CEN will be the mostly adopted one. A brief definition of those classes is presented below:

a) I, or W1 (ISRM), fresh rock – represents the unweathered rock massif, with no signs of weathering neither in rock matrix nor in joint surfaces;
b) II, or W2 (ISRM), slightly weathered – represents the rock massif, with small spots of weathering only in joint surfaces;
c) III, or W3 (ISRM), medium weathered – represents the rock massif, with weathering covering globally the joint surfaces;
d) IV, or W4 (ISRM), highly weathered – at this stage the weathering is extended to all massif, although it can have some rock boulders inside the residual matrix; the macro structures (joints) are still represented in the massif; it can be peeled by hammer;

e) V, or W5 (ISRM), decomposed – basically is the same of IV but with less overall strength; it can be removed by spoon;
f) VI, or W6 (ISRM), soil – this is the final stage of weathering processes, and it represents the soil-mass where the ancient macro-structures are no longer evident.

In any weathering process which converts rock into soil there will be a gradual transition with no fixed frontier dividing rock and soil typical properties and magnitudes. Globally, the first 3 stages correspond to a typical sound rock massif, whose global behaviour is controlled by the strength of the rock matrix and the characteristics of joint systems, while in stages IV and V rock matrix strength become so low that gets close to typical soil behaviour, although the relic structures are still present and may have important influence in global behaviour. In these intermediate stages, the response to some engineering situations can be mixed (soil and rock type), since the general mass is disaggregated enough to behave like a soil-mass but where weakness planes of old joints can control mechanical behaviour. Finally, stage VI represents a soil-mass behaviour, leaving a proper description to soil classifications.

2.5.2. Wesley Classification

One of the important goals on residual research works is the attempt to develop specific classifications for engineering purposes, since those applied to sedimentary soils are not adequate, as summarized by Wesley (1988):

a) The clay properties of some tropical and subtropical soils are not compatible with those normally associated to the Unified Soil Classification system;
b) The soil mass in-situ can be described as a sequence of materials ranging from a true soil to a soft rock depending on degree of weathering, which cannot be adequately described by systems based on classification of transported soils in temperate climates;
c) Conventional soil classification systems focus primarily on the properties of the soil in its remoulded state, while residual soils are strongly influenced by in-situ structures inherited from the original rock or developed as consequence of weathering, which are destroyed after remolding.

Furthermore, identification tests of this soil in remoulded conditions, such as Atterberg limits, relative density, grain size distribution or fines content, do not reveal or classify the real geotechnical behaviour of residual soils, as it happens in sedimentary ones

(Vaughan et al., 1988). In fact, remolding and preparation of samples clearly affect their characterization due to the strong influence of microfabric in mechanical behaviour. As a consequence, the application of these tests is very limited and may lead to erroneous classifications for the ultimate purpose of engineering behaviour.

Based on mineralogical composition and soil micro and macrofabric, Wesley (1988) proposed a very practical system to provide a division of residual soils into groups with similar engineering properties. The basis of this proposed classification will be described in the following lines.

The specific characteristics of residual soils, which distinguish them from transported soils, can generally be attributed either to the presence of specific clay minerals found only in residual soils, or to particular structural effects, such as the presence of unweathered or partially weathered rock, relict discontinuities and inter-particle bonds. These influences can be grouped under the general headings of composition and structure.

Composition refers to particle size, shape and mineralogical composition of the fraction and it can be divided into:

a) Physical composition, e.g. percentage of unweathered rock, particle size distribution, etc.;
b) Mineralogical composition;

Structure refers to the specific in-situ properties of soil, which can be subdivided as follows:

a) Macrofabric (or macro-structure) or discernible structure - This includes all features discernible to the open eye, such as layering, discontinuities, fissures, pores, presence of unweathered or partially weathered rock and other relict structures inherited from the parent rock mass;
b) Mass-structure or non discernible structure - This includes microfabric, interparticle bonding or cementation, aggregation of particles, pore sizes and shapes, etc.

The first step to classify residual soils consists in forming groups on the basis of mineralogical composition alone, without reference to their undisturbed state. The following three groups were suggested by Wesley (1988):

a) Group A: Residual soils without a strong mineralogical influence;

b) Group B: soils with a strong influence deriving from clay minerals also commonly found in transported soils;
c) Group C: Soils with a strong mineralogical influence deriving from clay minerals only found in residual soils.

Group A: Residual soils without a strong mineralogical influence

By eliminating those soils that are strongly influenced by particular clay minerals, a soil group can be settled, being expected to have similar engineering properties. In general, soils with a weathering profile like the one illustrated on Figure 2.8 (Little, 1969) presented above in this chapter will fall within this group. In relatively rare instances, weathering in the top layer (i.e. zone VI) may be sufficiently advanced for its properties to become strongly influenced by clay minerals, developed by extensive weathering. Group A soils can be further sub-divided on the basis of structural effects. It is convenient to separate structural effect into the two broad groups mentioned earlier, namely macro-structure and micro-structure. Group A can therefore be divided into three main sub-groups:

Sub-group (a) - Represents soils in which macro-structure plays an important role in the engineering behaviour of the soil; highly weathered to decomposed horizons (IV and V) fall into this group;

Sub group (b) - Represents a soil without pronounced macro-structure, with a strong influence of micro-structure; the most important form of micro-structure is the relict particle bonding or that arising from secondary cementation (laterization), and although this cannot be identified by visual inspection, it can be inferred from fairly basic aspects of soil behaviour; for example, sensitivity is a very good measure of micro-structure, since it measures the influence of a distinctive structure (involving some form of bonds) that is destroyed by remolding; residual soils presenting high liquidity index (or existing in an analogous state) are also those that shows pronounced bonding or similar effects, enabling soil to exist in a metastable state close to or above its liquid limit;

Sub group (c) - Residual soils not greatly influenced by macro or micro-structural effects are included here as a third sub-group, which is a very incipient group, since very few residual soils fall into this category.

The defined groups A (a) and A (b) are rather broad for grouping on the basis of similar engineering properties, and so further sub-divisions were suggested by Wesley (1988),

which should be based in engineering properties, where in-situ testing could play a major unifying role.

Group B : Residual soils with a strong mineralogical influence deriving from commonly occurring clay mineral

This group represents soils which are strongly influenced by clay minerals commonly found in transported soils; the most significant member of this group is the black cotton soils or 'vertisoils', which shows high shrinkage and swelling potential, high compressibility and low strength, due to their predominant mineralogical constituent, namely montmorillonite or similar mineral of the smectite group. The engineering properties of such soils are therefore usually very similar to those of any transported soil, consisting predominantly of clay minerals of the smectite group. Structures may have a strong influence on the behaviour of soils in this group, particularly on shear strength and permeability.

Information in the literature suggests that not many other residual soils belong to this group, although there are some residual soils derived from sedimentary rocks that have properties strongly influenced by mineralogical composition.

Group C: Residual soils with a strong mineralogical influence derived from special clay minerals only found in residual soils.

This group represents the soils that are strongly influenced by the presence of clay minerals not commonly found in transported soils. The two most important minerals involved here are the silicate clay minerals halloysite and allophane. Halloysite is a lattice (crystalline) mineral of tubular form and belongs to the same group as kaolinite. Allophane is a very distinctive mineral with unusual properties, described as amorphous (non-lattice) or gel-like that may have a poorly developed crystalline structure. In addition to these silicate mineral, tropical soils may contain non-silicate minerals (or 'oxide' minerals), in particular the hydrated forms of aluminum and iron oxide (the sesquioxides), gibbsite and goethite.

Chapter 3. Mechanical evolution with weathering

3. MECHANICAL EVOLUTION WITH WEATHERING

The continued actions described in the previous chapter give raise to mechanical degradation, which departs from the unweathered more or less fractured massif, exhibiting its maximum strength and stiffness and moving towards a generalized soil mass, with no signs of the original macrofabric. In fact, in the extreme limits, assumed behaviours are completely different, with the first three weathering degrees of ISRM classification (W_1 to W_3) being represented by principles and models, where macrofabric and rock matrix plays the fundamental role in strength and stiffness behaviour, while from this level on, chemical weathering is progressively extended to the whole massif and soil type behaviour arises.

The general mechanical evolution of massifs throughout weathering is mainly governed by an increasing porosity of rock material, the weakening of mineral grains and the existing bonding between grains is progressively loss. However, a residual interparticle cementation always remains. The rock massif tends to become more and more friable due to the development of fractures both between and within mineral grains. Furthermore, chemical weathering produces new minerals that may be deposited within pores, at grain boundaries or along fractures that may then be removed (leached) leaving a relict, highly porous structure of the original grains. As a consequence, the massif will looses strength and stiffness and its permeability may change depending on the nature of the rock and the type of weathering products (Geological Society, 1995). In this process, weathering degrees W_4 and W_5 most commonly represent the transition behaviour, where the presence of relic discontinuities inherited from the parent rock, often coated with low friction minerals and eventually creating some kind of structural anisotropy, can have an important influence on its engineering behaviour but always balanced with the matrix (microfabric) control. For this reason, these massifs can behave either as a soil or a rock mass, depending on each specific loading situation. As weathering proceeds, influence of microfabric becomes increasingly important in strength and stiffness control, as relic structures disappear.

Baynes & Dearman (1978), working on granitic massifs, pointed out that an unweathered rock matrix from granite has a large cohesion and high angles of shearing resistance due to the strength of the intergranular bonds and the interlocking texture. In

early stages, both cohesive intercept and angle of shearing resistance are only slightly reduced by the degree of weathering, since mineralogical changes and internal weakening of the grains are minimal. With advancing weathering both mechanical parameters decrease, showing a tendency for the cohesive intercept (in terms of Mohr-Coulomb failure envelope) to be reduced by opening of grain boundaries and micro-fracturing, while angles of shear resistance tend to be slightly higher than the same soil in a remoulded state as a consequence of surface roughness of mineral grains induced by weathering. Wesley (1988) presents a very comprehensive scheme (Figure 3.1) of the mechanical evolution from fresh rock (W_1) to saprolitic or lateritic soils, adapted from Tuncer & Lohnes (1997) and Sueoka (1988).

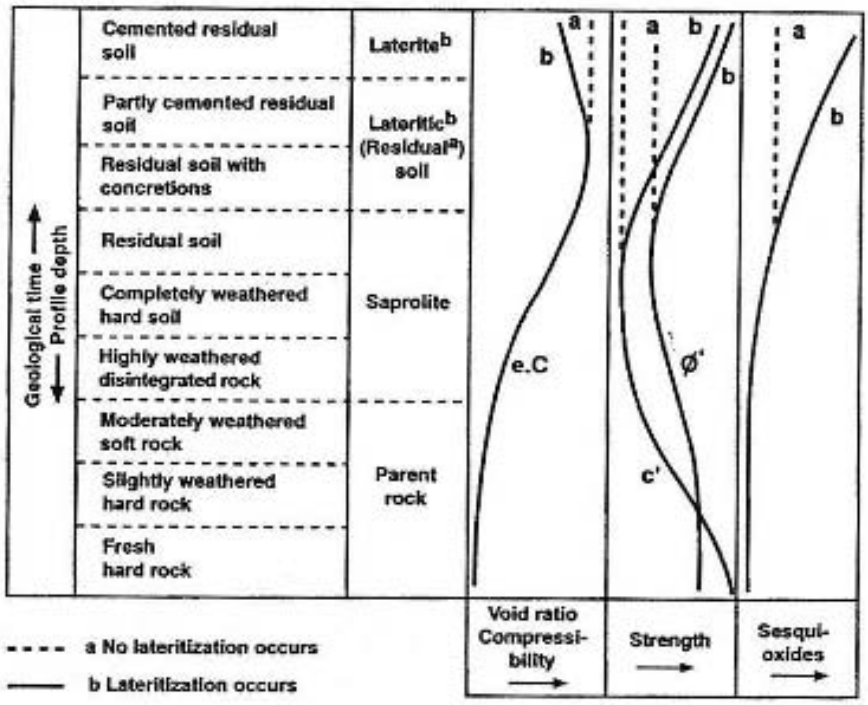


Figure 3.1 - Mechanical evolution through weathering (after Wesley, 1988).

3.1. Unweathered to medium weathered rock massifs

From the mechanical point of view, rock and soil present quite different fundamental behaviours, since the latter can be seen as a more or less homogeneous and isotropic massif characterized by the friction and a small cohesive intercept, while rock horizons generally stands for a heterogeneous massif with the overall strength dependent on both rock matrix and discontinuities combined with geo-environmental conditions, such as natural stresses and hidrogeological regimen. Moreover, the presence of tectonized zones weathered or with different mineralogy generates weakness planes and

anisotropy that may also imprint fundamental influence in mechanical behaviour (Rocha, 1981). Shear strength evaluation in unweathered to medium weathered rock massifs can be divided into 3 distinctive situations (Hoek & Brown, 1980), represented in Figure 3.2:

a) No discontinuities are involved in specific problem geometry, being the behaviour controlled solely by rock matrix, which can be isotropic or anisotropic;
b) One to three discontinuities sets are present, controlling the strength behaviour and introducing a strength anisotropy;
c) Three or more sets are present and shear strength is controlled by combined effects arising from rock matrix and discontinuities, being represented by an isotropic block system.

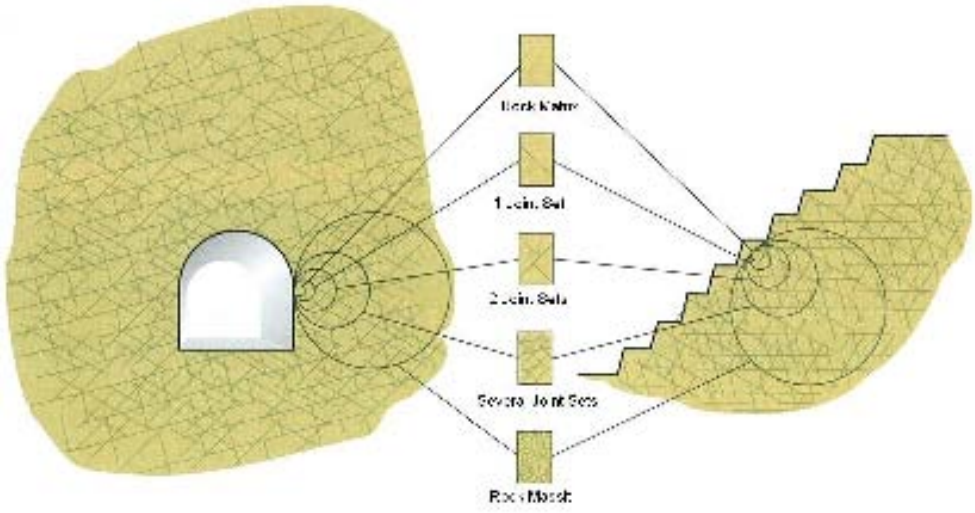


Figure 3.2 - Strength control as function of scale effects (after Hoek & Brown, 1980).

Some indications of the failure criteria that can represent these situations are presented in Table 3.1, adapted from Valejo et al. (2002). A brief description of the respective behaviours is presented in the following sub-chapters.

Table 3.1 - Failure criteria for typified situations (Valejo et al., 2002).

Rock massif	Discontinuity control	Rock matrix control
No discontinuities	Impossible	Hoek & Brown (1980)
Stratified (1 joint set)	Mohr-Coulomb (c and ϕ related to discontinuities)	Hoek & Brown (1980)
2 joint sets	Mohr-Coulomb (c and ϕ related to discontinuities)	Hoek & Brown (1980)
3 joint sets	Hoek & Brown (1994) (m, s and α)	Rarely Possible
At least 4 joint sets	Hoek & Brown (1994) (m, s and α)	Impossible

3.1.1. Massif controlled by rock matrix

In a massif area with no discontinuities, the overall strength depends on the strength of rock matrix which can develop isotropic or anisotropic behaviour, according to its microfabric. Rock matrix strength is mainly influenced by its basic chemical/mineralogical composition and weathering degree and shear strength is better evaluated by non-linear criteria. An example of non-linear criteria is the one proposed by Hoek & Brown (1980), valid for isotropic rock matrix under triaxial conditions:

$$\sigma_1 = \sigma_3 + \text{sqrt}\,(m_i\, q_u\, \sigma_3 + q_u^2) \qquad (3.1)$$

where σ_1, σ_3 are the maximum and minimum principal stresses, q_u is the uniaxial compression strength, while m_i stands for a rock type factor dependent on mineralogy and microfabric, determined by triaxial testing or selected from prepared tables like the one presented in Table 3.2(Hoek & Brown, 1997).

Table 3.2 - m_i parameter for the common rock types (Hoek & Brown, 1997).

Rock Family	Rock	m_i
Sedimentary	Conglomerate	22
	Sandstone	19
	Greywacke	18
	Limestone	8
Metamorphic	Marble	9
	Quartzite	24
	Schist	10
	Gneiss	33
Magmatic	Basalt / Gabbro	17/27
	Andesite/ Diorite	19/28
	Traquite/Syenite	17/30
	Rhyolite/Granite	16/33

As it can be observed in Equation 3.1, shear resistance depends on confining stress, cohesion (represented by uniaxial compressive strength) and the lithology type, where m_i can be seen as an adjustment factor dependent on the type of rock. Since this latter remains constant throughout weathering, shear behaviour is essentially controlled by the reduction rates of compression strength which are directly related to cohesion. Given the magnitude order of the latter and since bonding structure has to be broken before an effective mobilization of friction takes place, the usual construction loads rarely reach the needed magnitudes for a friction controlled behaviour and thus, in the earlier stages of weathering (W_1 to W_3), bonding is decisive for global shear strength.

When rock matrix is anisotropic (schist, gneiss, etc.) the equation that represents shear strength can be written in the following form:

$$\sigma_1 = \sigma_3 + q_u \text{ sqrt } [(m/\sigma_3 q_u)+s) \quad (3.2)$$

$$m = m_i \exp^{(GSI-100)/28} \quad (3.3)$$

$$s = \exp^{(GSI-100)/9} \quad (3.4)$$

where σ_1, σ_3 are the maximum and minimum principal stresses, q_u is the uniaxial compression strength, m_i stands for a rock type factor dependent on mineralogy and microfabric, while m and s are model parameters dependent on the Geological Stress Index (GSI), which is going to be discussed ahead in this chapter.

3.1.2. Massif controlled by discontinuities

In the cases of massifs including 1 to 3 joint sets, global strength is influenced either by rock matrix and discontinuities, revealing an anisotropic behaviour generally controlled by the conditions of discontinuities. In fact, discontinuities represent weakness plans, usually weathered by water flowing, generating a discontinuous and anisotropic response and thus, having a major influence on strength, deformability and hydraulic properties of rock massifs. To properly characterize them several key features are required to be described and/or measured, such as:

a) Wall roughness – results in dilatancy of discontinuities at low confining stresses; the respective numerical evaluation can be obtained by laboratorial testing (combined tilt and Schmidt hammer tests) or through pre-selected Joint Roughness Coefficients (JRC) profiles (Figure 3.3), as proposed by Barton & Choubey (1977);
b) Wall strength – with confining stress increase, shear must involve more and more considerable grain peak breakage; the wall strength will determine the turning point from where roughness rules the strength and can be determined by Schmidt hammer tests performed in the discontinuity surface;
c) Wall coating – low friction minerals may coat the surface and reduce frictional strength to sliding;
d) Infilling – if its thickness is greater than grain peaks amplitude, then its mechanical characteristics will dominate the process;
e) Water (or other incompressible fluids) – when a discontinuity is full with a fluid, shear strength will be reduced by the fluid pressure;
f) Persistence (continuity) – non-persistent discontinuities are characterized by rock bridges, increasing the cohesion component of shear strength.

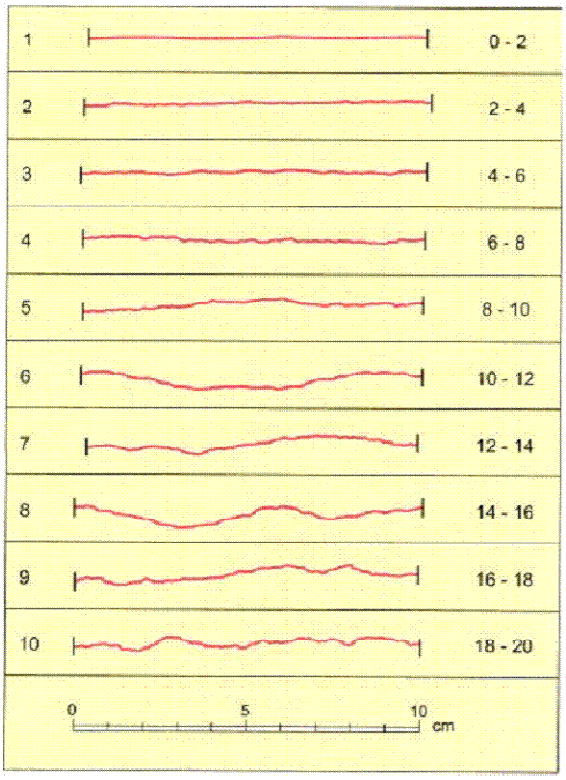


Figure 3.3 - JRC profiles. Strength control as function of scale effects (after Hoek & Brown, 1980).

In case of a massif controlled by discontinuities, its shear strength is represented by the friction developed along a contact surface and the behaviour can be adequately represented by Mohr-Coulomb criterion. In rock mechanics, the following friction angles of discontinuities can be defined:

a) Peak friction angle, ϕ_p, related to maximum shear strength determined by type of rock and roughness of the surface;
b) Basic friction angle, ϕ_b, characteristic of the rock mineralogy and related to a reference planar surface with no signs of weathering (W_1);
c) Residual friction angle, ϕ_r, related to minimum shear strength, after breakage of the rough peaks of the surface.

Direct shear tests are the best approach to determine friction, but unfortunately they are neither quick nor economical, disabling the possibility of having good friction profiles taking into account the local heterogeneities (Branco, 2008). A common alternative is to use direct and practical approach, such as Barton & Choubey's (1977) model, according to which, the shear strength, τ, of a discontinuity under a normal stress, σ_n, in a rock material with a basic angle of shearing resistance,ϕ_b , is given by:

$$\tau = \sigma_n \tan[JRC \log (JCS/ \sigma_n) + \phi_r] \quad (3.5)$$

$$\tau = \sigma_n \tan[1{,}7JRC + \phi_r \text{] if } (JCS/\ \sigma_n) > 50 \quad (3.6)$$

$$\phi_r = (\phi_b - 20) + 20\ r/R \quad (3.7)$$

where ϕ_b and ϕ_r represent respectively the basic and residual angle of shearing resistances, R and r are the rebound of Schmidt hammer respectively on an unweathered dry surface and on discontinuity surface, JRC is the Joint Roughness Coefficient and JCS is the uniaxial compression strength of the rock material in the vicinity of the surface, usually determined by Schmidt hammer, through the expression:

$$\log JCS = 0{,}00088\ \gamma_{rock}\ r + 1{,}01 \quad (3.8)$$

JRC provides an angular measure of the geometrical roughness in a scale 0 to 20, and can be estimated using pre-selected JRC Profiles (Barton & Choubey, 1977) or tilt tests together with Schmidt Hammer to back figure its value by the expression:

$$JRC = (\alpha - \phi_r) / \log (JCS / \sigma_n) \quad (3.9)$$

where α stands for the inclination angle at which the relative movement of a discontinuity starts.

Finally, ϕ_b can be determined by tilt tests or using tabulated values such as those proposed by Barton & Choubey (1977), presented in Table 3.3, as adopted by Hoek & Brown, 1997).

Table 3.3 - Basic friction angle, ϕ_b, for the common rock types (Hoek & Brown, 1997).

Rock Type	ϕ_b (dry)	ϕ_b (wet)
Sandstone	26-35	25-34
Siltstone	31-33	27-31
Limestone	31-37	27-35
Basalt	35-38	31-36
Fine granite	31-35	29-31
Coarse granite	31-35	31-33
Gneiss	26-29	23-26
Schist	25-30*	21-25*

*in schistosity planes

Strength degradation with weathering evolution is related to a decrease of both peak and residual angle of shearing resistances (Equations 3.6 to 3.9) and also the matrix compression strength. These friction angles should not be confused with matrix angle of shearing resistance, but seen as a combined response of surface roughness and the interparticle strength, being more than a physical friction resistance parameter. The maximum magnitude and respective intervals of variation are strongly influenced by the lithology type and microfabric, which are numerically represented by the basic friction angle. For a given unweathered massif, peak and residual friction angles depend exclusively on the type of rock and surface roughness, and the reduction of both magnitudes with weathering is related to the strength against breakage of grains that represent surface roughness. In fact, when installed stresses overcome strength reserve, the interparticle bonds break and roughness naturally decreases. Thus, even though friction has control on shear strength, its magnitude is directly dependent on lithology and cementation, with the latter being decisive in mechanical evolution and the former being independent of weathering.

3.1.3. Massif controlled by rock matrix and discontinuities

In a significative part of the current situations, however, the response of the massif is not depending on only one but both rock matrix and discontinuities. Figure 3.4 illustrates the variation in the strength of a massif with four joint sets (Brady & Brown, 1985, adapted from Valejo et al., 2002).

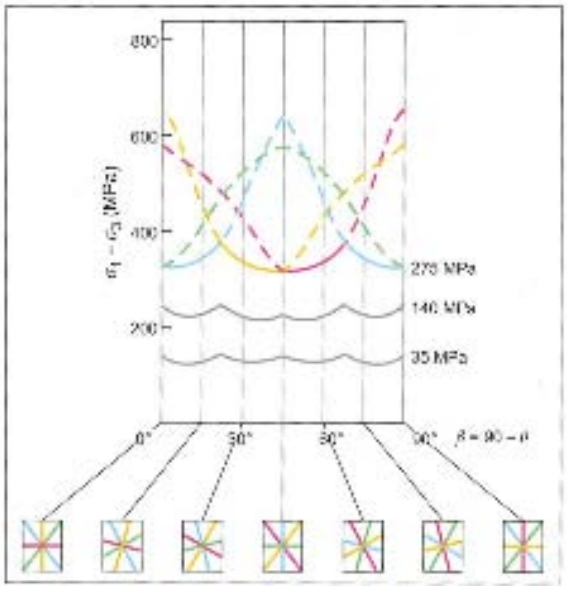


Figure 3.4 - Strength variation within a four joint set massif (after Valejo et al., 2002).

In such case, the massif works as a compartmented block system, where the nature, dimension and surface asperities of the blocks combined together control the strength behaviour. Being so, rock matrix strength and discontinuity characteristics, as well as rock type, should be considered in a proper failure criterion, such as the Hoek & Brown Modified Criteria (Hoek & Brown, 1994), and represented by the following equation:

$$\sigma_1 = \sigma_3 + q_u \, (m \, (\sigma_3/q_u) + s)^{\alpha} \qquad (3.10)$$

where m, s and α are the intrinsic strength parameters that depend on the type of rock, spacing of discontinuities, RQD, joint conditions (persistence, width, infilling, weathering degree, previous movements) and the presence of water.

Of course, it is not simple to incorporate all of these dependencies within the same analytic model, but empirical approaches previously developed to represent an overall "quality" of the rock massif, such as Rock Mass Rating (RMR), were used by Hoek & Brown (1994) to compose a *Geological Stress Index* (GSI) that could be used in these determinations. Even though this methodology is strongly empirical, it takes into account all the major factors that influence strength and so, it is reasonable to expect some confidence on the respective evaluation. Being so, departing from proper field characterization, RMR_{84} is evaluated using Figure 3.5 (Bieniawski, 1984), considering always dry conditions. This parameter is further used to evaluate the Geological Stress Index (GSI) through the following equation:

$$GSI = RMR_{84} - 5 \qquad (3.11)$$

Then, the parameters m, s and α of the model can be determined as follows:

$$m = m_i \exp^{(GSI-100)/28} \qquad (3.12)$$

$$s = \exp^{(GSI-100)/9} \quad \text{and } \alpha = 0.5 \text{ if } GSI > 25 \qquad (3.13)$$

$$s = 0 \quad \text{and } \alpha = 0.65 - (GSI/200) \text{ if } GSI < 25 \qquad (3.14)$$

CLASSIFICATION GEOMECHANIC RMR (BIENIAWSKI, 1984)

1	Compressive strength (unaxial test)	>250	250-100	100-50	50-25	25-5.	5-1.	<1
	rating	15	12	7	4	2	1	0

2	RQD	90%-100%	75%-90%	50%-75%	25%-50%	<25%
	rating	20	17	13	6	3

3	Spacing	>2m	0,6-2m	0,2-0,6m	0,06-0,2m	<0,06m
	rating	20	15	10	8	5

4	Descontinuities	Continuidade Continuity	<1m	1-3m	3-10m	10-20m	>20m
		rating	6	4	2	1	0
		Width	0	<0,1mm	0,1-1,0mm	1-5mm	>5mm
		rating	6	5	3	1	0
		Roughness	Very rough	Rough	Slightly rough	Smooth	Slickensided
		rating	6	5	3	1	0
		Infilling	None	Hard (<5mm)	Hard (>5mm)	Soft (<5mm)	Soft (>5mm)
		rating	6	4	2	2	0
		Weathering deg	Unweathered	Slightly w.	Medium	Highly	Decomposed
		rating	6	5	3	1	0

5	Presence of water	Dry	Damp	Wet	Dripping	Flowing
	rating	15	10	7	4	0

Figure 3.5 - Rock Mass Rating, RMR_{84} (after Branco, 2008).

As it happened in the previously discussed shear possibilities, the mechanical behaviour in the present situation is mainly controlled by cohesion and the type of rock, as globally expressed by the respective equations. Thus, from the strength point of view, the evolution through weathering is especially marked by the reducing bonding strength, sustained in high orders of magnitude within W_1 - W_3 weathering levels, significantly decreasing in intermediate geomaterials (IGM) range.

3.1.4. Stiffness

Stiffness of a rock masses is one of the most difficult parameter to evaluate within rock mechanics field, since it depends both on the deformability of rock matrix and the one produced by the presence of discontinuities (Rocha, 1981). The deformability of rock matrix can be represented by Young modulus adequately determined by laboratorial testing, while discontinuity is represented by the ratio between load and displacement (k), since its strains are very difficult to determine. In a massif with one joint set with a specific spacing (S), the inverse of its deformability can be obtained by the sum of the

inverse deformability of both rock matrix and discontinuities, following the equation below (Goodman, 1989):

$$1/E_m = (1/E_i) + (1/k_nS) \quad (3.15)$$

where E_m and E_i respectively represents the deformability modulus of massif and rock matrix, k_n the ratio obtained with one discontinuity and S the spacing of the joint family.

Although rock matrix modulus it is easier to determine, the other referred (massif and discontinuity) stiffness parameters are quite difficult, especially due to the scale effects arising from discontinuities disposition (Rocha, 1981). The methodologies available to estimate the massif modulus can be basically divided into direct and indirect. The former are represented by in-situ testing, while the latter are represented by geophysical methods and empirical expressions. Rocha (1981) indicates the basic in-situ testing techniques as the surface load tests, flat jacks (Rocha et al., 1969) and rock dilatometers (Rocha et al., 1969, 1970). The main problems with the interpretation of direct methods is their dependence on scale effects and on the measurement of strain level, which create serious difficulties in current situations (Rocha; 1981), while in indirect methods the strain level of measurement is usually unknown. For this reason, it is usual to use empirical correlations to evaluate the parameter for the most common situations. Several methodologies are available to empirically deduce massif modulus, such as those based in a factor of reduction applied to the rock matrix modulus (Bieniawaski, 1984; Johnson & De Graff, 1988), in RMR (Bieniawski, 1978; Serafim & Pereira, 1983) or GSI (Hoek et al., 1995), with the last two being the mostly applied, as represented in Table 3.4.

Table 3.4 - Empirical correlations for massif modulus determination, E_m.

Correlation	Reference	Field of application
$E = 2\ RMR - 100$	Bieniawski, 1978	Rock Massifs of good quality (RMR > 50)
$E = 10^{(RMR-10)/40}$	Serafim & Pereira, 1983	Rock Massifs of medium to good quality (25 < RMR < 50)
$E = \sqrt{(q_u/100)} * 10^{[(GSI-10)/40]}$	Hoek et al., 1995	Rock massifs of poor quality (q_u < 100 MPa)

These empirical correlations, based in observed situations, show that stiffness is highly dependent on compressive strength and fracturing characteristics, with the former being determinant. These considerations imply a gradual loss of stiffness with cement degradation, thus following a pattern identical to the one observed with strength.

3.2. Intermediate Geomaterials (IGM) and residual soils

3.2.1. Background

3.2.1.1. General Characteristics

Beyond the first three weathering degrees (W_1 to W_3), chemical weathering is extended to the whole massif, and so the mechanical evolution is mainly governed by an increasing porosity of rock material, the weakening of mineral grains and the reduction of bonding between grains, with the rock massif becoming more and more friable and weathered. Weathering degrees W_4 and W_5 represent transition behaviour where micro and macro fabrics have similar influence, towards a residual soil-mass where the relict macrofabric is no longer present. This process is followed by a mechanical degradation that leads to substantial reduction of strength and stiffness. Table 3.5 illustrates orders of magnitude of strength and stiffness parameters typically associated to rock and soil-masses.

Table 3.5 - Typical soil and rock index parameters ranges

	Uniaxial Strength (MPa)	Cohesion (MPa)	Young Modulus (MPa)
Rock	2 - 300	> 0,1	>400
Soil	< 2	< 0,1	< 300

When macrofabric is no longer presented, general cohesive-frictional soil behaviour takes place, with the overall mechanical behaviour being governed by a wide range of factors such as micro-structure, stiffness non-linearity, small and large strain anisotropy, weathering and destructuration, consolidation characteristics and flow rate dependencies (Schnaid, 2005). The main features of these soils can be summarized as follows (Schnaid et al., 2004):

a) Bonding and structure are important components of shear strength;
b) Cohesive-frictional nature;
c) Eventual anisotropy derived from relic structures of the parent rock;
d) Structure and fabric may be developed in-situ by weathering processes;
e) Highly variable fabric and mineralogy;
f) Destructuration under shear actions;
g) Low influence of stress history.

The interpretation of behaviour of these non-textbook materials is rather complex and cannot be supported only by classical soil models, fundamentally by the following reasons (Vaughan et al., 1988):

a) Presence of a component of strength and stiffness coming from bonding between particles, inherited from parent rock or due to precipitation, which may coexists with high void ratios; its level evolves continuously and it is only related with actual stress state;.
b) Constant variation of mineralogical content and grain size distribution, as a result of weathering, generates randomly variable void ratios and thus, stress history has little effect on its behaviour;
c) Behaviour mostly independent of initial porosity and stress history.

Bonded materials are strongly influenced by cementation structure and thus cemented soils (residual or sedimentary) and highly weathered rocks present similar mechanical response that led to the definition of an intermediate class in between soil and rock, designated by Intermediate Geomaterials (IGM) or non text-book materials. Brenner et al. (1997) summarized the influence factors that have different stress-strain and strength effects on residual and sedimentary soils, as presented in Table 3.6.

Table 3.6 - Residual versus transported soil responses.

Influence Factor	Effect on residual soil	Effect on transported soil
Stress history	Not important	Very important. Modifies initial grain packing. Causes overconsolidation
Grain strength	Very variable, as function of mineralogy	Uniform, because weaker particles are eliminated during transport
Bonding	Important component of strength, mostly due to inherited bonds. Causes cohesion intercept and a (precocious) yield stress. Can be destroyed by sampling	Occurs with geologically aged deposits. Causes cohesion intercept and a yield stress. Can be destroyed by sampling
Relict structure and discontinuities	Developed from pre-existing structure in parent rock, including bedding, flow structures, joints, slickenside	Developed from deposition cycles and from stress history. Possible formation of slickenside surfaces
Anisotropy	Derived from relict rock fabric	Derived from deposition and stress history
Void ratio / density	Depends on weathering level. Independent of stress history	Depends directly on stress history

Schnaid et al. (2004) identify IGM soils as those that satisfy at least one of the following criteria:

a) Classical constitutive models do not offer a close approximation of its true nature;
b) It is difficult to sample or to be reproduced in laboratory;
c) Very little systematic experience has been gathered or reported;
d) Values of geomechanical parameters are outside the range that would be expected for more common sands and clays;
e) The soil state is variable due to complex geological conditions.

From the considerations above, apart from residual soils and weak rocks, other soils can not be represented by classical soil models being also included in the same framework. In fact, both soft to stiff clays and granular soils are often found structured in nature, with cementation being developed by agents like silica, hydro-silicates, iron oxides, carbonates and hydroxides deposited under one of the following conditions (Clough et al., 1981, Leroueil & Vaughan, 1990):

a) At the porous contacts between sand grains;
b) Cementation-like effects resulting from dense packing;
c) Matrix of clays and silts;
d) Decreasing values of cohesion inherited from rock massif, while weathering and leaching progress.

As a consequence, the earlier studies of Clough et al. (1981), Vaughan & Kwan (1984), Vaughan (1985), Maccarini et al. (1988) and Vaughan et al. (1988), contributed to the conceptual framework presented by Leroueil & Vaughan (1990) to describe stress-strain behaviour of cemented soils, despite the way it was generated. Those authors have shown that stress-strain behaviour of both naturally and artificially cemented soils is mainly dependent on initial state and the critical state line of destructured material. Therefore, cemented structures and respective effects on soil behaviour should be considered as important as initial density and stress history. Basically, this conceptual work considers that the effects of a cemented structure on soil behaviour is similar to that exhibited from overconsolidation in clays, and thus, represented by an initial stiff behaviour followed by increasing plastic deformation as the soil moves towards failure. Departing from this point, extensive research has been carried on, pursuing specific geotechnical modeling adapted to these type of materials (Tatsuoka & Shibuya, 1992; Coop and Atkinson, 1993; Gens and Nova, 1993; Malandraki & Toll 1994, 2000; Viana

da Fonseca, 1996, 2003; Cuccovillo & Coop, 1997; Consoli et al., 1998; Rodrigues, 2003; Rodrigues & Lemos, 2002, 2003, 2004, 2006; Schnaid et al., 2000, 2004; Cruz et al., 2004, 2006, 2008; Toll & Malandraki, 2006; Viana da Fonseca et al., 1997, 2001, 2003, 2004, 2006, 2007, 2009).

3.2.1.2. Microfabric and sampling influences

To understand the evolution and influence behaviour of microfabric throughout the weathering process, Baynes and Dearman (1978) based on scanning electron microscope analysis, looked into microfabric of granitic masses in different stages, bringing to light very useful and comprehensive information, summarized below:

a) The initial incoming of weathering agents occurred along primary micro-voids probably caused by the cooling and exhumation of the granite, and along open mineral cleavages;
b) The initial stages of weathering increased porosity by dissolution along the grain boundaries and within feldspars. The weathering of the feldspars showed the formation of a structurally controlled intra-granular voids;
c) Weathering greatly increased the intensity of microfracturing of the rock by opening grain boundaries, expanding biotites and possibly de-stressing quartz crystals;
d) Continued weathering of feldspars evolving to clay, produced a variety of different microfabric features;
e) Very different microfabrics were found in the same specimen, indicating a high variability of weathering micro-environments;
f) Microfabric is related to the degree how feldspars have been weathered, the proportion of clay produced during decomposition, and also the extent to which particles have been removed from the system, all reflecting duration and intensity of weathering.

The important issue arising from this study is that generally weathering gives rise to a weak bonded structure of grains of varying strength and with somehow erratic arrangements. In fact, the soil particles resulting from weathering will be individual mineral grains or agglomerations of grains from the original rock in different stages of de-structuring, as well as grains or agglomerations of grains resulting from weathering. These can result in a wide range of particle strength, with quartz remaining stable throughout the weathering, while feldspars and biotites are substantially, or totally, altered mainly to clay minerals. Viana da Fonseca & Coutinho (2008), based on

micropetrographic studies reported in literature, state that in volcanic and granitic rock, quartz remains fairly constant throughout the weathering evolution, with the content of feldspar being gradually reduced to a clay parcel, while micro-fractures and voids increase with weathering. Furthermore, with the weathering evolution primary inter-particle bonds break and voids are generated, creating instability in the feldspars and micas, thus opening a way for leaching and producing a net of inter-granular void spaces. The result is a very heterogeneous mass with highly varying porosity, depending on its initial mineralogical distribution, different grain strength against weathering and different levels of exposure to water. Convergent information is given by Viana da Fonseca (1996), Rodrigues & Lemos (2004), Viana da Fonseca et al (2006), Ng & Leoung (2006) and Coutinho (2007), dealing with Porto, Guarda, Hong Kong and Brazilian granitic and gneissic formations, as result of the microscopic analysis performed within their respective research works.

Baynes & Dearman (1978) conclusions highlights two of the major problems faced to establish a framework of cemented sands mechanical behaviour based on natural samples, namely the variability of its microfabric and the existence of different particle strength, which creates a significant difficulty in establishing adequate laboratory testing programs. In addition, sampling disturbance in IGM materials is rather high and is often found to have intensive impact in interparticle bonding with natural consequences in its global mechanical behaviour. Aware of these problems, Vaughan (1985) proposed the use of artificially cemented soils as a way to overcome sampling, variability of microfabric and particle strength of natural samples, suggesting that destructured materials should be studied together in each framework to establish a reference and to evaluate the deviation from classical soil models. This proposal became the starting point for the main research works produced ever since, being the base for most experimental programs found in literature (Lade et al. 1987; Viana da Fonseca, 1988, 1996; Bressani, 1990; Leroueil & Vaughan, 1990; Coop & Atkinson, 1993; Gens & Nova, 1993; Cucovillo & Coop, 1997; Consoli et al., 1996; Futai et al., 2004, 2007; Martins, Toll & Malandraki, 2006; Rodrigues, 2003, Schnaid et al 2004, Schnaid 2005, Viana da Fonseca & Coutinho; 2008; Ferreira, 2009 among others).

Despite its unsuspected usefulness, it should be pointed out that this approach presents an important handicap resulting from the extreme difficulty of artificially re-creating natural microfabric. Cuccovillo & Coop (1997) tried to study the differences between naturally and artificially cemented sands using two differently cemented materials. One resulting from a cementation process developed in the early stages of

diagenesis, when small overburden was present, and a second related to a shallow marine environment with cementation developed in the later stages of diagenesis, marked by high overburden stresses. As a consequence of these environmental conditions, the former generates low densities and an open fabric, while the latter give rise to a very dense packing of cemented grains. Triaxial testing data revealed that naturally structured samples were found to consistently have higher shear stiffness than the reconstituted corresponding soil at comparable confining states, most probably related to microfabric differences, since all the other conditions were kept constant in the two sample types.

Another possibility had been previously proposed by Vaughan et al. (1988) and Maccarini et al. (1988), later developed by Bressani (1990) and recently used by Malandraki & Toll (1994, 2000), who tried to overcome this problem using artificially cemented soils obtained by mixing sand with a small amount of kaolin clay (13%) and firing at 500ºC for 5 hours, allowing a representative re-creation of natural cemented soils, since at this temperature the kaolin changes in nature and forms a weak bond between particles (Malandraki & Toll, 1994). However, the difficulty of recreating natural microfabric by remolding remains the same and so there is always an important gap between artificially and naturally bonded samples.

3.2.2. Strength behaviour

Classical soil mechanics admits a clay framework where density is presumed to be directly related to stress history and a granular framework whose behaviour is assumed to be dependent mostly on density. As discussed above, in residual soils stress history plays a minor role due to the continuous weathering, while initial porosity may generate important consequences in mechanical behaviour. In spite of that, this has to be combined with bonding, giving rise to a very similar behaviour to that observed in OC clays (Leroueil and Vaughan, 1990).

Despite this similarity, the usual (sedimentary) overconsolidation understanding cannot be applied to residual soils. In fact, the loss of weight during the weathering process will naturally result in some vertical unloading similar to overconsolidation of transported soil mechanics, but with grain size distribution and porosity of the soil being continuously modified, which greatly reduce the effect of previous stresses (Vaughan, 1985; Vaughan et al, 1988, London Geological Society, 1990, Viana da Fonseca, 1988, 1996, 2003, Rodrigues 2003, Rodrigues et al. 1997, 2000, 2001, 2002, 2004, among

others). Therefore, the break point designated by pre-consolidation stress in sedimentary soil mechanics is comparable to the breakage of cementation to a yield locus (Viana da Fonseca, 1996, 1998). The ratio between this yield stress and vertical effective initial stress is designated “virtual overconsolidation degree (vOCR)” (Vargas, 1953, Viana da Fonseca, 1988, 1996, 1998, Rodrigues, 2003) or “apparent overconsolidation degree (AOCR) (Mayne & Brown, 2003) thus differentiating it from the one physically sustained in the process of sedimentary soils generation with ‘stress memory’ (Viana da Fonseca et al. 2003; Cruz et al., 2006). In other words, it is reasonable to consider that the current density and structure of residual soil is in equilibrium with its actual state of stress, and the past stresses occurred during its evolution will have little influence on mechanical behaviour (Vaughan et al., 1988).

From the strength strict point of view, bonding condition gives rise to tensile strength, explaining the cohesive-frictional nature generally exhibited by residual soils. It is generally accepted that for a given range of stresses, cemented soils may be adequately represented by Mohr Coulomb envelope, typically showing a relatively stable angle of shearing resistance that seems to be independent of cementation level, and a drained cohesive intercept directly related with the bonding structure strength (Clough et al., 1981, Viana da Fonseca, 1988, 1996, 1998; Schnaid et al, 2004, Schnaid, 2005, Viana & Coutinho, 2008). This cohesive intercept is usually present, even when they show strong contraction during shear or when the same soil in a remoulded state doesn’t show any. As a consequence, the loss of strength with weathering degree can be represented by a reducing cohesion intercept, c’, due to weakening of contact forces between particles, giving continuity to the behaviour evolution observed in rock materials. However, it should be emphasized that in these non text-book materials, cohesion intercept can be a result of many other contributions apart from bonding, as described by Santamarina, (1997) and Locat (2003), and resumed by Viana da Fonseca & Coutinho, (2008):

a) Cementation due to chemical bonding, resulting from lithification of soil around particles and its contacts, as well as physical and chemical reactions related to both diagenesis and weathering; this cementation can be generated during or after the formation of soils, in cohesive or granular materials and stress-strain behaviour, strength, stiffness and volume change can be greatly affected by the level of cementation;
b) Presence of electrostatic forces (Van der Waals) providing contact strength (only in cohesive soils);

c) Adhesion of clay particles around some larger silt or sand particles (clay bonding);
d) Contact cementation developed with time and pressure (ageing);
e) Interaction with organic matter, where the fibbers can attract particles to form large strings or aggregates;
f) Suction due to development of negative pore pressures in unsaturated conditions, very common in residual soils, which has strong influence in strength and stiffness behaviours; due to the negative pore pressure, effective stresses become higher than total stresses, increasing strength and stiffness.

Despite this complexity, for most part of situations it is reasonable to assume that chemical bonding and suction (when it is present) give the fundamental contribution for the overall strength. Bonding structures can influence markedly strength and stiffness behaviour of frictional materials, but with failure modes varying with confining stresses, cementation agent and density (Clough et al.; 1981, Lade et al., 1987, Viana da Fonseca, 1996). Following Leroueil & Vaughan (1990) proposal, Coop & Atkinson (1993) defined three classes related to idealized behaviour of cemented soils (Figure 3.6) within specific ranges of confining stresses:

a) Class 1 – soil reaches yielding during isotropic compression, showing the same behaviour that is equivalent of non-structured material;
b) Class 2 – at intermediate states of stress, the cemented structure breaks during shear and the behaviour is controlled by friction of the equivalent non-structured material;
c) Class 3 – at low confining stresses, the stress-strain curve shows a peak value for small strains which is related to the cementation matrix; this peak appear usually prior to the highest dilatancy rate, which is a clear sign of the presence of cementitious bonds.

A similar approach is held by Santamarina (2001), which defines two basic regions of strength and stiffness control: at low or high confining stresses. Coop (2000) observed that strong and weakly cemented materials show some important differences that could be represented as presented in Figure 3.6.

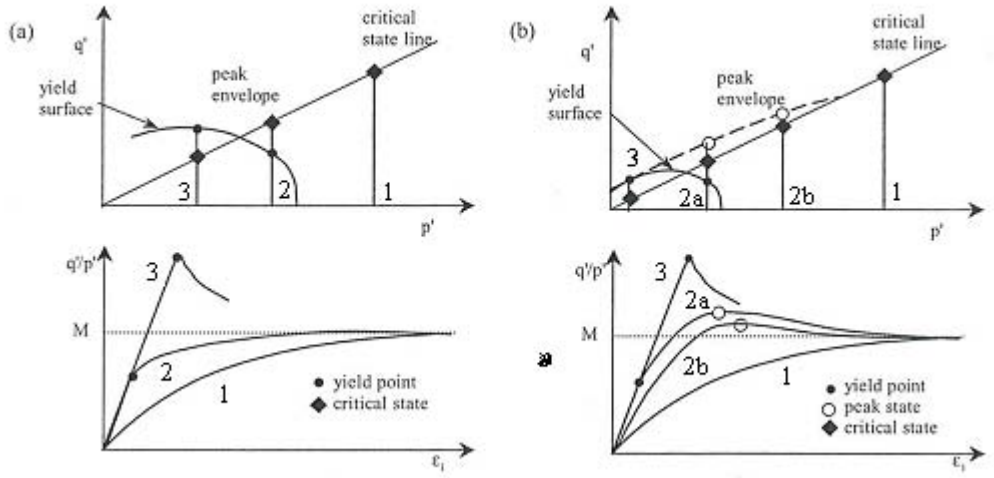


Figure 3.6 - Idealized behaviour of residual soils (after Coop, 2000)

At low confining levels, the presence of a cemented structure, even when weak, usually generates the development of a peak strength in the stress-strain curve, therefore enlarging strength envelope and some yield stress, generating different stress-strain ratios, as shown in Table 3.7 (Viana da Fonseca & Coutinho, 2008). Peak strength in deviatoric stress-strain curve is higher and occurs at successively lower strains, as cement content increases, for a given initial void ratio (Viana da Fonseca, 1988, 1996). The respective shear strains follow the opposite trend, decreasing with increasing cementation level. For a given cementation level, the confining stress increase usually produces the reduction of cohesive influence and thus, brittleness also reduces.

At high confining stresses, the behaviour changes from fragile to ductile and the peak strength disappears, converging to the response of destructured soils, with friction controlling mechanical response. This evolutive behaviour has implications in modeling numerical analysis based in hyperbolic “pseudo-elastic” model (Viana da Fonseca, 2003) or elasto-plastic hardening models such as Lade’s model (Viana da Fonseca, 1998).

Table 3.7 - Reference works in bonded soil strength (after Viana da Fonseca & Coutinho, 2008).

Reference	Type of parent rock
Sandroni, 1981	Gneiss
Coutinho et al. (1997, 1998)	Gneiss
Vaughan et al. (1988)	Basalt
Malandraki & Toll (2000) Toll & Malandraki (2006)	Granites
Cuccovillo & Coop (1997)	Sandstones and Calcarenites
Machado & Vilar (2003)	Sandstones
Schnaid et al. (2005)	Sandstones
Viana da Fonseca (1988, 1996, 1998, 2003) Viana da Fonseca & Almeida e Sousa (2002) Rodrigues (2003) Viana da Fonseca et al. (1997, 1998, 2006)	Granites

On the other hand, based in e- logσ'_v behaviour, Vaughan (1985) considered that it is possible for a residual soil to exist in three possible states, as a result of its natural void ratio, confining stress and bonding strength:

a) Metastable state, where the soil presents a void ratio impossible to occur for the respective destructured soil at the same confining level. This state is only possible because of inter-particular bonding;
b) Contractive state, represented by a soil with a void ratio possible for the respective destructured material, presenting volume decreasing in shear;
c) Dilatant state, represented by a soil with a void ratio possible for the respective destructured material, presenting volume increasing in shear.

As a consequence, microfabric and bond strength control the possibility for a soil to exist in one of these states, as illustrated by Anon (1995) in Figure 3.7.

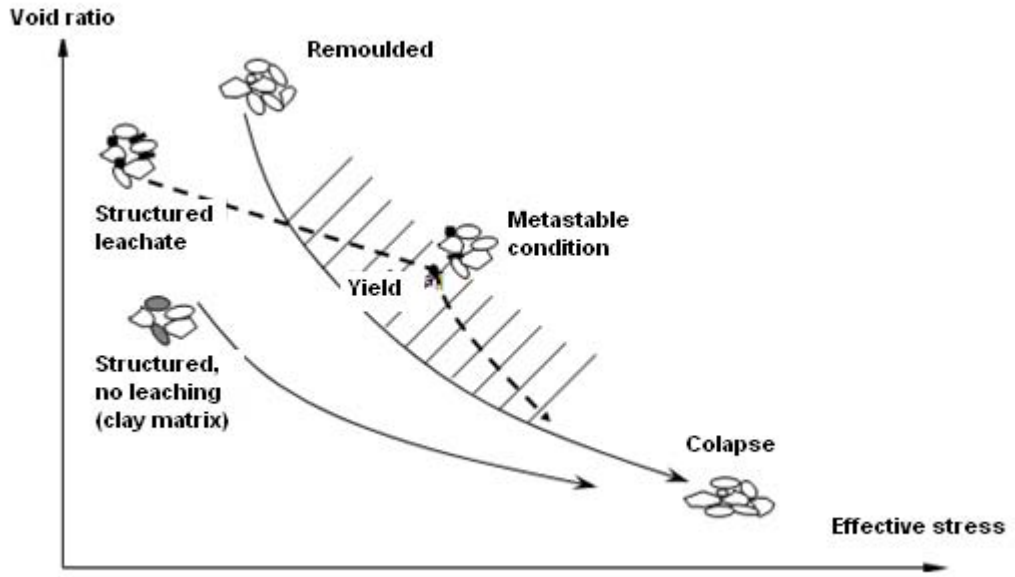


Figure 3.7 - Stress – void ratio possibilities in residual soils (after Anon, 1995).

Summarizing, it can be stated that general behaviour depends on the balance between cohesive (bonding and suction) and friction component influences, with the latter being dependent on confining stress. It is worthy to remind that component of strength (and stiffness) due to bonding is in equilibrium with current state of in-situ stress (Vaughan et al, 1988) and once broken by loading and strain, it is no longer recoverable. However, since the soil is altering as it contracts, another type of bonding may be continuously re-established, despite the large strains that may have occurred (Vaughan et al., 1988). In other words, bonded soils can be seen as evolutive with mechanical properties changing irreversibly with stress-strain level (Viana da Fonseca, 1998, 2003). Globally, a brittle behaviour is expected when shear is controlled by cohesive intercept, while ductility will be observed when friction takes control.

Representation of failure envelope in deviatoric stress-strain curve reveals a more or less straight line related to destructured material, while structured soils show curved envelopes, located as above the former as higher is cementation level. With increasing mean effective stresses, the structured envelopes converges towards the destructured one and at a certain value it overlaps the latter (Malandraki & Toll, 2000; Toll et al., 2006). Because in weakly cemented materials, the yield point is reached before failure, the respective yield surface doesn't cross the shear strength envelope of reconstituted samples. This point is identified by a transition between cementation and frictional control of mechanical behaviour.

The order of magnitude of cohesive intercept arising from the peak strength is as much relevant as the loading stress path is less dominated by volumetric compression (Viana da Fonseca, 1996; Viana da Fonseca et al., 2003). Figure 3.8 (Rios Silva, 2007) shows an example that highlights a definitive evidence of the cohesive tensile component when a compression path with decreasing of mean effective stress prevails, in opposition to others with increasing of mean effective stress. This is confirmed by the usually obtained differences of derived geotechnical parameters obtained for in-situ expansion tests (such as pressuremeters) versus compressive tests, such as penetrating tools (Viana da Fonseca et al., 1997; Viana & Coutinho, 2008).

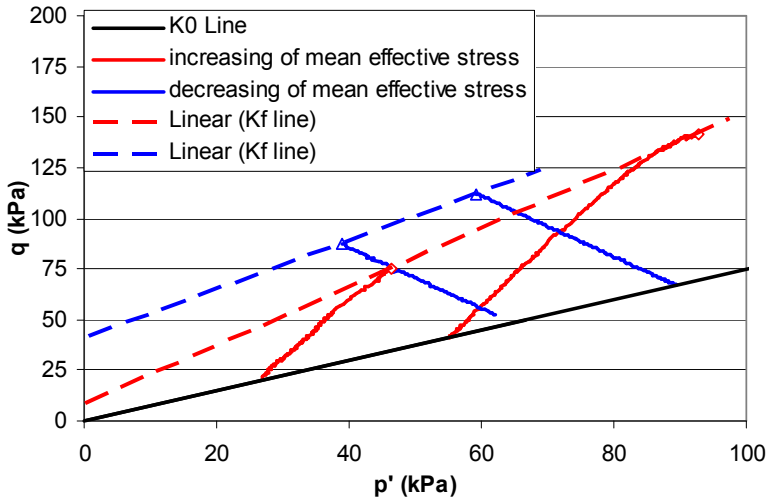


Figure 3.8 - Idealized behaviour of residual soils (Rios da Silva, 2007).

Gens & Nova (1993) proposed a discussion based on the role played by yield and the necessity of considering the cemented soil behaviour as being related to an equivalent uncemented material. Thus, the authors suggested the establishment of a constitutive law for the uncemented material, which would be modified according to cementation level, while the respective degradation would be simulated by assuming the level of cementation as function of strain level. Departing from this, Schnaid et al (2005) based in direct comparisons of remoulded samples versus artificially cemented and non-cemented soils subjected to low confining stresses, proposed that shear strength of cemented soils measured in conventional triaxial tests could be represented by the following equation:

$$q_f = [2\sin\phi/(1-\sin\phi)]p'_i + q_u \qquad (3.16)$$

where q_f represents the deviatoric stress at failure, p'_i the mean effective stress at failure of uncemented material and q_u the unconfined compressive strength.

From the above equation it can be inferred that as p_i' approaches to zero, deviatoric stresses tends to the unconfined compressive strength, while when q_u approaches to zero, deviatoric stress of cemented and uncemented soils with same initial mean effective stress (or density) tend to the same value. Of course, as deviatoric stress at failure in uncemented soils can be written as function of p_i' and angle of shearing resistance, the shear strength of cemented soil can be written as function of uncemented angle of shearing resistance and uniaxial compressive strength of cemented soil (Schnaid et al, 2005).

3.2.3. Critical or steady states

Another important feature to be looking at is the one related with the definition of strength parameters in limit states, which is far from being consensual. Critical state concepts were first developed in the sixties of last century by the research works of Roscoe et al. (1958), Roscoe & Burland (1968) and Schofield and Wroth (1968), generally based in tests performed in reconstituted and isotropically consolidated samples of clayey soils. These works gave birth to a Critical State Soil Mechanics (CSSM), representing saturated isotropic soils where the influences of structure and strain rates are negligible. Critical State Soil Mechanics considers that during shear the soil deforms homogeneously and reaches the critical state line at large strains (or deformations), whether the sample is initially normally or overconsolidated. In other words, Critical State can be defined as the state at which the soil continues to deform at constant stress and void ratio (Roscoe et al., 1958). The Critical State can be represented by a straight line (Critical State Line, CSL) in specific volume (1+e) versus logarithmic of mean effective stress (p') plots, defined by two mathematical parameters representing the specific volume for p' equal to 1 (Γ) and the slope of the critical state line (λ). Apart from this, Leroueil (2001) pointed out some extra important aspects to be considered with influence in limit states, such as:

a) Anisotropy and its influence on the limit state curves of natural soils;
b) Development of plastic strains within the limit state curve;
c) Influence of localization (shear banding);
d) Effects of crushing on the critical state lines of granular soils;
e) Effects of strain rates and temperature;
f) Effects of structure and discontinuities;
g) Influence of partial saturation.

Although the critical state concept has been often tried in sands, its application commonly reveals complex difficulties. However, its determination and validity is of considerable importance, since it provides the basis for failure criteria and post-failure behaviour of many constitutive models (Mooney et al, 1998).

Castro (1969) used undrained stress controlled triaxial tests on very loose sands to define a steady state line. The steady state of sands is defined as the state in which the mass is continuously deforming at constant volume, constant normal effective stress, constant shear stress and constant velocity. The steady state of deformation is achieved only after all particle orientation has reached a statistically steady state condition and after all the particle breakage is complete, so that shear stress needed to continue deformation and the respective velocity remain constant (Poulos, 1981). The steady state line (SSL) is defined as the locus of steady state points in void ratio / stress space. This reference line is represented by the slope of steady state points projection on e-logp' plane, designated by λ_{ss} and is usually determined by series of stress or strain controlled triaxial tests. Departing from this concept, a State Parameter (Ψ) was defined by Been & Jefferies (1985) to describe whether a sandy soil is contractive or dilative when shearing. The parameter represents the difference between the void ratio of a soil at a given mean effective stress and the void ratio on a steady state at the same mean effective stress, assuming positive values when a soil is contractive and negative when dilative, and thus positioned at the right or left side of SSL, respectively. For sands, it appears that steady state and critical states are fundamentally the same, only varying the respective form of determination (Been et al., 1991), with critical state relying on drained strain rate controlled tests on dilatant samples, while steady state is obtained from undrained tests on loose (contractive) sands, which is, in fact, just a formal approach.

However, characterizing the behaviour of soil near and beyond peak stress levels has been quite a challenge, mainly because of the development of localized strains, commonly designated by shear banding, which creates an important obstacle to determine reference Critical or Steady State Lines. In fact, the post peak behaviour, both in clays and sands, is often followed by strain localization into narrow bands, making experimental data difficult to interpret. Mooney et al. (1998), based on drained plane strain compression tests, observed that there is an abrupt formation of shear bands at the peak effective stress ratio as well as a decreasing dilatancy, suggesting that shear banding is the result of the approach to maximum strength, mobilizing its

peak friction. Post peak softening could be in part related to decreasing dilatancy in shear band.

Most part of available research on the subject (Coop & Atkinson, 1993; Viana da Fonseca, 1996, 1998, 2003; Viana da Fonseca et al, 1997; Cuccovillo & Coop, 1999; Cotecchia & Chandler, 2000) as been performed over metastable or stable-contractive (Vaugha, 1988). From the practical point of view, a comprehensive work related to a stable dilatant granular cemented soil (similar to the one within the present framework), based in undrained, constant σ'_3, constant mean effective stress (p') and constant σ'_1 was presented by Toll & Malandraki (Toll & Malandraki, 1993; Malandraki & Toll, 2000; Toll et al., 2006). The referred work revealed that in constant σ'_3 tests a dilating behaviour is observed, followed by a decrease of q and p' with the approach to Critical State conditions. When data is plotted in terms of void ratio against logarithmic scale of mean effective stress, it reveals a sharp change which was identified by the authors as representing strain localization and so, the Critical State points could be taken as the point before the referred sharp change (Toll et al., 2006), as illustrated in Figure 3.9. Viana da Fonseca (1996) had observed similar conditions in saprolitic soils of granite.

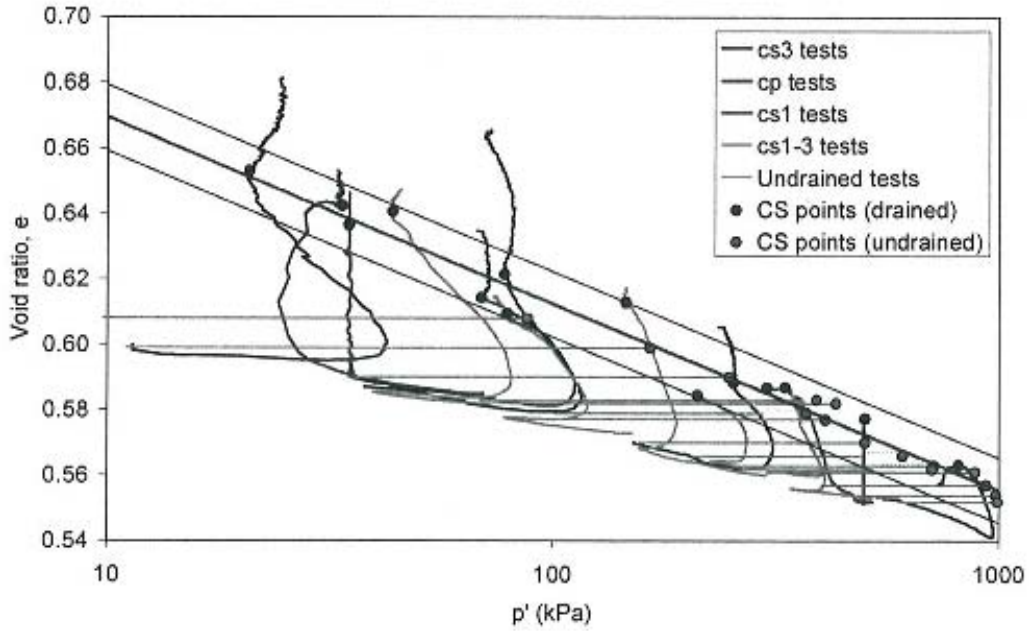


Figure 3.9 - Critical state point determination (after Toll et al., 2006)

Figure 3.9 also reflects another important aspect reported by other researchers (Vaid et al., 1989; Mooney et al 1998; Yamashita et al. 2000; Fourie and Papageorgio, 2001 and Hosseini et al., 2005) suggesting that in e-logp' space critical state void ratio for a given mean effective stress cannot be represented by a unique line, as it can be

observed in q-p' space, showing a band of values, in the case ranging within Γ = 1,726 $\pm$ 0,1 and a slope λ = 0,025.

A comprehensive summary of the basic ideas on the subject can be taken from Leroueil (2001) work:

a) Critical State Soil Mechanics is a powerful tool to understand and analyze soil behaviour; the concept of limit state can be applied to a wide range of materials, from clays to weak rocks;
b) Although there is some discussion on the matter, the concept of critical state and steady state (as defined by Poulos, 1981) seems to represent the same;
c) The shape of limit state curves of clays is influenced by the stress ratio prevailing during normal compression, with intermediate principal stress and stress rotation having major influence in the limit state; the stress-strain behaviour inside the limit state curve is highly non-linear and shows development of plastic strains; the whole limit state surface is strain rate dependent, while the critical state line is not;
d) The critical state line is probably represented by more than one line and could be influenced by the type of test, consolidation stress and stress axis rotation; moreover, it is strongly influenced by crushing becoming bi-linear in specific volume versus mean effective stress plot, or even tri-linear in the case of liquefiable soils (Bedin, 2009; Viana da Fonseca, 2009; Rocha, 2010);
e) At large deformations, states in the neighborhood of normal consolidation (or loose state in the case of sandy soils) can be identified as in accordance with Critical State Soil Mechanic concepts; in case of dense sands or overconsolidated clays, peak strength is reached when stress path touches the enlarged strength envelope, with failure developing along one or several shear bands (localization); this localization generates relative displacements of rigid blocks sliding over each other, introducing an important heterogeneity since the void ratio and/or moisture content tends to be different of the overall sample;
f) The behaviour of soils in shear bands (localization) depends a great deal in shape of particles, with round particles allowing the application of Critical State Soil Mechanics;
g) Bonded soils compared with the same destructured soils with identical void ratio show a larger limit state curve with the critical state line inside; stiffness

inside the limit state curve is also larger, but the general pre-yield behaviour can be described as a function of a “virtual” or “apparent” OCR;

h) Microfabric and discontinuities play a major role in soil behaviour;
i) Limit and critical state lines also depend on matrix suction;
j) Meter valores do artigo da soils and foundations do tó Viana

3.2.4. Stiffness

Interpretation for modulus evaluation is rather complex, since it varies with mean effective stress and shear strain amplitude, and the recently assumed modulus degradation curves in granular materials don´t fit in the observed patterns in cemented soils (Tatsuoka & Shibuya, 1992; Schnaid et al., 2005; Viana da Fonseca & Coutinho, 2008). A progressive de-structuring is a key feature in cemented granular soils giving diverse patterns of non-linearity in stress strain curves, for different effective confining stresses, as sustained by Viana da Fonseca (1996, 2003) and Fahey (2001; Fahey et al., 2003, 2007)

Clough et al. (1981), based on experimental laboratory work, observed that weakly cemented samples show brittle failures at low confining stresses with a transition for ductile failure at high confining stresses. Volume increasing during shear occurs at a faster rate and smaller strain than in uncemented samples, and density, grain size distribution, grain shape and microfabric play an important role on stiffness behaviour. On its turn, Cuccovillo & Coop (1997), comparing naturally and artificially cemented sands, brought another insight on the subject:

a) The contributions of the component of structure arising from cementation to shear stiffness are only due to the situations where yielding is prevented;
b) Yielding in structured sands is marked by a decrease of stiffness and progressive deterioration of cementation followed by plastic strains; the typical behaviour is the result of a progressive transformation of the cemented soil in a granular material, contrasting the strain-hardening response observed in the reconstituted samples;
c) In sands, where the influence of structure arises from cementation, the values of shear stiffness after a first yielding decrease with bonding degradation; when it arises from an interlocking fabric, shear stiffness remains high despite bond degradation, and even increase when mean effective stresses/density increase.

The term yield adopted herein represents marked changes in stress-strain behaviour, in natural or bi-logarithmic scales, allowing the possibility of having more than one yield, as suggested by Vaughan et al. (1988). In general, the typical stress-strain pattern of structured soils includes successive yield points, thus differing from the traditional sedimentary behaviour. The concept of more than one yield has been increasingly reported in literature (Maccarini et al., 1987; Bressani, 1990; Leddra et al. 1991; Jardine, 1992; Malandraki & Toll, 1994; Viana da Fonseca, 1996, 1998; Cuccovillo & Coop, 1997; Viana da Fonseca et al, 1997, 1998; Rodrigues, 2003; Toll & Malandraki, 2006), generally identifying the typical pattern as an initially stiff behaviour followed by successive yields. The position of yielding points differs according to the author. Vaughan et al. (1988) suggested the existence of 2 yields, due to the presence of bonding. The first yield represents the moment at which bonding starts to fail. Afterwards, bond strength decreases with further stress and strain, until a second and more significative yield occurs, which was defined by Vaughan et al. (1988) as the moment at which increasing stress equalizes the bond strength. However, it should be noted that this implies a homogeneous level of cementation between particles within the soil mass under load, which is unlikely to happen in natural soils, and thus second yield might, in some way, be dissimulated and so very difficult to determine. Despite what it may seem, second yield does not represent the end of bond strength, which will happen for much higher strains.

Jardine et al. (1991) and Jardine (1992) suggested the following three yield points, where the first two are kinematic and move according to the current stress path direction, while the third is static and independent of stress history:

a) Y1 – represents the limit of linear elastic behaviour;
b) Y2 – represents the limit of recoverable behaviour, meaning that behaviour up to Y2 can be non-linear but no plastic strains are generated;
c) Y3 – represents the complete destruction of any structure within the soil.

On its turn, Cuccovillo & Coop (1997) followed by Schnaid et al. (2005) highlighted the definition of a yield stress, by representing data in a bi-logarithmic plot of secant modulus against deviatoric stress, based on the observation that there is an initial portion where the modulus is roughly constant, followed by a yield and post-yield gradual reduction as a result of the progressive transformation of a bonded soil into a frictional material (Figure 3.10).

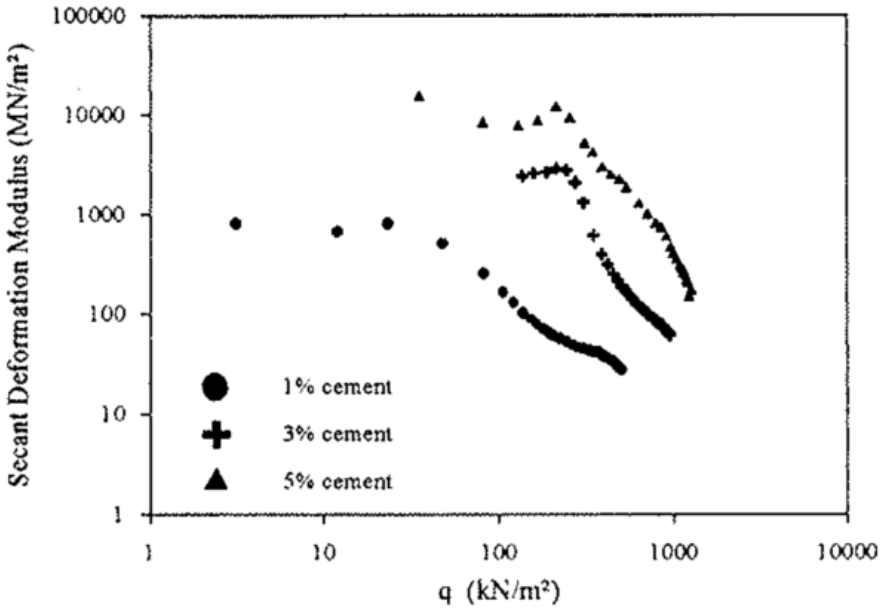


Figure 3.10 - Yield point determination (after Cuccovillo & Coop, 1997)

Another approach is given by Malandraki & Toll (1994, 2000), who proposed a model with 3 yield points, which were related with steps of the bonding breakdown. Figure 3.11 illustrates the three yield points defined in stiffness vs axial strain plot, using bi-logarithmic scale, which are function of initial bond strength, initial void ratio (Vaughan et al., 1988; Malandraki and Toll, 2000; Toll et al., 2006) and stress path (Silva Cardoso, 1986; Viana da Fonseca, 1988; 1996, Malandraki & Toll, 2000). An initially stiff behaviour is identified, represented by more or less stable elastic behaviour until a certain point (at very low axial strain) where a first drop occurs (first yield), which was identified as the beginning of bonding breakage representing the same first yield proposed by Vaughan et al. (1988), Jardine (1992), Viana da Fonseca (1996) or Rodrigues (2003). Up to this point cementation contribution remains the same and only very small changes in stiffness occur. After the first yield, while stress and strain increase, the cementation strength decreases with a slight reduction in stiffness, and when strength and stress fall within the same stress level, a major change in tangent modulus is observed (second yield). This yield is also coincident with the one defined by Cuccovillo & Coop (1997) and Schnaid et al. (2005). The respective axial strain position depends on the followed stress path, usually decreasing as stress paths rotate left (Malandraki & Toll, 2000). It should be emphasized that this second yield is not the same Y2 proposed by Jardine (1992), which is related with the end of an elastic non linear behaviour, and much more difficult to determine. Beyond second yield, tangent modulus decrease with axial strain, progressively converging to the one observed in destructured equivalent soil, until both reach a coincident final yield (third yield), which

is the same of Jardine (1992) and Vaughan et al. (1988). Since this model incorporates all the assigned possibilities, with exception to the difficult to determine Jardine's Y2 yield locus (1992), it was the one adopted to interpret modulus degradation and yielding within the present experience.

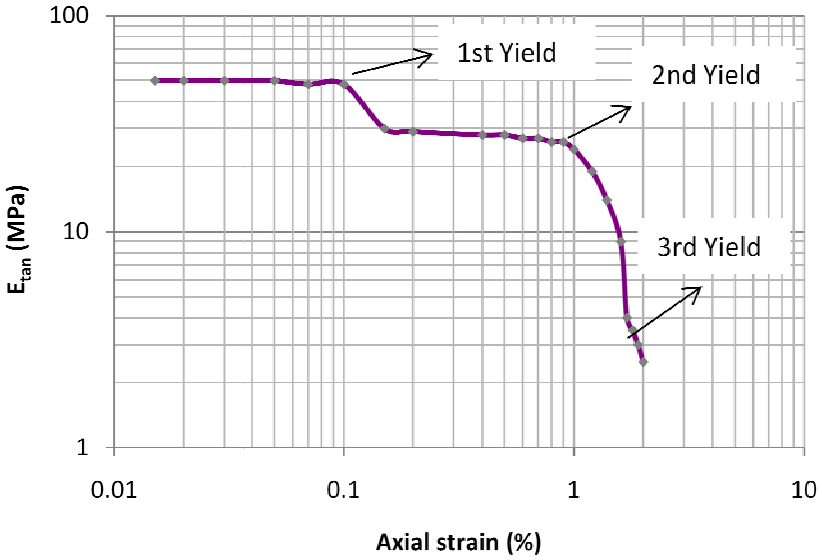


Figure 3.11 - Typical yield sequence purposed by Malandraki & Toll (1994, 2000).

At low confining stresses, cemented soil deformation modulus doesn't seem to be specially affected by its initial mean effective stress, and so the secant deformation modulus of cemented soils could also be represented by Janbu (1963) mathematical expressions, as referred by Schnaid et al. (2005).

$$E = k\, p_a\, (\sigma'_3 / p_a)^n \qquad (3.17)$$

where E represents the deformability modulus, σ'_3 is the effective confining stress, p_a is the atmospheric pressure, k and n are the adimensional factors of the model.

This kind of approach, however, is not easy to apply in day-to-day problems, since they depend too much on triaxial testing and, as a consequence, are strongly influenced by sampling disturbance. Moreover, cementation breakage is not a sudden phenomenon, with gradual evolution as the strain level increases, being generally accepted that the stress-strain behaviour of almost all soils is highly non-linear, even for stiff soils in the 'elastic' region of the stress-strain response (Fahey et al., 2003), leaving an important a role to continuous non-linear models. In general, it has been recognized that conventional testing deduced parameters are too conservative when compared with

real situations (Burland, 1989; Tatsuoka et al, 1997; Viana da Fonseca & Coutinho, 2008).

As sustained by many investigators (Fahey & Carter, 1993; Viana da Fonseca, 1996, 2001, 2003; Fahey et al. 2003; Mayne, 2006; Viana da Fonseca & Coutinho, 2008) the initial tangent modulus, G_0, is the fundamental parameter of the ground, a benchmark value, which reveals its true elastic behaviour and, if properly normalized, with respect to void ratio and effective stress, could be seen as independent of the type of loading, number of loading cycles, strain rate and stress/strain history (Viana da Fonseca & Coutinho, 2008). This parameter can be accurately deduced through shear wave velocities, since their magnitude are closely related to stiffness, as expressed in the equation below:

$$G_0=\rho \cdot v_s^2 \tag{3.18}$$

where ρ stands for density and v_s for shear wave velocity.

For uncemented sands G_0 has been shown (Hardin & Richard, 1963; Jamiolkowski et al., 1995, Fahey et al., 2003; Viana da Fonseca & Coutinho, 2008) to depend on the effective stress level raised to some power, *n*:

$$\frac{G_0(\mathrm{MPa})}{F(e)} = S \cdot \left[p'_0\,(\mathrm{kPa})\right]^n \tag{3.19}$$

$$F(e) = \frac{(C-e)^2}{1+e} \tag{3.20}$$

where p'_0 is the initial mean effective stress, *S* and *n* are experimental constants, *e* represents the void ratio, *F*(*e*) the void ratio function and C a constant depending on the shape and nature of grains. The value of 2.17 presented by Hardin & Richard (1963) for sands seems to fit well in the case of Porto granitic soils. The power *n* is generally around 0.4 to 0.6 for uncemented sand and it would be expected to be lower, or even zero for well-cemented sands (Fahey et al, 2003). A summary of reported *S* and *n* results can be seen in Table 3.8, as presented by Viana da Fonseca & Coutinho (2008), where it can be observed that parameter S is much higher than the value adopted for cohesionless soils, as result of local weathering conditions, while the exponent *n* is, in general very low, reflecting a substantially lower influence of the mean effective stress. These different values of n are consequence of different types of bonding between grains affecting the Hertz low type of behaviour existing in particulate

materials (Biarez et al. 1999, Viana da Fonseca, 2003; Schnaid, 2005; Viana da Fonseca et al. 2006,).

Table 3.8 - Stiffness vs stress state parameters for residual soil (Viana & Coutinho, 2008)

References	S	n
Alluvial sands, Ishihara (1982)	7.9 to 14.3	0.40
Saprolite from granite (Matosinhos,Porto,Portugal), Viana da Fonseca (1996, 2003)	110	0.02 p´<100kPa
Saprolite from granite (CEFEUP, Porto, Portugal), Viana da Fonseca et al. (2004)	65	0.07
Saprolite from gneiss (Caximbu, Sao Paulo, Brazil), Barros(1997)	60 to 100	0.30 p´<100kPa
Saprolite from granite (Guarda, Portugal), Rodrigues & Lemos (2004)	35 to 60	0.35
Competely decomp. tuff (Hong Kong), Ng & Leung (2007b)	37 to 51	0.20-0.26
Cachoeirinha lateritic soil (Porto Alegre, Brazil). Consoli et al. (1998) and Viana da Fonseca et al. (2008)	79	0.18
Passo Fundo lateritic soil (Porto Alegre, Brazil), Viana da Fonseca et al. (2008)	181	0

Direct application of small-strain shear modulus to evaluate deformations in most practical problems is rather difficult, due to its usual non-linearity. In fact, for every level of applied stress, a different secant shear modulus (G_{secant}, or simply G) is obtained and thus there is no single 'correct' value of soil stiffness for any specific situation, which depends on the loading (strain) level (Fahey et al., 2003), being useless to apply linear elastic models to a non-linear behaviour. The ratio between secant shear modulus (G) normalized by the initial tangent value, G/G_0, and a normalized shear strain (Fahey & Carter, 1993; Santos, 1999; Viana da Fonseca & Coutinho, 2008) can be seen as representing stiffness degradation, since it is not affected by the kind of soil, plasticity index, confining stress overconsolidation ratio and degree of saturation (Viana da Fonseca & Coutinho, 2008). As a consequence, plots of stiffness changes with strain level are a good approach to represent moduli, being often the use of plots of (G/G_o) versus shear strain or mobilized shear stress (Fahey et al., 2003).

Hardin & Drnevich (1972). verified that stress-strain ratios is not well described by hyperbolic model, but when the strain level is properly normalized by a reference strain, γ_r, stress-strain curves fit into two narrow bands related with cohesive and incoherent soils. The author's selected the reference strain as the strain related to the interception of the initial tangent of shear stress/shear strain ratio with the maximum shear stress line, but other possibilities could be selected such as the strain corresponding to G/G_0 equal to 0.7 proposed by Santos (1999), which seems to fit well in engineering practice, being used in some of the available commercial software for numerical analysis. The Modified Hyperbolic Model (Hardin & Drnevich, 1972) consists in applying a distortion to the strain axis, forcing the soil curves to fit into the hyperbolic curve, by means of a reference hyperbolic strain obtained by Equation (3.21):

$$\gamma_h = \frac{\gamma}{\gamma_r}\left[1 + a\,exp\left(-b\frac{\gamma}{\gamma_r}\right)\right] \tag{3.21}$$

where γ,, γ_r and γ_h are respectively the strain, the reference strain and hyperbolic strain, while *a* and *b* are soil constants (Table 3.9, adapted from Barros, 1997) and exp stands for the base of natural logarithmic.

Table 3.9 - Values of a and b (adapted from Barros, 1997).

Type of Soil	*a* value	*b* value
Dry clean sands	-0,5	0,16
Saturated clean sands	-0,2 log N	0,16
Saturated cohesive soils	1+ 0,25 log N	1,3

Applying this correction, degradation curves can be deduced through the following equation (Barros, 1997):

$$(G/G_0) = 1 / (1+\gamma_h) \tag{3.22}$$

Other alternatives can also be considered, such as plotting G/G_o versus mobilized shear stress normalized by a maximum shear stress, τ/τ_{max}, or deviatoric stresses, q/q_{max}, (Tatsuoka & Shibuya, 1991). One example of this approach is the proposal of Fahey and Carter (1993) that introduced a 'distorted hyperbolic modell', represented by the following equations:

$$G/G_0 = 1 - f\,(\tau/\tau_{max})^g \tag{3.23}$$

$$E/E_0 = 1 - f\,(q/q_{max})^g \qquad (3.24)$$

where *f* and *g* are the parameters that control the non-linearity of stress-strain curve.

The value *f* in the equation determines the value of the secant stiffness at peak strength (at τ_{max}), while *g* represents the rate at which the stiffness 'softens' with increasing mobilized shear stress ((τ/τ_{max}). In this equation, setting the 'distortion parameters' *f* and *g* to both be equal to 1, gives the straight-line hyperbolic model. Mayne (2001) pointed out that for monotonic loading in unstructured uncemented sands values of f=1 and g=0.3 seem to be representative (Figure 3.12). In Portugal, tests in resonant column of Porto granitic residual soils carried out by Viana da Fonseca (2006) revealed the same degradation curve of the one proposed for sands by Santos (1999), which actually is considered in some available commercial software for engineering analysis.

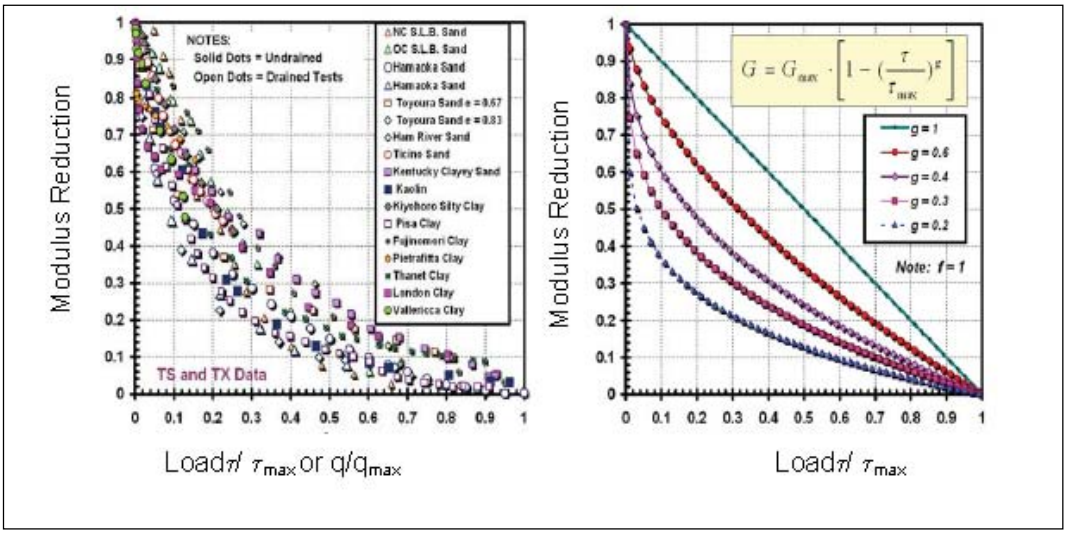


Figure 3.12 - Modulus reduction (adapted from Mayne, 2001).

Another approach to represent stiffness of cemented soils was developed by Liu and Carter (2002), introducing the Structured Cam Clay (SCC) model, a relatively simple, practical model to describe the response of structured soils to load increments. In this model four additional parameters are used to introduce the influence of soil structure into the Modified Cam Clay model (Roscoe and Burland 1968), namely the destructuring index, *b*, which quantifies the rate of destructuring, the size of the initial yield surface, $p'_{co'}$ the additional void ratio sustained by the structured soil when yielding begins, Δe_i and another parameter, ω, which describes the influence of soil structure on the plastic potential of the soil. The model has been applied with success, predicting foundation settlements in Perth

carbonate cemented sands, revealing some advantages in relation to other models, such as the similarity with the well-known Modified Cam Clay model, with only simple but significant changes and needs relatively few parameters to be quantified, all of which have a clear physical meaning (Carter, 2006). Comparing 6 different models in Perth cemented soils, Carter (2006) concluded Modified Cam Clay and Structured Cam Clay provide the best prediction of the stress-strain curve, and also reasonably accurate peak strengths, while the others (Lagoia & Nova, 1995; Islam, 1999) only at large strains provide good predictions, being too conservative at small strains. On the other hand, all the models provide reasonable predictions of the volume reduction, with the exception of Modified Cam Clay model, which identified dilation in samples contracting during shearing.

Apart from triaxial testing, which is the main tool used for stiffness characterization, some attempts have been made using correlation with penetration tests (SPT, CPT), direct measurement using pressuremeters (pre-inserted or self-bored) and semi-direct measurement with DMT, while the definition of small-strain stiffness modulus has been obtained through seismic wave velocities. Maximum shear (or Young) modulus (E_0 or G_0), obtained by non destructive methods, are related to small strains, typically in the order of 10^{-6} strain, while strain levels associated to DMT, pressuremeter and penetrometer in-situ tests of determination will be variable as shown in Figure 3.13 (Sabatany et al., 2002). The degradation curve can be expressed as function of soil plasticity and strain (Vucetic & Dobry, 1991), mobilized shear stress, τ/τ_{max} (Tatsuaka & Shibua, 1992; Fahey & Carter, 1993; Lo Presti et al., 1998), logarithmic strain (Jardine et al., 1986; Jardine, 2005) and ratios G/G_0 and τ/τ_{max} (Mayne, 2006).

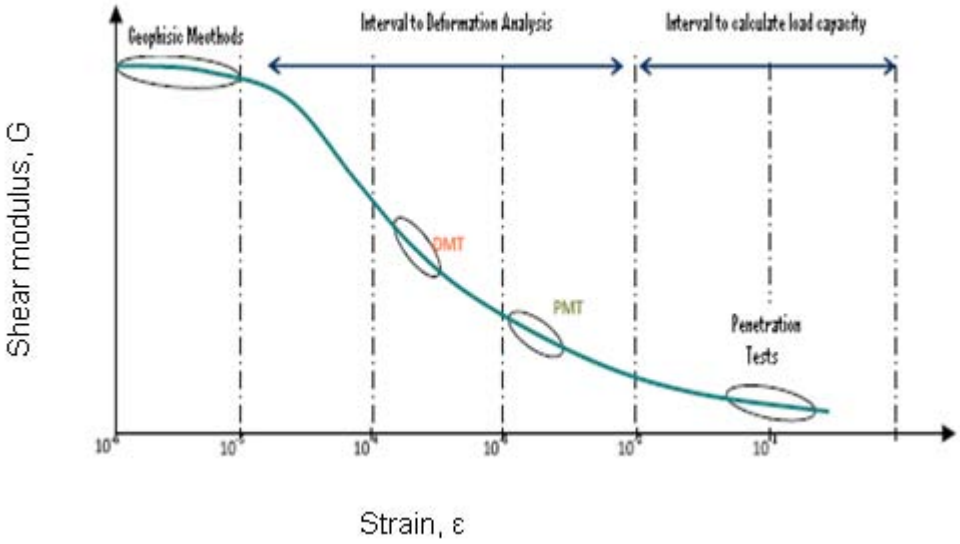


Figure 3.13 - Variation of shear modulus (G_0) with strain level (ε).

Another important issue brought to light by Viana da Fonseca & Coutinho (2008) is whether the yield locus is isotropic or anisotropic, and if this is, or not, centered in the K_0 stress axis. In natural clays, the shape of the yield curves is anisotropic centered in the K_0 stress axis due to the conditions prevailing during their deposition (e.g., Tavenas and Leroueil, 1977; Graham et al. 1983; Smith et al. 1992; Diaz-Rodriguez et al. 1992). In bonded soils this is not yet well known, as limited data are available. Viana da Fonseca & Coutinho (2008) identify some cases, reported in international references, where yield curves and residual soils and soft rocks may appear centered on the isotropic axis (Leroueil and Vaughan, 1990; Leroueil & Hight, 2003; Machado & Vilar, 2003), while Futai et al. (2006) showed that yield curves of tropical soils under saturated conditions may be isotropic or anisotropic with respect to the hydrostatic axis, depending on the degree of weathering, the respective original rock nature, and diagenesis. Viana da Fonseca et al. (1997a) reported some results of isotropic consolidation tests with local measurement of axial and radial strain, which provided values of the virtual isotropic preconsolidation stress slightly lower than the one deduced from the oedometer tests, taking K_0=0.38 (Figure 3.14a). Futai et al. (2006) show the limit state curves from gneissic mature and young residual soils presented Figure 3.14b. The expansion of the limit state curves with the increase of depth is quite clear in the figure. It is shown that limit state curves for soils from depths of 1.0 and 2.0m in horizon B are centered on the hydrostatic axis. Limit state curves of soils from horizon C (depths 3-5 m) are not centered on the hydrostatic axis, which may be due to the remaining 'mother' rock anisotropy, showing similar shapes observed for natural

clays that are anisotropic due to the K_{0nc} stress conditions prevailing during their deposition (Viana da Fonseca & Coutinho, 2008).

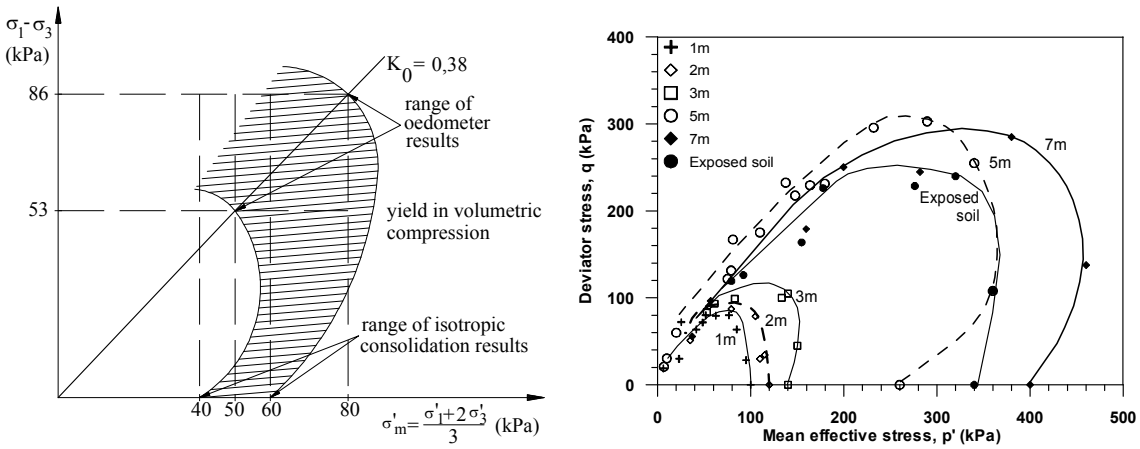


Figure 3.14 - Yield surfaces for volumetric compression (σ_1 = vertical stress, σ_3= horizontal stress) – a) Viana da Fonseca et al. (1997a); b) Limit state curve for saturated condition (Futai et al. 2006) (After Viana & Coutinho, 2008)

3.2.5. The role of suction

In many situations in nature, water table is not located near the surface, thus creating a zone of unsaturated conditions subjected to saturation degrees somewhere between 0 and 100%. This is a consequence of a property called surface tension that allows soil to have capillary water above the water level. The ground surface climate is a prime factor controlling the depth of the groundwater table and therefore, the thickness of the unsaturated soil zone.

Surface tension is a typical liquid property which generates tensile pull strength, at surface, resulting from intermolecular forces acting at air-liquid interface. The forces in the interior of the liquid acting on a molecule experiences a resultant force towards the interior of the liquid and an equilibrium tensile pull is generated along the surface (Montañez, 2002). The resulting force from these phenomena is commonly known as suction. Suction can be defined as the free water absorption capacity of a porous element, which mainly depends on mineralogy, density and water content (Topa Gomes, 2009) and generates a geotechnical behaviour different from those predicted according to the effective stress principle that has been developed for saturated soils and temperate climate (Viana da Fonseca & Coutinho, 2008).

Suction is responsible for an important difference between saturated and unsaturated soils, related to the development of negative pore pressures in the water of the pores that give an extra contribution to strength and stiffness. The presence of suction in a specific soil massif has a significative impact in geotechnical properties, and thus it should be considered in the interpretation of testing and design procedures (Viana da Fonseca & Coutinho, 2008). In fact, suction contributes to stiffening the soil against external loading, which can be interpreted as an increase in the apparent preconsolidation stress as suction increases, similarly to the cementation effect. As a consequence, a concept of a maximum past suction ever experienced by the soil, similar to the concept of pre-consolidation stress is proposed by Alonso et al. (1990), from where irreversible strains will begin to develop. Furthermore, if the natural depositional processes or the compaction method induce an open structure in the soil, a reduction in suction (wetting) for a given confining stress may induce an irrecoverable volumetric compression (collapse), while for a certain range of the confining stress the amount of collapse increases with the intensity of the confining stress (Alonso et al., 1990).

The strength behaviour of unsaturated soils can be evaluated according to the following four variables (Fredlund et al., 1978; Alonso et al., 1990; Viana da Fonseca & Coutinho, 2008):

a) Deviator stress (q);
b) Net mean stress ($p - u_a$);
c) Suction ($u_a - u_w$);
d) Specific volume (v).

Fredlund et al. (1978) proposed the following expression to evaluate the soil strength in unsaturated conditions, departing from classical Mohr-Coulomb concept:

$$\tau = c' + (\sigma - u_a) \tan\phi' + (u_a - u_w) \tan\phi^b \quad (3.25)$$

where c' and ϕ' stands for the Mohr-Coulomb criterion parameters, $(\sigma - u_a)$ the normal liquid stress, $(u_a - u_w)$ the matrix suction and $\tan\phi^b$ the non-lineal (Escario & Juca, 1989; Vanapalli et al., 1996 and Futai & Ito, 2008) suction angle of shearing resistance which represents the contribution of matrix suction to shear strength.

As it can be understood from the respective equation, there is a fundamental difference between shear strength of saturated and unsaturated soils related to stress variables, consisting in a behaviour (saturated soils) mainly governed by single effective stresses

(σ - u_w) and another (unsaturated soils) controlled by two independent stress variables, namely the matrix suction (u_a - u_w) and the net normal stress (σ - u_a) (Fredlund, 1973; Fredlund and Rahardjo, 1993a).

The term (u_a - u_w) represents the matrix suction and can be seen as a measure of the energy required to remove a water molecule from the soil matrix without water having a state evolution. When the removal of water is through evaporation (water changing state from liquid to gaseous), the term total suction is applied. The presence of dissolved salts in water reduces the tendency of evaporation to occur and the required energy to remove the water molecule from the soil liquid phase is increased, meaning an increase of total suction. The additional energy that is demanded to remove a single water molecule is called osmotic potential and it represents the difference between total and matrix suctions (Montañez, 2002).

One important tool to quantify suction contribution in unsaturated soils is the *Soil-water characteristic curve*, defined as the relation between volumetric water content and matrix suction. The definition of this curve is fundamental to understand soil behaviour in unsaturated conditions and can be decisive in the evaluation several parameters such us permeability, shear strength, volumetric strains or thermal conductivity (Frendlund & Xing, 1994; Fredlund et al., 1997).

Experimental data requested for its definition can be obtained by direct and indirect measurements of suction. Direct methods are those that measure the equilibrium state without involving the use of an external media for moisture equalization, while indirect methods are external based. Psychrometers, tensiometers and pressure plates fall in the first category, whereas filter papers and thermal conductivity sensors are included in the second. Table 3.10 (adapted from Ridley & Wray, 1995 and Guan, 1996) presents a summary of available devices and its respective advantages and limitations. Of course, direct in-situ measurements of suction matrix would be desirable, but it has been generally confined to 100 kPa ranges because of cavitation problems, which constitutes a fundamental problem in research programs on the behaviour of unsaturated soils.

Table 3.10 - Suction devices (adapted from Ridley & Wray, 1995 and Guan, 1996).

Device	Suction type and ranges (kPa)	Time for stabilization	Advantages	Limitations
Psycometer	Total (100-8000)	Minutes	Wide range	Constant temperature conditions Poor accuracy Only laboratorial
Filter paper (contact)	Matricial	7 days	Cover the entire range of measurement Low cost	Difficult handling Poor accuracy User dependent Only laboratorial
Filter paper (without contact)	Total	7 days		
Thermal conductivity	Matricial (0-400)	Weeks	Independent of dissolved salts and temperature Lab and field measurements	Equilibrium time Low accuracy above 150kPa Deterioration of thermal block
Pressure Plate	Matricial (0-1500)	Hours	No cavitation High suction measurement	Equilibrium time Diffusion difficult Only laboratorial Best suited for suction control
Suction plates and ordinary tensiometers	Matricial (0-100)	Days	Quick response Low cost Easy handling Lab and field measurements	Cavitation limit to 100kPa Air bubble conflict
Osmotic tensiometer	Matricial (0-1800)	Minutes	No cavitation High suction measurement	Poor reliability Strict temperature control Only laboratorial Expensive equipment

Futai et al. (2007) presented a very comprehensive work on basic understanding of suction influence in strength and stiffness properties. In Figure 3.15, soil-water retention curves of two gneissic residual soil (mature lateritic and young saprolitic) are presented, measured using the suction plate, for suction lower than 30 kPa, pressure plate (suction between 30kPa to 500kPa) and the filter paper technique (Chandler & Gutierrez, 1986) for higher suction levels. The differences between the two soils regarding grain size distribution, mineralogical composition and microstructure directly influence the water retention capacity. Porosimetry measurements appear to confirm

the results of the grain size analysis, since mature lateritic soil possesses smaller pores and higher clay content than young saprolitic. The overall analysis of grain size, soil microscopy and porosimetry suggests a meta-stable structure for the mature lateritic soil comprising micro and macro pores.

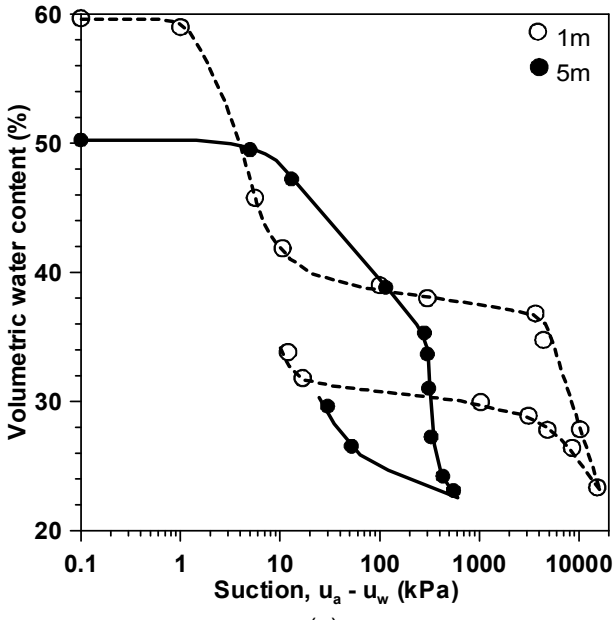


Figure 3.15 - Soil-water retention curve (after Futai et al. 2007).

From the strength point of view, the expected increase of cohesive intercept with increasing suction level (Santamarina, 2001, Fredlund, 2006; Futai et al. 2006; Vilar 2007, Viana da Fonseca & Coutinho, 2008; Topa Gomes, 2009) was observed as represented in Figure 3.16 (Futai et al., 2006), showing an important increase at small levels of suction (< 100 kPa). The same Figure also shows the increase of angle of shearing resistance with suction level (Lafayette, 2006; Futai et al., 2006, Viana da Fonseca & Coutinho, 2008), which has been less referred in literature.

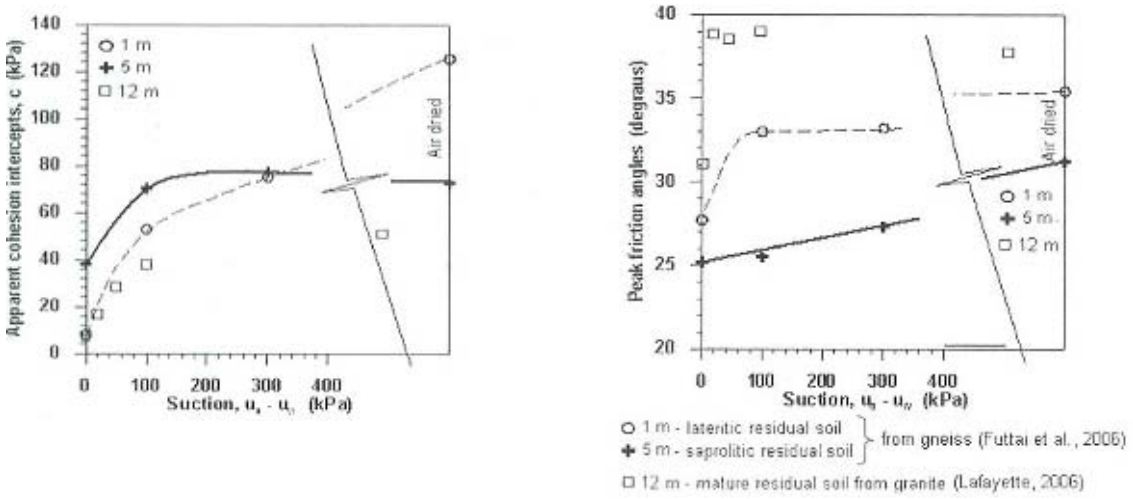


Figure 3.16 - Cohesion intercept and angle of shearing resistance versus suction (after Viana da Fonseca & Coutinho, 2008).

From stiffness point of view, the effect of increasing suction is to enlarge the yield curves, maintaining the shape (Futai et al., 2007). Neverthless, Topa Gomes (2009) observed that stiffness increases with increasing suction at smaller rates near saturation, as shown in Figure 3.17 Viana da Fonseca & Coutinho (2008), quoting international references on the subject, indicate that these yield curves can appear centered (Machado & Vilar, 2003) in natural residual soils or not centered in the hydrostatic axis (Cui & Delage, 1996; Maâtouk et al. 1995; Leroueil & Barbosa, 2000) in compacted and artificially cemented unsaturated soils.

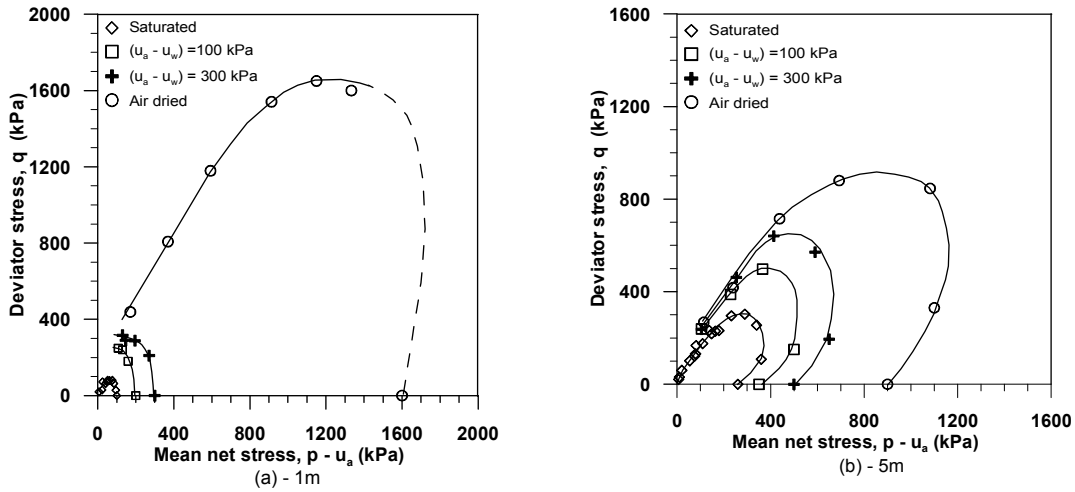


Figure 3.17 - Yield curves under constant suction (after Viana da Fonseca & Coutinho, 2008)

Finally, a reference is due to the constitutive model for partially saturated soils proposed by Alonso et al. (1990), although only a brief discussion will be presented since it was not included in this research frame. Departing from Modified Cam Clay Alonso et al. (1990) proposed a constitutive model based on the representation on deviatoric stress (q) – mean stress (p') – suction (s) space. The model is characterized by a loading-collapse (LC) and a suction-increase (SI) yield curves, both enclosing an elastic region in the (p, s) plane. A three dimensional view of the yield stresses in q:p:s space is presented in Figure 3.18. The application of this model requires nine constants, five more than the critical state model, related with the following stress states and parameters (Alonso et al., 1990)

a) Initial state: initial stresses (p_i, q_i, s_i), initial specific volume (v_0) and initial reference stress variables (strain hardening parameters) defining the initial position of the yield surfaces (p_{0i}*, s_{0i});
b) Parameters directly associated with the LC yield curve (isotropic stress): a reference stress (p^c), compressibility coefficient for the saturated state along virgin loading [$\lambda(0)$], compressibility coefficient along elastic (unloading-reloading) stress paths (κ), the minimum value of the compressibility coefficient (virgin states) for high values of suction (r), and a parameter that controls the rate of increase in stiffness (virgin states) with suction (β);
c) Parameters directly associated with changes in suction and the SI yield curve: compressibility coefficient for increments of suction across virgin states (λ_s) and compressibility coefficient for changes in suction within the elastic region (κ_s)
d) Parameters associated with shear stress changes: shear modulus within the elastic domain (G), slope of the critical state line (M) and a parameter that controls the increase in cohesion with suction (k).

The determination of the model parameters have to be based in suction-controlled testing with the following stress paths suggested by Alonso et al. (1990):

a) Tests that involve isotropic drained compression (loading and unloading) at several constant suction values, providing p^c, p_0*, $\lambda(0)$, κ, r and β;
b) Tests that involve a drying-wetting cycle at a given net mean applied stress, providing s_0, λ_s and κ_s;
c) Drained shear strength tests at different suction values, providing G, M and k.

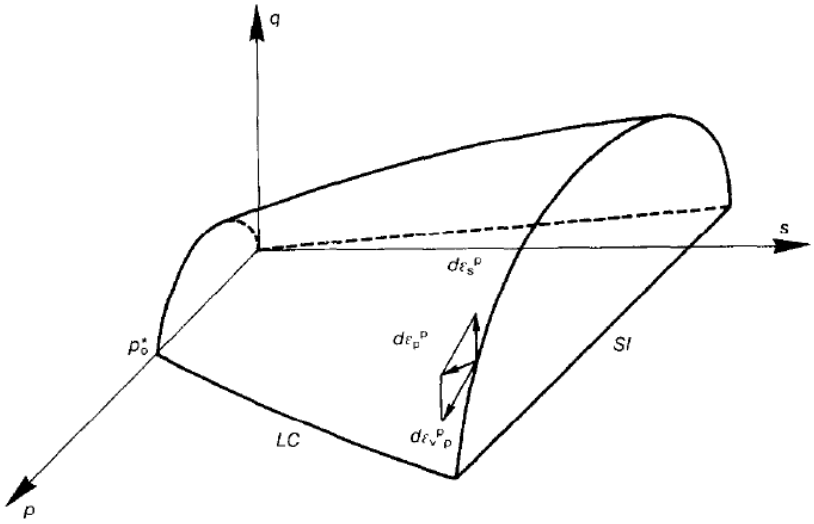


Figure 3.18 - Three-dimensional view of the yield stresses in q:p:s space.

Chapter 4.
Geotechnical parameters from in-situ characterization

4. GEOTECHNICAL PARAMETERS FROM IN-SITU CHARACTERIZATION

"Rates remain extremely competitive, restricting investment in new equipment and techniques. We must continue to encourage clients to consider best value rather than low cost." (Gabriel, 2001).

4.1. Overview

The comprehension and interaction of natural massifs depend greatly on the measuring capacity of its properties with adequate accuracy and with low levels of disturbance introduced by equipment installation. Ground investigations are the processes involved in the acquisition of information on ground properties and should be specifically designed for each individual situation (Simons et al., 2002). The main goals to be achieved in ground investigation could be presented as follows (Devincenzi et al, 2004):

a) Nature and sequence of the subsurface strata (geology);
b) Groundwater conditions (hydrogeology);
c) Physical and mechanical properties of the subsurface strata (engineering properties);
d) Distribution and composition of contaminants (geoenvironmental conditions).

These requirements can vary in volumetric extent depending on the nature of the proposed project and the perceived ground related risks. There are many techniques available to achieve the objectives of a ground investigation, including both laboratory and field tests. Before going into a deeper analysis it may be worth to remind the main requirements for the successful practice of geotechnical engineering, as referred by Peck (1962) in the early sixties:

a) Knowledge of site past history;
b) Familiarity with soil and/or rock mechanics;
c) Clear understanding of the geologic history and the effects that might come in the consequence of the building construction;
d) Search for all possible failure mechanisms;
e) Model and field conditions never match perfectly and so there will always be differences between field and predicted behaviour.

The mechanical characterization of soils can be based in laboratory and in-situ testing, ideally viewed as complementary rather than competitive. Geotechnical investigations during the first decade of XX century were marked by the execution of bore-holes with Standard Penetration Tests (SPT) eventually combined with simple laboratory mechanical tests, constituting the main source of information. Subsequently, there was an important development of laboratory test devices based in theoretical knowledge, supported by numerical quality data for characterizing strength, stiffness and hydraulic properties. To convert laboratory data in field performance and to sense spatial variation, SPT tests provided the conventional support for design purposes. Globally, laboratorial testing can be divided in those that test single elements of the ground (consolidation and triaxial testing, for example) and those that test large scale masses and structures, such as physical models (centrifuge tests), presenting the great advantages of controlling and defining boundary conditions, drainage and stress paths. However, some obstacles of difficult solution arise from laboratorial demands and limitations, such as those related to sampling, massif heterogeneity and non-continuous information, leading to an increasing interest on site techniques. In fact, in-situ testing covers quite well laboratory testing disadvantages, since they avoid sampling and some can identify ground heterogeneities continuously. In-situ tests can also offer some more extra advantages, such as low time consuming and commonly low cost. As a consequence, in the second half of XX Century, new in-situ devices were appearing in geotechnical practices, evolving from the rough SPT to more refined techniques such as Light, Medium, Heavy and Super-Heavy Dynamic Probing (respectively DPL, DPM, DPH and DPSH) Plate Loading Test (PLT), Field Vane Test (FVT), Cone Penetration Test (CPT), Menard Pressuremeter Test (PMT), Self-Boring Pressuremeter Test (SBPT), Piezocone test (CPTu), Marchetti Dilatometer Test (DMT), Cross-Hole seismic test (CH), Seismic Piezocone Test (SCPTu) and Seismic Dilatometer Test (SDMT).

SDMT and SCPTu tests are among the most useful in geotechnical characterization for design purposes, since they both combine, in one test, mechanical and geophysical measurements. Despite these developments, most of in-situ evaluation of geotechnical parameters is still based on empirical correlations with SPT data, which, in the author's opinion, should only be used as primary approach, considering the development of technologies in our days. Thus, modern geotechnical programs using those technologies are required to improve the accuracy, quality of results and, consequently, a consistent understanding of this behaviour.

4.2. Sampling

As it was referred, laboratory testing depend too much on sampling, which introduces soil disturbances that highly influences the estimation of ground properties (Baligh, 1985). Soil disturbance usually occurs in a wide variety of sampling stages, namely drilling, sampler penetration, transportation, extrusion and trimming, responsible for significative and complex damage. A comprehensive illustration, showing a typical sample stress path from its original location to final laboratory testing, is represented in Figure 4.1 (Ladd and Lambe, 1963).

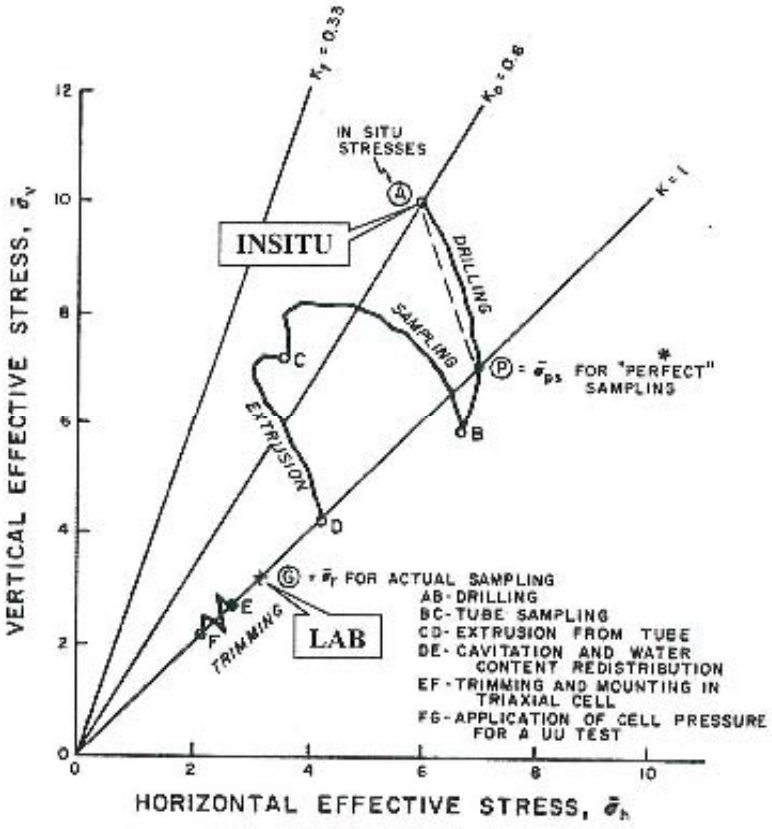


Figure 4.1 - Typical stress path associated to sampling (after Ladd & Lambe, 1963)

The disturbance effects are usually identified from variation of state of stress, mechanical strain, water content and void ratio variations, as well as eventual chemical alteration, being some of these unavoidable while other can be substantially reduced if proper procedures are undertaken. The level of disturbance and importance of each referred factors depends not only on the sampling process but also on the type of soil (Hight, 2000; Viana da Fonseca & Ferreira, 2001; Rodrigues, 2003). Clayton et al. (1995) summarized the main causes of disturbance due to sampling processes as described in Table 4.1.

Table 4.1 - Sampling disturbance (adapted from Clayton et al., 1995).

Before Sampling	During sampling	After sampling
Stress release	Stress release	Stress release
Expansion	Remolding	Water migration
Compression	Displacements	Variation of water content
Displacements	Crushing	Overheating
Bottom ruptures	Boulders in the tip	Vibration
“Piping”	Mixing or segregation	Chemical exchanges
Cavitation	Local ruptures	Extrusion Disturbance

In sandy soils, the sampling processes generate a drained answer and suction level is quite limited, thus the main consequences can be resumed as follows (Hight, 1995):

a) Void ratio (or volume) variations;
b) Mechanical disturbance of soil structure and cementation (normally presented in natural soils), generated by volumetric and shear deformations;
c) Significative decreasing of mean effective initial stress (p’);
d) Modifications of interparticle contact distribution.

Sampling techniques are usually divided according to its output quality, which can be described as follows (Viana da Fonseca & Ferreira, 2001):

a) Block Samples – blocks with larger dimensions than usual tube samplers; they are trimmed by hand in the field and with the lowest sampling disturbance; however, it is only possible to get these samples if some cohesion (structural, therefore effective, or apparent such as that due to suction) is present and at locations above water level, requiring highly skilled operators; Sherbrooke and Laval samples allow collecting samples with same level of quality
b) Statically driven tube samplers – thin wall open tube samplers (Shelby and piston samplers) statically pushed into soft and loose to medium soils, with high fine content and limited size of maximum grain particles, since the thin wall is easily damaged during penetration;
c) Driven tube samplers - thick wall open tube samplers installed by driving with hammer blows; the tube walls are stronger for penetration but introduce important sample damage, especially in bonded soils; appropriate for stiff/compacted materials;

d) Rotary double and triple (Mazier) samplers – double or triple wall samplers that are introduced by rotary drilling, usually with water, allowing for continuous sampling and low suction levels developed during extraction; on the other hand, the water is responsible for relevant disturbance reducing the mean effective stress, especially in equipments of frontal discharge; appropriate to stiff soils;
e) Disturbed samples – only for visual inspection.

With the exception of the block samples, which in practice are only used in limited situations, sampling is executed by means of driving samplers into the ground. The quality of the samplers can be defined through its Area Ratio (AR) and Inside Clearence Ratio (ICR), as defined in Figure 4.2 (Clayton et al., 1998), translating their specific geometry. The major factors influencing the magnitude of strains can be controlled by AR and the outside cutting edge for compression peak axial strain, as well as ICR in extension peak axial strain.

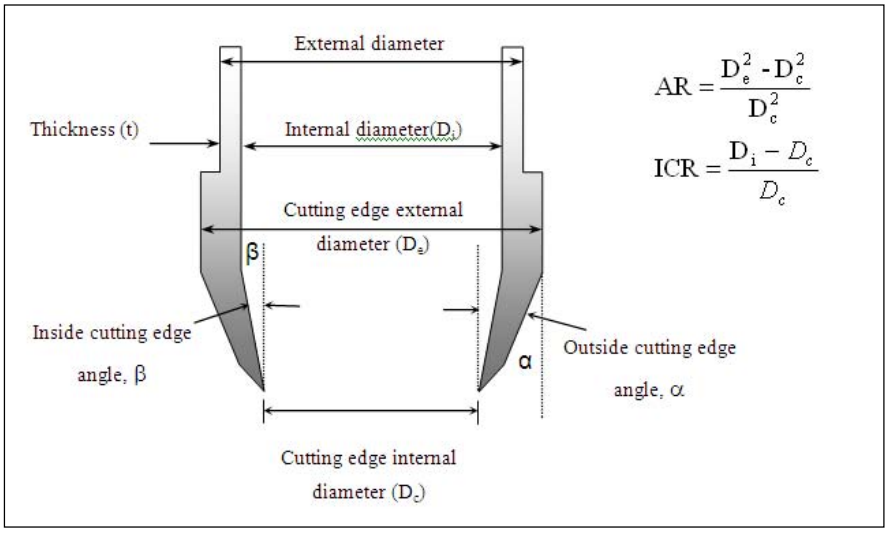


Figure 4.2 - Sampler geometric parameters (after Clayton et al, 1998).

The strain path analysis applied to the penetration of a cylindrical tube by Baligh et al. (1987) and the work of Clayton et al. (1998) constitutes a step forward in the subject, as highlightened by Hight (2000) and Viana da Fonseca & Ferreira (2001):

a) In the central line of a sampler with inside clearance the soil experiments complex triaxial strain distributions in the surrounding soil as a result of triaxial compression and unloading, thus introducing variations in the initial state of stress and partial destructuration of the soil, especially in the vicinity of the tube wall; a tube without inside clearance greatly reduces the strain and so it should be adopted

b) The maximum compression strain is related with the ratio between tube diameter and wall thickness, B/t;
c) In the surroundings of the tube wall there is intensive shear controlled mainly by the wall thickness;
d) The maximum strain in the central line are strongly influenced by the cutting edge angle;
e) A redistribution of water content occurs as a consequence of sampler penetration; depending on the type and density of soil the water content in the central line increases in soft clays/loose sands and decreases in hard clays/dense sands. These effects can somehow be reduced if the sample extrusion is done in the field followed by the removal of the sample periphery and adequate sealing and protection.

Taking this into account, to obtain good quality samples Hight et al. (2000) suggests a reference sampler composed by thin walls, no inside clearance, 5º (or less) cutting edge angle, large diameters and length of at least 0,5m (in order to reduce suction effects during the recovering process), designated as Modified Tube Sampler.

No matter the used methodology, it is fundamental to assess sample quality to calibrate laboratory parameter interpretation, especially when triaxial modeling based interpretation is undertaken (Long, 2001; Ferreira, 2009). Available methodologies for sample quality evaluation can be presented as follows (Hight, 2000):

a) Fabric inspection – visual inspection of soil fabric involves a great deal of subjectivity, which only enables the identification of “macro problems”;
b) Measurement of initial mean effective stress, p’ – quantitative evaluation based on effective stresses variation before and after sampling;
c) Measurement of strains during reconsolidation – quantitative evaluation based on strain variation, as proposed by Lunne et al. (1997), by means of the ratio of void ratio variation against initial void ratio;
d) Comparison of in-situ and laboratorial seismic wave velocities – the sensitivity of shear waves enables to distinguish different structure or fabric arrangements as well as stress conditions and void ratio; thus, direct laboratory and in-situ comparisons seem to be very promising for sample quality assessment, with emphasis in structured soils (Viana da Fonseca & Ferreira, 2002, 2001/4; Viana da Fonseca & Coutinho, 2008; Ferreira, 2009).

Generally this subject is very complex, especially in residual soils, with intensive research undergoing worldwide. It is not our purpose to go deep into the subject, since this research is within in-situ testing techniques and laboratory tests were performed on artificially cemented samples just for calibration purposes. Being so, the subject will only be generally commented in the following lines. In Chapter 6, a proposed classification for sample quality in residual soils (Ferreira, 2009) will be presented. For more detailed information, the works of Viana da Fonseca (1988, 1996, 1998), Viana da Fonseca & Ferreira (2002, 2004); Rodrigues (2003), Viana da Fonseca & Coutinho (2008), Topa Gomes (2009) and Ferreira (2009) in residual soils, or Lunne et al. (1997), Leroueil (1997), Hight (2000) in sedimentary soils are suggested.

4.3. In-situ testing

The information about in-situ testing is abundant and varied (e.g. Cestare, 1980; Mayne and Kulhawy, 1990; Bowles, 1988; Coduto, 1999, Schnaid, 2000; Mayne, 2007), looking into all the important details such as equipments, procedures, fields of application, sources of error, data interpretation, advantages, limitations, etc. It is not a purpose to repeat an exhaustive discussion about each in-situ test device in this document and so, after a brief overview on the matter, only the in-situ tests involved in the present work will be discussed. In this context, it will be given a special attention to DMT in Chapter 5 and Chapter 7, since it is the reference test selected for the basic model for residual soil characterization proposed herein, while some discussion on deriving geotechnical parameters from SCPTu tests will be provided within this chapter, due to its significant use combined with DMT in Porto granitic residual soils.

There are some different ways of looking into “in-situ” testing, ordering them by order of appearance, obtained parameters and fields of application, among others. In the following paragraphs, a simple overview is presented, starting from the early SPT and seeing how the others successively improve in-situ accuracy and efficiency, not necessarily ordered by their “date of birth”.

Standard Penetration Test is the most worldwide used in-situ test, and it is the main source for the basic knowledge of geotechnical ground properties and behaviour. In short words, it can be said that SPT is a device that senses the strength of the soil and soft rocks (including intermediate geomaterials, IGM) through a measurement of the number of blows needed to drive into the ground 300 mm of a standardized 50 mm outer diameter split barrel sampler, by means of a 760 mm free fall of a 63.5 kgf weight hammer. Although it is a normalized test, operators, driving devices and condition of

the sampler can deeply influence the results of the test, as highlightened by recent research on the subject (Cavalcante, 2002; Odebrecht, 2003; Odebrecht et al., 2004; Lopes, 2009; Rodrigues et al., 2010), giving raise to some important interrogations on its data analysis.

Taking the test procedure into account, it is expected that somehow SPT can represent the strength of the penetrated soils, while care must be taken deducing stiffness parameters since it really doesn't measure the stress-strain relations. It is a simple and rough test with no special measurement devices and capable of penetrating in almost all types of ground, which make it very easy to perform and very friendly to incorporate in the drilling campaigns. However, the obtained data doesn't allow special quality (with special emphasis in the case of soft/loose soils), the information is discontinuous and one single value (N_{SPT}) represents both tip and side internal and external friction resistances, which makes it inadequate whenever some precision is required. Furthermore, although the test is cheap, a campaign exclusively based on SPT testing becomes very expensive, since boreholes are needed to perform the test. The combination of the boreholes with some other modern testing devices can be much cheaper, faster and, at the same time, more reliable than a SPT based campaign. Finally, little evolution of the testing equipment has been introduced since its earlier appearance, and so modern technology is not incorporated in the testing device, which leads to the question "Is it not the time for SPT retirement?" (Mayne, 2001). More recently, however, a second breath of the test has arisen by the application of the concepts of energy transfer (Schnaid et al., 2009). On the other hand, the combination of limit equilibrium analysis and cavity expansion theory provided analytical formulations established from energy measurements in dynamic penetration tests that have shown the possibility to calculate a dynamic force transferred to the soil when a device is driven by the struck of a hammer blow. Departing from the dynamic force derived this way, it is possible to predict geotechnical parameters, such as angle of shearing resistance of sands or undrained shear strength of clays and also can be directly applied to bearing capacity of piles (Schnaid et al., 2009).

Dynamic probing (DP), represents almost the same as the SPT, although with some important changes. In fact, dynamic probing relies on the same method of penetration, but using a cone instead of a sampler, loosing the "identification" capacity by missing the soil recoiled in the Terzaghi sampler of penetrated ground but enabling quasi-continuous information and a no longer mixed side friction/tip resistance determination.

In alluvial areas or in other soft or loose grounds, the inadequacy of dynamic testing becomes evident. In fact, these soils usually reveal values of N_{SPT} typically lower than 4 blows, which disable efficient interpretations of drained and undrained shear strength. In soft clayey soils, the strength is so low that the only way of getting a proper value is to know quite well the applied force (with high sensitivity devices), the volume involved and the flow characteristics (Odebrecht, 2003, Odebrecht et al., 2004). Assuming that clays develop only undrained behaviour during test execution, then *Field Vane Test (FVT)* is a very useful tool for strength evaluation. The test consists of a vane blade, a set of rods and a torque measurement apparatus that allows accurate and reproducible readings in the form torque-angular deformation of a cylinder of soil with height equal to two times the diameter.

By the end of thirties of last century, those were the available in-situ tests that were combined with laboratory testing for geotechnical ground characterization. A second wave of developments started with Cone Penetration Test, CPT, which would become one of the most powerful tools on soil characterization of modern days, since it combines past experience, evolution on available test results, some theoretical solutions to support interpretation, incorporation of recent technology devices and it can work as installation guide for other type of devices (seismic cone, cone pressuremeter, visiocone, etc). Generally departing from three measurements (tip resistance, side friction and pore pressures) CPT test results allow the assessment to important geotechnical data with high quality, related with stratigraphy, stress history, strength and deformability. However, it should be said that adequate modulus evaluation should be obtained using seismic wave velocities (SCPTu), since the measurements taken in the common test procedures correspond to the pressure needed for shearing, and so reliability of results may be questioned. More detailed discussion will be provided ahead in this chapter.

Stiffness evaluations throughout dynamic (SPT and DPs) and static (CPTu) tests are not direct, being deduced through the idea of how a soil of a certain type and a certain strength would behave. On the contrary, a proper modulus determination should include measurements of both load and respective displacement/settlement with time. So, in the first half of last century the only adequate test for stiffness analysis was the *Plate Load Test, PLT*, which is just the simulation of a (usually circular) small direct foundation. The test is performed in a sequence of load levels applied to a circular steel plate, measuring the evolution of settlement with time for each applied load, through adequately precise deflectometers. At the end of the test, the obtained results provide

time - settlement curves related to each load increment and a load-settlement plot from where stiffness moduli can be deduced, and (if lucky) the ultimate resistance. Unfortunately the test covers only shallow depths and ground above phreatic level, which makes it only applicable to a very narrow band of engineering conditions. This difficulty of testing in depth was overcome in the second half of last century, by the introduction of a new device in France by Louis Menard (1956), designated by Menard Pressuremeter Test (PMT), and developed from an original idea of Kogler in 1933. The pressuremeter is a cylindrical rubber balloon, inserted in the ground by pushing, self-boring or pre-boring a hole into which the expansion cylinder is placed. Once in the ground, increments of pressure are applied, forcing the rubber membrane to inflate against the surrounding soil and thus forming a cylindrical cavity. A typical test is very similar to plate load tests and consists on the measurement of a series of incremental loads and the respective cavity wall volume change with time, which allows the definition of a loading curve that may be analyzed using rigorous solutions supported by cylindrical cavity expansion and contraction theories. Based on those interpretations, test provides information related to the horizontal effective stresses, pseudo-elastic moduli, creep and ultimate stresses, all used to evaluate in-situ stress, compressibility and strength of the tested materials. Besides those, solutions for direct applications on foundation (bearing capacity and settlement) and excavation analysis using test parameters are also available. Pressuremeter tests can be performed in a wide variety of soil types and weathered or soft rocks.

The ultimate developments in geotechnical measuring devices and techniques reveal a growing usefulness of geophysics not only through the traditional seismic wave velocities, but also with electrical and electro-magnetic (georadar) methodologies, representing a step further on site characterization, mainly because of its capacity for stiffness evaluation (seismic) and geotechnical mapping, at relatively low prices, when compared with some other in-situ tests. At the end of last century, back analysis around tunnels and excavations using finite element analysis have shown that in-situ stiffness of soils and rocks is much higher than that was previously perceived, and that stress-strain behaviour of these materials is non-linear in most cases and the strain levels in the ground around retaining walls, foundations and tunnels are small (Burland, 1989; Simons et al. 2002), typically in the order of 0.01 to 0.1% (Jardine et al., 1986). *Seismic tests* apply very small strains (10^{-6} to 10^{-4}) and thus it has been considered that they give relevant results to linear elastic phase of soil deformation (Viana da Fonseca et al., 1997; Simons et al., 2002). Mayne (2001), summarizing the importance of shear wave velocity determination, pointed out that it is a fundamental measurement in all

solids, including soils and rocks, provides small-strain stiffness represented by shear modulus and can be applied to all static and dynamic engineering problems at small strains under drained and undrained conditions. These considerations gave rise to the development of a large number of apparatus to measure compression and shear wave velocities and thus obtaining theoretical interpretations for small strain shear modulus evaluation. In saturated uncemented soils the propagation of compression waves (designated as P waves) will represent a short term undrained loading, where most of the energy travel through the pore water and the compressibility of water tend to dominate soil stiffness, showing P-velocities close to those exhibited by water (approximately 1500 m/s). Being so, in saturated soils shear waves (S waves) should be the only used, since they are not influenced by the compressibility of the fluid. In cemented soils, the stiffness of mineral skeleton increases and the first arrival of compression waves become representative of the material, since velocities tend to be higher than in pore water medium. In the limit, the elastic modulus of saturated rock obtained from P-wave will be representative.

Although seismic refraction methodologies are the most widely used in geotechnical surveys, other geophysical techniques, such as *seismic reflexion*, *electric resistivity*, *electro-magnetic (Geo-Radar)* and *gravimetry* are available and can be very powerful tools in soil characterization, especially in ground mapping. These techniques have been frequently used by the author in day-by-day practice of geotechnical campaigns where MOTA-ENGIL has been involved (Cruz et al., 2008c; Cruz et al., 2008d), providing an increasing confidence to its application in current characterization campaigns.

In Table 4.2 to Table 4.4, a synthesis of basic information related to in-situ testing is presented, in terms of general characteristics, domains of application and quality of derived parameters, adapted from Lunne et al. (1997).

Table 4.2 - Characteristics of in-situ tests

	SPT/DPs	PLT	FVT	SCPTU	PMT	DMT
Hardware	Simple and rough	Simple and rough	Simple and rough	Complex and rough	Complex and sensitive	Simple and rough
Execution	Easy	Easy	Easy	Easy	Complex	Easy
Profile type	Discont. Continuous	Discont.	Discont.	Continuous	Discont.	Continuous
Interpretation	Empirical	Theoretical	Theoretical	Theoretical Empirical	Theoretical Empirical	Theoretical Empirical
Type of soil	All types	Earthfill, Soils above the water level	Soft clays	Very soft to stiff clays, very loose to medium compact sands	All types	Very soft to stiff clays, very loose to medium compact sands, earthfills
Information type	Qualitative	Quantitative	Quantitative	Quantitative.	Quantitative	Quantitative
Geotech. information	Compactness and consistency derived design parameters	Moduli and Bearing capacity of shallow foundations and sub grading	Undrained shear strength	Continuous evaluation of Density and Strength. Discontinuous evaluation of Stiffness and Flow properties	Compressibility and Bearing capacity	State of stress, Stress history, Strength, Stiffness and Hydraulic properties

Table 4.3 - In-situ tests fields of applications

	Type of soil					
	Gravel	Sand		Silt	Clay	
		Loose	Dense		Soft	Stiff
SPT e DPs	2 to 3	1	1	2	3	3
PLT	4	1	1	1	1	1
FVT	4	4	4	3	1	2
CPT (Mec)	2 to 3	1	2	1	1	2
CPT(Elect)	3	1	2	1	1	2
SCPTU	3	1	2	1	1	2
PMT	2	2	1	1	1	1
SBPT	3	2	2	1	1	1
DMT	3	1	2	1	1	2

High; 2- moderate; 3- limited; 4- inappropriate

Table 4.4 - Quality of deduced parameters.

	Soil type/profile	u	γ	c_u	ϕ	I_D	M	G_0	K_0	OCR	c_v	k
SPT	Borehole	--	3	3	3	2	3	3	--	--	--	--
DPs	--	--	--	3	3	2	3	3	--	--	--	--
FVT	Borehole	--	--	1	--	--	--	--	--	2/3	--	--
PLT	--	--	--	2	3	--	1	1	--	--	--	--
PMT	Borehole	--	--	2	3	3	2	2	3	3	--	----
CPTu	1 / 1	1	2	2	2	2	3	3	--	3	1/2	2
SCPTu	1 / 1	1	2	1/2	2	1/2	1/2	1	--	2	1/2	2
DMT	1 / 1	3	1	1/2	2	1/2	1/2	2/3	2/3	2		
SDMT	1 / 1	3	1	1/2	2	1/2	1	1	2	2		
CH	Borehole	--	--	--	--	--	--	1	--	2	--	--

1- High; 2- moderate; 3- limited; -- inappropriate

Due to the existence of some contact points between in-situ tests, disadvantages of one can be covered by the advantages of another, suggesting that, when carefully selected, campaigns combining various test types (here designated by MultiTest or MT Technique) increases the level of efficiency of the in-situ testing whole package, bringing some important advantages such as (Cruz et al., 2004a):

a) More test parameters are available to combine, and so more possibilities for deducing geotechnical parameters that couldn't be obtained otherwise;
b) Increment on the number of assessed geotechnical parameters as a result of the sum of both test abilities;
c) Usually each test has its own advantages and limitations, which are different in every case; thus, combining pairs give the possibility of correcting or completing the information obtained, bringing reliability and confidence on selected design parameters;
d) Cross-confrontation of the same geotechnical parameter obtained by more than one test, allows the calibration of correlations as well as the detection of inappropriate applied deriving methodologies; this can be very useful in characterizing non-textbook materials or when the geological environment is quite different from those that gave raise to each specific correlation;
e) Possibility of combining tests adapted to local conditions, in order to assess good quality information on strata with different levels of penetration resistance; in some cases it is possible to achieve this with minimal extra-costs (e.g. DMT + CPTu).

In general, combinations should be selected including always at least one continuous type of test. DPSH used together with SPT can be an interesting methodology, since its similar working principle makes it easy to settle a local correlation between the two test's results, and provides continuous dynamic logging, which could be worked both via SPT traditional correlations and through a dynamic point resistance, q_d.

One of the best combining pairs is DMT/CPTu, since both individually can assess the most required parameters for design and because they can be pushed with the same rig, making it easy for field work in penetrable grounds. However, they have the same major limitation, thrust capacity, which cuts the access to some types of ground.

In difficult ground, PMT is an obvious solution, but DPSH can be a reasonable alternative. The problem could be solved using CPTu or DMT (or both) combined with PMT or DPSH, by calibrating the information where they both can be performed and

using the latter in the stiffer depth ranges. FVT or DMT, combined with CPTu, can also be very useful to calibrate correlation factors for c_u derived by the latter in soft clays.

As due to well compacted earthfills, PLT and DPSH together can provide a stiffness continuous profile, while for loose to medium dense soils, DMT (or CPTu) and PLT can give significant useful information (Cruz et al., 2006b, 2008a).

During last decade, geophysics became a geotechnical tool, gaining field on current design campaigns. Seismic techniques have been used quite often, but late technology evolutions made its application in a very comfortable way, as for SCPTu or SDMT. Moreover, electric and electro-magnetic have potential to be used in combinations either in soil or rock massif surveys (Cruz et al., 2008c). Some suggestions resulting from a strong field experience on applying this procedure both in sedimentary (Cruz et al. 2004a, 2006a) and residual soils (Almeida et al., 2004; Carvalho et al., 2004; Viana da Fonseca et al., 2004, 2006; Cruz et al., 2004b, 2004c, 2006b) as well as in rock massif characterizations (Cruz et al. 2008c, 2008d) are presented in Table 4.5.

Table 4.5 - Possible test combinations

	Foundation	Excavation	Fill over soft soils	Liquefaction	Special works
Soft clayey soils	DMT/SCPTu DMT/FVT SCPTU/FVT	DMT/SCPTu DMT/FVT SCPTU/FVT	DMT/ SCPTu DMT/FVT SCPTu/FVT Laboratory	DMT/SCPTu SPT/CH (V_s, V_p) Laboratory	DMT/SCPTu CH/Up-hole*
Hard clayey soils	DPSH/PMT DMT/PMT	DMT/PMT	DMT/PMT DPSH/PMT	--	DPSH/PMT CH/Up-hole*
Loose sandy soils	DMT/SCPTu	DMT/SCPTu	DMT/SCPTu	DMT/SCPTu SPT/CH (V_s, V_p)	DMT/SCPTu
Dense sandy soils	DMT/PMT	DMT/PMT	DPSH/PMT	--	PMT/Geophysics
Cemented soils	DMT/SCPTu DPSH/PMT	DMT/SCPTu DMT/PMT	DPSH/PMT Laboratory	--	BH/ Geophysics
Loose fills	DMT/PLT DMT/PMT	DMT/PLT DMT/PMT	--	DMT/SCPTu SPT/CH (V_s, V_p) Laboratory	BH/ Geophysics
Well compacted fills	DPSH/PMT DPSH/PLT	DPSH/PMT	--	--	--
Rock massifs	BH/ Geophysics /Lab	BH/ Geophysics /Lab	--	--	BH/ Geophysics /Lab
Karstic massifs	BH/ Geophysics /Lab	BH/ Geophysics /Lab	--	--	BH/ Geophysics /Lab

* to anisotropy evaluations

4.3.1. Cone Penetration Tests (SCPTu)

CPT is one of the faster and less expensive forms of in-situ testing in relatively soft or loose to medium soils and it's an interesting equipment that represented, by the time of its appearance, a high jump in the general quality of geotechnical data. Figure 4.3 shows the set of needed devices to perform a modern SCPTu test.









Figure 4.3 - Details on SCPTu testing devices

The earlier test started from a measurement of the load needed to statically push a normalized tip (10cm^2 cross-section area and an apex angle of 60º) into the ground, then introducing devices to measure side friction, pore water pressure and, more recently, shear wave velocity, or even other devices for geoenvironmental purposes, such as dielectric sensors. The earlier penetrometers were mechanical (Begemann, 1965), which required a double rod system. Nowadays this equipment is mostly out of service, due to the development of electrical cones with built-in strain gauges or

extensometers that record continuously the tip resistance, q(c), the local side shear, f(s), and pore-pressure, u. Typically, an electrical cable connects the cone and side friction sleeve (cross-section of 150cm^2) measuring gauges with data acquisition equipment at the ground surface, although other data transfer technologies are also available (radio transfer, for instance).

CPT is fundamentally a strength test since it registers penetration resistances, being therefore adequate to deduce drained or undrained strength properties. The addition of a pore-pressure gauge at the base of the cone (CPTu) provides important information enlarging its dimension to the interpretation of soil strata identification, strength and flow geotechnical parameters, especially in loose or soft soils (Konrad and Law, 1987). The determination of excess pore pressure generated during penetration is a useful indication of soil type and provides excellent mean for detecting “thin” layers and to stress history evaluation. In addition, when the steady penetration is stopped, the dissipation of the excess pore-pressure with time can be used to deduce the horizontal coefficient of consolidation, allowing the analysis of time-settlement rates, previously only achieved by the time-consuming laboratory consolidation tests. In Figure 4.4, various tip configurations with different locations for pore pressure measurements are presented (Mayne 2001).



Figure 4.4 - Different configurations of SCPTu cones (after Mayne, 2001).

More recently, evaluation of stiffness become possible with the introduction of shear wave velocity devices in the field equipment (SCPTu), greatly increasing its efficiency for design analysis. SCPTu test results (Figure 4.5) can be theoretical or empirically interpreted in order to give soil stratigraphy and classification as well as geotechnical parameters related to state and stress history, strength, stiffness (here the relevance of

the rigidity index, Ir, has a significant meaning) and flow characteristics of soils subjected to drained or undrained conditions.

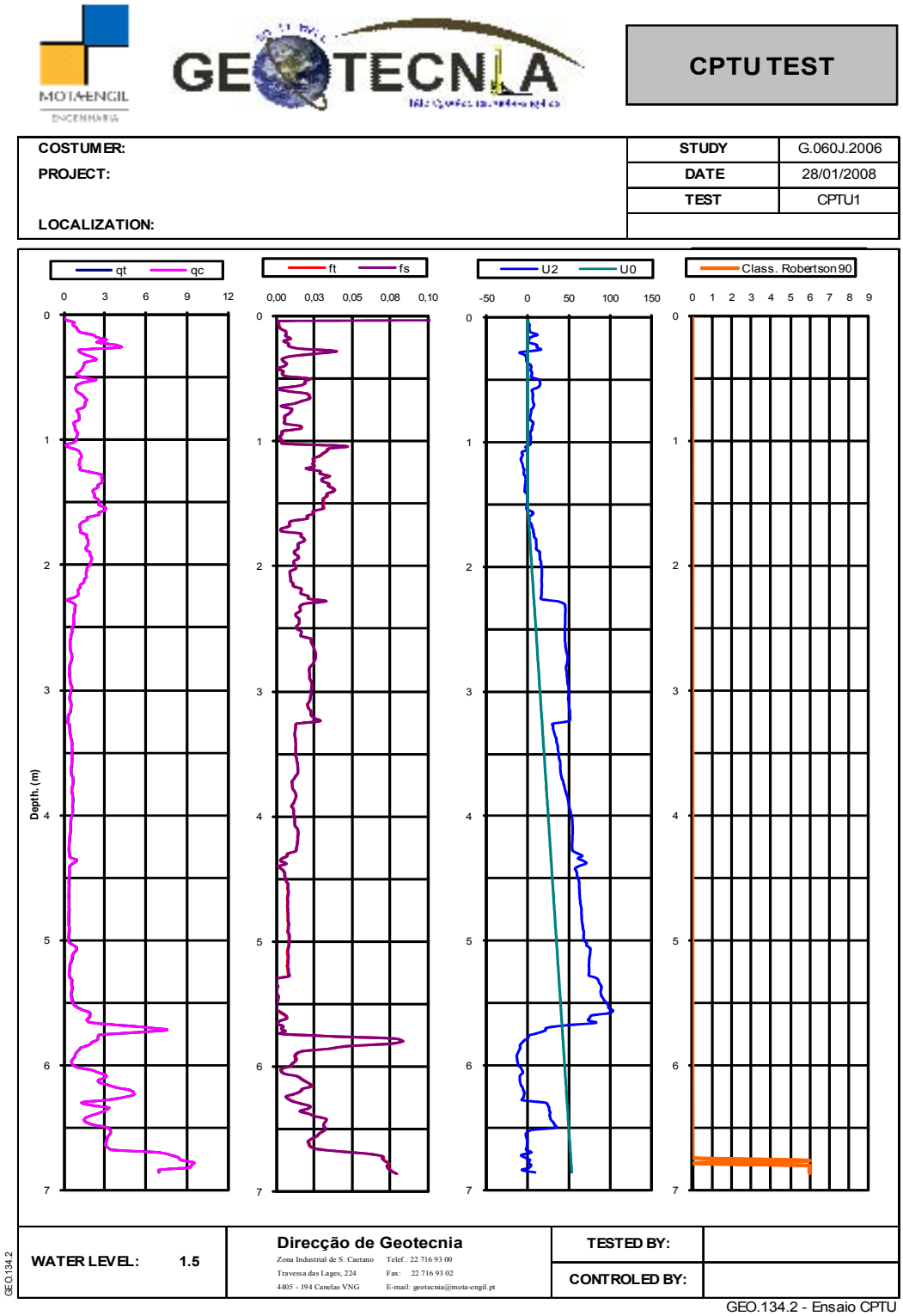


Figure 4.5 - Typical SCPTu data presentation (courtesy of Mota-Engil).

Besides those interpreted parameters, results of CPT/CPTu can also be directly applied to bearing capacity and settlements analysis of shallow and deep foundations, quality control of ground improvement and liquefaction potential analysis. More detailed information on the subject can be found in "*Cone Penetration Test in Geotechnical Practice*" (Lunne, Robertson & Powell, 1997).

CPTu test offers obvious advantages over other routine forms of in-situ testing, such as low cost, rapid procedures, continuous recording, high accuracy, repeatability and possibility of automatic data logging. Moreover, the possibility of assembling additional sensors to test equipment, allowed the introduction of several devices such as pH, temperature systems (envirocone) cameras (vision cones), and seismic modules (SCPTu) making it a mix of experience and modernity.

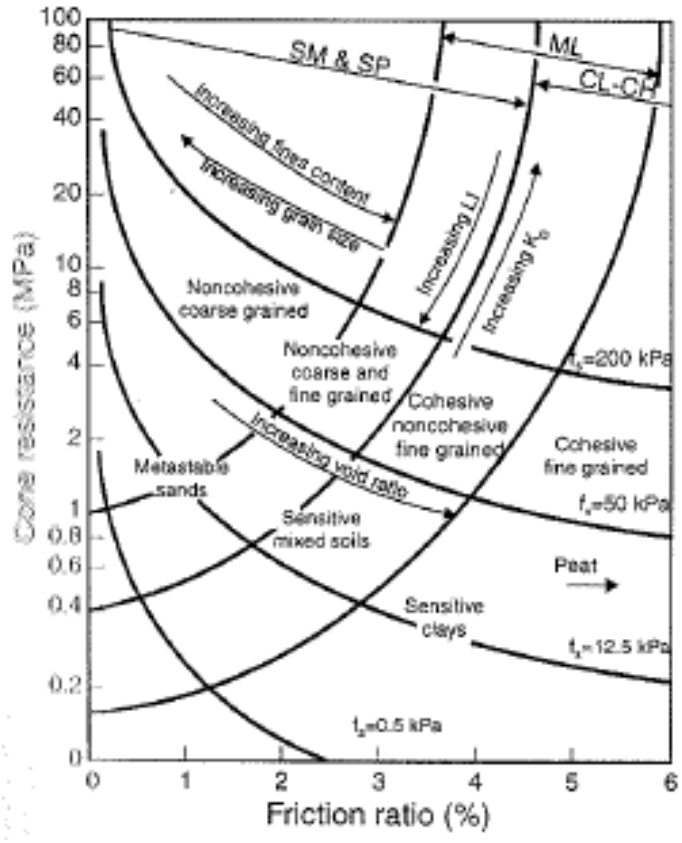
Naturally, some disadvantages can be pointed out to the test, being the most important related to the impossibility of sampling (although it gives stratigraphy information), the difficulty to penetrate very dense soils (or containing cobbles or boulders) and the possibility of drifting from vertical at depths higher than 15m (modern equipments include inclinometers for verticality monitoring). Comparing it with SPT it is correct to say that almost all the referred problems were solved with SCPTu tests. In fact the equipment includes modern measuring devices, the strength parameters are not deduced from a number of blows, provides continuous information, pore-pressure determinations, adequate sensitivity to soft/loose soils determinations and ability to discern tip from side friction resistance (so giving back at least two different measurements). Furthermore, the test is quite protected from human errors and it is easy to incorporate in general geological and geotechnical campaigns.

4.3.1.1. Classification and Stratigraphy

There are four different forms to describe soil stratigraphy: direct visual interpretation of CPT/CPTu parameters, diagrams based on CPT/CPTu parameters, application of a numerical equation and probabilistic approach. The mostly used is the second one, while the third gives the possibility of using a numerical value in identification which can be introduced in geotechnical parameters reduction formulae, in a similar manner of I_D (DMT), as described in next chapter. The first and the last just show a lower level of efficiency and so they are not going to be discussed here.

The first attempt to establish classification using a diagram was settled for the mechanical cone with friction sleeve by Begemann (1965), and that methodology was

followed by the international community when electrical cones and pore pressure measurements were introduced in the test equipment. Douglas and Olsen (1981), after an exhaustive study on this theme, confirmed an existing tendency to high cone tip resistances and low lateral friction developed in sandy soils, while the opposite could be drawn in fine grained soils (Figure 4.6).



1 - increases fine content

2 - increases size.

3 - increases liquid limit.

4 - increases K_0.

5 - increases void index

6 - mud formations

Figure 4.6 - CPTu Classification (Douglas & Olsen, 1981)

Robertson et al. (1986) complemented and improved this diagram by introducing pore-pressure influence in cone tip resistance, which gave rise to a corrected tip resistance (q_t), normalized lateral friction ratio (F_r) and pore-pressure ratio (B_q), defined as follows:

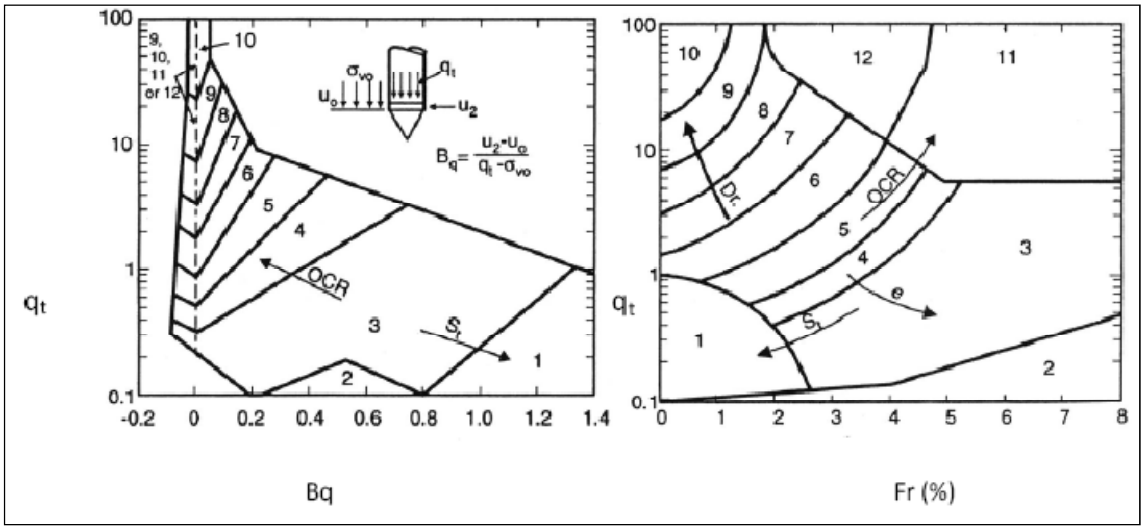
$$q_t = q_c\,(1-a) \tag{4.1}$$

$$B_q = (u_2 - u_0) / (q_t - \sigma_{v0}) \tag{4.2}$$

$$Fr = f_s / (q_t - \sigma_{v0}) \tag{4.3}$$

where u_2 and u_0 are respectively the pore pressure at tip level and in-situ pore pressure, σ_{v0} the in-situ vertical stress, q_c the net cone resistance and f_s the side friction.

The proposed classification is presented in Figure 4.7.



1 – Fine grained sensitive soils	7 - Silty sand to sandy silt
2 - Organic material	8 - Sand to silty sand
3 - Clay	9 - Sand
4 - Silty clay to silt	10 - Sand with pebble to sand
5 - Clayey silt to silty clay	11 – Fine grained hard soils *
6 - Sandy silt to clayey silt	12 - Sand to hard clayey sand*

*overconsolidated or cemented soils

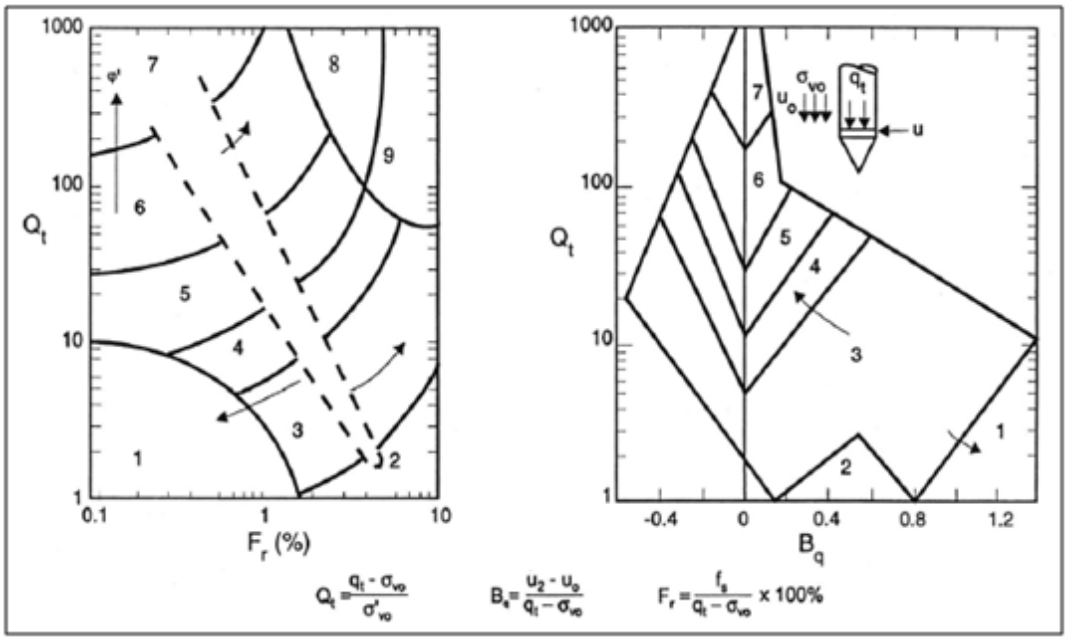
Figure 4.7 - CPTu Classification (Robertson et al. 1986)

In the late 80's, Robertson (1990) proposed a substitution of corrected cone resistance q_t, by the normalized cone resistance (Q_T) defined by equation below, changing the earlier diagram for the one presented in Figure 4.8:

$$Q_T = (q_t - \sigma_{v0}) / \sigma'_{v0} \quad (4.4)$$

Jefferies and Davies (1993) introduced a numerical Classification Index (I_c), combining the three normalized parameters (Q_t, F_r and B_q) into the following equation:

$$I_c = \{(3 - \log[Q_T (1-B_q)]^2 + (1.5+1.3*\log F_r)^2\}^{0.5} \quad (4.5)$$



1 – Fine grained Sensitive soils
2 - Organic soil
3 – Clay to silty clay
4 – Clayey silt to silty clay
5 – Silty sand to sandy silt
6 – Clean sand to silty sand
7 – Sand with pebble to sand
8 – Sand to very hard clayey sand
9 – Very hard fine grained soil

Figure 4.8 - CPTu Classification (Robertson et al. 1986)

Since this and Robertson's equations used the same input parameters, it is possible to relate one another, as shown in Table 4.6 (Saraiva Cruz, 2008).

Table 4.6 - Correlation between graphical and numerical methods (Saraiva Cruz, 2008).

Soil Classification	Zone (Robertson, 1990)	Ic ranges
Organic clayey soils	2	Ic > 3,22
Clays	3	2,82 < Ic < 3,22
Silty mixtures	4	2,54 < Ic < 2,82
Sandy mixtures	5	1,90 < Ic < 2,54
Sand	6	1,25< Ic < 1,90
Coarse sands	7	Ic < 1,25

4.3.1.2. Unit weight

Evaluation of unit weight is a very important issue for calculation purposes, although it can be roughly estimated with no important deviations. Deduction of this parameter from SCPTu test results can be obtained departing from classification diagrams (Robertson et al, 1986; Robertson, 1990), lateral friction and particles unit weight (γ_s) or from shear wave velocities (v_s).

Specific approaches were introduced by Robertson et al. (1986), when an estimation of the parameter was related to each of the defined zones of the soil type diagram presented in Table 4.7, later repeated with Robertson's (1990) classification. Mayne (2007) presented another approach for unit weight evaluation, based in lateral friction (f_s) and solids unit weight (γ_s), as presented in Figure 4.9. Finally, when shear wave velocity is available (SCPTu tests), a third approach becomes possible, as function of both v_s and depth, proposed by Mayne (2007).

Table 4.7 - Unit weight by Robertson, 1986

Zone	Approx. unit weight	Soil type
1	17.5 kN/m^3	Well graded sensitive soil
2	17.5 kN/m^3	Organic soil
3	17.5 kN/m^3	Clay
4	18 kN/m^3	Clayey silt to clay
5	18 kN/m^3	Silty clay to clayey silty
6	18 kN/m^3	Silty sand to silty clay
7	18.5 kN/m^3	Sand silty to silty sand
8	19 kN/m^3	Sand to sandy silty
9	19.5 kN/m^3	Sand
10	20 kN/m^3	Coarse sand to sand
11	20.5 kN/m^3	Fine grained hard soil *
12	19 kN/m^3	Sand to sandy clay *

* Over-consolidated or cemented

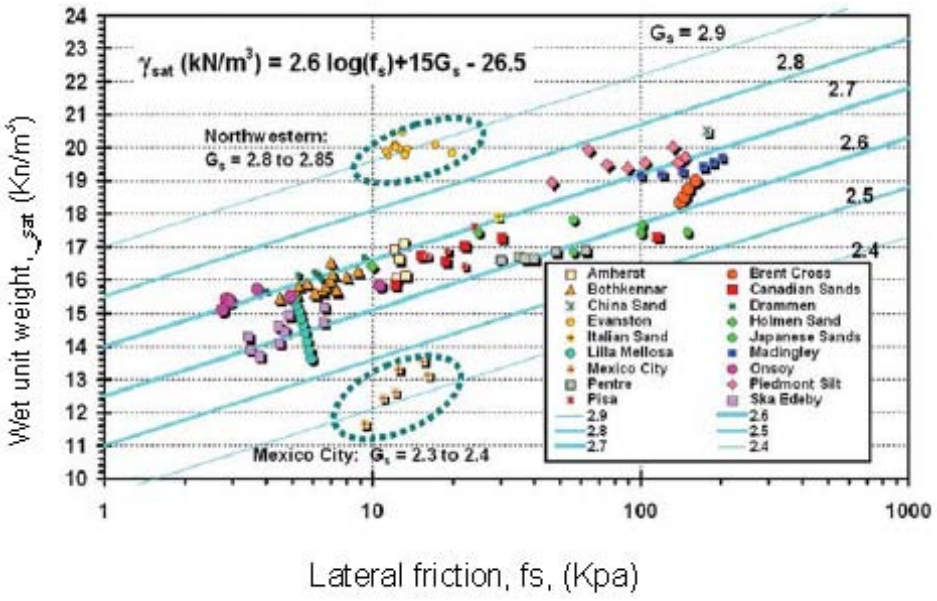


Figure 4.9 - Unit weight based in side friction (Mayne, 2007)

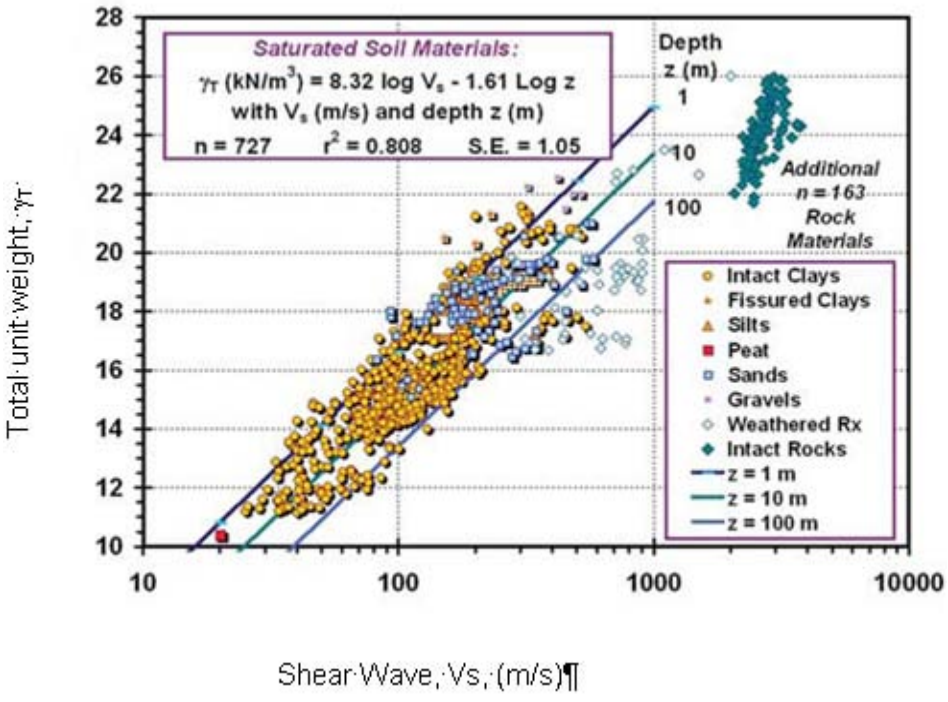


Figure 4.10 - Unit weight evaluation based in v_s and depth (Mayne, 2007)

Saraiva Cruz (2002, 2008) using the iterative process described below, proposed another interesting methodology, after adapting the unit weights proposed by Robertson (1986) to the Robertson's (1990) classification by joining together the groups 3 and 4, 6 and 7, 8 and 9 (Table 4.8):

a) Use of q_t, f_t, u_2 and water table position to determine Q_T and F_r; vertical stresses needed for their determination are provided by considering an initial estimated unit weight;
b) Soil classification using Robertson (1990) chart and determination of respective unit weight, based in Table 4.8.
c) Compare this unit weight with the initially estimated, correcting it by iterations until the differences are minimal.

Table 4.8 - Unit weight (Saraiva Cruz, 2008)

Zone	Approx. unit weight	Soil type
1	17.5 kN/m^3	Well graded sensitive soil
2	12.5 kN/m^3	Organic soil
3	17.5 to 18 kN/m^3	Clay to Clayey Silty
4	18 kN/m^3	Silty Clay to Clayey Silty
5	18 to 18.5 kN/m^3	Sand Silty to Silty Sand
6	19 to 19.5 kN/m^3	Sand to Sand Silty
7	20 kN/m^3	Sand to Thick Sand
8	19 kN/m^3	Hard Sand to Sand Clay
9	20.5 kN/m^3	Thin size Hard soil

4.3.1.3. Shear Strength

Evaluation of shear strength of soils through CPTu is based on the assumed drained or undrained conditions during the execution of the test. Thus, in sands where the conditions are assumed to be drained, the respective strength geotechnical parameter is the effective angle of shearing resistance (ϕ'), while for clays (undrained conditions) undrained shear strength, S_u, will be the reference parameter.

Undrained shear strength (S_u)

Undrained shear strength can be derived from cone penetration tests using both theoretical and empirical approaches. Theoretical solutions can be based in classical bearing capacity theories, cavity expansion, conservation of energy (Baligh, 1975), stress-strain curves (Ladanyi, 1963) and strain path (Baligh, 1985). However, since cone penetration is a complex phenomenon, all the theoretical solutions incorporate

several simplifying assumptions regarding soil behaviour, failure mechanism and boundary conditions. Hence, empirical correlations are generally preferred, although theoretical solutions have provided a useful framework for basic understanding (Lunne et al., 1997).

Empirical correlations for undrained shear strength are generally based in estimations through total cone resistance, net cone resistance or excess pore pressure. The value of undrained shear strength (S_u) may be calculated from tip resistance, net or corrected (q_t), reduced from total horizontal stress (σ_{h0}) and divided by a cone factor (N_k or N_{kt}), as follows:

$$S_u = [q_c - \sigma_{h0}] / N_k \quad (4.6)$$

$$S_u = [q_t - \sigma_{h0}] / N_{kt} \quad (4.7)$$

Senneset et al. (1982) and Campanella et al. (1982) suggested the use of effective cone resistance by introducing the pore water pressure measured during test (u_2) and a new cone factor (N_{ke}), expressed as follows:

$$S_u = [q_t - u_2] / N_{ke} \quad (4.8)$$

The third one is based on the difference between measured pore pressure (u_2) and hydrostatic pressure (u_0) divided by a cone factor $N_{\Delta u}$ (Vesic, 1972; Randolph & Wroth, 1979; Battaglio et al., 1981; Massarch & Broms, 1981; Campanella et al., 1985):

$$S_u = (u_2 – u_0) / N_{\Delta u} \quad (4.9)$$

The cone factors are the main problem to solve these equations, and usually extra tests are needed (FVT or DMT) to a proper calibration. In Tables 4.9 to 4.12 a summary of the international references related to cone factor ranges is presented.

Table 4.9 - Cone Factor N_k typical values

Factor Nk	Author
17 (triaxial testing)	Kjekstad et al. (1978)
(non fissured and overconsolidated clay)	
11-19 (FVT)	Lunne and Kleven (1981)
(normally consolidated clay)	

Table 4.10 - Cone Factor N_{kt} typical values

Factor N_{kt}	Author
8-16 (triaxial and direct shear tests) (plasticity index 3%<Ip<50%,	Aas et al. (1986)
11-18 (no evidence of relation with Ip)	La Rochelle et al. (1988)
8-29 (triaxial testing) (evidence of strong relation with OCR)	Rad and Lunne (1988)
10-20 (triaxial testing) (Ip dependent)	Powel and Quaterman (1988)
8.5 – 12 (triaxial testing)	Luke (1995)
6-15 (triaxial testing)	Karlsrud et al., (1996)

Table 4.11 - Cone Factor N_{ke} typical values

Factor N_{ke}	Author
9 +/- 3	Senneset et al., (1982)
1 – 13 (apparently related to B_q)	Lunne et al., (1985)
Graphic method (function of B_q)	Karlsrud et al., (1996)

Table 4.12 - Cone Factor $N_{\Delta u}$ typical values

Factor $N_{\Delta U}$	Author
4-10 (triaxial testing) (good relation with B_q)	Lunne et al., (1985)
7-9 (FVT)	La Rochelle et al., (1986)
6-8 (triaxial testing) (normally consolidated clay, with B_q >0,3)	Karlsrud et al., (1996)

Since the determination of undrained shear strength (S_u) by empirical approaches can be achieved through several solutions, it is important to define a process that allows the use of all correlations in a coherent mode, although the best approach is to define local specific correlations. Lunne et al. (1997) suggests that in geological formations where test results are not available, the approach based on q_t, with N_{kt} values between 15 and 20 should be used. On the other hand, in hard and fissured clays the same correction factor could reach values near 30. In soft to very soft formations, where some uncertainty associated to tip resistance ranges can exists (very low values), the approach based in excess pore pressure should be used, taking $7<N_{\Delta U}<10$.

Effective angle of shearing resistance

The shear strength of non cemented sandy soils is usually expressed by effective angle of shearing resistance, which can be deduced from CPTu following three methodologies:

a) Empirical and semi-empirical correlations, based on calibration chamber tests;
b) Bearing capacity theories;
c) Cavity expansion theories.

The first category can be based on a relative density (Dr) approach or in direct correlations with q_c and σ'_{v0}. The latter is commonly adopted, being obtained by comparisons of effective angle of shearing resistance and cone resistances measured in calibration chamber tests (Robertson & Campanella, 1983; Lunne & Cristophersen, 1983), and gave rise to the well-known diagram from Robertson & Campanella (1983), presented in Figure 4.11 that can be represented by the following equation:

$$\phi' = \arctan [0.1+0.38\log (q_c / \sigma'_{v0}) \quad (4.10)$$

where ϕ' stands for the angle of shearing resistance, q_c is the tip resistance and σ'_{v0} is initial effective vertical stress.

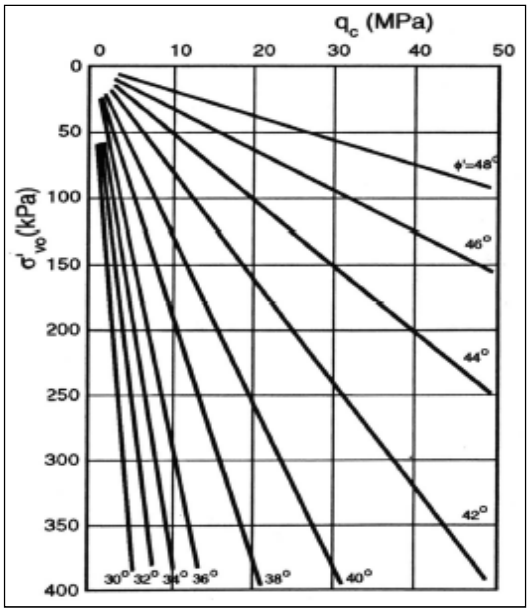


Figure 4.11 - Angle of shearing resistance based on q_c/σ'_{V0} (Robertson & Campanella, 1983).

The two main bearing capacity theories are related to the shape of failure zone (Janbu & Senneset, 1974) and to the effect of horizontal stresses and cone roughness (Durgunoglu & Mitchell, 1975). The latter presents lower complexity and thus has been preferred to the angle of shearing resistance deduced using the diagram presented in Figure 4.12 (Marchetti, 1988).

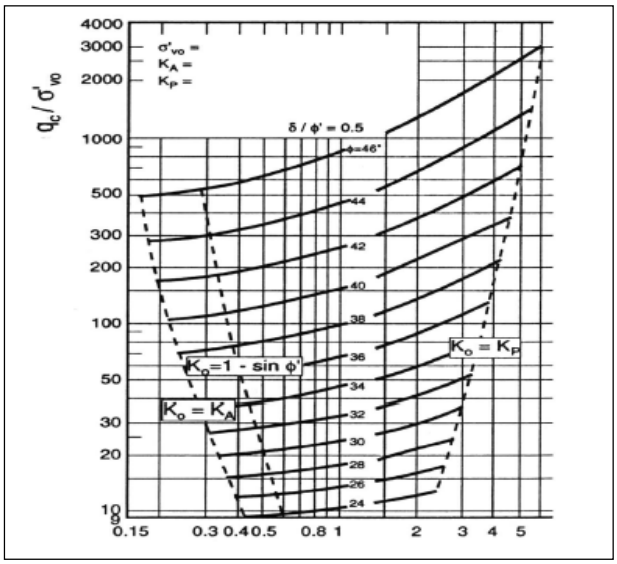


Figure 4.12 - Angle of shearing resistance based on qc/σ'_{V0} (Marchetti, 1988).

Kulhawy and Mayne (1990), reviewing representative calibration chamber data, suggested the following correlation:

$$\phi' = 17.6 + 11\log q_{t1} \quad (4.11)$$

$$q_{t1} = [(q_t/p_a) / \sigma'_{v0}/pa]^{0.5} \quad (4.12)$$

The third category (Vesic, 1972) is too complex to apply in day-to-day practice, requiring some very difficult to estimate parameters, such as volumetric changes and stresses in the plastic zone, thus rarely used.

4.3.1.4. Stiffness

Soil stiffness can be reduced with different accuracy by two different ways, depending on the type of test used: CPT/CPTu or SCPTu.

Regarding CPT/CPTu, no strain measurements are obtained, and thus it is only possible to access moduli through empirical correlations, which should be applied with caution, since they are strongly dependent on local conditions. The main correlations based in CPT/CPTu data relate tip resistance [qc or qt] with constrained modulus, M_0, or maximum shear modulus, G_0, with the basic equations being settled for different drainage behaviours, as presented below.

Lunne & Christophersen (1983), based on calibration chamber tests related to uncemented predominantly siliceous clean sands (drained behaviour), proposed the following correlation for deriving constrained modulus:

$$M_0 = 4 \times q_c \quad \text{if } q_c < 10 \text{ MPa} \quad (4.13)$$

$$M_0 = (2 \times q_c) + 20 \quad \text{if } 10 < q_c < 50 \text{ MPa} \quad (4.14)$$

$$M_0 = 120\text{MPa} \quad \text{if } q_c > 50 \text{ MPa} \quad (4.15)$$

For mixed soils (partially drained behaviour), Senneset et al. (1988) proposed the following correlation:

$$M_0 = (2 \times q_t) \quad \text{if } q_t < 2.5 \text{ MPa} \quad (4.16)$$

$$M_0 = (4 \times q_t) - 5 \quad \text{if } 2.5 < q_t < 5 \text{ MPa} \quad (4.17)$$

Mitchell & Gardner (1975) and Kullhawy (1990) presented correlations to derive M parameter in clayey to silt-clayey soils (undrained behaviour):

$$M_0 = \alpha_n \times q_c \quad (4.18)$$

α_n is dependent on tip resistance soil type and plasticity, can vary from 1 to 8.

$$M_0 = 8.25 \times (q_c - \sigma_{v0}) \quad (4.19)$$

In these equations, M_0 represents the initial constrained modulus, q_c is the tip resistance, q_t is the corrected tip resistance and σ_{v0} is the vertical total stress.

An attempt to derive maximum shear modulus (G_0) directly from CPTu was first presented by Mayne and Rix (1993) as function of normalized tip resistance (q_t) and initial void ratio (e_0), followed by Sabatani et al. (2002) who correlated the parameter with tip resistance (q_c) and vertical effective stress (σ'_{v0}). The respective equations are:

$$G_0 = 99.5\ p_a^{0.305}\ q_t^{0.695} / (e_0)^{1.130} \quad (4.20)$$

$$G_0 = 1.634\ q_c^{0.25}\ (\sigma'_{v0})^{0.375} \quad (4.21)$$

The extra seismic module recently added to the original CPT/CPTu has given an important improvement in stiffness evaluation, due to its direct dependency on seismic wave velocities. The seismic module is simply a receptor of compression (P) and shear (S) waves (Figure 4.13) generated at ground surface, at certain depth intervals (usually around 1,0m). In Figure 4.14 a general lay-out for seismic measurement is illustrated, while in Figure 4.15, the apparatus for generation of respectively P and S waves is presented

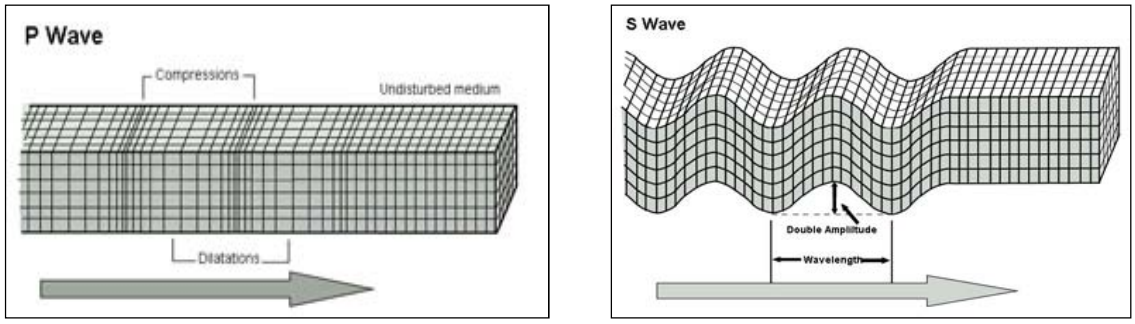
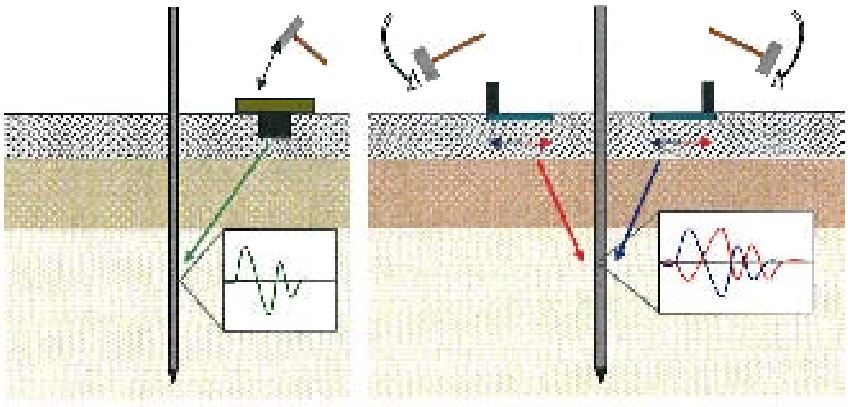


Figure 4.13 - P and S wave propagation

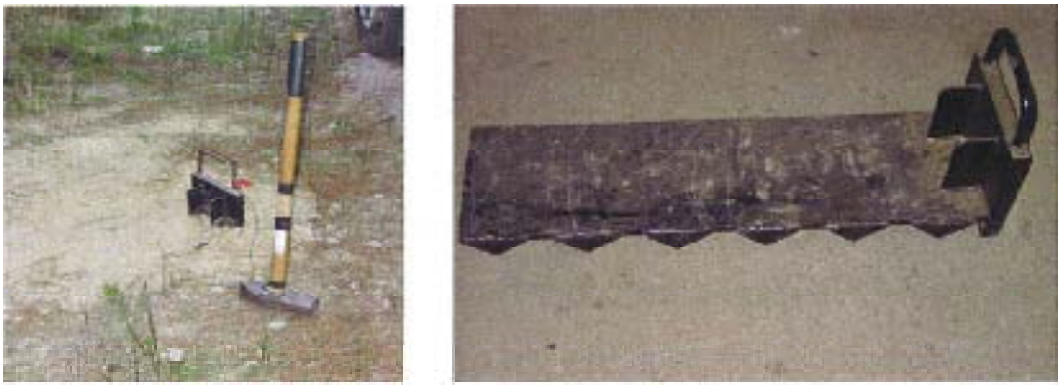


a) b)

Figure 4.14 - Wave generation: a) P waves; b) S waves (after Saraiva Cruz, 2008)



a)



b)

Figure 4.15 - Wave generation apparatus: a) P waves; b) S waves

In a considered isotropic elastic medium, compression (v_p) and shear waves (v_s) velocity can be related to deformability moduli by the following expressions:

$$v_p = [(K+1.25G)/\rho\ ]^{0.5} \quad (4.22)$$

$$v_s = (G/\rho)^{0.5} \text{ or } G_0 = \rho\ v_s^2 \quad (4.23)$$

$$K = E/(3-6\nu) \text{ and } G = E/(2+2\nu) \quad (4.24)$$

where v_p and v_s are respectively compression and shear wave velocities, G is the distortional modulus, E the elastic modulus, K the bulk modulus, ν the Poisson coefficient and ρ represents the mass density of surrounding ground.

One of the main advantages of these methods is that the tested soil remains at its in-situ stress and saturation level, thus practically undisturbed, even if boreholes are used for equipment installation. Even more, measured dynamic stiffness using geophysics is close to operational static values required for the calculation of displacement for a large range of civil engineering structures (Matthews, 1993; Clayton and Heymann, 2001; Fahey, 2001a). However, the accuracy of measurement is strongly dependent on time arrival interpretation, which requires time and knowledge of skilled geophysists to properly assess geotechnical data. Obviously, this has created some misleading around wave velocities and respective stiffness values.

To conclude, seismic methods have introduced a powerful tool that may provide the most reliable means of stiffness measurement in geomaterials that are difficult or impossible to sample, with the maximum shear modulus, G_0, assumed as being a benchmark for stiffness measurements using other methods (Simmons et al., 2002)

Chapter 5.
Marchetti Dilatometer Test

5. MARCHETTI DILATOMETER TEST

5.1. Introduction

Marchetti dilatometer test or flat dilatometer, commonly designated by DMT, has been increasingly used and it is one of the most versatile tools for soil characterization, namely loose to medium compacted granular soils and soft to medium clays, or even stiffer if a good reaction system is provided. The main reasons for its usefulness deriving geotechnical parameters are related to the simplicity (no need of skilled operators) and the speed of execution (testing a 10 m deep profile takes around 1 hour to complete) generating continuous data profiles of high accuracy and reproducibility. The test equipment exhibits high accuracy, and yet is very friendly and easy to use, robust to face the work in the field, and very easy to repair (even in the field) for most of common problems.

The DMT test was developed by Silvano Marchetti (1980) and can be seen as a combination of both CPT and PMT tests with some details that really makes it a very interesting test available for modern geotechnical characterization. In its essence, dilatometer is a stainless steel flat blade (14 mm thick, 95 mm wide and 220 mm length) with a flexible steel membrane (60 mm in diameter) on one of its faces. The blade is connected to a control unit on the ground surface by a pneumatic-electrical cable that goes inside the position rods, ensuring electric continuity and the transmission of the gas pressure required to expand the membrane. The gas is supplied by a connected tank/bottle and flows through the pneumatic cable to the control unit equipped with a pressure regulator, pressure gages, an audio-visual signal and vent valves. The equipment is pushed (or driven) into the ground, by means of a CPTu rig or similar, and the expansion test is performed every 20cm. The pressures required for lift-off the diaphragm, to deflect 1.1mm the centre of the membrane and at which the diaphragm returns to its initial position (closing pressure) are recorded. The general lay-out of the test and basic output are shown in Figures 5.1 to 5.3.

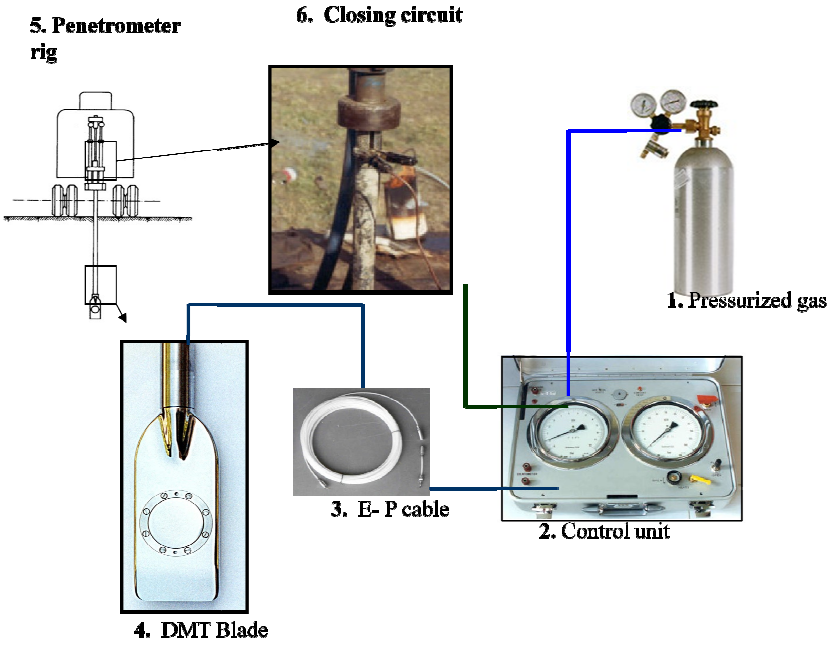


Figure 5.1 - DMT test lay-out

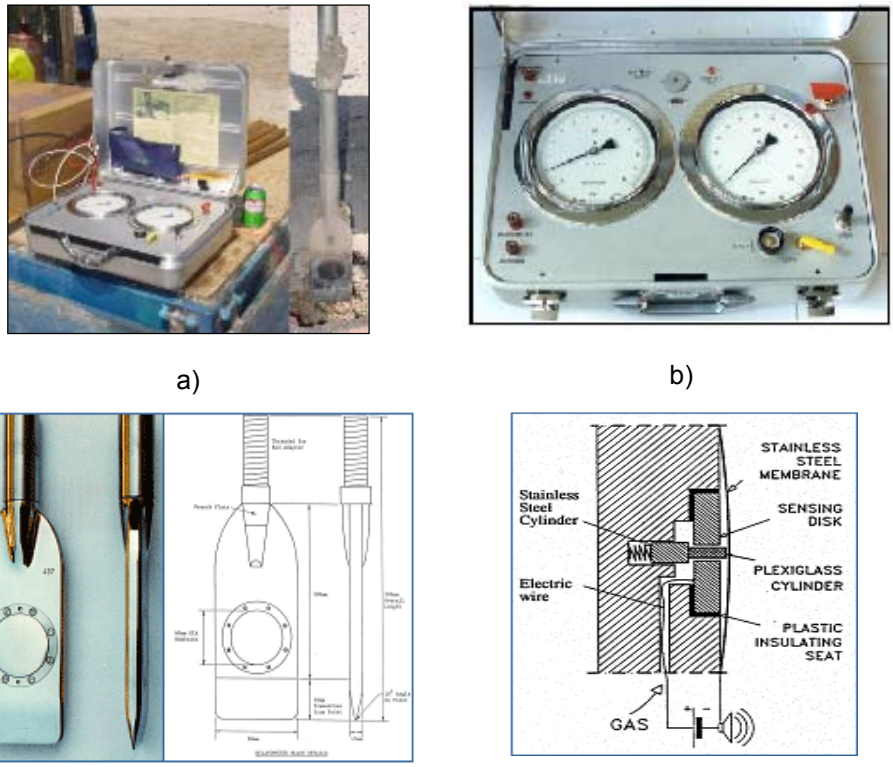


Figure 5.2 - a) DMT test equipment; b) acquisition unit; c) blade details.

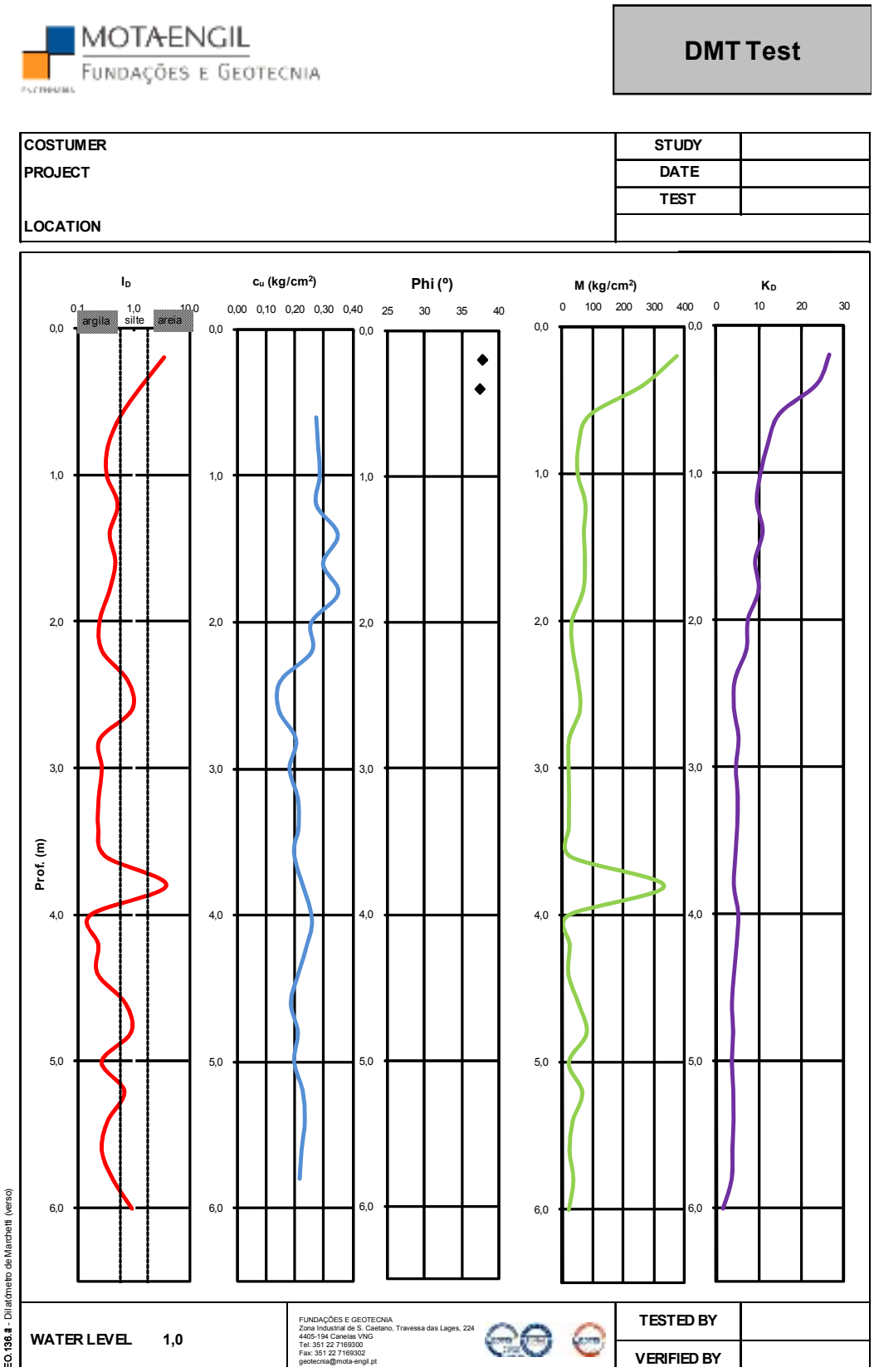


Figure 5.3 - DMT presentation data sheet (Courtesy of MOTA-ENGIL)

The field of application of DMT is very wide, ranging from extremely soft soils to hard soils or even soft rock, depending mainly in the thrust capacity of drill rig or penetrometer trucks (the latter being incomparable more efficient). The test is found suitable for sands, silts and clays where the grains are smaller (typically 1/10 to 1/5) compared to the membrane (Marchetti, 1997). Due to the balance of zero pressure measurement method (null method), DMT readings are highly accurate even in extremely soft soils, and at the same time the blade is robust enough to penetrate soft rock or gravel (in the latter, pressure readings are not possible), supporting safely 250kN of pushing force. Clayey soils can be tested from c_u = 2 to 4 kPa up to 1000 kPa (marls) and the constrained modulus typically is within 0.4 and 400 MPa. Although static push is preferable, DMT can also be dynamically driven, for instance by SPT hammers and rods. In addition, the blade was designed to introduce the minimum possible disturbance, being less invasive than CPT cones.

The test results are quasi-continuous and cover a wide range of properties of the soils, such as soil stratigraphy and classification, unit weight, stress state and stress history, strength, stiffness and flow characteristics, all supported by comprehensive approaches and much less dependent on local correlations. The original correlations (Marchetti, 1980) were obtained by calibrating DMT results in several test sites with soil parameters determined in high quality laboratory testing samples. This test is under the scope of the present research and thus a detailed discussion of its use in sedimentary soils will be presented in this chapter, while the application on residual soils will be presented in *Part B – The Residual Ground*.

5.2. Basic Pressures

As referred previously, the test starts by pushing (or driving) the dilatometer into the ground, with typical penetration rates similar to CPT's (2cm/s). At every 20 cm, the membrane is inflated and two basic measurements are taken (Figure 5.4):

a) A-pressure, required to begin to move the membrane against the soil ("lift off" pressure)
b) B-pressure, required to move the centre of the membrane 1.1 mm against the soil

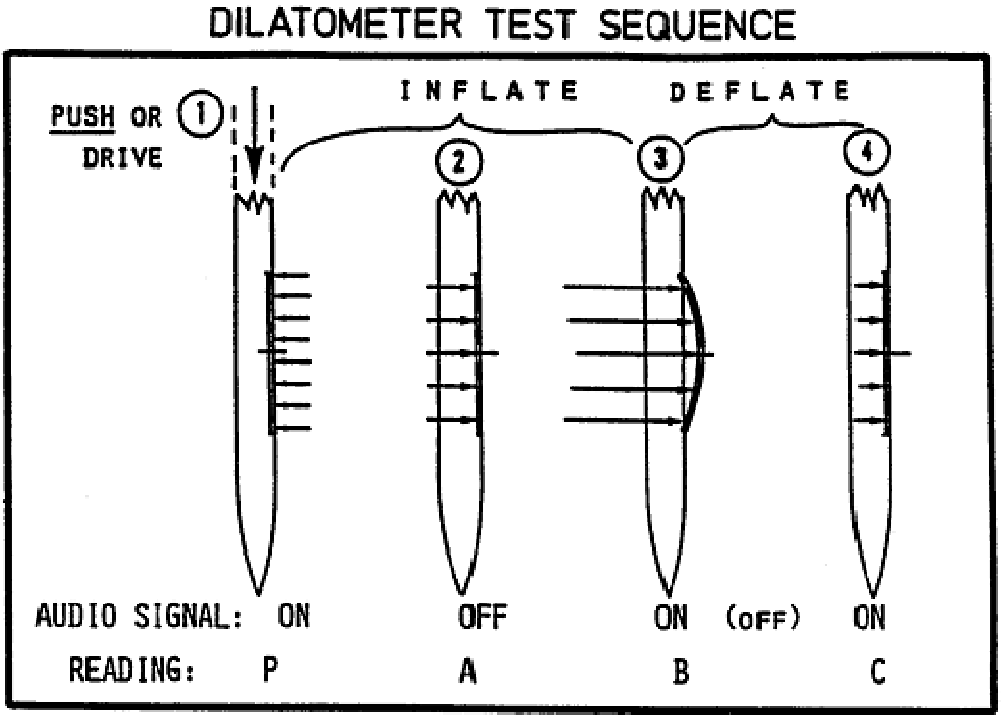


Figure 5.4 - A, B, C measurements (after Marchetti, 1997).

Following this expansion sequence an additional pressure, designated by “C-reading” (closing pressure), may be taken by slowly deflating the membrane soon after B position is reached until the membrane comes back to 0.05 mm position (A position).

These pressures must then be corrected by the values ΔA and ΔB, determined by calibration, to take into account membrane stiffness and thus converted in the three basic pressures P_0, P_1 and P_2, which are determined as follows:

$$P_0 = 1.05\ (A-Z_m-\Delta A) - 0.05\ (B- Z_m -\Delta B) \quad (5.1)$$

$$P_1 = B - Z_m - \Delta B \quad (5.2)$$

$$P_2 = C - Z_m - \Delta A \quad (5.3)$$

where Z_m is the pressure gage reading when vented to atmospheric pressure (Z_m should be taken equal to zero in all formulae, when calibration values and basic pressures are measured in the same gage, even if it is different from zero), ΔA is the gage pressure inside the membrane required to overcome the stiffness of the membrane and move it outward to a centre expansion of 0.05mm to the air and ΔB is the gage pressure required to overcome the stiffness of the membrane and move it outward to a centre expansion of 1.10mm to the air.

Four intermediate parameters, material Index (I_D), dilatometer modulus (E_D), horizontal stress index (K_D) and pore pressure index (U_D), are deduced from the basic pressures P_0, P_1 and P_2, having some recognizable physical meaning and some engineering usefulness (Marchetti, 1980), as it will be discussed along this chapter. The deduction of current geotechnical soil parameters is obtained from these intermediate parameters (and not directly to the basic P_0, P_1 and P_2), independently or combined together, covering a wide range of possibilities.

The first campaign of DMT tests in Portugal was performed 15 years ago, in the context of a MSc research work on DMT applications (Cruz, 1995) and it was the beginning of an extensive research program in sedimentary soils, which actually includes fifty experimental sites located in Portuguese territory, and some local spots in Spain (Cruz et al., 2006a). The aim of the research was to check the adequacy of DMT tests with regards to the accepted correlations established for parametrical derivation, and to contribute as base reference in data interpretation in residual soils (Cruz, 1995; Viana da Fonseca, 1996; Cruz et al, 1997). The sedimentary experimental sites included in this framework covered a wide range of soils, from clays to sands, organic to non-organic, stable to sensitive. Overall, more than 200 tests were performed (plus identification and physical index tests) including 57 DMT, 50 FVT, 40 CPTU, 6 SCPTU, 4 PMT, 3 cross-hole seismic, 9 triaxial and 37 oedometer tests.

Relying on this data base, the interpretation and application of intermediate DMT parameters deriving geotechnical properties of sedimentary soils will be presented later in this chapter. The adequacy of the test in Portuguese soils, illustrated by these research results, will be discussed in the following sections attempting to establish a reference basis to residual soil applications.

5.3. Material Index, I_D

Marchetti (1980), following the observation that P_0 and P_1 are close to each other in clayey soils and apart in sands, defined Material Index, I_D, as the difference between the two basic pressures, normalized in terms of the effective lift-off pressure, $P_0 – u_0$, (somehow related with horizontal effective stress):

$$I_D = \Delta P / (P_0 - u_0) \quad (5.4)$$

where u_0 is the pre-insertion in-situ pore pressure.

According to Marchetti (1980), the soil type can be deduced as follows:

a) $I_D > 3.30$ – sands;
b) $1.80 < I_D < 3.30$ – silty sands;
c) $1.20 < I_D < 1.80$ – sandy silts;
d) $0.90 < I_D < 1.20$ - silts;
e) $0.60 < I_D < 0.90$ – clayey silts;
f) $0.35 < I_D < 0.60$ – silty clays;
g) $0.10 < I_D < 0.35$ - clays;
h) $I_D < 0.10$ – peat and other sensitive soils.

I_D parameter is one of the most valuable indexes deduced from DMT, due to its ability to identify soils throughout a numerical value that can be easily introduced in specific formulae for deriving geotechnical parameters. This fact offers undoubtfully a lot of extra possibilities to model geomaterials and, at the same time, makes it easier to develop constitutive laws that can be applied to higher ranges of different soils, with particular emphasis in IGM (including silts or residual soils). As referred by Marchetti (1997), I_D is not a result of a sieve analysis but just a mechanical behaviour parameter (a kind of rigidity index) from which soil stratigraphy is deduced, and thus some deviation can occur in heterogeneous formations, when directly compared with classifications based on grain size distributions (a mixed clay and sand horizon can be described as a silt). In a simple form, it could be said that I_D is a "*fine-content-influence meter*", providing the interesting possibility of defining dominant behaviours in mixed soils, usually very difficult to interpret when only grain size is available, thus it may be associate to an index reflecting an engineering behaviour. Moreover, together with pore pressure index (U_D), the parameter allows the control of drainage paths, so very important in the strength (drained, partially drained or undrained) evaluation.

Some numerical analysis have been performed to compare I_D with CPTu classifications, namely F_r (Mayne & Liao, 2004) and I_c (Robertson, 2009), but no consistent results have been published yet. The recent literature review carried out by Robertson (2009) revealed a general tendency that can be represented by the following correlation:

$$I_D = 10^{(1,67 - 0,67Ic)} \quad (5.5)$$

The experience in Portugal (Cruz et al., 2006a) clearly shows that Marchetti (1980) original correlation globally represents the geological environment of the selected experimental sites, confirming international trends. In fact, DMT results show good

agreement with borehole information, laboratory identification tests by means of elementary triangular chart and Unified Classification for engineering purposes (ASTM D2487, 1998), and also with classical CPTu stratigraphy classification charts (Robertson et al., 1986; Robertson, 1990). The global data set obtained in Portugal whose representation in CPTu chart (Robertson, 1990) is presented in Figure 5.5, suggests that DMT can easily be used together with boreholes in general subsurface investigations, with the following advantages:

a) The global analyzed data can be referenced as function of each zone of Robertson (1990) CPTu chart; in that context 19.76% is associated to zone 1, 33.04% to zone 2, 9.97% to zone 4, 7.73% to zone 5, 20.69% to zone 6, 4.01% to zone 7, 1.42% to zone 8 and 3.27% to zone 9;
b) Accurate identification of soil type, which can be easily to correlate with borehole information, thus allowing to create cross sections with at least the same level of confidence obtained from drilling evaluations;
c) High accuracy in defining strata with interbedded thin layers, usually undetected in borehole information (a common advantage of penetration tests or pressuremeters);
d) I_D is a numerical via for classification of soils, similar to Ic in CPT/CPTu tests;
e) Together with identification, DMT capacity to give information about pore water pressure and unit weight creates a rare autonomy in the field characterization, similar to CPTu.

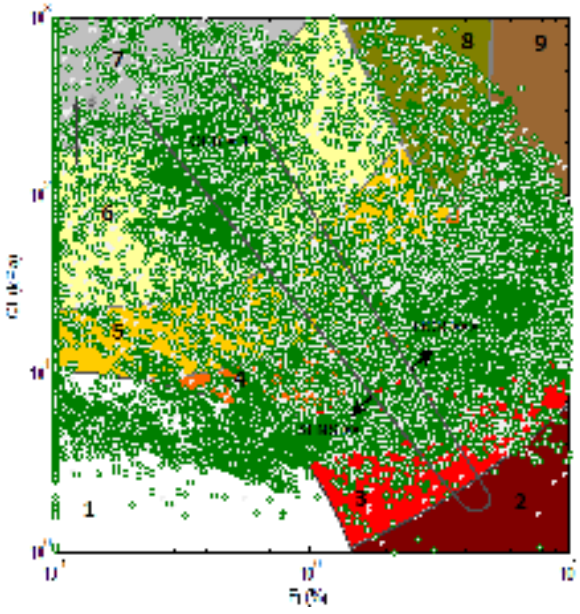


Figure 5.5 - Projection of sedimentary considered data in CPTu classification chart (Robertson, 1990).

5.4. Horizontal stress index, K_D

The horizontal stress index (Marchetti, 1980) was defined to be comparable to the *at rest earth pressure coefficient*, K_0, and thus its determination is obtained by the effective lift-off pressure (P_0) normalized by the in-situ effective vertical stress:

$$K_D = (P_0 - u_0) / \sigma'_{v0} \quad (5.6)$$

where σ'_{v0} represents the pre-insertion in-situ overburden stress and u_0 is the pore pressure at measurement depth.

Departing from the work of Kulhawy & Mayne (1990), Mayne (2001) and Yu (2004), Robertson (2009) proposed a correlation between this parameter and CPTu normalized tip resistance, valid for fine grained sedimentary soils:

$$K_D = 0.3 (Q_{t1})^{0.95} + 1.05, \text{ when } I_c > 2.60 \text{ (or } I_D < 0.85) \quad (5.7)$$

where Q_{t1} is the normalized cone resistance with a stress exponent for stress normalization equal to 1.0 and I_c the CPTu Classification index .

K_D is a very versatile parameter since it provides the basis to assess several soil parameters such as those related with state of stress, stress history and strength, and shows dependency on the following factors:

a) cementation and ageing;
b) relative density in sandy soils;
c) vibrations, in sandy soils;
d) stress cycles;
e) natural overconsolidation resulting from superficial removal.

The parameter can be regarded as a K_0 amplified by penetration effects, with the value of two representing normally consolidated (NC) deposit with no ageing and/or cementation structure (Marchetti, 1980). On the other hand, K_D typical profile is very similar in shape to the OCR profile and thus it gives useful information not only about stress history but also on the presence of cementation structures (Marchetti, 1980; Jamiolkowski, 1988), as illustrated in Figure 5.6. Since undrained shear strength of fine soils can be related and obtained via OCR and the relation between K_0 and angle of shearing resistance is well stated by soil mechanics theory, then the parameter is also used with success in deriving shear strength.

The basic assumptions to the evaluation of strength parameters by in-situ testing are related to the type of soil, using undrained shear strength, S_u, in fine grained soils (assuming that no dissipation of pore pressure occurs during test execution), and angles of shear resistance, ϕ', in granular soils (assuming free drainage). In this context, I_D can be used to control the deviation of a given soil, in relation to the pure behaviour, which is not possible in current in-situ tests such as SPT. In the following sections, geotechnical parameters deduced from this index will be discussed.

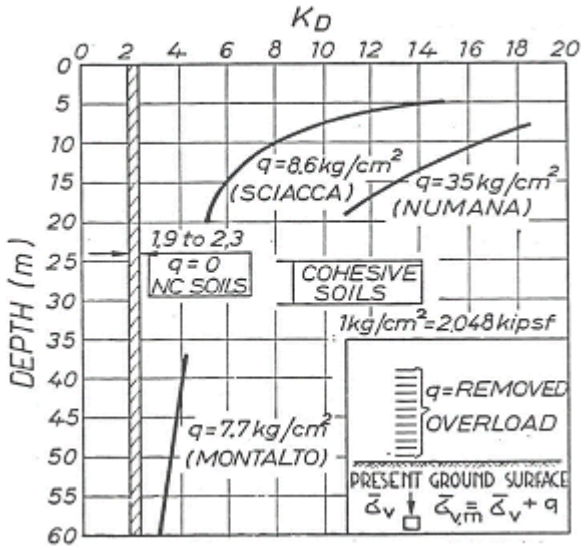


Figure 5.6 - Typical K_D profiles (after Marchetti, 1980).

5.4.1. Fine grained soils

5.4.1.1. State Characteristics

Overconsolidation ratio is commonly defined as the ratio of the maximum past effective stress and the present effective overburden stress, and represents soils where the only stress changes were due to the removal of overburden stress or the fluctuations of water level. In reality, creep is also a factor that has similar consequences in inducing identical overconsolidation patterns with soils gaining elastic reserve. This characterizes the “so called” aged soils, which can be present in fine to coarse materials. Cementation is another extra factor associated to a quality of mechanical behaviour typical of an overconsolidated pattern of behaviour. For cemented or aged soils OCR may reflect the ratio between yield and the present effective overburden stresses, with the former depending in direction and type of loading (Lunne et al., 1997).

State of stress installed in soil massifs can be considered as due to solely gravitic forces and so effective vertical stress (σ'_v) is determined simply through:

$$\sigma'_{v0} = \gamma * z \quad (5.8)$$

where γ represents the bulk unit weight and z the depth of analysis.

On the other hand, being horizontal stresses very difficult to be directly measured, which is decisive for the evaluation of the ratio of at rest horizontal and vertical effective stresses, commonly designated by at rest earth pressure coefficient:

$$K_0 = \sigma'_{h0} / \sigma'_{v0} \quad (5.9)$$

where σ'_{h0} and σ'_{v0} are the horizontal and vertical initial stresses, respectively.

The great challenge in geotechnical site investigation at this level is that faithful registration in fine grained soils, $K_{0,}$ is mainly dependent on the past loading history of the deposit (OCR). For sedimentary normally consolidated (NC) soils, K_0 is most likely lower than 1. Regarding overconsolidated (OC) soils, the changes in vertical effective stresses with load removal or water level variations follow a linear decrease, with horizontal effective stresses remaining relatively stable resulting in an increase of K_0 value. The determination of the parameter is quite complex, mainly due to device installation or just stress-relief destructuring (in-situ testing) and sampling disturbance (for laboratory testing) and only a few reliable methods are available. Based on the confrontation with laboratorial test results in clayey soils, Marchetti (1980) presented the following correlations to deduce K_0 and OCR, which are still mostly used nowadays. Both correlations are only valid for non-cemented soft to medium hard soils not affected by ageing or tixotropic hardening, being overconsolidation strictly due to superficial removal (Marchetti, 1980) and limited to soils presenting I_D values under 1.2 (Jamiolkowski et al., 1988):

$$K_0 = (K_D / 1.5)^{0.47} - 0.6 \quad (\text{for } K_0 > 0.3) \quad (5.10)$$

$$OCR = (0.5\ K_D)^{1.56} \quad (5.11)$$

These relationships have been confirmed as adequate by several researchers (Mayne & Martin, 1988; Mayne & Bachus, 1989; Smith & Houlsby, 1995; Mayne, 2001) and it is the mostly adopted in present days.

Powell and Uglow (1988) suggested the application of different methodologies according to the age of the deposits. For young clays (less than 60 000 years), the following equations were proposed:

$$K_0 = 0.34\ K_D^{0.55}, \quad (5.12)$$

$$OCR = 0.24\ K_D^{1.32}, \quad (5.13)$$

For old clays (over 60 000 years), the authors suggested the determination of two or three values, from which a parallel line (to young clays line) could be drawn, valid for both parameters.

Lacasse et al. (1990) suggested a similar approach, this time based on undrained cohesive ratio (c_u / σ'_{v0}):

if $c_u / \sigma'_{v0} \leq 0.8$

$$K_0 = 0.34\ K_D^{0.54} \quad (5.14)$$

$$OCR = 0.3\ K_D^{1.17} \quad (5.15)$$

if $c_u / \sigma'_{v0} > 0.8$

$$K_0 = 0.68\ K_D^{0.54} \quad (5.16)$$

$$OCR = 2.7\ K_D^{1.17} \quad (5.17)$$

As it can be understood from those equations, in NC deposits the correlations are quite the same and very similar to Marchetti's formulations. As a consequence, Marchetti´s equations are the most generally accepted and seem to represent well this type of soils around the globe (onshore). In OC clays, Marchetti's correlations (1980) are not valid and the proposals of Lacasse et al. (1990) is easier to apply, but probably reflects only a very particular environment, thus requiring local validation. Powell and Uglow's (1988) can provide an interesting methodology to characterize OC soils.

In the course of sedimentary data collection (Cruz, 1995; Cruz et al., 2006a), it was not possible to experimentally determine K_0, namely through Self-Boring Pressuremeter and/or K_0 triaxial testing, and thus the main comparisons are limited to some empirical correlations applied to fine grained soils, providing convergent information with DMT data. The mostly used empirical correlations, adopted in this framework, are those proposed by Brooker & Ireland (1965), deduced from plasticity index and OCR, and the

more recent one by Mayne (2001), based in OCR and in the angle of shearing resistance (ϕ') expressed as follows:

$$K_0 = (1- \sin\phi') \, OCR^{\sin\phi'} \quad (5.18)$$

OCR needed in both correlations may be derived from CPT or DMT and for the first case, the angle shearing resistance of clays was derived from Kenney (1967) proposal relying in the plasticity index, IP. Although the reference values are empirical and non-negligible scattering is obtained (Figure 5.7), both methodologies converge to the results obtained by DMT, thus giving some credit to the parameter, which is also supported by local experience.

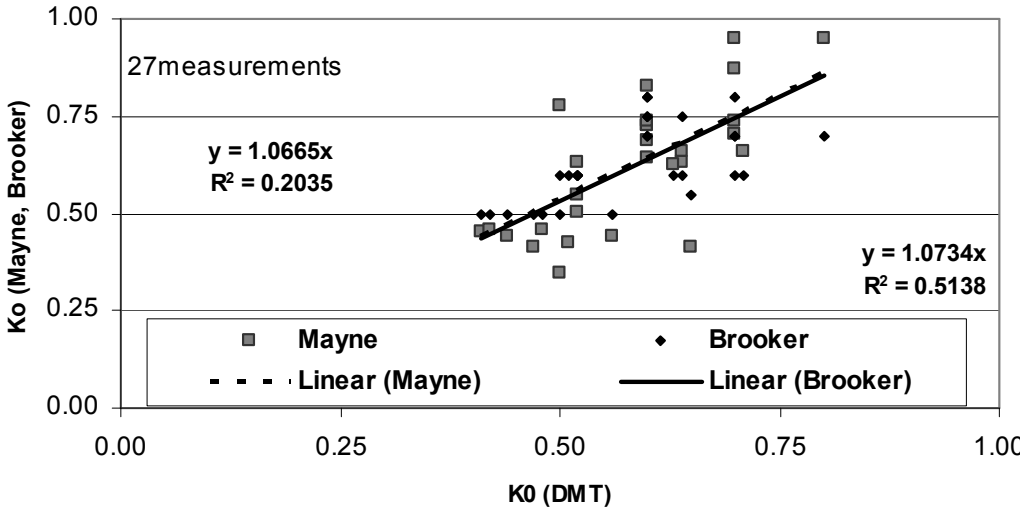


Figure 5.7 - K_0 comparisons

Stress history was analyzed by comparing OCR_{DMT} results with those obtained by oedometer tests, which generally fit together. It should be remembered that the research framework covered a narrow band of OCR values (1-3), corresponding to normally (NC) to slightly overconsolidated (LOC) soils. Figure 5.8 and 5.9 show the OCR estimated from DMT results in the Mondego and Vouga river alluvial deposits and are compared with those from oedometer tests performed in high quality samples, revealing an evident convergence that confirms the observed global efficiency of DMT on normally consolidated clays.

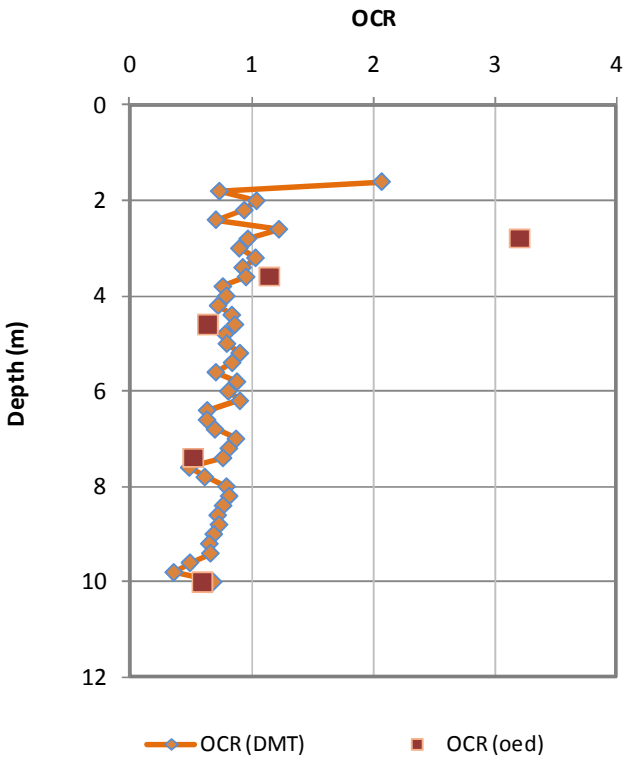


Figure 5.8 - OCR results in Mondego's alluvial deposits.

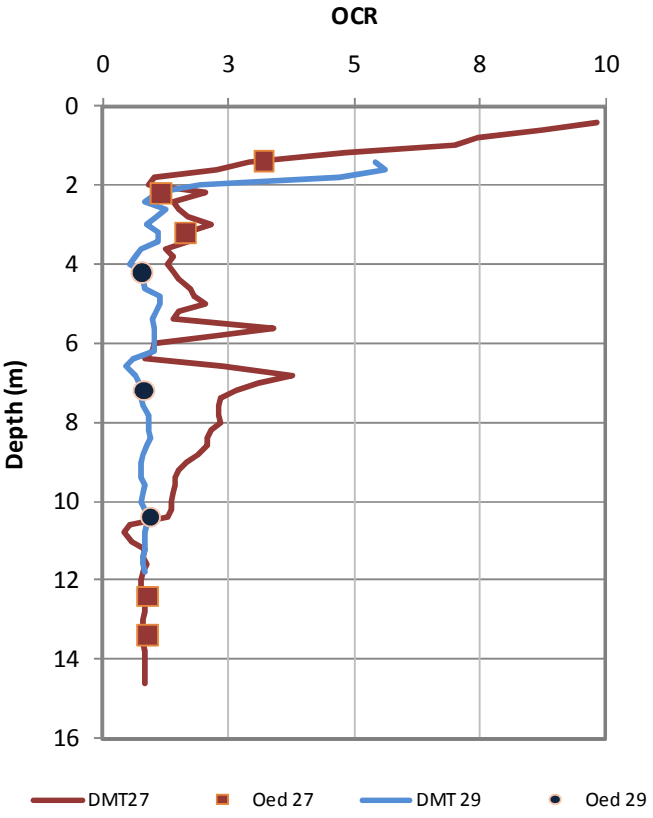


Figure 5.9 - OCR results in Vouga's alluvial deposits.

5.4.1.2. Undrained shear strength

The load application on clayey soils generates an excess of pore-pressure that dissipates at a slow rate due to its low hydraulic conductivity. Thus, undrained loading conditions are installed. If the soil is fully saturated and exhibits a full undrained behaviour, a total stress analysis can be applied. However, it is important to remember that undrained shear strength can assume different forms, since it depends on the mode of failure, soil anisotropy, strain rate and stress history, and thus can vary on each specific problem (Lunne et al., 1997). Being so, it is important to index DMT results to classical tests, in order to have a reference for application purposes.

Based on Ladd´s (1977) and Mesri (1975) works, Marchetti (1980) deduced a correlation for fine grained soils undrained shear strength via OCR, written in the form:

$$c_u / \sigma'_{v0} = 0.22\ (0.5\ K_D)^{1.25} \qquad (5.19)$$

Comparing the results with those obtained by FVT and triaxial compression tests, Marchetti (1980) observed a very reasonable consistency of results and a tendency of DMT to produce conservative values. Since then, this parameter has been studied by several investigators (Fabius, 1985; Grieg et al, 1986, Lutenegger and Timian, 1986; Ming & Fang, 1986; Lacasse & Lunne, 1988; Lutenegger, 1988) and it was verified that DMT prediction based on the Marchetti's original correlation compares well with FVT results in saturated soft to medium hard clays. Furthermore, Powell & Uglow (1988) confirmed Marchetti´s correlation for young clays, while for old clays suggested the application of the same methodology proposed for K_0 and OCR. On their turn, Lacasse & Lunne (1988) suggested a sub-division of the initial correlation taking into account the followed stress path:

$$c_u / \sigma'_{v0} = 0.17 \text{ to } 0.21\ (0.5\ K_D)^{1.25} \quad \text{(FVT)} \qquad (5.20)$$

$$c_u / \sigma'_{v0} = 0.20\ (0.5\ K_D)^{1.25} \quad \text{(Triaxial comp.)} \qquad (5.21)$$

$$c_u / \sigma'_{v0} = 0.14\ (0.5\ K_D)^{1.25} \quad \text{(Direct shear)} \qquad (5.22)$$

Based on triaxial compression results performed in the Norwegian Glava clay, Roque et al. (1988) proposed a completely different approach, relying upon bearing capacity theories and using an approach similar to the usually applied with CPTu results. In DMT, c_u would be dependent of P_1 parameter (instead of P_0, used on K_D

determination), horizontal total stress (derived from DMT, through K_0) and a blade factor (N_c) depending on the plasticity of soils:

$$c_u = (P_1 - \sigma_{h0}) / N_c \quad (5.23)$$

where σ_{h0} stands for the total horizontal stress, evaluated from K_0 obtained by DMT, and N_c is a coefficient that depends on brittleness of soil (5 for hard clay and silt, 7 to medium clay and 9 to non sensitive plastic clay).

In this approach, instead of using N_C and introducing some subjectivity, the methodology followed by CPTu practice is strongly suggested, that is the use of calibrated N_c parameter by classical tests, such as field vane or unconsolidated undrained (UU) triaxial tests.

The presented data reduction is based on the principle that developed shear strength is mobilized under fully undrained conditions. The distinction between drained and undrained conditions really depends on the rate of loading against rate of drainage (if rate of loading is slow compared with rate of drainage then drained conditions prevail, or the other way around). However, a clear frontier between both conditions can´t be settled, meaning that there is a transition zone (mixed soils) positioned between drained and undrained conditions, developing some excess of pore water pressure, but not as much as would occur in a pure undrained answer. These intermediate soils typically include SC, GC, SC-SM, GC-GM and ML (ASTM Unified Classification), and require some extra judgment for proper shear strength analyses. In such cases, I_D and U_D DMT parameters offer the possibility of discerning between drained, partially drained and undrained behaviour, thus controlling model applications. Lutenegger (1988), comparing DMT/FVT results, showed that there is an accuracy decrease as I_D increases, reaching an optimum point when $I_D < 0.33$ (pure clay). As a guide line, true undrained conditions should be expected in soils with I_D lower than 0.35, while from that value to 0.6, conditions are mostly undrained and deviation increases with I_D. Above 1.2 it is probable that drained conditions prevail, and so this parameter is no longer effective. Between 0.6 and 1.2, Cruz et al (2006a) suggested that the best approach is to consider both drained and undrained analysis and try to crosscheck with reference laboratory tests or simply considering the worst situation.

Sedimentary Portuguese data obtained along three of the main Portuguese rivers (Cruz, 1995, Cruz et al, 2006a) generally confirmed the good adaptability of the test to reproduce undrained characteristics. The overall results revealed significant scatter

when first plotted altogether, suggesting complex interpretation. However, when divided in two groups, organic and non-organic soils, the results showed quite different trends, as represented in Figure 5.10.

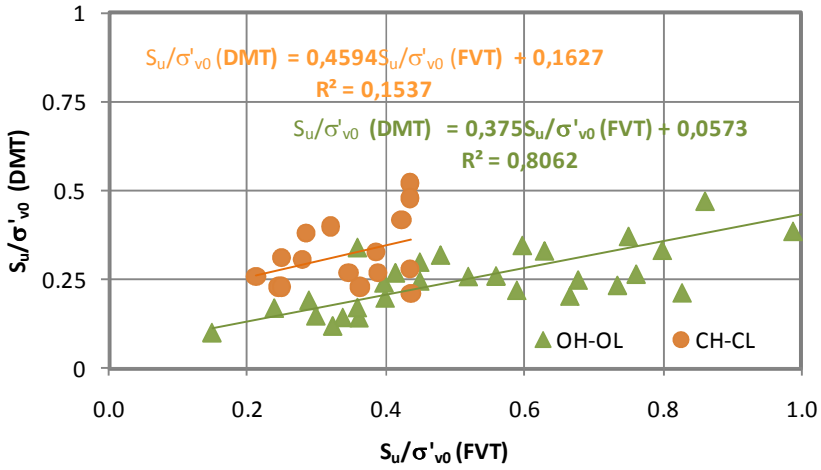


Figure 5.10 - Undrained shear strength, S_u (DMT) for organic and non-organic soils, compared with FVT.

In inorganic soils it is quite clear that results confirm the international experience, with the values from Marchetti's correlation being comparable to FVT results corrected by IP Bjerrum factor. The same conclusion can be applied when the results are compared with those from triaxial tests (Figure 5.11).

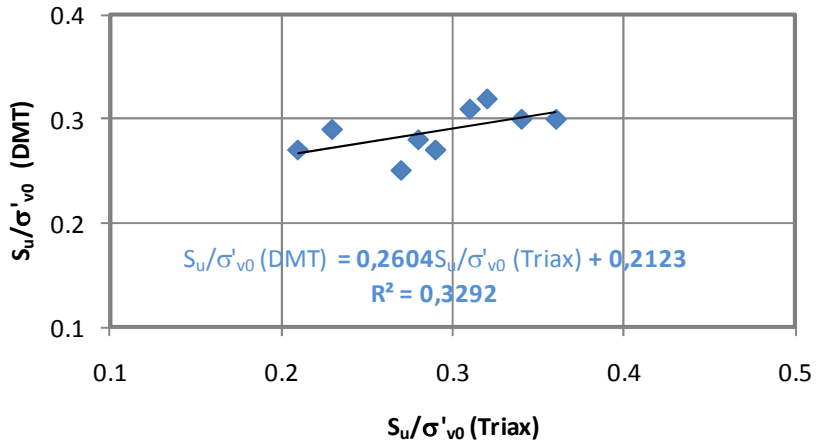


Figure 5.11 - Results from Marchetti's correlation, compared with triaxial testing

Moreover, when compared with FVT results in organic soils, data obtained by Marchetti´s correlation reveals itself too conservative, while Roque's correlation seem to converge to FVT results (Figure 5.12).

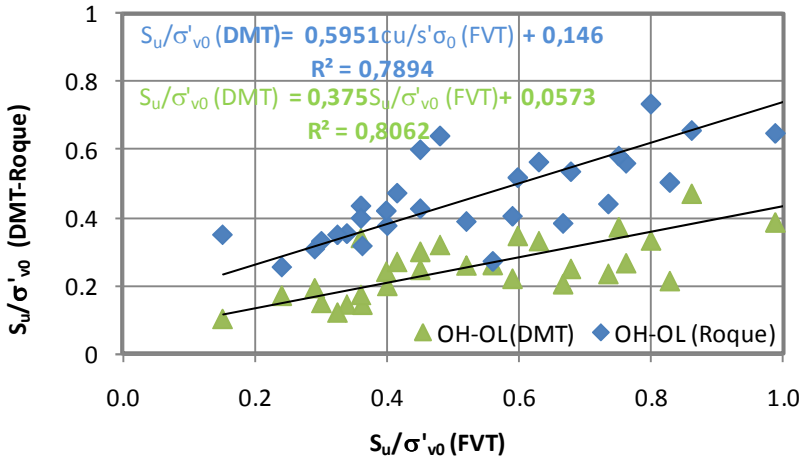


Figure 5.12 - Results from Marchetti's and Roque's correlation, compared with FVT

Finally, the ratio s_u/σ'_{v0} (DMT) / s_u/σ'_{v0} (FVT) seems to increase with increasing OCR_{DMT} as it becomes clear from Figure 5.13. OCR values lower than one represented in the same figure, correspond to soils loaded by a recent earthfill, where consolidation hasn't been concluded.

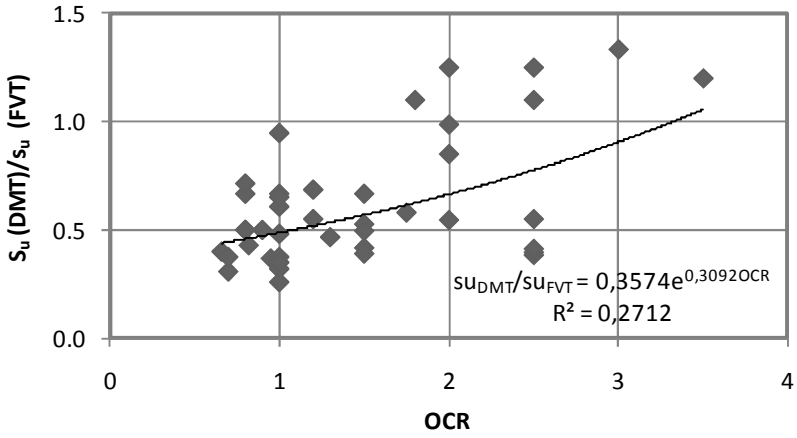


Figure 5.13 - Ratios S_u (DMT) / S_u (FVT) versus of OCR.

5.4.2. Coarse-grained soils

5.4.2.1. State Properties

The behaviour of sands follow a different path from clays, with the concept of OCR loosing its meaning, since those soils don't show significative dependency on stress history, except for the ageing processes that can only be associated to secondary or creep consolidation. However, OCR reflects mainly a density state, loose for NC and dense for OC or aged sands. This parameter may be a useful tool to determine the form of the stress-strain curves (presence or absence of a peak strength, naturally depending on confining stresses) related to dense or loose materials, as well as for evaluation of strength due to cemented structures of residual soils, as it will be discussed in *Part B – The Residual Ground*. In that sense, no matter the real meaning of the parameter, it is important to take a look to the possibilities of deducing OCR, in its broad sense, in coarse grained soils. Departing from the correlation established for clayey soils, Marchetti & Crapps (1981) defined different correlations between OCR and DMT results, covering all types of soils:

$I_D<1.2$ (cohesive soils) $\quad OCR = (0.5\ K_D)^{1.56}$ (5.24)

$I_D > 2$ (sandy soils) $\quad OCR = (0.67\ K_D)^{1.91}$ (5.25)

$1.2 < I_D < 2$ (mixed soils) $\quad OCR = (m\ K_D)^n$ (5.26)

$m = 0.5 + 0.17\ P$ (5.27)

$n = 1.56 + 0.35\ P$ (5.28)

$P = (I_D - 1.2) / 0.8$ (5.29)

As it can be observed, the respective formulae incorporates K_D and I_D, meaning that both fine content and density are represented, based on the general knowledge of OCR. This might also be useful to sense the behaviour of mixed soils and its proximity to either coarse-grained or fine grained soils.

Another possibility of evaluating OCR in sands is to combine DMT and CPTu test results, namely through M/q_c, as suggested by Baldi et al. (1988), based on calibration chamber tests and by Jendeby (1992), based on in-situ monitoring during compaction works. In fact, constrained modulus (M) shows higher sensitivity to density variations when compared to the corrected tip resistance (q_t), where values within the range of 5

to 10 should be seen as representative of normally consolidated (loose) soils, whereas values between 12 and 24 represent overconsolidated soils (Marchetti, 1997).

5.4.2.2. Drained Strength

Following classical soil mechanics approach, the general failure under drained conditions can be represented by Mohr-Coulomb failure criterion, where angle of shearing resistance (ϕ') is the representative soil strength parameter. Besides, this frictional strength, some soils (for instance, cemented or aged soils) may develop another type of strength related to attraction forces between particles, and denominated cohesive intercept. In the general case, Mohr-Coulomb shear strength is represented by the known classical formulae:

$$\tau = c' + \sigma \tan \phi' \qquad (5.30)$$

where τ stands for shear strength, c' the cohesive intercept, σ the normal stress and ϕ' the angle of shearing resistance.

The value of ϕ' depends on both frictional properties of the individual particles and the interlocking between particles affected by many factors such as mineralogy, shape of the grains, gradation, void ratio and the presence of organic material. Cohesive intercept can represent a wide range of phenomena within the soil mass, being usual its differentiation in real and apparent cohesion. Real cohesion may result from cementation (chemical bonding), electrostatic and electromagnetic attractions (with small meaning in the overall shear strength) and primary valence bonding or adhesion (cold welding in overconsolidated clays). On the other hand, apparent cohesion can be due to different sources such as suction, negative pore pressures due to dilation and apparent mechanical forces resulting in additional energy necessary to overcome particle interlocking.

In sedimentary sandy soils, drained shear strength is usually represented solely by angle of shearing resistance which, by means of confining state influence, shows a strong inter-dependency with K_0. Due to the difficulty of determining this value demandfull for more or less complex methods, the two values are temptatively determined together, as proposed by different authors (Marchetti & Crapps, 1981; Schmertmann, 1983; Marchetti, 1985; Campanella and Robertson, 1991; Marchetti, 1997), which gave rise to the following three methodologies suggested by ISSMGE TC 16 (1989).

Iterative method (Schmertmann, 1983), Method 1a

This method is based on K_D and thrust penetration of the blade, being applied to deduce both K_0 and ϕ'. It is a very complex method, as presented below, and requires the measurement of a penetration force that is not always available (CPT thrust forces can be used instead). Thus, this methodology is the least considered in deriving this geotechnical parameter deduction.

$$\tan(\phi_{ps}/2) = [F - (\pi/4)*D^2*u_0*1.019 - (S+\pi\, d^2/4 - B_t\, d)q_f+W\,(Z+2)]/FH \quad (5.31)$$

$$FH = P_0 - u_0 * \alpha * 1.019 \quad (\alpha = 355) \quad (5.32)$$

$$q_f = \gamma avg * B\, N\gamma q / 10 \quad (5.33)$$

$$N\gamma q = A\, B\, (C + D\, E\, F - G\, H + G\, I) \quad (5.34)$$

$$A = \cos(\psi-\delta) / \cos\delta \quad (5.35)$$

$$B = (1 + \text{sen}\phi_{ps}\, \text{sen}\,(2\gamma-\phi_{ps}) / \cos\phi_{ps} \cos(\gamma-\phi_{ps}) \quad (5.36)$$

$$C = [\cos^2(\gamma-\phi_{ps})\, I\theta / 4 \cos2\psi \cos2\phi_{ps}] \quad (5.37)$$

$$D = [3 \cos(\gamma-\phi_{ps}) / 4 \cos\psi \cos\phi_{ps}] \quad (5.38)$$

$$E = e^2\theta_0 \tan\phi_{ps} \quad (5.39)$$

$$F = (m - 0{,}66\, m') \quad (5.40)$$

$$G = K[\cos\psi \cos\phi_{ps} / \cos(\gamma-\phi_{ps})] \quad (5.41)$$

$$H = (m - m')^{2\,*\,(m + 2m')} \quad (5.42)$$

$$I = m^3 \quad (5.43)$$

$$J = \tan(\psi) / 4 \quad (5.44)$$

$$m = D / B \quad (5.45)$$

$$m' = \text{sen}\beta \cos(\gamma - \phi_{ps}) * e\, \theta_0 \tan\phi_{ps} / 2 \cos\psi \cos\phi_{ps} \quad (5.46)$$

$$\tan\gamma = (\text{sen}\phi_{ps} + \sqrt{}\, 1+2\cos\phi_{ps}) / (2 + \cos\phi_{ps}) \quad (5.47)$$

$$\psi = 90 - \alpha \quad (5.48)$$

$$\theta 0 = 180 - (\psi + \gamma) + \beta \quad (5.49)$$

$$I\theta=\{3\tan\phi_{ps}\,[e^{3}\tan\phi_{ps}\cos\beta-\cos(\theta_0-\beta)]+[e^{3}\tan\phi_{ps}\,\mathrm{sen}\beta+\mathrm{sen}(\theta_0-\beta)]\}/1+9\tan 2\phi_{ps} \quad (5.50)$$

where ϕ_{ps} is the angle of shearing resistance in plane strain conditions, F represents the thrust force (kg), D the rod diameter (cm), P_0 is the basic DMT parameter, u_0 the pore-pressure before blade penetration (kg/cm^2), S the DMT membrane cross section (cm^2), d the friction reducer diameter (cm), B_t the blade thickness, q_f the bearing capacity factor according to Durgunoglu e Mitchell (kg/cm^2), W the rod weight (kg), Z the test depth (m), FH the horizontal force (normal to the blade), γ_{avg} the average unit weight above the measurement depth, $N_{\gamma q}$ the bearing capacity factor, ψ the blade angle,α the half of the blade angle, β the angle of the tangent to shear surface with the vertical (assumed = ϕ_{ps}), γ the shear plane angle (assumed = $\phi_{ps}/2$), δ the friction soil/dilatometer (assumed = $\phi_{ps}/2$), m the ratio depth/ blade thickness, θ_0 the logarithm of the angle of shear plane and K the at rest earth pressure coefficient.

To solve the system, Schmertmann (1983) indicates the following steps:

a) Estimate ϕ'_{ps};
b) Evaluate K_0;
c) Calculate ϕ_{ps};

Perform iterative calculations until assumed and determined ϕ_{ps} fall in the same range and reduce plane strain (ϕ_{ps}) to axially symmetric angle of shearing resistance (ϕ_{ax}), as follows:

$$\phi'_{ps} < 32 \qquad \phi'_{ax} = \phi'_{ps} \quad (5.51)$$

$$\phi'_{ps} > 32 \qquad \phi'_{ax} = \phi'_{ps} - [(\phi'_{ps} - 32) / 3] \quad (5.52)$$

Combined CPT and DMT tests (Marchetti, 1985), Method 1b

The method first derives K_0 from q_c and K_D through Baldi's correlation (1986) and then applies the theory of Durgonuglu & Mitchell (1975) to estimate ϕ' from K_0 and q_c. The evaluation begins by deriving K_0 by:

$$K_0 = 0.376 + 0.095\, K_D + C_3\, q_c / \sigma'_v \quad (5.53)$$

with q_c representing the tip resistance of CPT, σ'_v the effective vertical stress and C_3 is a constant equal to – 0.002 (freshly deposited sand) or – 0.0017 (seasoned sand).

Once K_0 is determined it is possible to use the chart shown in Figure 5.14, worked out by Marchetti (1985) from Durgunoglu & Mitchell's work and readapted by Campanella & Robertson (1991) with the introduction of right scale of K_D, that was based on their observation of $q_c / \sigma'_{v0} = 33\ K_D$.

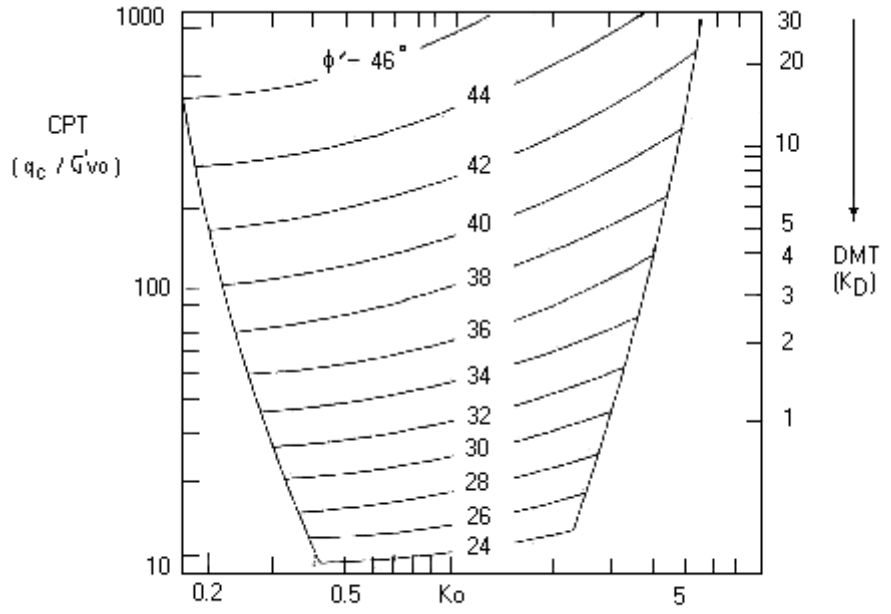


Figure 5.14 - Re-adapted Durgonuglu & Mithcell diagram (Robertson & Campanella, 1991)

Lower bound approach (Marchetti, 1997), Method 2

This method does not look for a high precision value of the parameter, but just a safe value. In fact, Marchetti (1997), based in self-boring pressuremeter data proposed a conservative equation based only in K_D (thus avoiding CPT testing), which also allows for further evaluation of K_0 (Figure 5.15). Numerical expression of this correlation is presented in Equation 5.53. Although not so accurate as the other two, Marchetti (1997) suggests this method for practical applications since it has the advantage of being much easier to apply than the previous and because the expected deviation is of small influence in bearing capacity final calculations for daily common problems. Another similar approach was presented by Mayne (2001), expressed by Equation 5.54.

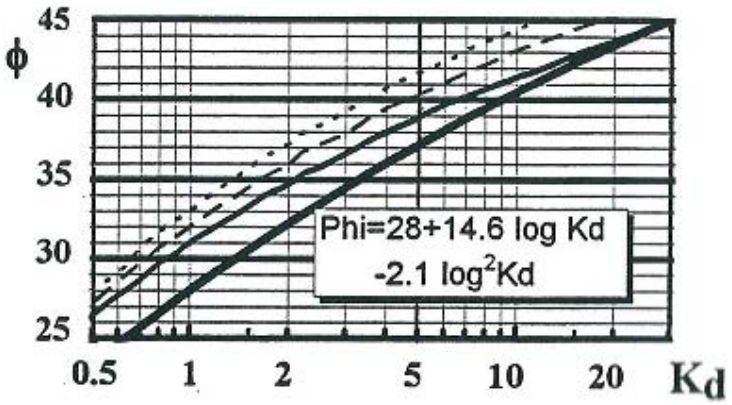


Figure 5.15 – Angle shearing resistence, ϕ, from K_D

$$\phi' = 28 + 14.6 * \log(K_D) - 2.1 * \log^2(K_D) \tag{5.54}$$

$$\phi' = 20° + \frac{1}{0.04 + \frac{0.06}{K_D}} \tag{5.55}$$

Method 2 is the usually adopted in Iberian Peninsula and thus global results obtained both in Portugal and Spain (Cruz et al, 2006a) were plotted against reference ϕ'_{CPTu} evaluated by Robertson & Campanella chart (1983). Figure 5.16 shows the respective results, revealing a clear convergence between Spanish and Portuguese data, with ϕ'_{DMT}/ϕ'_{CPTu} ratio being a little lower than 1. Statistical analysis revealed results expressed by 0.95 $\pm$ 0.1, globally within the interval 0.76 to 1.33.

These considerations are based on the principle that soils are saturated but in many engineering situations, unsaturated soils can be found, and thus different approaches are required. However, the strength behaviour of unsaturated soils is much more difficult to evaluate, since standards and practice are not yet as well established as for saturated soils. Globally, the strength of unsaturated soils is often greater, due to negative pore water pressures (suction) developed above water levels, which increase effective stresses and, consequently, shear strength.

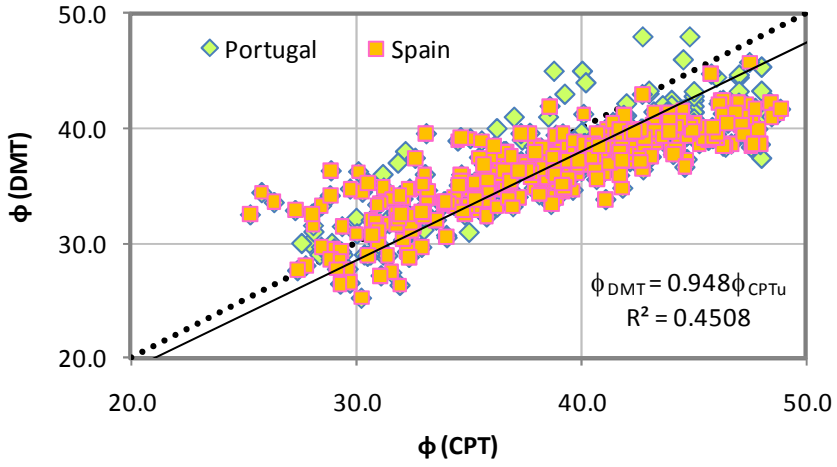


Figure 5.16 - Marchetti lower bound determination of ϕ' compared with CPTu results (Portugal and Spain)

5.5. Dilatometer modulus, E_D

Stiffness behaviour of soils is generally represented by soil moduli, and thus the base for in-situ data reduction. Generally speaking, soil moduli depend on stress history, stress and strain levels, drainage conditions and stress paths. In practice, the more commonly used moduli are constrained modulus (M), drained and undrained compressive Young modulus (E' and E_u) and small-strain shear modulus (G_0), this one being assumed as purely elastic and associated to dynamic low energy loading. In sandy soils, in-situ determinations are the only available methodologies for deducing stiffness, since undisturbed sampling in these soils is very difficult, or even impossible. In that sense, in-situ tests that measure both applied stresses and consequent deformations are mostly preferable, such as plate load, pressuremeter and dilatometer tests. S-modules in DMT or CPTu tests and CH tests are very valuable, since the determination of shear wave velocities can be directly related to small-strain shear modulus, as discussed in Chapter 4.

The determination of stiffness parameters by DMT is primarily based in the dilatometer modulus. In DMT, the usual complexity for efficient field devices to measure displacements is overcome by imposing a specific displacement through the use of Plexiglas cylinders, which remain fairly stable both with time and temperature, providing a rare accuracy in displacement determination. Theory of Elasticity is used to derive dilatometer modulus, E_D (Marchetti, 1980), by considering that membrane expansion into the surrounding soil can be associated to the loading of a flexible

circular area of an elastic half-space, and thus the outward movement of the membrane centre under a normal pressure Δp can be calculated by (Gravesen, 1960):

$$s_0 = (2\ D\ \Delta p / \pi) * (\ 1 - \nu^2) / E \quad (5.56)$$

where s_0 is the displacement (1,05mm) in normal direction to membrane plane, D is membrane diameter (60mm), Δp the differential pressure, ν Poisson's ratio and E the Young modulus. Introducing DMT geometric characteristics the equation takes the form:

$$E_D = E / (1 - \nu^2) = 34.7\ \Delta p \quad (5.57)$$

This theoretical background supporting E_D, together with its calibration by the type of soil (I_D) and the stress history (K_D), provides high accuracy in moduli evaluations, so well documented and accepted by scientific community. In fact, to obtain constrained modulus, M (equivalent to E_{oed} or $1/m_v$), Marchetti (1980) introduced a correction factor, R_M, to dilatometer modulus, E_D, justified by the following reasons:

a) E_D is derived from soil distorted by the penetration;
b) The direction of loading is horizontal, while M is vertical;
c) The variation of stress history with type of soil have to be considered; thus it is fundamental to consider K_D and I_D, besides E_D, in the evaluation of M_{DMT};
d) In clays, E_D is derived from undrained expansion, while M_{DMT} is a drained modulus; as it is hard to find reliable E_u (the preferential path) one must rely on M_{DMT} / E_D relation, which is a complex function of many parameters, such as pore pressure, anisotropy, soil type, stress history and can somehow be represented by I_D and K_D.

Based on these assumptions, Marchetti (1980) outlined the following correlation to derive constrained modulus, M, which has been widely used with very good reported results:

$$M_{DMT} = R_M\, E_D \quad (5.58)$$

$$R_M = 0.14 + 2.36 \log K_D, \text{ for } I_D \leq 0.6 \quad (5.59)$$

$$R_M = R_{M0} + (2.5 - R_{M0}) \log K_D, \text{ for } 0.6 < I_D < 3.0 \quad (5.60)$$

$$R_M = 0.5 + 2 \log K_D, \text{ for } I_D \geq 3.0 \quad (5.61)$$

$$R_M = 0.32 + 2.18 \log K_D, \text{ when } K_D \geq 10 \quad (5.62)$$

$R_{M\,0} = 0.14 + 0.36\,(I_D - 0.6) / 2.4$ (5.63)

R_M is always ≥ 0.85. (5.64)

A typical M_{DMT} profile compared with oedometer results is represented in Figure 5.17, as a sign of the common adjustment of this DMT approach (Marchetti, 1980).

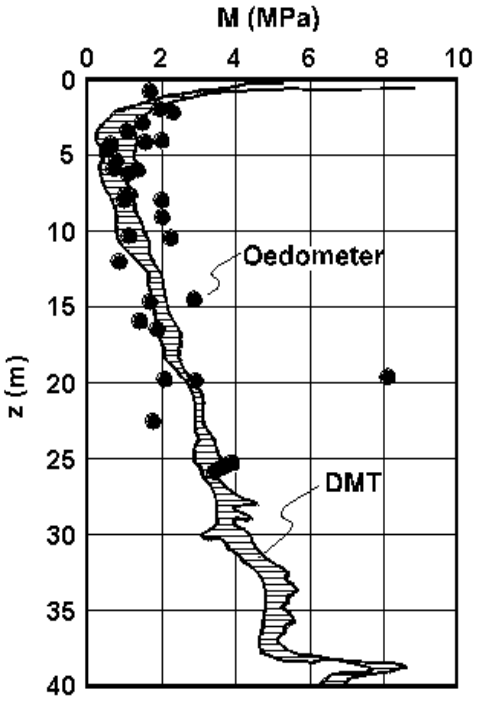


Figure 5.17 - Comparison between M_{DMT} and E_{oed} (after Marchetti, 1980)

Starting from constrained modulus and considering the coefficient of Poisson, ν, it is possible to derive Young modulus (Marchetti, 1997) and shear modulus (Monaco et al, 2009) by applying Theory of Elasticity. Taking Poisson's coefficient equal to 0.25, then E_{DMT} and G_{DMT} can be derived through the following equations

$E_{DMT} \approx 0.8\ M$ (5.65)

$G_{DMT} \approx M/3$ (5.66)

M_{DMT} can be considered as a reasonable estimate of the *operative* or *working strain modulus*, i.e. the modulus that, introduced into the linear elasticity formulae, predicts with acceptable accuracy the settlements under working loads, as concluded by Monaco et al (2009) based in reported case histories (Schmertmann, 1986, Monaco et al., 2006) that showed average ratios (using the Ordinary 1-D Method) DMT calculated/observed settlement to fit within 1.18 and 1.30.

Portuguese data, related within this sedimentary framework (Cruz et al, 2006a) and obtained from 37 high quality consolidation tests, was used to check and calibrate M_{DMT}, with the results confirming the high accuracy of the parameter, as it is shown in Figure 5.18.

Besides, DMT results were also compared with CPTu data, by means of M and q_t, as presented in Figure 5.19, with Portuguese and Spanish experimental data fitting in the same correlation, thus confirming the general adequacy of the parameter, quite independent of local peculiarities.

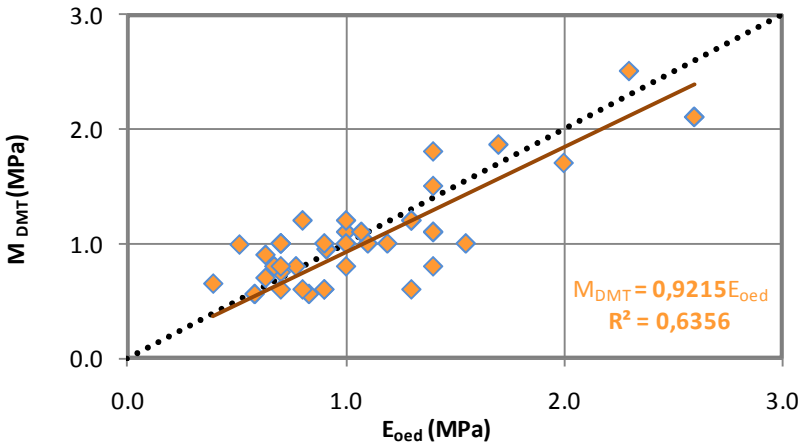


Figure 5.18 - Comparison between M_{DMT} and E_{oed}

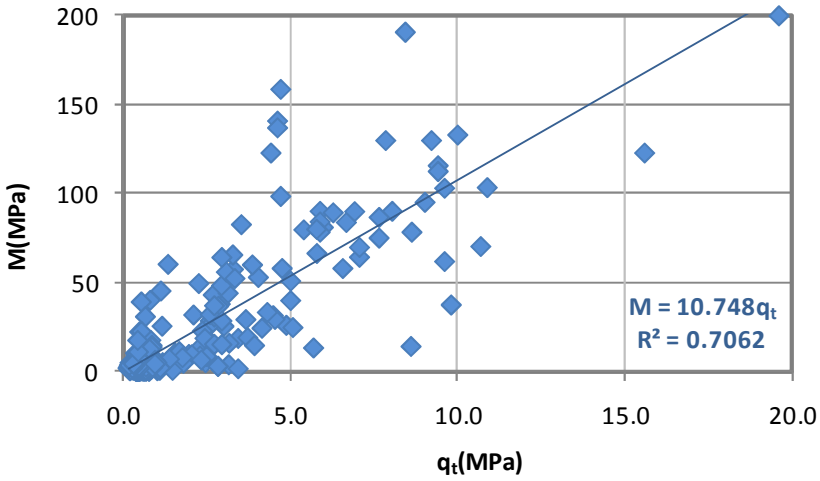


Figure 5.19 - M/qt correlations

Robertson (2009), departing from the work in Piedmont residuum (Mayne & Liao, 2004) presented the following correlation between DMT and CPTu results:

$$E_D / \sigma'_{v0} = 5 (Q_{t1}) \quad (5.67)$$

where Q_{t1} and σ'_{v0} is the initial vertical effective stress.

More recently, with the increasing use of seismic measurements to determine small-strain modulus, some attempts have been made to correlate DMT parameters with initial or dynamic shear modulus, G_0, with recourse to calibrations based in cross-hole and seismic SCPTu tests. In particular, the research works of Jamiolkowski et al. (1985) Sully & Campanella (1989), Baldi (1989), Tanaka & Tanaka (1998), Marchetti et al. (2008), Monaco et al. (2009) and the well documented method by Hryciw (1990) can be pointed out as main references. The reference work on this subject shows two different approaches for calibrating DMT results in terms of G_0 determination, namely through the ratio G_0/E_D (designated by R_G) or based in Hardin & Blandford (1989) indirect method. These methodologies are discussed below with some detail.

The first approach considers the coefficient (R_G) based on the ratio G_0/E_D and tries to define typical values as function of type of soils (Jamiolkowski, 1985; Lunne et al. 1989; Sully & Campanella, 1989; Baldi et al, 1991; Tanaka & Tanaka, 1998; Cavallaro et al. 1999, Ricceri et al. 2001). During the global research performed by the author in sedimentary soils, it was possible to have some seismic data together with DMTs, in alluvial clayey and sandy deposits. The results obtained following this approach show a local trend for G_0 to increase with both E_D and M (and also q_t from CPTu) with the first one showing less scatter (Figure 5.20). Furthermore, the ratio G_0/E_D (Figure 5.21) is in the vicinity of 7.0, close to Tanaka & Tanaka's (1998) results (R_G = 7.5), while for silica sands R_G is within 1.9 $\pm$ 0.6, being close to Jamiolkowski's (1985) and Baldi's (1986) results (2.2 $\pm$ 0.7 and 2.7 $\pm$ 0.57, respectively).

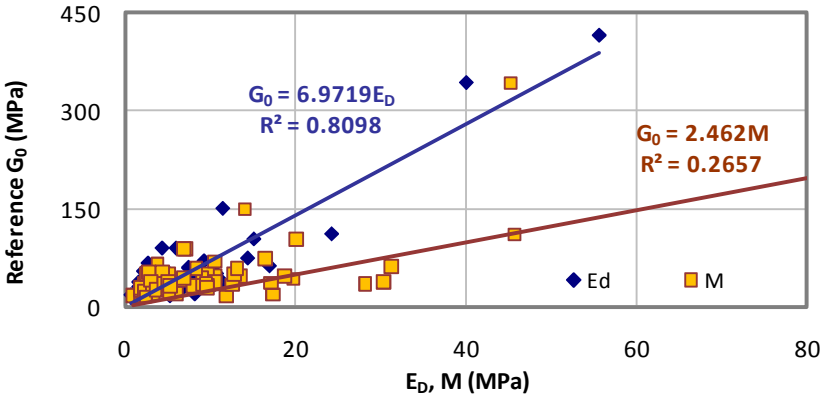


Figure 5.20 - Ratios G_0/E_D and G_0/M_{DMT}

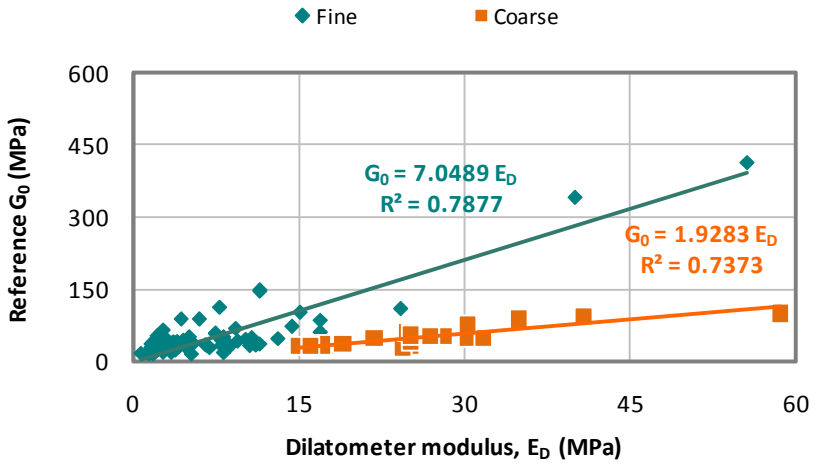


Figure 5.21 - Comparison between reference G_0 and E_D

Cruz et al. (2006a) using exclusively portuguese data and using the ability of the test to represent soil type by a numerical value, found out that R_G could be correlated with I_D as shown in Figure 5.22. Resulting data revealed a general decrease of R_G with the increasing presence of silty and/or sandy fraction, marked by a significant drop as the soil goes from clay to silty clay. Information arising from DMT international database, kindly granted by Prof. Marchetti, confirms the trend (Figure 5.23) and it allows a more robust correlation represented in Figure 5.24. In Figure 5.25 global data is represented in 3D plot (G_0-E_D-I_D space).

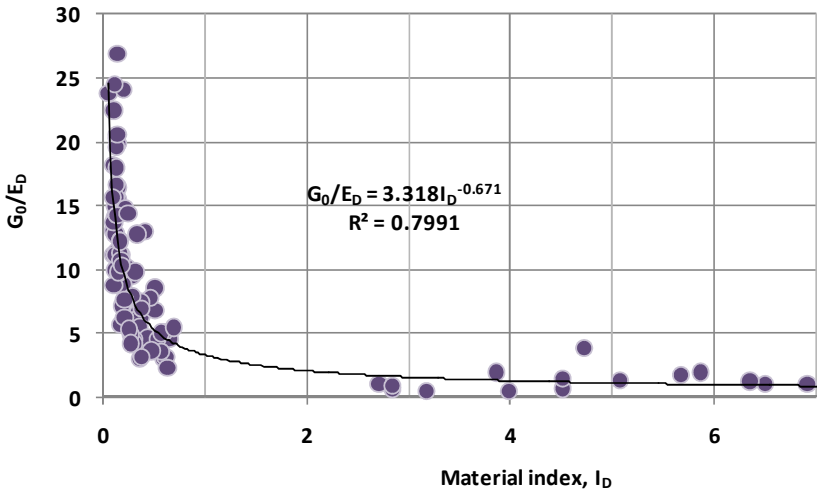


Figure 5.22 - G_0/E_D ratio versus I_D in Portuguese soils (Cruz et al., 2006a)

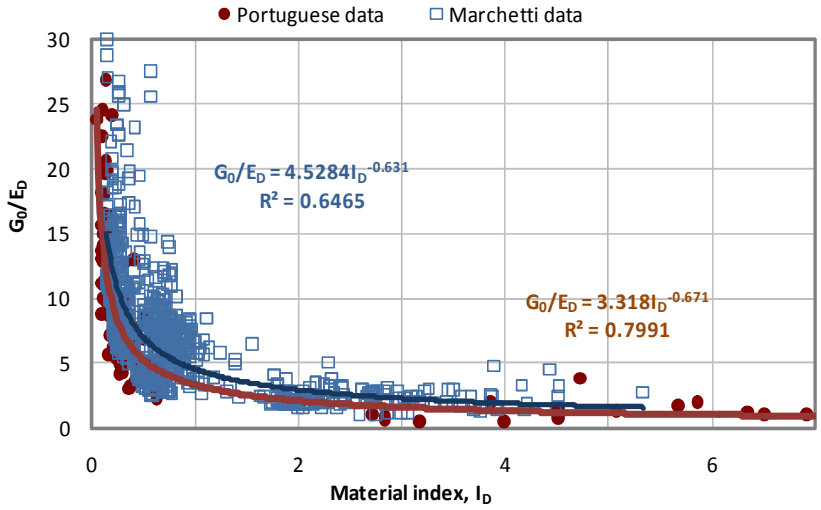


Figure 5.23 - G_0/E_D ratio versus I_D (Marchetti & Cruz data)

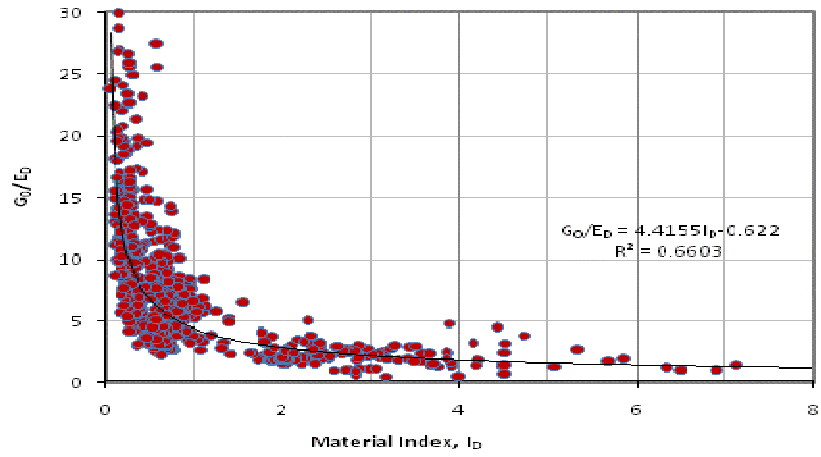


Figure 5.24 - Comparison between G_0/E_D and I_D (global data)

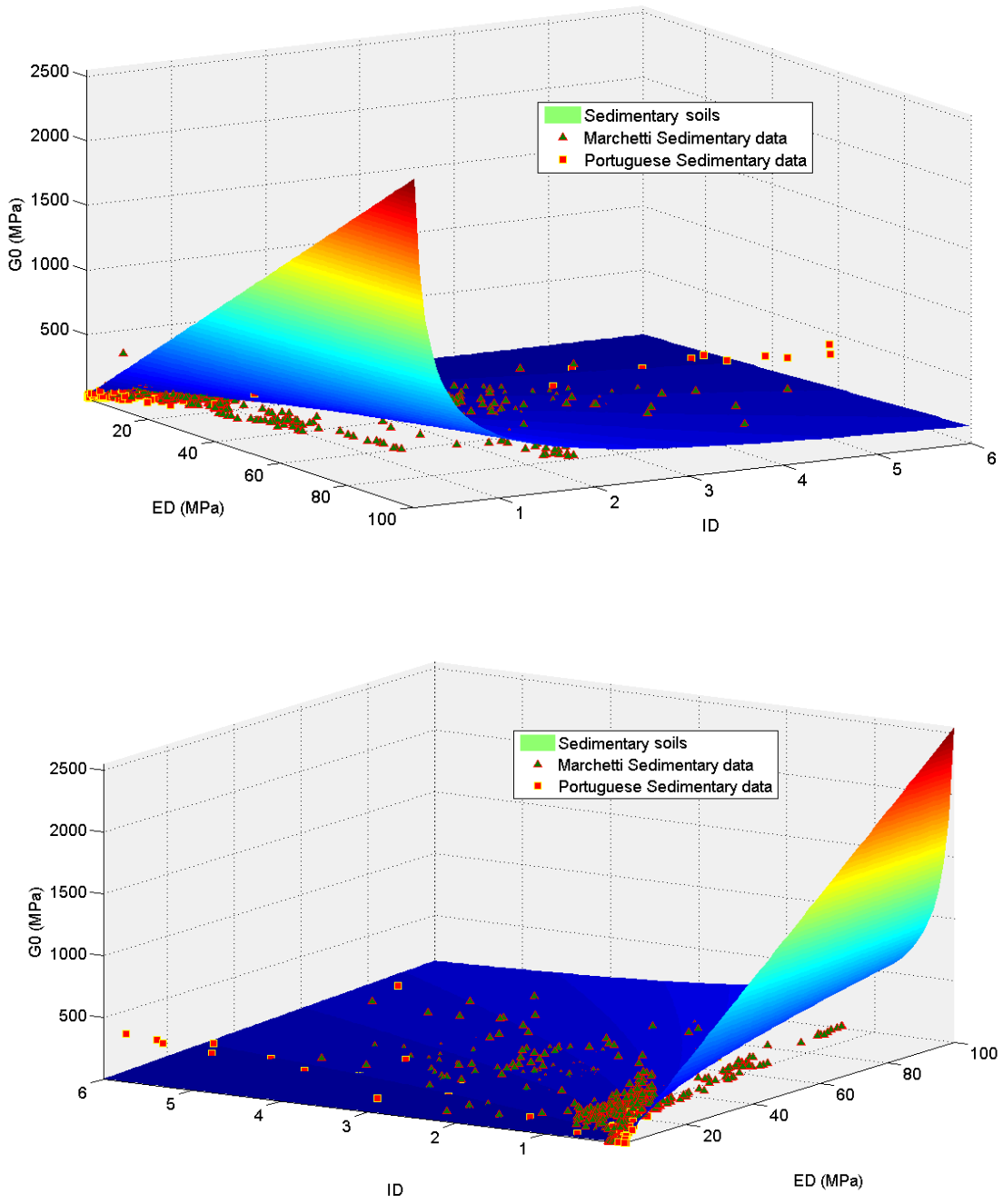


Figure 5.25 - Global data in 3D plot

Taking into account the relation of K_D with initial density, it is likely that this parameter can be successfully introduced in G_0 deducing formulae from DMT. Marchetti et al. (2008), plotted both ratios G_0/E_D (Figure 5.26) and G_0/M_{DMT} (Figure 5.27) against K_D and also as function of I_D, finding out that the correlation degree related with the former are lower, thus recommending the latter to be used in deriving G_0 from DMT.

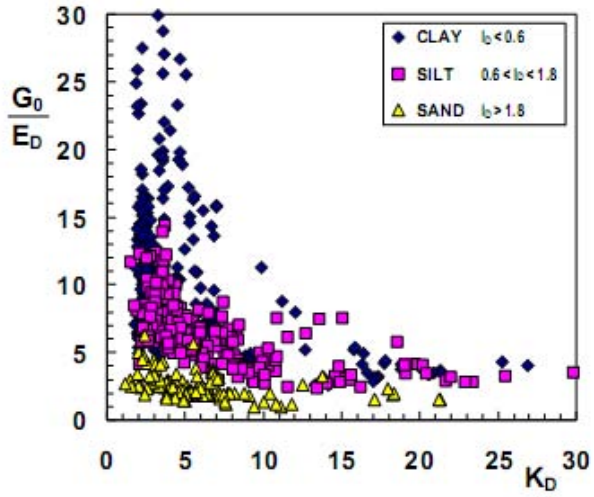


Figure 5.26 - G_0/E_D ratios as function of K_D (after Monaco et al., 2009)

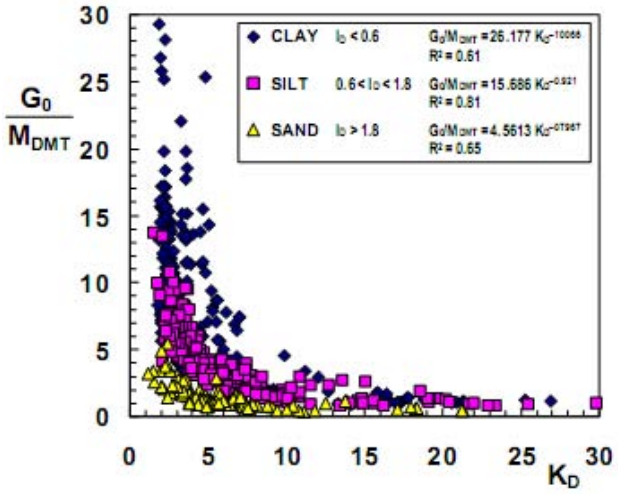


Figure 5.27 - G_0/M_{DMT} ratios as function of K_D (after Monaco et al. (2009)

The integration of these correlations under a unique equation (as function of I_D and K_D) is also possible with a few simplifications. Considering that frontier I_D values, namely 0.3 (clay-silty clay), 1.2 (clayey silts-silts-sandy silts) and 3.3 (silty sands-sands) can represent a reasonable mean, then it is possible to write the following expression:

$$G_0/M_{DMT} = a\ K_D^{\ b} \tag{5.67}$$

$$a = 31.42\ e^{-0.587\ I_D} \tag{5.68}$$

$$b = 1.021\ e^{-0.076\ I_D} \tag{5.69}$$

where *a* and *b* are the correlation factors depending on the type of soil (Figure 5.28)

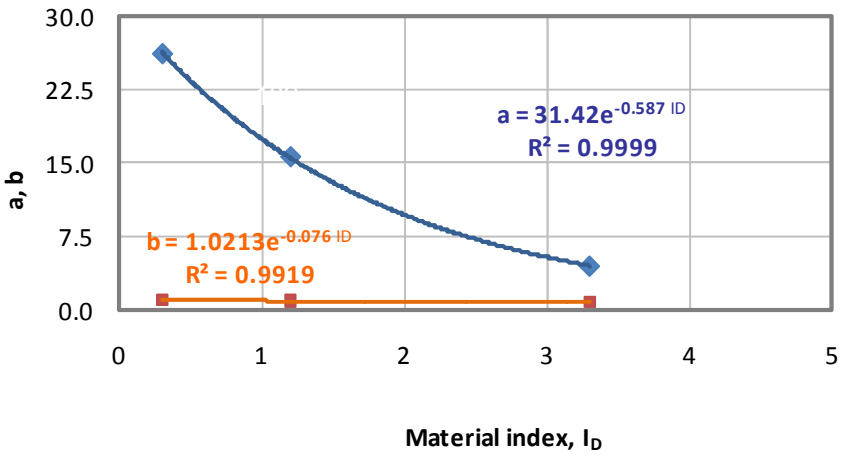


Figure 5.28 - Factors a and b variation with I_D

Cruz et al. (2006a) also attempted this approach, but K_D variation in Portuguese available data was too narrow and so, not conclusive. However, data reasonably fits in Marchetti's correlations, as it can be observed in Figure 5.29, from where it is clear that Portuguese clay data is placed around both clay and silt curves.

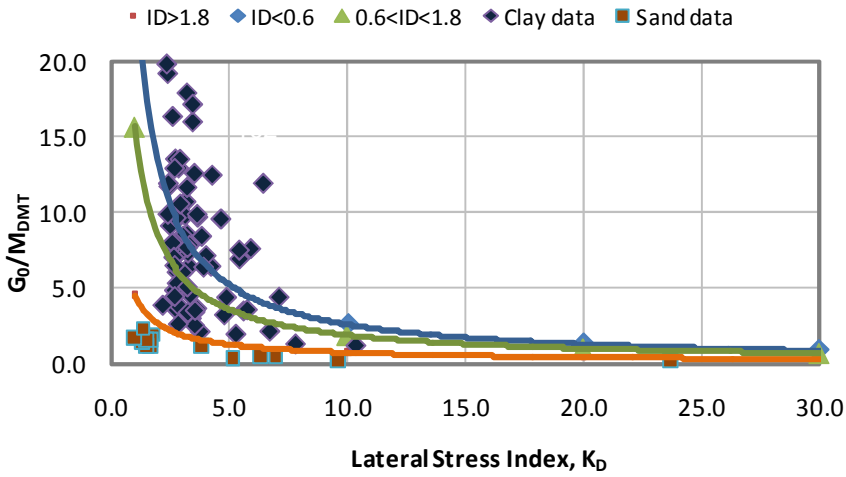


Figure 5.29 - Portuguese sedimentary data plotted against Marchetti's (2008) correlations.

The possibility of gathering together Portuguese (Cruz et al., 2006a) and international data (Marchetti, 2008) gave rise to a deeper study based on more powerful mathematical tools. Being so, a first step for numerical analysis was established from the correlations considering G_0 as function of (I_D, E_D, K_D) :

$$\begin{aligned} g: \quad & R^3 \quad \rightarrow \quad R \\ & (I_D, E_D, K_D) \rightarrow \widetilde{G_0} \end{aligned} \tag{5.70}$$

where $\widetilde{G_0}$ denotes the approximation given by the function g , to the measured parameter G_0. Many possibilities were considered (over than 150), but the approach

considering the definition of the dilatometric modulus (Marchetti, 1980) and its relation with soil moduli through Theory of Elasticity was followed. (the following approach was established to this analysis).This analysis was performed using the data collected in many different locations (Portugal, Spain, Italy, Belgium, Poland and United States) totalizing a sample of 860 measurements, modeling the ratio $\left|\frac{G_0-E_D}{E_D}\right|$ (which is strictly positive) as function of I_D and K_D. As so,

$$\left|\frac{G_0-E_D}{E_D}\right| = F(I_D, K_D). \tag{5.71}$$

This because,

$$\frac{G_0}{1-\left(f(I_D,K_D)\right)^2} = E_D \Leftrightarrow G_0 = E_D - E_D\left(f(I_D,K_D)\right)^2 \underset{E_D\neq 0}{\Longleftrightarrow} -\frac{G_0-E_D}{E_D} = \left(f(I_D,K_D)\right)^2 \tag{5.72}$$

After several numerical experiments, four functions were found to represent well the referred ratio, as presented in Table 5.1.

Table 5.1 - Base functions considered in MatLab® analysis.

Designation	Function Type
F1	$\frac{G_0-E_D}{E_D} = \exp\left(\alpha + \beta * \mathrm{I_D} + \gamma * \mathrm{K_D}\right)$
F2	$\frac{G_0-E_D}{E_D} = \exp\left(\alpha + \beta * \mathrm{I_D} + \gamma * \ln\left(\mathrm{K_D}\right)\right)$
F3	$\frac{G_0-E_D}{E_D} = \left(\alpha + \beta * \sqrt{\mathrm{I_D}} + \gamma * \sqrt{\mathrm{K_D}}\right)^2$
F4	$\frac{G_0-E_D}{E_D} = \exp\left(\alpha + \beta * \mathrm{I_D} + \gamma * \sqrt{\mathrm{K_D}}\right)$

The mean and the median of the relative errors $\frac{|G_0-\widetilde{G_0}|}{G_0}$ for all the data considered were sustained by values of 0.28 and 0.21, respectively. In this context and due to the high variability of the data considered (geographically and within its values) it's probably more advisable to point out the median instead of the mean as a control parameter. A summary of the constants, correlation factors, median and mean of errors are presented in Table 5.2, while Figures 5.30 to 5.33 show the best fitting planes related to the four designated functions. As it can be observed, the results are very similar, although F2 and F4 are slightly better.

Table 5.2 - Statistical parameters and constants related the four designated functions

Function Name	α	β	γ	Correlation factor, R^2	Relative Residuals	
					Median	Mean
F1	2.5920	-0.6968	-0.0761	0.6774	0.2074	0.2885
F2	3.0206	-0.6934	-0.5777	0.6923	0.2043	0.2878
F3	4.5813	-1.5328	-0.4014	0.6427	0.2079	0.2962
F4	3.1720	-0.6923	-0.4553	0.6892	0.2060	0.2861

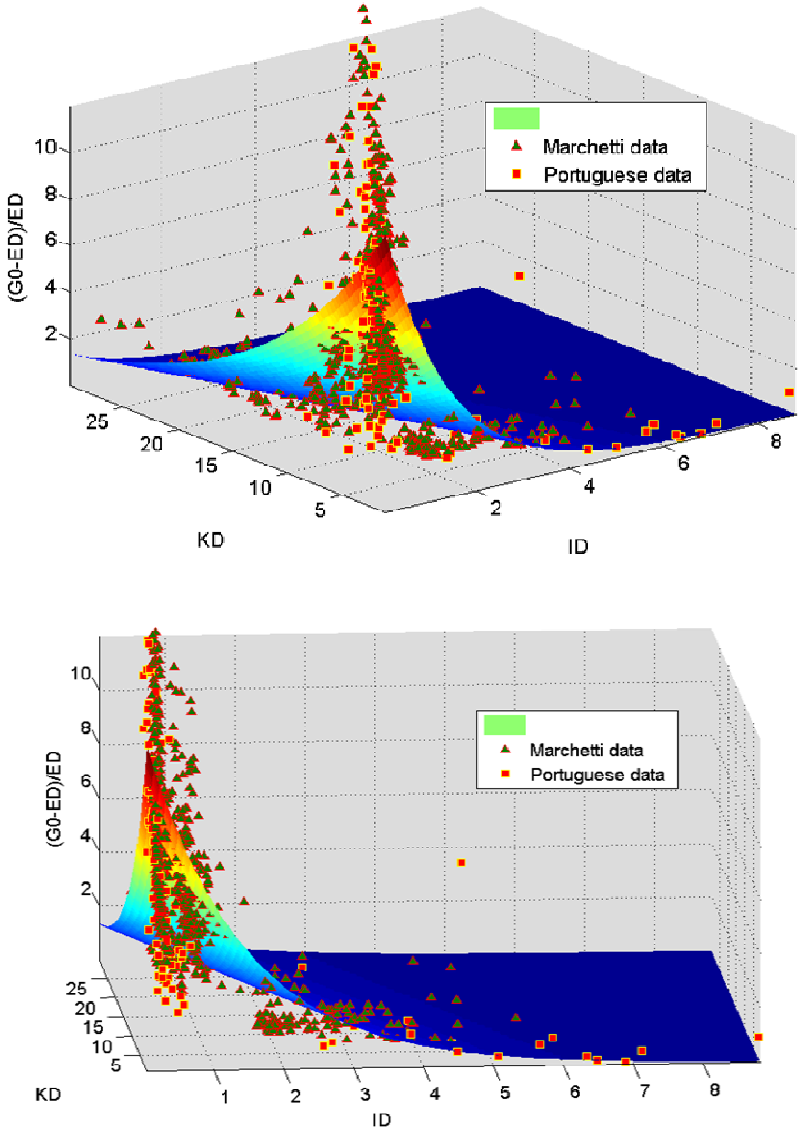


Figure 5.30 -3D representation of function F_1

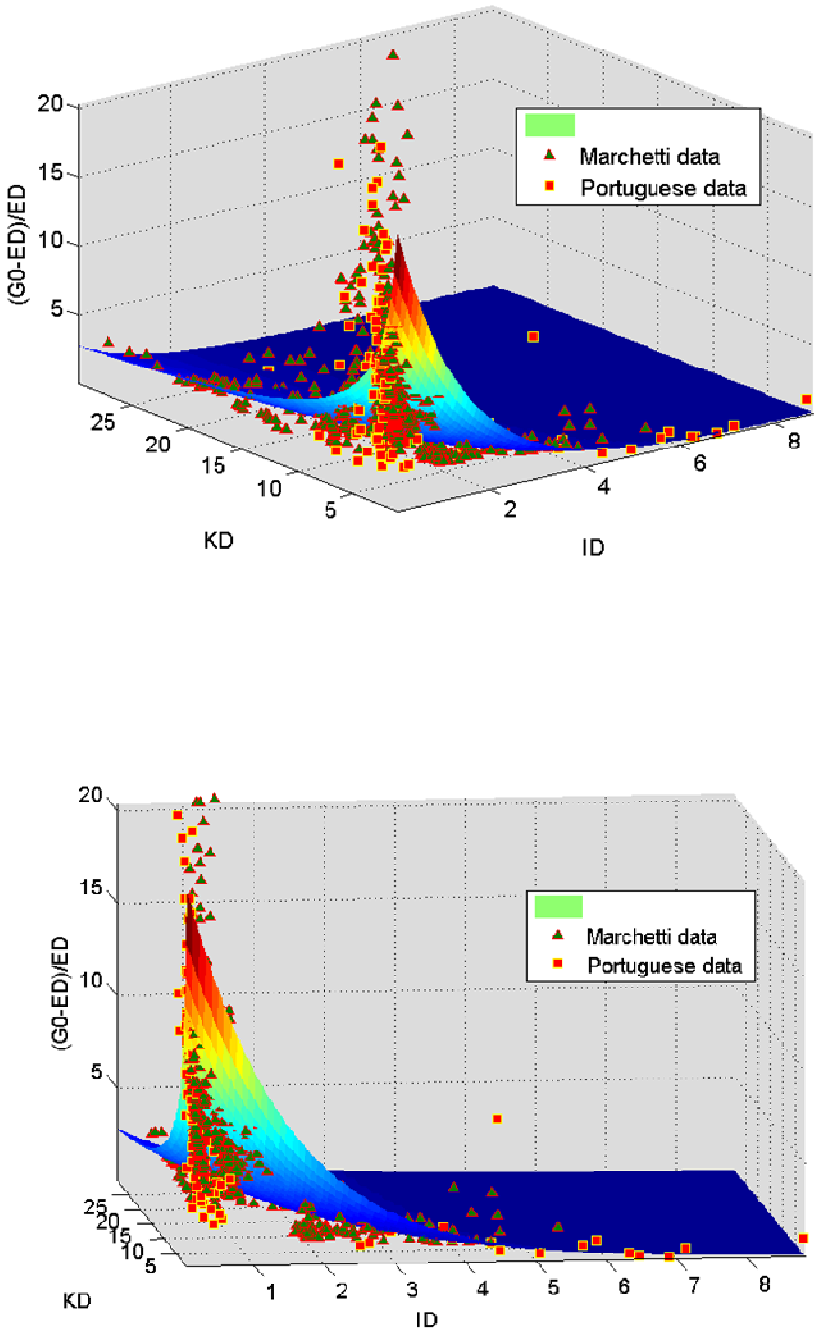


Figure 5.31 -3D representation of function F_2

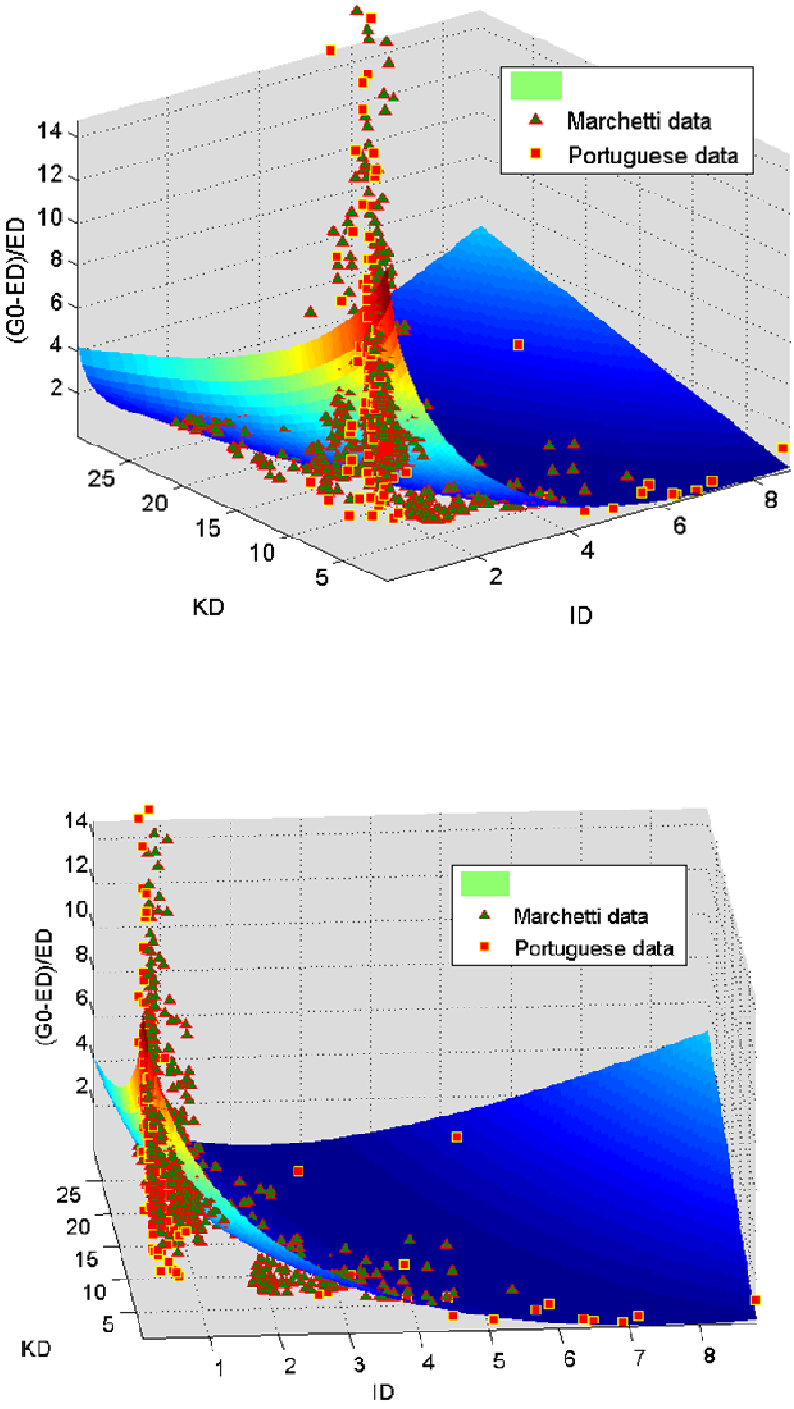


Figure 5.32 -3D representation of function F_3

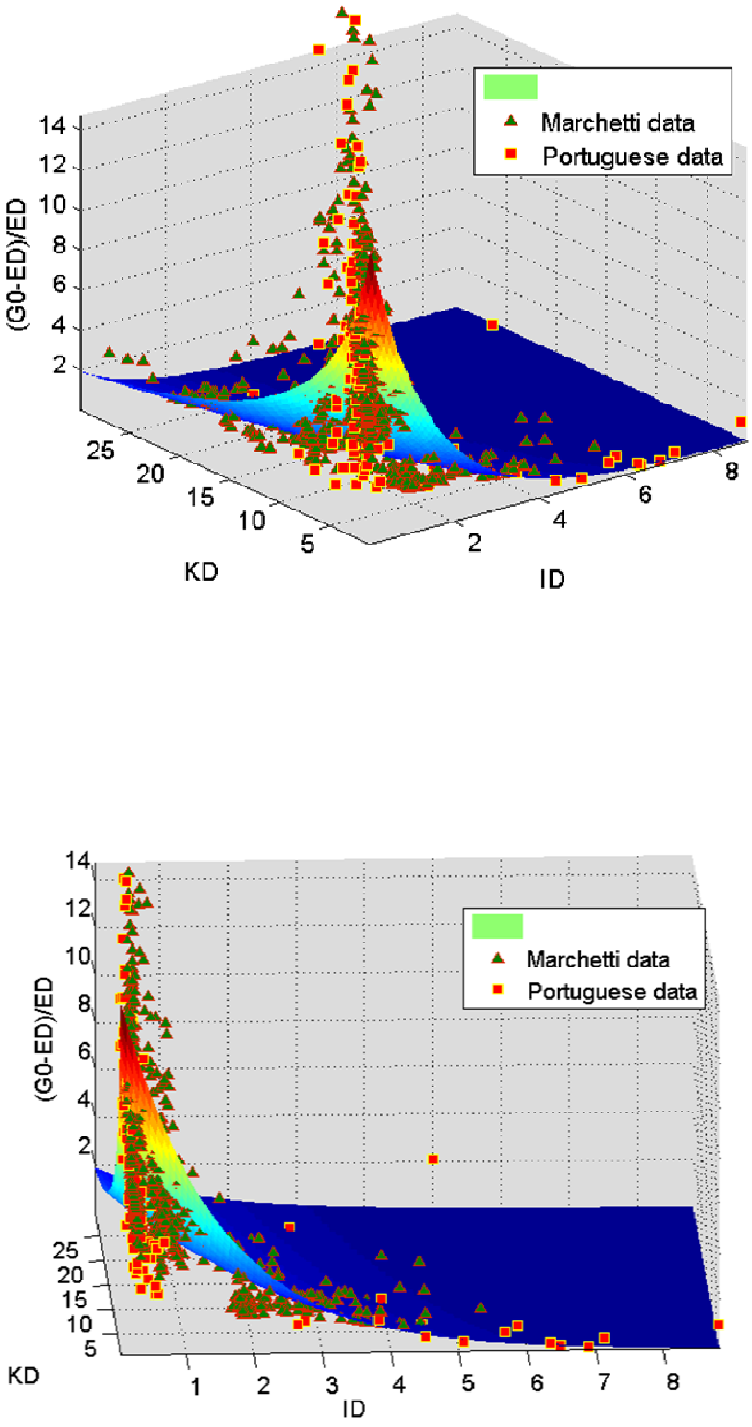


Figure 5.33 -3D representation of function F_4

An alternative correlation to evaluate R_G was proposed by Baldi et al (1989), with application only in normally consolidated sedimentary sands, through a correlation between G_0/E_D and an adimensionalized DMT "lift-off" pressure (P_{0N}), written as follows:

$$G_0/E_D = 4.9 – 3.7 \log (P_{0N}/10), \text{ for NC sands} \quad (5.73)$$

$$G_0/E_D = 9.7 – 8.3 \log (P_{0N}/10), \text{ for river sands} \quad (5.74)$$

where P_{0N} can be determined by the equation below:

$$P_{0N} = P'_0 / \sqrt{(\sigma'_{v0} * p_a)},\ p_a = 1 \text{ kPa} \quad (5.75)$$

In a more theoretical approach, Hryciw (1990) pointed out that correlations based on E_D would be affected by the DMT working strain level. Taking this observed behaviour into consideration, Hryciw (1990) proposed a new methodology for all type of sedimentary soils, developed from indirect method of Hardin & Blandford (1989), working with the variables K_0, γ e σ'_{v0}, (all derived from DMT) taking the place of σ'_0 and void ratio (*e*) on the original correlation. The respective correlation can be written as follows:

$$G_0 = [530/(\sigma'_{v0}/P_a)^{0.25}] * [(\gamma_d/\gamma_w)-1]/[2.7- (\gamma_d/\gamma_w)]*[K_0^{0.25}(\sigma'_{v0}*P_a)^{0.50} \quad (5.76)$$

where K_0 is the at rest earth pressure, γ_D and γ_w, respectively the dry and water unit weight, σ'_{v0} is the initial vertical effective stress and P_a the atmospheric pressure.

The comparison of Hryciw proposal with seismic data showed a set of results overlapping those presented by the same author, indicating the adequacy of the method for this particular case (Figure 5.34). Using the same error definition used by Hryciw ($G_{0predicted} – G_{0observed} / G_{0observed}$), 62% of the total data points have an error less than 25% and 93% less than 50%.

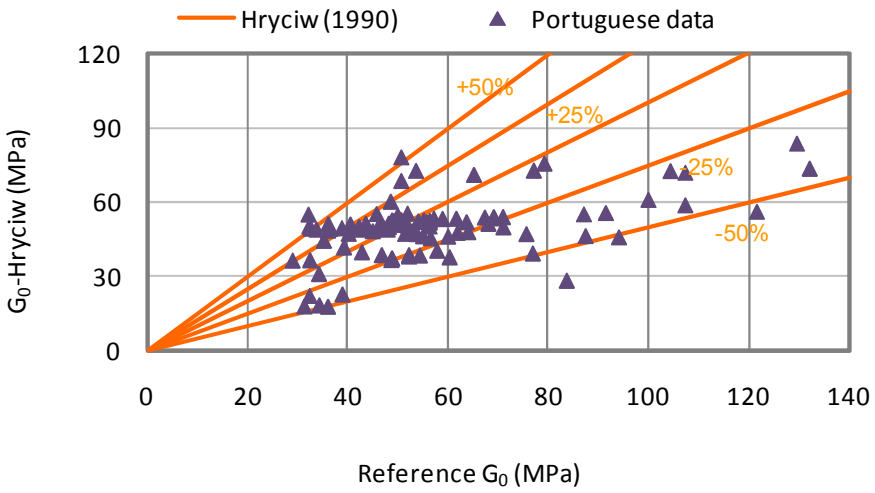


Figure 5.34 - Experimental results comparing with Hryciw's determination

Aware of the fundamental role of G_0 in modern design, and despite the discussed available correlations, Marchetti recently introduced a seismic module in DMT, re-naming it as SDMT (Figure 5.35).

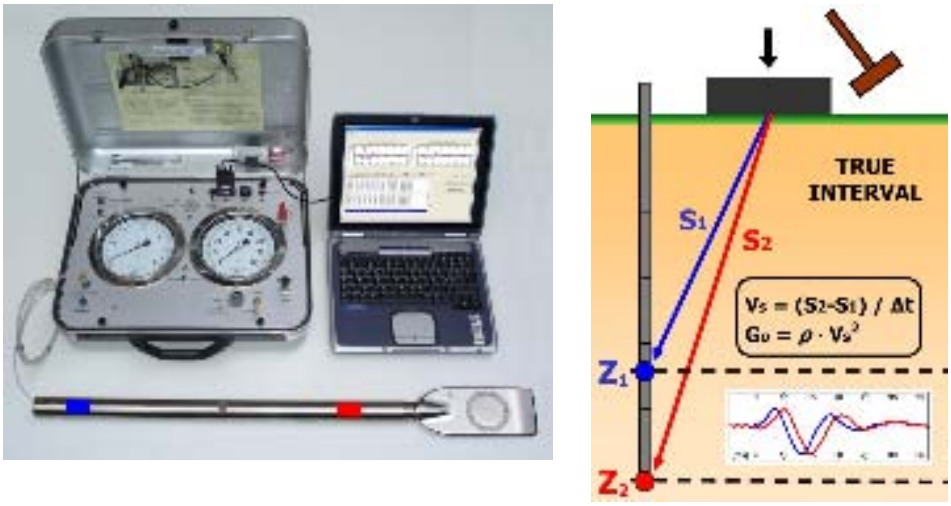


Figure 5.35 - Seismic Dilatometer, SDMT

Since the accuracy of results is directly dependent on the arrival time and the energy source, the seismic module was conceived using two geophones instead of one, guaranteeing the same level of energy in each pair of results related with each velocity determination. This provides the possibility of working with a true time range, avoiding the need of determining the time arrival, which is a source of uncertainty in seismic wave velocity determination. In fact, since the beginning of time of impact is the same for both geophones, then the phase difference corresponds to the extra time needed to reach the lower geophone, as illustrated in Figure 5.36.

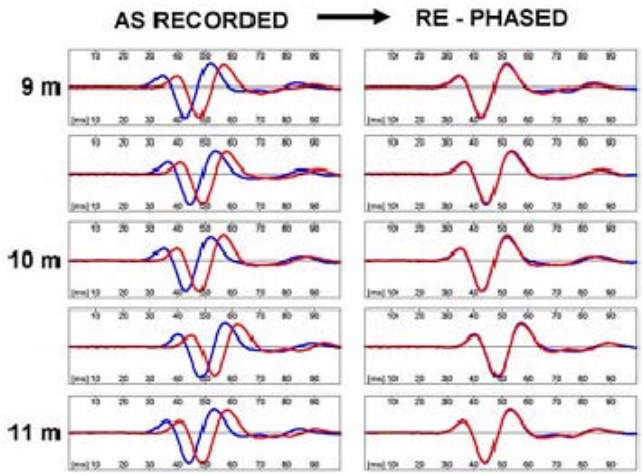


Figure 5.36 - Adjustment of time arrivals obtained in a two-geophone device (after Marchetti, 2006).

As discussed in Chapter 3, due to stiffness non-linearity direct application of small-strain shear modulus to evaluate deformations in most practical problems is not possible, which gave rise to the development of modulus (E_0 or G_0) degradation curves. Since G/G_0 is the usual ordinate of the normalized *G*-γ decay curve, Monaco et al. (2009) proposed the use of G_{DMT}/G_0, where G_{DMT} is deduced from M_{DMT} using Theory of Elasticity. Monaco et al. (2009) argued that since M_{DMT} is a working strain modulus, G_{DMT}/G_0 could be regarded as the shear modulus decay factor at working strains. If this is found acceptable, Figure 5.37 could be used to provide rough estimates of the decay factor at working strains. Plotted data reveals that the decay in sands is much less than in silts and clays, silts and clays decay curves are very similar and in all cases the decay is maximum in the NC or lightly OC region (low K_D).

The possibility of having two independent measurements of stiffness in only one test, related with different strain levels (G_0 from V_s and G_{DMT} from M_{DMT}) opens a way to attempt deriving in-situ decay curves of soil stiffness with strain, as suggested by Monaco et al. (2009). To do so, it is important to locate, even if roughly, the shear strain corresponding to G_{DMT}, which seems to be globally within intermediate level of strain (0.01 to 1%) as sustained by many researchers (Mayne, 2001; Ishihara, 2001; Sabatany et al., 2002; Monaco et al., 2009).

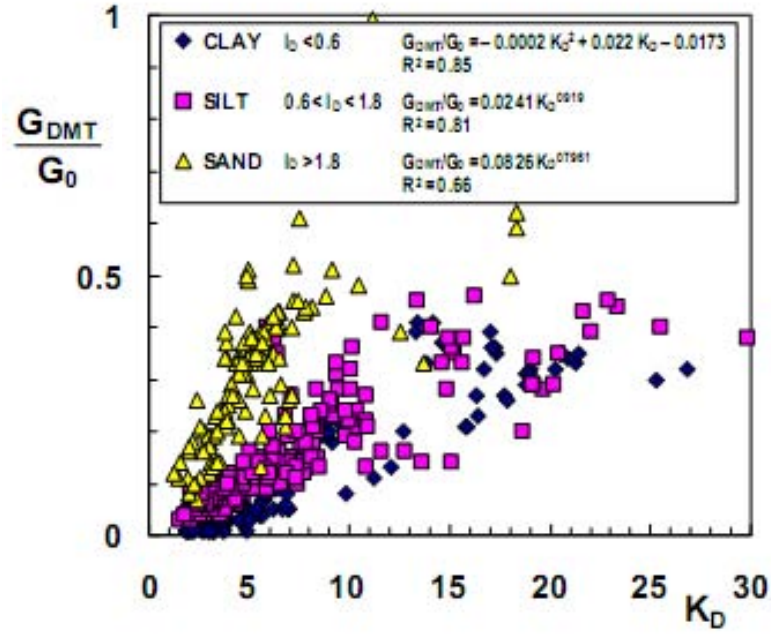


Figure 5.37 - Decay ratio G_{DMT}/G_0 vs. K_D for various soil types (after Monaco et al., 2009).

On the other hand, monotonic static loading show faster degradation rates than those observed in cyclic loading (Figure 5.38), as sustained by some researchers in the field (Lo Presti et al., 1993; Mayne et al., 1999, among others).

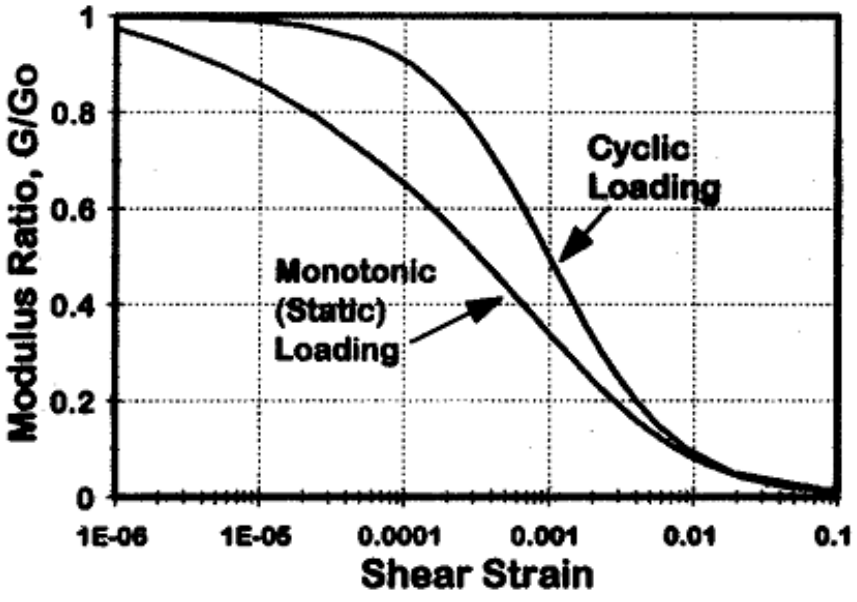


Figure 5.38 - Monotonic cyclic degradation response with logarithm of shear strain(after Mayne et al., 1999).

Mayne et al. (1999) proposed to use the modified hyperbola model proposed by Fahey & Carter (1993) already discussed in Chapter 3, to deduce stiffness response departing

from SDMT results. For unaged, uncemented and insensitive under monotonic loading, Mayne et al. (1999) states that *f* and *g* factors should be taken equal to 1.0 and 0.3, respectively and thus modulus degradation could be deduced through the following equations:

$$G/G_0 = 1 - (\tau/\tau_{max})^{0.3} \quad (5.77)$$

$$\tau_{max} = \sigma'_{v0} \tan(\phi') \quad (5.78)$$

where G_0 is derived from shear wave velocities, while the angle of shearing resistance, ϕ', can be deduced by Marchetti (1997) correlation.

5.6. Pore Pressure Index, U_D

Although a direct measure of pore pressure is not provided by DMT testing, P_2 can be used to estimate pore pressure in sands. In fact, during inflation the membrane displaces the sandy particles away from the blade while during deflation they tend to remain in the displaced position and, therefore, the pressure on the membrane is that of the water in the pores. As clays tend to rebound and thus, contribute equally to pressurize the blade, P_2 should only be used qualitatively (Marchetti, 2001).

The comparison of P_2 with u_0 allows the differentiation of more or less draining layers, with the drained condition represented by $P_2 = u_0$ and $P_2 > u_0$ reflecting increasingly partially drained and undrained behaviours. Naturally, this ability can also be used in soil identification, supporting and cross-checking I_D determinations.

These considerations led Lutenegger & Kabir (1988) to define one additional parameter related to pore pressure condition, namely Pore Pressure Index, U_D, which is similar to B_q of CPTu tests. When U_D is equal to "0" a drained condition is attained, while increasing values of U_D reflect a drop in draining ability (Benoit, 1989):

$$U_D = (P_2 - u_0) / (P_0 - u_0) \quad (5.79)$$

Portuguese data (Cruz et al., 2006), including piezometric and CPTu (u_2 type) measurements, allowed outlining the following trends:

a) Direct comparisons of P_2 and u_2 revealed a general parallel increasing pattern, although with some scatter for lower values (Figure 5.39). It is interesting to observe that generally the obtained correlation leads to higher

values of u_2, suggesting the influence of tip geometry in the excess of pore pressure generated by penetration.

b) In fine grained soils, represented by I_D lower than 0.9, the plotting of the ratio P_2/u_2 against I_D reveals a clear drop-down of the ratio with increasing I_D, approaching gradually to a lower level of 0.5 (Figure 5.40). In sandy soils, the overlapping of P_2 and u_0 profiles can be easily recognized, confirming the efficiency of the parameter to detect water table depth when drained conditions are installed. The general plot shows a distribution that could be useful to interchange P_2 and u_2, mostly in silty soils.

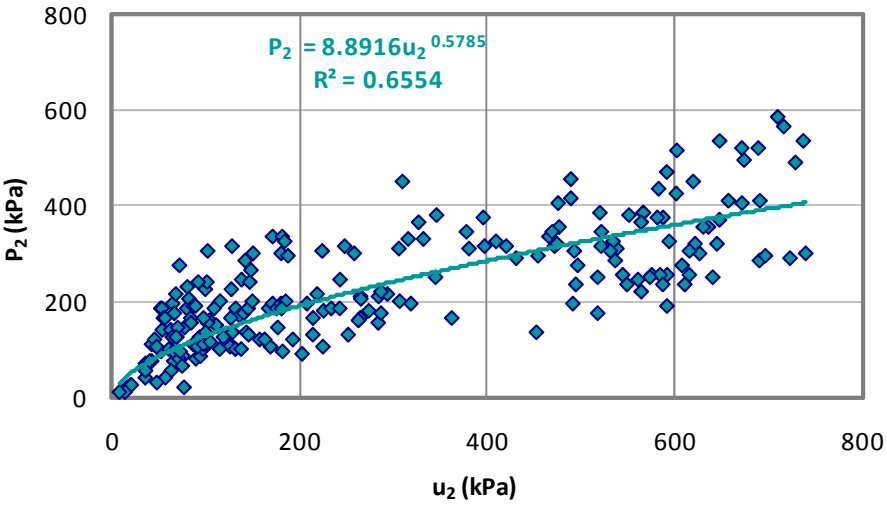


Figure 5.39 - P_2 (DMT) - u_2 (CPTU) comparing results

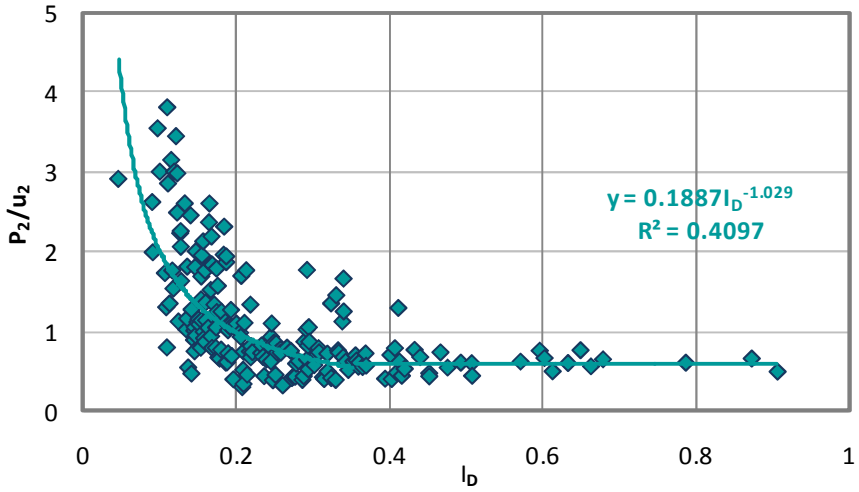


Figure 5.40 - Variation P_2 / u_2 with I_D in fine grained soils.

Pore Pressure Index, U_D, evaluations are presented in Figure 5.41, with the black line representing the evolution of mean values for each interval of soils defined by Marchetti (1980) and represented by I_D.

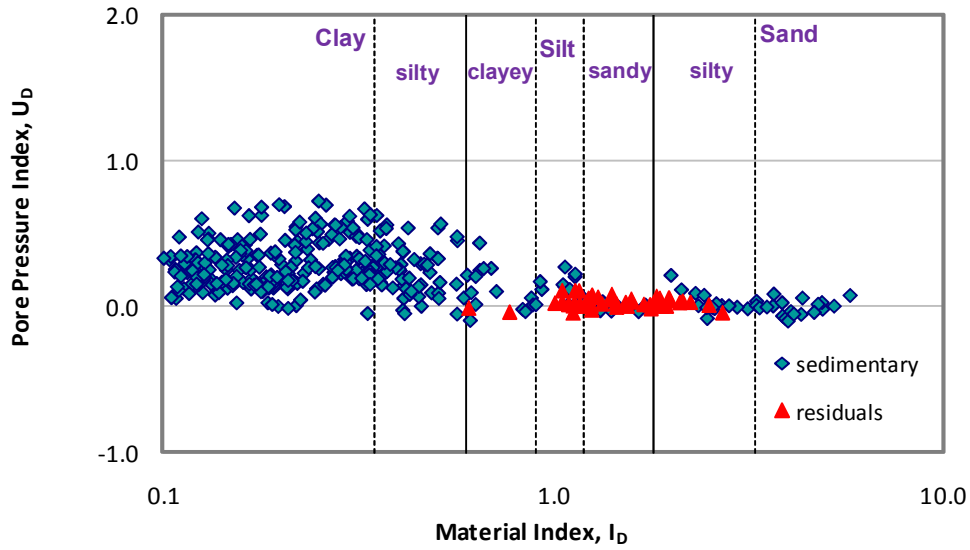


Figure 5.41 - Variation of U_D with I_D

The respective data suggests the following considerations:

a) Pure undrained conditions are settled for soils with $I_D < 0.35$, meaning clayey soils; within this interval, U_D decreased globally from a maximum of 0.65 to 0.25;
b) Pure drained behaviour ($U_D = 0$) was identified for soils with $I_D > 1.8$, meaning sands to silty sands;
c) Partially undrained behaviour (transition curve) for the intermediate soils, have shown U_D values decreasing from 0.25 to 0, with growing values of I_D.

5.7. Unit Weight (combining E_D and I_D)

Another valuable parametric determination is the unit weight, since it is (directly or indirectly) needed in some DMT calculations, namely for initial stresses, and also because it is a primary value for any geostatic stress state dependent analysis. Marchetti and Crapps (1981) combined E_D and I_D parameters to establish the chart of Figure 5.42 to evaluate the unit weight of the soil. Theoretically, this combination offers interesting potential for successful unit weight evaluation, since it combines type of soil (I_D) and stiffness (E_D),. Therefore, it reveals a great potential to represent void ratios, and consequently unit weight.

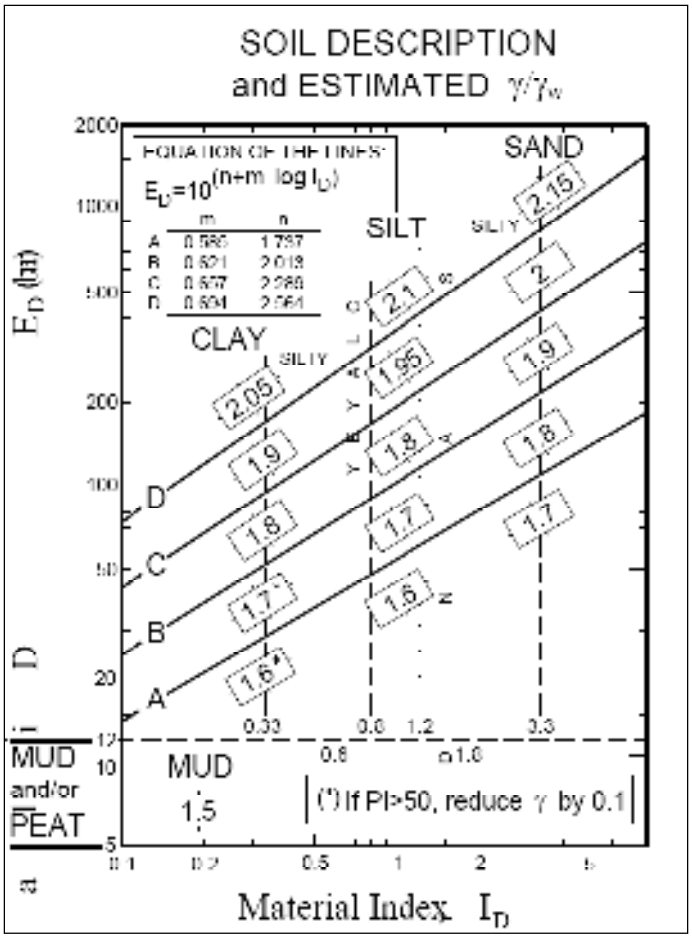


Figure 5.42 - Soil unit weight after Marchetti & Crapps (1981)

Portuguese data obtained in laboratory from undisturbed samples (Cruz et al., 2006a) revealed variations globally less than 1kN/m^3, and only in a few cases $\pm$2kN/m^3 (Figure 5.43). Of course, in sandy soils undisturbed sampling is very difficult, so the results reflect mainly cohesive soils (clays and silts). Despite these discrepancies, the results show reasonable accuracy for vertical effective stresses evaluations, turning the test more independent from external factors and/or more efficient than a simple “best guess evaluation”. In soft clays, Lacasse & Lunne (1988) compared values estimated by this proposal with those obtained from high quality laboratory samples direct measurements and concluded that the chart tends to underpredict results.

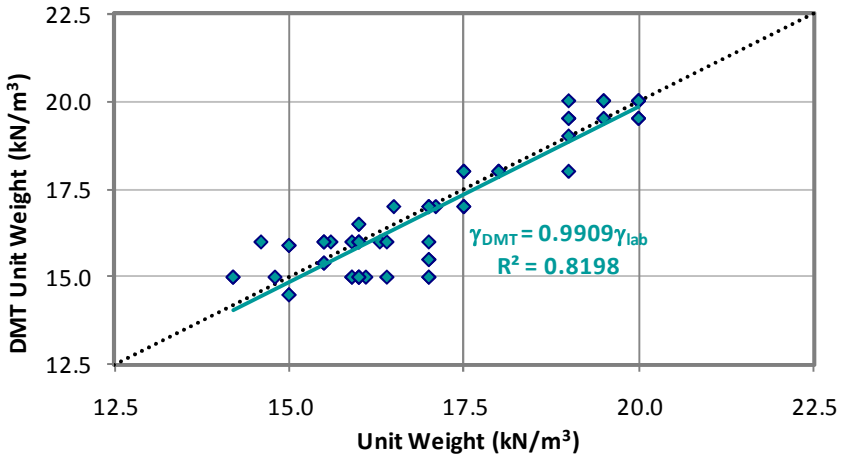


Figure 5.43 - Unit Weight comparisons

5.8. Summary

The main important conclusions arising from the presented work can be summarized as follows:

a) Classification of soils can be made through a quantitative value (I_D), which represents an important tool for numerical data analysis and to interpret mechanical behaviour of difficult soils, such as intermediate (mixed) soils or residual soils;
b) Possibility of determining water level depth in sandy soils and to distinguish drainage types from U_D, which can also be used to cross-check I_D classification;
c) The evaluation of stiffness properties is supported by Theory of Elasticity and numerical values are obtained by a high resolution measurement system;
d) K_D can represent well stress state, since it is obtained from a lift-off horizontal pressure and its calculation can be associated to in situ at rest stress state (K_0); moreover, the respective profile is very similar to OCR evolution and therefore, it provides valuable information on the stress history of clays and, density of sands;
e) As a consequence of the previous, K_D can also be indirectly used to derive strength properties through OCR (undrained shear strength) or coefficient of horizontal stress (drained angle of shearing resistance); OCR can also be used to derive cohesion intercept in residual soils, as discussed in Chapter 7;

f) The combination of some or all those parameters can simultaneously represent the influence of type of soil, stiffness, density and pore-pressure;
g) Since the basic determinations are at least two (P_0, P_1), it is expectable that it could be used to evaluate angle of shearing resistance and cohesion intercept in intermediate and overconsolidated materials, characterized by cohesive-frictional behaviour.

On the other hand, combining tests generates important possibilities for assessing information that otherwise couldn't be attained, as well as for cross-checking results. Besides, due to a very similar form of execution, the combined use of information of penetration processes and dilation of membranes is easy to implement in the field.

Portuguese data obtained in the last 15 years, resulting from a great variety of laboratory and in-situ tests, revealed its adequacy for geotechnical characterization, as presented below:

a) DMT gives accurate definition of soil stratigraphy and unit weight, following the general patterns described above;
b) P_2 correlates well with u_2 from CPTu, and the ratio between them seems to decrease with increasing I_D;
c) At rest earth pressure coefficient, K_0, derived from DMT was concluded to be reliable, both by ϕ' and OCR correlations (Mayne, 2001) and OCR in combination with IP (Brooker & Ireland, 1965);
d) Angles of shearing resistance deduced from DMT (Marchetti, 1997) matches well those obtained from CPTu solutions (Robertson & Campanella, 1983), with DMTs being slightly conservative;
e) Undrained shear strength showed two patterns, according to the percentage of organic content, which seem to reduce S_u(DMT)/S_u(FVT) ratios; in this case, Roque's (1988) data seem to over predict the peak FVT value, while Marchetti's (1980) correlation tends to underpredict residual FVT values;
f) Constrained modulus, M, derived from DMT reveals high efficiency, confirming the international observations and conclusions on the subject;
g) Small strain modulus, G_0, seems to correlate well with E_D, presenting rates similar to Tanaka & Tanaka's data for clayey soils and to Jamiolkowski and Baldi´s data for silica sands; data also revealed that G_0/E_D can be successfully calibrated by I_D and K_D, and revealing the utility of the former to control changing behaviours with fine content increase.

What I hear, I forget
What I see, I remember
What I do, I learn

(Confucius)

PARTE B – THE RESIDUAL GROUND

Chapter 6. Geotechnical characterization of Porto and Guarda granitic formations

6. GEOTECHINCAL CARACTERIZATION OF PORTO AND GUARDA GRANITIC FORMATIONS

6.1. Introduction

The whole experience in which the present research work is based relied upon residual soils from granites, quite often used in cemented soil frameworks. In fact, the great majority of DMT in-situ residual data was collected in Porto Granitic Formation, while the controlled experience presented in *Part C – The Experience*, was carried out on residual soils from Guarda Granitic formations.

The information about Porto granites is rich and abundant, due to the existence of a geotechnical map (Porto Geotechnical Map, here designated as PGM) that covers the urban area (COBA, 2003), becoming a very useful tool to study mechanical evolution through weathering presented in this chapter. Although one should be careful interpreting this data (due to its diverse origin), it globally allows for the identification of the most important physical and mechanical trends, thus finding trustable global behaviour evolution with weathering. Taking this into account, PGM (COBA, 2003) data will be presented in terms of statistic median (considered more robust than mean values) and 1st (25%) and 3rd quartiles, aiming to give a realistic idea of the more frequent ranges.

A relevant research work on these granitic residual soils has been developed in Faculdade de Engenharia da Universidade do Porto, FEUP (Silva Cardoso, 1986; Viana da Fonseca, 1988, 1996, 1998, 2001, 2003, 2004, 2005; Begonha, 1989; Ferreira, 2009; Topa Gomes, 2009), being highlighted by the internationally recognized experimental site (CEFEUP/ISC2, 2004). Also relevant contributions were given by other institutions/contractors, such as Laboratorio de Geotecnia e Materiais de Construção (LGMC) of CICCOPN (Cruz, 1995; Cruz et al., 1997; Cruz et al., 2000, Viana da Fonseca et al., 2001; Vieira, 2001; Ferreira, 2009) and MOTA-ENGIL (Cruz et al., 2004ª, 2004b, Cruz & Viana da Fonseca 2006ª; Cruz et al., 2008, Viana da Fonseca et al., 2007, 2009). In fact, the important construction held in the city during last decade (European Football Championship, European Capital of Culture and Metro do Porto network) offered a opportunity to obtain significant amount of field data and, thus, allowing important research possibilities. This has allowed for the calibration PGM data greatly improving its usefulness either for research or design practice and thus, a

step forward in understanding physical and mechanical behaviour of Porto residual soils. Finally, research work developed in Instituto Politecnico da Guarda, IPG (Rodrigues, 2003; Rodrigues & Lemos, 2000, 2001, 2002, 2004; Rodrigues & Sousa, 2002; Rodrigues et al., 2002), has allowed comparing Porto and Guarda granitic residual soils, particularly important for the calibration work presented herein.

The global characterization of these granitic formations was ordered in terms of geomechanical evolution with weathering, following the criteria presented below:

a) Strength and stiffness variation with weathering is primarily based in PGM data (2003), being organized by geotechnical groups; rock materials will be represented by its weathering degrees (W1 to W5), while residual soils designations respect the references mentioned in PGM (COBA, 2003), namely G8 (compact), G4 (medium compact) and G4K (intensively kaolinized) residual soils, with density levels according to Skempton (1986) classification, based on SPT results;
b) Residual soils from Porto granites tend to show mostly a granular behaviour, but there are three spots of intense kaolinization, where a global clay matrix takes control (G4K); this situation represents both the lower limit of stiffness and strength and the upper limit of weathering degree of local soils; therefore, it is of relevance to define its basic mechanical behaviour; for this purpose, due to different criteria used in borehole descriptions, PGM data seems to mislead G4K and G4 and so it was not considered; instead, G4K ranges were obtained in one of the above mentioned kaolinized spots (Senhora da Hora), where experimental data was obtained and controlled by the author (Technical Report BDF 10/05, 2005 – Porto Metro Network);
c) Data related to the same geological and geotechnical units obtained by CICCOPN and MOTA-ENGIL in their regular activities, was used to enlarge the global characterized ground and also to cross-check with PGM data; finally, CICCOPN, Hospital de Matosinhos and CEFEUP experimental sites provided high quality data very useful for the calibration point of view; this sequence ensured the control of PGM data ranges creating an important and efficient tool in deducing geotechnical parameters, not only for the present work but also for supporting practical design applications;

Guarda available information was compared to the whole package of Porto numerical data in order to place the former within weathering levels defined for the latter and to establish a cross-link between previous DMT testing and the calibration experiment.

In Table 6.1 adopted designations throughout this document are presented, in order to identify main units and experimental sites. The overall existing results will be presented in the course of this chapter, with exception to DMT (alone or combined with CPTu) results that will be treated separately in the next chapter.

Table 6.1 – Adopted class designations in the present work

Unit / Experimental site	Designation	References
Unweathered rock	W_1	ISRM
Slightly weathered rock	W_2	
Medium weathered rock	W_3	
Weathered rock	W_4	
Highly weathered rock	W_5	
Compacted residual soil	G8	PGM (COBA, 2003)
Medium compacted residual soil	G4	
Loose residual soil	G4K	Cruz, 2005
CICCOPN/MOTA-ENGIL data	CME	Cruz e tal., 2004a, 2006b
FEUP experimental site	CEFEUP	Viana da Fonseca et al., 2004
IPG experimental site	IPG	Rodrigues, 2003
Casa da Musica Metro Station (Porto network)	Av. França	Viana da Fonseca et al., 2007, 2009

6.2. Geology

6.2.1 Porto Region

The north-western region of Portugal is largely dominated by upper layers of residual soils from different nature, namely originated in granite and schist. The field work for the present research is located in Porto Metropolitan area, including Porto, Gaia, Matosinhos, Maia, Vila do Conde and Póvoa de Varzim, where Porto Granite Formation is dominating.

Globally, the geomorphology associated to this area is based in a set of hills that are going smoothly down in height towards the Atlantic Ocean, while the Douro valley is confined by abrupt side walls. Up north, after the Ave Valley, the platform is covered by marine erosion deposits that cover the Granite of Póvoa de Varzim. In Figure 6.1 the global studied area is presented.

The overall platform defines a hercinic NW-SE alignment and is laterally confined by two metamorphic complexes: Schist – Grauvaquic Complex at Northeast and Foz-do-Douro Metamorphic Complex at Southwest. It is interesting to observe that the latter is connected with the fault Porto-Tomar, one of the main geotectonic contacts of Iberian Peninsula that divides the Centre-Iberian Zone to the Ossa-Morena Zone of the old Hesperic massif. The studied area is placed in the border of the former. In general, it can be said that actual topography is the result of a long surface modeling, starting at the end of Hercinic orogeny (270 million years ago). Porto Granites are approximately 300 million years old and were installed of around 10 km depth. Due to the joint and fault systems generated by Hercinic or later movements, the granitic mass has arisen way up to the surface where it mostly rest today. In Figure 6.2 regional geology of the whole area included in the present work is presented, while Porto Granite Formation is shown in Figure 6.3, as represented in *Carta Geológica de Portugal* (1:1.000.000 and 1:25.000). In both figures, granites are represented by pink and orange spots, while green spots represent the Schist – Grawack complex



Figure 6.1 - Partial views of the studied area: a) from south; b) from west.

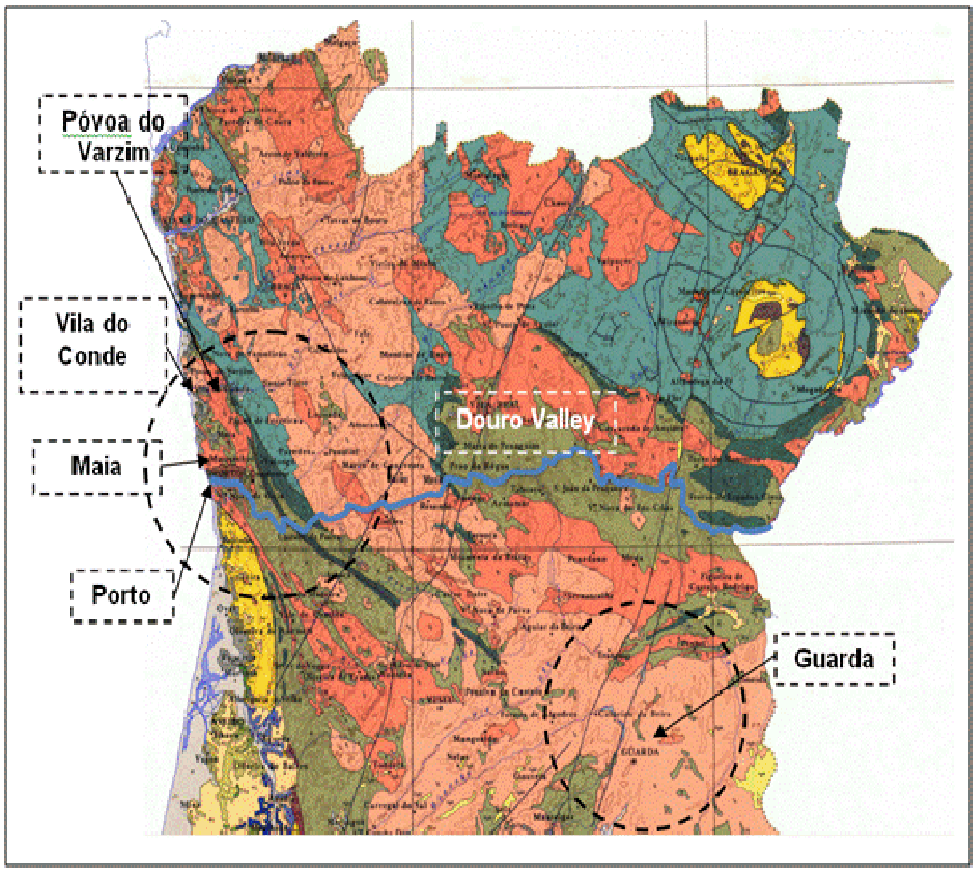


Figure 6.2 - Geologic Map of Portugal (1:1.000.000)

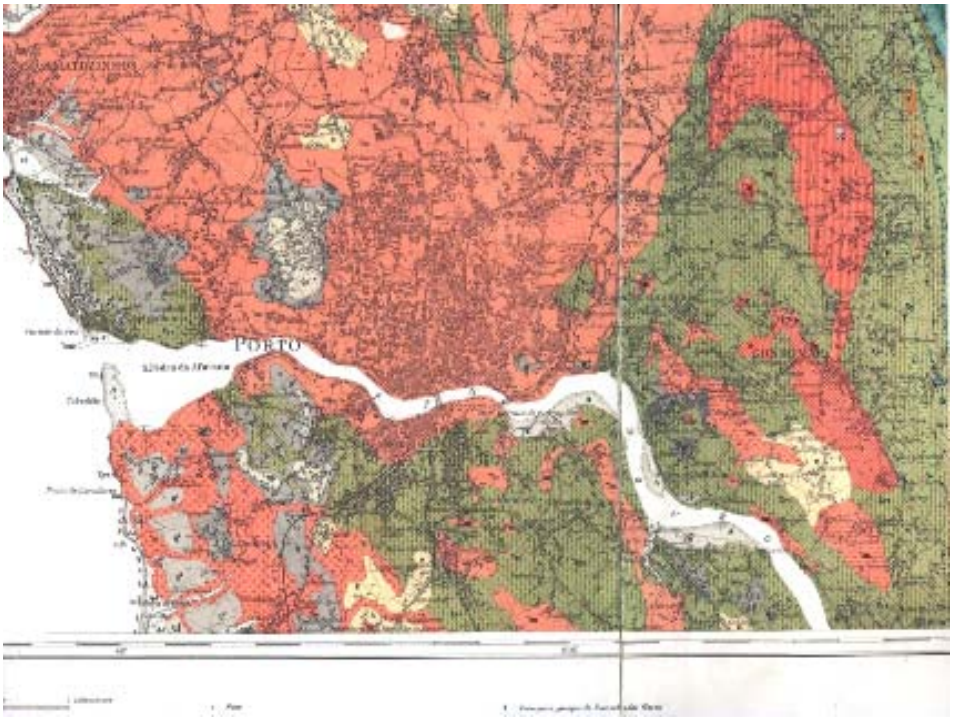


Figure 6.3 - Geologic Map of Porto (1:25.000).

The fundamental geological Porto unit (Porto Granitic Formation) can be described as a leucocratic alkaline rock, comprising a mixture of glassy quartz, white alkali-feldspar often in mega-crystals, biotite and muscovite with the latter prevailing, white sodic plagioclase and minor amounts of dark minerals. The alkali feldspar usually presents the higher grain size and is mostly orthoclase, sometimes microcline. As for plagioclases, oligoclase-albite and albite are commonly present (Begonha, 1989; PGM, 2003; Viana da Fonseca et al., 2004). Other variations of the main formation are present, showing small differences and having a minor representation, such as the Granite of Contumil (mega-crystals of feldspars), Granite of Póvoa de Varzim (sometimes with a gneissic texture), and the Granite of Campanhã, all showing gradual transitions to the main body.

The residual soils arising from these formations are the result of mechanical and chemical weathering, respectively by means of grain dismantling and hydrolysis of K-feldspar and Na-feldspar, which lead to the formation of kaolinitic clay, while quartz and muscovite remain stable due to their high weathering resistance. Biotite (and amphibole, if present) undergoes oxidation to form iron oxides. The consequent soil is sand evolved by a kaolin matrix with frequent less-weathered rock boulders. The natural particle arrangement is characterized by more or less open voids on a cemented structure.

The relation of all these transient constituents to the stable amount of quartz is usually used as a classification index, but other primary elements such as zircon and tourmaline can also be used (Ferreira, 2009). As it was stated, Lumb (1962) petrographic index (X_d) is the only one that can be used with some geotechnical expectations. The values obtained for the respective index in residual soil from Porto range between 0.59 and 0.63 (Viana da Fonseca, 1996), reflecting high degrees of weathering, as presented in Figure 6.4.

From mechanical point of view, Porto granitic masses are very complex and mostly characterized by its gradation from upper levels to lower sound rock, improving its behaviour with depth. Typical weathering profiles in the area show a global decrease of its levels to deeper sound rock, and so, inherent improvement of its geomechanical properties, from upper residual soils to the correspondent slightly weathered (W_2) rock. Commonly the weathered zones are very irregular in extension and magnitude, showing quite frequently the presence of granitic boulders inside highly weathered masses. This is related to the characteristics of discontinuities, especially its spacing,

allowing water to flow into and through, thus accelerating chemical processes and creating differential weathering.

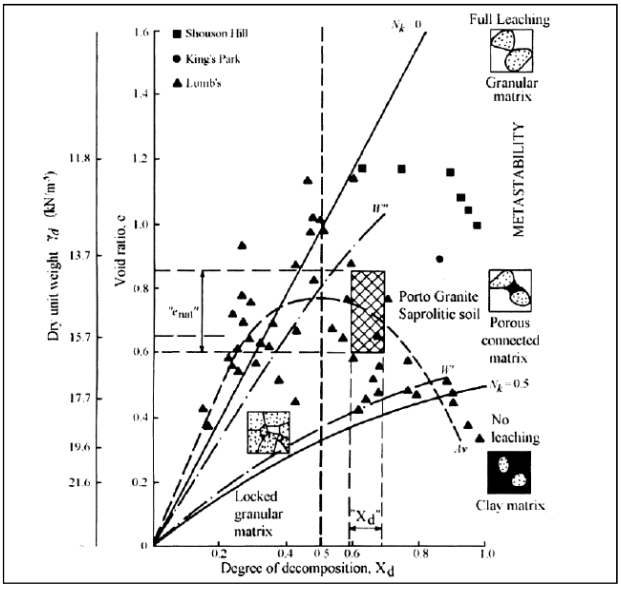


Figure 6.4 - Microstructure characterization by degree of decomposition (Viana da Fonseca, 2003).

In general, the usual local profile fits in Little (1969) reference profile, and can be described as follows:

a) A thin layer of top soil (< 3.0m);
b) A thick layer of medium compact residual soil, referenced by N_{SPT} values ranging between 10 and 30 blows (G4), often followed by a compact transition layer corresponding to N_{SPT} between 30 and 50 (G8), where the marks of old joint alignment are not present (Figure 6.5); according to PGM data (2003), this medium compact layer can reach 15 to 20 m of thickness and it's common to find boulders within this soil mass; the transition layer tends is thinner than 5m.



Figure 6.5 - Typical residual medium compacted to compacted residual soils from granite

c) Decomposed (W_5) to highly weathered (W_4) rock massif, where the traces of old joint alignment can be observed, represented by N_{SPT} values typically higher than 60. When remoulded, the resulting soil presents the same basic properties (grain size, Atterberg limits, compaction properties, etc) of those referred in (b). The main differences in natural state are the presence of joints and a stronger cemented matrix (Figure 6.6).



Figure 6.6 - Typical decomposed to highly weathered granite

d) Medium (W_3) to slightly weathered (W_2) granite (Figure 6.7)



Figure 6.7 - Typical medium weathered granite

Although this may suggests an homogeneous evolution with depth, these formations show erratic profiles (Figure 6.8), either horizontally or with depth as a consequence of diverse weathering factors, such as composition of the parent rock, intensity and continuity of joint systems (in other words, degree of water penetration in the massif) and climate conditions. In temperate zones, as it is the case, the water flow into the joints with percolation and seasonal gradients of the water levels represent the main factors for the existence of differently weathered soil. The specific genesis of the soil in each location leads to a high variability of microfabric.

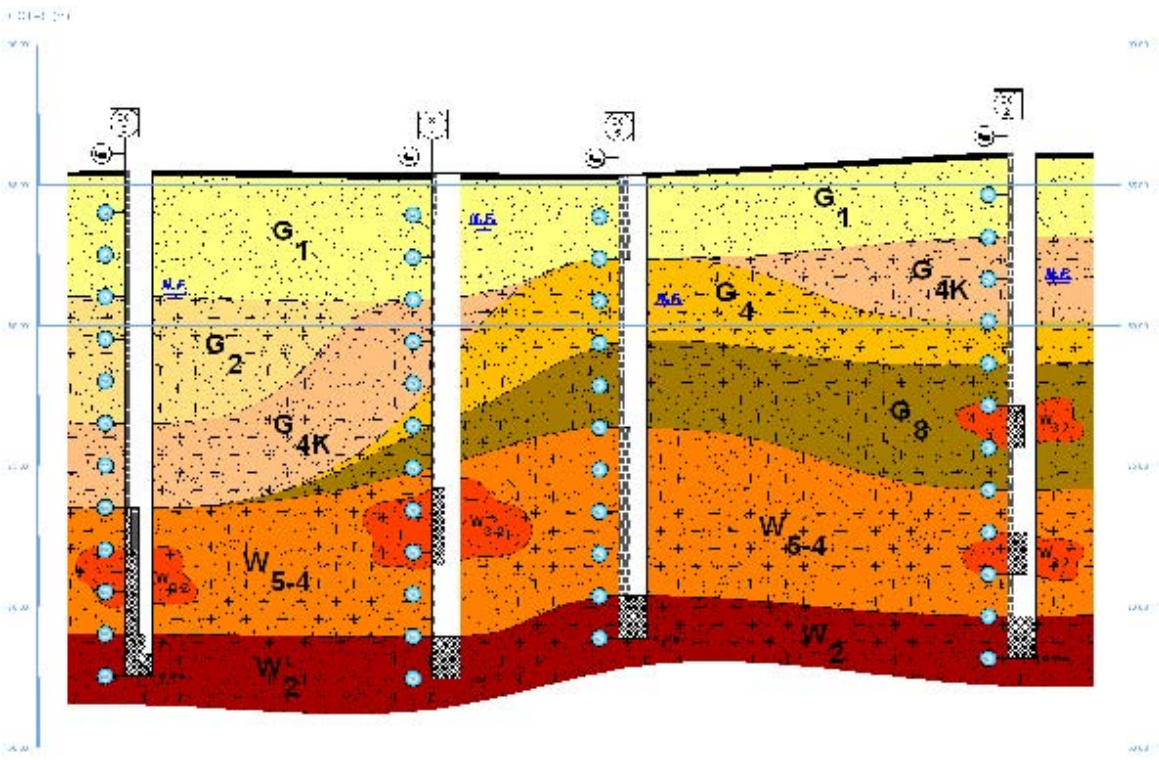


Figure 6.8 - Typical cross section of Porto Granitic Formation showing different weathering degrees

6.2.2 Guarda region

Guarda granitic formation is within the geological complex responsible for the formation of Estrela massif, the highest mountain in Portuguese mainland. The geologic history of the massif started in the Precambric (650 million years) with marine deposition that kept going on through the Cambric (500 million years), followed by diagenesis and metamorphism responsible for the formation of schist and grawack sequences, very typical in Portugal. Afterwards, 3 phases of Hercinic orogeny took place, during which the main granitic mass was developed, followed by erosion and the uplift of the granite masses. Finally, in the Quaternary, the area was submitted to intense glaciation that gave rise to the actual geomorphology. In Figure 6.9 a schematic representation of this history is presented (after Rodrigues, 2003).

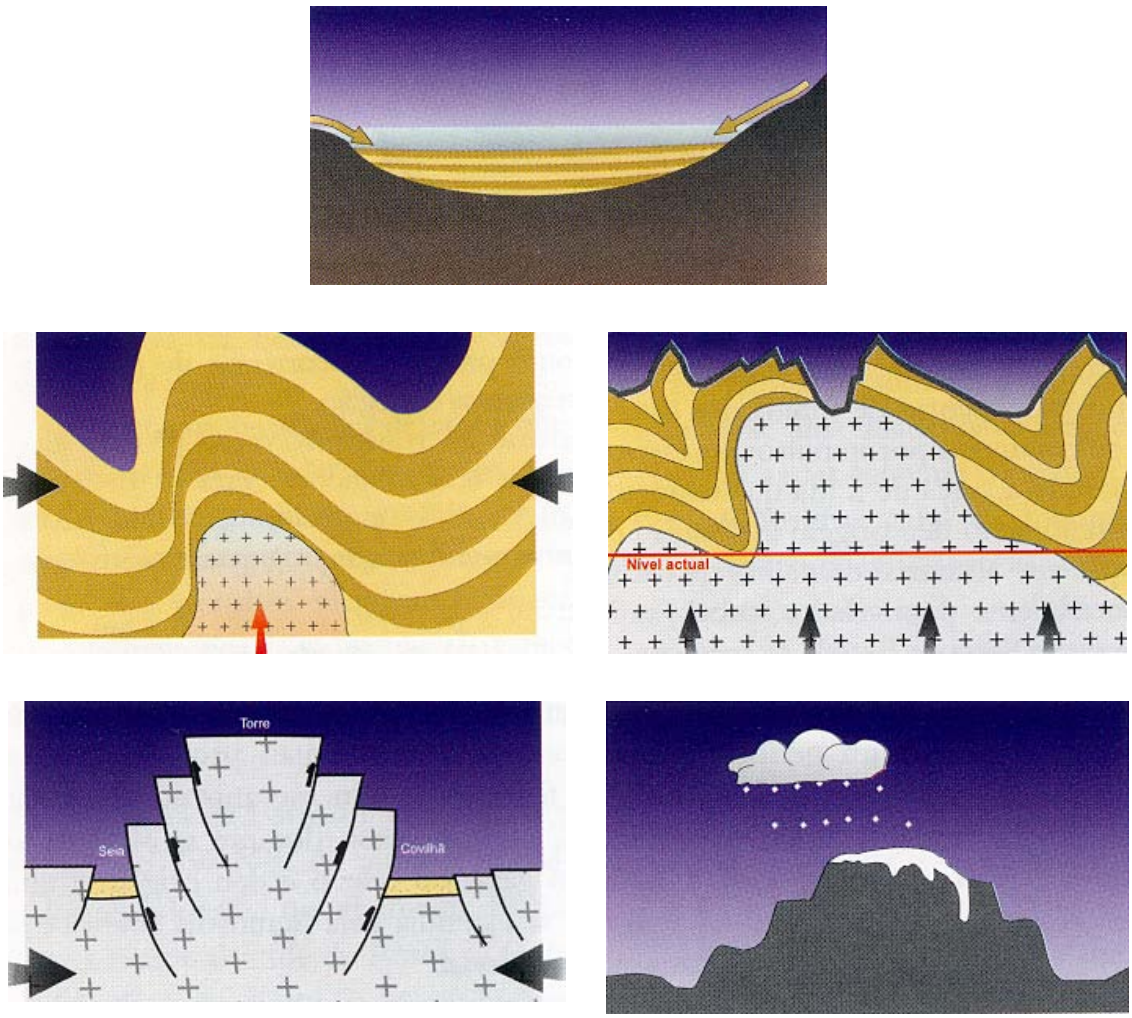


Figure 6.9 -Sequence of geologic evolution of Estrela massif (after Rodrigues, 2003): a) Diagenesis and Metamorphism; b) Installation of granites; c) Erosion and uplift of granitic masses; d) Formation of the mountain complex; e) Glaciation

The city of Guarda is located in a granitic mass designated as Guarda Granitic Formation (Figure 6.10). This geologic unit is constituted by a leucomesocratic granite with quartz (25%), sodic and potassic feldspars (39,1%) commonly in mega crystals), biotite (4,8%) and muscovite (2,6%), and mainly kaolin, sericite and clorite as main secondary minerals (Rodrigues, 2003). The values obtained for the respective index (X_d) in residual soil from Guarda granitic residual soils range between 0.27 and 0.64 (Rodrigues, 2003), reflecting high degrees of weathering, as presented in Figure 6.11. In Figure 6.12, a typical cross-section is presented (Rodrigues, 2003), whose main geotechnical features are very similar to the ones described for Porto Granitic Formation.

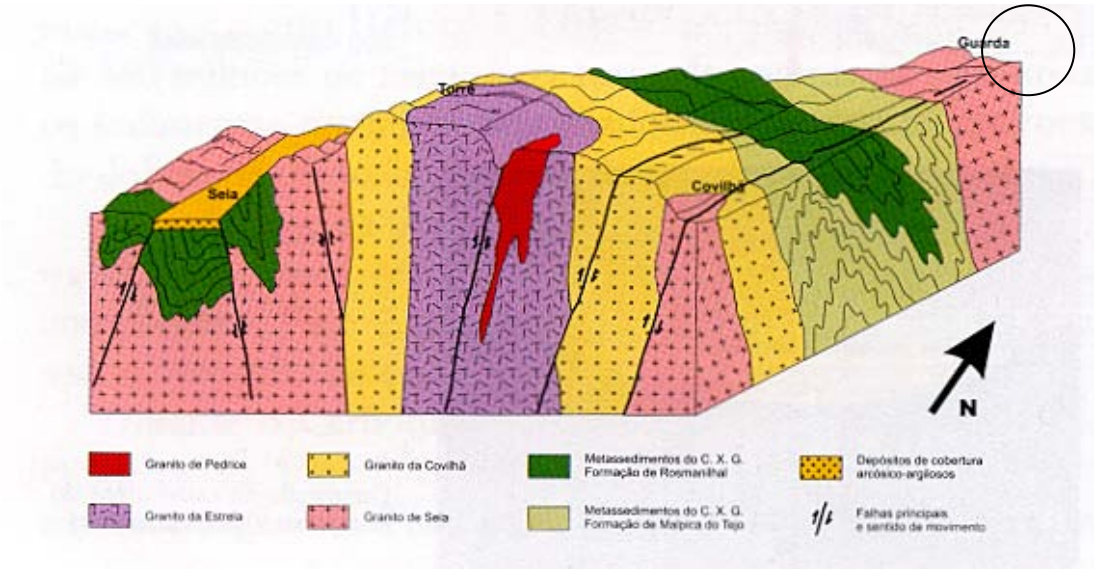


Figure 6.10 -3D schematic diagram of Serra da estrela Geologic complex (Ferreira e Vieira, 1999)

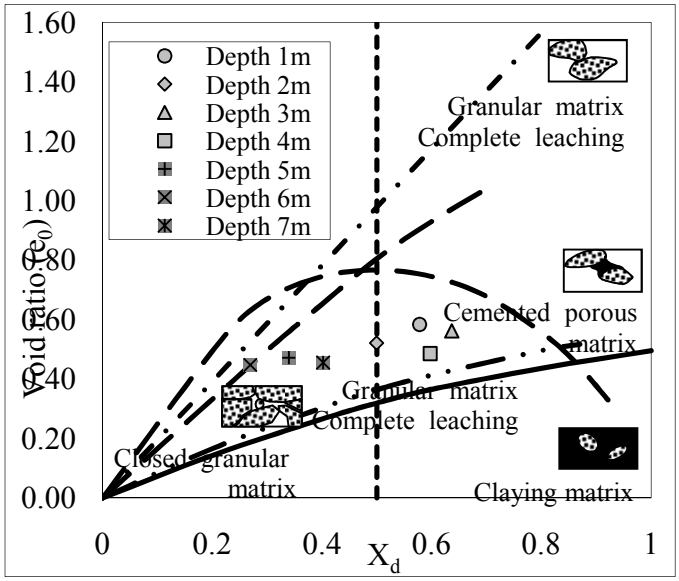


Figure 6.11 - Microstructure characterization by degree of decomposition (after Rodrigues, 2003).

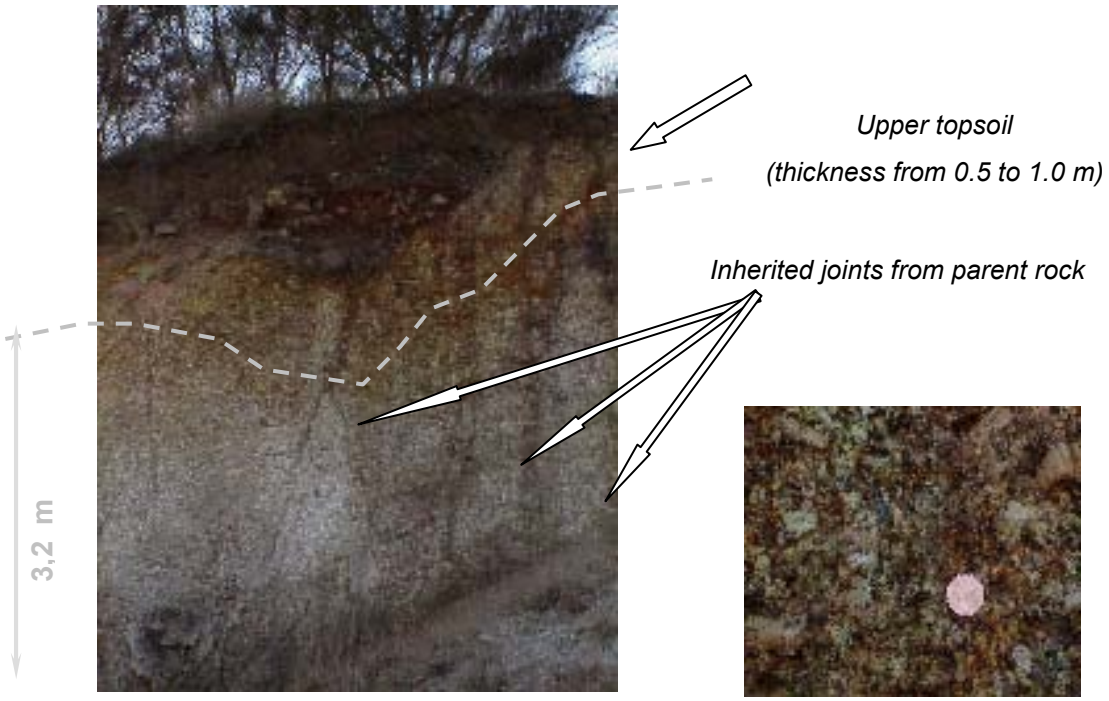


Figure 6.12 - Typical cross-section of Guarda residual soils (after Rodrigues, 2003)

6.3. Sampling disturbance and quality control

Sampling is a critical process for ensuring the quality of laboratorial test results, as discussed in Chapter 3. Sampling disturbance evaluation in residual soils is even more complex than in sedimentary soils, since besides the typical problems related to stress release and possible generation of differential pore pressures, it deeply affects the cementation matrix to an unknown extent. Naturally this has a strong influence in measured strength and stiffness parameters. It is not our purpose to go deeper in the subject, since laboratory testing was performed over artificially cemented soils, within this research work. However, it is important to highlight the relevant work that is undergoing in Porto (Viana da Fonseca & Ferreira, 2002; Viana da Fonseca et al., 2006, Viana da Fonseca & Coutinho, 2008; Ferreira, 2009) and Guarda (Rodrigues, 2003; Rodrigues & Lemos, 2003, 2004) granites, whose conclusions on the influence of sampling and laboratory testing preparation in strength and stiffness behaviour can be summarized as follows:

a) Sampling using open tube samplers induce significant disturbance of the soil structure;

b) Sample quality improves significantly when using samplers with a bigger diameter (100 mm) than the triaxial sample (70 mm) and carefully molding down the sample to the pretended diameter;
c) Block sampling is normally accepted as the best technique to obtain undisturbed samples; however, if the right methodology of sample preparation is not used for light cemented soil, the end quality can be poorer than the obtained through the 70 mm open tube sampler;
d) Sampling and sample preparation methodology influences the respective quality by decreasing shear resistance and stiffness, and by increasing the stress strain non-linearity as a result of an increase of the deformation to attain the peak;
e) When soil stiffness results are obtained from Cross-Hole and triaxial testing with internal measurement, respective results can be within the same order of magnitude, if the quality of the undisturbed sample is high, or if an artificially cemented soil is used;
f) Artificially cemented soils show great potential as a physical model to investigate the behaviour of granite saprolitic soils.

Also relevant is the recently published research work of Ferreira (2009) on sampling disturbance in Porto residual soils. Working in two experimental sites of the present research (CEFEUP and CICCOPN), Ferreira (2009) observed significative discrepancies between laboratory and in-situ shear wave velocities, as presented in Figure 6.13 and 6.14. As a result, a fundamental contribution to control laboratorial data through a sample quality classification was proposed based in shear wave velocity (vs*) normalized to the respective void ratio (Table 6.2)

Table 6.2 - Classification for sampling quality and sample condition (Ferreira, 2009)

Quality Zone	% Loss in Vs*	Vs*lab/Vs*in-situ	Sample quality	Sample condition
A	< 15%	>0.85	Excellent	Perfect
B	15% - 30%	0.85 – 0.70	Very good	undisturbed
C	30% – 40%	0.70 – 0.60	Good	Fairly undisturbed
D	40% - 50%	0.60 – 0.50	Fair	Fairly disturbed
E	>50%	>0.50	Poor	Disturbed

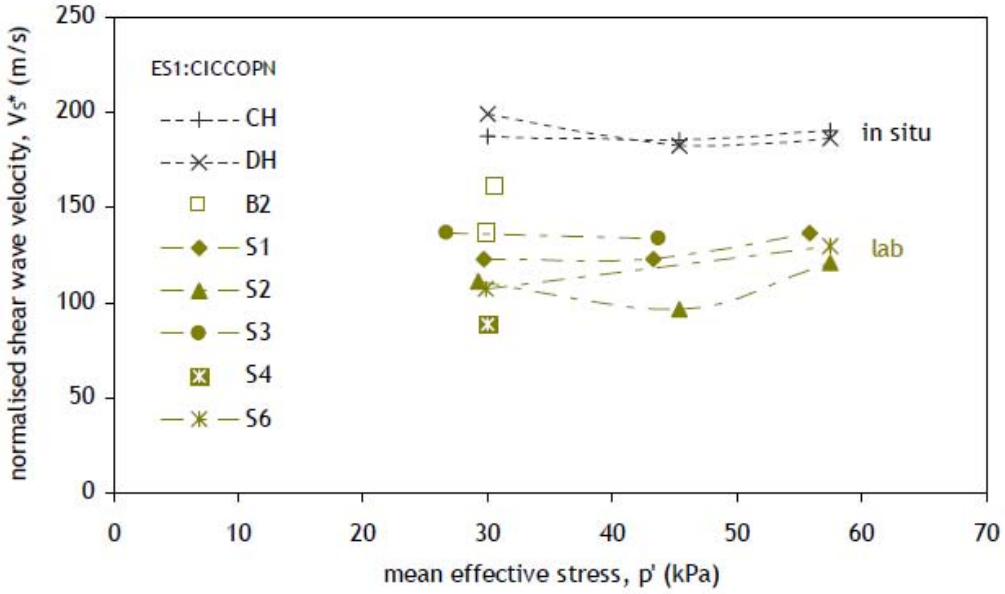


Figure 6.13 - Normalized shear wave velocities CICCOPN specimens (after Ferreira, 2009)

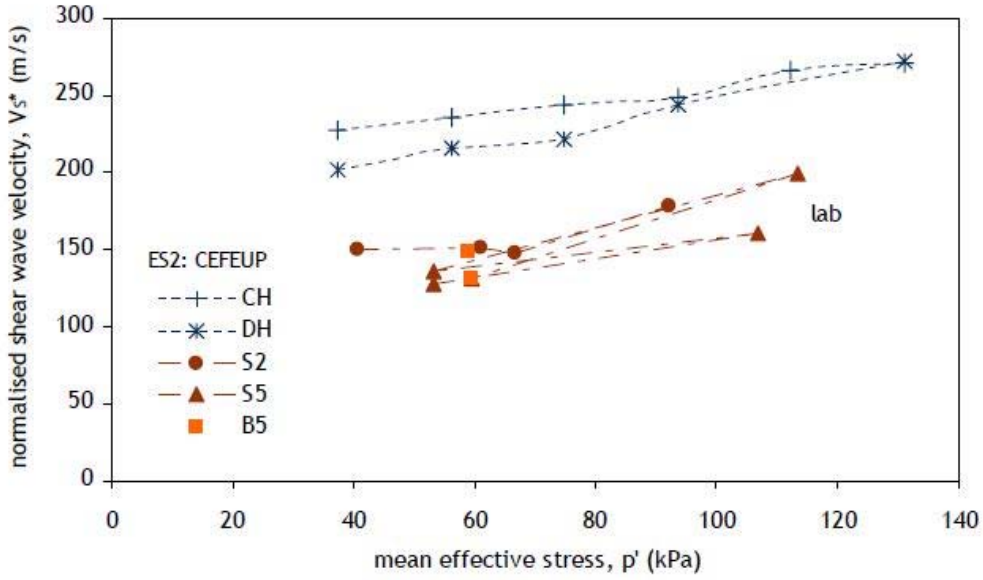


Figure 6.14 - Normalized shear wave velocities CEFEUP specimens (after Ferreira, 2009)

6.4. Identification and classification

Identification and physical properties of local soils and highly weathered rock massifs are abundant, since its determination is usually included in regular geotechnical campaigns, and also because of their good ability to use in earthfills. Identification undertaken by sieve analysis reveal that these soils are mostly classified as sandy silts to silty sands, sometimes clayey sands, with generally low plasticity, which has been widely confirmed by CPTu and DMT classifications. Figure 6.15 represents 290 grain size distributions associated to the geotechnical units of PGM (COBA, 2003), showing a well graded material, where fine content increases with weathering degree. CEFEUP data shows a mean grain size curve that fits in this global behaviour, while Guarda's seems to represent a lower bound (coarser grained) of the three sets of data, confirming the differences observed in the respective parent rocks. Guarda grain size coefficients show C_u values higher than 100 and C_c varying between 1 and 3, both higher than CEFEUP (0.8 a 1.5) and G4K of PGM (0.5 to 1.0).

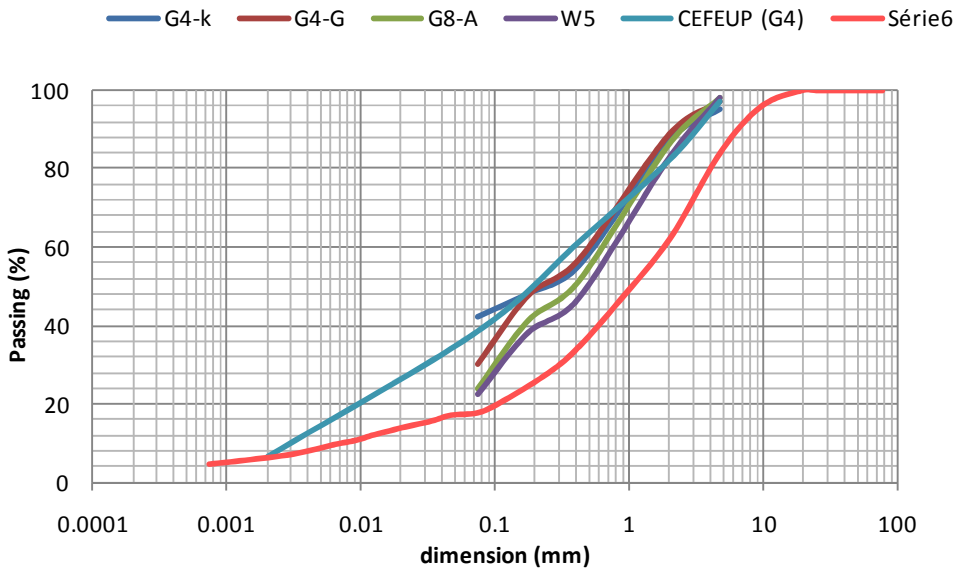


Figure 6.15 - Grain size distribution

In Figure 6.16, relative frequencies of Atterberg limits of the various geotechnical units and reference experimental sites are presented, obtained from 220 tested samples. A general distribution of the results in Casagrande chart is presented in Figure 6.17.

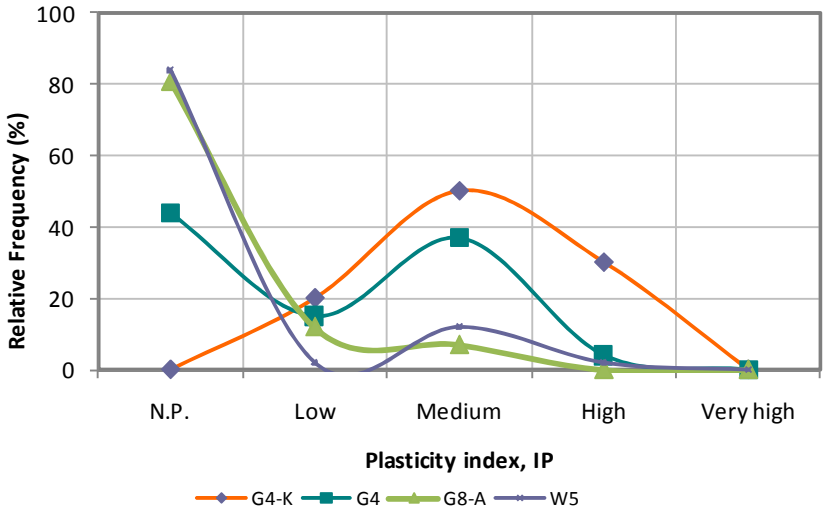


Figure 6.16 - Plasticity Index, IP

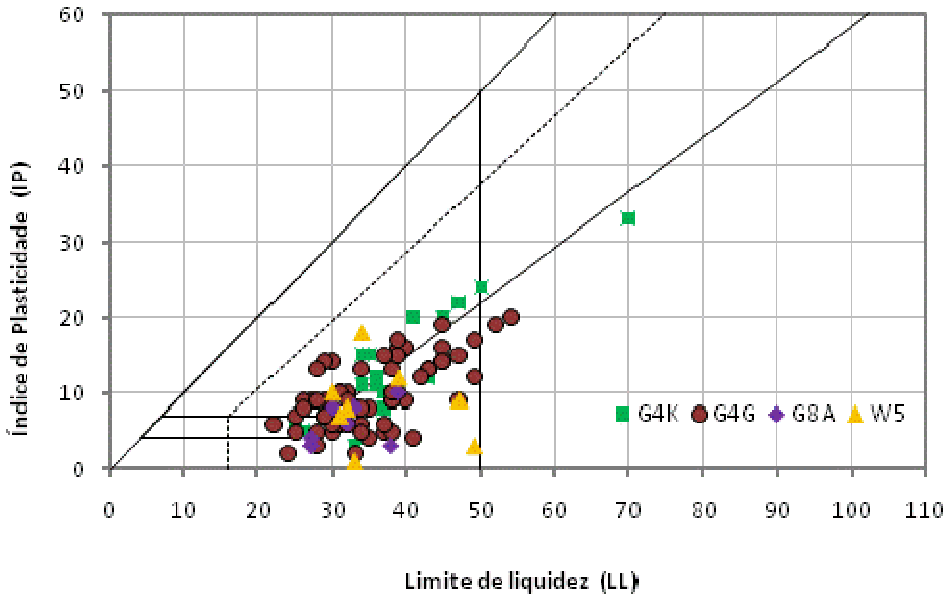


Figure 6.17 - Representation of consistency limits in Casagrande Chart

The global results suggest the following observations:

a) Presence of high percentage of non-plastic or low plasticity soils in G4 and G8 units, while G4K is represented by medium plasticity;

b) CEFEUP soils are placed within G4 limits, while Guarda exhibits a rather curious high plasticity (IP 15-20%); this observation is supported by activity index (At) results, which in Guarda is within 1.5 and 3.0, while in Porto (ISC2 and Srª da Hora-G4K) varies from 0.5 to 1.0; these results converge to the expected kaolinite – ilite type of clay (0.5 to 1.5) in Porto soils, while Guarda

soils seem to be slightly more active than the typical behaviour of these type of clays;

c) Globally, identification tests (grain size distribution and Atterberg limits) reveal that for high density levels (G8) the soils tend to be non-plastic, with lower fine content (generally below 30% passing #200); for higher weathering degrees, as a result of chemical weathering of feldspars into clay, fine content and plasticity gradually increases, up to respectively 40% fine content and medium to high plasticity in G4K (maximum found IP of 17%);

d) Another interesting observation is that the ratio <0.002 mm / #200, here designated as clay-fine ratio, CFR, can possibly be explored as an index parameter for the intensity of weathering and might be related to some engineering properties; in fact, since the fine content is generally produced from the weathering of original feldspars crystals and the maximum weathering level should be represented by clay, the referred ratio can be seen as a proportion of particles in late stages of weathering in relation to a reference mass (passing #200) of potential weathering material; although PGM data (COBA, 2003) only include a few sedimentation grain size analysis, but CEFEUP, Guarda and G4K experimental results support this proposal, with the first two (G4) showing CFR ranging between 10 and 25%, while in the latter the ratio is clearly higher, from 30 to 40%, which is in accordance with Triangular Classification indexed behaviour.

From the classification point of view, ASTM Classification for Engineering Purposes (D2487, 1998) and AASHTO Classification (American Association of State Highway and Transportations Officials) were applied, showing a high percentage of silty sands (SM), with 70 to 90% of relative frequency. As suspected, soils with high kaolin content (G4K) are an exception, showing clayey sands (SC) and silts of low plasticity (ML). As for the AASHTO classification, unit G4K ranges from A-4 to A-7, while the remaining (G4 and G8) are almost exclusively A-1 and A-2, showing why these latter are the most convenient soils for earthfills.

However, these classifications are not fully applicable to residual soils, as widely recognized by residual soil researchers. From the engineering point of view, the classification proposed by Wesley (1988) adapts better to these soils, and thus a special emphasis will be given to this subject. For now, it is only important to keep in mind that the all range of soils in this framework belong to Group A of Wesley Classification, representing soils where mineralogical influence is small.

6.5. Physical Properties

Physical parameters with influence in strength and stiffness behaviour such as porosity, void ratio and unit weight show a global increasing void ratio and porosity and decreasing unit weight, with weathering. The available laboratorial testing results provide important information on the evolution of unit weights (dry, solids and total), void ratio (soil) and porosity (rocks) with weathering, representing respectively 172, 83 and 62 samples.

Figure 6.18 represents the evolution of solid, dry an total unit weights with weathering. Solids unit weight remains fairly stable throughout weathering and can be seen as a unit weight upper bound. Dry and total unit weights reveal a more or less stable value within G4 and G8, increasing towards W_3 from where it remains fairly stable up to W_1, approaching the value of solids unit weight. Figure 6.19 and 6.20 seem to corroborate these results showing stable porosities from W_1 to W_3 levels, where a sudden break is observed as a consequence of weathering extended to whole massif (W_4), stabilizing again for higher degrees of weathering. This observed trend is supported by Baynes & Dearman conclusions (1978) research with electronic microscope. CEFEUP and CME data confirm results within G4 (PGM, 2003).

Referring to the same geological environment, Viana da Fonseca et al. (1994) presents a summary of the main physical properties of Portuguese North-Western granites, which are in accordance with the discussed ranges (Table 6.3).

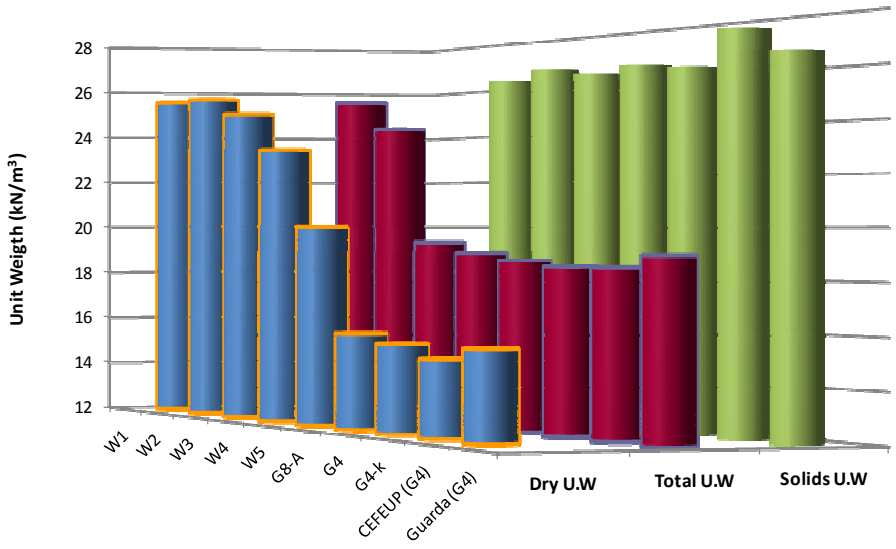


Figure 6.18 - Representative unit weights in Porto and Guarda Granite Formations

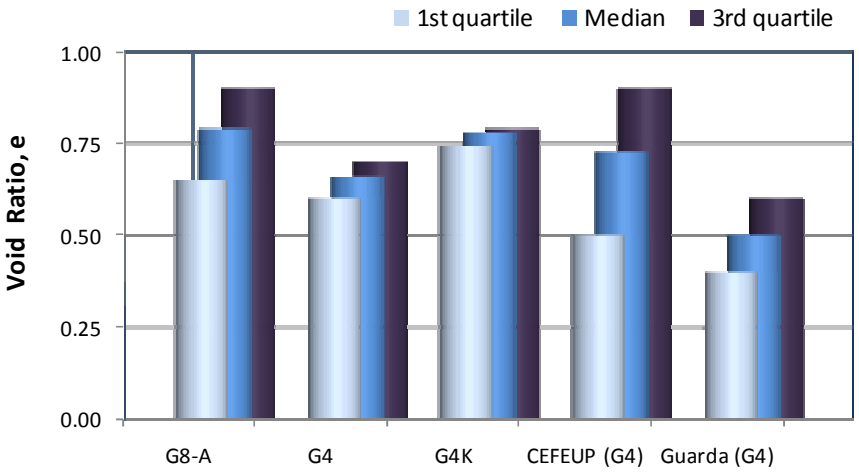


Figure 6.19 - Representative void ratios in Porto and Guarda Granite Formations

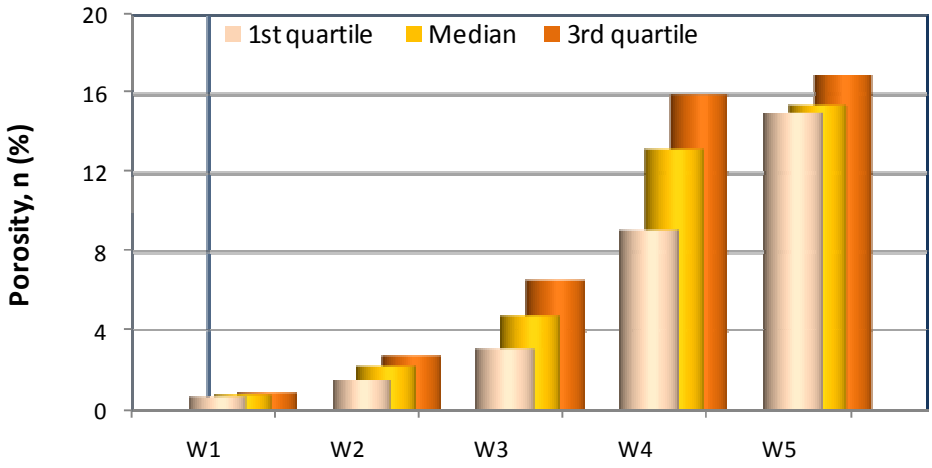


Figure 6.20 - Representative porosities in Porto Granite Formation

Table 6.3 - Typical ranges of granitic physical properties (Viana da Fonseca et al., 1994)

γ_s (kN/m3)	w_L (%)	IP (%)	w (%)	S (%)	e	γ (kN/m3)
25,5 – 26,7	25 – 40	< 13	10 – 30	60 –100	0,40 – 0,85	17,0 – 22,0

From the flow point of view, available permeability results were obtained mainly by in-situ determinations (470 tests against 13 in laboratory), but that is usually considered the most appropriate for characterizing these soils, since both macro and micro-structural variability controls the in-situ behaviour (Costa Filho & Vargas, 1985; Viana da Fonseca, 2003; Ferreira, 2009). The global in-situ trend is represented in Figure 6.21, revealing a slight decrease of in-situ permeability with weathering (higher scatter in lower weathering levels), always in the same order of magnitude, which might be related to the increasing infilling of joints by weathering products and expansions, somehow compensated by the gain in porosity and/or void ratios that will transform fissure permeability (W_1 to W_3) into a global pore permeability (W_4 or higher). In Figure 6.22 data representation in depth is presented, revealing a considerable scatter.

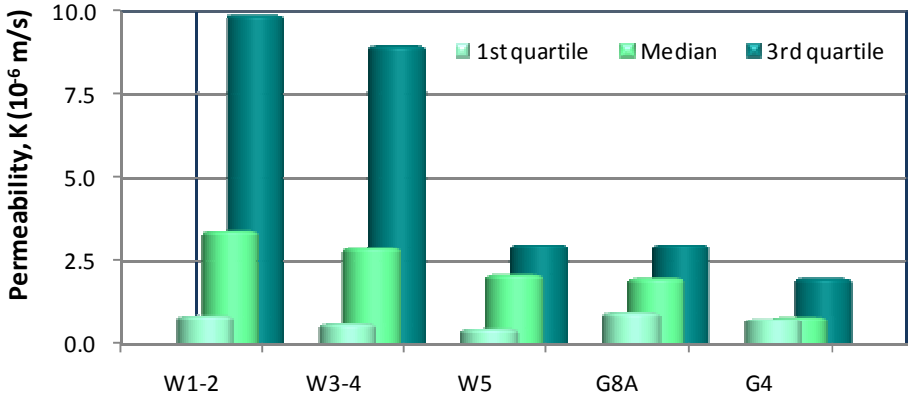


Figure 6.21 - Representative permeability coefficients in Porto Granite Formation.

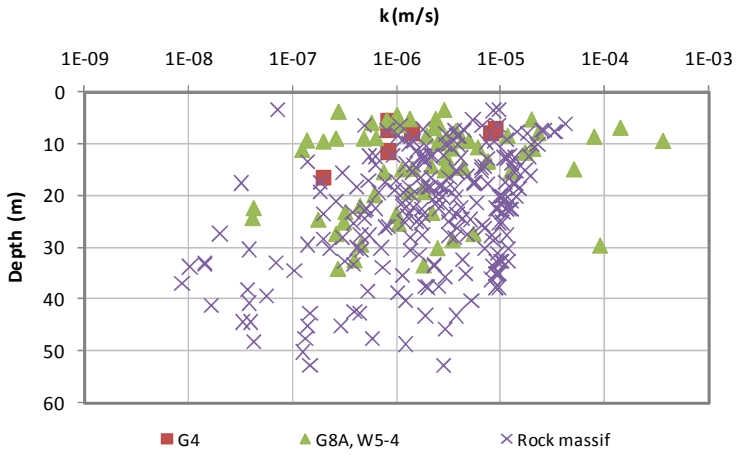


Figure 6.22 - PGM (COBA, 2003) in-situ permeability in Porto Granite Formation.

Table 6.4 resumes a synthesis of extensive experimental data in the urban area of Porto arising for the Metro lines presented by Viana da Fonseca (2003), revealing convergent classification as intermediate permeability (Schnaid et al., 2004; Schnaid, 2005). The main differences between the two data sets are observed in materials were macrofabric become significant (fissure permability), which could be related to different fracturing degrees, not described in PGM data (COBA, 2003). Convergent results were also reported by Ferreira (2009) and Topa Gomes (2009) dealing with the same Porto Granite formation.

Table 6.4 - Trend values of permeability by classes of weathering of Porto Granite (after Viana da Fonseca & Coutinho, 2008)

Class of rock weathering (ISRM, 1981)	Permeability (m/s)
Decomposed rock – soil with no relic structure (G4 to G8A)	10^{-7}
Completely weathered rock – saprolitic soil (W5)	10^{-6} to 10^{-5}
Highly weathered (W4) and fractured rock (F4-F5)	10^{-5} to 10^{-4}
Moderatly weathered (W3) and fractured rock (F3-F4)	10^{-5} to 10^{-6}
Slightly weathered rock (W2)	10^{-6} to 10^{-7}

6.6. Strength and stiffness

Both laboratory and in-situ tests have been widely used in research and design practices in the massifs of the area, therefore offering to PGM (COBA, 2003) a wide variety of data and providing an insight of strength and stiffness evolutions with weathering. Strength and stiffness properties can be evaluated by means of a wide range of laboratory and in-situ tests, which could be grouped as follows:

a) Laboratory tests suited for soils and rocks – triaxial and uniaxial compression tests, with the latter being the mostly used;
b) Laboratory tests suited only for rocks – point load and Schmidt hammer tests;
c) In-situ tests – commonly suited for soils, although possible in rocks; generally, in-situ tests in rocks are very expensive and time-consuming and so its usage is limited only to special construction such as dams and tunneling; in the present case, only in-situ soil testing was considered representative to be analyzed.

6.6.1. Laboratory testing

Uniaxial compression strength is one index property that can be evaluated either in soil or rock, and thus it is an important reference for defining weakening stages generated by weathering. The other relevant test is the diametral compression test, an indirect procedure to evaluate tensile strength, most important to cemented soils and other mixtures, directly related to cohesion intercept (Viana da Fonseca, 1996). Alternative tests are the point load test and Schmidt hammer, applied to rock materials only. Uniaxial tests can also provide deformability modulus determination, and so strength and stiffness can be analyzed from only one simple test. In the context of this data presentation, deformability modulus (E) was determined by the linear section of stress-strain (σ-ε) curve measured by the usual equipments referred in ISRM (rock materials) or by external measuring devices (soils).

The global data obtained from 200 uniaxial compression tests, 300 point load tests, 70 diametral compression (tensile) tests and 70 Schmidt hammer tests is presented in Figure 6.23 to Figure 6.26. Results reported by Viana da Fonseca (2003) on the same background confirm the general tendencies.

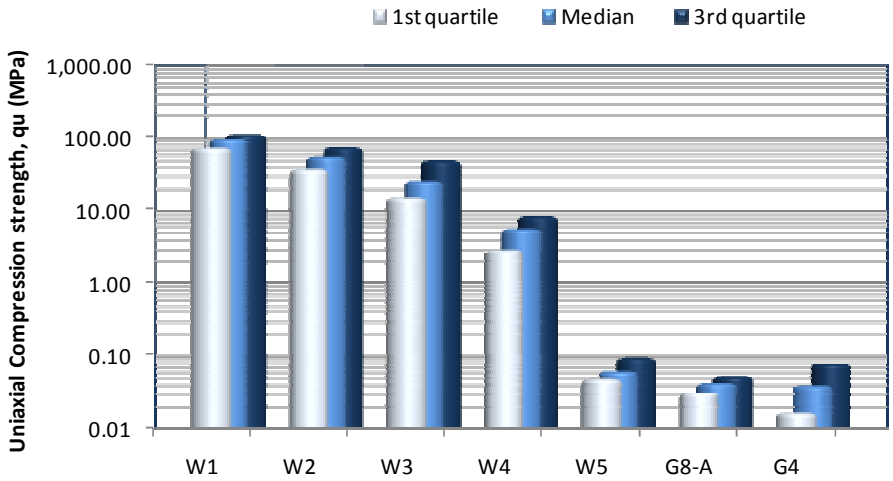


Figure 6.23 - Representative uniaxial compressive strength in Porto Granite Formation

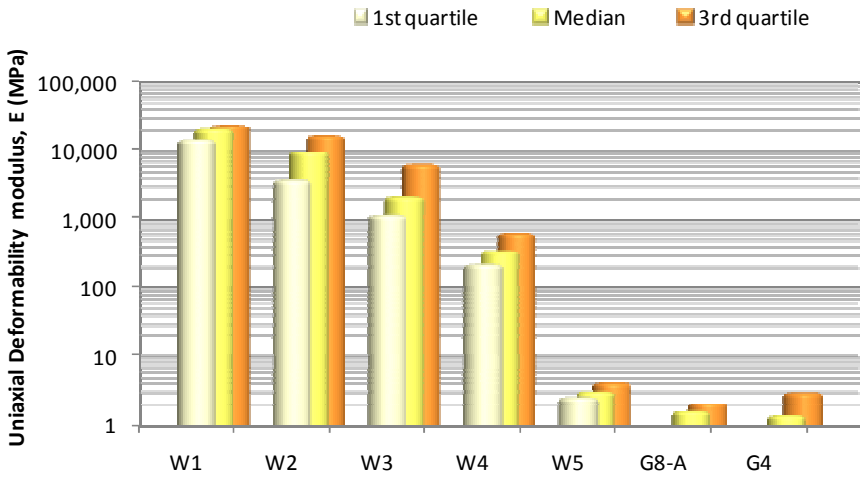


Figure 6.24 - Evolution of uniaxial deformability modulus in Porto Granite Formation

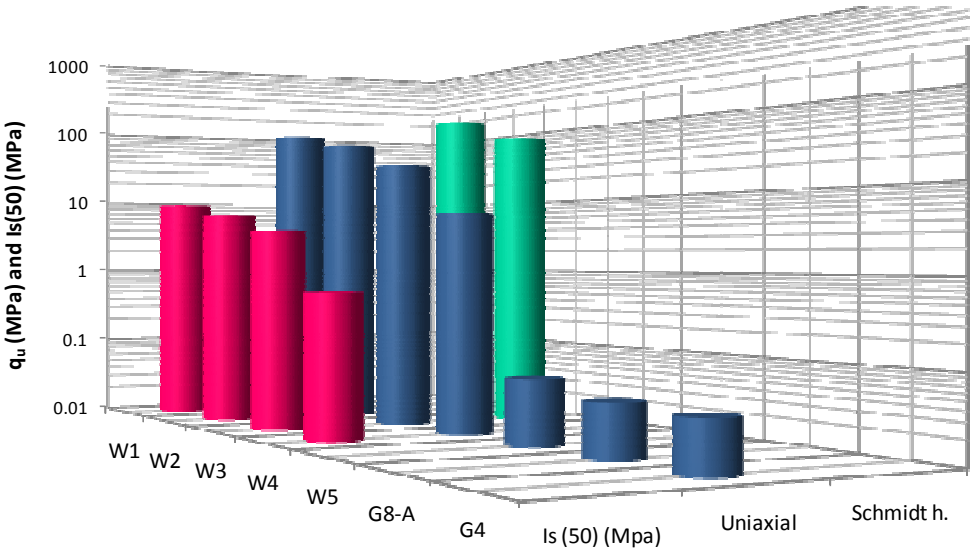


Figure 6.25 - Representative uniaxial compressive strength obtained from uniaxial compression, point load and Schmidt hammer tests, in Porto Granite Formation

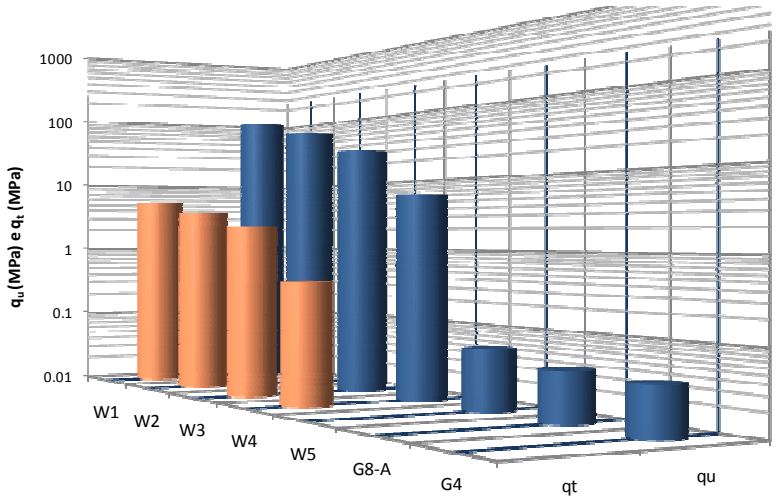


Figure 6.26 - Evolution of uniaxial compressive strength, tensile strength in Porto Granite Formation

Global data obtained from this wide range of quantified strength and stiffness parameters, crossing all weathering profile, strongly suggests a logarithmic global decrease with increasing weathering, where W_4 - W_5 represent a transition zone that shows a main drop on strength and stiffness properties. The rate of decreasing is in the same order of magnitude within W_1 – W_4 and G8 - G4 ranges, while within W_4 and G8 a drop of one logarithmic cycle is observed. In W_1 to W_4 range, point load test index, Is (50), and tensile strength assume values of 10% of uniaxial strength values, while Schmidt hammer are almost the double of the same reference.

Triaxial testing confirms the above results, showing the same pattern, pointing out again the W_4-W_5 transition zone. In this context, cementation strength represented by cohesion intercept follows a logarithmic evolution represented by two stable levels separated by a sudden drop observed between W_4 and W_5, confirming the higher influence of cementation in the weakening process (Figure 6.27). On the other hand, angles of shearing resistances displayed by rock or soil matrix are within 35º and 50º (Figure 6.28) while the same parameter in discontinuity surfaces is globally within 35 to 45º (Figure 6.29).

Table 6.5 presents some published data related to triaxial testing performed by Viana da Fonseca (1994), Rodrigues (2003) and Cruz et al. (2004b), which globally fits in the general ranges revealed by PGM (COBA, 2003) data. Moreover, some extra results from triaxial testing, reported by Viana da Fonseca & Coutinho (2008) and Topa Gomes (2009), reveal ranges of ϕ_{cv} between 31.5 to 34.0º in Porto granites young residual soils, fairly reasonable when compared with the presented results.

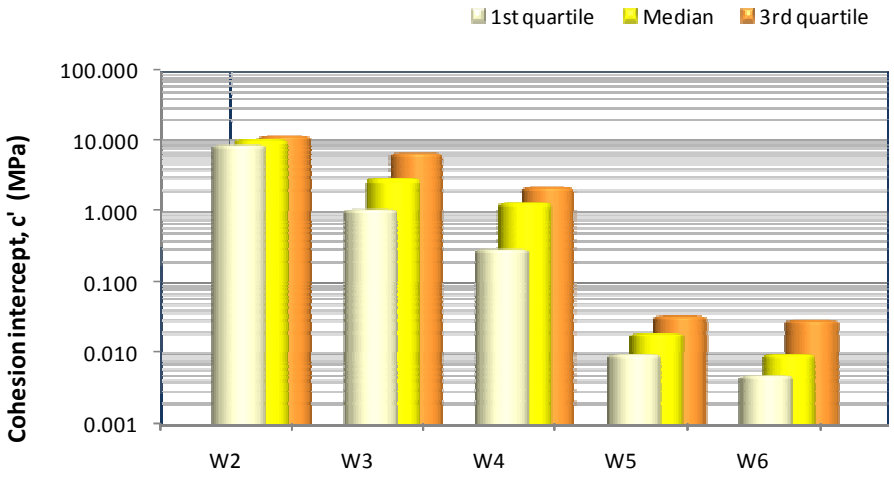


Figure 6.27 - Evolution of effective cohesion in Porto Granite Formation

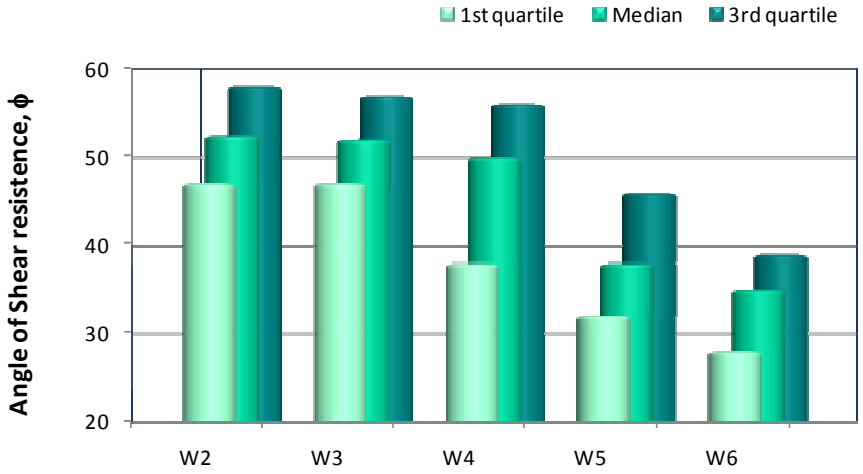


Figure 6.28 - Angles of shearing resistance of rock matrix in Porto Granite Formation

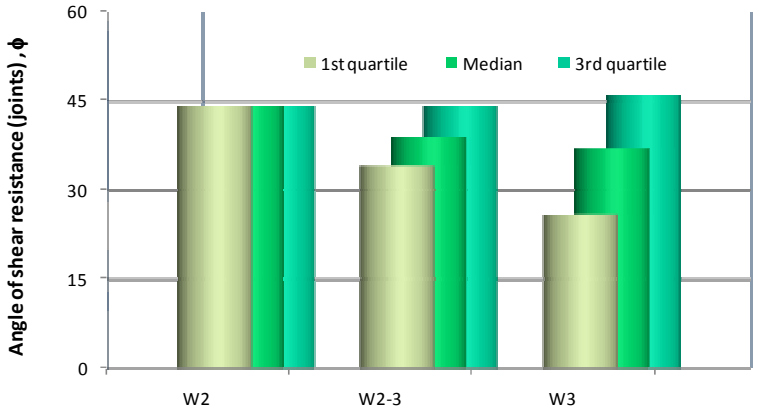


Figure 6.29 - Evolution of angle of shearing resistance of joint in Porto Granite Formation

Table 6.5 - Some local strength parameters

Site	Type of test	Reference	c' (kPa)	ϕ' (º)	N_{SPT}*
S. João Madeira	CIU (compression)	Viana da Fonseca et al (1994)	2 - 45	34 - 35	7 - 15
Porto (city)	CID (compression)		17 – 34 23 5	28 – 31 32 37	12 – 17 15 – 20 > 60
Porto (city)	CIU (compression)		24 25 32	33 27 37	10 – 16 17 22 - 32
Leixões harbor	CIU (compression)		2 – 5 6 – 9 16	36 – 39 45 – 47 46	15 – 30 30 – 60 > 60
Gaia (Railway tunnel)	CIU (sat) CID (w_{nat}) CID (w_{nat})		5 – 55 6 – 43 25	29 – 38 27 – 39 35	20 – 40 20 – 40 3 - 24
Braga	CIU CID		0 – 3 4 - 46	32 – 41 25 - 32	---
Guarda	CIU, CID	Rodrigues (2003)	30 - 40	34 - 36	10 - 30
CICCOPN Maia	CID Ck0D	Cruz et al. (2004)	5 – 10 12	36 – 37 42	10 – 30 10 - 30
Porto	Ck0D		24	32	20 - 35
Vila do Conde	Ck0D		11	35	15 - 30

* associated to N60

6.6.2. In-situ testing

SPT's are an obvious in-situ reference in soils and this is noticeable in PGM data (Coba, 2003), being represented by 15825 tests. In Figure 6.30, statistic ranges of uncorrected N_{SPT} indexed to each specific weathering unit are presented. Confirming the trend, dynamic point resistance (q_d) derived from 11688 dynamic probing tests show identical pattern (Figure 6.31). In Figure 6.32 the correlation between both tests is presented, obtained from the granitic residual soils data base created by the author within CICCOPN and MOTA-ENGIL (CME) geotechnical surveys, revealing that it is also representative of PGM (COBA, 2003) data.

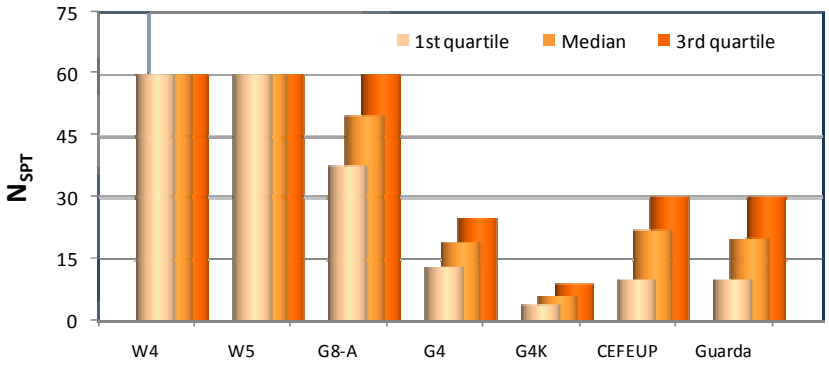


Figure 6.30 - Evolution of N_{SPT} in Porto and Guarda Granite Formations

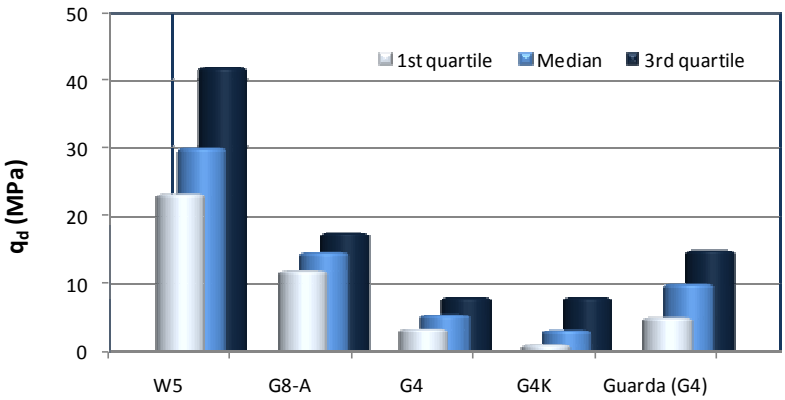


Figure 6.31 - Evolution of dynamic point resistance, q_d, in Porto and Guarda Granite Formations

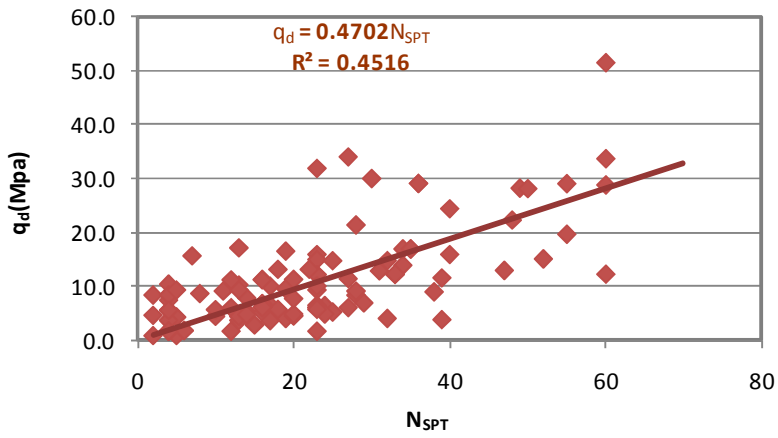


Figure 6.32 - Correlation between N_{SPT} and q_d in granitic residual soils

The general observed trends can be resumed as follows:

a) 99% of the tests were within 0 and 18m depth in G4K and G4 units, while G8 can go up to 22,5m, within the usual recognized depth of weathering.
b) Global decrease of mean values (and intervals of occurrence) with weathering at a roughly constant rate of variation with weathering
c) W_5 unit is represented by N_{SPT} values always higher than 60, G8 within $30<N_{SPT}<50$, G4 within$10<N_{SPT}<30$ while G4K varies from 4 to 9. The same units (by the same order) expressed in terms of dynamic point resistance, q_d, are within the intervals, respectively of [>20MPa], [10-20MPa], [5-10MPa] and [< 5MPa]. CEFEUP and IPG units are within the medium compacted G4 range. Following the trend of the 6.32 (CME database), for the given SPT ranges, q_d would be higher than 25 Mpa (W5), within 15 to 25 MPa (G8), 5 to 15 MPa (G4) and lower than 5 MPa (G4K), globally confirming PGM data.
d) CEFEUP and IPG SPT profiles are represented by upper levels that fit in G4 unit overlying directly W5 unit.
e) All PGM (COBA, 2003), CME, CEFEUP and Guarda results reveal increasing values with depth and effective overburden stress, which is consistent with the regional practice.

Static penetrometers, by means of CPT tests have been used quite frequently in Porto, so the amount of data is quite fair for the purpose (568 tests). However, PGM data refers mainly to the mechanical tip (Begemann, 1965), which is no longer used in actual practice. The general behaviour (Figure 6.33) follows the same pattern of the other penetrometers (SPT, DP) with q_c increasing with overburden and with the ranging values related to each geotechnical units within the same intervals of q_d. Side friction (f_s) shows irregular pattern with values ranging from 0.3 to 0.4MPa.

Begemann and Olsen's Classifications, adequate to mechanical tips, show a general convergence (PGM) in classifying the soils as slightly overconsolidated sandy silts, which is also confirmed by the ratio q_d/q_c of 1, representative of overconsolidated sedimentary sands (Cestare, 1982). These observations are consistent with the usually observed pattern, where cementation seems to be represented as an overconsolidation when sedimentary approaches are used.

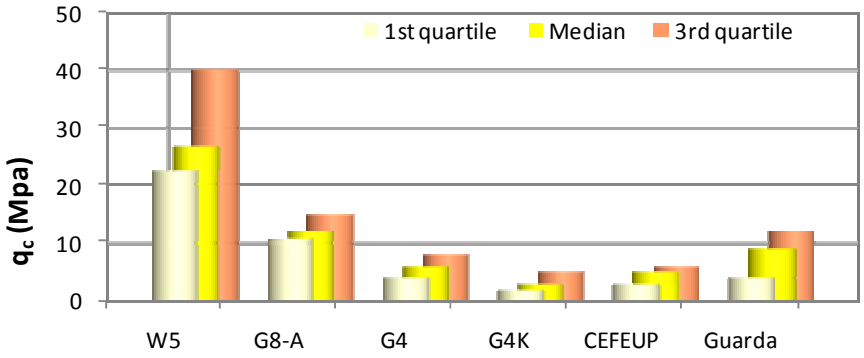


Figure 6.33 - Evolution of static point resistance, q_c, in Porto and Guarda Granite Formations

When electrical CPTu cone tips are used, the correlation derived from CME data, generates quite different ranges when compared to those from mechanical cone (Figure 6.34), which is supported by reference literature.

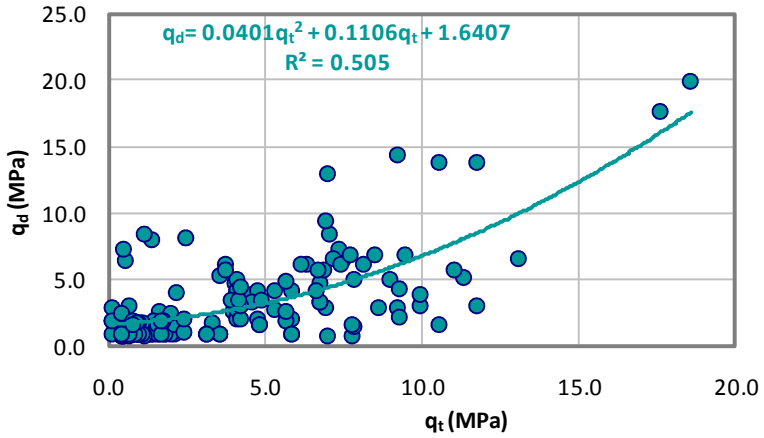


Figure 6.34 - Correlation between q_t and q_d in granitic residual soils

Menard Pressuremeter tests are rarely used when compared with penetrometers. Even tough, 75 PMT tests were available in PGM data, allowing some confidence in data analysis. The results (Figure 6.35 to 6.37) confirm the global trend observed in penetrometers, where stiffness increases with decreasing weathering degrees. Yield pressure (P_y) and limit pressure (P_l) show a smooth growth within the same order of magnitude, while PMT modulus reveals a logarithmic increase.

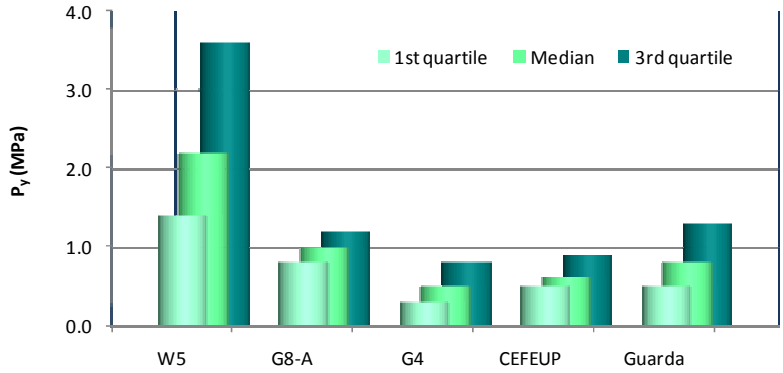


Figure 6.35 - Evolution of PMT yield pressure, P_Y, in Porto and Guarda Granite Formations

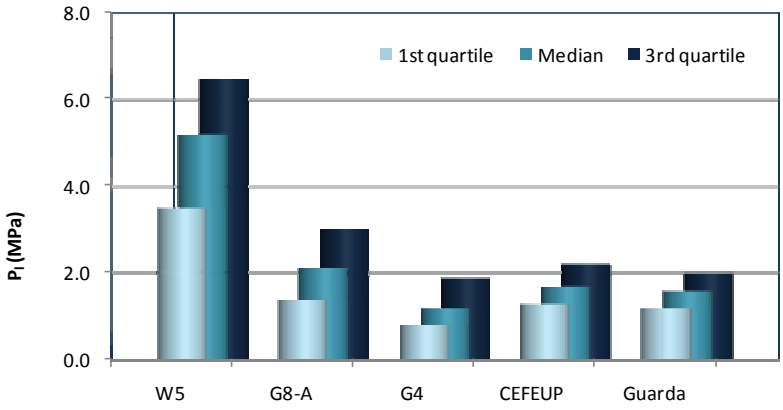


Figure 6.36 - Evolution of PMT limit pressure, P_l, in Porto and Guarda Granite Formations

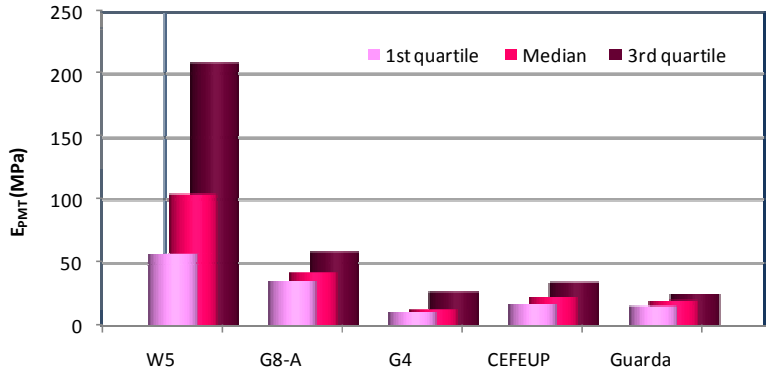


Figure 6.37 - Evolution of PMT parameters in Porto and Guarda Granite Formations

These values are also supported by the correlations between PMT and the ratio N_{SPT}/N_b (N_b represents the number of blows/cm, in the context of this work), obtained from CME database, as shown in Figure 6.38 and 6.39. Based on the same database, pressuremeter modulus in sedimentary soils within the same grain size distribution is also presented, revealing the known influence of cementation in stiffness. CEFEUP and IPG soils fall within the G4 range, again confirming the adequacy of PGM data.

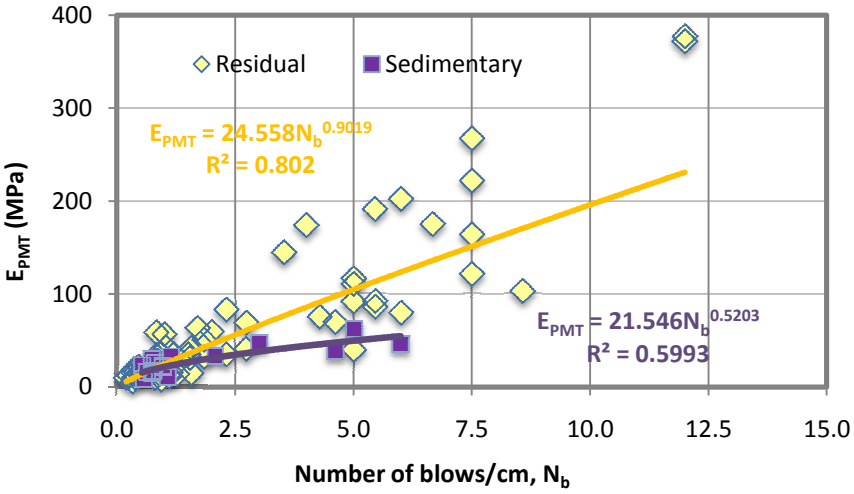


Figure 6.38 - Correlation between E_{PMT} and N_b (CME))

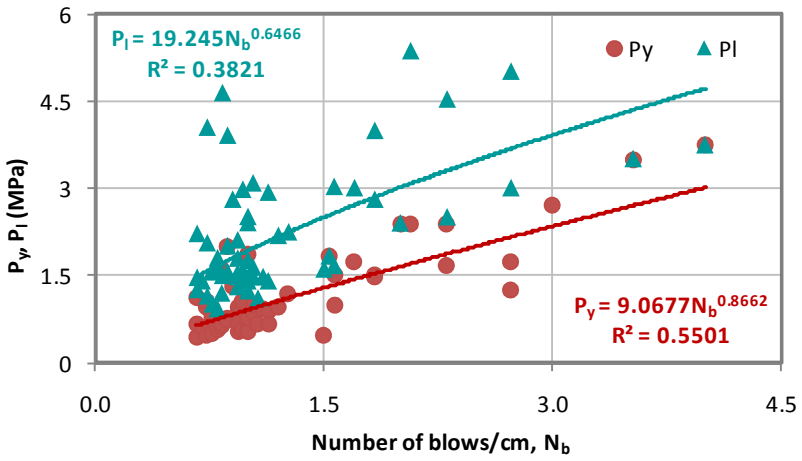


Figure 6.39 - Correlation between P_y/ P_l and N_b (CME)

Concerning seismic wave velocities, PGM (COBA, 2003) available data only refers to compression waves (v_p). Figure 6.40 reveals an increase of compression wave velocities with the weathering decrease, confirming the generally observed ranges related to the weathering degrees of granites.

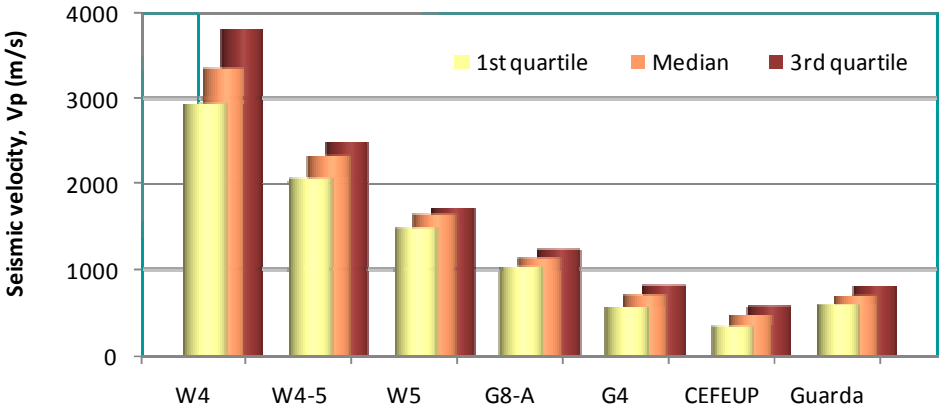


Figure 6.40 - Seismic wave velocities in Porto and Guarda Granite Formations

6.7. Proposal for a modified Wesley Classification

Even though behaviour classifications (such as those obtained by CPT/CPTu, DMT or PMT) generally identifies reasonably the residual soils, the common classifications applied to sedimentary soils (Unified and AASHTO Classifications, based in grain size distribution and Atterberg limits) are frequently useless in residual soils, because they don't take into account some distinctive characteristics, such as macrofabric or mineralogy. As already discussed in Chapter 2, Wesley (1988) proposed a more adequate approach for residual soil classification, based in mineralogy, macro and micro fabric and plasticity, suggesting that further sub-divisions on the basis of similar engineering properties should be implemented, since the basic groups are rather broad. The classification starts from a first division of soils into three main groups on the basis of its mineralogical composition, as follows:

a) Group A: Soils without a strong mineralogical influence;
b) Group B: Soils with a strong influence deriving from clay minerals also commonly found in transported soils;

c) Group C: Soils with a strong mineralogical influence deriving from clay minerals only found in residual soils.

Considering the extensive and well calibrated data, a proposal for further division of A sub-groups within Wesley Classification is suggested (here designated as Modified Wesley Classification), as presented in the following lines.

Globally Porto and Guarda granitic residual soils fall within Group A, so this is going to be the only one that will be analyzed herein. According to Wesley Classification, Group A is further divided into two broad groups, based in its macro [A(a)] and microfabric [A(b)] influences in mechanical behaviour. In that context, A(a) represents soils in which macro-structure plays an important role in the engineering behaviour with W_4 and W_5 massifs falling generally in this category, while A(b) represents soils with a strong influence of micro-structure (G4 and G4K). The most important form of micro-structure is the relict particle bonding or that arising from secondary cementation, and although this cannot be identified by visual inspection it can be inferred from fairly basic aspects of soil behaviour (Wesley, 1988), such is the case of sensitivity, in the case due to the destructuration resulting from remolding. A minor group [A(c)] represents those A soils that don´t fit in the former. Porto and Guarda granitic residual soils are within A(a) and A(b).

The available data, complemented by the author's experience in Porto granites suggests that N_{SPT} could represent an important index parameter for grouping according to the weathering level. The local reality, as it was shown, is represented by a profile of a usually thick layer (10 to 20 meters) of medium compact soils either overlaying a transition compact soil unit usually within 3 and 5m, or directly over highly weathered massif (W_5). Besides, the influence of macrofabric decreases with advance weathering, due to the extension of chemical actions, meaning that weaker units shall be most likely microfabric controlled. Taking this into account, a suggestion for sub-division of A(a) and A(b) groups is discussed below.

Sub-group A(a) is represented by N_{SPT} higher than 60 blows, identifying W_5 to W_4 massifs where, by the ISRM definition, macrofabric is still present and can influence engineering behaviour. This sub-group could be further subdivided considering the rate of penetration. In fact, analysed data shows that the difference between W_5 and W_4 is mainly due to the loss of cementation strength, with direct consequences in penetration rates, and so it is reasonable to assume the middle term as a reference border line:

a) A(a1) – represented by N_{SPT}>60 with penetration lower than 15cm;

b) A(a2) – represented by N_{SPT}>60 with penetration higher than 15cm.

Sub-group A(b) is represented by N_{SPT} lower than 60, identifying saprolites where microfabric probably controls the general behaviour. According to the presented database, this sub-group could be further divided in 3 main categories:

a) A(b1) – represented by the transition layer (G8) with 30< N_{SPT} <60;
b) A(b2) – represented by the typical unit (G4) with 10< N_{SPT} <30;
c) A(b3) – represented by the ultimate observed weathering degree, with NSPT lower than 10, where a clay matrix controls general behaviour; apart from SPT, the ratio between the amount of clay (<0.002 mm) and the fines percentage (passing ASTM #200 sieve) could also be explored to distinguish this unit, although more data is needed to confirm this proposal and to define adequate ranges of variation.

Sub-group A (c) remains as in the original classification.

Using this Modified Classification, the previously defined groups would be written as presented in Table 6.6, where some index ranges based on in-situ testing are also included.

Table 6.6 - Index parameters for Modified Wesley Classification

General classification	Proposed Wesley Modified Classification	Possible Index Parameters		
		N_{SPT}	qc (MPa)	E_{PMT} (MPa)
G4K	A (b3)	< 10	< 5	---
G4	A (b2)	10 - 30	5 - 10	10 - 40
G8	A (b1)	30 – 60	10 - 20	40 - 80
W_5	A (a2)	>60 (15-30cm)	> 20	80 - 200
W_4	A (a1)	> 60 (< 15 cm)	---	200 - 300
$W_3 – W_1$	Rock	Not applicable		

Of course, these N_{SPT} reference values don't define a clear change in weakening, but just the probability of a macrofabric, microfabric or clay matrix controlled behaviours to be more or less present. This proposal has been implemented for several years by the author as a basis for geotechnical zoning, confirming itself as a very useful and appropriate framework, generally fitting in local practice. In this case, given the

extensive available data, it is also possible to use DP, CPT and seismic shear wave velocities (v_s) as index parameters, while care should be taken using longitudinal waves (v_p), due to its susceptibility to water. Furthermore, E_{PMT} can also be explored as a control parameter, although PMT scarce use reduces its practical utility. CPTu and DMT parameters that can be related with G8, G4 and G4K groups will be discussed in the next chapter.

6.8. Geotechnical parameters deduced from in-situ and laboratory tests

Evaluation of strength and stiffness parameters from laboratorial in-situ tests is quite difficult to control since some distinct parameters are needed to obtain the final result, which faced some difficulties due to the diversity of origin of collected data (COBA 2003). Bearing this in mind, the criteria discussed below was established to select the available PGM data related with strength and stiffness properties of these granitic formations.

From the strength point of view, triaxial test data was considered to offer the most credible results to serve as a reference, both to cementation (cohesion intercept) and frictional (angles of shearing resistance) contributions. Deriving cohesion from in-situ tests is not an easy or common task, although some approaches have been tried with PMT (Schnaid and Mantáras, 1995), DMT (Cruz et al., 2004, 2006), or SBPT (Fahey et al., 2003; Topa Gomes, 2007; Topa Gomes et al., 2008) as well as the ratios of in-situ results (N_{SPT}, q_c), proposed by Schnaid (2003) and indicial/typological classifications based on in-situ tests, such as CPTu charts (Viana da Fonseca et al, 2004). However, this derivation implies specific procedures impossible to be followed by using PGM (COBA, 2003) in-situ data, disabling its application. Being so, strength evaluation was obtained considering only a hypothetical angle of shearing resistance, which includes cementation and dilation contributions, by using some well-known in-situ correlations for transported soils, namely based in SPT (Peck et al., 1953, 1986; Décourt, 1989 and Hatanaka & Uchida, 1996), CPT (Robertson & Campanella, 1983) and PMT (Baguelin et al, 1978) test parameters. The selected correlations are presented in Figure 6.41.

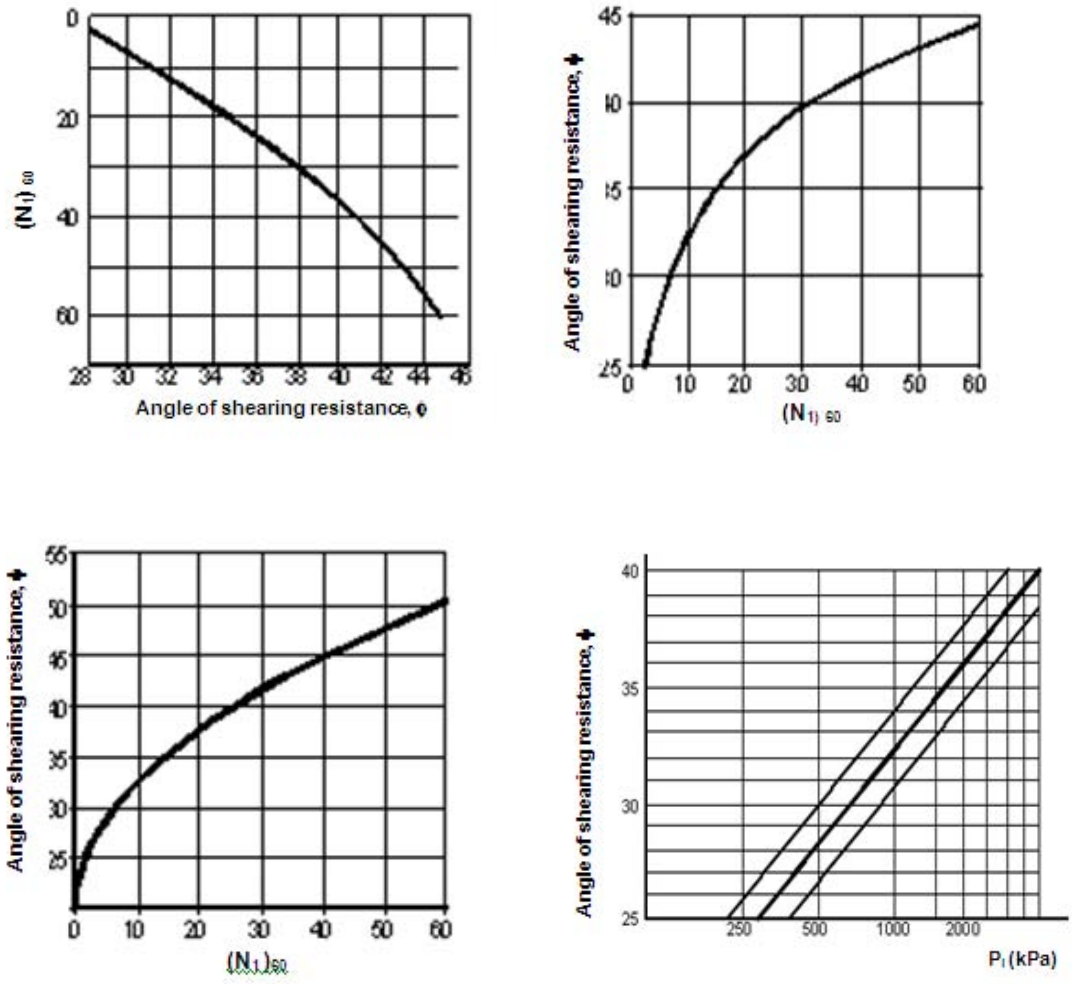


Figure 6.41 - Angles of shearing resistance from in-situ tests: a) Peck et al., 1953; b) (Decourt, 1989); c) Hatanaka & Uchida (1996); d) Baguelin et al., 1978

Evaluation of angle of shearing resistance of granular soils from SPT tests is based on the corrected N_{SPT}, designated $(N_1)_{60}$ by ISSMFE-TC16 (1989), which can be written as follows:

$$(N_1)_{60} = C_n N_{60} \quad (6.1)$$

$$C_n = [(\sigma'_{v0})_1 / (\sigma'_{v0})]^{0.5} \quad (6.2)$$

$$N_{60} = N_{SPT} * ER_r/60 \quad (6.3)$$

$$ER_r = 100 * E_r / E_p \quad (6.4)$$

where $(N_1)_{60}$ is the corrected blow count, C_n is the normalization factor to a reference in situ effective vertical stress of 98 kPa, N_{60} is the blow count normalized to 60% efficiency of the the Energy Ratio, ER_r. Finally, E_r and E_p stand for respectively the real delivered energy to the rods and the potential energy resulting from the hammer weight and falling height (474 J, in the case of standardized SPT test).

The first correction factor is possible to be applied with success, since test depths were available and a good guess of unit weights could be obtained from borehole information. However, for the second correction it had to be assumed that SPT equipments used presented the referred energy ratio of 60%, as it is usually considered in Portugal. This consideration can be quite erroneous, since the real energy ratio may be considerably different from 60%, despite the information provided by suppliers. Recent research based in SPT analyzer determinations reported by MOTA-ENGIL (Rodrigues et al. 2010) has shown significant discrepancies to the reference value. Naturally, procedures and equipments of PGM data used in the analyzed data couldn´t be controlled and thus some deviation may have occurred when applying the selected correlations since they all depend on the corrected number of blows, $(N_1)_{60}$. Estimation of in-situ effective stress, needed for deriving the parameter from SPT, as well as from CPTu, followed the usual procedures considered reasonable in geotechnical practice.

Finally, the selected correlation to derive the parameter from PMT (Baguelin et al., 1978) depends only in the respective test parameters, namely E_{PMT} and P_l. Figure 6.42 reveals that in-situ based correlations usually exhibit higher values of angles of shearing resistance than those obtained by triaxial tests, with the differences expectedly increasing with cementation, due to the inclusion of the effect of cementation strength in friction parcel of Mohr-Coulomb criteria.

Globally, the results fall within a upper bound represented by directly derived SPT and CPT parameters and a lower one represented by PMT (Baguelin et al, 1978), which presents the same order of magnitude or even slightly lower than triaxial results.

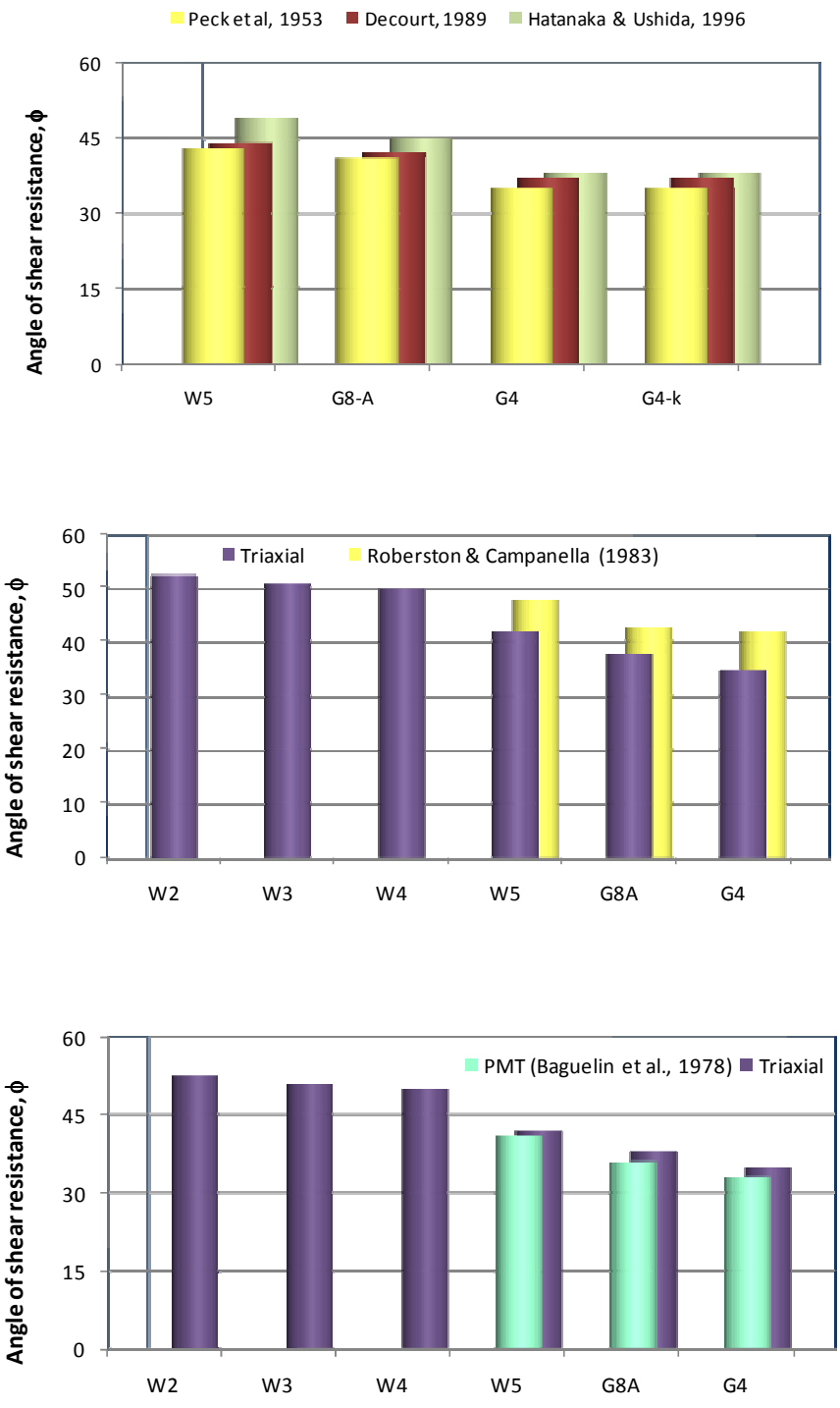


Figure 6.42 - Comparisons of angle of shearing resistance deduced from in-situ and laboratorial test results.

Concerning to deformability, mostly of the available triaxial information didn´t allow for a definitive conclusion about the strain or stress levels to which the modulus should be referred to, and so these data was not included. On the other hand, SPT and CPTu are mainly strength tests capable of providing only rough estimations and so not considered as well. Being so, deriving modulus from in-situ testing was only attempted based in PMT data, which was then compared with laboratory uniaxial testing results. Deformability modulus was derived from PMT tests following the correlation expressed below:

$E = E_{PMT}/\alpha$

where E is the deformability modulus, E_{PMT} is the pressiometric modulus and α a correction factor (Amar *et al*., 1991), dependent on ratio E_{PMT} / $P_{l,}$ that is pressiometric modulus and limit pressure. Values of α are represented in Table 6.7

Table 6.7 - Values of α to derive deformability modulus (Amar *et al*., 1991)

Soil type	Clay		Silt		Sand and cobble	
	Em/pl	α	Em/pl	α	Em/pl	α
OC	>16	1	>14	0,67	>10	0,33
NC	9 a16	0,67	8 a 14	0,5	6 a 10	0,25

The observed pattern for strength properties with advancing weathering was also followed by stiffness, reflected either by laboratory or in-situ test results (Figure 6.43). Even though differences between in-situ and laboratorial results should be expected, as a consequence of sampling disturbances (strongly affects cementation), results suggest the combination of uniaxial and PMT as a reasonable approach for practical evaluations. In fact, rock materials, from W_1 to W_4 uniaxial tests are the only practical possibility for most common situation. From this latter to the highest weathering level (W_4 to G4K) moduli evaluated from uniaxial tests is increasingly affected by its low sensitivity.

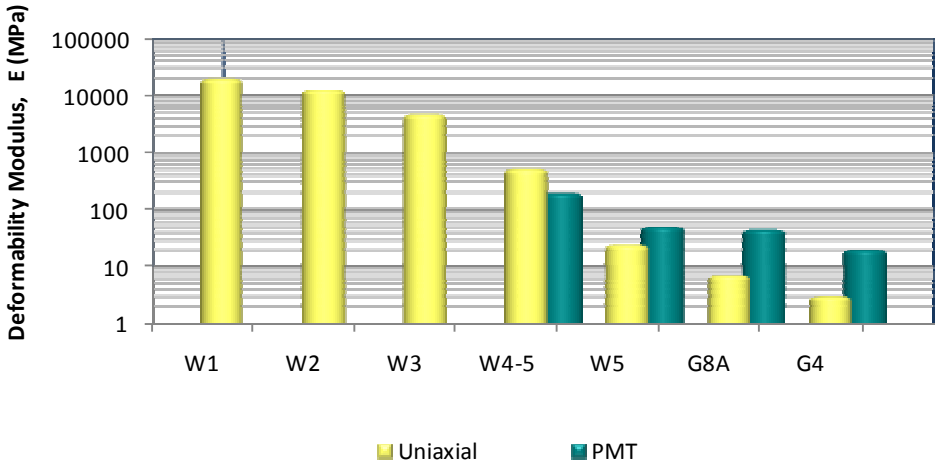


Figure 6.43 - Deformability modulus deduced from in-situ (PMT) and laboratorial (uniaxial) test results

The overall strength and stiffness evolution with weathering degree displayed by PGM (COBA 2003) data, seems to fit with the explanation given by Vaughan & Kwan (1984) of a global decrease of strength and stiffness with weathering, mainly associated to loss of cementation between particles represented by a logarithmic reduction of cohesion intercept and a smoother decrease of angle of shearing resistance, in a Mohr-Coulomb failure criteria. In fact, laboratory triaxial and uniaxial available data reveals a similar pattern through weathering evolution, with a general logarithmic decrease of global strength (uniaxial tests) and cohesion (triaxial tests), while angle of shearing resistance tend to vary at low rates. This general pattern is in accordance with the physical parameters evolution described earlier in this chapter.

The distinctive drop in strength and stiffness between W_4 and W_5 classes was also observed in the main trends of selected in-situ strength and stiffness correlations, representing the connection between weathering confined to the vicinity of discontinuity surfaces and a globally weathered massif. The reference experimental sites for this data calibration (CICCOPN, Hospital de Matosinhos, CEFEUP and Guarda) globally converge and confirm all test ranges associated to A(b2)/G4 class to which they belong, thus giving sustainability to the observed trends.

6.9. Other available geotechnical test parameters

Recently published research works on Porto granitic residual soils (Topa Gomes, 2009; Ferreira, 2009) brought some insight to the state of stress evaluation, namely through K_0, confirming the general considerations related to these materials (Viana da Fonseca et al., 1994; Viana da Fonseca, 1996; Viana da Fonseca & Almeida e Sousa, 2002). In fact, based in extensive and high quality laboratory testing program (G4 and G8 soils), Ferreira (2009), although exclusively based in discussable laboratorial radial strain controlled triaxial tests, reports values of 0.41 for lower vertical stresses of 50 kPa and an average of 0.30 which is in the vicinity of 0.35 – 0.50, the local reference range (Viana da Fonseca, 1988; Viana da Fonseca et al., 1994; Viana da Fonseca, 1996; Viana da Fonseca & Almeida e Sousa, 2001) for residual soils and W_5 massifs. These results are also supported by theoretical considerations related to the condition of zero horizontal strain, which would be around 0.30 if Poisson's ratio is assumed equal to 0.25 (Vaughan, 1988; Viana da Fonseca, 1988, 1996). In W_5 and W_4 weathering levels, Topa Gomes (2009) reported values ranging between 0.55 and 0.7, obtained from SBPT tests, confirming the general decrease of the parameter with increasing weathering degree which would be closed to one in the W_4-W_3, as reported by Viana da Fonseca (1996) and Viana da Fonseca & Almeida e Sousa (2001). These results were obtained in a very thorough campaign of self boring pressuremeter tests and have great significance, since it become the second campaign (first one performed in 1994 by Viana da Fonseca in Matosinhos experimental site) to be performed in portuguese residual soils.

Another important issue arising from Topa Gomes work (2009) is the one related with suction resulting from unsaturated conditions. Figure 6.44 presents' retention curves of Porto residual soils obtained by filter-paper technique, pressure plate cells and triaxial testing (Topa Gomes, 2009). In Table 6.8 the respective strength parameters in unsaturated conditions, including ϕ_b taken from triaxial tests, are presented together with those obtained in Hong Kong granites and riolites (Ho & Fredlund, 1982).

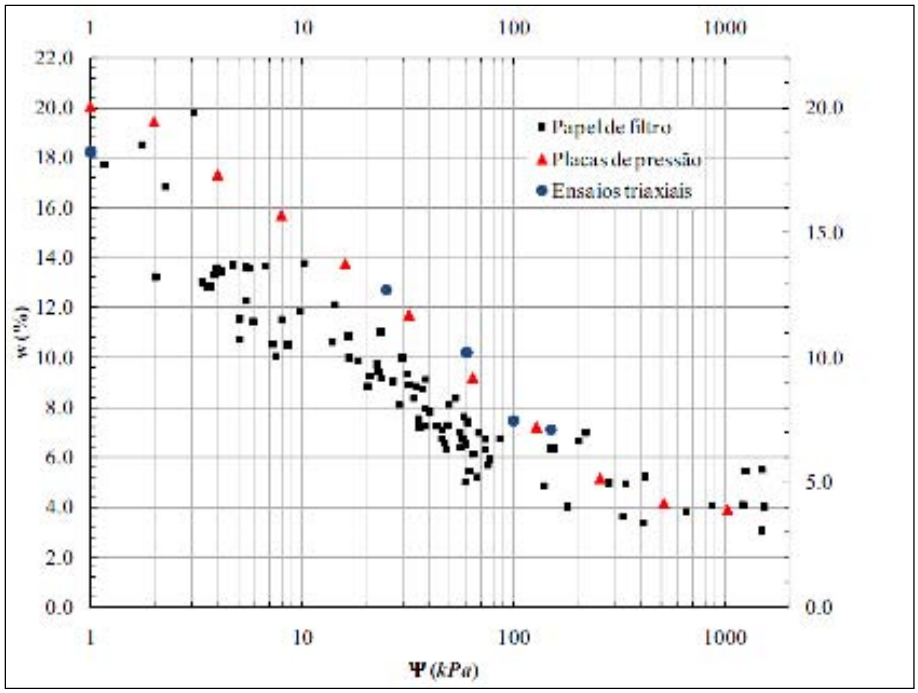


Figure 6.44 - Retention curves of Salgueiros Metro Station (after Topa Gomes, 2009).

Table 6.8 - Summary of some strength parameters in residual soils

Soil Description	c´(KPa)	ϕ´ (º)	ϕb (º)	Test type	Reference
Decomposed granite (natural) Porto	1 – 4,5	39 – 41	13,7 – 14,1	CD	Topa Gomes (2009)
Decomposed granite (natural) Hong Kong	28,9	33,4	15,3	CD	Ho & Fredlund (1982)
Decomposed riolite (natural) Hong Kong	7,4	35,3	13,8	CD	Ho & Fredlund (1982)

6.10. Summary

A summary of the discussed results is presented in Tables 6.9 and 6.10, which are organized according to the proposed Modified Wesley Classification, as discussed before in this chapter. The global set of analyzed data arising from Porto Geotechnical Map, research work carried on by FEUP and IPG, and also from general controlled campaigns performed by LGMC of CICCOPN and MOTA-ENGIL (CME), gave rise to the following conclusions:

a) The evolution of general mechanical properties is gradual and represented by continuous ranges related to each specific weathering level;
b) From identification point of view, the studied soils are usually well graded, revealing an increase of fine content and plasticity through weathering; ASTM and AASHTO classifications show convergent information, outputting silty sands to sandy silts related to W5 and G8, while G4 and G4K show a tendency to be sandy clays to silts of low plasticity;
c) Physical characterization, on its turn, reveals an expected increasing porosity with weathering, that is increasing void ratios and decreasing unit weights (dry, humid and saturated); solids unit weight remains fairly constant throughout weathering;
d) In-situ permeability seem to reduce itself with increasing weathering, although with significative scatter;
e) Laboratorial strength and stiffness testing is consistent with physical characterization, revealing very similar ranges within W_1 and W_2 weathering degrees, which consistently decrease for higher levels, represented by ranges evolving in continuity at more pronounced rates within W_4 and W_5; moreover, the mechanical degradation observed with weathering evolution is mainly related with decreasing cohesion and more or less stable angles of shearing resistance, confirming the theoretical background discussed in Chapter 3; however, it should be stressed that there is a concentrated break between W_3 and W_4, which can somehow be related to different concepts of the parameter within soil and rock massifs;
f) In-situ testing data reveals convergent information, although significant differences in magnitude between laboratory and in-situ testing can be observed in deformability modulus, which might be related to sampling and also to some differences associated to strain levels; in each type of test it varies according to the interpretation and stress-strain level, for what the indexation to deformability may be quite cumbersome;
g) Experimental sites data (CEFEUP, CICCOPN and IPG) fits in A(b2) or G4.

Table 6.9 - Summary of geotechnical parameters global ranges (laboratorial)

PGM data								Experimental sites		
	W_1	W_2	W_3	W_4	W_5	G8	G4	G4K	FEUP	IPG
Mod. Wesley Classification	Not applicable			A(a1)	A(a2)	A(b1)	A(b2)	A(b3)	A(b2)	A(b2)
#200	---	---	---	---	10-30	10-30	30-40	35-45	38-47	20-35
<0,002	---	---	---	---	---	---	---	14-16	3-10	2-7
Cu	---	---	---	---	---	---	---	> 200	> 100	> 200
Cc	---	---	---	---	---	---	---	0.5-1.0	0.8-1.5	1,5-3.5
CF rate (%) (Cruz, 2010)	---	---	---	---	---	---	---	30-40	10-20	12-25
IP	---	---	---	---	NP	NP -10	NP-15	8-18	NP-14	5-10
At	---	---	---	---	---	---	---	0.5-1.0	0.9-1.5	1.8-3.4
γs	---	---	---	2.6-2.7	2.6-2.7	2.6-2.7	2.6-2.7	2.6-2.7	2.7-2.8	2.6-2.7
γ	25-26	23-26	23-25	19-24	18-21	18-20	17-20	16-19	16-20	18-21
Void r.	---	---	---	---	---	0.7-0.9	0.6-0.7	0.4-0.7	0.6-0.8	0.4-0.6
n	---	1.5-3.0	3.0-7.5	7.5-15	---	---	---	---	---	---
K (m/s)		10^{-6} a 10^{-7}						---	---	---
ASTM	---	---	---	---	SM	SM	SM-SC	SC	SM-SC	SM
AASHTO	---	---	---	---						
q_u (MPa)	50-150	50-150	10-90	1-20	0.1-1.0	0.05-0.1	0.01-0.08	---	---	---
E (MPa) Uniaxial	10000-25000	10000-25000	1000-10000	500-1500	5-25	1.5-5.0	0.5-3.0	---	**---**	**---**
q_t (MPa)	3-10	1-6	0.5-5	0.2-1.0	---	---	---	---	---	---
Is (50) (MPa)	6-12	0.5-8.0	0.5-5.0	0-2.0	---	---	---	---	---	---
c' (MPa)	---	9-12	1-7	0.5-2.5	0.01-0.05	0.005-0.03	---			
ϕ' (º)	---	47-58	47-57	38-56	35-40	35 - 38	---			
K_0			0.9* (W4-3)	0.70 – 0.55* (high quality data)		0,35 (high quality data)**				

*Topa Gomes (2009); ** Viana da Fonseca (1996)

Table 6.10 - Summary of geotechnical parameters global ranges (in-situ)

	PGM data							Experimental sites		
	W1	W2	W3	W4	W5	G8	G4	G4K	FEUP	IPG
Mod. Wesley Classification	Not applicable			A(a1)	A(a2)	A(b1)	A(b2)	A(b3)	A(b2)	A(b2)
NSPT	---	---	---	> 60*	> 60**	30-60	10-30	<10	10-30	10-30
qd (MPa)	---	---	---	---	>20	10-20	5-10	<5		5-15
qc (MPa)	---	---	---	---	---	10-20	5-10	<5	2,5-7,5	5-25
fs (MPa)	---	---	---	---	---	0,3-0,4	0,3-0,4		0,1-0,3	
py (MPa)	---	---	---	---	1-6	0,5-1,5	0,5-1,5	---	0,5-1,0	0,8-1,3
pf (MPa)	---	---	---	---	1,5-10	1-4	1-3	---	1-2,5	1,2-2,0
EPMT (MPa)	---	---	---	---	80-200	40-80	10-40	---	15-35	15-25
vp (m/s)	2750 - 7500			1800-2700	1250-2000	800.1500	400.800	---	350-600	600-800
vs (m/s)	---	---	---	---	---	---	---	---	250-350	350-400

*penetration rate lower than 15cm; ** penetration rate higher than 15cm

Chapter 7.
Residual soil in-situ characterization

7. RESIDUAL SOIL IN SITU CHARACTERIZATION

7.1. Introduction

As it has been emphasized, residual soils characterization it's not an easy task, due to its cohesive-frictional nature and because disturbance effects by both sampling and installation of in-situ devices usually are significative. The sampling problems and the discontinuous information related to laboratory tests leave an important role to in-situ testing.

There are a lot of different manners of classifying in-situ tests, following its nature, the type of parameters assessed, installation characteristics, etc. Among these, Schnaid et al. (2004) proposed a basic division considering the disturbance level during installation, as follows:

a) Non-destructive or semi destructive tests are carried out with minimal overall disturbance of soil structure and small changing on initial mean effective stress with installation; seismic (or other geophysical tests), self boring pressuremeter and plate load tests are within this group and with some simplifying assumptions of their results can be interpreted by theoretical approaches;
b) Destructive tests, which deeply affects the massif by installation methods (penetration or boreholes), such as dynamic and static dilatometers and penetrometers, PMT and FVT; these tools are usually robust, easy to perform and of low cost although it's rather difficult to theoretically interpret them since the mechanisms associated to installation are difficult to control.

Concerning the non-destructive group, Viana da Fonseca & Coutinho (2008) synthesize some accumulated experience in granitic residual soils characterization (Portuguese and Brazilian) with non destructive geophysical tests, as follows:

a) Tomographic surface refraction is adequate for average 2D distributions (P and S waves) and to deduce elastic parameters such as shear modulus and Poisson´s ratio; depending on depth ranges, geological mapping is also a possibility;
b) Conventional cross-hole (CH) tests have the same purpose of last item, but are limited to a single 1D profile;

c) Seismic refraction and electrical methods seem to be adequate to map underground heterogeneities, both horizontally and vertically;
d) Varying saturation degree seem to play an important role on S-wave CH profiles, due to the influence of capillarity forces or suction effects;
e) Soil full saturation is represented by high frequency effects in the horizontal component of CH.

Mechanical in-situ tests within the same group are less used due to some known reasons. In fact, SBPT tests are quite difficult to apply in common practice due to its complexity, high cost, time-consuming and non-continuous information, although they have been used in research frameworks in residual soils with important benefits. As a consequence, the amount of available information related to these tests is scarce, hence disabling the possibility to assess global mechanical massif behaviour. However, some important work dealing with these tests in residual soils have been undergoing, such as the new cavity expansion model that incorporates the effects of structure and its degradation (Mantaras & Schnaid, 2002; Schnaid & Mantaras, 2003), the extension of cavity expansion theory to unsaturated soils (Schnaid & Coutinho, 2005) and the overall fitting SBP pressure-expansion curve (Fahey & Randolph, 1984; Viana da Fonseca & Coutinho, 2008; Topa Gomes, 2009). Viana da Fonseca (1996) highlights the utility of PLT, by performing series of tests with different plate sizes allowing the determination of strength parameters (c' and ϕ') as well as the obvious stiffness evaluation, although time-consuming and limitation to very superficial horizons makes it less actractive.

As a consequence, other in-situ tests that introduce reduced disturbance during installation and allow deformability measurements, such as PMT and DMT or the ones with seismic devices (SDMT, SCPTu) can play an important role on residual soil characterization for routine analysis. In fact, these tests generate higher disturbance during installation when compared with the ones of the first group, but they have the great advantage of providing a reasonable amount of data that can be used in statistical analysis and, somehow, attaining quite reasonable levels of efficiency.

DMT devices provide high level of precision for displacement measurements and its response can be explained by semi-spherical expansion theories. The information is quasi-continuous and can be easily combined with any type of in-situ and laboratorial test. Thus, in the context of this work, DMT was selected to be the reference base in characterization models for loose to compact residual soils.

Although it has not been possible to combine DMT+CPTu in the course of this experience, the multi-test approach (*MT technique*) can play an important role in characterizing residual soils, since the presence of cementation structures increases the number of geotechnical variables that can be balanced if more than one type of test is performed. Furthermore, the recent introduction of (double) seismic devices in both tests provides an excellent and valuable tool (seismic wave determination) for characterizing stiffness with quality. This is very important for the global quality of routine campaigns, since both tests provide very sustainable data in a wide variety of determinant geotechnical properties, related with state of stress, stress history, strength, deformability and flow. In the present situation, the mechanical level (medium compact to compact) of the majority of residual soils in the area under research, allowed the static penetration of both DMT and CPT equipments.

For strata with higher stiffness ranges, combination with PMT testing, directly correlated with SDMT or SCPTu within the strata where both could be performed, can be seen as a promising technique. SPT and/or DPSH may be used for the same purpose, but naturally with lower quality. From the author's own experience, some indicative information on the quality of these tools when used in residual soils is presented in Table 7.1, adapting the sedimentary soil approach presented by Lunne et al., (1997). Combined DMT and CPTu tests are also included.

During the last 15 years, the author studied the efficiency of combined testing in portuguese granitic residual soil characterization (Cruz, 1995; Cruz et al. 1997, 2001, 2004b 2004c, 2006d and 2008a, Cruz & Viana da Fonseca, 2006a, 2006b), trying to establish paths for data interpretation, as suggested by Schnaid et al. (2004):

a) Use of classical empirical or theoretical approaches in residual soils and evaluate its applicability;
b) Development of new specific methodologies;
c) Development of experimental databases to validate engineering applications.

From the practical point of view, the main goals for the referred research have been related to the development of specific correlations to determine effective cohesion intercept and to define correction factors for the angle of shearing resistance, which is usually over-predicted when sedimentary approaches are used, as a result of cementation effects on shear strength. Since at least two basic parameters (P_0 and P_1) are obtained from DMT, it is expectable the possibility of differentiating frictional and cohesive parcels fundamental for a proper strength parameterization. Besides strength,

the influence of cementation structure on stiffness behaviour of soils was also under scope, namely through its effect in constrained (M) and small-strain (G_0) moduli results.

Table 7.1 - In-situ efficiency in residual soil characterization

	Soil type/profile	u	γ	c'	ϕ'	I_D	M	G_0	K_0	OCR	c_v	k
SPT	Borehole	--	3	Global strength		3	3	3	--	--	--	--
DPs	--	--	--	Global strength		2	3	3	--	--	--	--
PLT	--	--	--	--	3	--	1	1	--	--	--	--
PMT	Borehole	--	--	2/3	2/3	3	2	2	3	3	--	----
CPTu	1 / 1	1	2	Global strength		2	3	3	--	3	1/2	2
SCPTu	1 / 1	1	2	Global strength		1/2	1/2	1	--	2	1/2	2
DMT	1 / 1	3	1	2/3	2	1/2	1/2	2/3	2/3	2	--	--
SDMT	1 / 1	3	1	1/2	2	1/2	1	1	2	2	--	--
DMT+CPTu	1	1	1	2/3	2	1/2	1	2	2	2	1/2	2
CH	Borehole	--	--	--	--	--	--	1	--	2	--	--

u – pore pressure; γ - unit weight; c' – cohesion intercept; ϕ' – angle of shearing resistance; I_D - density index; M – constrained modulus; G_0 – small-strain shear modulus; K_0 – at rest earth pressure; OCR – overconsolidation ratio; c_v – consolidation coefficient; k – coefficient of permeability

1- High; 2- moderate; 3- limited; -- inappropriate

The research undergone aimed to establish specific correlations with state of stress, strength and stiffness geotechnical parameters and included 15 site experimental programmes carried out between Porto and Vila do Conde (20-25 km to the North of Porto). Overall, a total of 40 drillings with regular SPT, 36 DMT, 22 CPTu, 4 PMT, 5 DPSH and 10 triaxial tests, all performed in granitic residual soils located in the region of Porto arising from the physical and chemical weathering of Porto Granite Formation, whose characteristics were discussed in the last Chapter. To those, important contribution with PLT and more high quality data from triaxial testing was provided by Viana da Fonseca (1996). In Table 7.2, CPTu and DMT global data ranges of basic and intermediate test parameters obtained in Porto granitic residual soils are presented, ordered according to the usual weathering classifications adopted herein.

Table 7.2 - CPTu and DMT ranges obtained in Porto Formation

Group	N_{SPT}	q_c	f_s	P_0	P_1	I_D	E_D	K_D
		MPa	kPa	MPa	MPa		MPa	
A(b1)/G8	30 - 60	10 - 20	> 300	> 0.5	> 2	1.5 -4.5	>50	>15
A(b2)/G4	10 - 30	1-10	250-400	0.1-0.5	0,5 - 3	1.5-4.5	5 - 60	5 - 20
A(b3)/G4K	5 - 10	< 5	100-250	0.05-0.3	0.2-1.5	1.0 -1.75	3 - 20	3 - 7
q_t and f_t – tip resistance and unit side friction obtained by CPT tests; P_0 and P_1 – DMT basic pressures; I_D, E_D and K_D – DMT intermediate parameters								

In what follows, the trends revealed by the whole amount of data are going to be presented and discussed with detail and at the end of the chapter a very well documented case (Viana da Fonseca et al., 2007; Viana da Fonseca et al., 2009) related to the finite element modeling of the excavation of *Casa da Musica Metro Station (*Porto Network*)* will be used to illustrate the efficiency of discussed correlations.

7.2. Basic Test parameters, P_0 and P_1 (DMT) and q_c and f_s (CPTu)

Before going into a detailed discussion, it is important to take a look into the basic CPTu and DMT parameters. From the global data analysis, the following trends became evident (Cruz et al., 2004b, 2004c, 2006b):

a) q_c slightly grows with depth, generally ranging from 1 and 10 MPa;
b) P_0 and P_1 increase with depth, following the usual pattern established for sedimentary soils, with P_1 increasing at higher ratios than P_0, respectively ranging from 0.5 to 3.0 and from 0.1 to 0.5 MPa;
c) The increase of P_0 and P_1 generally follows the increase of q_c, according to the pattern in b), suggesting a high ability of DMT test to, on its own, sense the influence of cementation structure; Figure 7.1 presents typical q_c versus P_0 and P_1 profiles.

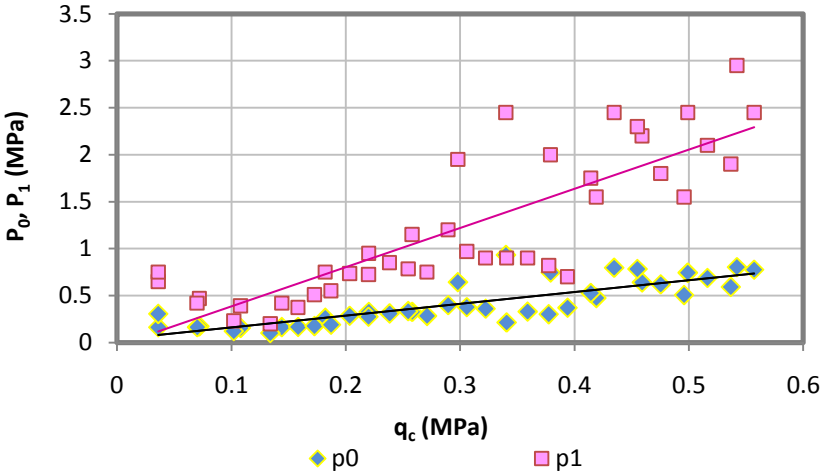
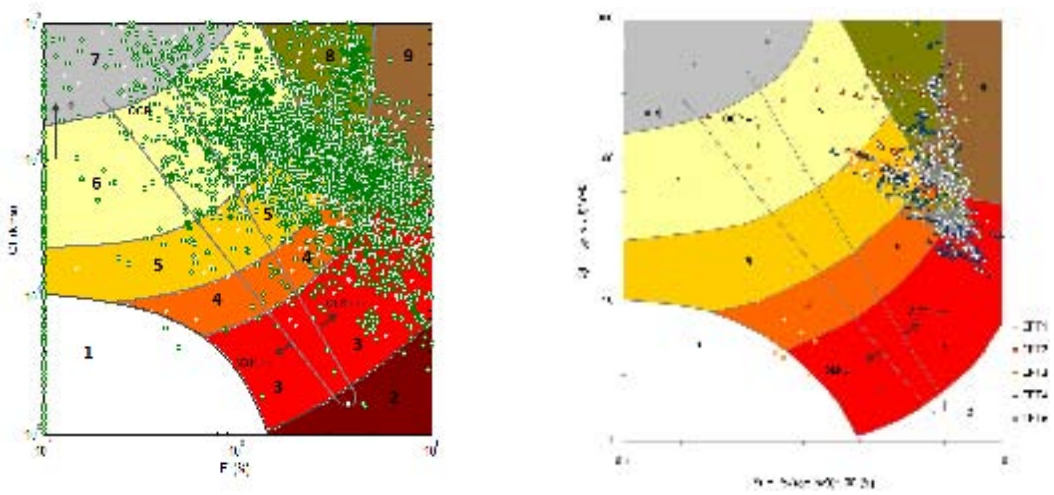


Figure 7.1 - Typical P_0 and P_1 profiles related to q_c

7.3. Stratigraphy and unit weight

As discussed in Chapter 5, a very important detail of DMT in soil characterization is its ability to provide information related to the basic properties (identification and physical indexes) of soils, thus creating a rare autonomy in field characterization. In the course of this research, the overall data set have shown the same level of accuracy found in portuguese sedimentary soils (Cruz et al., 2006a), revealing no need for specific approaches for residual soils. In fact, soil identification based on both DMT (and CPTu) tests generally revealed the presence of granular soils, firmly converging to the general data obtained from drillings and identification laboratory tests such as grain size distributions and Atterberg limits. Globally, DMT results (Marchetti, 1980) identify silty sands and sandy silts, while CPTu results (Robertson, 1990) reveal sands to silty mixtures (zones 3, 4, 5 and 6), frequently affected by cementation and ageing (zones 8 and 9 of the proposed diagram). Figure 7.2a represents the overall results from CPTu in residual soils within the present framework, showing a global tendency for soils to be within groups 5, 6, 8 and 9, identified respectively as sandy silts, silty sands to sands, cemented clayey sands and cemented fine grained soils. Scattering data may be extended to groups 4 and 3, related to the presence of higher fine contents. Figure 7.2b shows the representation of data obtained by Viana da Fonseca et al. (2006) in Porto granites, namely CEFEUP and Casa da Música experimental sites. In addition, DMT data also reveal that I_D reflects well the increase of fine content in the [silt, sandy-silt, silty-sand, sand] range, suggesting that it may be further explored as an index of weathering degree.



a) b)

Figure 7.2 - Porto granitic residual soils after Robertson (1990) classification: a) Cruz et al. (2006); b) CEFEUP and Casa da Música (after Viana da Fonseca et al., 2006)

Unit weight evaluation also revealed high efficiency, with differences between DMT and laboratory test results being globally smaller than 1kN/m^3, or 2kN/m^3 in few cases, laying in the same order of accuracy observed in transported soils, presented in Chapter 5. This data quality on stratigraphy and unit weight is very useful not only for the independence of the test, but also when dealing with test data cross-correlated with borehole information or other in-situ tests.

7.4. Strength evaluation

As previously described, residual soils behaviour is deeply marked by the presence of a cemented structure, and it is generally accepted that strength behaviour of these soils can be represented by Mohr-Coulomb strength envelope, where cohesion intercept (c') reflects the cementation and suction between particles and angle of shearing resistance (ϕ') represents both the frictional component between particles and their space arrangement, that is density and interlocking (Schnaid et al., 2004). This reality brings the following implications for deriving strength parameters from DMT:

a) Cohesion intercept is not considered in the basic DMT data reduction;
b) Angle of shearing resistance derived from transported soils formulae, represents the overall strength instead of the parameter on its own, thus displaying higher values than reality, as widely recognized by specialized scientific community;

c) DMT is a two-parameter test and thus it is reasonable to expect the possibility of deriving both c' and ϕ' (Cruz et al., 2004b, 2004c).

7.4.1. Virtual overconsolidation ratio, vOCR

According to DMT references for transported soils (Marchetti, 1980), K_D profiles present the following typical patterns:

a) K_D profiles tend to follow the classical shape of the OCR profile;
b) Normally-consolidated (NC) soils tend to present values of K_D around 2;
c) Over-consolidated (OC) soils show values of K_D above 2, decreasing with depth and converging to NC values;
d) Normally consolidated soils affected by cementation or ageing structures show values of K_D higher than 2, remaining fairly stable with depth.

Cruz et al. (1997), based in two well documented cases reflecting the same weathered level of Porto Granite (G4) included in a MSc thesis (Cruz, 1995) and a PhD thesis (Viana da Fonseca, 1996), observed identical I_D and E_D values, but with clearly divergent K_D. Furthermore, K_D profiles revealed a general tendency to remain stable with depth, with values significantly higher than 2, ranging from 5 to 15. This led to the conclusion that K_D could really reflect the effects of cementation in strength properties, confirming Marchetti's considerations (Cruz et al., 1997). However, representative K_D profiles showed limited efficiency in accessing cementation (cohesion intercept) variations, and so a different approach was attempted by Cruz et al. (2004c) and Cruz & Viana da Fonseca (2006a), based on OCR parameter derived from DMT (which in fact is an amplification of K_D). Although the concept of overconsolidation does not have the same meaning for sedimentary and residual soils, the presence of a naturally cemented structure gives rise to a behaviour very similar to overconsolidated clays, as sustained by Leroueil and Vaughan (1990). For this reason, the concept is usually designated as "virtual" or "apparent" overconsolidation, being designated by vOCR (Viana da Fonseca, 1988, 1996) or AOCR (Mayne, 2006). Besides, vOCR is I_D and K_D dependent (that is P_0 and P_1), reinforcing the confidence on the simultaneous determination of both angle of shearing resistance and effective cohesion intercept. Having this in mind, OCR derived from DMT in sandy sedimentary soils (Marchetti & Crapps, 1981) was used to obtain correlations for evaluate cemented structure strength. On the other hand, since combination of CPTu and DMT tests can also provide important references on OCR in sandy soils, based on the ratio between

Constrained Modulus (M_{DMT}) and CPTu tip resistance (q_c) (Baldi et al.,1988; Jendeby, 1992), this approach was also taken into account. Marchetti (1997), synthesizing the work of different authors, suggests that in sedimentary soils values of between 5 and 10 correspond to normally consolidated soils, whereas values of M/q_c between 12 and 24 would represent overconsolidated soils. In the context of the present work, measurements above and below water level were taken and so, it was considered that it would be preferable the use of the corrected tip resistance q_t, changing the ratio to M/q_t. The same referred NC and OC ranges may be considered, since the reported experiences were performed in non-saturated conditions and so q_c and q_t assume identical numerical value. The importance of using this ratio may be sustained as follows:

a) The M parameter is calculated on the basis of three DMT test intermediate parameters, i.e. the calculation is dependent on I_D (type of soil) and on K_D (reflects the cementation structure), besides dilatometer modulus E_D;
b) M parameter shows higher sensitivity than q_t to reflect increasing stiffness resulting from compaction level, revealed by an increase in the relation with compaction; it seems logical to expect an identical effect in terms of the parameter's response to commentated structure;
c) NC/OC is a reference frontier in mechanical behaviour and so it could be useful in characterizing different behaviours, especially to distinguish between cemented and non-cemented layers.

Global DMT and CPTu related data, obtained from Porto loose to medium compact granitic residual mass, revealed some important and sustainable trends, as pointed out by Cruz et al. (2004b, 2004c):

a) M/q_t ratio is close to the frontier NC/OC (10 to 12, according to Marchetti, 1997); overall, data shows a homogeneous distribution, with the respective ratios equally distant from NC/OC frontier;
b) It is clear that M (DMT) increases with depth at higher ratio than q_t; Figure 7.3 represents a summary of the obtained results, divided according to the NC/OC frontier;
c) K_D profiles are typical of normally consolidated soils, but varying from 3 to 15, revealing the presence of cementation, according to Marchetti's (1980) conclusions; K_D value corresponding to the NC/OC frontier of M/q_t (10-12) is between 5 and 6;

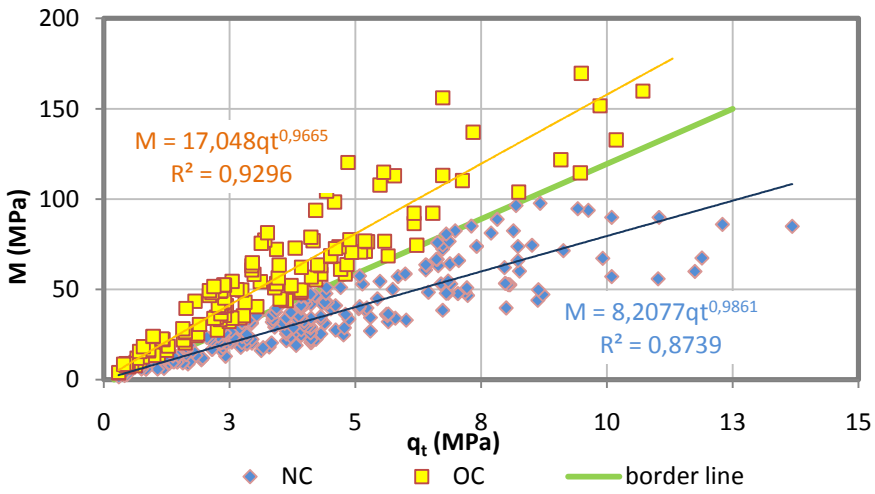


Figure 7.3 - Representative K_D, vOCR, and M/q_c profiles

Figure 7.4 illustrates a representative situation of the evolution of K_D, vOCR, and M/q_t with depth, suggesting the higher sensitivity of vOCR and M/q_t to variations in soil condition, when compared with K_D.

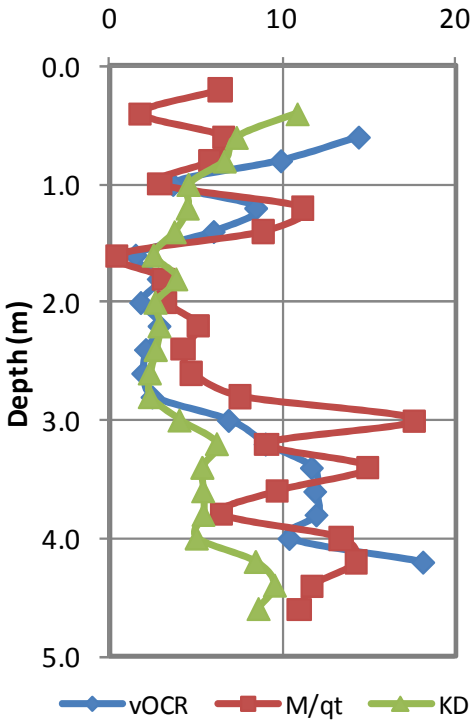


Figure 7.4 - Representative K_D, vOCR, and M/q_t profiles

7.4.2. Coefficient of earth pressure at rest, K_0

The definition of confining stresses is needed to distinguish the basic type of expected behaviour (Coop & Atkinson, 1993). Therefore, the definition of horizontal effective stresses or at rest earth pressure coefficient (K_0) becomes very important for the geotechnical analysis and design. The determination of this parameter is one of the most complex and controversial tasks of soil characterization, either through laboratory or in-situ tests, due to the disturbance effects on sampling or to the equipment installation processes. However, the parameter is often needed for design purposes and so even a rough experimental estimation is better than a "best guess" approach, as far as local or more generalized correlations can be used with other parameters. In general, it could be said that the best approach for this determination should be based in SBPT tests or in back-analysis of real situations. Unfortunately, none of these were possible during the present research and thus, the usually observed local practice was the only reference used, pointing out to values within 0.35 – 0.5 range in residual soils closer to the G4 ($10<N_{SPT}<30$) class (Viana da Fonseca, 1996), increasing to 0.6 - 0.7 in G8 ($30<N_{SPT}<60$) class (Viana da Fonseca & Almeida e Sousa, 2001, 2002) and close to 1.0 in W_5 to $W_{5\text{-}4}$ massifs (Topa Gomes, 2009).

The combination of DMT and CPTu tests seems to provide an important possibility for deriving K_0 parameter, departing from Baldi's (1986) proposal for transported soils:

$$K_0 = C_1 + C_2 \cdot K_D + C_3 \cdot q_c/\sigma'_{v0} \quad (7.1)$$

where $C_1 = 0.376$, $C_2 = 0.095$, $C_3 = -0.00172$, q_c represents the CPT tip resistance and σ'_v stands for the effective vertical stress that can be derived from DMT results; q_c has here the same meaning of q_t, since cone point resistance when using CPTu was always corrected by the area ratio (Lunne et al., 1997).

Global results from the application of this correlation were clearly out of the referred local ranges, leading to much higher values (2 or 3 orders of magnitude), generally higher than 1. On the other hand, it was found (Viana da Fonseca, 1996; Cruz et al., 1997) that data from Porto residual framework clearly showed that q_c/σ'_v ratio was quite different from 33 K_D as suggested by Campanella & Robertson (1991). Thus, a correction for C_2 constant of Baldi´s correlation was introduced (Viana da Fonseca, 1996; Cruz et al., 1997), expressed by the following equation:

$$C_2 = 0.095 * [(q_c/\sigma'_v) / K_D] / 33 \quad (7.2)$$

The application of this correction to global data revealed an unsuspected accuracy as shown in Figure 7.5, which represents the following three methodologies:

a) Direct use of the expression deduced by Baldi (1986), applied to sedimentary soils of granular nature and equivalent in terms of grain size to the soils under study (K_0 Baldi, in the figure);
b) Evaluation of the parameter exclusively based on DMT, taking the q_c/σ'_v relation equal to 33 K_D as established by Campanella & Robertson (1991); the parameter is named $K_{0\text{-}DMT}$;
c) The third approach is based in the application of Baldi's expression with C2 correction proposed by Viana da Fonseca (1996) and Cruz et al. (1997); the respective result is designated by $K_{0\text{-}rs}$.

The expressed results clearly shows the adequacy of the $K_{0\text{-}rs}$ (third approach), while the other two approaches display quite higher K_0 than local references.

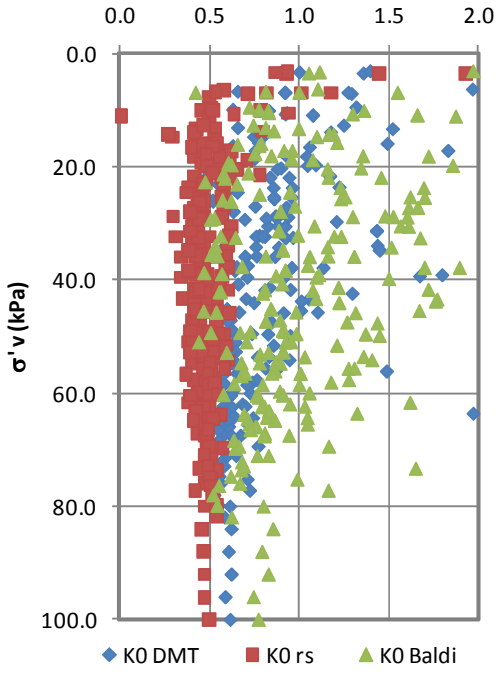


Figure 7.5 - K_0 results derived from sedimentary and residual correlations.

7.4.3. Cohesion Intercept, c'

A special framework to derive cohesion intercept was established using combined DMT and CPTu and comparing the obtained results with reference triaxial and PLT tests. For that purpose, lateral stress index (K_D) "virtual overconsolidation ratio" ($vOCR_{DMT}$) and the ratio M/q_t were selected. The reference database included four experimental sites where cohesion intercept and angle of shearing resistance were determined, namely in CICCOPN (three locations in different weathering stages) and Hospital de Matosinhos experimental sites and two other located in Porto (Cunha Junior) and Vila do Conde (Cruz et al., 2004). The mechanical characterization of the studied areas was based on "in-situ" (DMT, CPTu and PLT) and laboratory (CK_0D and CID triaxial) tests performed in samples obtained by Shelby samplers pushed into the ground and, in the case of Hospital de Matosinhos, directly from block samples. The determination of reference effective cohesive intercept, c', was established by triaxial tests and, for Hospital de Matosinhos, through the performance of a set of three plate load tests up to failure under different loading areas (Viana da Fonseca, 1996, Viana da Fonseca et al., 1998). A summary of the results is presented in Table 7.3 (DMT/CPTu data) and Table 7.4 (triaxial data).

Table 7.3 - DMT and CPTu reference values of studied sites

Site	I_D	K_D	$vOCR^{(1)}$ (DMT)	M/q_t	ϕ' (°)$^{(1)}$ (DMT)	ϕ'(°)$^{(2)}$ (CPT)
Maia 1	1.5–2.5	4.5–7.5	5–20	5–15	37–39	35–36
Maia 2	1.8–2.0	3.5–5.0	5–10	10–15	35–40	35–39
Maia 3	2.0–3.5	7.5–11.0	10–25	10–15	39–40	37–40
V. Conde	1.8–2.0	11.0–15.0	20–50	10–15	39–41	44
Porto	1.8–2.1	7.5–15.0	50–100	10–15	42	38–41
Matosinhos	1.5–2.0	7.0–11.0	10–25	10–20	39–41	42–44

(1) Marchetti's (1997); (2) Robertson and Campanella's (1983)

Table 7.4 - Triaxial reference values of studied sites

Experimental site	σ'_3 (kPa)	$\sigma'_1 - \sigma'_3$ (kPa)	c' (kPa)	ϕ' (º)
Maia 1 CID	19 23 33 40 58	85 90 120 119 200	5	37
Maia 2 CID	30 77 90 125 150	125 289 297 381 490	10.3	36.3
Maia 3 CK_0(=0.4)D	18 23 33 40 58	106 146 150 190 288	11.9	42.1
Porto CK_0(=0.4)D	8 15 30	109 114 156	24.3	32
V. Conde CK_0D	9 12 30	48 67 96	10.8	35.4
H. Matosinhos Multiple size PLT and triaxial tests (Viana da Fonseca, 1996)	-	-	9 - 12	37

Figures 7.6 to 7.8, present the deduced correlations between reference effective cohesion intercept and K_D, vOCR (DMT) and M/q_t, reinforcing the lower efficiency of K_D to cementation variations already mention in this chapter. Nonetheless, vOCR shows better adjustment to variations, since it numerically incorporates the type of soil through I_D. In the same figures, correlations with c'/σ'_{v0} (true values of this latter multiplied by 100 to be represented in the same scale, are also represented. As it can be seen the correlating factors generally decrease, but tend to show the same tendencies.

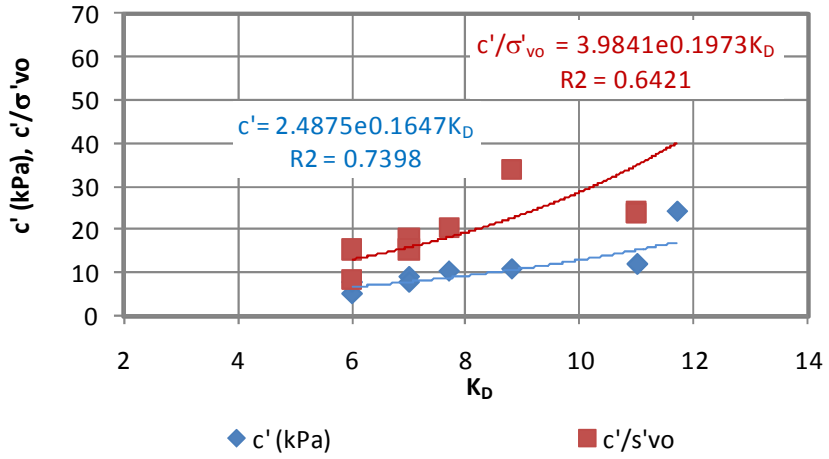


Figure 7.6 - c' vs K_D and c'/σ'_{vo} (*100) vs K_D correlations

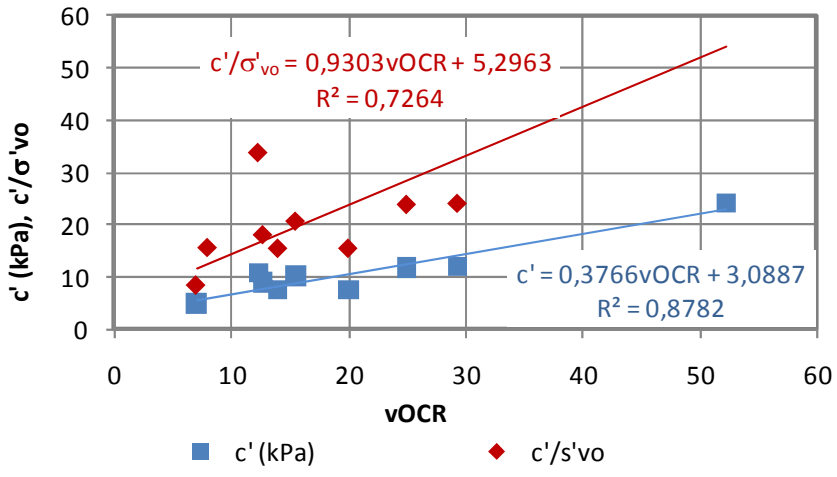


Figure 7.7 - c' vs vOCR and c'/σ'_{vo} (*100) vs vOCR correlations

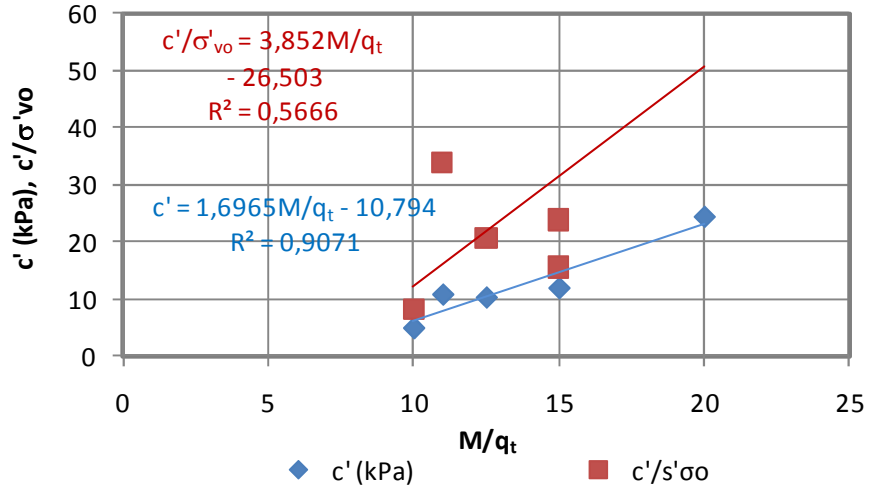


Figure 7.8 - c' vs M/q_t and c'/σ'_{vo} (*100) vs M/q_t correlations

On the other hand, the relation between the effective cohesion intercept and DMT preconsolidation stress, σ'_p (Figure 7.9), is equal to 0.011, quite lower than those observed by Mayne & Stewart (1988) and Mesri et al (1993), respectively 0.03 to 0.06 and 0.024, in overconsolidated clays, which in some way may be explained by the under-estimation of effective cohesion intercept due to sampling disturbances. This suggests the ability of the test to reflect the cementation structure.

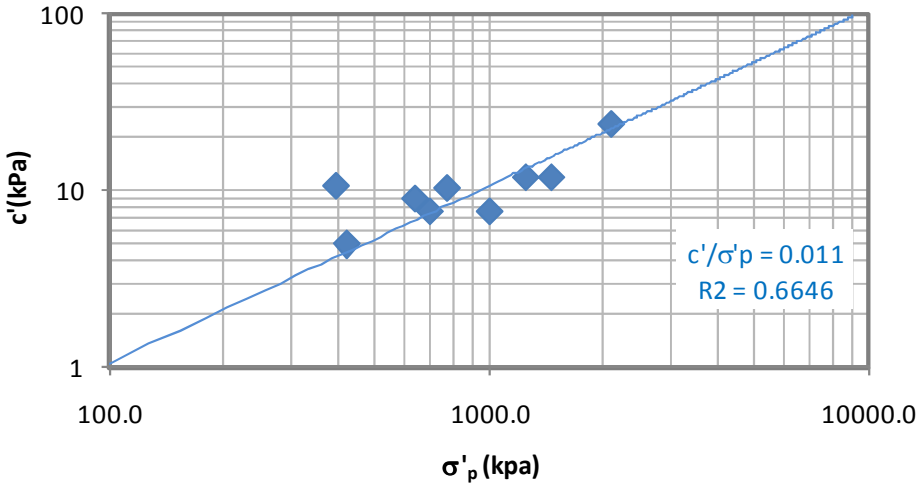


Figure 7.9 - Relation between c' and σ'_p

7.4.4. Angle of shearing resistance, ϕ'

Although, for practical purposes and for low level of cementation, bonding has little influence in variations of angle of shearing resistance, the presence of a cemented structure creates a serious obstacle to derive the parameter through in-situ tests (SPT, CPTu, PMT and, of course, DMT), when sedimentary soils expressions are used, mainly because they were developed on the principle of a (unique) granular strength (Cruz et al., 2004b, Cruz & Viana da Fonseca, 2006a, Viana da Fonseca et al., 2007, 2009), and thus, cementation resistance is "assumed" as merely granular, increasing fictionally the values of a overall angle of shearing resistance.

Taking global database it might be worth to observe global cross checking DMT and CPTu results derived respectively from Marchetti (1997) and Robertson & Campanella (1983) correlations. M/q_t reference ranges for NC/OC soils were also included in data analysis. Data analysis (Figure 7.10) revealed that ϕ_{CPTU} is higher than ϕ_{DMT}, for M/q_c below 12, and lower when M/q_c is within 12 and 24, suggesting a greater sensitivity of DMT to the cementation structure.

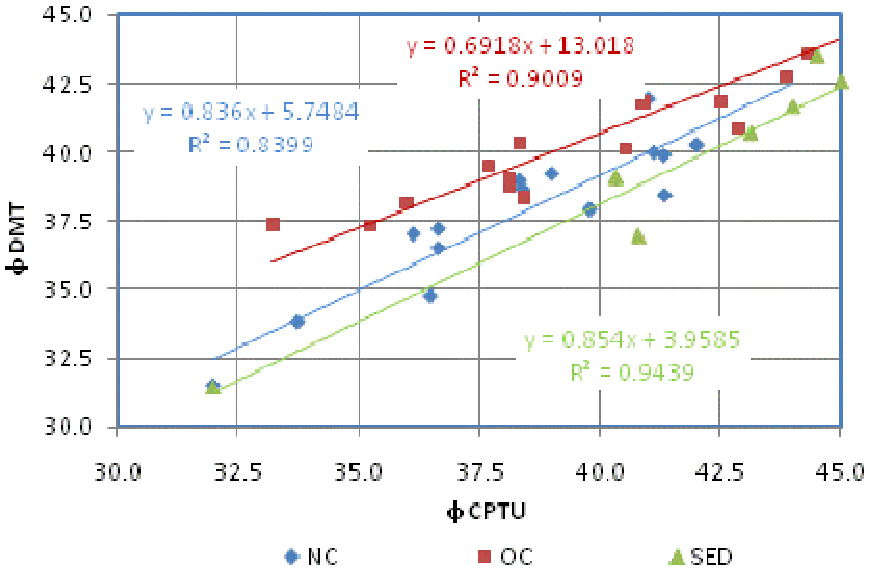


Figure 7.10 - Comparison between ϕ_{DMT} and ϕ_{CPTU}

All these trends of $\phi_{CPT(U)}$ and ϕ_{DMT} with M/q_t were also compared with those of portuguese and spanish sedimentary soils, within the same I_D interval (Cruz et al. 2006a). This comparison reveals a rough overlapping of the NC and transported soils correlations and a tendency for both to converge with the OC correlation at high angle

of shearing resistance values. The correlation factors (R^2) obtained were 0.84, 0.90 and 0.94 for NC and OC residual soils and sedimentary soils, respectively.

As expected, data confirmed the previous considerations, displaying an output range from 35º to 45º, globally higher (about 2–3º) than the reference (triaxial and multiple PLT) values. Considering the low influence that sampling has on the evaluation of angle of shearing resistance (Viana da Fonseca et al., 2001; Cruz & Viana da Fonseca, 2006a; Ferreira, 2009), the difference registered on ϕ' is mainly due to the influence of cementation structure on q_c and K_D parameters. Thus, once the cohesive intercept is obtained, it is reasonable to expect that it can be used to correct the over-estimation of ϕ', derived by transported soil correlations. In fact, taking the difference between ϕ_{DMT} (represents the global strength) and $\phi_{triaxial}$ (represents solely ϕ) and comparing it with c' (Figure 7.11), it becomes clear the good correlation between them (Cruz et al, 2004b), indicating a good ability to correct overestimated DMT derived values. Using only DMT results, the correction factor can be obtained by the following equation:

$$\phi'_{corrected} = \phi'_{DMT} - 0.138*OCR-1.16 \quad (7.3)$$

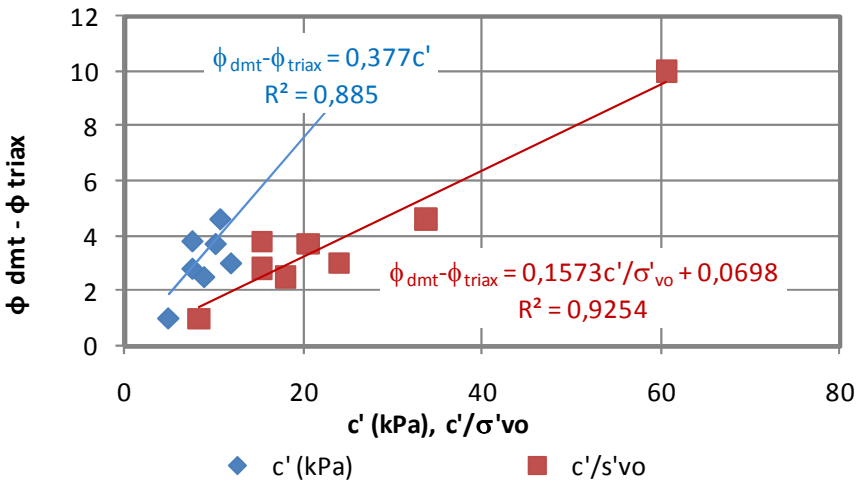


Figure 7.11 - Trends between (ϕ_{DMT}-ϕ'_{triax}) and c', 100* c'/σ'_{vo}

7.5. Deformability

Soil deformability from DMT is classically obtained by constrained modulus, M, that sometimes is used to deduce Young modulus, E, based on Theory of Elasticity (Marchetti, 1980; Marchetti, 2001). More recently, the maximum shear or distortional modulus, G_0, became an important reference for design purposes, due to the significative developments on seismic devices and criteria to discern cemented from

non-cemented soils based on this parameter has been frequently used (Schnaid et al., 2004). Being so, in the course of this research program, both parameters were analyzed and respective correlations evaluated.

7.5.1. Constrained modulus, M

The determination of stiffness parameters through DMT in transported soils has been obtained with considerable success with M (Marchetti, 1980), mainly because of the following reasons:

a) M is a parameter that includes information on soil type (I_D), overconsolidation ratio (K_D), as well as the modulus itself (E_D); in residual soils, it is reasonable to accept that cementation structure is also represented by K_D, as explained before;
b) E_D represents a ratio between applied stress and resulting displacement, with the latter presenting a highly accurate measuring system;
c) DMT insertion creates a lower level of disturbance than usual penetrometers like CPTu (Baligh & Scott, 1975).

In that context, M_{DMT} was first cross checked with (Lunne & Christophersen, 1983). Figure 7.12 presents the obtained results, revealing results significantly disperse with much lower $M_{0(CPTu)}$ (lower than 50 MPa) than M_{DMT} (5 and 150 MPa) values.

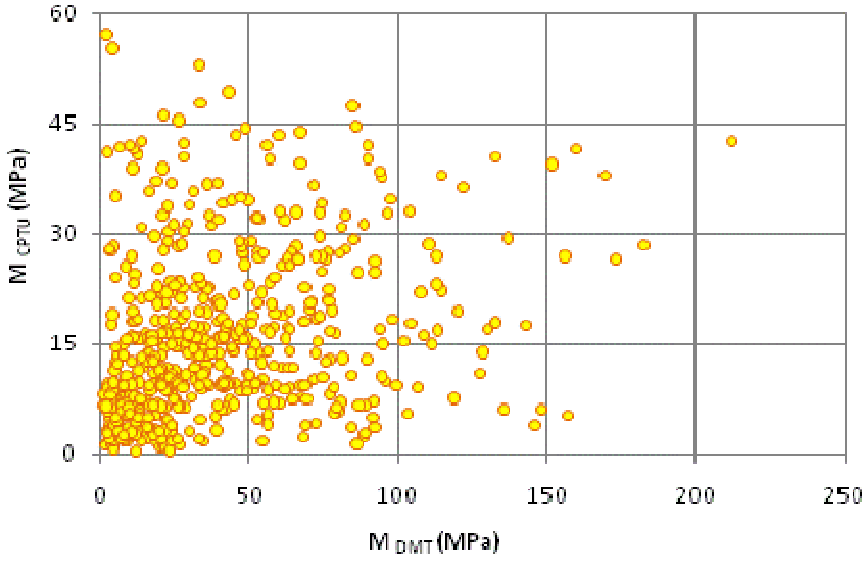


Figure 7.12 - Relation between M derived through DMT and CPTu tests

The rather difference in these values of M may be justified by the following reasons:

a) Lower disturbance levels produced during DMT insertion than CPT's (Baligh & Scott, 1975);
b) Conceptually, DMT is more adequate for the evaluation of deformability than CPTu, and M is a parameter that includes information on soil type (I_D) and cementation structure (K_D), as well as deformability (E_D), whereas M_0 is only based on q_c; triaxial test ($E_{s0.1\%}$) results clearly converge with those from DMT (Cruz & Viana da Fonseca, 2006a);
c) M is derived from DMT following a theoretical basis, while in CPTu the approach is purely semi-empirical.

A different approach was proposed by Viana da Fonseca (1996), based on data from triaxial tests related with two of the locations within the scope of this framework. The dilatometer modulus, $E_{D,}$ was correlated with the deformation modulus at 10% of shear strain, $E_{s10\%}$, using a normalized lift-off pressure, P_{0N}. The general correlation can be written in the form:

$$E_{s10\%} / E_D = 2.35 – 2.21 \log (P_{0N}) \quad (7.4)$$

The respective correlations lead to higher values than the ones proposed by Baldi et al. (1989) and Jamiolkowski & Robertson (1988) for NC transported soils and lower than correspondent OC soils (Baldi, 1989).

7.5.2. Maximum shear modulus

The ratios between a stiffness modulus and a specific stress-strain in-situ test parameter are higher in over-consolidated and cemented soils than in normally consolidated ones (Baldi et al., 1989), because these modulus have a good sensitivity to stress history of the soil when compared to other in-situ test parameters. However, if stiffness modulus is not elastic, correlations become dependent of several other factors, besides stress history. On the contrary, if the correlation is made with small strain shear modulus ($G_{0)}$, it depends exclusively on the combination of the void ratio and the average effective stress, represented by the State Parameter, ψ (Viana da Fonseca, 1996; Cruz et al., 1997). As a consequence, in the last decade maximum shear modulus (G_0), easily determined by seismic tests with geophysical techniques, became the main reference stiffness parameter for design purposes. This was also

potentiated by the perception that non-linear methods for geotechnical analysis rely on this “starting point” for competent modeling.

As already discussed in Chapter 5, Cruz et al. (2006a), taking the advantage of having a numerical identification, introduced I_D in the correlations for sedimentary NC soils, concluding that R_G (G_0/E_D) globally decreases with increasing I_D. A similar approach was applied to three residual soils well referenced experimental sites within the present scope (CEFEUP, IPG Guarda and Casa da Música in Porto), where seismic cross-hole data was available. To confirm the presence of cementation, the data obtained in these experimental sites was plotted on the charts presented by Schnaid et al. (2004), where the variations of G_0 with $(N_1)_{60}$ (SPT) and $(q_c)_1$ (CPT) are represented in a space within two bounds. These diagrams plotted in Figure 7.13 and Figure 7.14, confirm the presence of the cemented structure, revealing that these soils are not strongly structured, lying near the lower bound line for cemented materials (Viana da Fonseca et al., 2007, 2009).

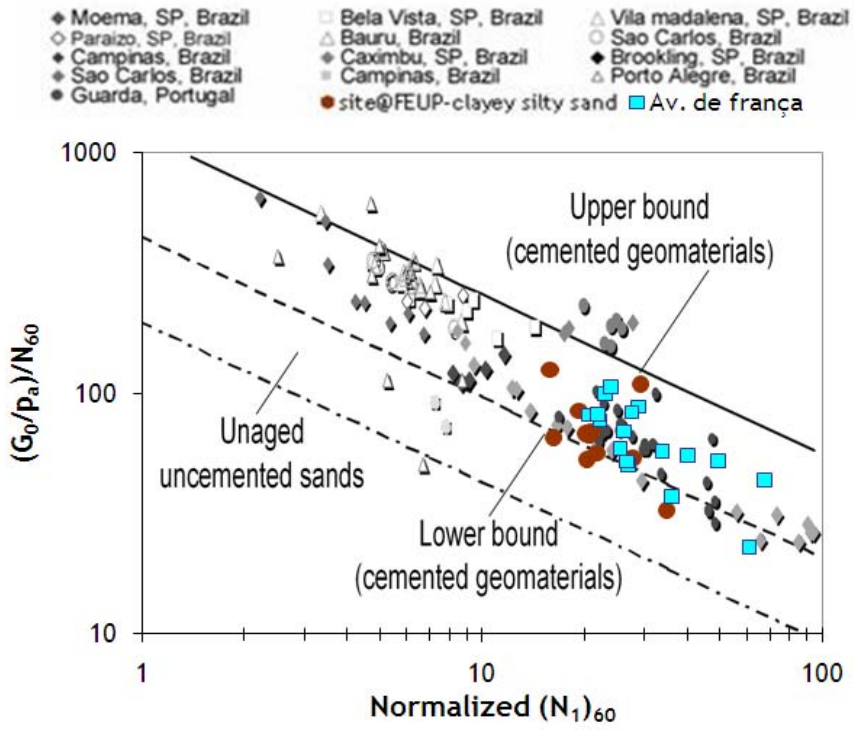


Figure 7.13 - Relations between G_0 and N_{60} for structured soils (after Viana da Fonseca et al., 2007)

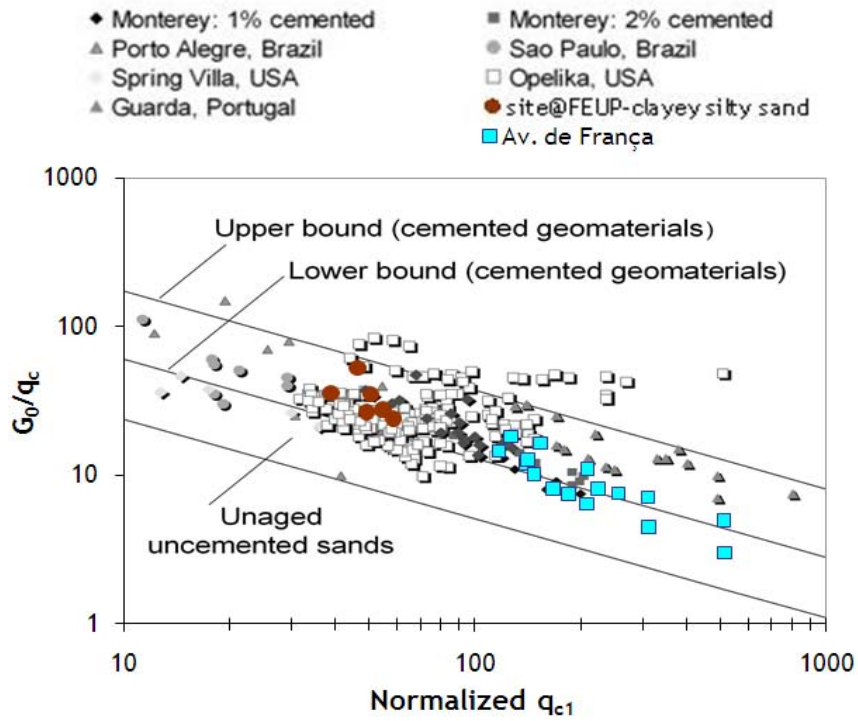


Figure 7.14 - Relations between G_0 and q_c for structured soils (after Viana da Fonseca et al., 2007)

In Figure 7.15, R_G versus I_D plot is presented, revealing a similar pattern to the one followed by sedimentary soils, but with higher absolute R_G values, confirming the expected higher stiffness with the increase of cementation level. The same data is represented in the 3D plot of Figure 7.16.

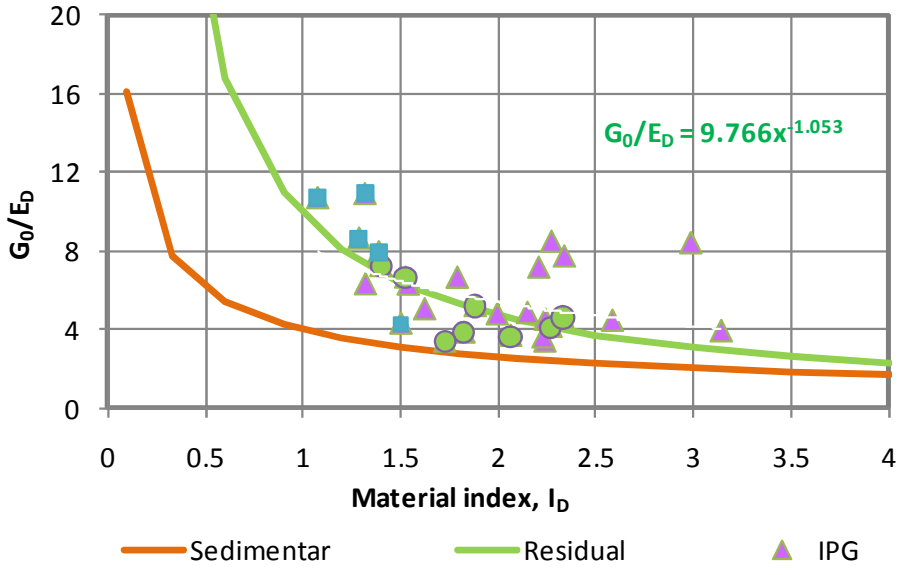


Figure 7.15 - Relations between G_0/E_D vs I_D

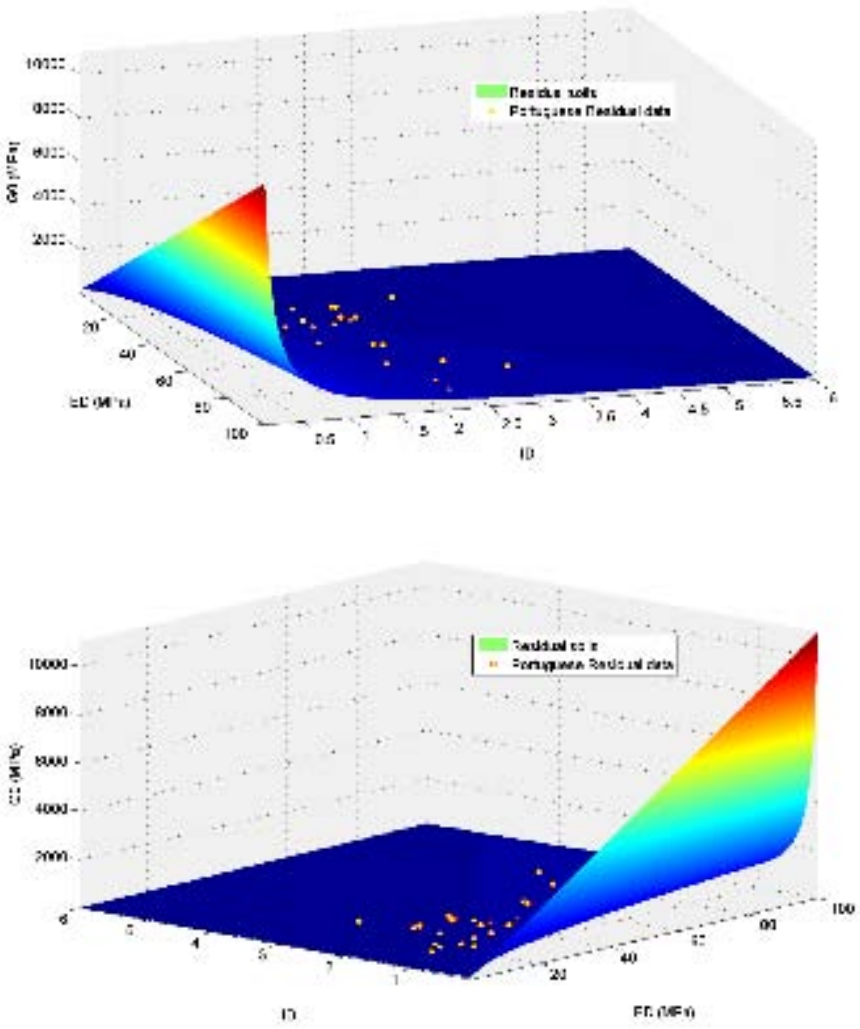


Figure 7.16 -3D plot of G_0 as function of E_D and I_D

Following the same approach applied to sedimentary soils (Chapter 5) a deeper mathematical analyisis was performed using MatLab ®. However, since the available data is scarce and confined to a very narrow band of I_D values ($1<I_D<3$), the possibilities of retrieving significant adjustments in that attempt were not expected. To overcome this problem a choice was made of using the same mathematical best fitting surfaces found in the sedimentary case, once the same kind of trends had been observed in the R_G vs I_D analysis (Figure 7.15) and thus giving some expectation on this procedure. In Table 7.5 and Figure 7.17, the respective analysis output is presented, also including the sedimentary data for comparison purposes. Even though the obtained correlations cannot be considered robust by the simplifying adopted procedure, they might be of some help to develop future research works with more quantity and variety of data.

Table 7.5 - Function parameters and statistics.

Soil Type	Function	α	β	γ	Correlation Factor, R^2	Relative Residuals	
						Median	Mean
Sedimentar	F1	2.5920	-0.6968	-0.0761	0.6774	0.2074	0.2885
	F2	3.0206	-0.6934	-0.5777	0.6923	0.2043	0.2878
	F3	4.5813	-1.5328	-0.4014	0.6427	0.2079	0.2962
	F4	3.1720	-0.6923	-0.4553	0.6892	0.2060	0.2861
Residual	F1	1.4492	0.2267	0.0623	0.3522	0.2731	0.2364
	F2	0.6895	0.2108	0.6080	0.3896	0.2097	0.2329
	F3	2.0701	0.7667	0.4171	0.3863	0.2007	0.2342
	F4	0.8188	0.2178	0.3992	0.3735	0.2426	0.2326

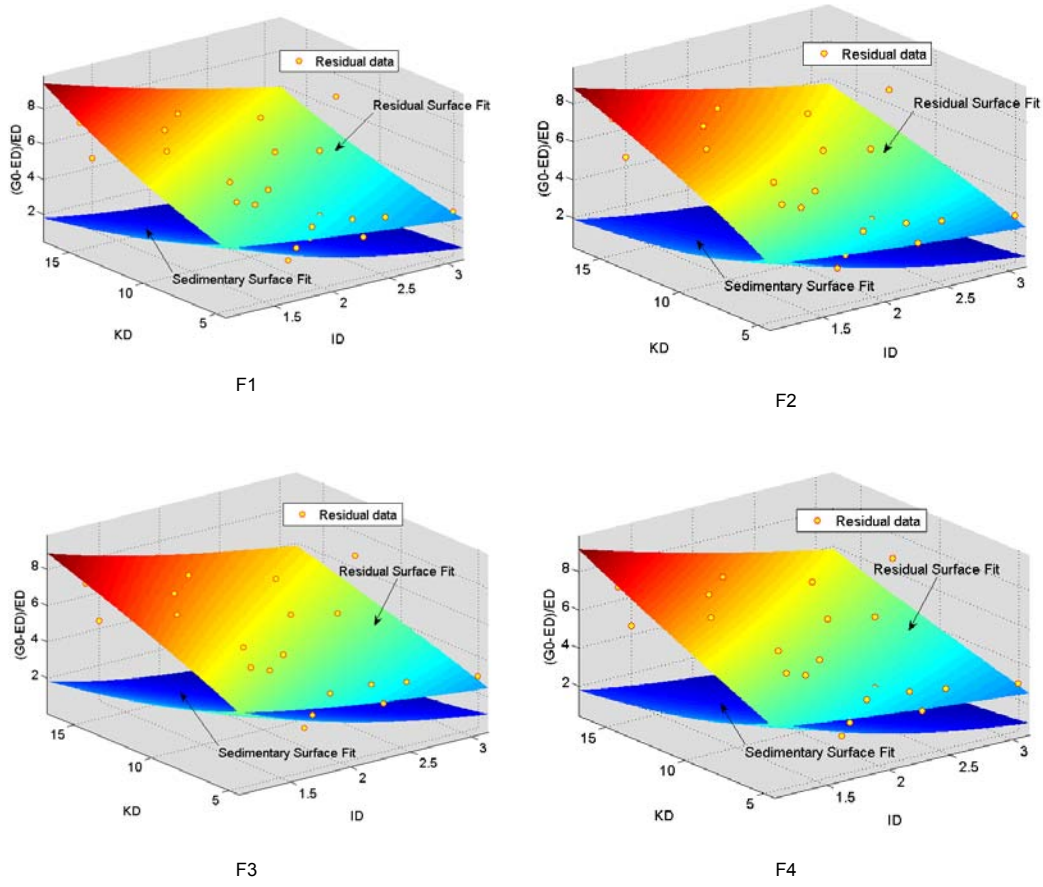


Figure 7.17 -3D Representation of best fitting surfaces.

Viana da Fonseca (1996), following the proposal of Baldi (1989) for sedimentary sands, obtained a correlation between G_0/E_D and the dimensionless DMT "lift-off" pressure (P_{0N}), expressed as follows:

$$G_0/E_D = 16.9 - 16.3 \log (P_{0N}/10) \quad (7.5)$$

where P_{0N} can be determined by the equation below:

$$P_{0N} = P'_0 / \sqrt{(\sigma'_{v0} * p_a)},\ p_a = 1kPa \quad (7.6)$$

Taking another point of view, Hryciw (1990) pointed out that correlations based on E_D would be affected by DMT strain working level, which may be too large to be related to small-strain behaviour. Thus, the author proposed a new method for all types of soils, developed from an indirect method proposed by Hardin & Blandford (1989), by substituting the variables σ'_0 and void ratio (*e*) for K_0, γ e σ'_{v0}, (all derived from DMT), as expressed below:

$$G_0 = [530/(\sigma'_{v0}/P_a)^{0.25}] * [(\gamma_d/\gamma_w)-1]/[2.7- (\gamma_d/\gamma_w)]*[K_0^{0.25}(\sigma'_{v0}*P_a)^{0.50} \quad (7.7)$$

However, global data obtained from this equation was to low when compared to reference values (blue marks in Figure 7.18) pointing out the need for a correction factor. Once again, vOCR became a very useful parameter for that purpose. A global correction factor obtained from the same experimental sites could be expressed by (bordeaux marks in Figure 7.19):

$$G_{0\ correct} = G_{0\ (Hryciw)} * 2.5 * OCR^{0.12} \quad (7.8)$$

or individually, for each site (data compared with 1:1 line in Figure 7.18).

Casa da Música - $G_{0\ correct} = G_{0\ (Hryciw)} * 3.9 * OCR^{0.15}$ (7.9)

CEFEUP - $G_{0\ correct} = G_{0\ (Hryciw)} * 1.6 * OCR^{0.25}$ (7.10)

IPG Guarda - $G_{0\ correct} = G_{0\ (Hryciw)} * 2.1 * OCR^{0.15}$ (7.11)

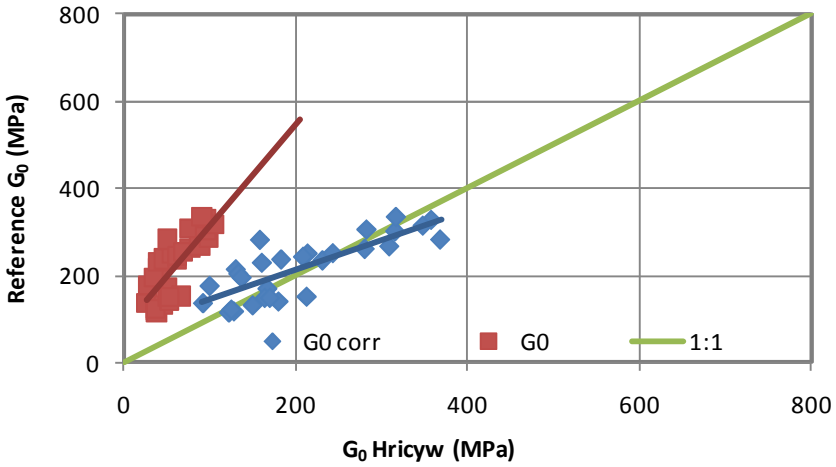


Figure 7.18 - Global G_0 deduced by Hricyw correlation compared with reference values

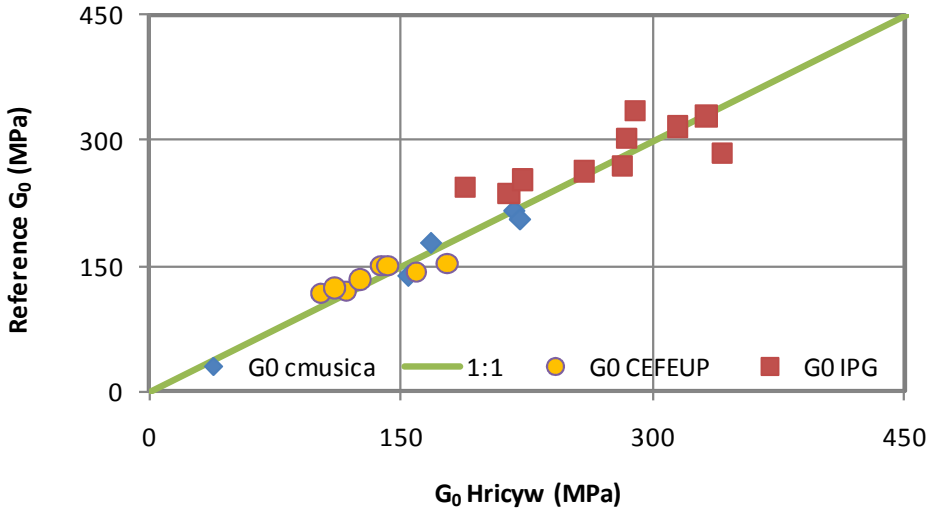


Figure 7.19 - G_0 deduced by Hricyw correlation, for each experimental site

7.6. A case study – Casa da Música Metro Station

An illustrative case study (Rios Silva, 2007; Viana da Fonseca et al., 2007, 2009) for evaluation of the proposed correlations efficiency is related to the characterization studies conducted for the design and subsequent back-analysis based on real time monitoring of a strutted excavation in Porto Metro Network (Casa da Música Metro Station).

The location of this case study is geologically dominated by heterogeneous weathered granite masses with deep residual soil profiles, within the general characteristics of

geological and mechanical properties of Porto granitic formation. The study included the interpretation of a significant volume of in-situ test results, triaxial tests over undisturbed samples and monitoring data, giving rise to specific correlations between testing and design parameters.

7.6.1. Geological and geotechnical site conditions

The geological and geotechnical site conditions of this area are representative of the general pattern observed within this work. The local is characterized by a thick residual soil layer (15m depth) overlaying the granitic rock massif (weathering degree W_5, W_4) of the dominant Porto Granite Formation, rather heterogeneous, with a predominant kaolin matrix with frequent boulders of less weathered rock mass. The residual mass is constituted by medium to coarse resistant quartz grains bonded by fragile clayey plagioclase bridges generating a soil with medium porosity fabric (details in Rios Silva, 2007). The evaluation of geomechanical properties of this residual soil was made by a detailed cross-correlation between in-situ and lab tests parametric results, as well as back-analysis based on finite element (FEM) simulation of the instrumented excavation (Viana da Fonseca et al., 2007, 2009). Apart from DMT tests, the in-situ testing program included dynamic (SPT, DPSH and DPL) and static (CPTu) penetration tests and cross-Hole tests (CH). In Table 7.6 the main ranges of in-situ test parameters are presented, while Table 7.7 shows the DMT results.

Table 7.6 - In-situ test parameters at Casa da Música Metro Station (Rios Silva, 2007; Viana da Fonseca 249ehav., 2007, 2009)

Depth	$N_1(60)$	qt (Mpa)	ft (kPa)	Qt	Vs (m/s)
0.0 – 15.0	10 – 30	2.5 – 6.0	100-250	20 – 100	250-300
>15.0	> 60	>10	>300	---	>300

Table 7.7 - DMT parameters at Casa da Música Metro Station (Viana da Fonseca 249ehav., 2007, 2009)

Depth	I_D	E_D (Mpa)	K_D (kPa)	Type of soil
0.0 – 1.0	1.80 – 2.60	20 – 45	30.0 – 40.0	Silty sand
1.0 – 5.5	1.00 – 1.85	10 – 30	6.0 – 10.0	Sandy silt to silt
5.5 – 6.5	1.25 – 1.75	40 – 45	6.0 – 10.0	Sandy silt

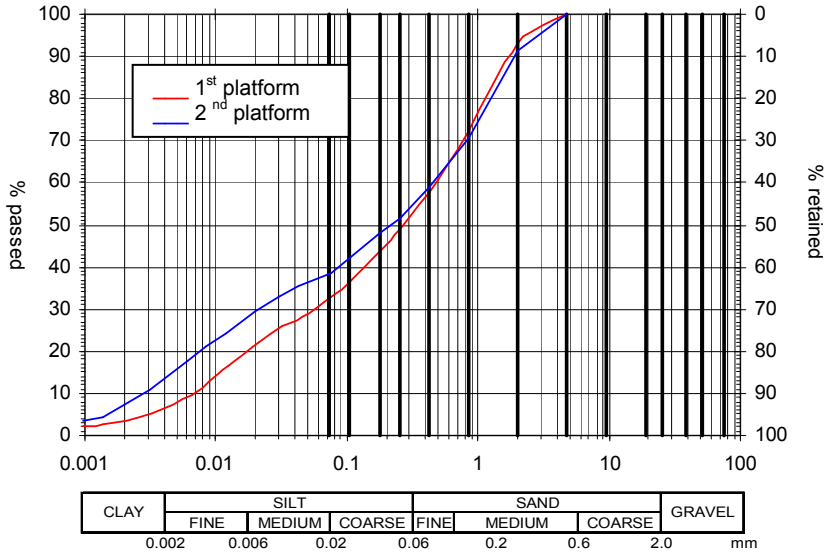
The experimental data revealed the following general mechanical behavior (Viana da Fonseca et al., 2007, 2009):

a) The level of cementation of the soil was not high, although exhibiting higher absolute values, especially concerning strength parameters and maximum shear modulus.
b) The local soil is characterized by low stiffness values at “medium to high” strain levels, revealing a strong non-linearity in the stress-strain “degradation” revealed both by triaxial and FEM simulation; data confirmed the general observed pattern of Porto residual granitic soils are characterized by a high initial stiffness (high G_0) followed by a sharp drop when the bonded structure is broken.

7.6.2. In-situ tests correlations

7.6.2.1. Soil classification and unit weight

The grain size distribution curves presented in Figure 7.20 reveals that this is a fine to medium grade and low plasticity material, mainly referenced as silty sand (SM) according to the typical classification of Porto residual soil (Viana da Fonseca et al., 1994).



(1st platform = 6.5 m; 2nd platform =11 m)

Figure 7.20 - Granulometric curves of the soil at two different depths

The classification of these materials using CPTu charts (Robertson, 1990) revealed very stiff sand to clayey cemented sandy soils. I_D values clearly converged (as usual) to those, classifying the soil as sands, silty sands or even sandy silts. Confirming the conclusions presented by Cruz & Viana da Fonseca (2006a), DMT unit weight (Marchetti & Crapps, 1981) revealed differences to laboratory tests globally lower than 1kN/m^3 (Table 7.8 and Table 7.9). Determination of the parameter based on shear waves velocity (V_s), following Mayne's (2001) proposal for sands, converges to the same order of magnitude (19 kN/m^3):

$$\gamma_{sat}\ (kN/m^3) = 8.32\log(v_s) - 1.61*\log(z) \qquad (7.12)$$

Table 7.8 - Unit weight determinations (Cross section 1)

Prof (m)	γ (kN/m^3)	γ_{DMT} (kN/m^3)
0 – 0.9	---	18.5
0.9 – 3.5	20.2	19.3
3.5 – 9	19.5	---
9 – 13.4	19.4	---
13.4 – 16.5	20.2	---

Table 7.9 - Unit weight determinations (Cross section 2)

Prof (m)	γ (kN/m^3)	γ_{DMT} (kN/m^3)
0 – 0.8	---	18.6
0.8 – 2.3	---	18.3
2.3 – 4.5	20.1	18.1
4.5 – 6.8	19.3	19.3
6.8 – 10.4	19.3	---
10.4 – 13.4	19.4	---
13.40 – 13.65	19.7	---
13.65 – 19.5	20.4	---

7.6.2.2. Stress state at rest and vOCR

The coefficient of earth pressure at rest was evaluated by one methodology already discussed in an earlier section of this chapter (Viana da Fonseca, 1996, Cruz et al., 1997), consisting in correcting the second term of the proposal of Baldi et al. (1985). Figure 7.21 represents both correlations, illustrating the inadequacy of sedimentary approach to residual soils. It is quite clear that the corrected correlation give rise to more realistic results, confirming the trends in similar soils reported by Viana da Fonseca et al. (2004, 2005).The estimation of the virtual over-consolidation ratio (vOCR) in sands is more complex than in clays, as it results from a complex history of preloading, desiccation and other effects difficult to quantify (Marchetti et al., 2001, 2006). The obtained results are presented in Figure 7.22.

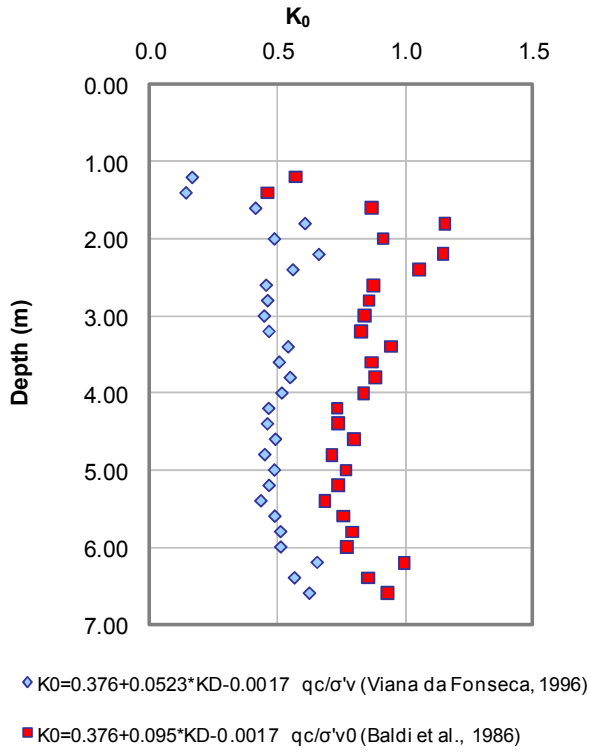


Figure 7.21 - Estimation of the coefficient of earth pressure, K_0 (adapted from Viana da Fonseca et al., 2007, 2009).

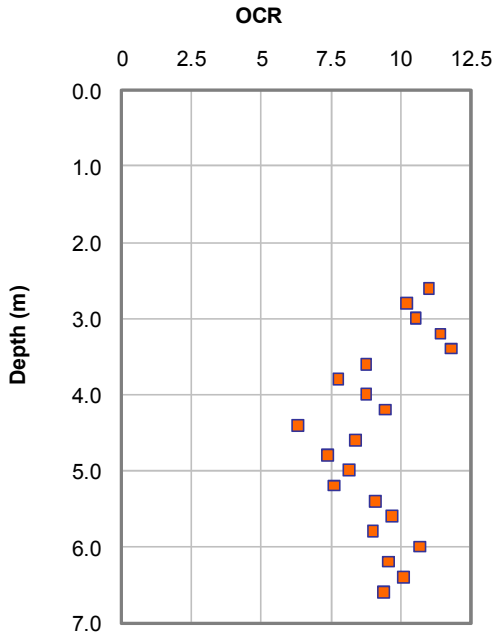


Figure 7.22 - vOCR profile estimated from DMT parameters (adapted from Viana da Fonseca et al., 2007)

7.6.2.3. Shear strength

The strength parameters used for this type of soil are those of Mohr-Coulomb criteria: the angle of shearing resistance (ϕ') and the effect of the effective cohesion intercept (c'), as it can be assumed to be loaded in drained conditions. Figure 7.23 presents the values of ϕ' obtained according to Mayne et al. (2001) for SPT, CPTu and DMT parameters (respectively, Eq. 7.13, 7.14 and 7.15) and of that proposed by Marchetti et al. (2001) based on DMT results, as indicated in Eq (7.16).

$$\phi' = [15.4*(N_1)_{60}]^{0.5}+20 \quad (7.13)$$

$$\phi' = \text{atan}[0.1+0.38*\log(q_c/\sigma'_{v0})] \quad (7.14)$$

$$\phi' = 20 + [1/(0.04+0.06/K_D)] \quad (7.15)$$

$$\phi' = 28 + 14.6 \log/(K_D) – 2.1 \log^2(K_D) \quad (7.16)$$

$$\phi'_{corrected} = \phi'_{DMT} – 0.138*OCR-1.16 \quad (7.17)$$

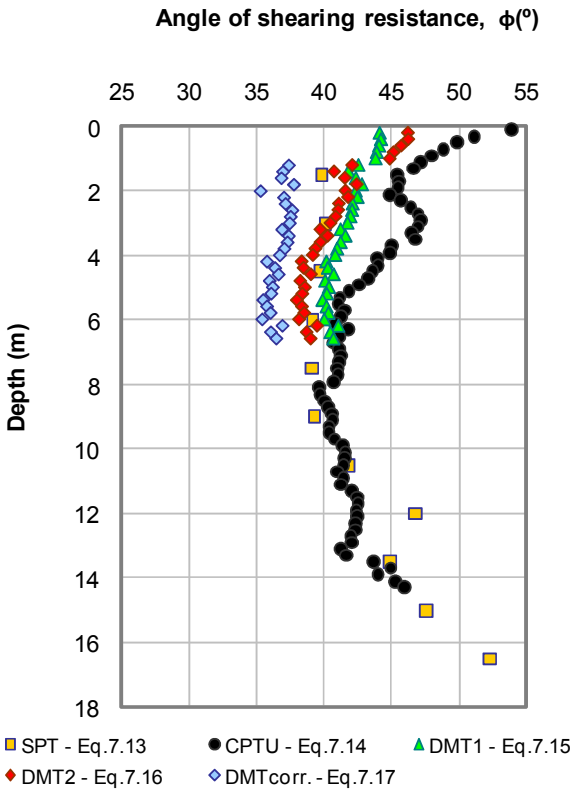


Figure 7.23 - Angle of shearing resistance obtained with various correlations (adapted from Viana da Fonseca et al., 2007, 2009)

As expected, the results from CPTu are the less conservative, reflecting the sensitivity of this test to cementation. The other three correlations converge towards the same results. It should be noted that correlations based on DMT – equations (7.15) and (7.16) – give the lowest values, with particular emphasis on the second one. A reasonable explanation for this fact, is that equation (7.16) was proposed by Marchetti (2001), as the lowest bound on ϕ'/K_D diagrams. It should be noted that, even so, correlations based on DMT results are more sensible than CPT to damage during installation. Eq. 7.17, in the same figure represents the correction proposed by Cruz & Viana da Fonseca (2006a), already defined in the course of the present chapter.

As expected, all the results are quite high, when compared to the triaxial tests results (ϕ'=37º), with the exception of results from Eq. 7.17 (Cruz & Viana da Fonseca, 2006a), revealing values close to triaxial test results, supporting the application of this expression.

Some authors (Lacasse & Lunne, 1988) defend that in granular soils DMT's K_D parameter should be complemented by q_c values from CPT or CPTu. It's curious to observe that plotting the ratio (q_c/σ'_{vo}) as a function of K_D, these results stand between

the proposal of Campanella & Robertson (1991) for sedimentary silty sands and the one proposed by Viana da Fonseca (1996) for residual soils (Figure 7.24).

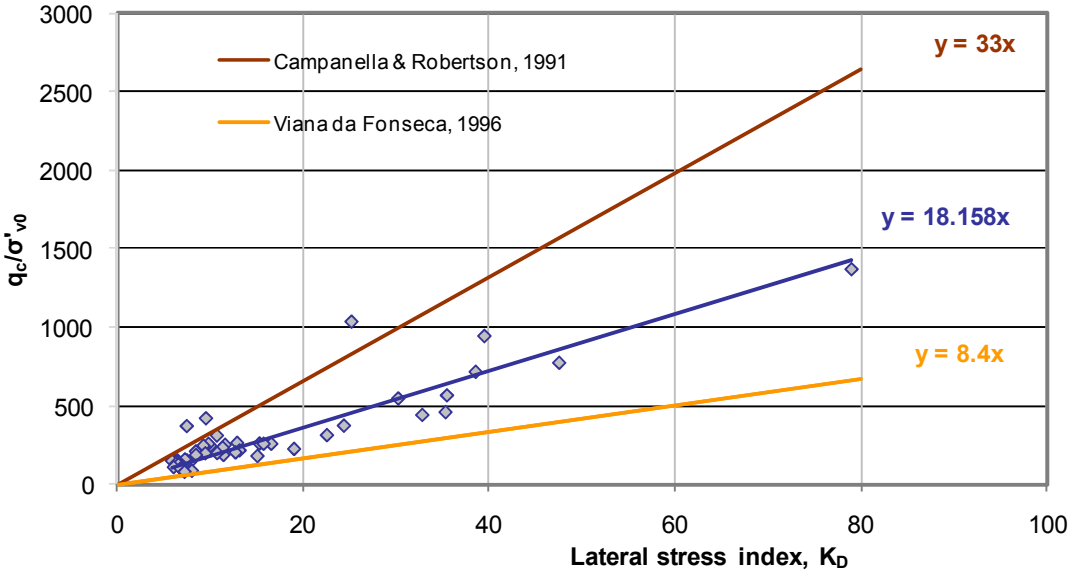


Figure 7.24 - Relations between q_c/σ'_{vo} e K_D (after Viana da Fonseca et al., 2007, 2009)

Finally, results from CPTu were inserted in the curves of Robertson & Campanella (1983) within the data presented by Viana da Fonseca et al. (2006), showing higher absolute values, mainly in the most superficial horizons (Figure 7.25).

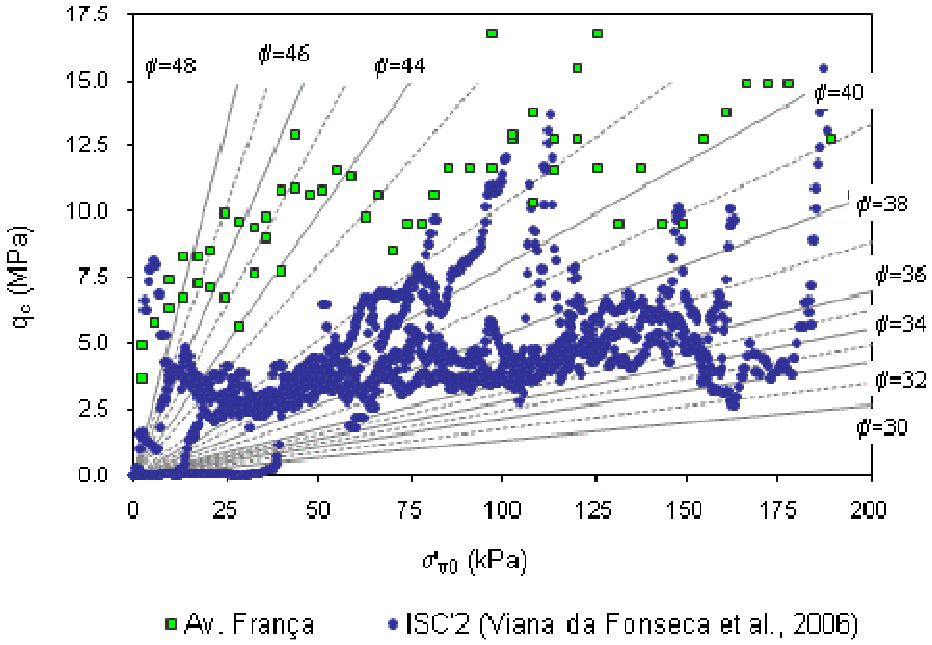


Figure 7.25 - Angle of shearing resistance from CPT data (adapted from Viana da Fonseca et al., 2007, 2009)

The increase in strength due to the cemented structure is provided by the effective cohesive intercept, c', that is not related to the presence of clayey/fine material. Cruz et al. (2004) and Cruz & Viana da Fonseca (2006a) proposed correlation based on the vOCR revealed an average value of 7 kPa, as plotted in Figure 7.26. This is within the range frequently found in this class of soils, although triaxial tests provided a much lower value (c'=2 kPa), associated to sampling disturbance (in the present case by means of Shelby tubes), which seem to be higher than that due to DMT insertion.

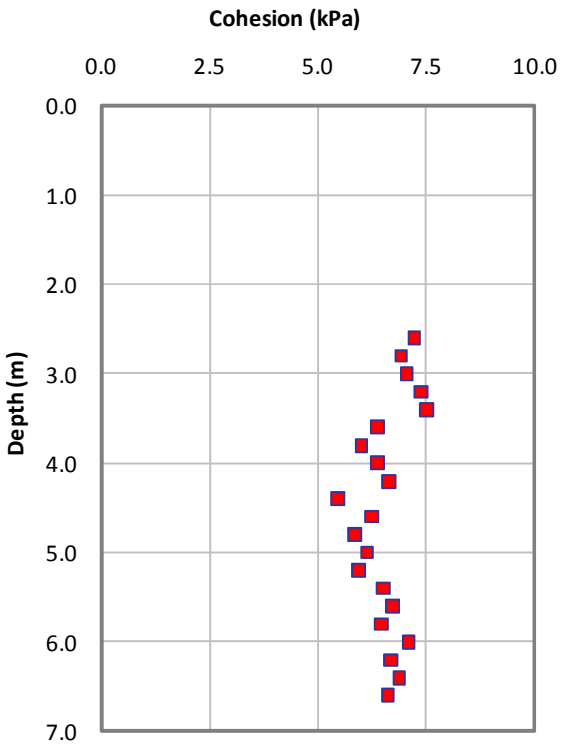


Figure 7.26 - Cohesive intercept derived from Cruz et al. (2006). Profile in cross-section 2 (adapted from Viana da Fonseca et al., 2007, 2009)

7.6.2.4. Stress-strain relations

The maximum shear modulus (G_0) is the reference stiffness parameter and can be easily obtained from shear wave velocities by means of seismic tests such as cross-hole test or down-hole seismic devices integrated in dilatometer (SDMT) or cone penetrometer (SCPTu). Figure 7.27 shows the comparison between the values directly determined by cross-hole (Eq. 7.18) and from the correlations proposed by Viana da Fonseca (1996) for Porto residual soils (equations (7.19), (7.20) and (7.21)):

$$G_0 = \rho \times V_s^{\,2} \tag{7.18}$$

$$G_0 = 98 + 0.42 \times N_{60} \tag{7.19}$$

$$G_0 = 57 \times N_{60}^{\,0.2} \tag{7.20}$$

$$G_0 = 3.2 \times q_c + 95.7 \tag{7.21}$$

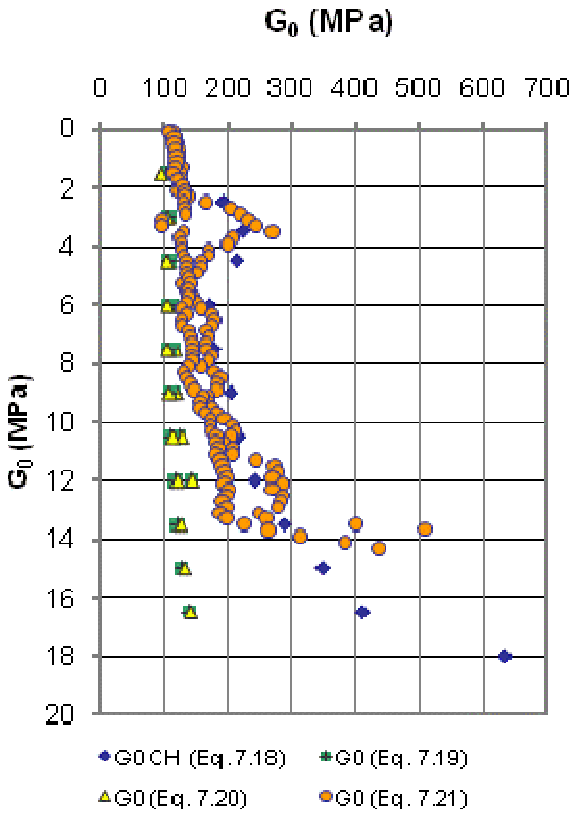


Figure 7.27 - Comparison between G_0 (CH) and correlated G_0 (after Viana da Fonseca et al., 2007, 2009)

It is clear that cross-hole test leads to higher values, but fairly close to those taken from CPTu correlation. In opposition, the correlations based on SPT provided similar results but rather lower than the others. It's also clear that stiffness is quite constant or increase smoothly in depth until 13.4 m, but greatly increases after that point indicating a less weathered rock.

As already explained, there are two different approaches to assess G_0 from DMT results. Concerning to G_0/E_D versus I_D approach (Cruz & Viana da Fonseca, 2006a), the respective analysis was already discussed, since this experimental site was included in the base correlated data.

On its turn, Hryciw (1990) proposed approach show quite low values when compared with reference G_0, which might be due to the application of a correlation developed for sands. Meanwhile the plot of the ratio $G_0^{CH}/G_0^{(Hryciw)}$ versus OCR, shows that the trend is similar to the one obtained for CEFEUP experimental site (Viana da Fonseca et al., 2006), although with some differences in absolute values. Nevertheless, applying the correction found in that chart and expressed in Eq. (7.22), the values become quite convergent to the ones obtained in seismic cross-hole tests (Figure 7.28).

$$G_{0\,(correct)} = G_0^{\,(Hryciw)} * 1.96 * OCR^{0.396} \qquad (7.22)$$

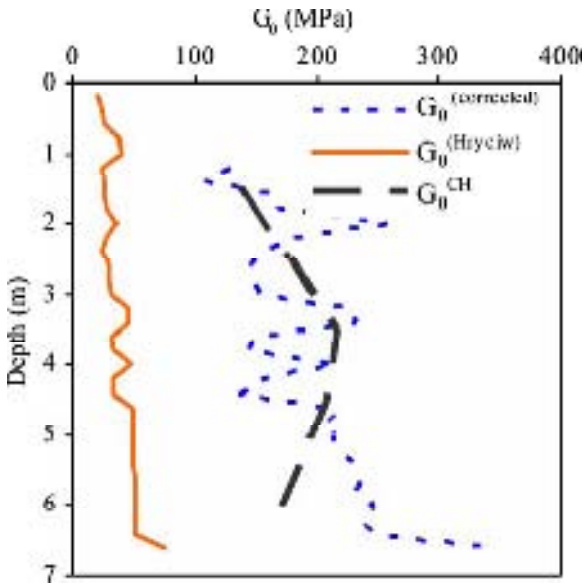


Figure 7.28 - Comparison between Cross-Hole G_0, Hryriw G_0 and corrected G_0 (adapted from Viana da Fonseca et al., 2007, 2009)

Finally, Figure 7.29 presents the relation between G_0/E_D and the dimensionless ‘‘lift-off’’ pressure of the DMT (p_{0N}), revealing higher absolute values than those obtained by Viana da Fonseca (1996, 2003) for Porto residual soil and by Baldi et al. (1989) for sands. In the present case reference G_0 was assumed constant (200 Mpa) according to the results obtained from the Cross-Hole tests in the same depth range.

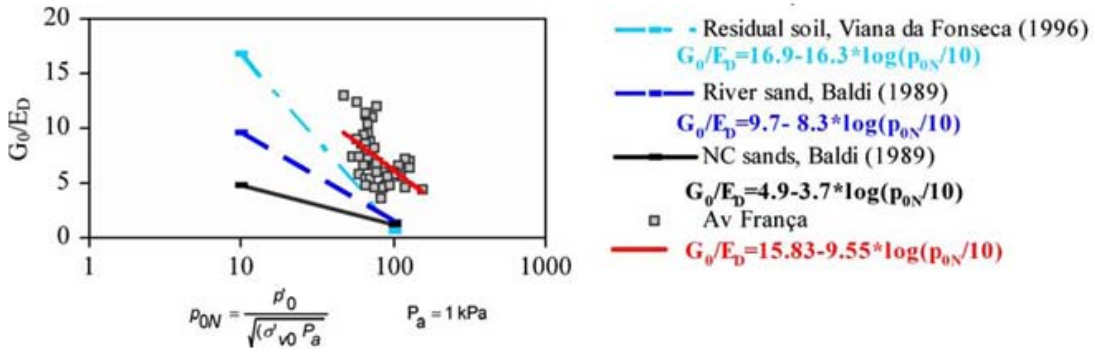


Figure 7.29 - Relations between G_0/E_D and p_{0N} (after Viana da Fonseca et al., 2009)

7.7. Summary

Fifteen years of practice with DMT in residual soils, combined with other in-situ and laboratorial tests allowed deducing sustainable regional correlations for granitic residual soils, as synthesized in Table 7.10.

Globally, data have proven that characterization campaigns based on DMT or combined DMT and CPTu tests are an effective tool for the characterization of medium compact to compact granitic residual soils essentially because:

a) Both tests give important information about stratigraphy profile, easily integrated within borehole information, and with higher capacity for detecting thin layers; unit weight can also be deduced by both tests individually;
b) Globally data has shown to be consistent and reproducible and in good agreement with other in-situ test trends;
c) State of stress can be evaluated by combined CPTu and DMT tests with reasonable adequacy.
d) From the strength point of view, DMT alone (through vOCR) or combined with CPTu (M/q_t) provide numerical information related to cementation (effective cohesion intercept) and may adequately derive angles of shearing resistance, revealed by proper calibration using triaxial test results. However, the reference values are expected to deviate from reality, at least due to sampling processes.
e) It is possible to deduce from DMT, high quality and varied numerical data related to stiffness, such as constrained, deformability and maximum shear modulus.

f) The number of combined DMT and CPTu basic parameters (four mechanical and two related with water) allows a wider sort of combinations, which might be useful to quantify some other properties of residual (or other non-textbook) soils, such as suction in unsaturated soils.

Table 7.10 - Correlations for granitic residual soils from Porto and Guarda

Parameter	Correlation	Author
Unit weight, γ (kN/m^3)	Same used in sedimentary soils	Marchetti & Crapps,1981
At rest pressure coefficient, K_0	$K_0 = C_1 + C_2 \cdot K_D + C_3 \cdot q_c/\sigma'_{v0}$ $C_1 = 0.376$, $C_3 = -0.00172$ $C_2 = 0.095 * [(q_c/\sigma'_v) / K_D] / 33$,	Viana da Fonseca, 1996
Cohesion intercept, c' (kPa)	c' = 0.3766*vOCR+3.0887 c' = 1.6965*M/qt-10.794	Cruz et al., 2004, 2006
Angle of shear resistance, ϕ'	Factor of correction to apply to Marchetti´s (1997) correlation: $\phi'_{corrected} = \phi'_{DMT} - 0.377*c'$	Cruz & Viana da Fonseca, 2006[a]
Constrained modulus, M (Mpa)	Same used in sedimentary soils	Marchetti, 1980
Secant deformability moduli, E_s (Mpa)	$E_{s10\%} / E_D = 2.35 – 2.21 \log (P_{0N})$	Viana da Fonseca, 1996
Small-strain shear modulus, G_0 (Mpa)	$G_0/E_D = 9.766*I_D^{-1.053}$ $G_0/E_D = 16.9 – 16.3 \log (P_{0N}/10)$	Cruz et al., 2004, 2006 Viana da Fonseca, 1996

Chapter 8.
Accuracy of results

8. ACCURACY OF RESULTS

The efficiency of a test measurement device depends on some different issues that may be useful to analyze and discuss. Apart from usual considerations about quality control of measurement devices (such as precision, accuracy, etc), some characteristics of DMT strongly influence final results:

a) Blade geometry;
b) Modes of penetration (pushing or driving);
c) Measurement devices.

In what follows, a general discussion on these issues will be presented, based in previously published studies (a) and in specific frameworks established within the scope of this work, in order to evaluate their influence (b and c).

8.1. Influence of blade geometry

The most important cause of error or result deviation is related to the distortion induced by blade penetration, even though this distortion is much lower in DMT than in common and most frequent testing procedures, excluding self-boring pressuremeter and geophysical systems. Figure 8.1 (Baligh & Scott, 1975) shows the difference between the distortion caused by CPT tip and DMT blade, revealing that the fundamental strains are located near the edge and also that lower apex angles generate lower shear strains. In fact, high apex angles mean sharp transitions that fall rapidly to a zone of residual stresses leading to plasticization levels far from the repos condition, and thus the equipment becomes less sensitive to the evaluation of horizontal effective stress, therefore to at rest earth pressure coefficient. DMT measurements are obtained in the face of the blade, where the strain is lower. Identical conclusions were reported by Davidson & Boghrat (1983) and Huang (1989).

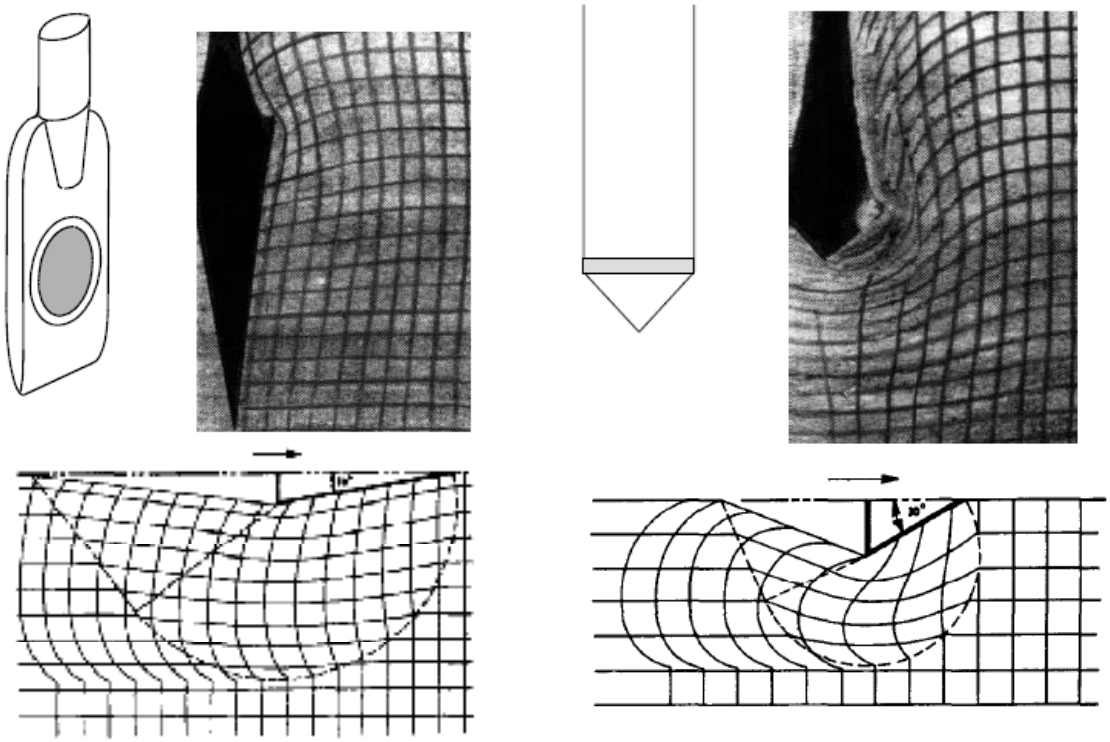


Figure 8.1 - Distortions caused by CPT and DMT (Baligh & Scott, 1975)

Although no numerical approaches to correct final results are available, the referred study suggests that disturbance during installation of DMT is lower than that observed in other in-situ tests, as presented in the following lines:

a) Baligh & Scott (1975) framework clearly reveals the lower level of disturbance of DMT during penetration, when compared with SCPTu;
b) Dynamic probing cones (DPL, DPM, DPH or DPSH) exhibits an apex angle similar to CPTu's and so at least the same level of disturbance is expected; in these cases, dynamic insertion gives an extra level of disturbance;
c) Concerning SPT tests, it is difficult to establish a comparison, Terzaghi sampler is an open cutting edge below cylinder and a significative part of tested soil is not laterally displaced, remaining inside the sampler; however, it is not difficult to believe that drilling associated to dynamic insertion will produce higher disturbance effects;
d) PMT tests have the great advantage of measuring a much larger volume variation, but are also difficult to compare and, again, the effects of pre-drilling can produce quite rough conditions, especially in soft/loose soils; furthermore, the deviation from perfect circular boreholes, when materials are non-homogeneous and difficult to cut, will create a heterogeneous stress distribution with important implications in data interpretation.

8.2. Influence of penetration modes

In order to penetrate DMT blade into the soil a hydraulic jack system or a hammer is required, with preference for the former. However, the possibility of driving the equipment by hammer fall can be very useful to overcome rigid layers of heterogeneous soils, as it is the case of residual soils. Usually the thrust capacity needed (or number of blows/inch) ranges between 2 tons for soft soils (5 blows) and 15 tons (45 blows) for very hard soils (Briaud & Miran, 1992). As stated, a static penetration is preferable, but in heterogeneous soils the possibility of using dynamic insertion in DMT enlarges its field of application, making easier to overcome rigid layers interbedded in loose strata, and increases the depth range of in-situ high quality characterization when thrust capacity is overcome.

8.2.1. Basic considerations

So far, the discussion of DMT role in soil characterization has been developed considering a static insertion into the ground, which is undoubtfully preferable. However, this type of installation is only possible in more or less homogeneous ground, free from blocks or boulders, represented by grain sizes not coarser than sand and with density levels represented by N_{SPT} values generally lower than 40. In residual soils (or other heterogeneous ground), where the weathering processes can give rise to a very heterogeneous massif with frequent boulders or stiff layers among highly weathered masses, the static insertion can be a significant limitation, and the use of dynamic penetrometers becomes a necessity, with important disadvantages in the quality of results, especially in stiffness evaluation. In that case, the possibility of combining both types of insertion should be regarded as an important feature since it enlarges its field of application. Taking into consideration that DMT induces a horizontal deformation after a vertical penetration, it can be expected, at least, some preservation of the intrinsic characteristics of natural soils and thus, DMT could also be seen as a superior substitute of dynamic penetration conventional testing, in materials where dynamic insertion is the unique possibility.

DMT specific references on the subject are restrained to some considerations referred by Marchetti (1980), Schmertmann (1988) and a deeper research performed by Davidson et al. (1988). These researches can be described by a couple of considerations such as (i) driving the blade tends to reduce P_0 and P_1 proportionally and P_2 seems to be unaffected, (ii) the effect of driving is more prevalent in loose to

very loose soils, and (iii) is important to have at least one pushed DMT performed together with a driven DMT for calibration purposes.

Aiming to find out the real efficiency of parametric evaluation with dynamic push-in, Cruz & Viana da Fonseca (2006b) developed a specific research work based in parallel dynamic and static pushed-in DMT tests (1.0 to 1.5 m apart), both in granitic residual soils and reference earthfills constituted by soils of the same nature, which can also be seen as representative of different behaviours developed by cemented and non-cemented materials. This study was based in a comparative analysis of results obtained in three different sites, namely CEFEUP experimental site, V.N. Gaia and Vila do Conde (20 km north from Porto), all located within the geologic formation of the present research. The field work consisted in performing DMT static/dynamic pairs, followed by SPT, DPSH (as defined by, TC16, 1989) and PMT tests, homogeneously distributed.

The mechanical ranges of the tested soils can be summarized as function of the results of SPT, DPSH and PMT tests. Table 8.1 shows the basic data obtained, including the data related to the number of blows (SPT hammer) to penetrate the soil with DMT blade. This results show a very similar strength profile in the case of V. Conde and V.N. Gaia's sites, being the CEFEUP site clearly weaker.

Table 8.1 - Mechanical characterization of the sites

Site	N_{60}	$(N_1)_{60}$	$N_{20\ DPSH}$	N_{60}/p_l	N_{60}/E_{PMT}	$N_{20\ DMT}$
CEFEUP	8 - 25	10 - 25	5 - 15	5 - 15	0.5 - 1.5	12 - 20
V. Conde	20 - 35	25 - 35	---	10 - 15	1.5 - 2.5	15 - 30
V.N.Gaia	25 - 30	20 - 35	---	10 - 20	1.5 - 3.0	20 - 30

The dynamic insertion of the blade was obtained using the same normalized hammer of SPT and the respective number of blows needed for 0.20m penetration ($N_{20\ DMT}$), compared with SPT (N_{60}) and DPSH ($N_{20\ DPSH}$) blow counts, in order to analyze possible correlations between them.

As expected, the compared results considering all the conditions show a good correlation between DMT and both SPT and DPSH blow counts. These correlations are reinforced by CICCOPN/MOTA-ENGIL (CME) collected data N_{60} and $N_{20\ DPSH}$ data obtained in Porto granitic residual soils independently of the present study. The trends

observed for the three situations are linear and can be expressed by the ratios (Figure 8.2):

$$N_{20\ DPSH} = 0.58\ N_{60} \quad (8.1)$$

$$N_{20\ DMT} = 1.58\ N_{20\ DPSH} \quad (8.2)$$

$$N_{20\ DMT} = 0.88\ N_{60} \quad (8.3)$$

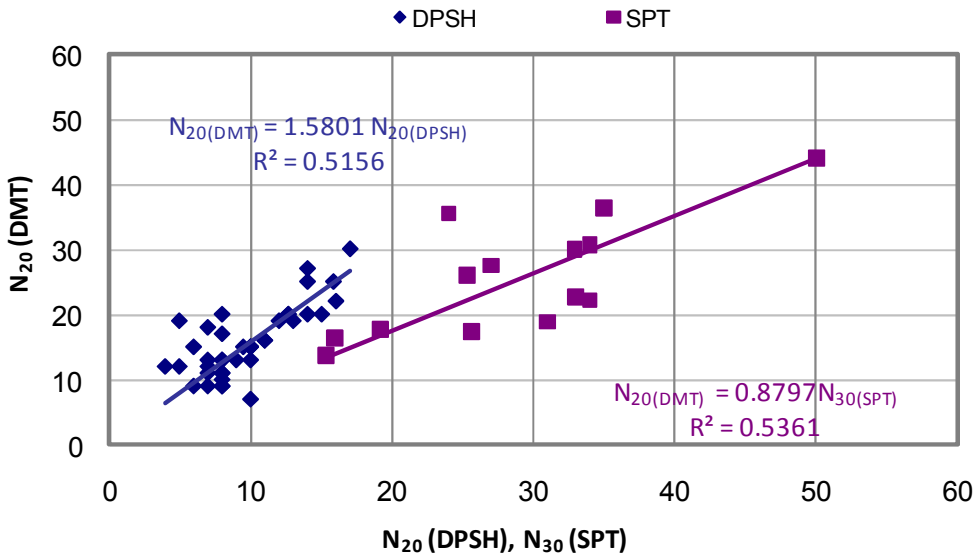


Figure 8.2 - Ratios N_{20} (DMT) versus N(60) and N_{20} (DPSH)

8.2.2. Typical Profiles

The superficial level of CEFEUP experimental site (1.5-2.0m) is characterized by an earthfill composed by identical grain size distribution of the granitic residual soils involved in this work (sandy silt to silty sand). As it will be shown, results from the earthfill showed completely different behaviour, although the amount of data was too limited. Therefore, some extra parallel tests were performed in a silty sand to loose to medium compacted sandy silt earthfill (10m high), denominated as reference earthfill in this document, which allowed both dynamic and static insertion. Table 8.2 summarizes basic and intermediate DMT parameter ranges, obtained by static and dynamic penetration modes (Cruz & Viana da Fonseca (2006b)). Concerning to variation with depth, profiles clearly show the same values ranges despite the mode of insertion, with smoother peak values in dynamic case.

Table 8.2 - Basic and intermediate DMT parameters obtained after static and dynamic penetration of the blade

Site (measured pairs)	Insertion	P_0 (bar)	P_1 (bar)	I_D	E_D (MPa)	K_D
CEFEUP (20)	static	2.5 - 4.0	7.5 – 20.0	1.5 - 2.5	20 - 50	5.0 - 10.0
	dynamic	2.5 - 4.0	7.0 – 15.0	2.0 - 3.0	15 - 40	3.5 - 5.0
V. Conde (15)	static	4.0 - 10.0	15.0 - 30.0	1.5 - 3.5	45 - 70	10.0 - 15.0
	dynamic	2.5 -7.0	10.0 - 25.0	2.0 - 4.0	30 - 60	6.0 - 15.0
V.N. Gaia (21)	static	4.0 – 10.0	15.0 – 30.0	2.0 – 3.5	45 - 65	7.0 – 10.0
	dynamic	3.0 - 5.0	15.0 - 25.0	2.5 - 4.5	35 - 60	4.0 - 7.5
CEFEUP earthfill (8)	static	1.5 - 2.5	3.5 - 7.0	1.7 - 1.9	6 - 16	5.0 - 7.5
	dynamic	1.5 - 2.5	5.0 - 10.0	2.0 - 3.0	15 - 25	6.0 - 9.0
Reference earthfill (48)	static	1.5 - 3.5	2.5 - 15.0	1.0 - 2.5	5 - 30	2.5 - 5.0
	dynamic	1.0 - 4.0	3.0 - 20.0	1.5 - 4.0	5 - 45	1.5 - 6.0

The data obtained from each pair of tests was compared and after elimination of spurious values, followed by a proper statistical analysis. In the following sections, the respective data and conclusions arising from that analysis are discussed in detail, as function of parameter type (basic, intermediate and geomechanical).

8.2.3. Basic parameters

In Table 8.3 and Table 8.4 statistical analysis on basic DMT test parameters (P_0 and P_1) is presented, organized by static/dynamic ratios, $P_x(S)/P_x(D)$ and discussed thereafter.

Table 8.3 - Statistics on P_0 (S)/P_0 (D)

Site	Maximum	Minimum	Std. Deviation	Mean
CEFEUP (20)	2.4	0.8	0.41	1.42
V. Conde (15)	1.8	0.8	0.34	1.26
V.N. Gaia (21)	1.5	1.0	0.13	1.28
CEFEUP earthfill (8)	1.2	0.4	0.24	0.84
Reference earthfill (48)	1.3	0.4	0.27	0.79

Table 8.4 - Statistics on P_1 (S)/P_1 (D)

Site	Maximum	Minimum	Std. Deviation	Mean
CEFEUP (20)	2.2	0.8	0.41	1.24
V. Conde (15)	1.5	0.9	0.22	1.10
V.N. Gaia (21)	1.7	1.0	0.22	1.15
CEFEUP earthfill (8)	1.1	0.4	0.30	0.77
Reference earthfill (48)	1.6	0.3	0.42	0.75

The major considerations resulting from these direct comparisons can be outlined as follows:

a) In residual soils, the ratio P_0(S)/P_0(D) is always greater than 1, and seem to drop with increasing level of compaction;
b) In earthfills the same ratio is lower than the unity, which means that P_0 values increase with dynamic insertion;
c) A similar behaviour is observed with P_1, but with lower variation rates.

These observations suggest that dynamically driving the blade into residual soils generates a loss of strength most probably due to the breakage of cementation structure, leading to a weaker state, since its void ratios are high. The higher variation of P_0 than P_1 ratios seem to reveal a decrease in disturbance as it gets away from the centre of the membrane. On earthfill materials, which can be used as reference of uncemented soil, data follows an opposite trend, with P_0 and P_1 being always lower in static insertion, probably related with dynamic compaction effects (Figure 8.3).

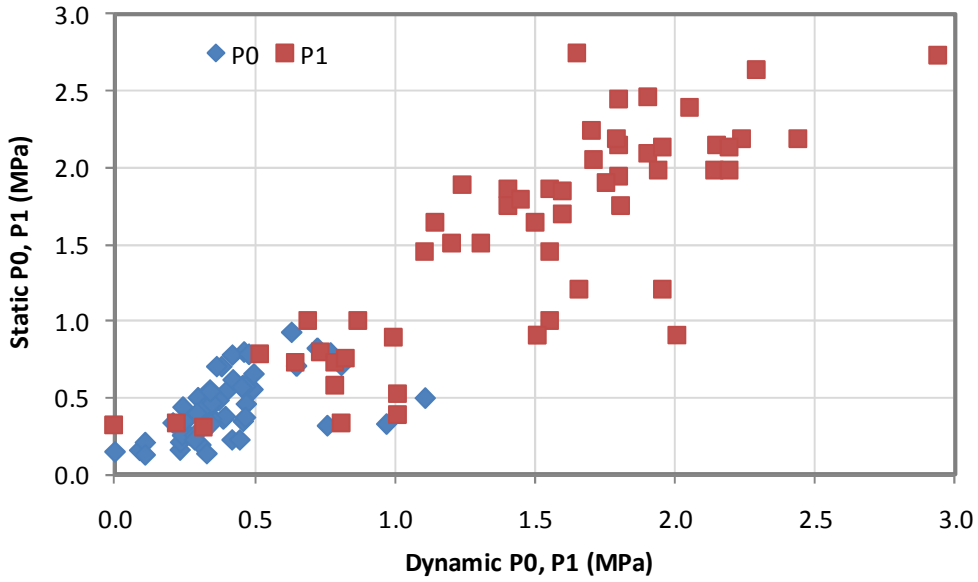


Figure 8.3 - Evolution of static/dynamic basic parameters

8.2.4. Intermediate Parameters

Concerning to intermediate parameters, I_D, E_D and K_D, the overall results seem to follow the general trends observed in basic parameters, revealing its direct dependency and suggesting the following considerations (Table 8.5 to Table 8.7):

a) $I_D(S)/I_D(D)$ clearly shows the general tendency of being lower than the unity, both in residual soils and earthfills, which may be related with the higher variation of P_0 in relation to P_1;
b) $K_D(S)/K_D(D)$ shows the same ability of P_0 to detect variations (K_D is highly dependent on P_0), and clearly reveals the loss of cementation by approaching the NC profile (Marchetti, 1980); this seems to confirm the adequacy of DMT to detect cementation structures (Cruz et al. 2004b, 2006b), as discussed in last chapter; in earthfill, this ratio is typically smaller than one, confirming a tendency for densification with dynamic insertion (higher K_D, higher stiffness);
c) $E_D(S)/E_D(D)$, shows a very stable mean value (>1) in residual soils (E_D amplifies the difference between P_0 and P_1), while in earthfill materials the results are higher when the insertion is dynamic, leading to the same conclusions pointed out for K_D.

Table 8.5 - Statistics on I_D (S) / I_D (D

Site (reading sets)	Maximum	Minimum	Std. Deviation	Mean
CEFEUP (20)	1.5	0.5	0.27	0.85
V. Conde (15)	1.2	0.5	0.20	0.86
V.N. Gaia (21)	1.2	0.7	0.16	0.89
CEFEUP earthfill (8)	1.1	0.4	0.21	0.85
Reference earthfill (48)	1.5	0.4	0.41	0.82

Table 8.6 - Statistics on K_D (S) / K_D (D)

Site (reading sets)	Maximum	Minimum	Std. Deviation	Mean
CEFEUP (20)	2.1	1.0	0.41	1.42
V. Conde (15)	1.6	0.8	0.29	1.23
V.N. Gaia (21)	1.5	1.0	0.13	1.25
CEFEUP earthfill (8)	1.2	0.4	0.25	0.84
Reference earthfill (48)	1.3	0.4	0.27	0.80

Table 8.7 - Statistics on E_D (S) / E_D (D)

Site (reading sets)	Maximum	Minimum	Std. Deviation	Mean
CEFEUP (20)	2.1	0.7	0.41	1.20
V. Conde (15)	1.5	0.8	0.23	1.10
V.N. Gaia (21)	1.5	0.9	0.21	1.13
CEFEUP earthfill (8)	1.2	0.4	0.33	0.74
Reference earthfill (48)	1.8	0.2	0.53	0.71

8.2.5. Geomechanical Parameters

The geotechnical parameters derived from DMT included within this framework were the unit weight, γ (Marchetti & Crapps, 1981), angle of shearing resistance, ϕ' (Marchetti, 1997) and constrained modulus, M (Marchetti, 1980). Moreover, OCR was also included in the study, given its special meaning in compaction control of earthfills (Cruz et al., 2006b) and in deriving bond strength in residual soils, as discussed in last chapter. The resulting ratios between static and dynamic values are presented in Table 8.8 to Table 8.11.

Table 8.8 - Statistics on γ (S)/γ (D)

Site (reading sets)	Maximum	Minimum	Std. Deviation	Mean
CEFEUP (20)	1.1	1.0	0.05	1.01
V. Conde (15)	1.1	0.9	0.04	1.00
V.N. Gaia (21)	1.1	1.0	0.03	1.02
CEFEUP earthfill (8)	1.1	0.9	0.06	0.95
Reference earthfill (48)	1.0	0.9	0.04	0.97

Table 8.9 - Statistics on ϕ' (S)/ϕ' (D)

Site (reading sets)	Maximum	Minimum	Std. Deviation	Mean
CEFEUP (20)	1.1	1.0	0.03	1.04
V. Conde (15)	1.1	1.0	0.03	1.02
V.N. Gaia (21)	1.1	1.0	0.01	1.03
CEFEUP earthfill (8)	1.0	0.9	0.04	0.98
Reference earthfill (48)	1.0	0.9	0.05	0.97

Table 8.10 - Statistics on M (S)/M (D)

Site (reading sets)	Maximum	Minimum	Std. Deviation	Mean
CEFEUP (20)	2.3	0.6	0.54	1.37
V. Conde (15)	1.8	0.9	0.33	1.15
V.N. Gaia (21)	1.8	1.0	0.26	1.18
CEFEUP earthfill (8)	1.2	0.4	0.39	0.71
Reference earthfill (48)	1.5	0.3	0.49	0.71

Table 8.11 - Statistics on OCR (S) / OCR (D)

Site (reading sets)	Maximum	Minimum	Std. Deviation	Mean
CEFEUP (20)	3.0	1.0	0.70	1.74
V. Conde (15)	2.5	0.8	0.65	1.40
V.N. Gaia (21)	2.0	1.0	0.29	1.48
CEFEUP earthfill (8)	1.4	0.4	0.45	0.68
Reference earthfill (48)	1.5	0.3	0.42	0.69

Globally obtained data suggest the following considerations:

a) Unit weight, depending on I_D and E_D, is fairly insensitive to dynamic insertion (mean values around 1);
b) The same conclusion is applied to the angle of shearing resistance, exclusively dependent on K_D;
c) M and OCR are sensitive parameters, respectively obtained by amplification of E_D and K_D throughout the application of correction factors; the correction factor applied to M is a function of soil type (I_D) and overconsolidation ratio (K_D), while OCR correction is function of soil type; Figure 8.4 illustrates these assumptions;
d) Both OCR and M confirm their ability to detect signs of natural bonding structures, with implications in stiffness and strength properties observed in other studies (Marchetti 1980; Marchetti 1997; Cruz et al., 2004b, 2006b).

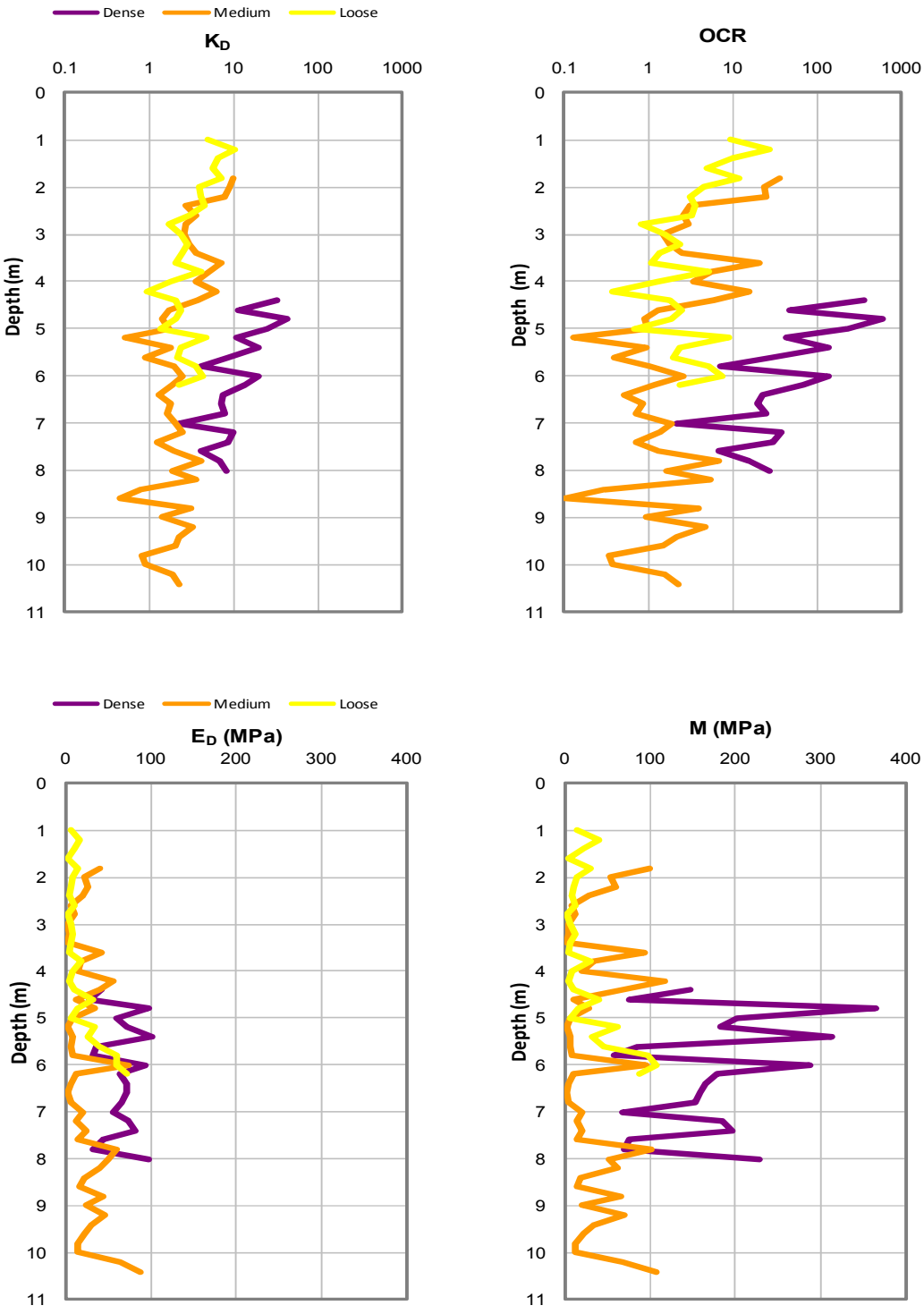


Figure 8.4 - K_D - OCR and E_D-M relations.

This specific research led to some useful considerations about using driven DMT's in granular soils, such as:

a) Dynamic insertion of DMT blade is responsible for an important loss of bonding in residual soils, leading to a decreasing of stiffness and strength properties; with the exception of I_D, all analyzed DMT parameters presented smaller values for dynamic insertion tests;
b) Earthfill (uncemented) soils react in an opposite way to dynamic insertion, which creates a densification of the soil; all parameters showed higher values in dynamic tests, explained by their initial density (loose to medium compacted), with densification becoming natural and expected; for higher levels of compaction it is possible that the mentioned ratios can change;
c) I_D intermediate parameter increases with dynamic insertion, both in residual and earthfill soils, meaning that soil type is classified coarser than reality;
d) The variation rates of unit weight and angle of shearing resistance are very small, revealing the low sensitivity of these two parameters to dynamic insertion;
e) M and OCR act as amplification of E_D and K_D, inducing higher sensitivity to variations, confirming OCR (once again) as a key parameter to deduce bond strength;
f) The number of blows to penetrate DMT blade in 20cm ($N_{20\ DMT}$) may be used as a control parameter, although some normalization taking into account friction reducers should be recommended.

8.3. Influence of measurement devices

The quality control of measuring devices is a common practice in modern industry. However, it is important to recognize that the accuracy of measurement devices may condition quite differently in the wide range of parameters or other calculations obtained from direct test measurements. Thus, a numerical framework was included in the global research program in order to evaluate the error propagation, starting from the accuracy of test measurement devices (Mateus, 2008). The accuracy and reproducibility of the test is usually high, due to the following reasons, as referred by Marchetti (1997):

a) The test is displacement controlled, and so the strain system imposed to any soil is approximately the same;
b) The membrane is just a separator (passive) soil – gas, so the accuracy of the measured pressures are the same of the gage; that means one can choose the desired level within the available precisions;

c) The blade works as an electric switch (on/off), and is not a transducer;
d) Displacements are determined as the difference between a Plexiglas cylinder height and a sensing disk thickness, machined to 0.01 mm accuracy, while temperature dilation of such components is less than 0.01 mm.

As a consequence of d), the displacement will be 1.10 mm $\pm$ 0.02 mm, which is not an accuracy value easily obtained by a transducer. When temperature corrections are taking into account; the maximum error displacement would cause a negligible error in the derived E_D parameter (max. 2%), even in the softest soils.

The study was performed gathering together 99 tests, carefully selected to cover the main types of soils. Thus, four reference groups were selected – sedimentary clay, sedimentary sand, granite residuals and earthfill. Data distribution is presented in Table 8.12.

Table 8.12 - Summary of measurements distributions (global values).

Soil Type	Group designation	Depth		Thickness		Readings	
		Minimum	Maximum	Σgroup	Total	Σgroup	Total
Earthfill	A	0.2	12.8	94.2	721	409	3304
Residuals	B	0.2	10.6	167.8		809	
Sed. Clay	C	0.2	26.8	255.4		1134	
Sed. Sand	D	0.2	13.0	203.6		952	

The first step was to determine in-situ reading accuracy, based on precision associated to each measurement system (gages, displacement measurement system, depth, water level) defining a basis for error calculation. Using an arithmetic double precision, reading error approximation was calculated (absolute and relative) related to each available parameter (I_D, E_D, K_D, γ, σ'_v, M, k_0, OCR, c_u, c', ϕ', G_0), resulting in 190391 estimated values. The calculations were made by means of MatLab© using *symbolic toolbox* for partial derivatives calculation.

The fundamental input parameters for calculation were the readings of equipment gages. An error reading is associated to these values is associated, which depends on the smaller scale of the instrument. Table 8.13.and Table 8.14 present maximum errors related to the basic output data of the test.

Table 8.13 - Maximum absolute errors of DMT devices

Name	Variable	Maximum absolute error
Reading ΔA (displacement 0.05m)	ΔA	$\delta \Delta A \leq 0.025$
Reading ΔB (displacement 1.1m)	ΔB	$\delta \Delta B \leq 0.025$
Reading A (displacement 0.05mm)	A	$\delta A \leq 0.025$
Reading B (displacement 1.1mm)	B	$\delta B \leq 0.025$
Reading C (displacement 0.05 – unloading)	C	$\delta C \leq 0.025$

Table 8.14 - Maximum absolute errors of current used devices

Name	Variable	Maximum absolute error
Water unit weight	γ_w	$\delta \gamma_w \leq 0.01 KN/m^3$
Top unit weight,	γ_{top}	$\delta\gamma_{top} \leq 0.1 KN/m^3$
Depth	z	$\delta z \leq 0.005$ m
Water Level	WL	$\delta z \leq 0.005$ m

Table 8.15.to Table 8.17 show the range of variation and average of relative errors related to each basic, intermediate and geotechnical parameters, grouped by soil origins.

Table 8.15 - Relative error range of basic parameters (%).

	Earthfill		Residual soils		Sedimentary Clay		Sedimentary Sand	
	Range	Average	Range	Average	Range	Average	Range	Average
P_0	1 - 11	3	0 - 11	2	0 - 5	2	1 - 7	3
P_1	0 - 4	1	0 - 5	1	0 - 4	1	0 - 3	0
ΔP	1 - 13	2	0 - 18	2	1 - 67	16	0 - 12	1
P_2	---	---	0 - 50	13	1 - 25	6	3 - 33	11
u_0	---	---	2 - 21	6	1 - 21	3	2 - 21	5

Table 8.16 - Relative error range of intermediary parameters (%).

	Earthfill		Residual soils		Sedimentary Clay		Sedimentary Sand	
	Range	Average	Range	Average	Range	Average	Range	Average
I_D	1 - 23	5	1 - 29	4	2 - 73	18	1 - 19	5
E_D	0 - 13	2	0 - 18	2	1 - 67	16	0 - 12	1
K_D	1 - 12	4	1 - 16	5	1 - 26	9	1 - 16	5
U_D	---	---	1 - 143	41	2 - 356	15	4 - 630	119

The overall results reveal some consistent and interesting trends of how the basic errors propagate throughout all calculations until each specific final result. Considering that design parameters are selected by averages of results associated to a specific geotechnical unit, then it is reasonable to assume the average as representative. The major considerations arising from this research are presented below (Mateus, 2008; Cruz et al, 2008b, 2009):

a) Adequate precision of basic pressures (P_0 and P_1) measurement, reflected by a mean relative error smaller than 5%; P_2 pressure can present higher ranges of error, especially for low measured values; the other parameters needed for basic calculations are depth and water level (also a depth measurement), and for these a precision of decimeter is enough, since higher precision doesn't generate significant improvement;

b) The evaluation of soil type from I_D parameter reveals good efficiency, since the influence of error does not introduce significant deviations in soil classification;

c) From geotechnical point of view, there are a lot of different situations depending on each specific parameter and type of soil; thus, maximum relative errors associated to unit weight, vertical stresses, at rest earth pressure coefficient and angles of shearing resistance are lower than 20%, with average values lower than 10%, guaranteeing reasonable estimation of design values;

d) When the maximum values of relative error exceed 20% (OCR, c', M and G_0), the average values are globally lower than 15%, with exception to deformability parameters (G_0 and M) in clayey soils (20 and 30%, respectively).

Table 8.17 - Relative error range of geotechnical parameters (%).

	Earthfill		Residual soils		Sedimentary Clay		Sedimentary Sand	
	Range	Average	Range	Average	Range	Average	Range	Average
γ	0 -8	1	0 - 8	1	0 - 13	4	0 - 6	1
σ	0 -6	1	0 - 12	2	0 - 22	7	0 - 7	2
K_0	0 - 8	1	0 - 12	2	0 - 21	7	0 - 16	1
OCR	1 - 49	9	2 - 52	13	2 - 40	14	2 - 57	11
c_u	---	---	---	---	0 - 54	18	---	---
c'	---	---	1 - 42	8	---	---	---	---
ϕ'	0 - 3	1	0 - 3	1	---	---	0 - 4	1
M	0 - 13	2	0 - 14	0	0 - 80	21	0 - 15	2
G_0 (*)	1 - 26	5	1 - 36	5	2 - 111	27	1 - 24	4
G_0 (++)	0 - 36	5	0 - 39	6	0 - 67	21	- 31	5

*(Cruz et al, 2004, 2006); ** (Hryciw, 1990)

The variation of parametric efficiency with pressure gauge accuracy was also studied, showing that currently used devices are adequate for earthfills, sandy and residual soils, while for clayey soils a precision increase up to 10 millibars should be adopted to reduce average errors for a lower desirable limit of 10%. Furthermore, relative errors of DMT parameters depend on soil type, showing a global increase with decreasing I_D.

Kruskal-Wallis test applied to the four selected soil groups revealed that mixed soils can be clustered (silty sands, sandy silts and silts + silt-clays and clay silts), while clayey and sandy statistically differ. The Kruskal-Wallis test is a non-parametric test proposed by William Kruskal and W. Allen Wallis which (1952) for testing equality of means of *k* continuous distributions that are obviously abnormal, and with independent samples. Shortly, the test works by sorting in ascending order the $n = \sum_{i=1}^{k} n_i$ observations and ranking it, (that is, substituting the appropriate rank from 1, 2, ... n for each observation). In the case of ties, the usual procedure is to replace the ranks of the tied observations by the mean of the ranks (e.g. if the observations 19 and 20 have the same value after being ordered, it will be assigned to them the rank 19.5). With this procedure, it is defined a new random variable, R_i, that represents the sum of the ranks get by the observations in the sample *i*. Kruskal and Wallis, proposed the statistic,

$$V = \frac{12}{(n)(n+1)} \sum_{i=1}^{k} \frac{R_i^2}{n_i} - 3(n+1) \tag{8.4}$$

observing that, if the *k* samples came from the same population and $n_i > 5, \forall i = 1, \ldots, k$, *H* is reasonable approximated by the χ^2_{k-1}. As so, they proposed the test reject:

$$H_0 : (\mu_1 = \mu_2 = \cdots = \mu_k) \text{ if } v = \frac{12}{(n)(n+1)} \sum_{i=1}^{k} \frac{r_i^2}{n_i} - 3(n+1) > \chi^2_{k-1,\alpha} \tag{8.5}$$

where α is the required significance level (in this work α was assumed equal to 0.05).

The success of this propagation error analysis gave rise to its application to other in-situ tests, such as PMT (Vieira, 2009) and CPTu (Mateus et al., 2010), highlighting how important this type of analysis can be in data quality control as well as for adequate design parameter selection. It is important to recall that error propagation doesn´t mean deviation from ground reality, but only to a final deviation due to a specific measurement.

Table 8.18. presents the error results related to the main fundamental geotechnical parameters (Mateus et al., 2010) obtained from these three in-situ tests, suggesting the following considerations:

a) PMT reveals the more stable values, independently of analyzed geotechnical parameter and type of soil; globally relative errors in these tests are placed within 12 and 25%.
b) DMT maximum relative erros are quite lower than PMT's in cemented and no cemented sandy soils (< 5%), considering both strength and stiffness

parameters; on the other hand, DMT error's in clayey soils are higher, ranging from 20 to 35% ;

c) CPTu maximum relative errors are similar to DMT's except for the constrained modulus that can reach values of 33% in sedimentary sands and clays, higher than those exhibited by DMT; it should be noted that the low value related to undrained cohesion derived by CPTu is not precise, because N_k correction factor was considered with error "zero" and thus, not including the errors associated to this calibration (through FVT, DMT or triaxial testing);

d) Considering all the tests under scope, stiffness parameters are usually more affected by the propagation of error than (drained or undrained) strength's; clays represents the situation with higher deviations;

Table 8.18 - In-situ test error propagation (Mateus et al., 2010)

Soil type	Test type	E	M	c_u	ϕ	G_0
Residual soils	DMT	2%	2%	--	1%	5%
	PMT	17%	17%	--	13%	17%
	CPTu	---	2%	--	1%	5%
Sedimentary clay	DMT	21%	26%	20%	--	35%
	PMT	18%	18%	16%	--	18%
	CPTu	---	33%	1%	--	4%
Sedimentary sand	DMT	2%	2%	--	1%	5%
	PMT	24%	24%	--	12%	25%
	CPTu	---	33%	--	4%	4%

In Deserts, that which seems eternal
may change overnight
And that which is least expected
is always a possibility

(in Living Earth Book of Deserts, Susan Arritt)

(…and we have always to be prepared to react)

PARTE C – THE EXPERIMENT

Chapter 9.
Laboratorial Testing Program

9. LABORATORIAL TESTING PROGRAM

The laboratorial testing program within this research work was established in order to characterize with detail the granitic soils used in the experience and to act as a reference for calibrating DMT strength and stiffness geotechnical correlations.

As discussed in Chapter 3, Vaughan (1985) proposed the use of artificially cemented soils for studying the effects of cementation matrix in mechanical soil behaviour, in order to minimize variability and sampling consequences. This approach has been followed in several research programs produced ever since (Vaughan et al., 1988; Viana da Fonseca; 1988, 1996; Leroueil and Vaughan, 1990; Coop & Atkinson, 1993; Schnaid et al., 2001; Rodrigues, 2003; Schnaid, 2005; Viana da Fonseca & Coutinho, 2008, among others), although it doesn´t overcome the different fabric observed in naturally and artificially cemented soil. In fact, a natural cemented structure is represented by a specific weakening condition (in the case of granites resulting from the weathering of feldspars), which is variable with the local content of the weathered mineral (or minerals), while in artificial sands cementation increases with time until stabilization, showing tendentially homogeneous distribution. Bressani (1990) and Malandraki & Toll (1994, 2000) tried to mitigate this problem using artificially cemented soils obtained by mixing sand with small amounts of kaolin clay and heating at 500ºC for a couple of hours. Unfortunately, this methodology was not possible to be settled in the current research work, due to the obvious difficulties of preparing 1.5m^3/per sample needed for the experience in the CemSoil box, described in the next chapter. However, since one of the main purposes of the present work is to calibrate DMT measurements (and its respective data reduction) with the real in-situ strength and stiffness, then the similarity between DMT and triaxial testing samples ensures a proper base for comparison. Being so, soil-cement samples used in the present experience were obtained by mixing granitic residual soils with commercially available cements, following similar remolding conditions both in the box as in laboratory testing sample preparation. The experimental work was defined aiming an efficient determination of the geotechnical parameters that represents strength and stiffness in residual soils, as well as the evaluation in suction effect on them.

From strength point of view, the separation of global strength into two variables (c' and ϕ') is the main goal to be achieved. The estimation of a practical and useful effective cohesion intercept (herein designated by cohesion for simplicity) was based in a

reference stress-strain behaviour of sedimentary clays as suggested by Leroueil & Vaughan (1990). The previous research work based in field experiences (Cruz et al., 1997; Cruz et al., 2004c and Cruz & Viana da Fonseca, 2006a) allowed the establishment of correlations between c´ obtained by triaxial testing (performed on high quality samples) and DMT (OCR and K_D) or combined DMT and CPTu (M/q_t) results. Correction equations for the angles of shearing resistance derived from sedimentary formulae were also achieved (Cruz & Viana da Fonseca, 2006a). However, the reference value used for deriving cohesion was affected by both variability of natural samples and sampling disturbance, inducing the partial breakage of cementation. Thus, the proposed correlations were affected by an unknown deviation from in-situ real conditions.

On the other hand, the possibility of evaluating suction contribution was also taken into account, since unsaturated conditions are very common in residual soils and can play an important role in soil behaviour. Naturally, this creates an extra challenge of trying to separate (again) apparent cohesion in two components, which means trying to deduce three different strength contributions from only one test. Being so, since tensiometers are of small dimension and important knowledge on DMT efficiency could arise from the resulting data, a profile of six (or two profiles of three) measuring points was included in the main experience. By this time, it is noteworthy to mention that combination of CPTu and DMT tests should be efficient in separating the different strength contributions, since at least two more reliable parameters are obtained, with the possibility of being used together with DMT results. Unfortunately, it was not possible to “build” a larger CemSoil samples, so each experiment had to be repeated (CPTu and DMT performed in separate samples), which was not possible to guarantee in a reasonable period of time. A specific research experimental work is already being prepared in MOTA-ENGIL, to achieve this goal, interpreted on ongoing research program (MOTA-ENGIL ReSoil Project sponsored by QREN, 2009/2010).

Besides these strength implications, stiffness properties are also influenced by cementation and suction and so the respective correlations should also be calibrated. In fact, the reference values taken for developing stiffness correlations with DMT parameters were obtained by triaxial and shear wave velocity measurements (Cruz & Viana da Fonseca, 2006a), respectively influenced by sampling and suction.

In summary, the main objectives of the research were to evaluate how DMT results can reflect the effects of bonding and suction in strength and stiffness behaviour, globally and/or separately, as well as the influence of insertion of DMT blade on final results.

Thus, taking into account the above considerations, the laboratorial experience was established, as discussed below.

In the first place, Department of Civil Engineering of Instituto Politécnico da Guarda (IPG) kindly offered specially suited conditions for the main frame and subsidiary elements, including a two-floor facility, allowing to locate the experimental apparatus in the base floor while the upper level was used to push-in DMT blades using a penetrometer rig. A global view of local conditions is illustrated in Figure 9.1.

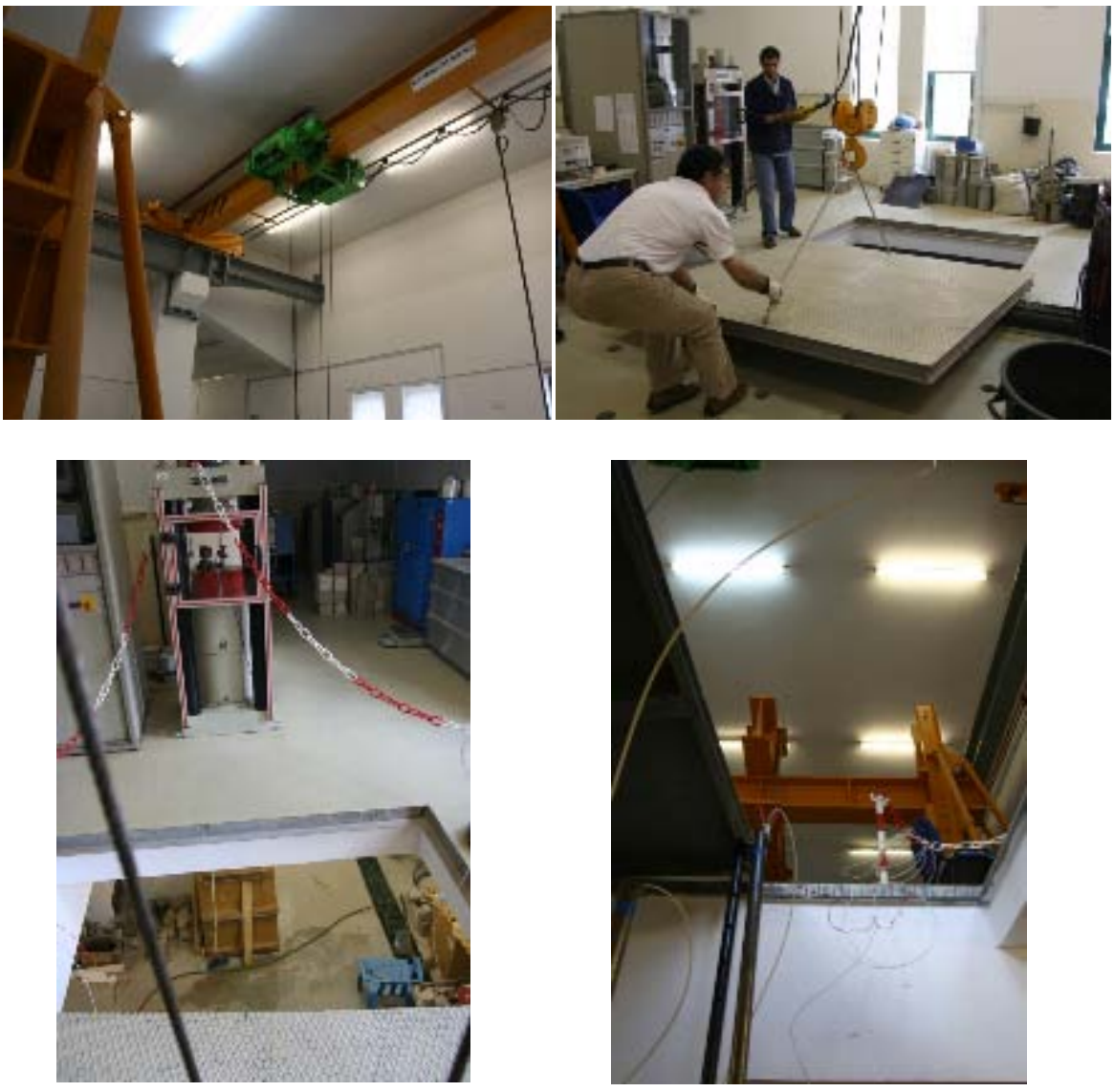


Figure 9.1 - IPG local facilities for the assembly of CemSoil box.

The experimental main frame, here designated as IPG CemSoil Box or simply CemSoil, was based in a system conceived together by the author and Prof. Carlos Rodrigues (IPG), in order to remould a sample as bigger as possible, adequate to be penetrated by DMT blades and adaptable to local facilities. CemSoil experimental work should include pre-installed and pushed-in DMT blades under saturated and unsaturated conditions, piezometric and suction control, and shear wave velocity measurements. Details of the cell and respective device installation conditions will be discussed in Chapter 10.

A combined testing program based in CemSoil and triaxial testing samples was established, aiming to simulate different cementation levels and calibrate specific correlations for deriving strength and stiffness properties. In this context, apart from the usual laboratory testing equipments, IPG Geotechnical Laboratory owns an advanced triaxial system, worked by skilled and creative personnel, allowing the whole research work to be performed in the same facilities, and thus providing excellent flexibility for interaction in the course of the main experience. In fact, based on soil-cement mixtures obtained following the standards or reported procedures for artificial cementation, it was possible to create comparable controlled conditions, namely in curing times, compaction procedures, final unit weights and void ratios, avoiding the undesirable scattering and deviations resulting from sampling and sample variability influences.

The laboratorial program was also established to contribute to a deeper understanding of residual soil behaviour, beyond the main purpose of this work (establishment of a characterization model based on DMT testing). Four different compositions of soil-cement mixtures and one uncemented were prepared to be tested in CemSoil Box, followed by an exhaustive laboratorial program, including uniaxial, tensile and triaxial testing at low and high confining stresses. Uniaxial and tensile strengths were selected to be used as cementation reference indexes.

Uniaxial and tensile strength tests were performed under almost saturated (no prior system for imposing back pressures was used) and unsaturated conditions, while triaxial tests were executed in complete saturated samples, isotropically consolidated, followed by shearing under a conventional compression path at constant confining stress (constant σ'_3). Characteristic retention curves for suction influence evaluation were also determined in FEUP laboratory taking advantage of the knowledge arising from Topa Gomes (2009) recently published works.

Within these global conditions the following objectives could be defined:

a) Evaluation of the effects caused by DMT penetration on cemented structures;

b) Calibration of specific correlations for strength and stiffness parameters, departing from the previous in-situ DMT data-base in residual soils (Cruz et al., 1997a, 1997b, 2000, 2004b, 2004c; Viana da Fonseca, 1996, 2001, 2003; Cruz & Viana da Fonseca, 2006a; Viana da Fonseca et al, 2001, 2007; Viana da Fonseca & Coutinho, 2008) established using high quality triaxial testing;

c) Evaluation of suction and its influence on cohesive intercept and determination of DMT sensitivity to evaluate its magnitude, by creating saturated and unsaturated zones within the CemSoil box;

d) Evaluation of suction and cohesion influences (globally and/or separately) in compression and shear wave velocities, obtained from the installed geophysical devices (as described in next chapter), both in saturated and unsaturated zones;

e) Incorporation of local high quality data in similar soils (Rodrigues, 2003), within this experimental work, aiming to compare artificially and naturally cemented soils, implicitly affected by sampling and microfabric effects.

f) Cross-calibration of the results with Porto Geotechnical Map (COBA, 2003) data

g) Establishment of a model for geomechanical characterization based on DMT and seismic tests, adequate to residual soil peculiarities, taking into account cementation factors and suction effects on strength and stiffness properties, specifically with those characteristics related to stress-strain levels.

9.1. Sample Preparation

9.1.1. Soils

The materials used in the laboratorial experience were collected in a natural slope of Guarda granitic residual soils (Figure 9.2), located in the surroundings of IPG facilities, and previously used in several research works (Rodrigues, 2003; Rodrigues & Lemos, 2005). Total grain size was preserved in order to represent the natural soil. The mineralogical composition of the soil mass obtained by X-ray diffraction (Rodrigues,

2003) is represented in Figure 9.3. Identification and physical parameters of natural samples, following the usual laboratory procedures, revealed the information presented in Figure 9.4 and Table 9.1 and 9.2.



Figure 9.2 - Experimented soils in its natural ground.

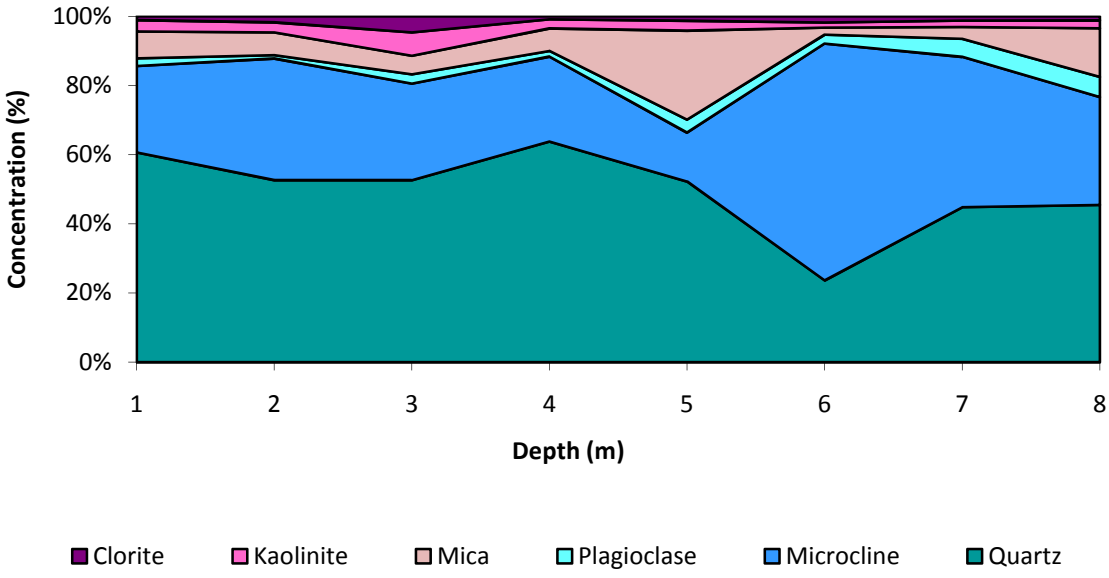


Figure 9.3 - Mineralogical composition obtained by X-ray diffraction (Rodrigues, 2003)

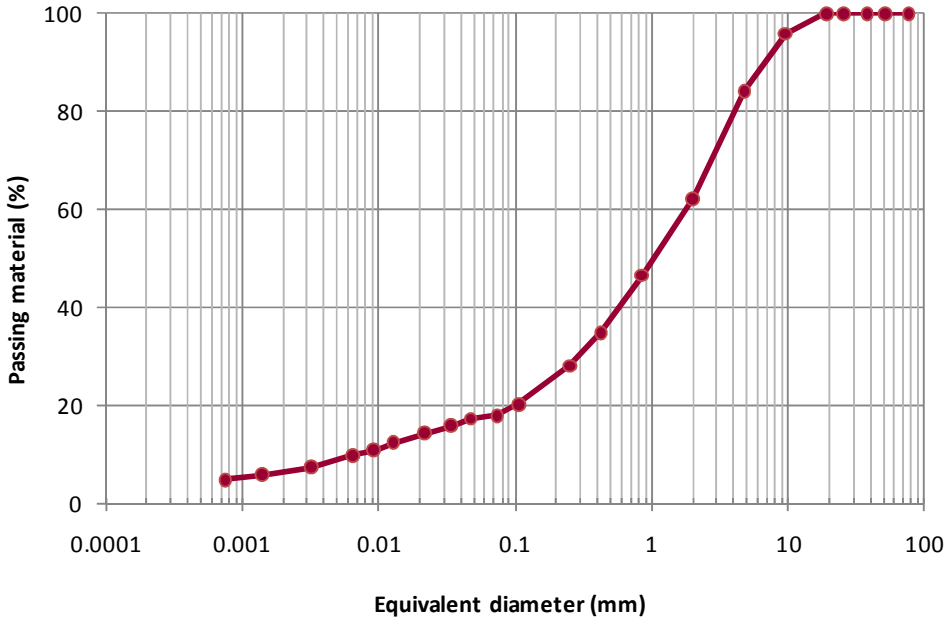


Figure 9.4 - Grain Size Distribution

Table 9.1 - Identification and physical properties of natural soil used in the main experiment (after Rodrigues, 2003)

Sample depth	Clay %	Silt %	Sand %	Gravel %	D_{10}	C_u	C_c
1.1 m	9.63	23.3	40.3	26.8	0.002	390	0.9
1.5 m	3.99	17.8	44.3	33.9	0.009	180	3.0
2.1 m	5.34	22.4	38.5	33.8	0.005	216	1.5
2.6 m	2.57	15.8	42.7	38.9	0.005	198	1.6
3.1 m	3.37	16.3	41.2	39.1	0.011	186	2.1
3.5 m	4.37	18.8	40.2	36.6	0.006	254	1.9
4.1 m	5.77	16.0	40.2	38.1	0.005	360	3.6
5.1 m	5.36	20.4	44.4	29.8	0.005	198	1.8
6.1 m	7.56	16.8	39.7	35.9	0.003	424	3.1
7.1 m	5.30	17.5	43.2	34.0	0.007	191	2.2
8.1 m	4.75	19.2	38.8	37.2	0.006	266	1.6

Table 9.2 - Identification and physical properties of the soil used in the main experiment

Moisture content w (%)	Unit weight γ (kN/m3)	Dry Unit weight γ_d (kN/m3)	Saturation degree Sr (%)	Void ratio e_0
13.2	18.4	16.2	57.1	0.61

Soil-cement sample remolding

Preparation of soil started with air drying of unique sample of natural soil, which was then desegregated, mixed and separated in grain size homogeneous portions. Each of these samples was then mixed with different portions of cement and prepared through static compaction (four 35x70mm layers, with interface scarification) in order to obtain a similar void ratio of the respective natural soil. Samples were remoulded by static compaction in order to represent the natural density level and with moisture content determined by previous Modified Proctor Tests, following the Portuguese standards and recommendations (LNEC E 197-1966). Taking global results (Figure 9.5) the reference values assumed in the experimental work were:

Max. dry unit weight, γ_{dmax} = 18.5 kN/m^3; Opt. moisture content, w_{opt} = 10.4 %.

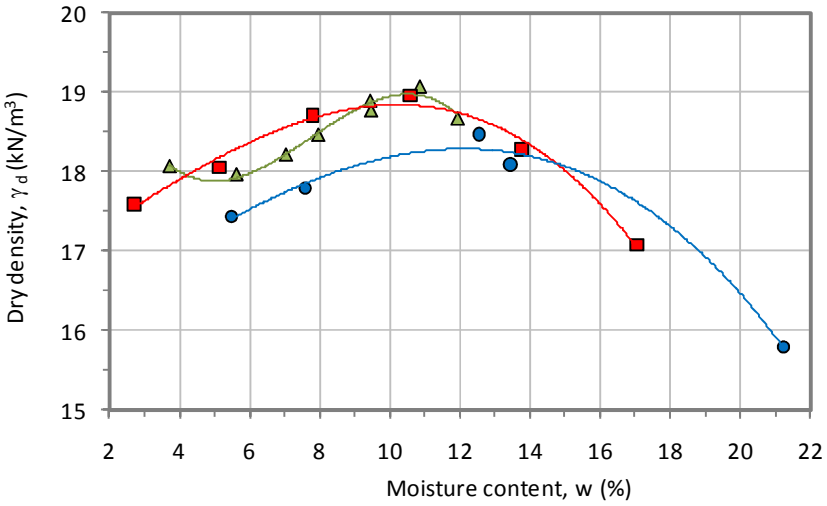


Figure 9.5 - Compaction test results

9.1.2. Cements

Samples were prepared aiming to obtain different levels of inter-granular bonding, representing different levels of the cohesive component of strength. Different percentages of cement (0% to 6%) were mixed with the pre-selected residual soil samples, followed by compaction (directly in the molds) for uniaxial and diametral compression tests. The used cement was a commercial product of SECIL, S.A., designated as CIM I/52.5R. This is a grey cement of high performance, usually used in the composition of rapid curing concrete when short curing times are needed to achieve final strength, with high hydration temperatures (Figure 9.6).

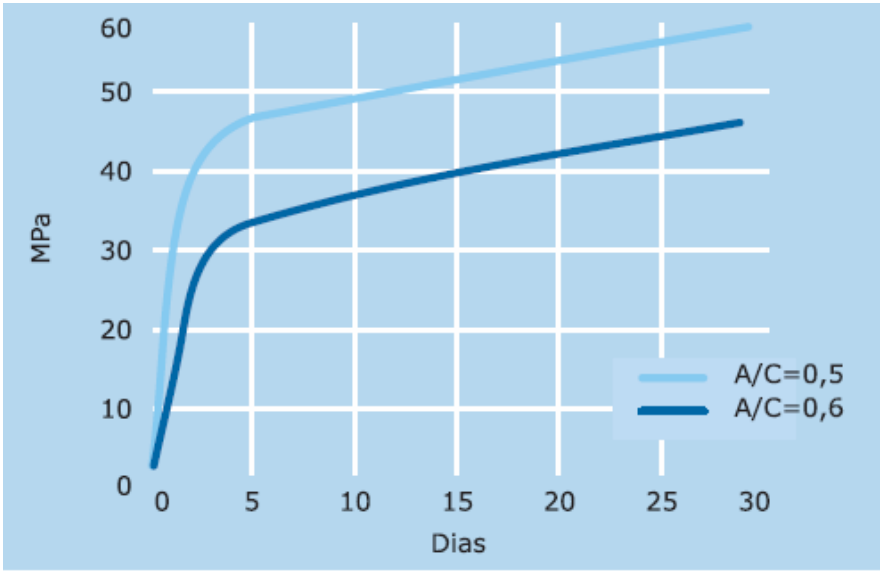


Figure 9.6 - Indicative values of uniaxial strength of concrete produced with 350 kg/m^3 of CIM I 52.5R (adapted from Secil catalogue)

Then, uniaxial and diametral compression (an indirect approach to tensile strength) tests were performed over samples with different percentages of cement. The results of this preliminary testing program aimed to settle conditions for compaction processes and curing times during the main experiment and to calibrate the respective strength with the one of natural soil.

Three groups of cylindrical samples with 14cm height and 7 cm diameter were prepared, with compositions indicated in (Table 9.3). The preparation of these samples was based in 4 layers of 3.5cm, statically compacted (Figure 9.7) using a split mold for adequate extrusion. Samples were then placed in a curing chamber with automatic control of environmental conditions (20 ±1ºC of temperature and moisture content of 95 ± 5%), maintained during the experimental programme (Figure 9.8).

Table 9.3 - Soil-cement sample constitution

Cement CIM I 52.5R			
Cement (%)	2	4	6
Dry soil weight (g)	861.62	844.03	826.45
Cement weight (g)	17.58	35.17	52.75
Water weight (g)	91.44	91.44	91.44



Figure 9.7 - Sample preparation process



Figure 9.8 - Chamber used for curing of artificially cemented samples.

Uniaxial and diametral compression tests were performed at curing times of 7 and 21 days. Uniaxial compression tests were based in a commercial load apparatus (ELE Digital Tritest 100) with a load capacity of 100 kN (Figure 9.9). The samples were placed inside the empty cell and a displacement transducer was then positioned. Load was applied at a constant rate of 0.5mm/min, with data acquisition rates of 5 s.



Figure 9.9 - Uniaxial compression test apparatus.

Diametral compression tests were performed using a device composed by two rigid metallic plates that can rotate against each other by means of two cylindrical axis. These latter are fixed to the lower plate, avoiding rotations during the loading phase. The upper plate includes a longitudinal metallic vein through which the linear load is applied to the sample. A displacement transducer is placed in upper plate to measure axial strain (Figure 9.10), while the 10 kN load cell is placed over it. Following the experience obtained in these soils by Rodrigues (2003) supported by other research works in FEUP, the load was applied at a constant rate of 0.04mm/min with 10 s of data acquisition rates. Obtained results at 7 and 21 days of curing time are presented in Tables 9.4 to 9.7 and Figures 9.11 and 9.12.





Figure 9.10 - Diametral compression test apparatus

Table 9.4 - Physical characterization of samples used in compression strength (CIM I 52.5R, 7 e 21 days).

Compressive strength		% of cement		
		2	4	6
γd(kN/m^3)	7 days	15.63	16.32	16.68
W (%)		21.71	19.56	17.99
e_0		0.670	0.599	0.564
Sr (%)		86.23	86.90	84.82
γd(kN/m^3)	21 days	15.87	16.30	16.78
W (%)		17.14	16.33	14.69
e_0		0.644	0.601	0.555
Sr (%)		70.81	72.30	70.42

Table 9.5 - Maximum uniaxial compression strength (CIM I 52.5R, 7 e 21 days)

CIM I 52.5R	Uniaxial compression strength qu (kPa)		qu 21/qu 7
% of cement	7 days	21 days	
2%	49	76	1.55
4%	330	527	1.56
6%	670	807	1.20

Table 9.6 - Physical characterization of samples used in diametral compression strength (CIM I 52.5R, 7 and 21 days)

Tensile strength		% of cement		
		2	4	6
γd(kN/m3)	7 days	15.27	16.35	16.57
W (%)		21.60	19.00	18.01
e_0		0.709	0.596	0.575
Sr (%)		81.04	84.87	83.27
γd(kN/m3)	21 days	15.73	16.38	16.45
W (%)		15.90	15.40	13.84
e_0		0.659	0.593	0.587
Sr (%)		64.19	69.08	62.76

Table 9.7 - Maximum diametral compression strength (CIM I 52.5R, 7 and 21 days)

	Tensile strength q_t (kPa)		$q_{t\,21}/q_{t\,7}$
% of cement CIM I 52.5R	7 days	21 days	
2%	4.4	8.2	1.86
4%	41.1	56.5	1.37
6%	88.0	98.0	1.11

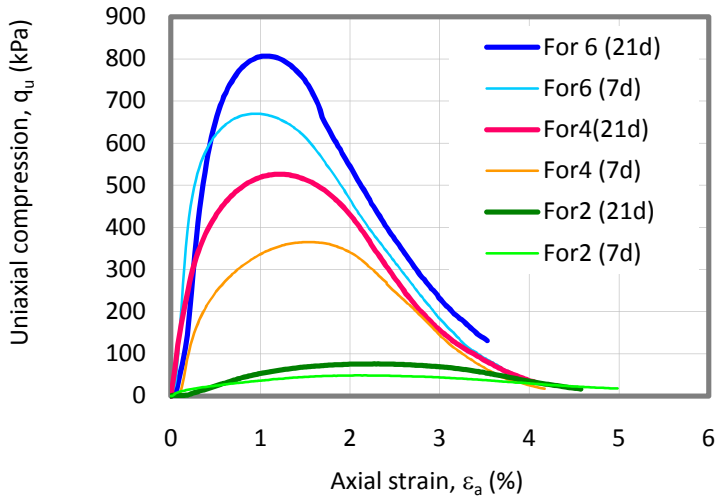


Figure 9.11 - Compression test results of 2, 4 and 6 % of CIM I 52.5R at 7 and 21 days

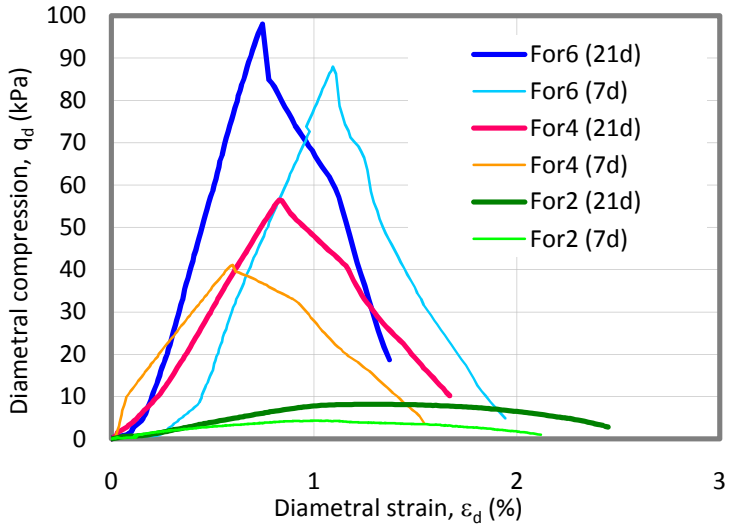


Figure 9.12 - Tensile strength results of 2, 4 and 6 % of CIM I 52,5R at 7 and 21 days

Test results clearly show that both uniaxial and diametral compression strengths follow the usual behaviour reported in literature (Clough et al., 1981; Consoli et al, 2001; Rodrigues, 2003; Schnaid et al. 2005; Consoli et al., 2010; among others) revealing increasing peak strength obtained for lower axial strains, with the increase of cement content. Naturally cemented samples show a range of results close to the observed for 2%.

Reference values of SECIL cement (Figure 9.6) are 1.25 and 1.15, respectively for A/C (rate water/cement) of 0.6 and 0.5. Thus, and taking into account the obtained results, it was decided that 14 days would be adequate to the analysis of bonding influence in DMT results.

During the experimental work in CemSoil box, the thrust capacity was overcome when inserting the blade on a testing sample (sample “For2”), posing a new problem to solve. In fact, working with intervals of 0.5% of cement content would probably generate very unstable situations (especially under 1%) due to an almost erratic cementation arising from the small quantity of needed cement. In these circumstances, a decision was taken of considering lower strength cement that could be used in higher quantities. The choice was made for Portland Cement CIM II/B-L 32.5N of CIMPOR, which is indicated to concrete strength classes C12/15 a C25/30, and is a product of low initial strength evolution and high workability with small rates of water/cement (Figure 9.13).

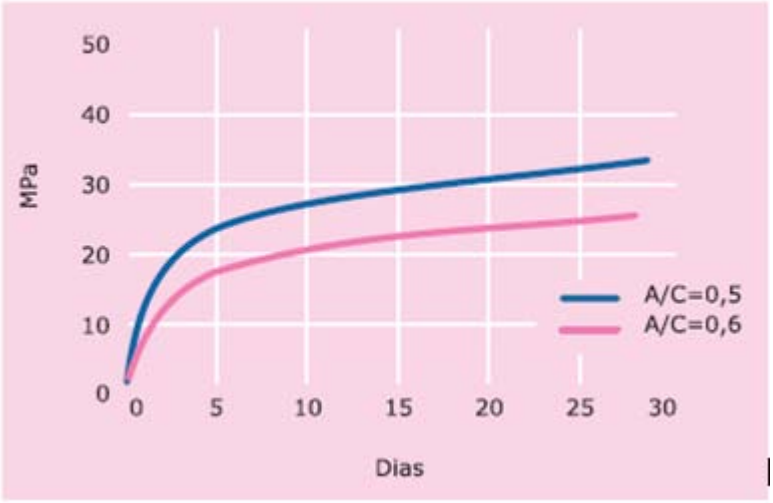


Figure 9.13 - Mean values of compressive strength produced with 350 kg/m^3 of CEM II/B-L 32.5N.

It should be noted that the whole research program was based in considering exactly the same curing time of each pair of samples (laboratory and respective CemSoil), considering that tensile strength could be used as the main parameter for indexation.

Being so, if the accuracy of index parameter and the similarity of CemSoil and laboratory samples was ensured, for research purposes it would be reasonable to combine results of both cement types.

Comparing both performance curves, it seemed reasonable to consider 21 days of curing time for the mixtures with this new cement.

With the exception of cement type and curing time, all the other conditions of preparation were the same, and three more samples were prepared with no cement and 2 and 3% of CIM II/B-L 32.5N, as presented in Table 9.8.

Table 9.8 - Cement compositions for CEM II/B-L 32.5N.

	No cement	CIM II/B-L 32.5N	
Cement (%)	0	2	3
Dry soil weight (gf)	879.20	861.62	852.83
Cement weight (gf)	0	17.58	26.38
Water weight (gf)	91.44	91.44	91.44

New uniaxial and diametral compression tests were performed for no cement, 1% and 2% of CIM I 52.5R and 2% and 3% of CIM II/B-L 32.5N. To test the adequacy of using both cements in one experience, CIM I 52.5R samples were tested at 14 and 35 days of curing times, while CIM II/B-L 32.5N samples were tested at 21 and 35 days. Results are presented in Figure 9.14 and 9.15 and Tables 9.9 to 9.12.

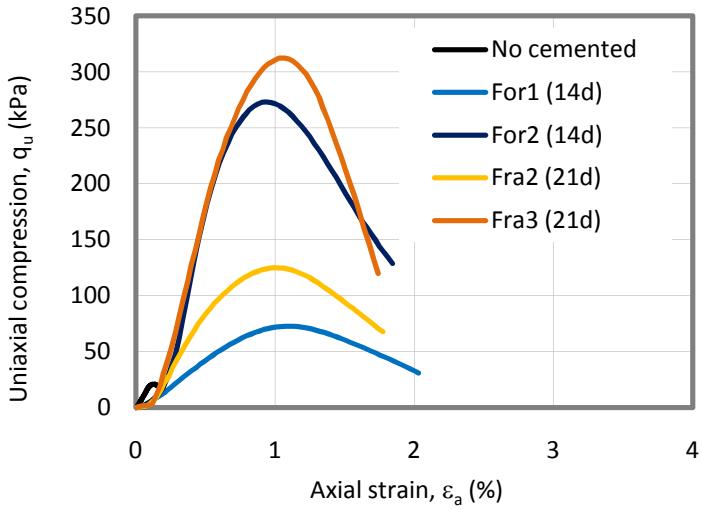


Figure 9.14 - Uniaxial compressive strength of soil mixtures

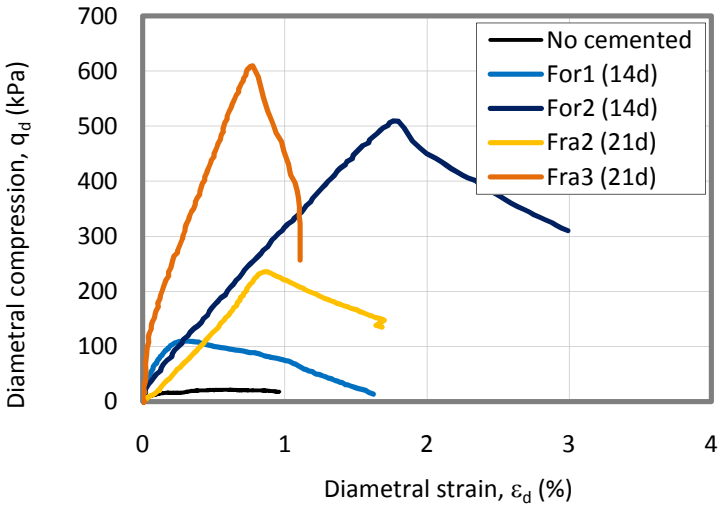


Figure 9.15 - Tensile strength of soil mixtures

Table 9.9 - Physical characterization of samples used in compression strength

Compressive strength		Cement type				
		No cement	Cim 52.5R		Cim 32.5 N	
% of cement		0	1 (For1)	2 (For2)	2 (Fra 1)	3 (Fra 2)
γd(kN/m^3)	14 or 21 days (W% nat)	15.79	15.64	15.56	15.47	15.50
W (%)		11.24	11.14	10.71	14.04	13.72
e_0		0.653	0.669	0.677	0.687	0.683
Sr (%)		45.81	44.30	42.05	54.34	53.41
γd(kN/m^3)	14 or 21 days (Saturated)	-	15.84	15.83	15.82	15.87
W (%)		-	21.90	21.98	22.06	21.71
e_0		-	0.647	0.648	0.649	0.645
Sr (%)		-	90.03	90.23	90.41	89.56
γd(kN/m^3)	35 days (W% nat)	-	15.72	15.92	15.85	15.88
W (%)		-	8.12	7.29	8.26	7.54
e_0		-	0.660	0.639	0.646	0.643
Sr (%)		-	32.72	30.35	34.01	31.21

Table 9.10 - Uniaxial compression test results

		Cement type				
		No cement	Cim 52.5R		Cim 32.5 N	
% of Cement		0	1 (For1)	2 (For2)	2 (Fra1)	3 (Fra2)
Uniaxial compressive strength q_u (kPa)	14or 21 days	20.8	72.6	273	124.9	312.3
	35 days	20.8	111.7	379.1	180.8	383.7

Table 9.11 - Physical characterization of samples used in diametral compression strength

Tensile strength		Cement type				
		No cement	Cim 52.5R		Cim 32.5 N	
% of cement		0	1 (For1)	2 (For2)	2 (Fra 1)	3 (Fra 2)
γd(kN/m^3)	14 or 21 days (W% nat)	16.07	15.69	15.77	15.65	15.58
W (%)		10.76	11.02	11.33	11.62	11.50
e_0		0.624	0.663	0.655	0.667	0.675
Sr (%)		45.84	44.23	46.00	46.33	45.29
γd(kN/m^3)	35 days (W% nat)	-	15.73	15.91	15.85	15.90
W (%)		-	6.89	7.22	7.21	7.98
e_0		-	0.659	0.640	0.647	0.642
Sr (%)		-	27.81	29.98	29.64	33.10

Table 9.12 - Diametral compression test results

		Cement type				
		No cement	Cim 52.5R		Cim 32.5 N	
% of Cement		0	1 (For1)	2 (For2)	2 (Fra1)	3 (Fra2)
Tensile strength q_t (kPa)	14 or 21 days	1.5	7.2	33.2	15.3	39.2
	35 days	1.5	8.9	33.8	17.5	39.4
Ratio qt/qu (%)		7	10	12	12	13

Figure 9.16 clearly shows how both types of cement fit in the same line of evolution, no matter the type of cement used, confirming the adequacy of selected curing times, which were maintained through the entire experimental work.

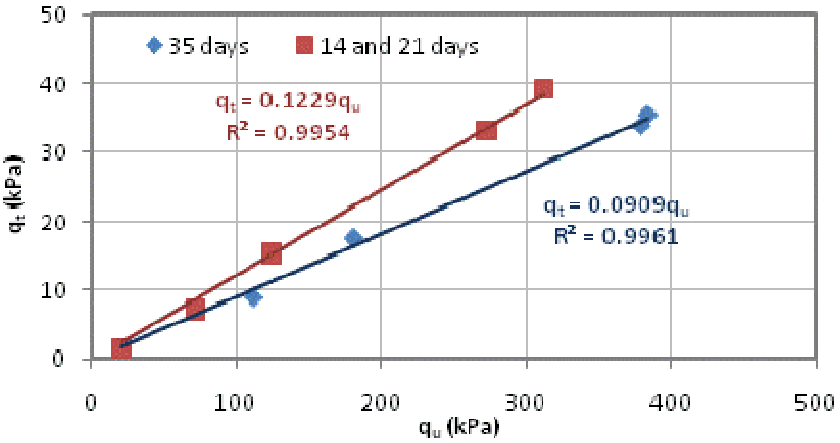


Figure 9.16 - Strength evolution of samples mixed with the two different cements

The results confirm all the tendencies revealed in the previous tests, revealing increasing peak strengths obtained at decreasing shear strains, as cementation level increases. Results also reveal increasing values for both strengths following the order: no-cement, 1% CIM52.5R (For1), 2% CIM32.5N (Fra2), 2% CIM52.5R (For2), 3% CIM32.5N (Fra3). Comparing the ratios between tensile and compressive strengths of cemented samples, it can be observed that they are within the same range (10 to 13%), converging for the results in artificially cemented sands reported by Clough et al. (1981), Schnaid et al. (2005), Rios da Silva (2009) and Consoli et al. (2010), the latter deducing a value of 0.15 from their proposed correlations based in the voids/cement ratio (η/C_v). Moreover, tests in Porto (COBA, 2003) and Guarda (Rodrigues, 2003) naturally cemented granitic soils reveals identical ratios.

Comparing these results with PGM (Coba, 2003) data, it becomes clear that they fall within medium compacted (G4 - For1) compacted (G8 - Fra2) and W5 (Fra3 and For2) ranges. Furthermore, results obtained in the same experimental site used in this experiment (Rodrigues 2003) revealed 9 to 17 kPa and 65 to 100 kPa, respectively, for diametral and uniaxial compression strengths, situating these natural soils between For1 and Fra2 tested samples.

In order to find out how suction affects compressive strength, new samples were prepared following exactly the same procedures and curing conditions used in previous

samples. For that purpose samples were emerged 24 hours before testing, generating a convergence value of saturation degree of 90%, controlled after testing. To reach a value of 100% for saturation degree, vaccum back pressures had to be applied, probably leading to some deviations on basic conditions, and so the option was to test with these saturation levels, where very low values were accepted. In Figure 9.17, stress-strain curves are represented together with the same curves related to non saturated conditions. In Table 9.13, global results related to saturated and non saturated conditions are presented.

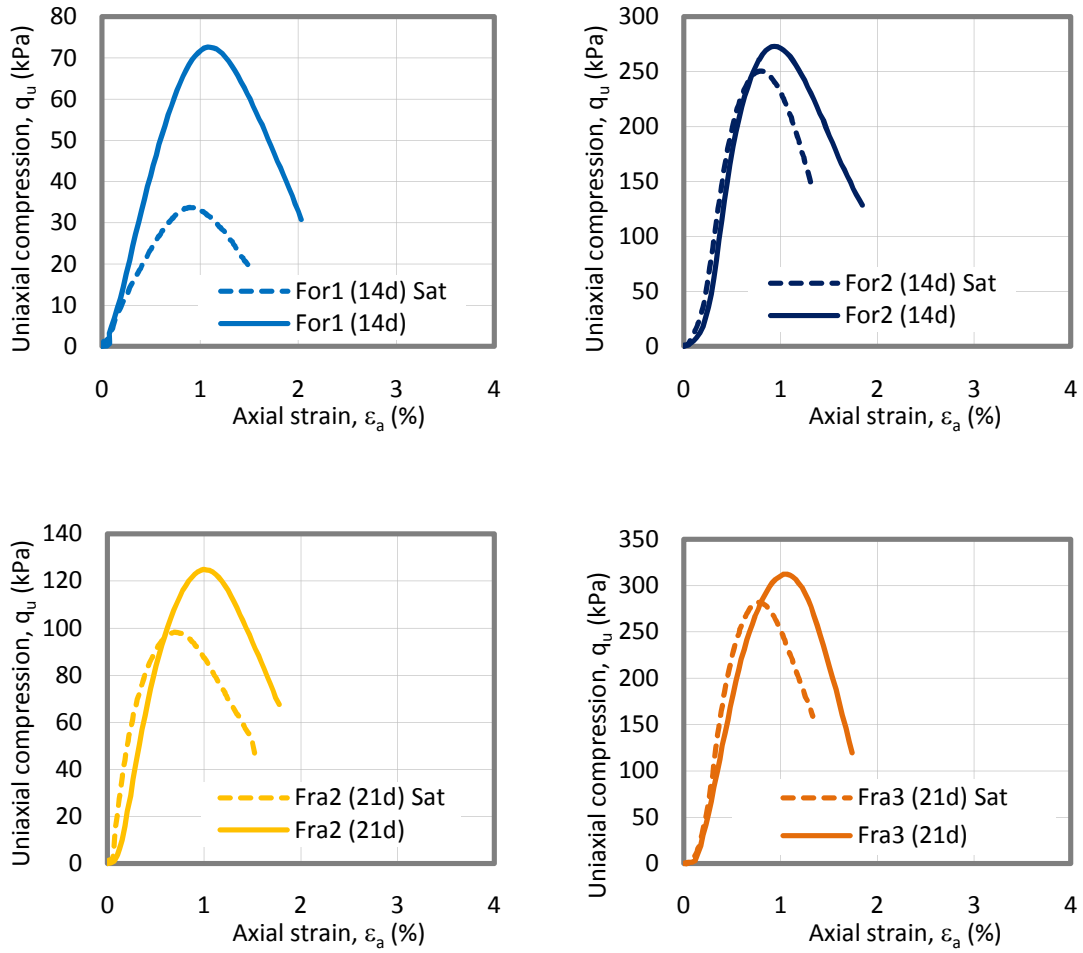


Figure 9.17 - Uniaxial compression strength in saturated and non saturated samples.

The overall data reveals lower peak values reached at lower strain level on saturated samples. Since sample preparation follows the same methodology and a homogeneous microfabric between the two types of samples is expected, then those differences shall be related with suction. If the lowest cement content sample is disregarded, there is a tendency for highly saturated sample results to be lower 20 to 25 kPa than those obtained in remoulded moisture conditions, generating a clear

difference due to suction influence. The reason for the deviation on the first sample may be justified by the small amount of cement causing some variation on the distribution of cement within the sample. This indicates that for a specific type of soil with the same void ratio, suction effects are independent of cement content, with lower influence of the former as the latter increases.

Table 9.13 - Compressive strength test results under different saturation conditions

		Cement type				
		No cement	Cim 52.5R		Cim 32.5 N	
% of Cement		0	1	2	2	3
Uniaxial compressive strength q_u (kPa)	Moisture content (%)		11.14	10.71	14.04	13.72
	14 or 21 days	20.8	72.6	273	124.9	312.3
	Moisture content (%)	…	21.90	21.98	22.06	21.71
	14 or 21 days	…	33.8	250.6	98.3	281.8
q_u unsat - q_u sat		…	38.2	22.4	25.6	20.5

Summarizing, uniaxial and diametral tests performed allow outlining the following considerations:

a) q_u and q_t increases with cementation level, following a single trend line, no matter the type of cement used; it should be noted that time curing levels are different since used cements react differently with time;
b) Peak strengths are higher and brittleness increases with cement content in both uniaxial and diametral compression tests;
c) Uniaxial and diametral compression magnitudes fall within the range found by Rodrigues (2003), when dealing with the same granitic site material that were used in this experience, allowing to compare naturally and artificially cemented sample results;

d) Ratios q_t/q_u fall within 10 to 13% range converging to some results presented in reference works on artificially cemented samples;

e) Different results were found in uniaxial compression strengths tested under different saturation degrees, highlighting the influence of suction, which seems to be independent of cementation level; for the tested samples, differences between unsaturated and almost saturated (> 90%) conditions varies between 20 and 25 kPa, as presented in Figure 9.18.

f) High saturation degrees are always related to lower peak values reached at higher shear strains, which is in agreement with the expected suction influence.

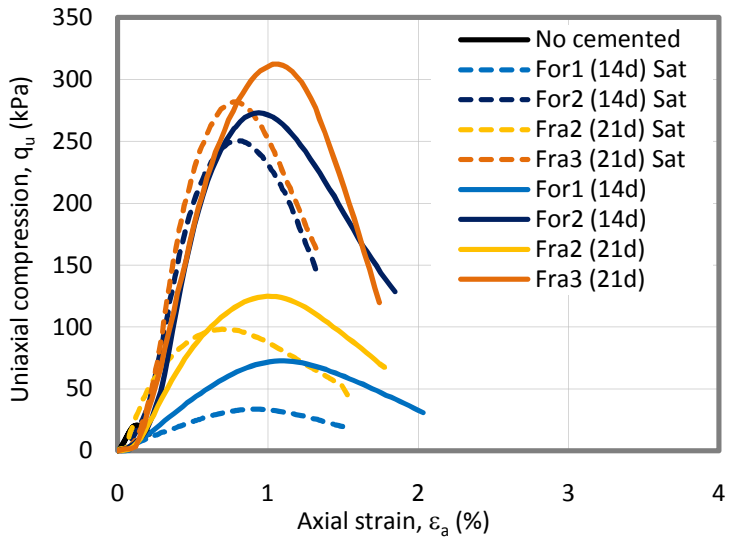


Figure 9.18 - Global results of compression tests in saturated and unsaturated samples

9.2. Triaxial testing

9.2.1. Equipments and methodologies

For each cement content of the samples placed in CemSoil Box, laboratory (isotropic) consolidated-drained (CID) triaxial testing was performed in representative remoulded samples. Overall, 20 samples were tested in IPG Laboratory over saturated samples with confining stresses of 25, 50, 75 and 300 kPa applied to 0%, 1% and 2% of Cement 52.5R and 2 and 3 % of Cement 32.5N. IPG Laboratorial triaxial testing apparatus (Figure 9.19) is constituted by a ELE International triaxial cell, equipped with an extended special ring to allow the installation of three LVDT transducers (GDS), two for axial strain and one for radial strain evaluations, the latter connected to a Bishop

ring. The cell is connected to a testing control system produced by the Imperial College of London, which can be described as follows:

a) Two air-pressure controllers equipped with step engines that allows to control cell and back pressures, through air/water interfaces, with 0.07 kPa incremental adjustments up to a maximum value of 820 kPa;
b) One analogical/digital (A/D) convertor of 16 channels. Eight of them work at 100 mV, for load cell, pressure transducers and displacement transducers (LSD). The remaining are 10V channels, in order to supply internal and external displacement transducers (LVDT) and a 100 ml automatic volume controller, commercialized by ELE;
c) A safety switch for triaxial load system, connected to software I/O board, developed by Durham University (Toll, 1995), enabling to stop the loading automatically.



Figure 9.19 - IPG triaxial apparatus

The general characteristics related to the components of triaxial apparatus are presented in Table 9.14. The software used in the triaxial testing control was developed by Durham University (Toll, 1995).

Table 9.14 - Characteristics of devices used in triaxial testing

Device	Reference	Range	Accuracy
Pressure transducers (3)	ELE	1000 kPa	0.01 kPa
Submersible load transducer (1)	ELE	10 kN	0.01 kN
External axial strain transducer (1)	ELE	±25.0 mm	0.001 mm
Electronic volume change unit (1)	ELE	80 cc	0.01 cc
Internal axial strain transducer (2)	GDS	±5.0 mm	0.1% FRO
Internal radial strain transducer (1)	GDS	±5.0 mm	0.1% FRO
Load frame (1)	ELE Digital Tritest 100	100 kN	-

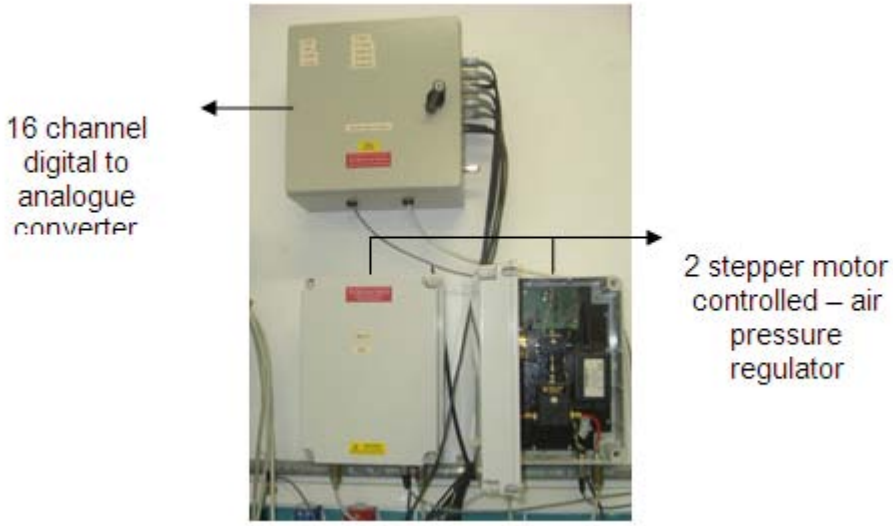


Figure 9.20 - Triaxial control system

Sample remolding for triaxial testing followed the same sequence executed in diametral and uniaxial compression tests, with 70mm diameter and 134 to 140mm height. The sequence of preparation and installation of testing samples is illustrated in Figure 9.21.











Figure 9.21 - Remolding conditions: 1st row - Static compaction; 2nd and 3rd rows – Mounting the cell; 4th row – Placing LVDT's

As stated, the curing time of CemSoil and laboratory testing samples were exactly the same in the whole experiment, in order to avoid strength and stiffness differences between cell and laboratory tests. All triaxial tests were performed under saturated conditions, achieved in two stages. In the first stage, the water was forced to flow, by applying a 10 kPa back-pressure in the base, while the top was at atmospheric pressure. During this stage, cell pressure was maintained at 15 kPa pressure to avoid swelling. A volume of water of at least twice the volume of voids was percolated, aiming an efficient air expelling from the pores. In a second stage, cell and back-pressures were increased in controlled increments of 25 kPa/hour, with a gap of 5 kPa between them, until Skempton B parameter reached at least 0.93, which was achieved for reference values of 250 kPa of cell pressure. During this stage, volumetric changes were registered through the internal instrumentation system.

After saturation, specimens were submitted to isotropic consolidation, following the pre-selected confining stresses, during which volume changes were registered by external and internal systems. Then, shear phase was implemented at low strain rates of 0.02mm/min, in order to ensure drained conditions (in a double drainage path).

9.2.2. Presentation and Discussion of Strength Results

In Figures 9.22 to 9.25, stress-strain and volumetric vs axial strain are presented and compared. Maximum deviatoric stress were determined by the maximum σ'_1/σ'_3, although no special differences was found when maximum q value is considered directly.

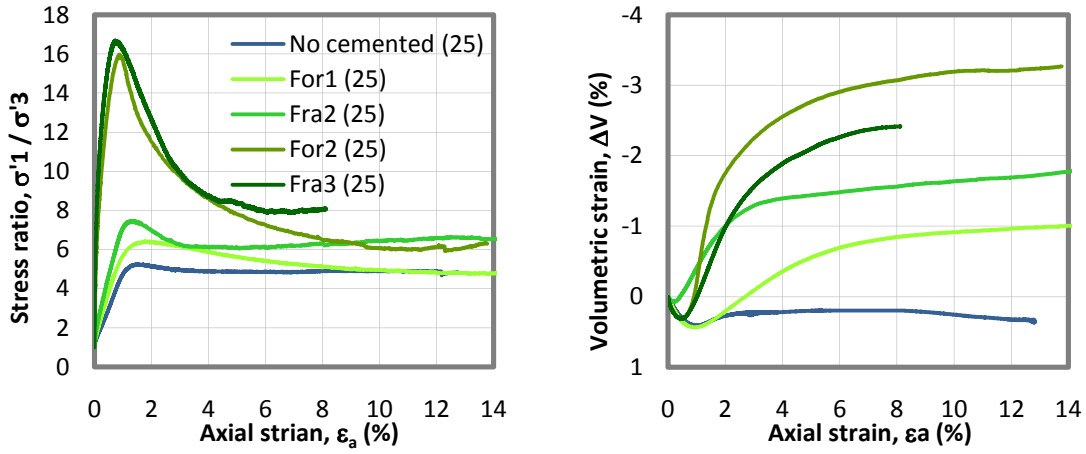


Figure 9.22 - Stress and strain curves for 25 kPa of confining stress

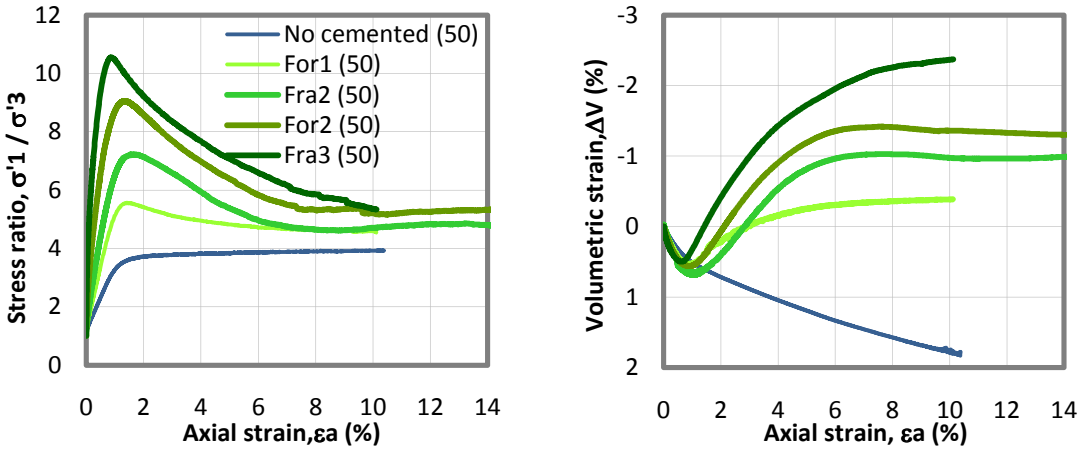


Figure 9.23 - Stress and strain curves for 50 kPa of confining stress

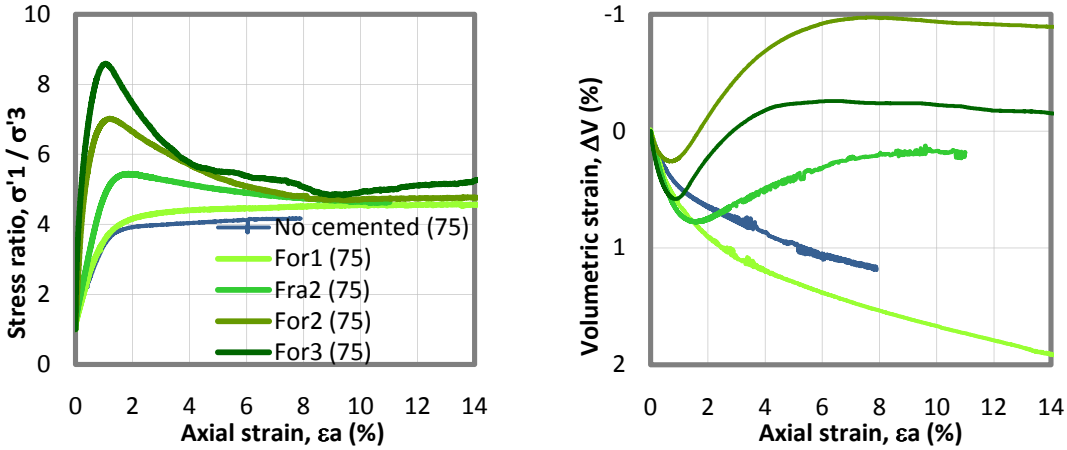


Figure 9.24 - Stress and strain curves for 300 kPa of confining stress

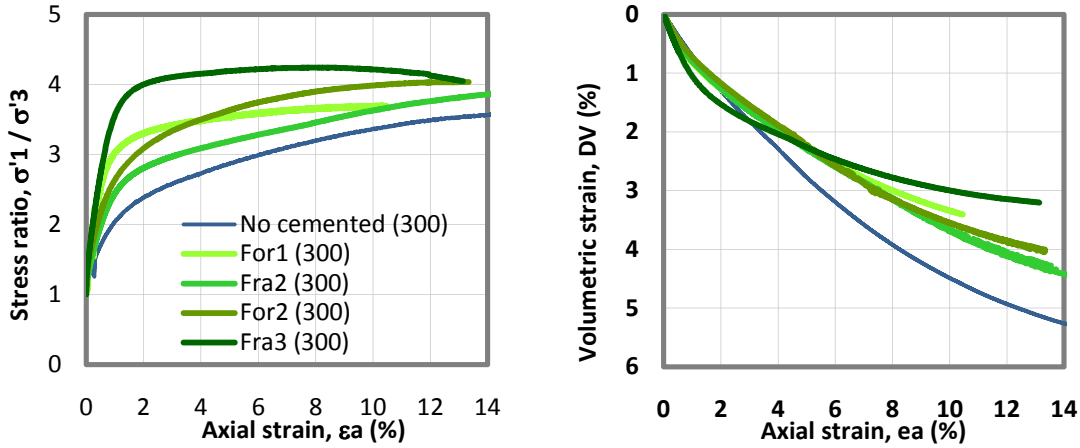


Figure 9.25 - Stress and strain curves for 300 kPa of confining stress

In Tables 9.15 and 9.16 a summary of relevant results is presented, including those obtained by Rodrigues (2003) on Guarda granitic residual soil used as reference to reconstitute the samples of the present experience. The latter is represented by an upper level located from ground surface up to 4.5m depth, and was tested for confining stresses varying from 15 to 550 kPa. To make the comparison between naturally and artificially cemented soils easier, comparable results are marked in the respective table in different colors, red and blue respectively for low and high confining stresses. In the Table 9.15, e_0 represents void ratio, w the moisture content, γ the unit weight, p'_i the initial mean effective stress, p'_f and q_f respectively the mean effective and deviatoric stresses at failure, ε_a the axial strain, d ($d = \delta\varepsilon_v^p / \delta\varepsilon_s^p$ according to Coop & Cuccovillo, 1997) the dilatancy, ε_d and Δv respectively the strain and volume change related to maximum dilatancy.

The main trends revealed by stress-strain and volumetric-axial strain curves are globally consistent with the behaviour usually reported in reference works (Vaughan, 1988; Clough et al. 1981, Ladd, Cuccoville & Coop, Malandraki & Toll, 2000; Rodrigues, 2003; Viana da Fonseca, 1996, 1998, 2003; Schnaid, 2005, Toll & Malandraki, 2006, Ferreira, 2009, among others), also confirming the uniaxial and diametral compression tests. In fact, global data reveals that, with the exception of a smooth peak at lower confining stress (25 kPa), explained by the approach of uniaxial condition, destrucutred samples show ductile behaviours, while cementation seems to induce the development of an increasing peak strength with cementation level, which, in turn, is limited by a certain level of initial mean effective stress. Beyond this level, soil behaviour is progressively governed by frictional strength, shifting from fragile to ductile type stress-strain curves.

At low confining stresses (25 to 75 kPa) stress-strain curves reveal brittle failure modes, followed by dilatant behaviour, with increasing values with cementation level, while peak axial strains decrease with cement content, ranging between 2 and 0.8%. On the other hand, at high confining stresses (300 kPa), stress-strain curves reveal ductile behaviour and respective volumetric strain is always of contractive type. Maximum σ'_1/σ'_3 is reached for much higher strains (8 to 18%) than those at low confining stresses. In other words, the value of 300 kPa of confining stress seems to be in the transition of bond structure controlled soil behaviour (pre-yield state) to a granular frictional response (post-yield state). Stress-strain curves also reveal an increasing initial stiffness with cementation level, while dilatant behaviour increases with cementation level and decrease with initial mean effective stress.

Table 9.15 - Global laboratory testing results

Sample (q_t, kPa)	e_0	w	γ	p'_i	p'_f	q	ε_a	d	ε_d	ΔV_d
		%	kN/m^3	kPa	kPa	kPa	%		%	
No cement. (1.5)	0.616	12.4	18.0	25	60.4	106.1	1.5	0.218	1.48	0.342
	0.656	12.0	17.5	50	97.5	144.7	10.4	…	…	…
	0.602	11.3	18.0	75	151.7	233.7	7.8	…	…	…
	0.570	11.9	18.4	300	557.5	776.8	16.0	…	…	…
For1 (7.2)	0.684	21.8	18.7	25	68.6	132.3	1.8	0.274	2.65	0.015
	0.659	21.4	18.9	50	127.3	230.4	1.4	0.520	1.41	0.422
	0.650	15.9	18.2	75	160.3	261.5	13.4	…	…	…
	0.569	11,8	18.4	300	570.2	811.4	10.3	…	…	…
Fra2 (15.3)	0.640	11.8	17.6	25	80.7	165.3	1.3	0.679	1.06	0.451
	0.640	16.8	18.4	50	154.8	313.4	1.6	0.467	2.73	0.059
	0.632	10.8	17.6	75	183.7	329.0	1.9	0.722	2.57	0.692
	0.621	20.3	19.2	300	587.7	871.5	17.2	…	…	…
Guarda residual soil 1,5-4,5m (9-17)	0.548	14.7	19.0	15	47.2	95.3	3.5	0.562	3.69	-0.588
	0.489	11.2	19.4	25	94.3	203.4	2.8	0.746	3.86	-1.354
	0.428	10.9	20.0	50	150.4	304.6	2.6	0.682	3.04	-0.523
Guarda residual soil (4.5-7.0m) (12.3)	0.539	15.7	19.3	150	346.5	594.1	6.8	0.285	8.59	0.302
	0.467	12.8	19.8	350	719.5	1105.6	6.9	0.161	8.49	1.235
	0.562	18.1	19.4	500	959.7	1378.4	9.4	…	…	…

Table 9.16 - Reference strength parameters.

Sample	q_t	q_u	q_t / q_u	ϕ'_p	c'
	kPa	kPa		º	kPa
No cement	1,5	20.8	7	35	2.5
For1	7.2	72.6	10	33	23.8
Fra2	15.3	124.9	12	34	38.4
For2	33.2	273.0	12	30	63.2
Fra3	39.2	312.3	13	30	107.7
Guarda (25-350 kPa)	9-17	65-100	…	36	30.4
Guarda (25-550)	12.3	81.3	15	34	37.1

Axial strains at failure reveal a strong difference between dilatant and non-dilatant types, with the former reaching maximum value for axial strains globally placed between 1 and 2%, while the latter tend to fail in shear for much higher strains (8 to 10%). Naturally cemented soils show the same order of magnitude although a bit higher than artificial mixtures. The observed differences could probably be related to the different fabric of naturally and artificially cemented samples, since destrucutred sample results, in this case, converge to those presented by Rodrigues (2003). These trends are also reported in bibliographic references on the subject reported by Cuccovillo & Coop (1997), Viana da Fonseca (1996, 1998), Rodrigues (2003). In Figures 9.26 to 9.27, test curves of maximum ratio σ'_1/σ'_3 and volumetric changes against axial strain are presented for the lower (25 kPa) and higher (300 kPa) confinement stresses, where peak strength and maximum dilatancy are marked. Figures 9.28 and 9.29 represent the evolution, with cementation level, of q/p' against strain level and volume change corresponding to maximum dilatancy. From those figures the following trends can be pointed out:

a) Considering the same confining stress, with increasing cement content, it can be observed that the maximum ratio σ'_1/σ'_3 (máx) increases with cement content and its mobilization occurs at decreasing axial strains; brittle behaviour is present in cemented samples at low confining stresses and increases with cementation level;

b) None of the samples tested at 300kPa (high) confining stresses showed dilatancy; at low confining stresses, no cemented samples show dilatancy for the lower confining stress (25 kPa), while cemented samples show dilatancy in almost all probes;
c) The dilatancy increases with cement content, with decreasing confining stresses (as sustained by Lade et al., 1987) and increasing q/p' (as sustained by Clough et al., 1981);
d) At low confining stresses, the increase of cementation level gives rise to a decrease of initial decreasing volume change, followed by dilation, that will be higher in stronger cemented samples;
e) Increasing cementation level leads to a higher gap between peak and maximum dilatancy strain;
f) Volumetric strain curves also indicate that rates of dilation at failure decreases with increasing confining pressure, which becomes positive (compression) at high confining stresses; this is due to destructuring by increase of mean effective stress, thus volumetric yield;
g) Volume changes tend to decrease with both increasing q/p' and cementation level and decreasing confining stresses;
h) There is a clear difference between mixtures with high (For2 and Fra3) or low (non cemented, For1 and Fra 2) cementation level; the former shows stable values of strain needed to reach maximum dilatancy indicating that cement prevails, while the latter shows a tipically destructuring effect by volumetric yield due to istropic effective stress increase.
i) Similar and convergent behaviour is revealed by comparing q/p' ratios and volume changes; in fact, the drop in q/p´ with volume changes is only visible in highly and preserved cemented mixtures, since the effect of destructuring is only observed during shearing, while in low cemented mixtures the drop is not detected since the loss of structure has already started during consolidation.

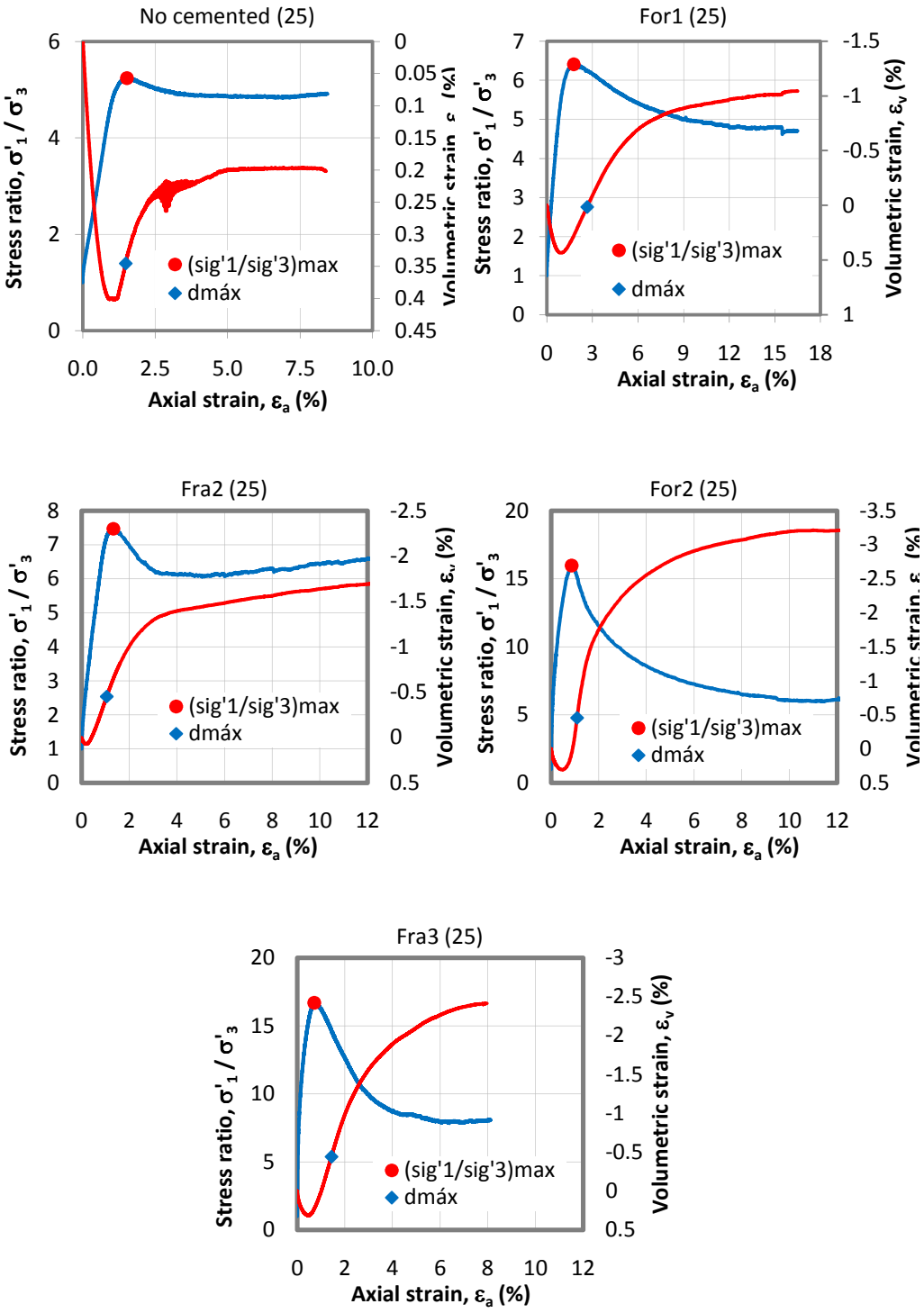


Figure 9.26 - Peak strength and maximum dilatancy for 25 kPa of confining stress

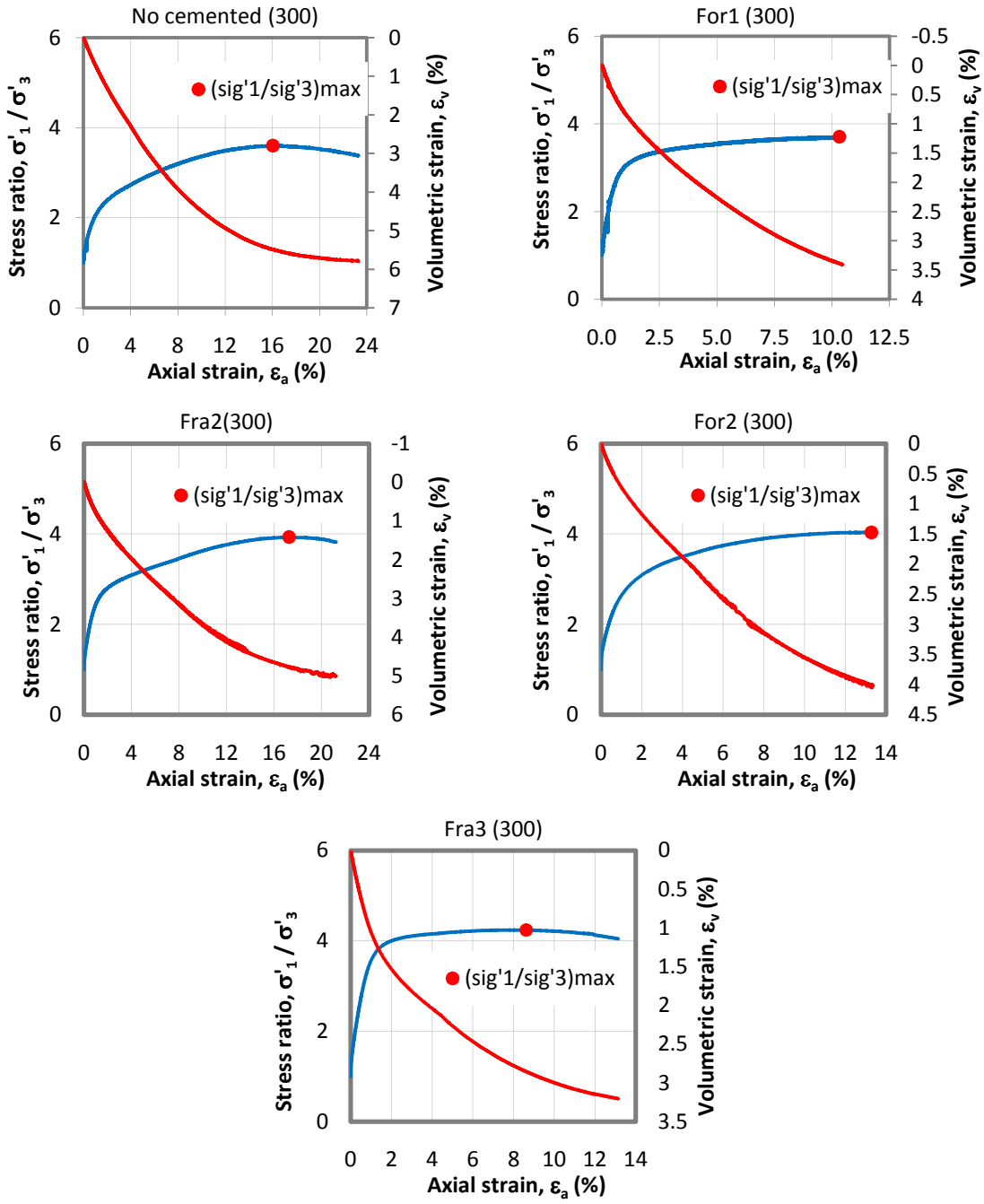


Figure 9.27 - Peak strength and maximum dilatancy for 300 kPa of confining stress

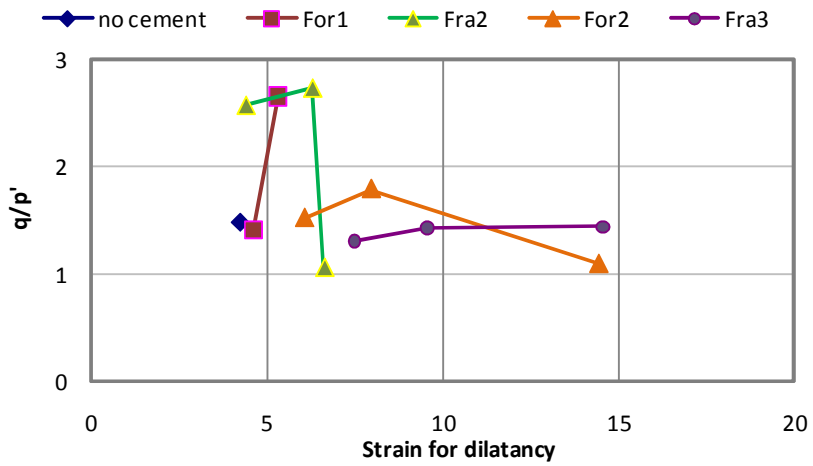


Figure 9.28 - Evolution of strain for maximum dilatancy with normalized deviatoric stress

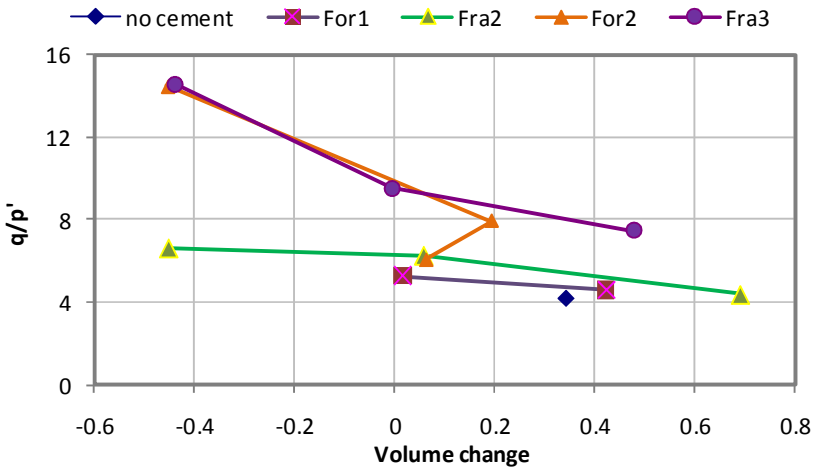


Figure 9.29 - Evolution of volume change related to maximum dilatancy with normalized deviatoric stress

The aforementioned interpretations are convergent to Toll et al. (2006) proposal for the explanation of the behaviour of bonded soils. This could be characterized by an initial yield locus where the stress-strain behaviour shows a drop in stiffness and represents the beginning of bonding breakdown. However, cementation keeps affecting soil behaviour and it reaches a higher level of strength than the observed in destrucutred soils. As mean stress increases, the curve goes down until it reaches the destrucutred surface, being an obvious consequence of de-structuring due to high confining effective stress. This pattern was found by those researchers to be similar to the effect of rotation of stress path direction on constant σ'_3 tests, to constant p' and constant σ'_1 tests, that show a shrinkage of yield surfaces, so yield occurs for lower deviator stresses. Data from the present framework can be represented by this model, with failure envelopes of cemented samples showing curved lines, as referred by many

researchers (Lade et al., 1987, Vaughan, 1988; Clough et al, 1981; Viana da Fonseca, 1996; Cuccovillo & Coop, 1997; Malandraki & Toll, 1994, Rodrigues, 2003; Schnaid et al., 2005), with increasing deviatoric stress with cementation level. In other words, the representation of failure envelope in p'-q space (Figure 9.30) reveal that destructured samples follow a straight line with deviatoric stress, which increases either with cementation level and mean initial effective stresses, converging to prior cited references. The strength envelope related with naturally cemented soils (Rodrigues, 2003) is represented in Figure 9.31.

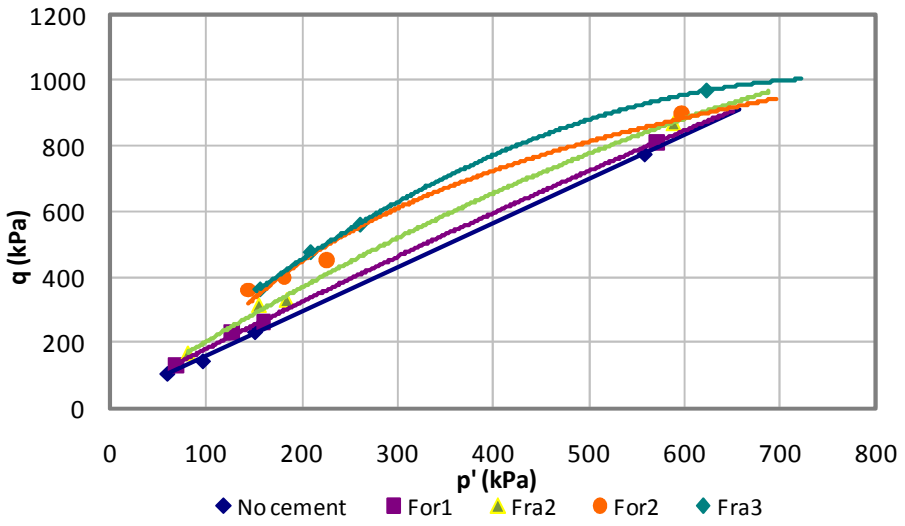


Figure 9.30 - Strength envelopes in q-p' stress space (artificial samples)

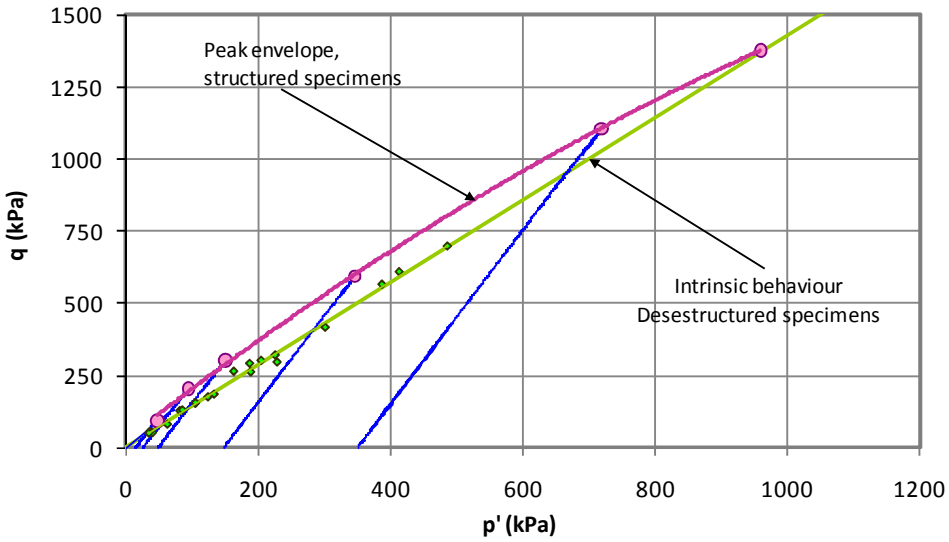


Figure 9.31 - Strength envelopes in q-p' stress space (natural samples – Rodrigues, 2003)

Furthermore, it is important to refer the great potential of Lade model, in modeling this multi-yield process, by separating isotropic and deviatoric plastification; hardening laws in these two vertents are successfully applied in cemented soils, as discussed by Viana da Fonseca (1996, 1998) and Viana da Fonseca et al. (2001).

As previously mentioned, it is generally accepted that cemented soil strength can be represented by Mohr-Coulomb envelope (Clough et al., 1981; Leroueil & Vaughan, 1990; Rodrigues, 2003; Schnaid et al, 2005; Viana da Fonseca & Coutinho, 2008), thus it is interesting to compare the influence of cementation on effective cohesion determined by triaxial tests. However, this assumption must be used with some caution, always related to a certain range of confining stresses, as suggested by the figures above. In fact, obtained results clearly highlight the non-linearity of cemented soils, deviating from Mohr Coulomb criterion and converging to the origin when mean effective stress (p') tends towards "0", which suggests the lower influence of cohesive contribution in the shear strength of these materials. An attempt to compare triaxial fundamental results with those from uniaxial and diametral compression tests is hereby presented (Figure 9.32 and Table 9.17), as it may be a simplified approach for the use of simple tests as index parameters of resistance gains due to cementation.

Concerning to cohesion, as expected, data clearly reveals that there is a direct relationship with compression and tensile resistances, as usually reported in cemented soils studies. In the present case, cohesion results are one third of unconfined compression and 2.5 times higher than tensile strength. Moreover, data converges to Clough et al. (1981) observations that tensile test results are lower than cohesion derived from ultimate states in stress paths obtained in triaxial testing, which can be related with the mentioned non-linearity of strength envelope.

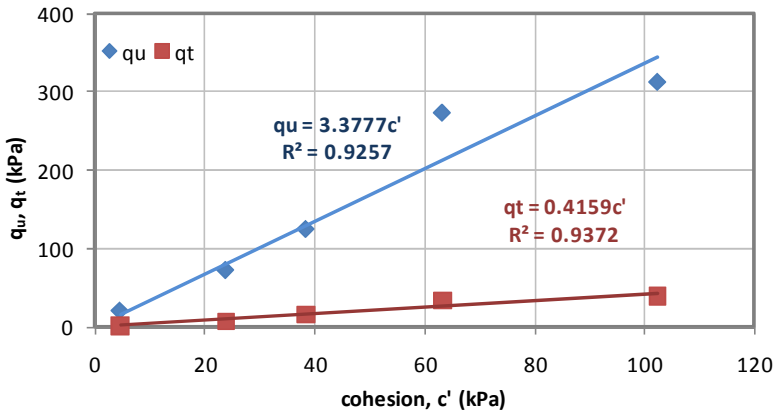


Figure 9.32 - Correlations between cohesion and compressive and tensile stresses.

Table 9.17 - Determined and deduced tensile strengths

Tensile strength (14 and 21 days)	Tensile strength test (35 days)	Tensile strength from triaxial results	Ratios
1,5	1,49	6,35	0,24
7,2	8,87	36,42	0,20
15,3	17,45	57,84	0,27
33,2	33,84	83,41	0,40
39,2	38,71	174,29	0,23

When comparing deviatoric stresses with uniaxial compression strength, it becomes clear that data converges well to Schnaid et al. (2005) conclusions, as shown in Figure 9.33. At low confining stresses, obtained results follow parallel straight lines with q_f increasing with q_u, while at high confining stress, correlation between the two parameters also follow a straight line, but at smoother rates, which can be related to a decrease of cementation influence in strength in favor of microfabric control. Low confining stress results obtained in the present research match quite well Schnaid et al. (2001) results, as proved by the respective correlation expressions (Figure 9.34):

$q_f = 3{,}32\ p_i' + 1{,}01 q_u$ (Schnaid et al., 2001) (9.1)

$q_f = 2{,}7\ p_i' + 1{,}05\ q_u$ (9.2)

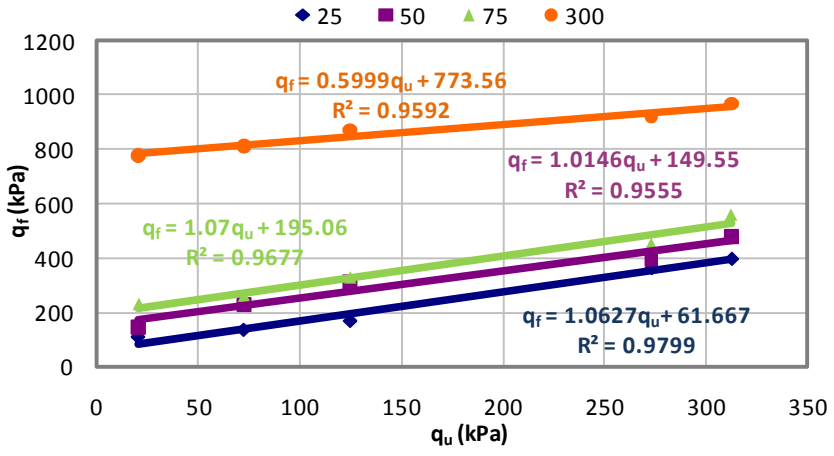


Figure 9.33 - Peak deviatoric stresses versus uniaxial compressive stress.

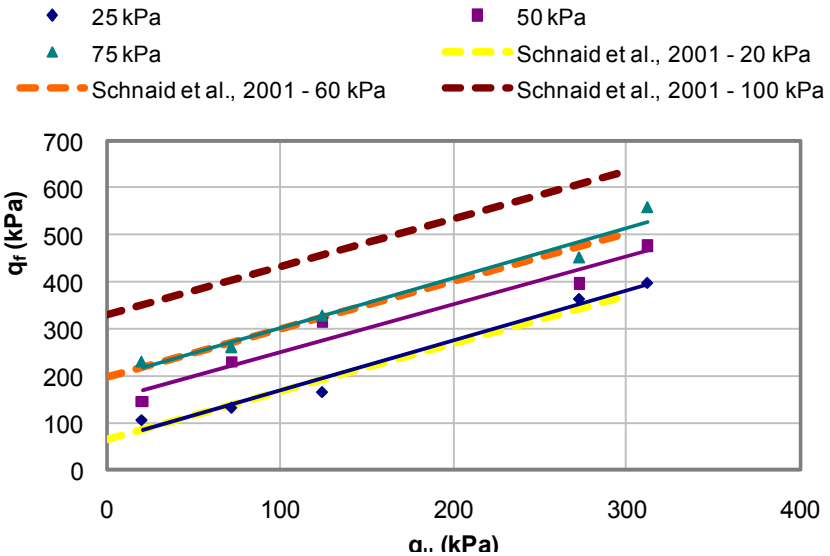


Figure 9.34 - Peak deviatoric stresses versus uniaxial compressive stress: actual data represented by full lines and Schnaid et al (2001) data represented by dashed lines.

If q_u combined with initial mean effective stress can be used to deduce deviatoric stresses, it is expectable that tensile strength can serve the same purpose, as illustrated in Figure 9.35. The parallel trends at low confining stresses and the lower slope of correlation at high confining stresses shows the same trends that were found in unconfined compressive strength, naturally with a different magnitude. In the present case, the respective correlation takes the following form:

$$q_f = 2{,}9\ p_i' + 8{,}14\ q_t \qquad (9.3)$$

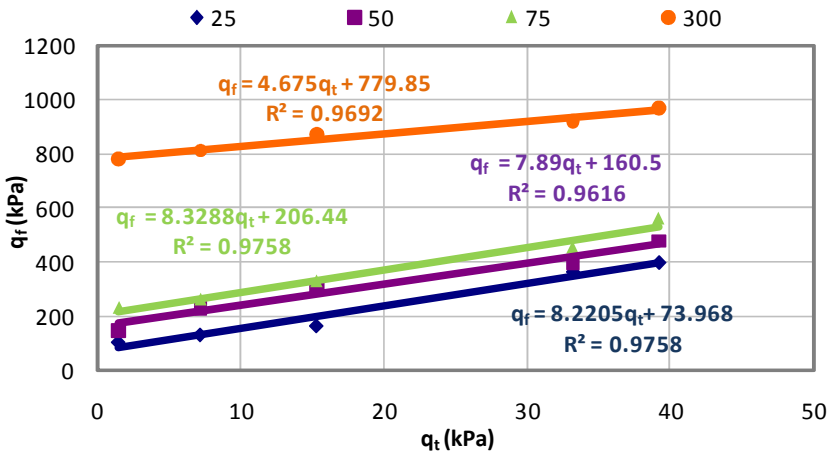


Figure 9.35 - Peak deviatoric stresses versus tensile strength.

Although the calibration work doesn´t really need critical state analysis, determination of strength parameters at critical state was attempted, since data obtained from triaxial testing revealed some interesting features enabling some discussion on this matter. The critical state lines represented in specific volume versus mean effective stress (log) are presented in Figure 9.36, while Figure 9.37 represents the critical state line obtained from all the performed tests.

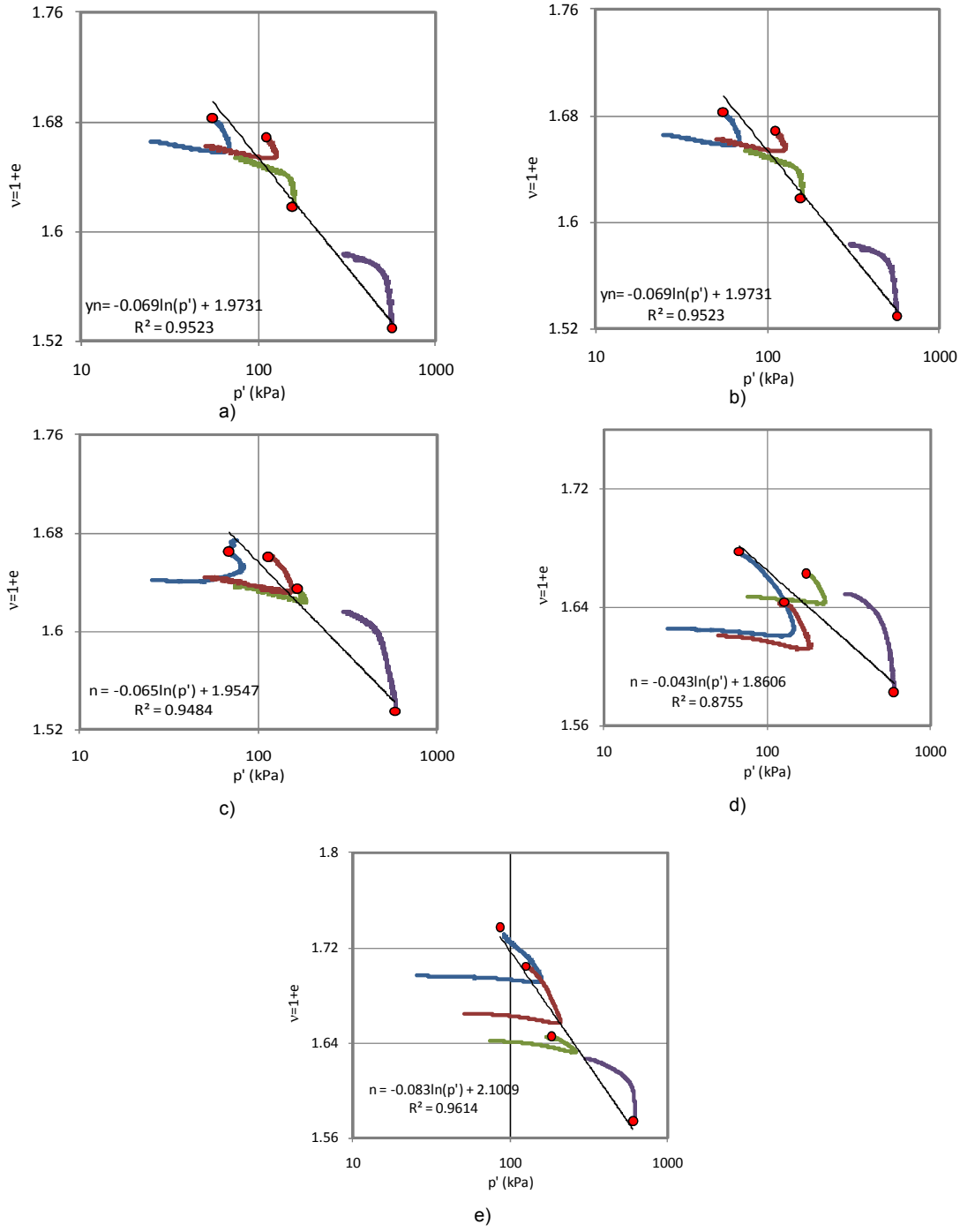


Figure 9.36 - Critical State Line (CSL) of: a) non-cemented; b) For1; c) Fra2; d) Fra3; e) For2

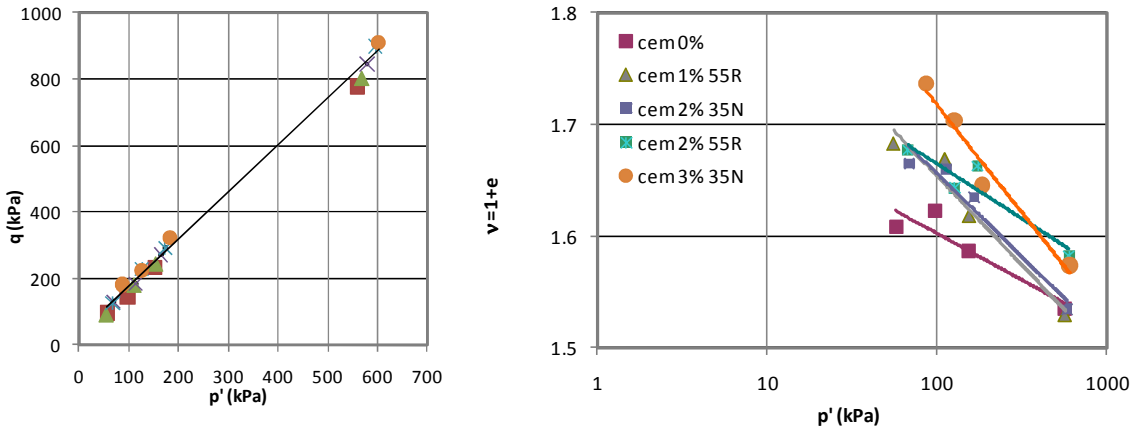


Figure 9.37 - Critical State Line (CSL) representation.

The overall results can be summarized as follows:

a) The representation of critical state points in q:p' space seems to define a unique line;
b) The representation of critical state points in ν: lnp' space shows that points related to the same cement content converge well to a narrow band;
c) Different cement contents generate different critical state lines, with increasing cementation levels giving rise to steeper slopes; this is a clear sign that in these high cemented levels in the low confining stresses there is a clear state evolution with eminent shear band, showing global convergence at high confining stresses;
d) Critical state parameters of non-cemented samples seem to constitute a lower bound of the whole situation; these observations indicate that changes in cement content might generate a different soil, both due to direct grain size variations resulting from cement addition and also to grain aggregation (as stated by Leroueil et al., 1997) that expectedly should vary with cement content, which may be assigned that in the cemented mixtures ultimate states, particles may be still aggregated, forming coarser grains.

Artificially and naturally cemented soil behaviours was also studied by comparing the results obtained in this experience with Rodrigues (2003) data. From the physical point of view, both situations are characterized by moisture content in the same range (10 to 20%), while void ratios range from 0.45 to 0.55 and 0.55 to 0.65, respectively, for natural and artificial soils.

Results obtained for non-cemented samples in the present work were primarily compared to destrucutred samples obtained by remolding natural granitic soils (Rodrigues, 2003), revealing a common trend assumed by global results (Figures 9.38 and 9.39) and thus, reinforcing the possibility of comparing both situations already assigned with compression and tensile strength tests.

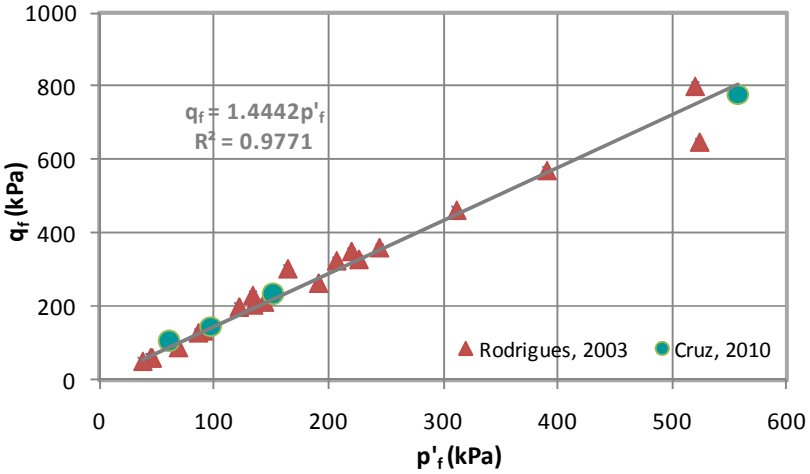


Figure 9.38 - Failure envelopes of destructured samples (present work and Rodrigues, 2003)

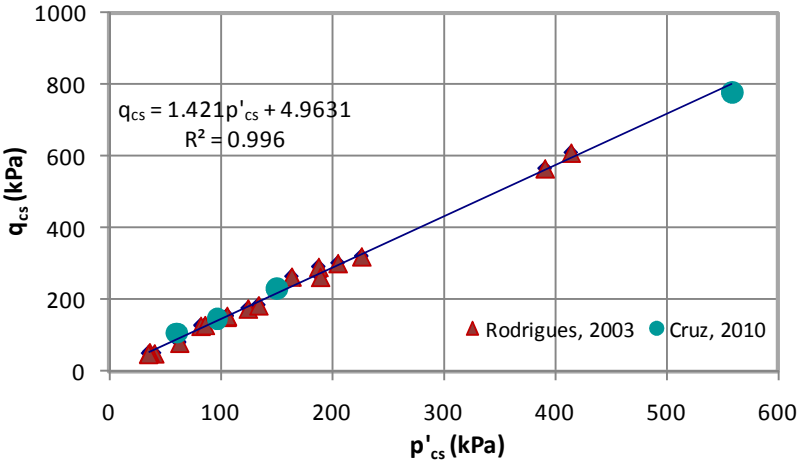


Figure 9.39 - Critical State Line of destructured samples (present work and Rodrigues, 2003).

For comparison purposes, the selection of the artificial sample equivalent to natural soil was attempted by similarity of maximum deviatoric stress, uniaxial compression and tensile strengths, pointing out to Fra2 sample. Comparing evolution of both materials in (1+e) vs lnp' space it becomes clear that there are important differences in critical state behaviour, with artificially soils presenting higher values of both critical state parameters, λ and Γ, while naturally cemented soils show a higher dispersion of critical state points (Figure 9.40).

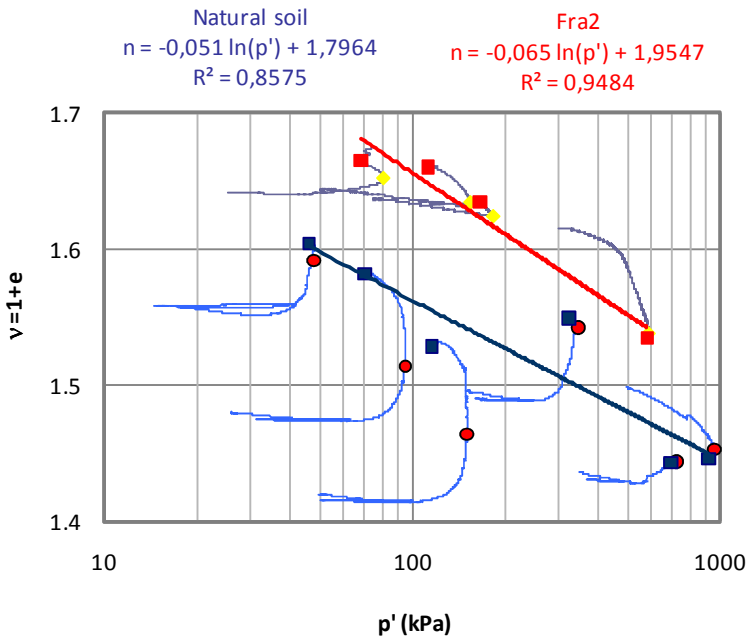


Figure 9.40 - Naturally and artificially cemented samples behaviour as approaching Critical State

The Figure 9.43 suggests that in natural soils, critical state approaching is preceded by shear banding responsible for the definition of more than one critical state line, while artificially cemented samples converge to a unique state line. The final look of tested (triaxial) samples, are presented in Figure 9.41, where the lower row represents the artificial samples, while the upper rows stand for the natural ones. In Figure 9.42 peak stress ratio (q/p') against maximum dilatancy is presented, as suggested by Cuccovillo & Coop (1999).

Figure 9.42 reveals the higher maximum dilatancy of naturally and artificially cemented soils when compared with destrucutred soils. Furthermore, in artificially cemented soils maximum dilatancy and peak stress ratio (q/p') increase with cement content and, for similar levels of cementation, dilatancy is higher in naturally cemented soils, suggesting the determinant influence of micro-fabric in these soils behaviour.



Figure 9.41 - Final look of naturally and artificially cemented samples after failure

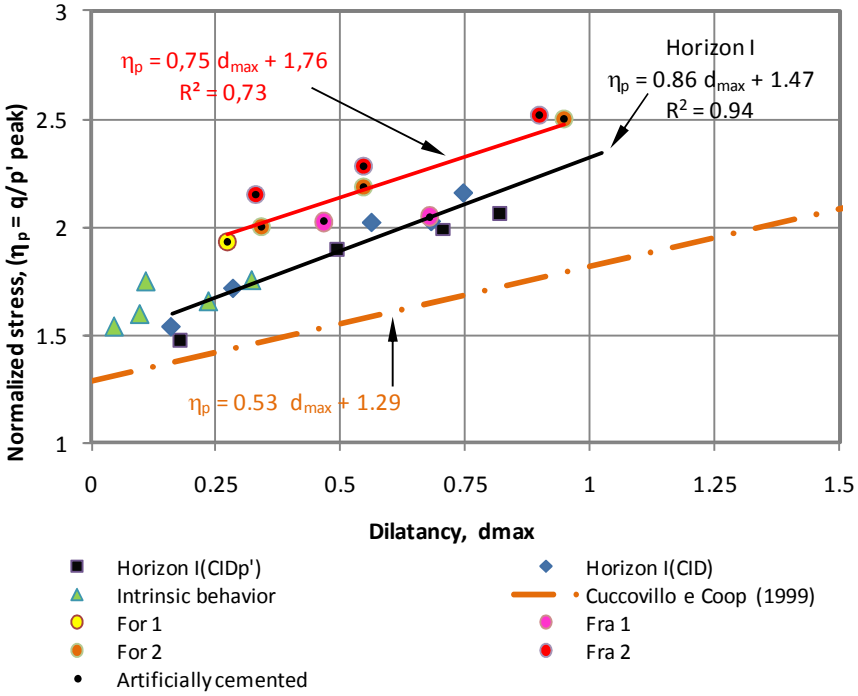


Figure 9.42 - Normalized deviatoric stress against maximum dilatancy of naturally and artificially cemented samples.

9.2.3. Presentation and discussion of stiffness results

The monitoring of displacements during triaxial testing was made by recouring to internal LVDT transducers and at very small acquisition intervals, which allowed to define very precise stiffness degradation curves, as it can be inferred from Figure 9.43 to Figure 9.46, where Young moduli are plotted against axial strains using bi-logarithmic scales and grouped by the same initial mean effective stresses. In order to follow Toll and Malandraki (2000) proposed analysis, discussed in Chapter 3, yield points defined by these authors are represented by red dots in the respective figure. In Table 9.18, derived results of tangent and secant moduli are also presented. Stiffness curves confirm the strength results, as they show different behaviours of high and low cemented mixtures. In fact, the high cemented mixtures clearly reveal the control of cementation at 25 kPa confining stresses. The increase of confining stresses shows mixed control of isotropic and deviatoric stresses (50 and 75 kPa), attaining a condition of complete loss cementation for 300 kPa.

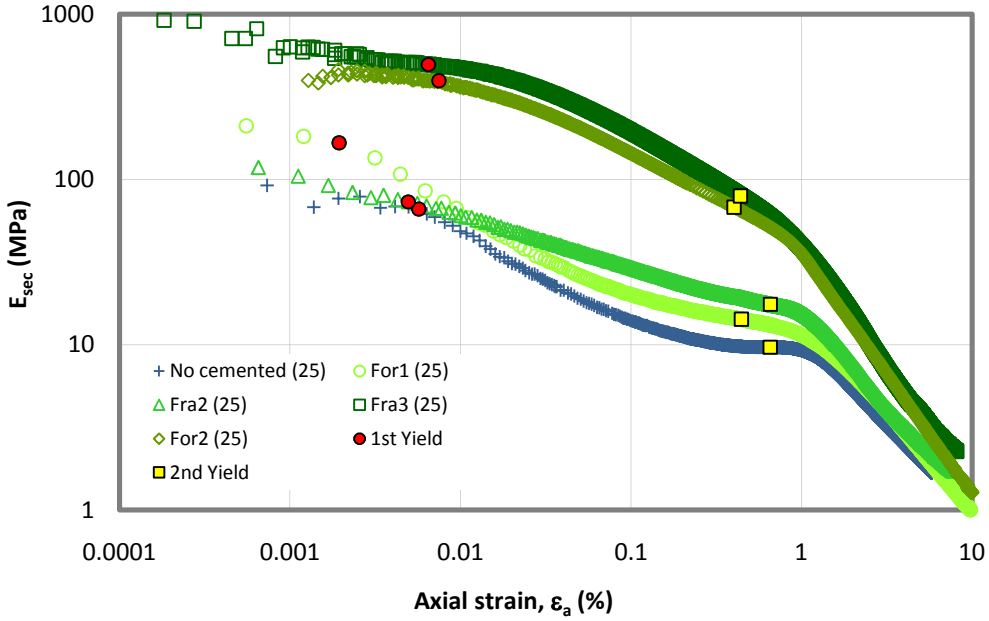


Figure 9.43 - Secant modulus obtained for confining stresses of 25 kPa.

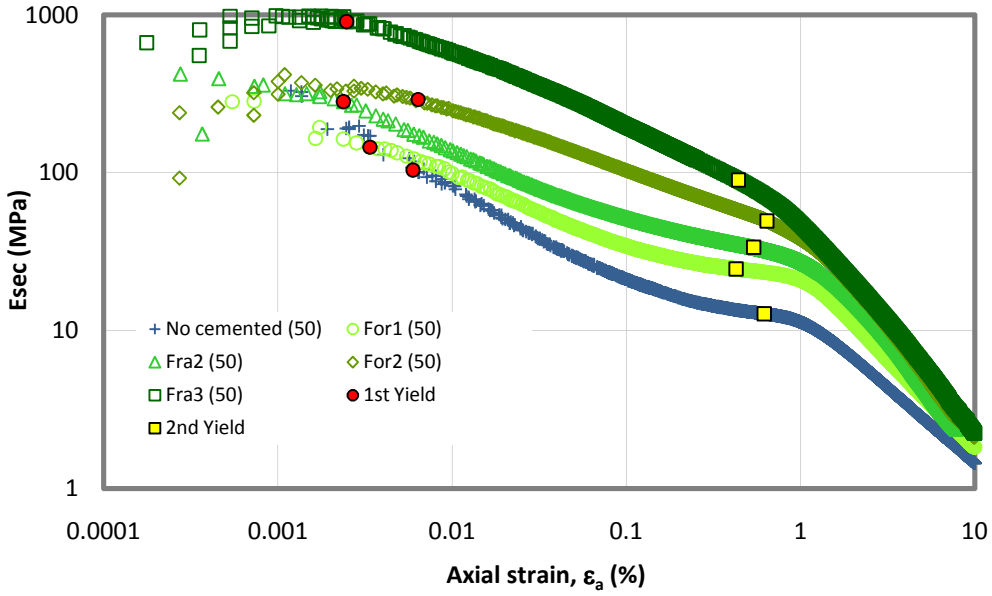


Figure 9.44 - Secant modulus obtained for confining stresses of 50 kPa

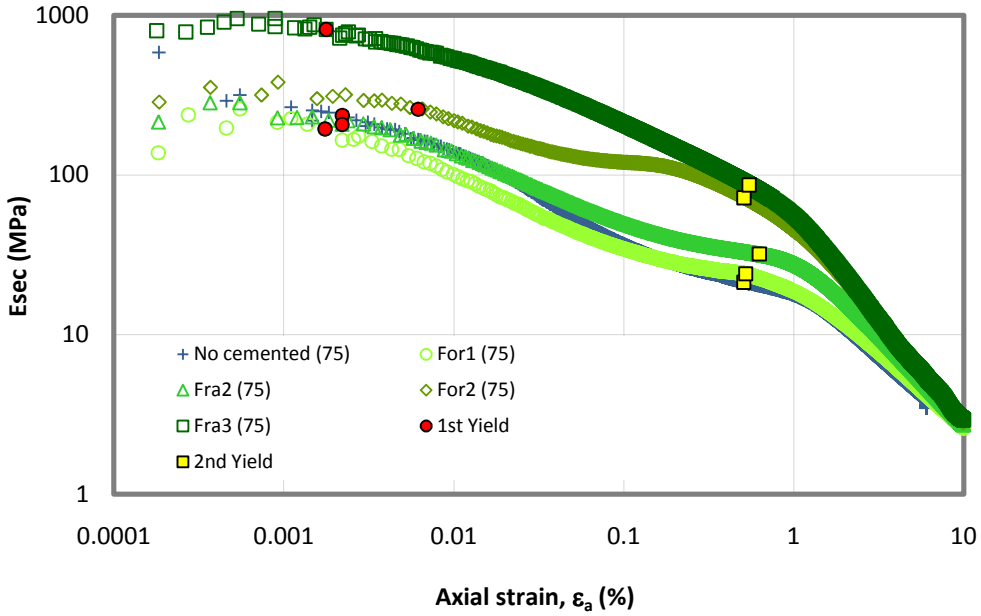


Figure 9.45 - Secant modulus obtained for confining stresses of 75 kPa.

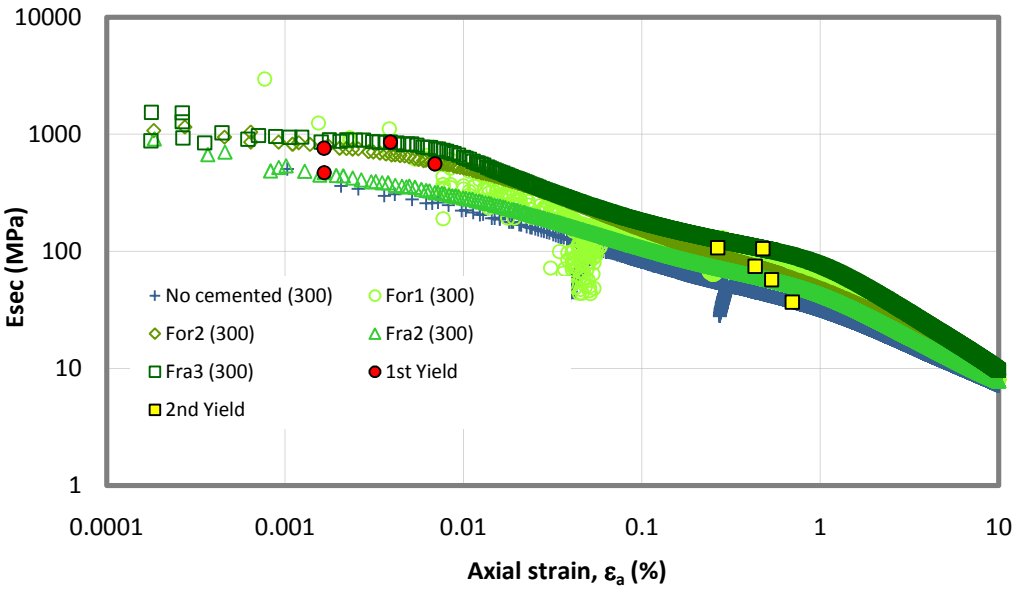


Figure 9.46 - Secant modulus obtained for confining stresses of 300 kPa.

Table 9.18 - Reference Moduli and Janbu parameters

Sample	q_t	p'_i	E_0	$E_{0,1\%}$	E_{50}	Modulus parameter	
	kPa	kPa	MPa	MPa	MPa	K	n
No cement.	1.5	25	91.8	13.9	9.7	2518.04	0.15
		50	294.9	21.1	13.0		
		75	291.0	36.8	20.7		
		300	361.0	80.7	23.4		
For1	7.2	25	210.7	19.9	14.1	3760.8	0.48
		50	283.0	34.2	24.2		
		75	260	34.4	23.5		
		300	873	129.1	98.8		
Fra2	15.3	25	118	29.2	19.5	3360.6	0.34
		50	360	52.2	35.2		
		75	284	49.7	33.3		
		300	667	107.5	42.6		
For2	33.2	25	462	143.4	109.6	4975.9	0.17
		50	419	103.4	67.3		
		75	381	120.2	107.8		
		300	1148.8	151.5	54.07		
Fra3	39.2	25	905	194.8	194.0	9751.7	0.016
		50	1026	197.6	161.6		
		75	955	209	156.9		
		300	1029	178.5	107.2		
Guarda residual (1.5-4.5m)	9.25 to 16.55	15	135	9.8	5.1	1742	0.817
		25	209	10.9	10.3		
		50	244	17.0	14.4		
		150	178	33	19.1		
		350	470	42	38.5		
		500	230	46	32.6		

In Figure 9.47 and Figure 9.48 the representation of first and second yield surface in deviatoric versus mean effective stress plot is presented, clearly revealing the influence of both cementation level and confining effective stresses in the position of second yield, while first yield does seem to be less sensitive to both. As for second yield, the increase in cement content enlarges the respective surfaces, while the confining stress increase tends to make this yield to fall within limit state surfaces.

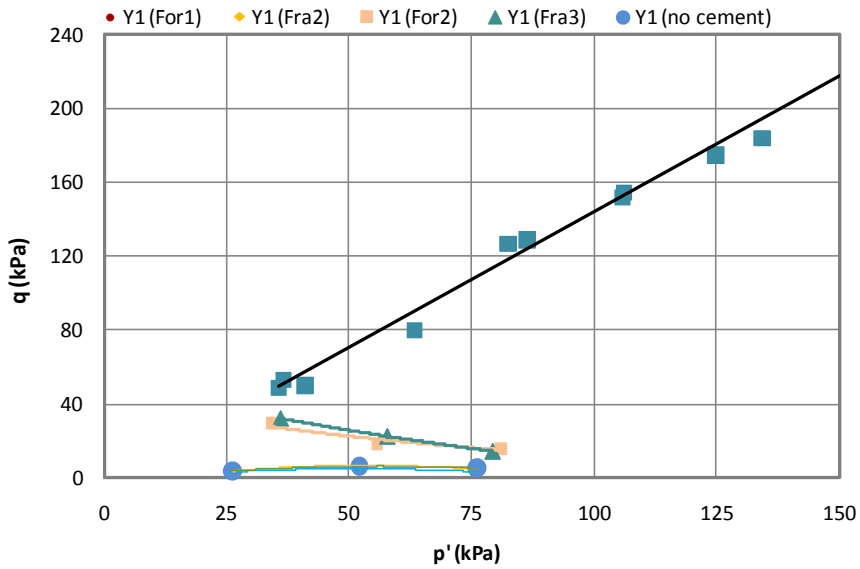


Figure 9.47 - Representation of first yield in q-p' space.

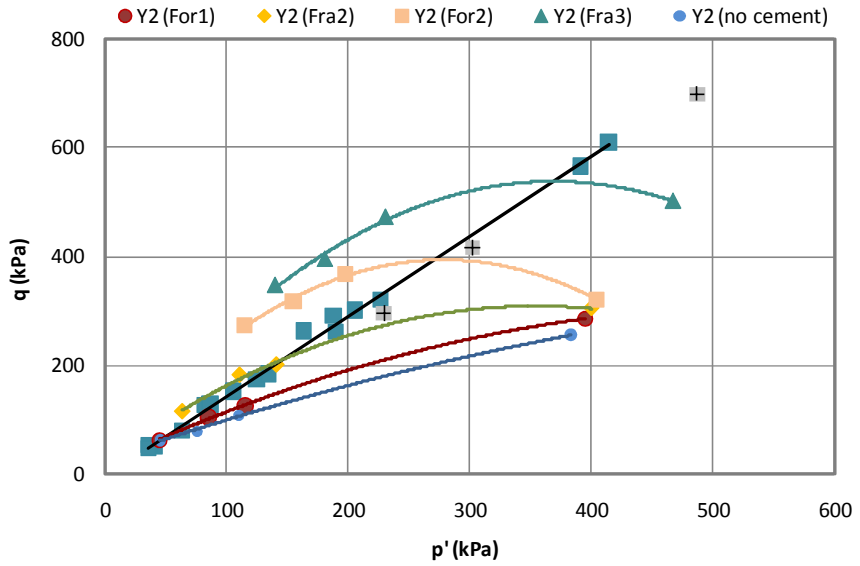


Figure 9.48 - Representation of second yield partial surface in q-p' space

Global results confirm the adequacy of this methodology to data analysis in the present situation, revealing the following trends:

a) Globally, it is clear the presence of distinctive slope changes in the curves allowing the determination of both first and second yield, as proposed by Malandraki and Toll (2000);
b) First yield is usually reached between 0.001 and 0.01% (10^{-5} to 10^{-4}) of strain level for all samples; second yield is globally placed within 0.1 to 1% (10^{-3} to 10^{-2});

c) The highly cemented sample (Fra3) maintains the magnitude (1000 MPa) of the first yield for all range of mean effective stress; the most similar mixture corresponding to For2, presents low values at low confining stresses, reaching the same order of magnitude at high mean effective stress; for weaker cementation or non cemented samples, the magnitudes are much smaller increasing both with cementation and mean initial effective stress;
d) The increase of mean effective stress generates increase of stiffness for lowest cemented samples, converging to the strongest cemented mixture, following an increasing order of magnitude with cementation level;
e) The global moduli at second yield is one order of magnitude lower than the first yield, and in general the correspondent axial strains tend to increase with cementation level reduction;
f) After second yield, there is a trend of different mixtures to converge, independently of its respective mean effective initial stress, for axial strains equal to 10% (high confinement) or even higher (low confinement).

A coherent pattern of an increasing tangent modulus with both mean effective initial stress and cementation level was observed, converging to the global understanding expressed by many other researchers (Clough et al, 1981; Ladd et al., 1987; Leroueil & Vaughan, 1990; Viana da Fonseca, 1996, Cuccovillo & Coop, 1997; Rodrigues, 2003, Consoli et al., 2007 among others). Moreover, cemented samples always show higher stiffness than equivalent non-cemented ones, both for tangent and secant moduli. The latter ($E_{0,1\%}$ and E_{50}) are significantly lower than tangent modulus, respectively 10 to 30% and 5 to 20% of the former. Finally, highly cemented samples display degradation patterns with different shape from those of low to moderate level of cementation, which become identical at high confining stresses, due to the progressive evolution to granular condition.

The interpretation of data in terms of Janbu's parameters (1963), K and n, revealed an increase of the former and decrease of the latter with cementation level, which is supported by Clough et al (1981), Viana da Fonseca (1996, 1998, 2001, 2002, 2003), Rodrigues (2003) and Schnaid et al (2005) experiments. A more detailed analysis reveals that reference moduli normalized by effective initial mean stress show a global decrease with the increase of mean effective initial stress. When represented in semi-logarithmic scale, the evolution of normalized modulus follows a straight line with increasing slope with cementation level but converging to the same interception point (Figure 9.49 to Figure 9.51), and representing granular condition after complete

destructuration of cementation arrangement. For increasing values of confining stresses, the behavior is controlled progressively by friction. The same figures also reveal a significative gap between For2 and Fra3 and the other weaker cemented and non cemented samples. In the figures, E_i represents the initial tangent modulus, $E_{s0.1\%}$, the modulus at a strain level of 0.1%, and E_{s50} the secant modulus at 50% of maximum deviatoric stress. In Table 9.19 the global found correlations are presented.

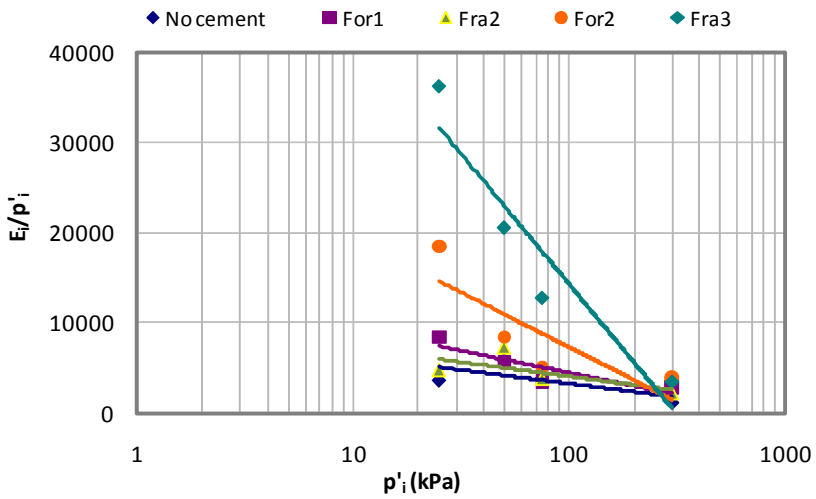


Figure 9.49 - Normalized E_i moduli plotted against initial mean effective stress.

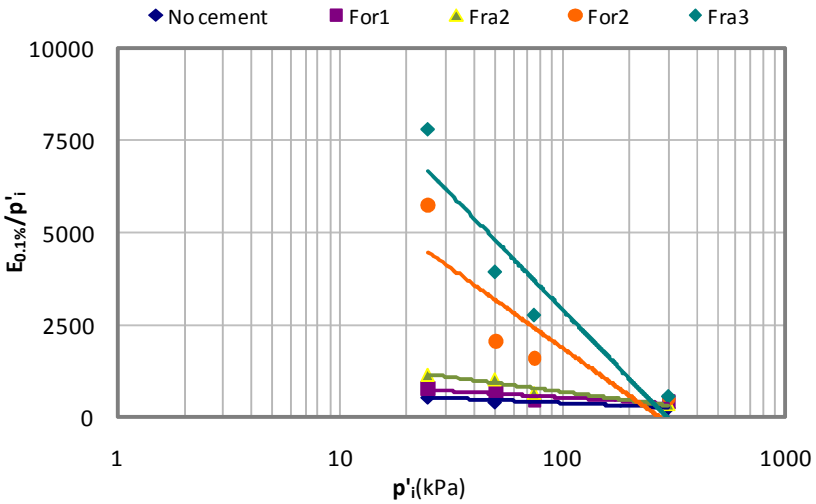


Figure 9.50 - Normalized $E_{s0.1\%}$ moduli plotted against initial mean effective stress.

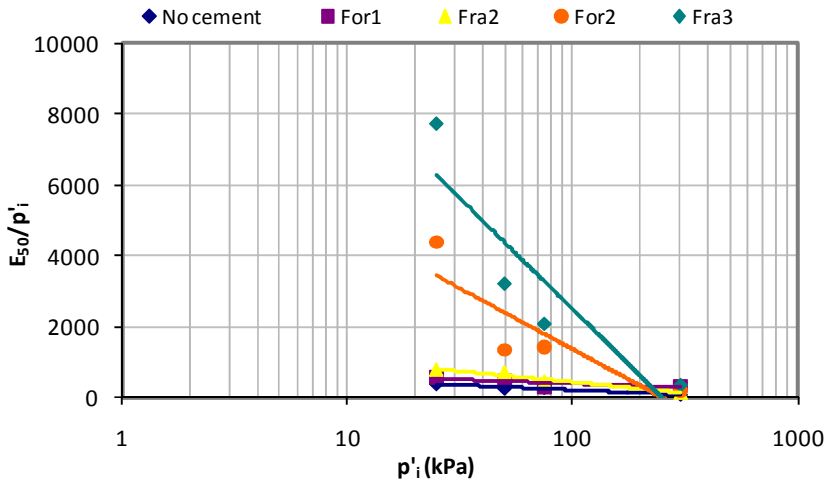


Figure 9.51 - Normalized E_{s50} moduli plotted against initial mean effective stress.

Table 9.19 - Moduli correlation parameters and factors

$E_x/p'_i=a*\log(p'_i)+b$		No Cement	For1	Fra2	For2	Fra3
E_i	a	-1315.0	-2102.7	-1336.3	-5270.0	-12521.0
	b	9302.0	14133.0	10341.0	31543	71910.0
	R^2	0.5128	0.7715	0.4713	0.6905	0.8931
$E_{s0,1\%}$	a	-108.8	-147.6	-338.8	-1868.0	-2703.2
	b	900.8	1225.1	2261.0	10402.0	15373.0
	R^2	0.8562	0.7623	0.9241	0.7441	0.8819
E_{s50}	a	-119.8	-94.1	-268.9	-1488.2	-2719.0
	b	764.1	826.1	1670.5	8218.4	15019.0
	R^2	0.9554	0.6559	0.9510	0.7564	0.8107

Another interesting pattern is observed when reference moduli is plotted against deviatoric stress normalized by initial mean effective stress, q/p'_i. There is a general decrease of moduli with q/p'_i, more accentuated in low degrees of cementation. Again, when plotted in a bi-logarithmic scale, despite some recognizable scattering for E_{50}, correlations tend to increase radially until a constant level is reached, at a certain cementation level (Figure 9.52 to Figure 9.54). Obtained equations and the respective correlation factors are presented in Table 9.20.

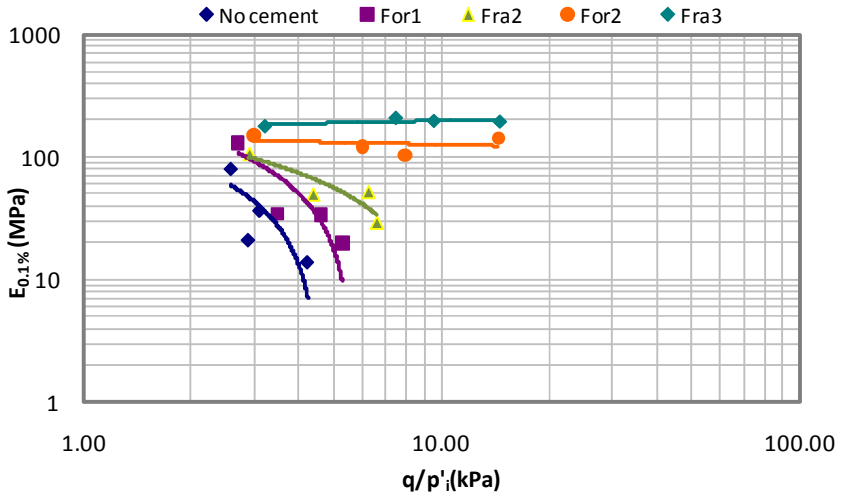


Figure 9.52 - Reference Ei moduli plotted against normalized deviatoric stresses.

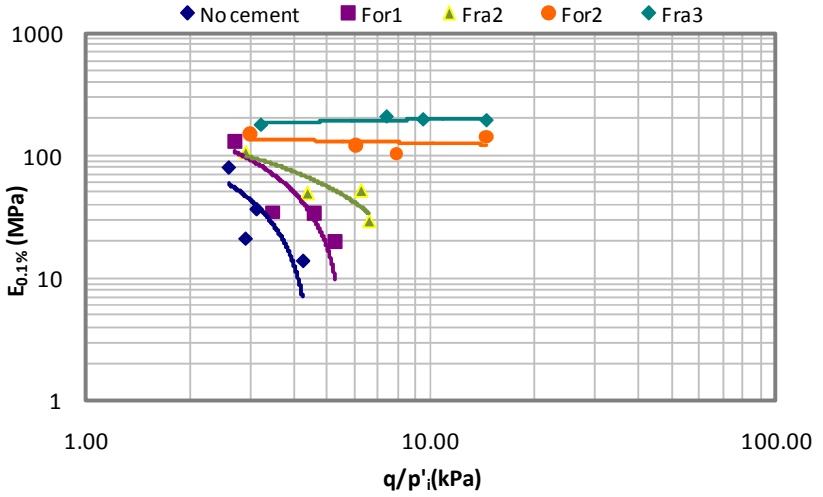


Figure 9.53 - Reference $Es_{0.1\%}$ moduli plotted against normalized deviatoric stresses.

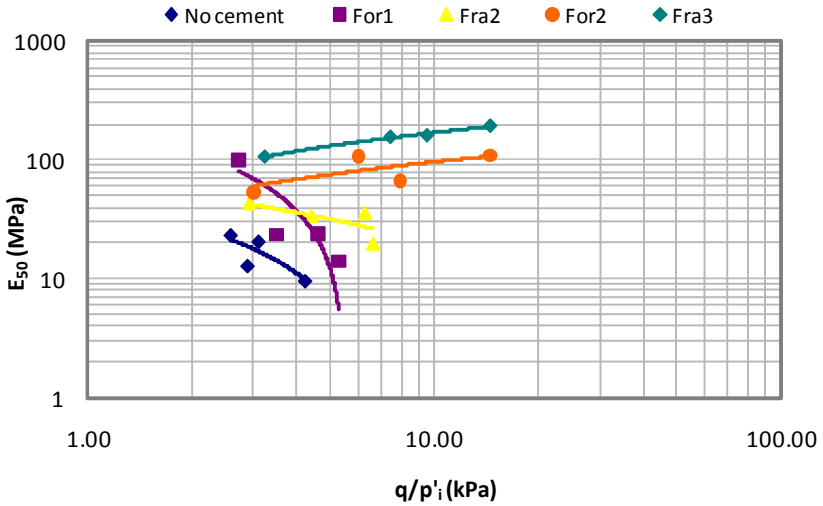


Figure 9.54 - Reference Es_{50} moduli plotted against normalized deviatoric stresses

Table 9.20 - Moduli correlation parameters and factors

$E_x=c*\log(q/p'_i)+d$		No Cement	For1	Fra2	For2	Fra3
E_i	c	-1171	-2066	-1337	-1474	-182.1
	d	763.7	1487.1	1158.9	1636.1	1109.8
	R^2	0.9627	0.7718	0.7608	0.7427	0.3244
$E_{s0,1\%}$	c	-238.5	-341.5	-338.8	-39.8	51.8
	d	140.8	233.0	184.3	157.5	157.7
	R^2	0.6034	0.8146	0.8651	0.7441	0.5942
E_{s50}	c	-50.8	-265.0	-49.3	92.4	179.2
	d	38.6	178.8	62.2	20.0	26.0
	R^2	0.5961	0.7996	0.5893	0.4883	0.8772

Taking into account that both q/p'_i and E/p'_i ratios decrease with confining stresses, these representations interpreted together reveal that cementation level increases q/p'_i. This produces higher stiffness at low confining stresses that generates a higher ratio of modulus reduction with the increase of mean effective initial stress. No matter the cementation level, all the curves tend to a convergent point marked by initial mean effective stress, seeming to represent the point from where fabric takes control of mechanical behaviour, as concluded by Cuccovillo & Coop (1997).

Finally, the evolution of tangent modulus with mean effective stress, p'_i, both normalized to atmospheric pressure (Figure 9.55), show a lower bound represented by non-cemented samples and upper bound by the stronger cemented sample (Fra3). For the upper bound, tangent modulus seems to be independent from p'_i, while the remaining cemented samples start from a lower value that globally increase with cementation level, and converge to the upper bound, following an evolution trend similar to the one exhibited by non-cemented samples. Apparently, in the upper bound (Fra3), cementation level controls the maximum magnitude of moduli, being expectable that it will show evolution for higher p'_i.

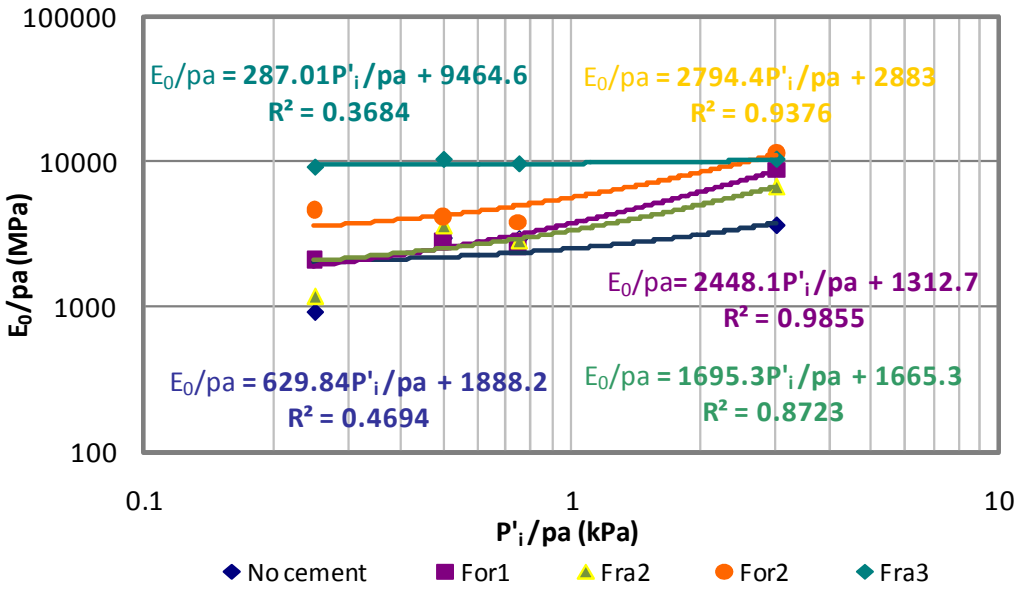


Figure 9.55 - Reference moduli plotted against normalized deviatoric stresses.

Another interesting detail can be observed in Figure 9.56, where although some scattering, data suggests that moduli evolution is directly related to tensile strength, confirming its adequacy as index parameter of cementation effects also in the case of stiffness. In fact, data reveals that there is an evolution with cementation, suggesting that moduli at small strains is marked by a clear distinct influence at low and high consolidation stresses, with decreasing differences as the strain level for moduli determination increases. The differences become smoother (blue line), maintaining parallel trends related to high or low confinement stresses.

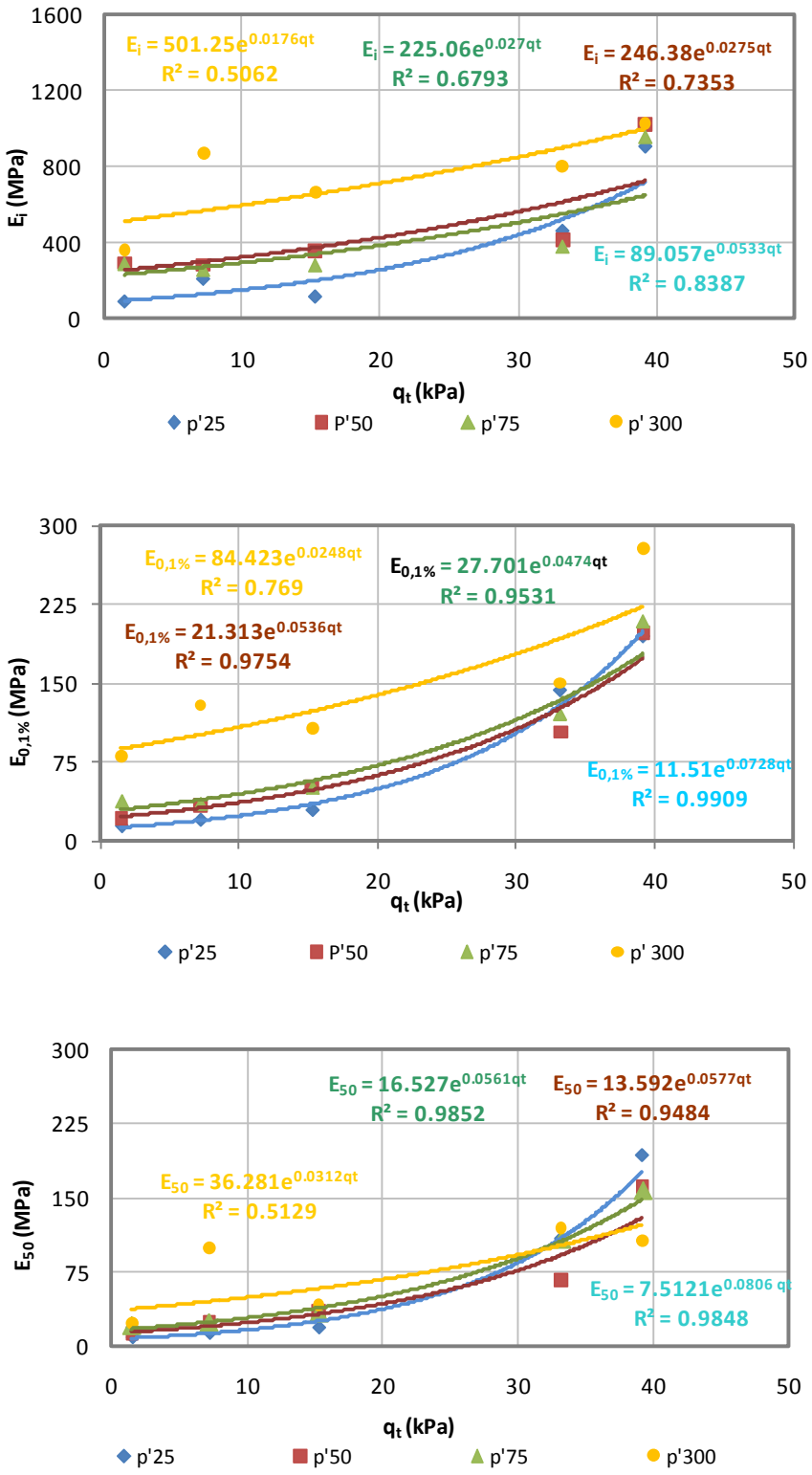


Figure 9.56 - Reference moduli plotted as function of tensile strength: a) E_i; b) $E_{s0,1\%}$; c) E_{s50}.

As discussed in Chapter 3, moduli evolution is non-linear, since stiffness varies with strains and thus, the definition of a modulus reduction is much more suitable for design purposes than any other multi yield model, too much complicated to be implemented. For this purpose, triaxial data was analyzed, using Fahey & Carter (1993) proposed approach:

$$E/E_0 = 1 - f\,(q/q_{max})^g \qquad (9.4)$$

where E / E_0 represent the normalized modulus, q/q_{max} is the normalized deviatoric stress, while f and g are the hyperbolic distortion parameters (Fahey & Carter, 1993).

In Table 9.21 and Figures 9.57 and 9.58 results of data analysis are presented.

Table 9.21 - *f* and *g* hyperbolic distortion parameters

Sample	Confining stress (kPa)	f	g
No cemented	25	0.90	0.050
	50	1.00	0.050
	75	1.00	0.025
	300	1.00	0.050
For1	25	0.95	0.025
	50	0.95	0.050
	75	0.95	0.050
	300	1.00	0.050
Fra2	25	0.90	0.100
	50	0.95	0.050
	75	0.90	0.050
	300	1.00	0.050
For2	25	0.90	0.200
	50	0.90	0.150
	75	0.85	0.150
	300	1.00	0.100
Fra3	25	0.95	0.300
	50	0.90	0.300
	75	0.85	0.250
	300	1.00	0.100

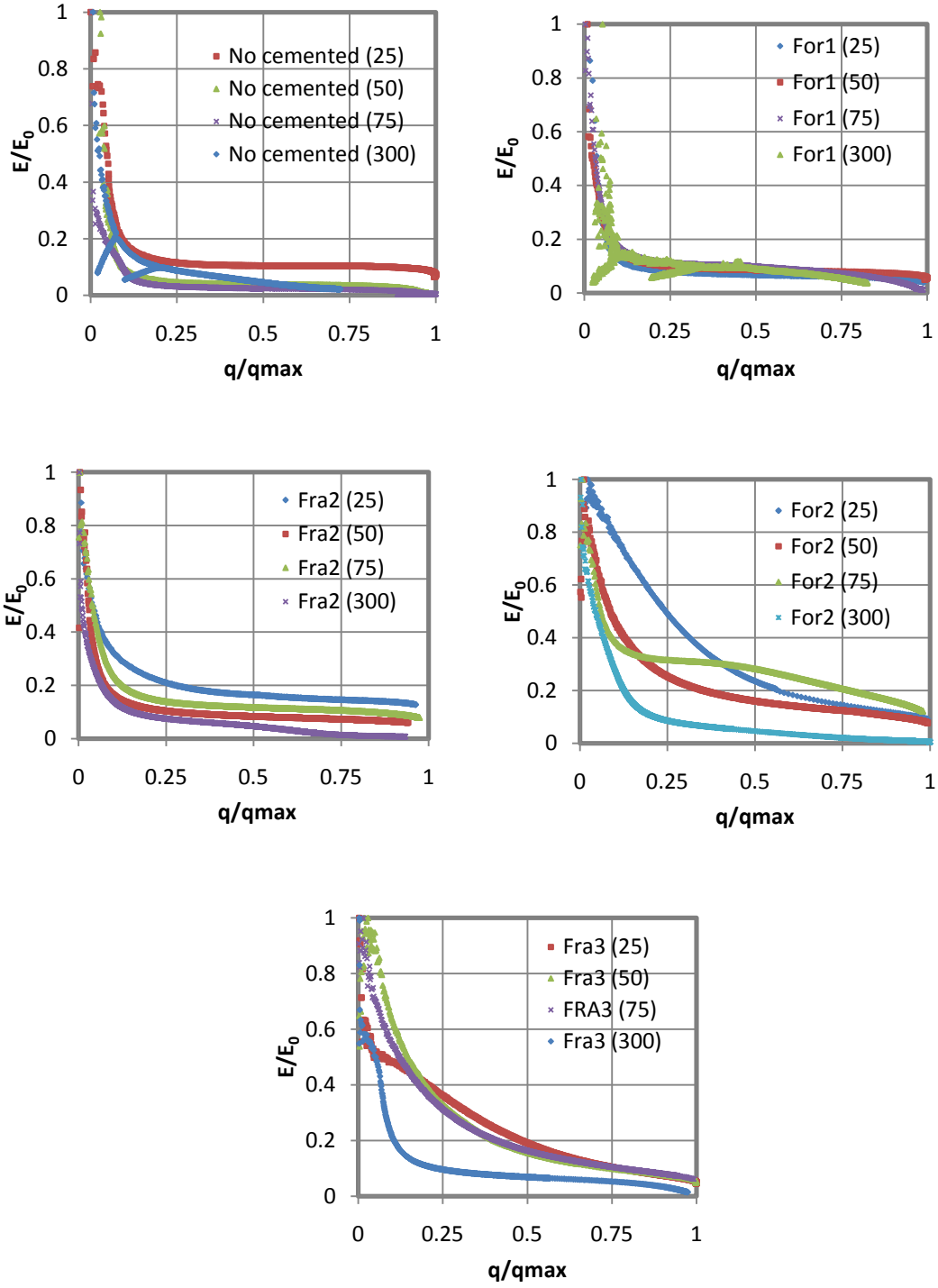


Figure 9.57 - Modulus reduction as function of normalized deviatoric stress, ordered by cementation level.

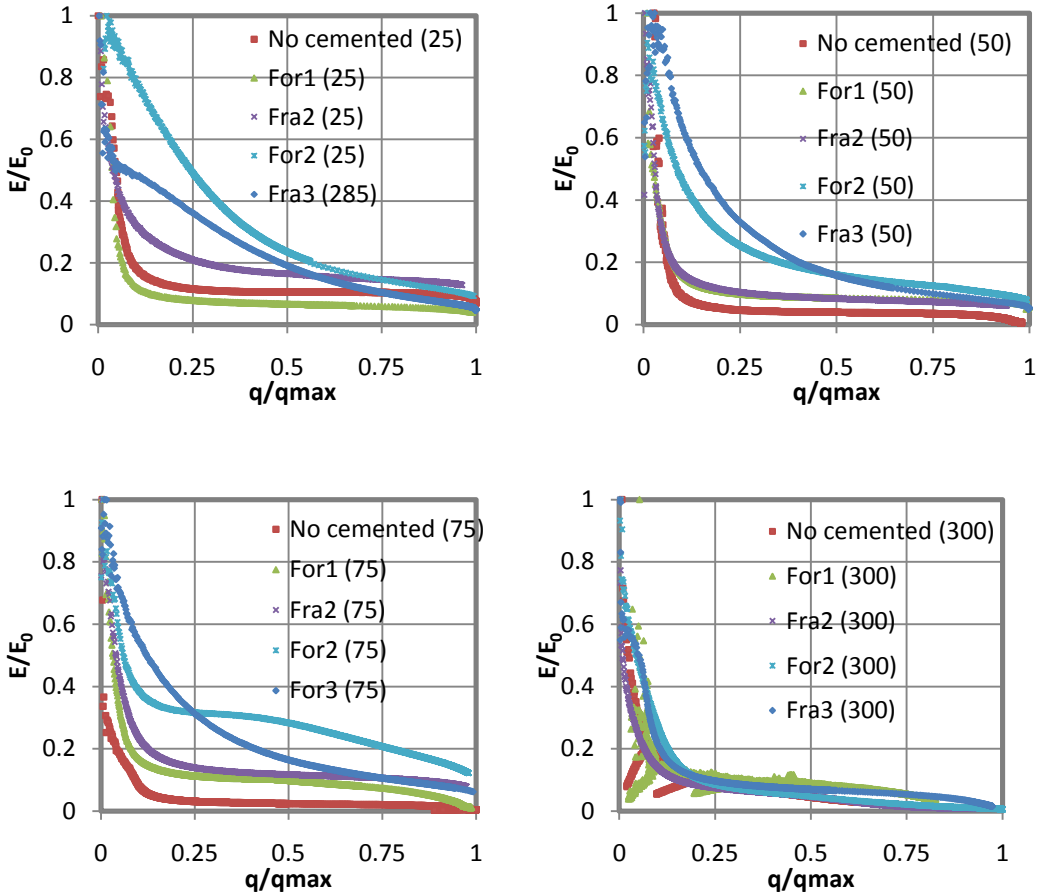


Figure 9.58 - Modulus reduction as function of normalized deviatoric stress, ordered by confining stress

Data analysis indicates some interesting observations and conclusions, as described below:

a) Non-cemented samples reveal very similar decay rates, no matter the confining stress, generally showing consistent *f* (1.0) and *g* values (0.05);
b) There is a clear distinction between modulus decay at low or high confining levels in cemented mixtures;
c) At high confining stresses, modulus reduction seem to follow the same hyperbolic curve, no matter the cement content; *f* parameter remains constant and equal to 1.0, while *g* parameter shows a small variation between 0.05 and 0.1;
d) At low confining stresses, cementation level influences modulus reduction; the higher the cement content, the higher will be the minimum normalized modulus that will be attained at higher normalized deviatoric stress;

e) The increase in cement content also generates higher differences in curves with different confining stresses; in general, for each cementation level, the confining stress increase leads to higher decays;
f) At low confining stresses, the increase in cementation level seems to generate a decrease in *f* parameter (from 1.0 to 0.85, in the present case) and an increase in *g* parameter (0.050 to 0.300), while confining stress increase leads to a decrease of both parameters

In conclusion, cementation induces variations in magnitude decay and in the level of deviatoric stress at which the minimum is attained, up to a certain limit of confining stress, to where distorted hyperbolic curves seem to converge. Data also suggests that this limit might change with cementation level. Globally, in the present experience, *f* parameter is within 0.85 and 1.00 while *g* varies between 0.025 and 0.300.

9.2.4. Naturally and artificially cemented soil behaviours

Using the same approach followed for critical state, results obtained in this experience were directly compared to Rodrigues (2003) data. In this context, the selection of the artificial sample equivalent to the natural soil was attempted by similarity of maximum deviatoric stress, uniaxial compression and tensile strengths, pointing out to Fra2 sample. Strength and dilatancy comparisons are presented in Figure 9.59.

Data analysis suggests that failure envelope follow the same trend, showing no special deviations from naturally to artificially cemented samples. As a consequence, strength geotechnical parameters, c' and ϕ', reveal a 20% decrease on cohesion magnitude from artificial to natural samples (38.4 to 30.4), while angles of shearing resistance are higher (34º to 36º) in naturally cemented samples, probably as a result of the different interparticle cementation that may generate larger particle diameters, and displaying a higher interlocking in natural samples.

At low confining stresses axial strains for peak deviatoric stresses show some variation that globally increase with mean effective stress at failure and decrease with the ratio q/p'. As for dilatancy, in the present work, dilatant behaviour was only observed at low confining stresses, in contrast to natural samples, developping this kind of behaviour in all range of confining stresses. Data seem to follow the same trend line, no matter the

type of cemented samples (naturally or artificially) revealing an expected general decrease in maximum dilatancy with increasing q/p'.

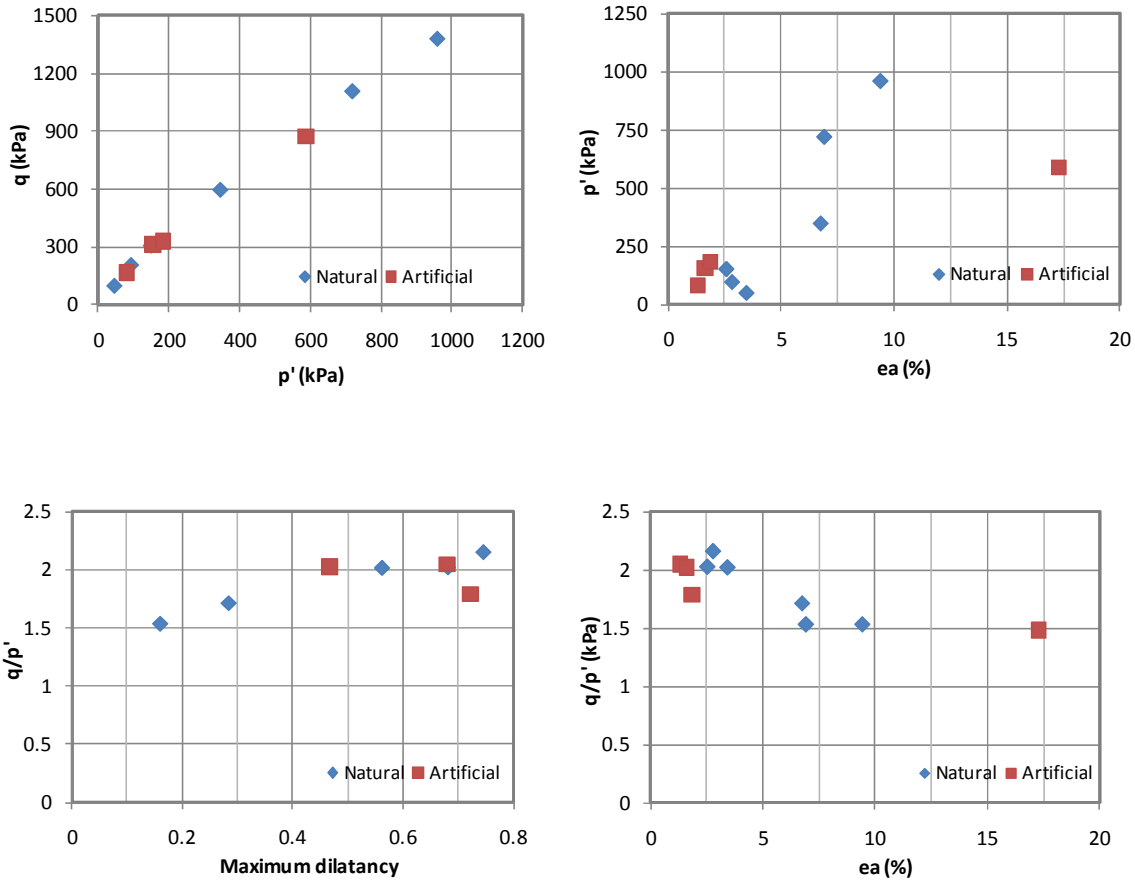


Figure 9.59 - Naturally and artificially cemented soil strength behaviours.

Stiffness comparative analysis was based in two different representations, namely normalized reference moduli as function of logarithmic initial mean effective stress and moduli against logarithmic normalized deviatoric stress as presented in Figure 9.60.

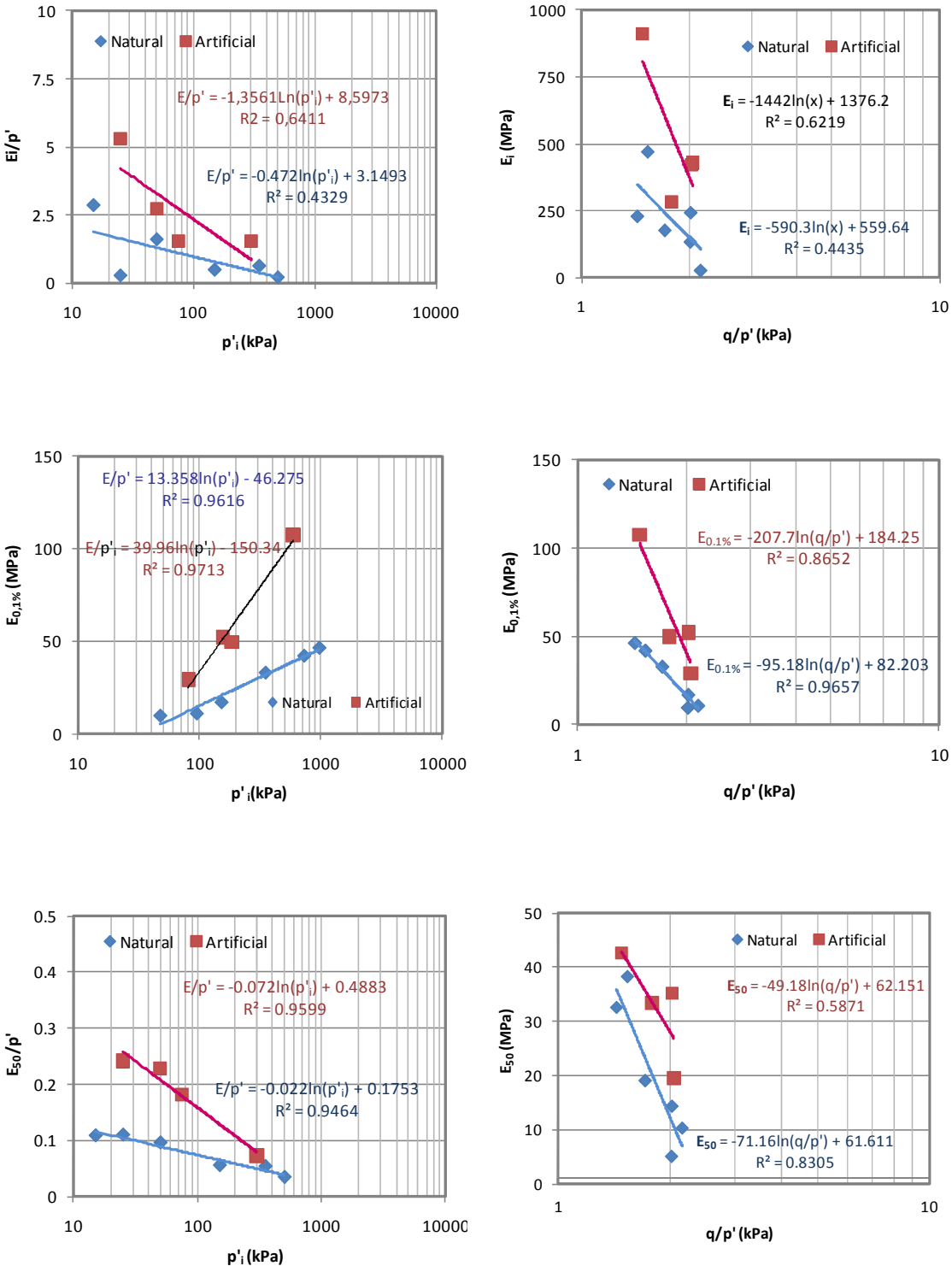


Figure 9.60 - Naturally and artificially cemented soils stiffness behaviours.

Obtained data reveals the following trends:

a) Both representations show higher magnitudes and rates of variation in the case of artificially cemented soils, with natural soils revealing orders of magnitude ranging from 30 to 60% of former;
b) Artificial and natural soil observed trends seem to converge at high confining stresses;
c) Artificial and natural soil evolution rates increase with decreasing strain level;
d) Initial tangent moduli related rates show magnitudes ten to twenty times higher than secant moduli;
e) The modulus degradation with strain level seem to follow the same order of magnitude for naturally or artificially cemented samples, as reflected by the ratios of $Es_{0,1\%}/E_i$ and Es_{50}/E_i , respectively 10 to 20% and 4 to 12%;
f) Stiffness always increases with cementation level at similar rates for low and high confining stresses, but with magnitude of initial tangent modulus clearly higher for the latter.

Chapter 10
Cemsoil Box Experimental Program

10. CEMSOIL BOX EXPERIMENTAL PROGRAM

10.1. Introduction

One of the most challenging steps to accomplish in this experience was to reproduce in-situ conditions of cemented materials in such a way that turn possible comparisons with triaxial reference tests on artificially reconstituted samples. In fact, for this calibration purpose, it is important to avoid the usual problems responsible for important scattering when in-situ and laboratorial testing are compared, related to sampling disturbance, soil heterogeneity and microfabric differences. From this point of view, calibration chambers described in literature were obviously a reference to follow, especially those related to CPT and (more rarely) DMT on sands. Summarizing reference literature related with calibration chambers for CPTu tests, it is possible to divide them into rigid wall, flexible wall and scale model categories, with the flexible wall chambers largely dominating (Holden, 1992; Puppala et al., 1992; Lunne et al., 1996; Balachowski, 2006).

Scale models are very confortable to work with but introduce undesirable scale effects, generating an extra variable difficult to control, especially in the present case where data of different origins should be considered in the main analysis. On its turn, proper calibration chambers are complex devices that should include at least load frames for applying horizontal and vertical stresses and strain measurement systems. However, the development of a calibration chamber is quite expensive and out of the budget available for this research program. Therefore, two possibilities for establishing adequate calibration conditions were considered:

a) To open a trench in-situ, and place remoulded cemented soil controlled samples by compacting to similar in-situ void ratios; this would have the great advantage of working in a controlled sample integrated within the in-situ massif, and thus reducing the uncertainties related to boundary conditions and size effects;
b) To create a high dimension block sample to fit within laboratorial controlled conditions, with a confining system conceived to be adaptable to local facilities and to respect, as much as possible, the international recommendations for calibration chambers.

The first approach is very interesting, especially in terms of size and boundary conditions control, which in the present case would be represented by the real “in-situ” massif with infinite dimension. However, the development of this approach had to overcome other important problems, such as control of remolding, compaction and especially curing conditions. Since these problems could not be solved satisfactory, important uncertainties would arise in data analysis and calibrations. Furthermore, IPG facilities allowed preparing a sample and a penetrometer rig in different connected stages, and thus the second choice was selected. The experience was idealized considering that thrust capacity would be obtained by means of a penetrometer rig placed in an upper floor from where the blade would be pushed into a Big Block (BB) sample prepared in the lower one. The obvious required confinement of this block sample was achieved throughout a box (CemSoil box), conceived to ensure adequate conditions for remolding, compacting and curing cemented samples, as well as for testing it by DMT, tensiometers and geophysical devices. As referred, the available budget was not enough to build a calibration chamber, but solely a confinement border to hold the block tight. Even tough, international calibration chamber experience was taken into account whenever it was adequate, especially in size options. Some references on large scale chambers were published after the first “truly” advanced calibration chamber built up at Country Road Board (CRB) with 76cm diameter and 91cm height (Holden, 1971), revealing that chambers developed ever since are typically round shaped and follow the same general principles of CRB’s with diameters and heights ranging respectively between 76 to 150cm and 80 to 150cm (Holden, 1992; Lunne et al., 1996).

Due to mounting and after-test dismantling operations, a square cross section was believed to be the one that would offer better working conditions. Thus, CemSoil box was constructed taking into account that weight and size should be adequate to its placement by available mechanical means. CemSoil box can be described as a 1.5m height steel box with a square cross section of 1.0m, with 3 mm thick steel walls, reinforced by metal bars placed at 1/3 and 2/3 of its height. Each panel was fixed to the adjacent with a profile of 5 screws (10mm) with 150mm of influence radius. Due to the wall-wall fixation system, in two of the faces this reinforcement system was in contact with the wall by a central 7mm thick H beam (100X50mm) placed vertically. This system aimed to reduce horizontal displacements during compaction processes. In Figure 10.1 and Figure 10.2, geometric details of the cell are illustrated.



Figure 10.1 - CemSoil box: General view of CemSoil box (upper row); location of central beam (mid row); placing the central beam (lower row)



Figure 10.2 - Fixation details of the interior of CemSoil box

The inner surfaces (vertical walls and bottom surface) of the cell were covered with a plastic film, in contact with the steel wall, followed by 15mm Styrofoam plates in order to create a gradual transition from the soil to the external frontier (Figure 10.3).



Figure 10.3 - Details of the interior of CemSoil box

Considering the main goals of the experiment, two DMT blades, two open tube piezometers, one profile of six tensiometers (or two profiles of three) and three pairs of accelerometers for compression/shear wave velocities measurements (during the whole process and when considered necessary) were ought to be installed. A discussion on the criteria for location and distribution of all these measuring devices within CemSoil box is presented in the following paragraphs.

Marchetti (1997) stated that DMT could be considered a two-stage (independent) test, being the first related to insertion and the second to membrane expansion, which is not a continuation of the former. The main references on DMT penetration (1st stage) modeling are scarce and seem to be related only to tests in undrained clay, but yet with some important findings. The available studies were based on either strain path analysis (Huang, 1989; Finno, 1993; Whittle and Aubeny, 1992) or flat cavity expansion methodologies (Yu et al., 1992; Smith and Houlsby, 1995), both converging to the conclusion that blade dimension seem to induce a three dimensional action that should be better represented by axisymmetric models (Whittle & Aubeny, 1992; Yu et al., 1992; Finno, 1993; Marchetti, 1997). Huang (1989) gave an important contribution by implementing a numerical technique to conduct strain path analysis for arbitrary three-dimensional penetrometers.

Numerical modeling of the penetration stage, using the strain path methodology (Whittle & Aubeny, 1992), pointed out some useful indications about the soil volumes that may be influenced by the dilatometer insertion. From this study, it was concluded that effects in the surrounding soil would be negligible at ratios between influenced zone and respective blade thickness higher than 10, as shown in Figure 10.4.

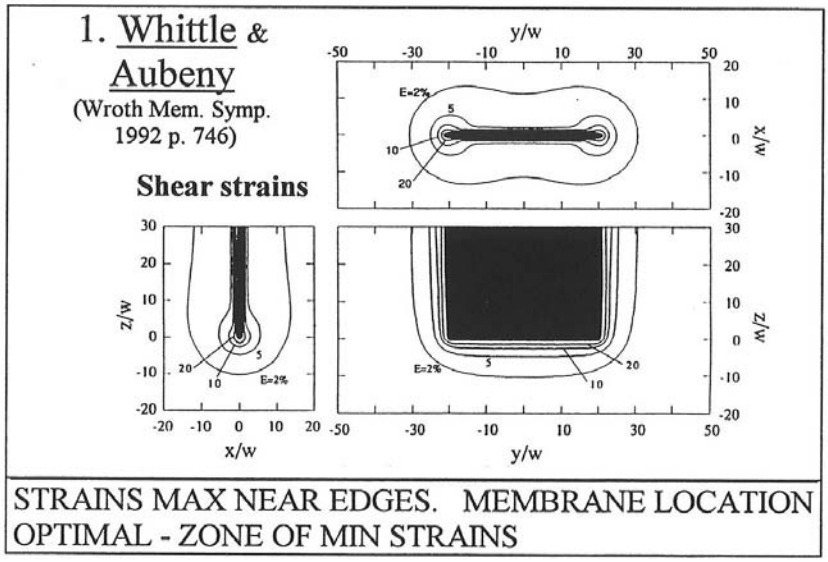


Figure 10.4 - Shear strains due to penetration (Whittle & Aubeny, 1992)

On its turn, in an attempt to use a simpler model, Yu et al. (1993) used the cylindrical cavity expansion model applied to cone pressuremeter installation (Houlsby and Withers, 1988) and proposed that installation of flat dilatometer could be simulated as a flat cavity expansion process. Therefore, stresses close to the tip of the dilatometer blade are affected by disturbance, but at some distance behind the dilatometer tip predicted stresses would be reasonably accurate concluding that two-dimensional flat cavity expansion method could be used in both clay and sand (although no analytical solutions are available for flat cavity expansion in sandy soils) and suggesting three-dimensional strain path methods to be used in theoretical frameworks for modeling the installation of the flat dilatometer.

Taking the aforementioned considerations, it seemed fair to place the blade at a distance of 250mm from the lateral and the back panels, since it represents a diameter ratio higher than 10 (at least 17) and leaves a significant soil thickness between expansion membrane and the cell wall placed in its front, guaranteeing the good quality of measurements during expansion. In fact, for a 60mm diameter membrane and 1.1mm of expansion in its centre, the respective ratios are at least 10 for the former and 600 for the latter. Being so, location of blades and measuring devices were

selected considering both penetration effects and expansion. In the case of penetration, it is ensured a diameter ratio at least 70% higher than the observed in clays using strain path method (Yu et al., 1993), and so a negligible influence of the wall is expected. Finally, assuming that DMT penetration effects are somehow comparable to CPTu, then the experimental trend observed on Hokksund sand (Parkin & Lunne, 1982) in which the effects on loose sands of this diameter ratio were found to be negligible on cone resistance. An extra safety factor against significative distortions due to proximity of walls is hereby expected.

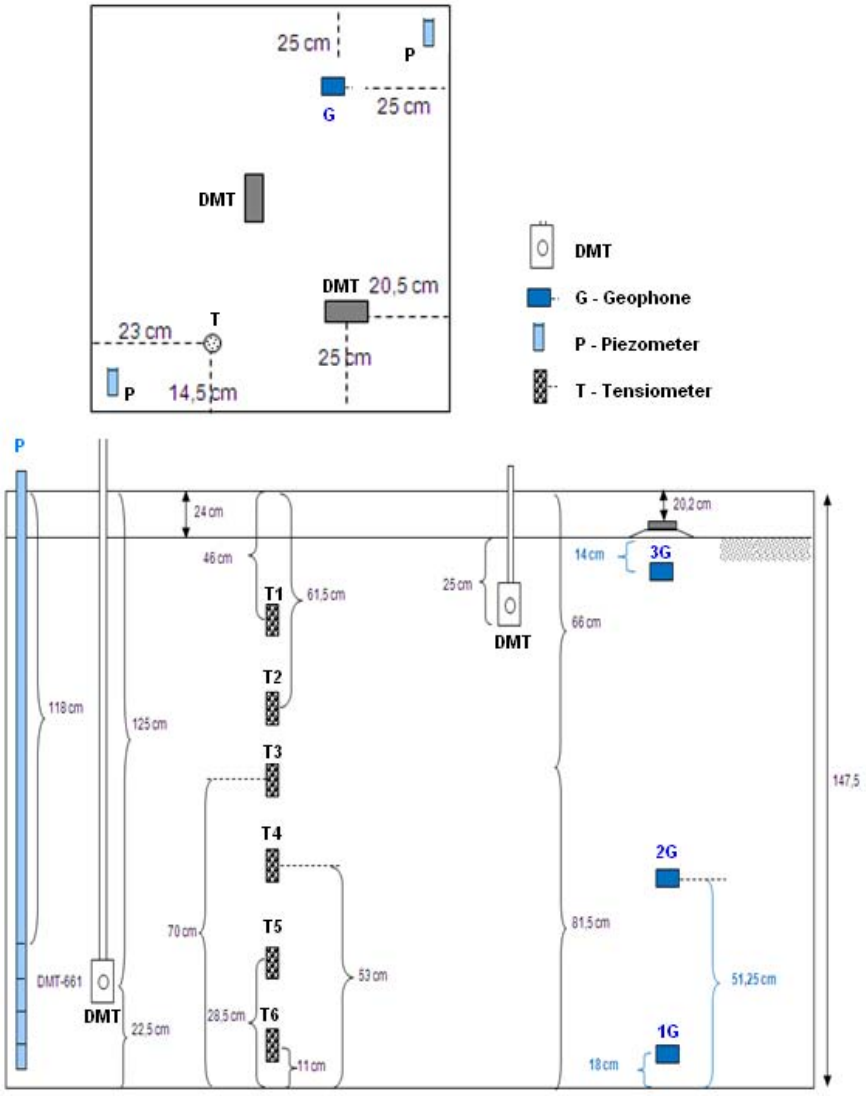


Figure 10.5 - Plant and Cross section of Cemsoil instrumentation

Guarda granitic residual soil was used to prepare remoulded soil-cement mixtures under similar conditions and identical curing time conditions used in triaxial samples (described in Chapter 9). CemSoil block samples were produced and compacted (in pre-defined conditions of moisture content) in homogeneous layers of 70-80mm,

aiming to produce similar void ratios in CemSoil and triaxial testing, in order to create comparable situations (Figure 10.6). The compaction was handmade, using a round wood hammer with 40cm diameter. It should be referred that in general, the last two upper layers (placed above blade locations) were not cemented, except for the sample with higher cement content where, occasionally, cementation was applied to all layers. This had no special purpose but yet it confirmed seismic measurements efficiency, as it will be explained in a further section.



a)



b)



c)

Figure 10.6 - CemSoil sample preparation; a) preparing the mixtures; b) filling the CemSoil; c) compaction of mixtures.

Two DMT blades were positioned during the compaction processes, one being placed 20cm above CemSoil base level and the other 25cm below the surface upper level of the cemented soil. Meanwhile, two open tube PVC piezometers were installed, one located nearby the water entry and another in the opposite corner, in order to control

water level and respective stabilization during the main experiment (Figure 10.7). In addition, six tensiometers (one profile of six or two profiles of three) and three pairs of geophones for seismic survey (one profile) were also installed, respectively for suction and seismic wave velocity measurements. Regular measurements of suction pressures and seismic wave velocities were made for different curing times, before and after saturation phase, which was settled two days before each test. Finally, at each pre-selected testing day, DMT measurements of the first and second installed blades were taken, followed by the second blade testing proceeding pushing-in towards the first blade testing depth. Detailed presentation and discussion of obtained results will be presented in the following sections.

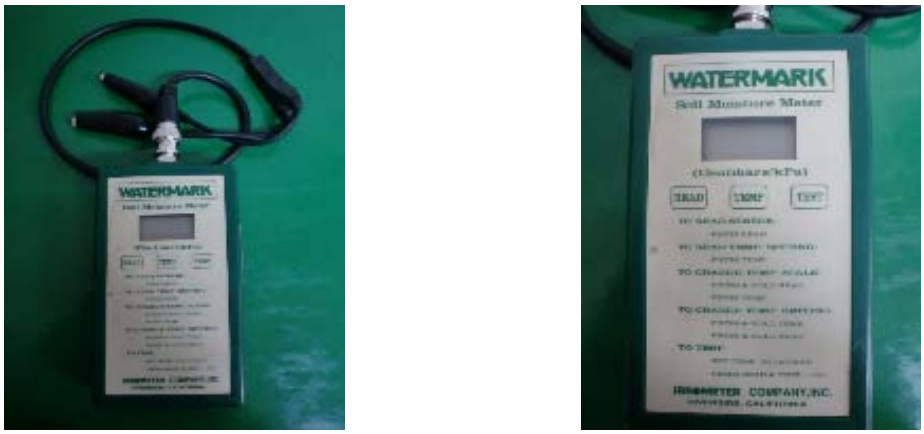


Figure 10.7 - Device installation: a) first blade; b) second blade; c) detail of open piezometric tubes; d) installation of piezometers.

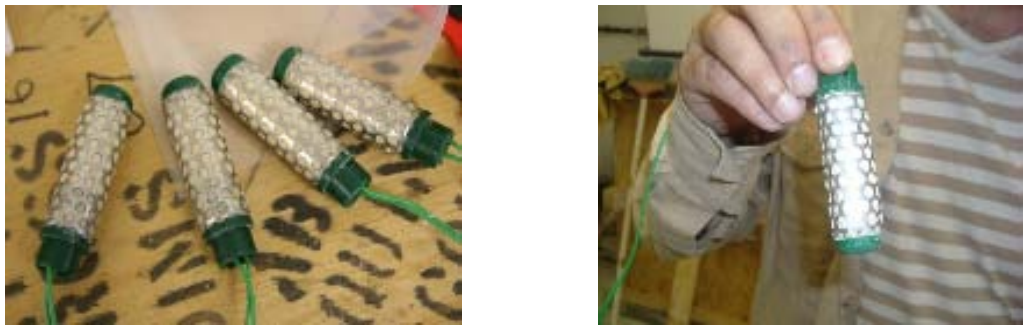
10.2. Matrix suction measurements

Since the dimension of the cell expectedly creates low levels of suction (below 100 kPa) it was considered adequate to use tensiometers for matrix suction evaluation. Initially a set of six tensiometers was placed in one vertical alignment, with more or less 20cm spacing, five above and one below water level. However, homogeneity of suction inside the cell was important to be checked and so, alternative profiles were adopted in

Fra2 and Fra3 samples, composed by two vertical alignments with three tensiometers, one with the same location of the previous and the other in the center of the cell. The devices used in the experiment (model ® Watermark – soil moisture meter) are a product of Irrometer Company, Inc. and are composed by the tensiometer itself and a measuring device for suction and temperature (Figure 10.8).



a)



b)



c)

Figure 10.8 - Suction measurements: a) reading device; b) tensiometer; c) tensiometer installation

Measurements of suction were taken regularly starting with the installation, namely the first three days, the value immediately before and after saturation, and twice a day afterwards, until completion of test. The obtained results are presented in Figure 10.9 respectively representing the three different experimental set-ups: sample with no cement and mixtures Cement 52R and Cement 32,5N.

These registers globally confirmed the overall expected values, taking into account recently published results in granitic residual soils (Topa Gomes, 2009), as presented below:

a) Non-cemented sample revealed very stable results after three days in place, showing a rapid answer to saturation (day 12);
b) The same time to initial and final suction stabilizations were observed in cemented samples, confirming three days after compaction and less than one day after saturation (in fact saturation stabilization was very fast, in just a couple of hours); also similar is the sharp drop when approaching saturated level;
c) The order of magnitude of stabilized values is similar in all samples; the respective results show a slight suction variation with depth (5 to15 kPa), converging to expectable results if linear negative evolution is considered up to water level (Topa Gomes, 2009);
d) These results are convergent with the retention curve shown in Figure 10.10a); the curve was determined by means of pressure plates in Laboratório de Geotecnia da FEUP;
e) Observed differences between lateral and center measurements show an initial gap that reduces to a minimum in three days, with no significant differences afterwards; in Figure 10.10 b) suction results obtained for each testing time are presented.

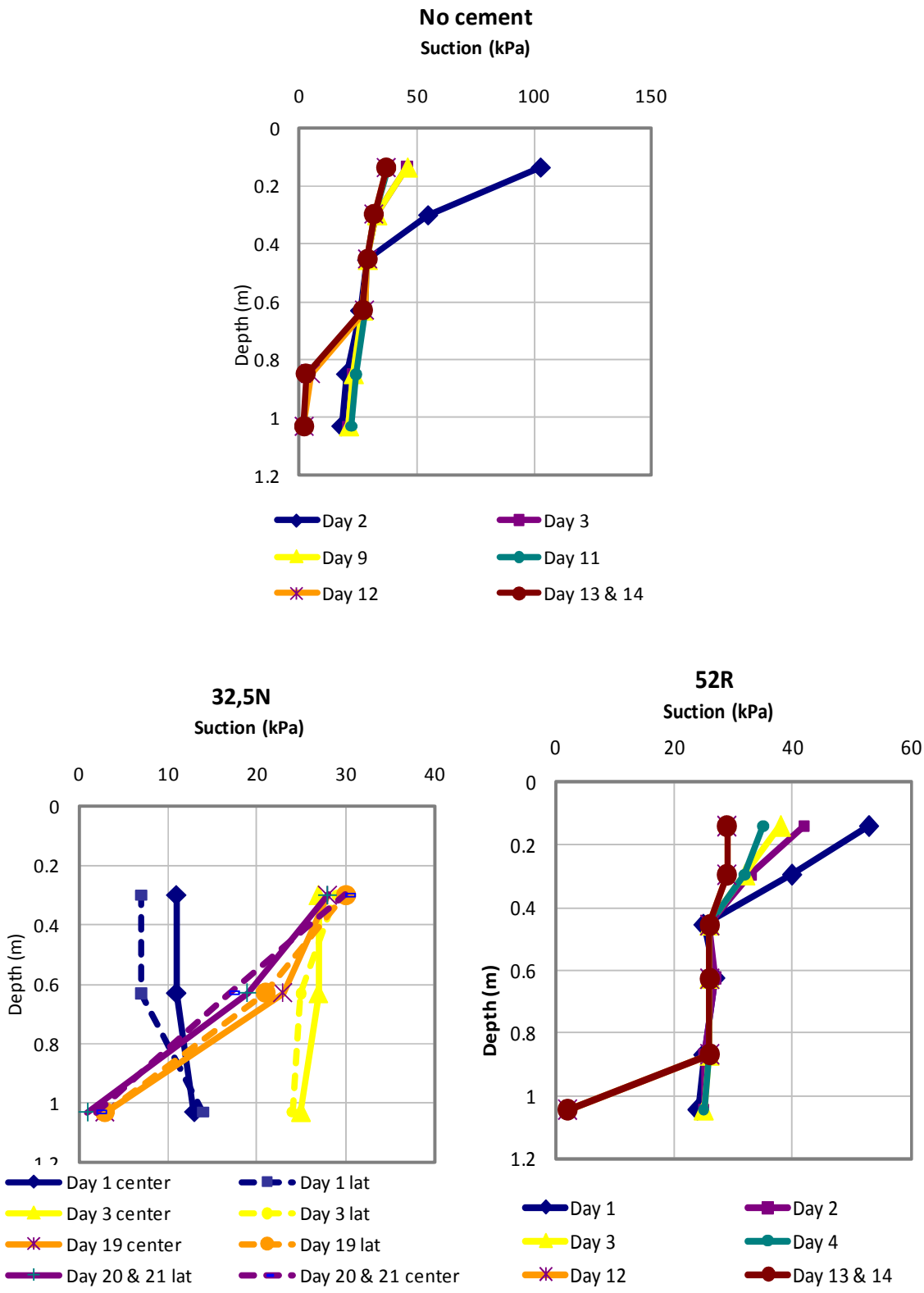
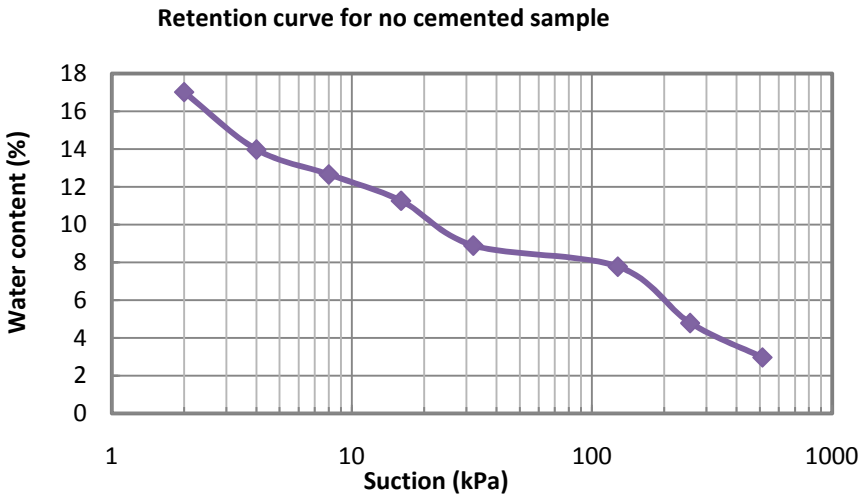
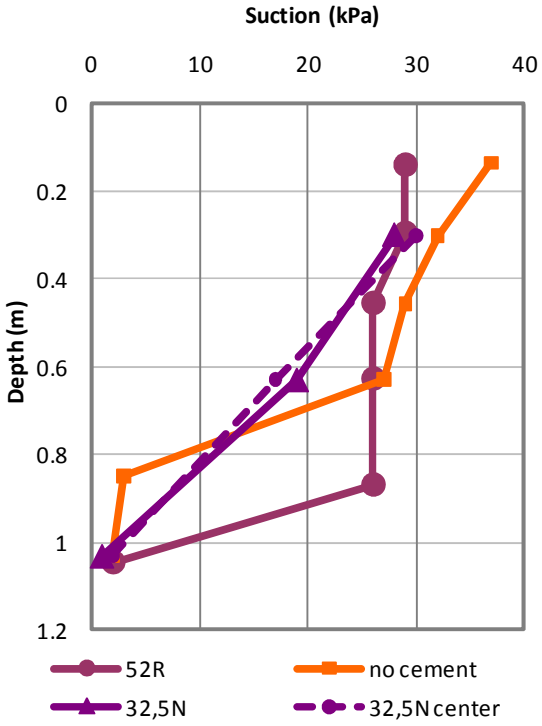


Figure 10.9 - Suction measurements.



a)



b)

Figure 10.10 - Suction results: a) retention curve (no cemented) b) suction at testing times.

10.3. Seismic wave velocities

As previously defined, compression and shear wave velocity measurements were made when the blade was installed, before and after saturation and during testing time. A set of geophones installed in a vertical alignment was used for this purpose, which location was already presented. At each testing point, two geophones were placed, one for each P and S wave velocity determinations, placed horizontal and vertically as shown in Figure 10.11. The source for generation of S-waves was composed by a block of 12kgf and an impact plate lying under rolling bars, as represented in Figure 10.12. This work was made in partnership with Prof. Fernando Almeida, geophysicist of Geoscience Department of University of Aveiro



Figure 10.11 - Seismic devices installation.

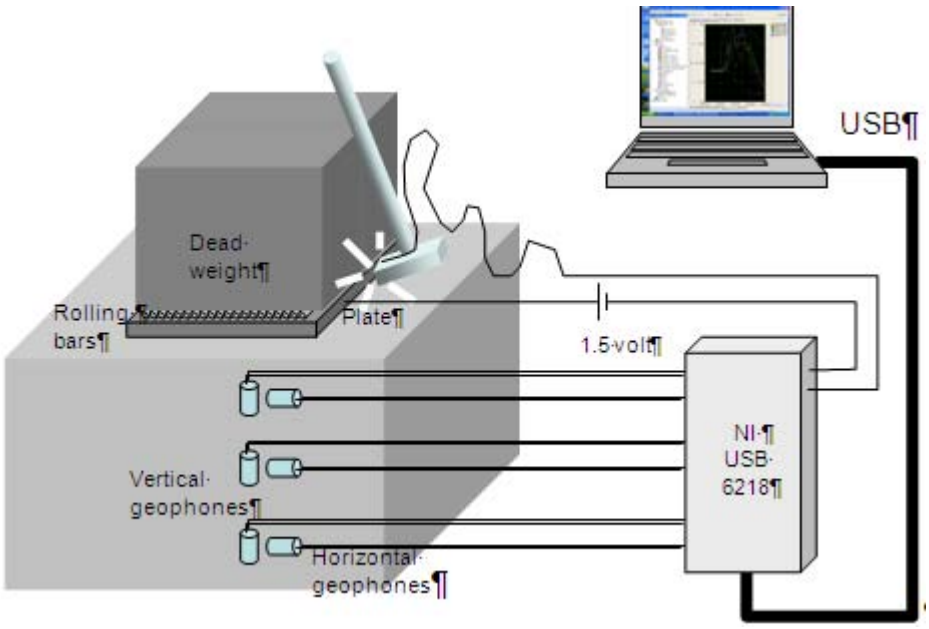


Figure 10.12 - Schematic representation of seismic wave apparatus

The dead weight load pressures the impact plate, and consequently, friction reaction increases, improving the quality of wave propagation. The blow in the impact plate generates a vibratory action with higher acceleration than the one that would be obtained considering a fixed total mass of plate and dead weight. This creates sharper signals and thus higher efficiency in first arrival determination.

Seismic solicitations were obtained by means of two polarities, creating hammer impacts in an unique path but opposite directions, allowing to verify the polarity variations. Despite the source has been conceived to amplify horizontal movements, it became clear during the experience that the system could also be used to vertical energy generation. The dynamic load generated P and S_v waves in vertical and S_h in horizontal geophones, allowing the evaluation of both wave velocities with a unique hammer impact (Figure 10.13).



Figure 10.13 - Details of seismic wave measurement apparatus.

The main difficulties found in time arrival determination, can be summarized as follows:

a) There is a change in the shape of the wave as it propagates within the medium, with higher modification near by the energy source; high frequencies becoming weaker than low frequencies and thus, generating a wave form where the instantaneous frequency decreases; however, during data analysis it became clear the resulting scatter could be greatly reduced when

logarithmic time scale is used, showing coincidence of the respective transformed function;

b) Reflexions of P waves occurring at confining walls disturb the spectrum of the waves propagating between the source and the measurement devices, creating some extra difficulties in estimating S waves first arrival; on the other hand, S-wave propagation is slower than in P-wave, being also vulnerable to P waves reflected in the wall; luckily, these undesirable (but inevitable) events show a oscillatory scattering pattern that allows filtering in relatively simple way.

Data acquisition was based with NI USB-6218 de 16-bit 250Ksamples/s device and a VI logger Task, developed from Measurements and Automation Explorer software, commercialized by National Instruments. Registered signals (Figure 10.14) were exported to MatLab® by means of an Excel® file, based in a script developed to determine P and S waves first arrivals and to calculate wave velocities.

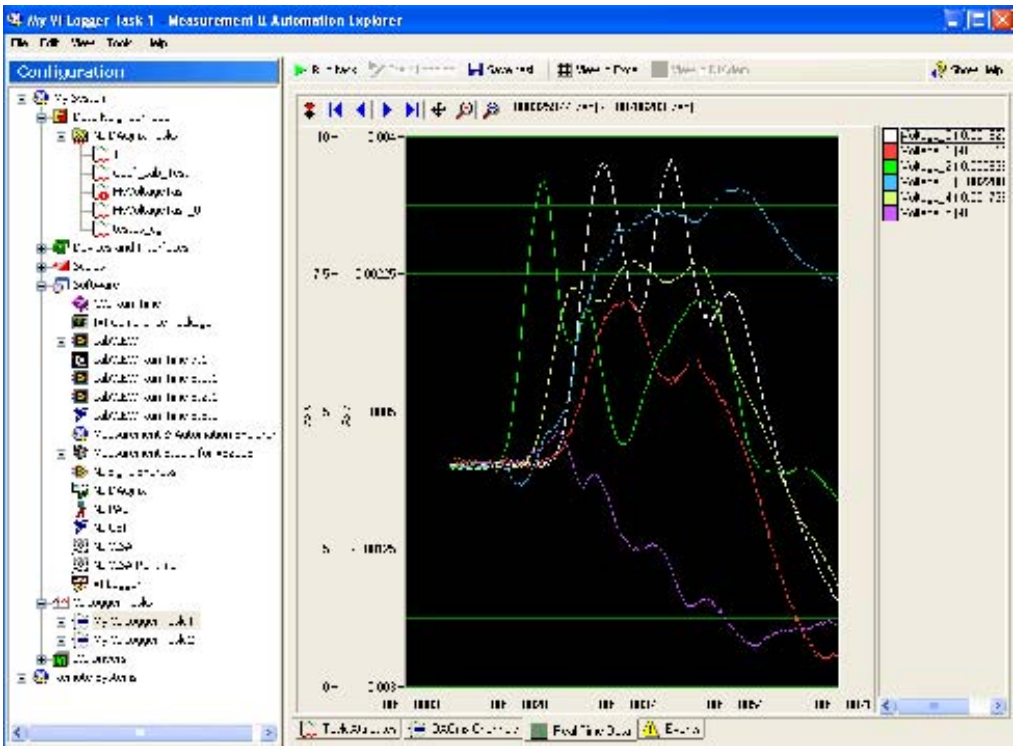


Figure 10.14 - Wave registration

Data processing in the script can be described as follows:

a) Importation of Excel files with opposite polarities;
b) Separation of channels and polarities;
c) Signal normalization;
d) Switching time scale from natural to logarithmic;
e) Re-sampling of transformed function;
f) Application of Fourier series to the signal;
g) Filtering frequencies;
h) Summing and subtracting of polarized spectra;
i) Plotting first arrivals;
j) Calculation of P and S waves and Poisson's ratios.

At each depth location, several tests were performed, in order to have enough data to statistical analysis. Overall, 50 pairs of measurements were obtained, allowing a significant amount of data. Sets of measurements obtained in the same experimental conditions were plotted against depth and median statistical parameter was taken as reference value, aiming a reduction of the effects of abnormal values in the final results. An example of this procedure is presented in Figures 10.15 and 10.16. The convergence of all data around the same trend becomes clear in Figure 10.17, where shear waves are plotted against compression waves values, with the larger markers representing the median obtained by statistical analysis.

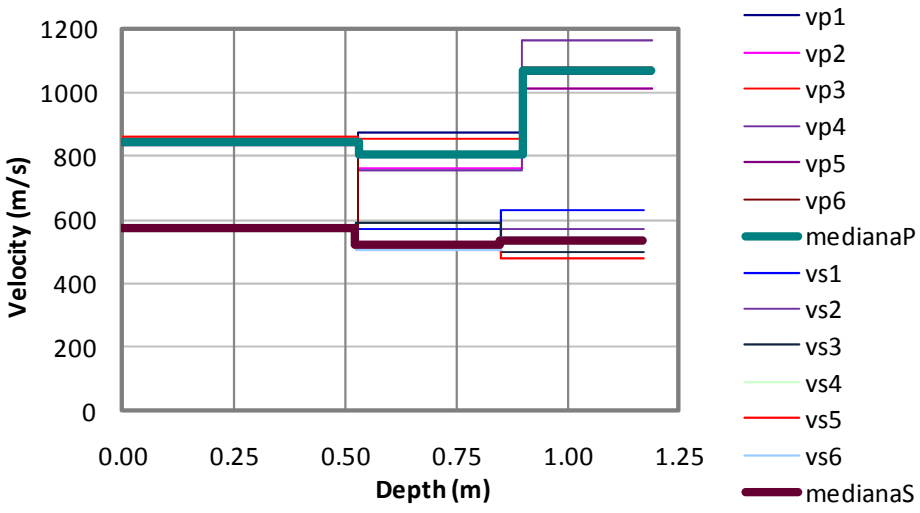


Figure 10.15 - Example of seismic wave velocity statistical analysis

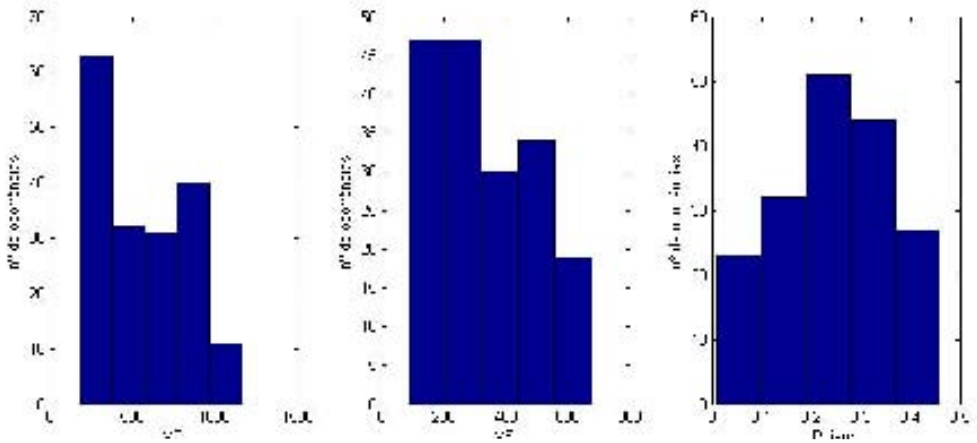


Figure 10.16 - Frequency of events

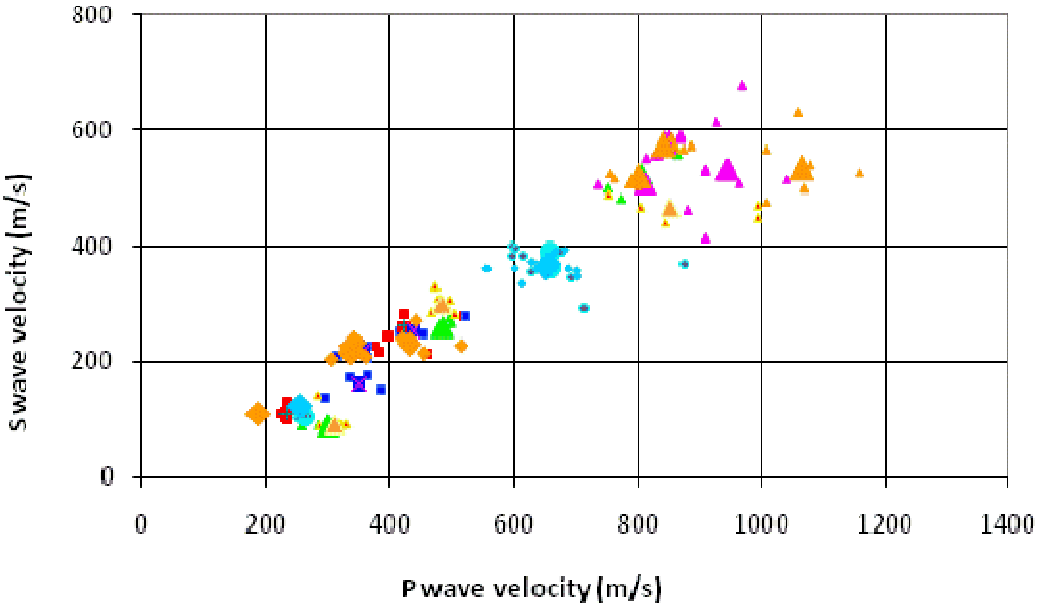


Figure 10.17 - S wavess versus P wave velocities variation.

Representation of obtained compressive and shear wave velocities and derived Poisson coefficient, revealed a significant variation when individual or singular values were considered. This apparent dispersion is, however, explained by the fact that P wave velocities in saturated conditions are non representative of the soil skeleton (and therefore of the effective stress behaviour) because the water level is distanced of the source. If this data is excluded, Poisson coefficient range becomes 0.25 to 0.40, as represented in Figure 10.18 (3D MatLab®).

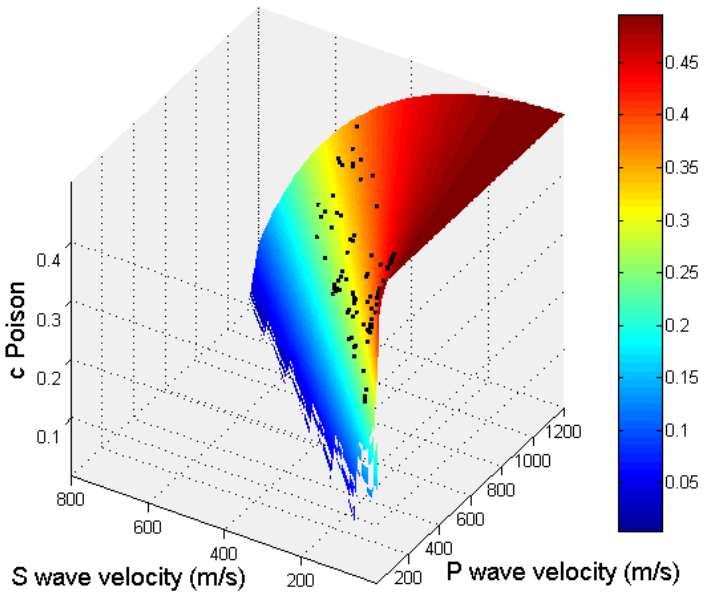


Figure 10.18 -3D representation of shear / compressive waves and Poisson's ratio.

Seismic wave velocities plotted as function of tensile strength are presented in Figures 10.19 to 10.22 and resumed in Figure 10.23. These plots suggest the following considerations:

a) Both compression and shear waves increase with cementation level, either in saturated or unsaturated conditions;
b) Results at the higher level correspond to uncemented layers, except for the highest cementation level where occasionally all layers were cemented; this is clearly detected either by P and S waves, with all measurements converging for the same value;
c) Apart from a singularity observed in the set of geophones placed at mid height of block sample, S wave velocities increase with cementation level; however, differences between saturated and unsaturated conditions seem to be not relevant and could be represented by the same trend line as shown in Figure 10.23; this is a obvious consequence of the low values of suction, with small influence of effective stress variation on very small strain deviatoric stiffness;
d) In the lower set of geophones, shear wave velocities displayed the same order of magnitude before and after saturation, while compressive waves clearly increase after saturation;
e) P and S waves show a parallel evolution with cementation level, as it can be seen in Figure 10.23.

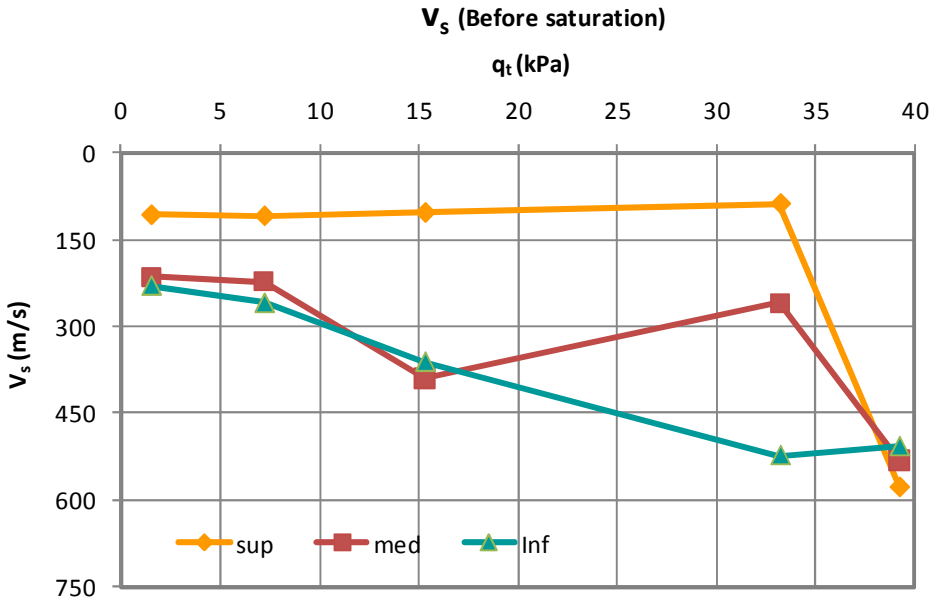


Figure 10.19 - Shear wave velocities obtained before saturation.

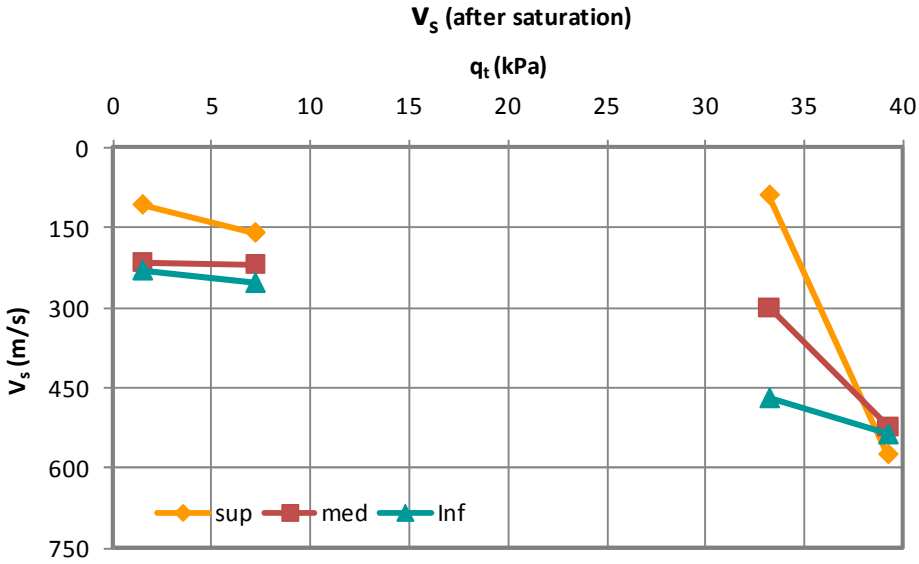


Figure 10.20 - Shear wave velocities obtained after saturation.

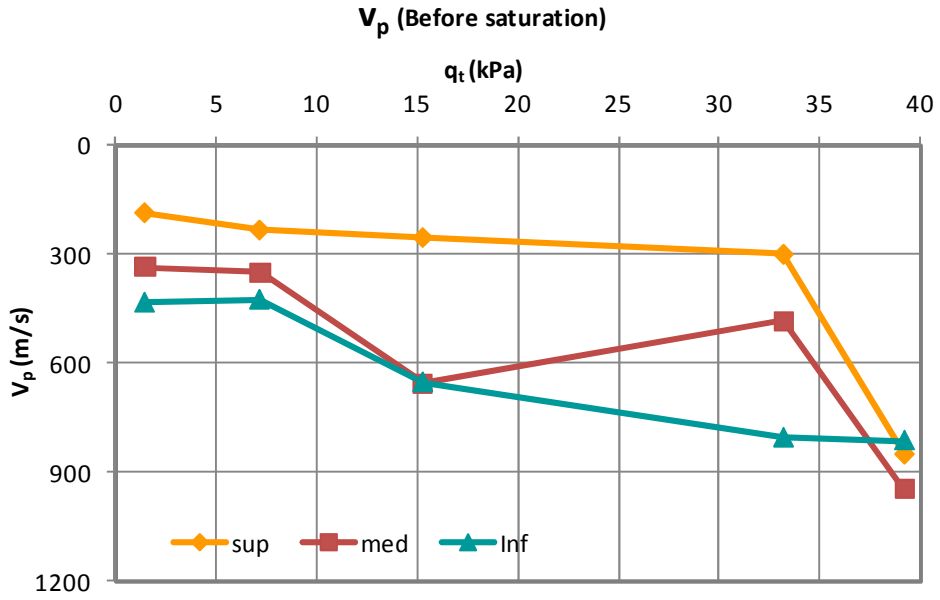


Figure 10.21 - Compression wave velocities obtained before saturation.

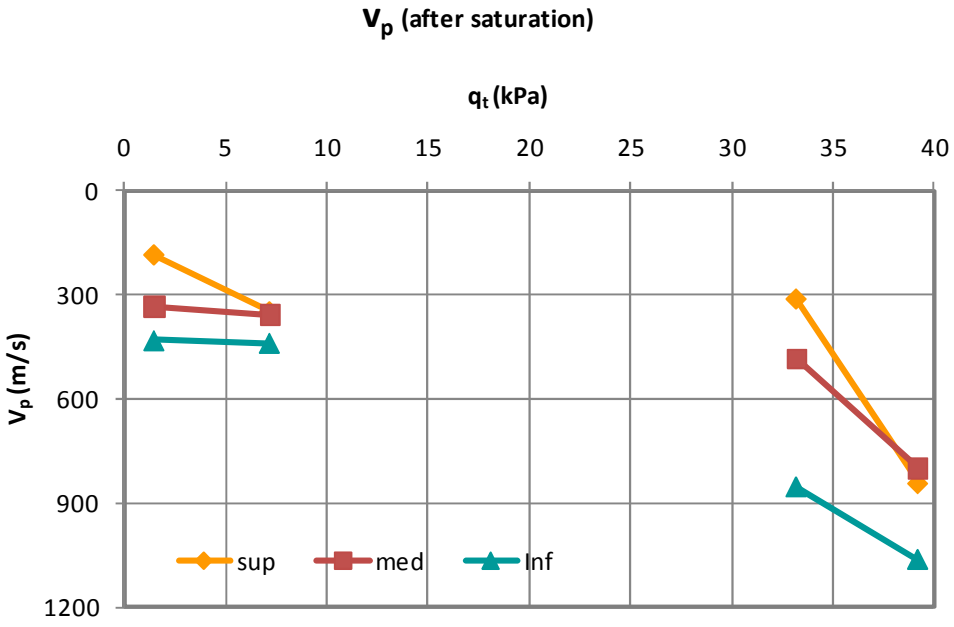


Figure 10.22 - Compression wave velocities obtained after saturation.

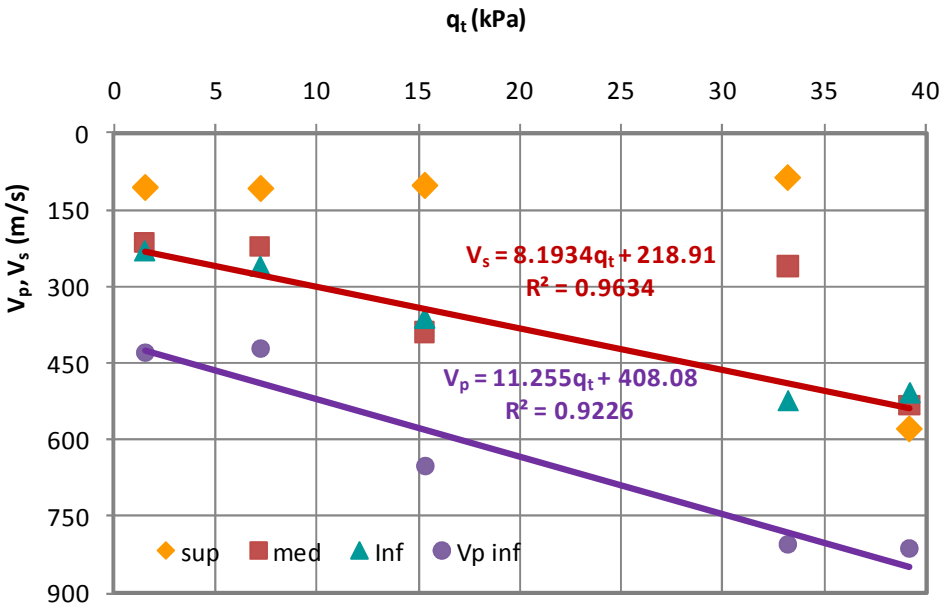


Figure 10.23 - Compression and shear wave comparisons.

The obtained results globally fits in the weathering ranges related to the different cementation levels as presented in Chapter 9 (For1 – medium compacted soil; Fra2 – medium compact to compact soil; For 2 – compacted soil; Fra3 – W_5, following the N_{SPT} indexation presented in Chapter 6).

10.4. DMT Testing

10.4.1. Introduction

According to the type of cement, at 14th or 21st day after suction, water level and seismic wave velocity measurements were taken and the main testing phase started. Two days before (12th or 19th), saturation of the last 35cm of CemSoil material was accomplished, controlled by means of two open tube PVC piezometers installed in CemSoil box. In these conditions, the first blade was placed below water level while the second blade was situated above, which opened the possibility of studying suction influence on DMT measurements and the respective results. Figure 10.24 and Figure 10.25; illustrate the final aspect of the soil mass (Fra2) after removing one of the test vertical panels at the end of testing phase.



Figure 10.24 - Final aspect of the instrumented block sample.



Figure 10.25 - Final aspect of a CemSoil sample (Fra2).

The first DMT test was always the one with the blade positioned below water level (pre-installed under saturated conditions), followed by the second one (pre-installed under unsaturated conditions) aiming to ensure undisturbed conditions due to penetration effects. Then, using a penetrometer rig, this second blade was (statically) pushed down and test readings were taken in intervals of 20cm, as usual in common DMT test procedures. Figure 10.26 illustrates some details of these DMT test conditions.



Figure 10.26 - DMT testing conditions: penetrometer rig (upper row), partial views from lower and upper stages (mid row) and penetration test conditions (lower row).

10.4.2. Basic Parameters

In Table 10.1 and Table 10.2, DMT obtained results are presented, ordered by installation, saturation conditions and cementation levels, the latter represented by tensile strength values, used as a reference index.

Table 10.1 - Results obtained in pre-installed conditions

qt (kPa)	Conditions	A-reading (kPa)	B-reading (kPa)	P_0 (kPa)	P_1 (kPa)
1.5	Pre-installed saturated	60	160	63.63	92.5
	Pre-installed unsaturated	80	560	64.63	492.5
7.2	Pre-installed saturated	80	1100	32.75	1025
	Pre-installed unsaturated	155	1100	110.80	710
15.3	Pre-installed saturated	80	1350	21.05	1280
	Pre-installed unsaturated	90	750	59.00	1060
35.2	Pre-installed saturated	130	2150	31.00	2110
39.2	Pre-installed saturated	155	3200	- 45.70	3140

To properly visualize results obtained in pushed-in conditions for each sample, P_0 and P_1 versus depth are displayed in Figure 10.27, were the profiles obtained on the Guarda's natural soil massif in which this experience is based (Rodrigues, 2003) were included. It is important to refer that the first 1.0m of in-situ data corresponds to a superficial earthfill, and so the comparable results should be seen shifted by 1.0m. Taking this into account, data reveals that in-situ Guarda's P_0 and P_1 results are within the range of cemented samples For1 and Fra2, that is medium compacted to compacted soil, which is in agreement with indication based on local N_{SPT} profiles (Rodrigues, 2003). This potentate the attempt to correlate these soils when artificially and naturally cemented.

Table 10.2 - Results obtained in pushed-in conditions.

qt (kPa)	Conditions	A-reading (kPa)	B-reading (kPa)	P_0 (kPa)	P_1 (kPa)
1.5	Pushed-in saturated	107.9	160	107.9	257.5
	Pushed-in unsaturated	200.0	690	184.1	622.5
		210.0	800	189.1	732.5
		190.0	690	173.6	622.5
		110.0	375	105.4	307.5
7.2	Pushed-in saturated	102.8	1100	102.8	465
	Pushed-in unsaturated	90.0	750	59.0	710
		170.0	800	140.5	760
		245.0	950	211.8	910
15.3	Pushed-in saturated	231.6	1350	231.6	1060
	Pushed-in unsaturated	235.0	1200	189.8	1169
		270.0	1350	219.1	1310
		450.0	1700	390.6	1660

From the same figure it is possible to infer that general obtained P_0 and P_1 profiles on pushed-in conditions are very similar in trend for all the hereby studied structured conditions, having increasing values up to the mid-height, and then decreasing until the deepest level, below water level. Generally, it can also be observed that P_1 reflects quite well the increase in cementation, while P_0 reveals a smoother variation.

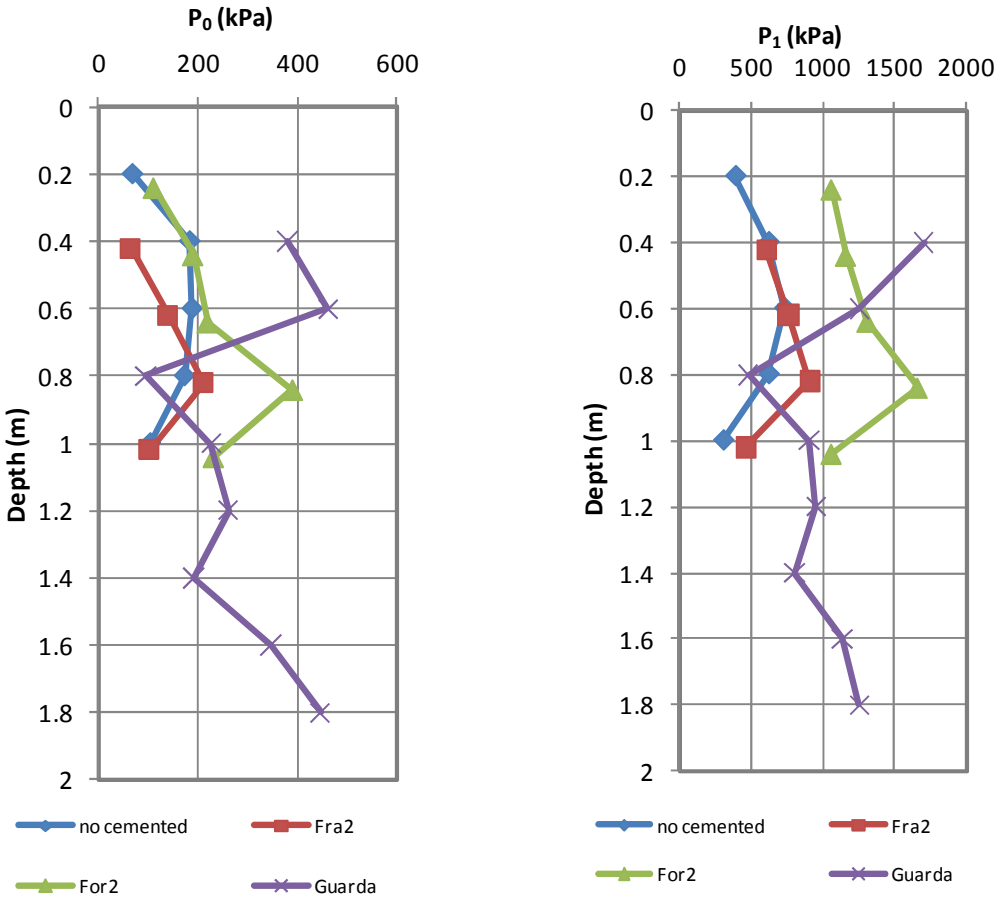


Figure 10.27 - Basic pressures obtained after static pushing in-situ and in CemSoil

Individual basic parameters obtained in installed and pushed-in blades are shown in Figure 10.28 to Figure 10.30, showing some gaps between pairs of readings. It should be noted that the first result in pushed-in profile corresponds to pre-installed unsaturated conditions.

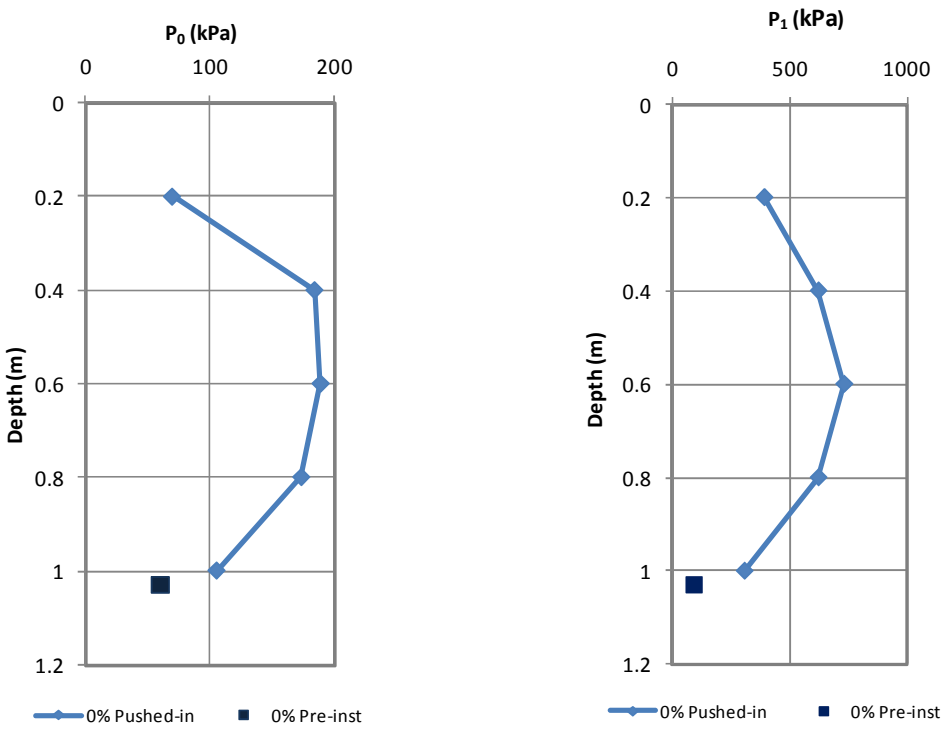


Figure 10.28 - Basic pressures obtained in pre-installed and static pushed-in conditions (no cemented).

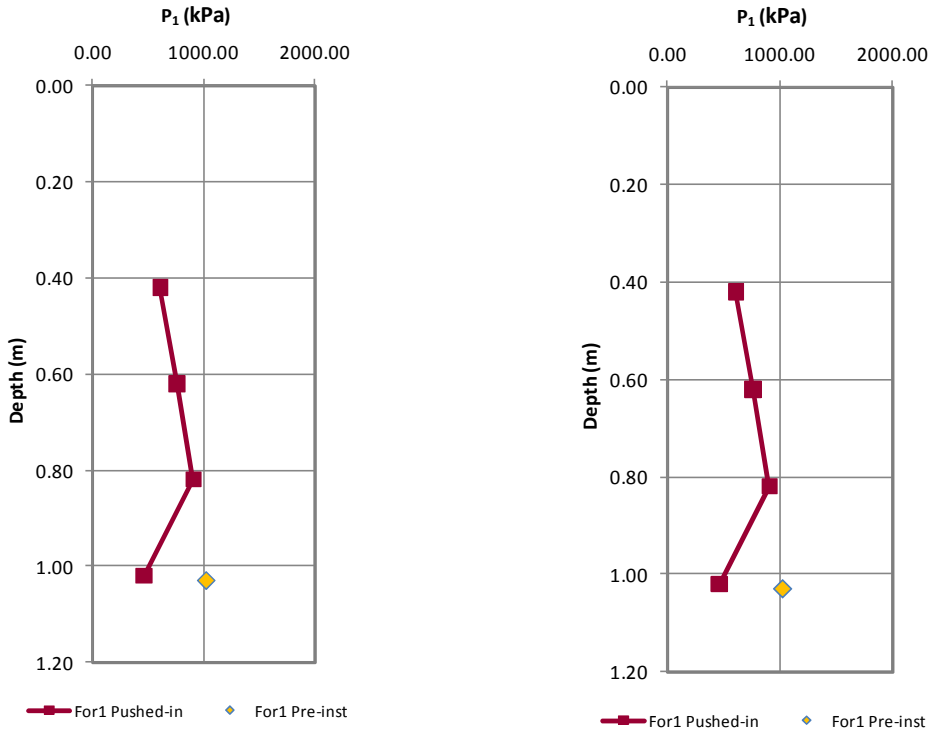


Figure 10.29 - Basic pressures obtained in pre-installed and static pushed-in conditions (For1).

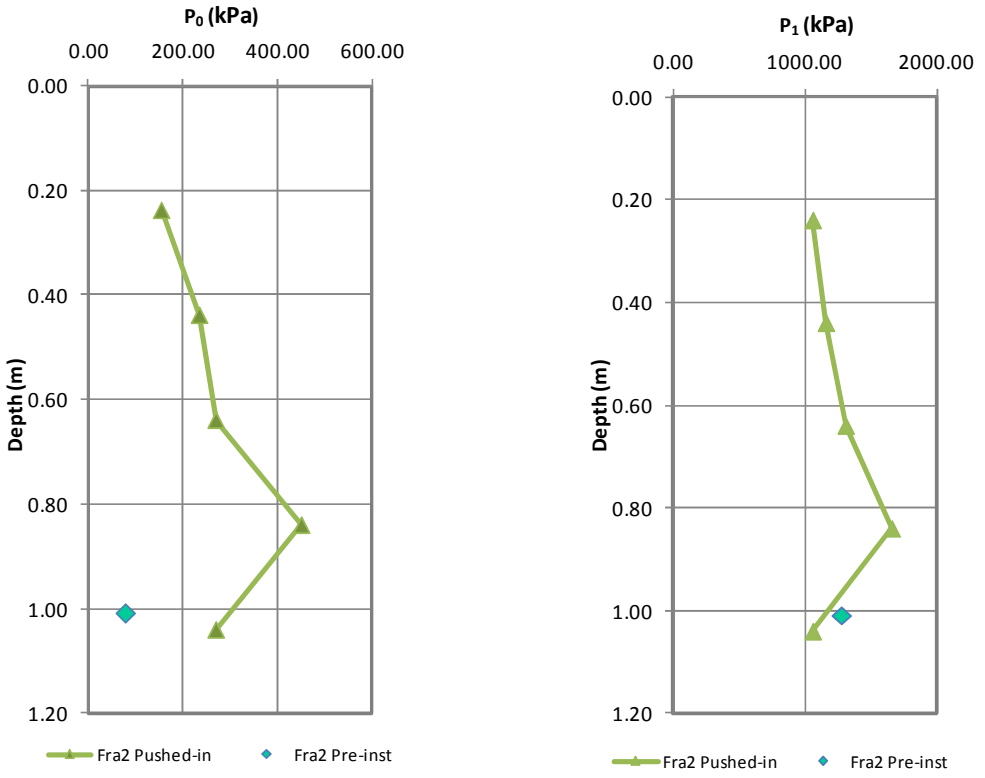


Figure 10.30 - Basic pressures obtained in pre-installed and static pushed-in conditions (Fra2).

The comparison of P_0 and P_1 results shows the trends summarized below:

a) Uncemented samples in saturated conditions show that both parameters are always lower in the case of installed blade, which somehow would be expected since penetration generates a compression of the surrounding soil;
b) In cemented samples P_0, is always lower in pre-installed blade, indicating that in the most incipient compression levels the processes that precede the DMT test (pre-installed or pushed-in) have higher influence; P_1 shows the opposite trend, with the observed differences explained by the loss of cementation;
c) P_0 differences between pre-installed saturated and unsaturated samples are small, showing no dependency on suction level, while P_1 differences seem to be affected by suction; this is not surprising since the confining effective stress has an obvious influence on mechanical paramaters, such as modulus and strength (and P_1 reflects them) while, in opposition, the influence in stress state is scarce (P_0).

These observations suggests that the effects of penetration in uncemented saturated samples generate a soil densification around the measuring membrane, which gives rise to higher values of P_0 and P_1. Even though a similar densification of the soil around the blade is expected when pushing-in the blade in cemented soils, results reveal an opposite trend in the case of P_1, where pre-installed values are higher. Considering that the only difference between tested situations is the presence of cement, P_1 results suggest that the loss of interparticle bonding due to matrix partial destructuration during penetration not only compensates but even overpasses densification effects. The reason why the opposite trend is displayed by P_0 might be explained by the lower strain level of its measurement. Being so, it should be considered that compression, by one side, and loss of cementation strength, by the other, seems to produce opposite effects, somehow partially compensating each other.

Diagrams of A and B readings evolution were analyzed and compared with corrected pressures, as presented in Figure 10.31, from where it becomes obvious the overlapping of B and P_1, with B slightly higher than P_1, as a consequence of membrane rigidity.

On its turn, comparison of A and P_0, shows an opposite evolution with selected cementation index (q_t), which is quite more complex to interpret. In fact, available experience on the evolution of at rest lateral stress in sandy mixtures shows that it decreases significantly with increasing cement content (Zhu et al., 1995), which seems to be confirmed by the global decrease of the pre-installed P_0 results obtained in the present research (Table 10.1 presented at the beginning of this section). However, membrane rigidity correction to obtain P_0 from A-readings depends on P_1 (or B readings) and thus, in these pre-installed conditions there is an increasing influence of the latter as the cementation level increases, which becomes negative in the higher cemented mixture. Since a negative value founds no logical explanation in field mechanical behaviour, it can be concluded that this influence of P_1 on P_0 evaluation can significantly affect the magnitude of final results and thus the respective interpretation in pre-installed conditions. Being so, for comparative purposes between pre-installed and pushed-in tests, it should be preferable to use A-readings instead of corrected P_0.

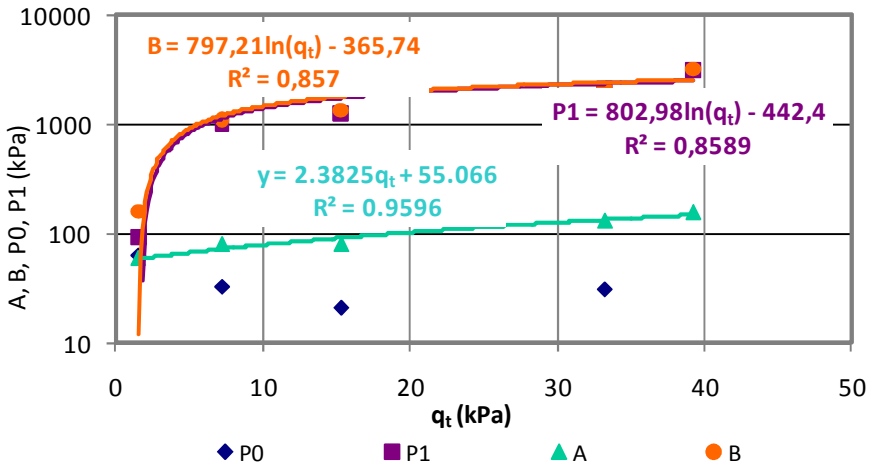


Figure 10.31 - Evolution of basic pressures and readings with cementation level

The respective A, B, P_0 and P_1 parametric results are presented in Figures 10.32 to 10.35, plotting all data against q_t index results and taking into account the different conditions of the samples, namely pre-installed-saturated (pre-inst sat), pre-installed-unsaturated (pre-inst unsat) and pushed-in-saturated (pushed-in sat) conditions. Since the conditions of remolding and void ratios are all alike and cementation level is the same for each specific sample, then it is reasonable to admit that differences between *pre-installed saturated* and *pushed-in saturated* results should reflect the penetration disturbance while between *pre-installed saturated* and *pre-Installed unsaturated* should be related to suction contribution.

Figure 10.32 reveals that A-reading values generated by pre-installed saturated conditions represent the lower level of results, which increase when saturation is not complete, as a result of suction influence, and also when the testing equipment is pushed (reflecting the penetration disturbance). In all the observed situations A reading values increase with cementation content, which may reflect an higher influence of membrane rigidity than lateral stresses on final results, since a decrease should be expected, if Zhu et al. (1995) conclusions are considered. A-reading differences between the tested situations globally increases. On the other hand, the same analysis applied to B-readings (Figure 10.33) shows the opposite trends with pre-installed saturated conditions displaying the higher values, which decrease both with unsaturation level and penetration, with the latter representing the lower level. This suggests that the main penetration effect is related to the partial loss of cementation strength, which shows a higher impact than stiffness increase around the blade, due to

unsaturation or penetration. The respective percent differences in these conditions are smoother than in A-reading case.

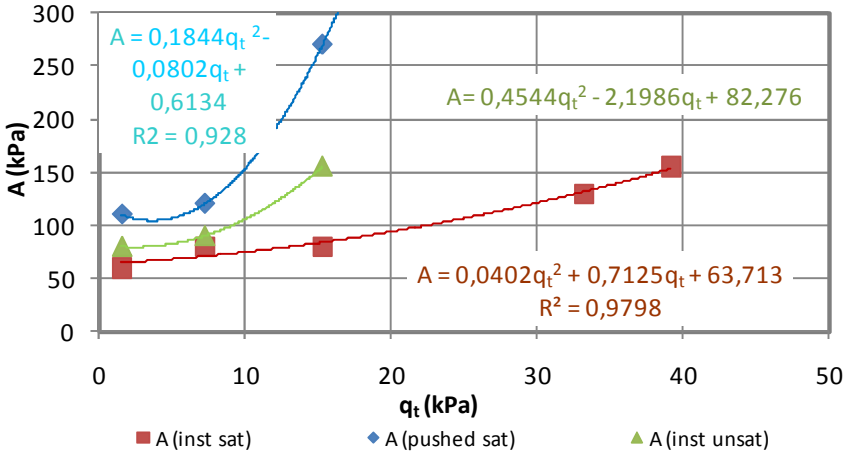


Figure 10.32 - Global A-readings

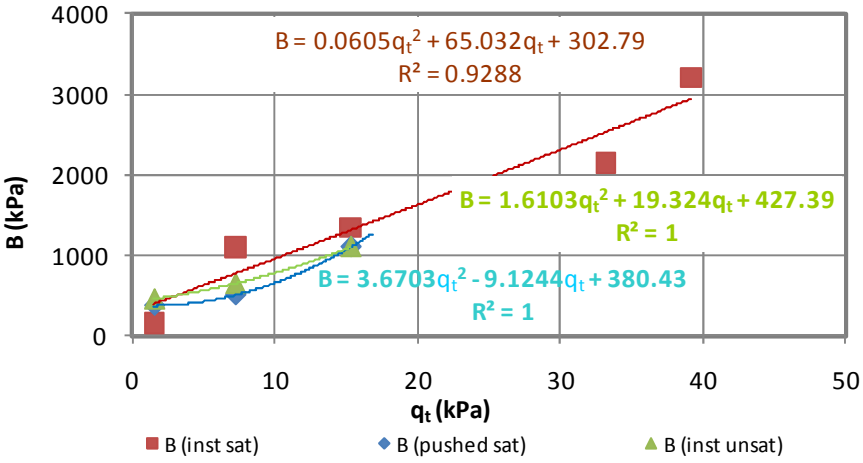


Figure 10.33 - Global B-readings.

In Figure 10.34 and 10.35, P_0 and P_1 evolutions are also represented, showing the already referred similarity P_1 and B, while P_0 and A follow similar patterns for pushed-in conditions and diverge when the blade is pre-installed, due to the reasons explained above.

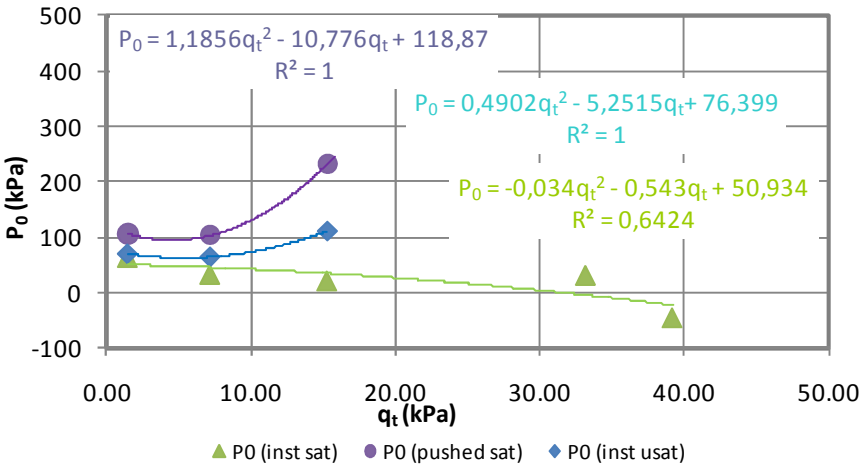


Figure 10.34 - Evolution of P_0 corrected parameter related to different penetration and saturation conditions..

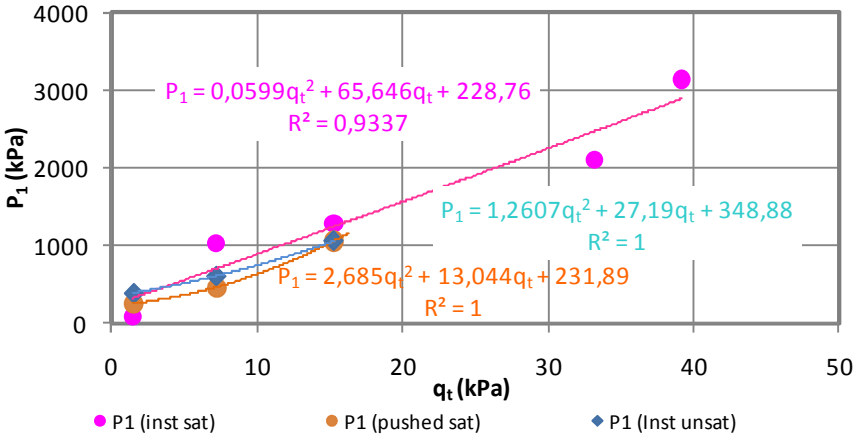
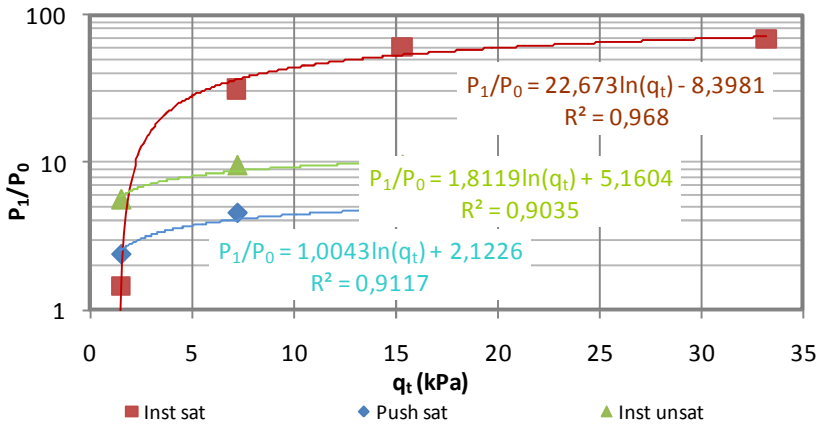
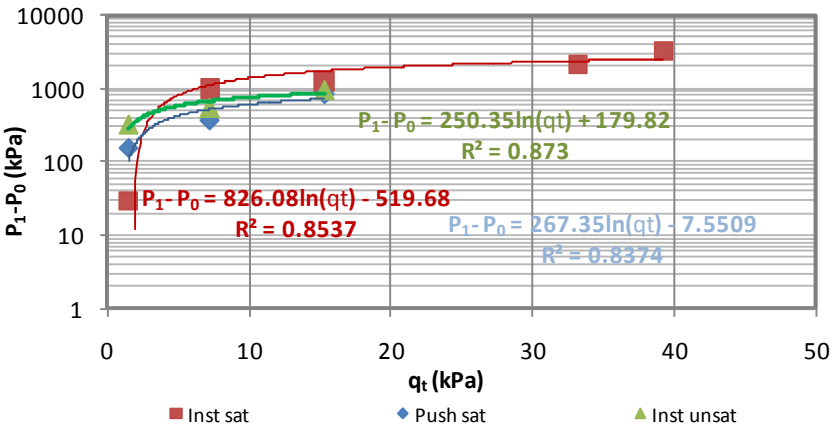


Figure 10.35 - Evolution of P_1 corrected parameter related to different penetration and saturation conditions.

Finally, in Figure 10.36 the evolution of the ratio (P_1/P_0) and the difference (P_1-P_0) between both basic parameters with cementation level are presented, revealing similar logarithmic trends in both situations. However, results also reveal a different behaviour between non-cemented soils and cemented mixtures, with pre-installed saturated results lower in the former and higher in latter cases, exactly as it happens with P_1 results.



a)



b)

Figure 10.36 - Evolution of basic pressure ratios with cementation level: a) P_1/P_0; b) P_1-P_0

Summarizing, it seems fair to say that test results reveal accuracy to detect variations due to the influence of pushing disturbance, cementation strength and suction effects, supported by reasonable explanations. In fact, penetration of testing equipment should impose a compression to the soil around the inflating membrane and thus, a higher lift-off (P_0) pressure after pushing is expected, reflected by the final results. Recognizing that the stress state in granular uncemented soils increases with density, the increasing in P_0 from pre-installed to pushed-in conditions is natural. However, in cemented conditions the insertion denotes both the densification and de-structuring. Thus the only real sensitivity to K_0 drop with cementation is obtained in pre-installed conditions.

On the other hand, P_1 or B results, which are obtained after deform the soil in 1.1mm of membrane expansion, clearly show that the penetration in cemented samples affects intensely the properties of cemented materials, specifically those with high void ratios, due to partially destructuration. Globally, P_0 and P_1 (as well as P_1-P_0) in pushed-in or pre-installed conditions, saturated or unsaturated, always reflect the increase of cementation level. P_0 only follows this trend in pushed-in tests, while in pre-installed conditions the parametrical calculation is greatly affected by the order of magnitude of P_1, decreasing with cementation levels (even reaching negative values).

On its turn, the presence of suction should increment the global strength and stiffness, being confirmed by the results in unsaturated conditions that globally are higher than saturated conditions. It is also interesting to compare P_1 results in saturated and unsaturated conditions. To do so, unsaturated values were normalized by the value obtained below water level in pushed-in saturated conditions (P_1*), as represented in Figure 10.37.

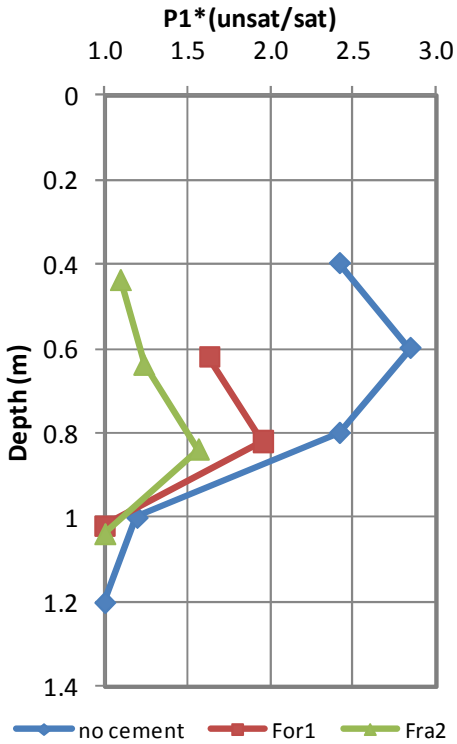


Figure 10.37 - P_1* normalized parameter obtained in pushed-in conditions.

Normalized P_1* results for different levels of cementation were plotted against depth, revealing its general decrease with cementation level increase. This trend is expected since the order of magnitude of cohesion intercept (well represented by such ratio) increases with cementation level while suction remains essentially the same.

10.4.3. Intermediate parameters

Due to the deviation of P_0 and to the differences with P_1, intermediate parameters in installed conditions although havin the same meaning, will not correlate with engineering properties with the same patterns. In fact, the very low values of A-readings and P_0 values due to the absence of densification in pre-installed conditions are associated to low horizontal stresses that have a strong effect on the parameters depending highly on P_0. These considerations have great impact in I_D and K_D, while results of E_D parameter can be seen as representative of stress-strain behaviour observed in pre-installed conditions. In Figure 10.38 it is possible to compare the "normal" behaviour of I_D represented by pushed-in conditions and the inadequacy of results obtained in pre-installed saturated conditions. For non-cemented specimens the value is around 0.5 (typical of silty clays), while for cemented increases to abnormal values (50, 100), which is a direct consequence of a simultaneous lower P_0 and higher P_1, when compared to "pushed-in values".

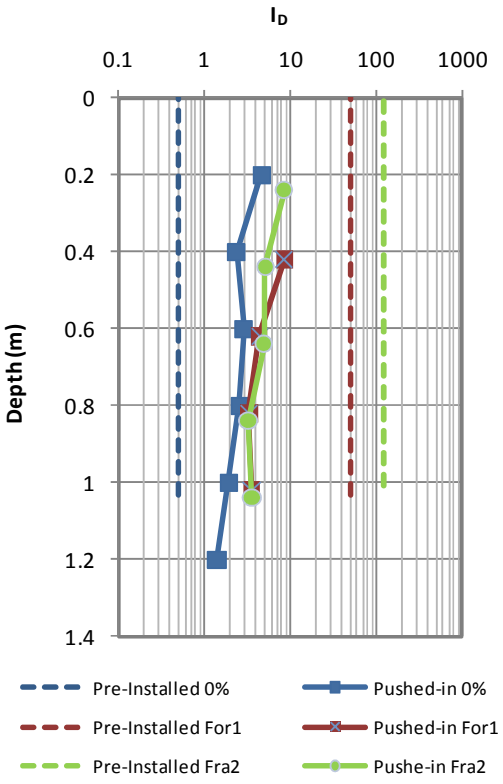


Figure 10.38 - I_D parameter obtained in installed and pushed conditions.

K_D parameter is strongly dependent on P_0, and so, its interpretation will be affected by these unusual values. Figure 10.39 highlights the weight of cementation level on the discrepancy of results, showing that for non cemented soils the parameter obtained in

saturated conditions displays the same values for both pre-installed and pushed-in conditions (blue line), while cemented mixtures present an increasing deviation with cementation level. It is also interesting to note that there is a general decrease of the parameter with depth, suggesting some sensitivity for suction evaluation. However, Figure 10.40 clearly shows a non consistent correlation between K_D values on both conditions, with inverse proportionality, showing again the inadequacy of the interpretation in pre-installed conditions. This is just a corollary of the high empiricism of K_D values, a well stated inlet for the conventional testing procedure (pushing and expanding), but totally unfit to the ideal condition of an “intact state”.

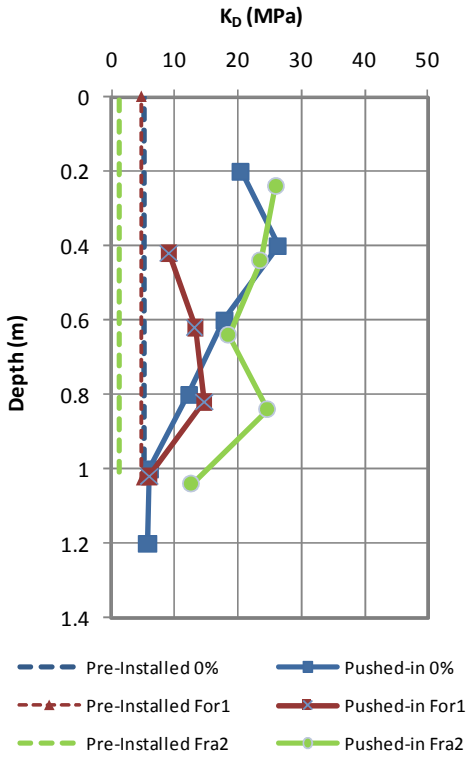


Figure 10.39 - K_D parameter obtained in installed and pushed-in conditions.

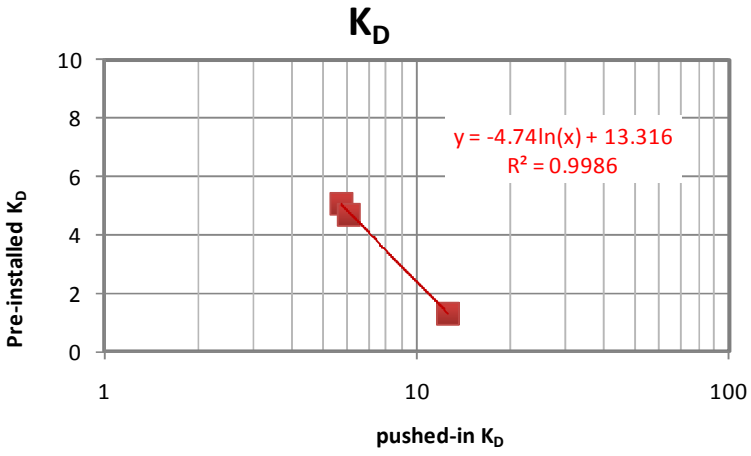


Figure 10.40 - K_D comparison in installed and pushed conditions

E_D value, however, makes a difference, since it really reflects stiffness under the plane deformation of the membrane. Figure 10.41 represents E_D results, revealing that both pushed-in and pre-installed conditions are sensitive to cementation level. Furthermore, the comparison between them reveals that in non-cemented conditions, the values of such a stiffness increases with the densification induced by pushing-in the blade, while in cemented mixtures there is a clear drop in stiffness due to the partial loss of cementation structure created by the insertion of the blade, partially minimized by some stiffness expected increase related to densification and increase in induced stress state during installation.

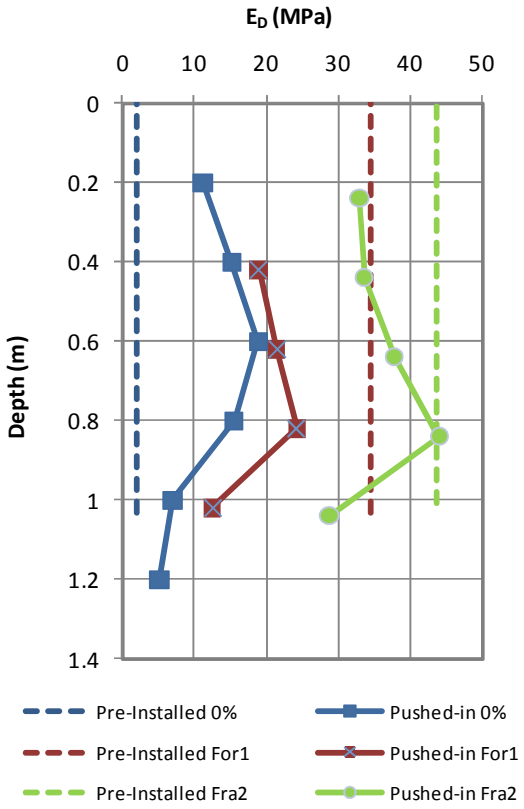


Figure 10.41 - E_D parameter obtained in installed and pushed-in conditions.

Following the approach followed in the analysis of basic parameters, in-situ and CemSoil intermediate parameters obtained after insertion by pushing were compared as shown in Figure 10.42. Keeping in mind that there is a gap of 1.0m between comparable results, data clearly reveals the expected equivalent condition of natural soil between For1 and Fra2 mixtures in what concerns to strength and stiffness parameters (respectively, K_D and E_D), while all the situations are coincident in terms of identification parameter (I_D).

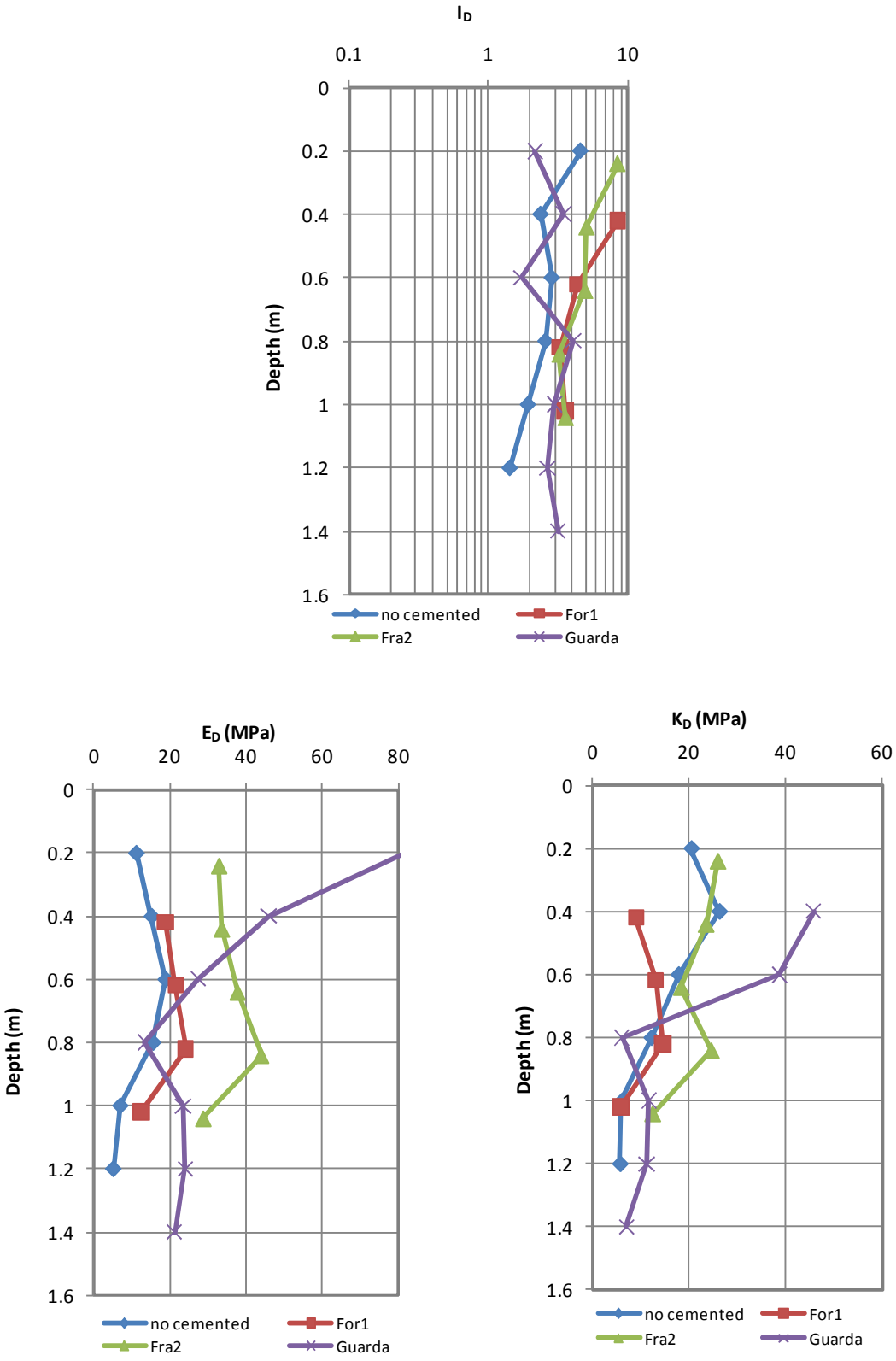


Figure 10.42 - Intermediate parameters obtained in pushed conditions.

In Figure 10.43 unsaturated values normalized to saturated ones (I_D*, E_D*, K_D*) are presented, aiming the analysis of the influence of saturation levels.

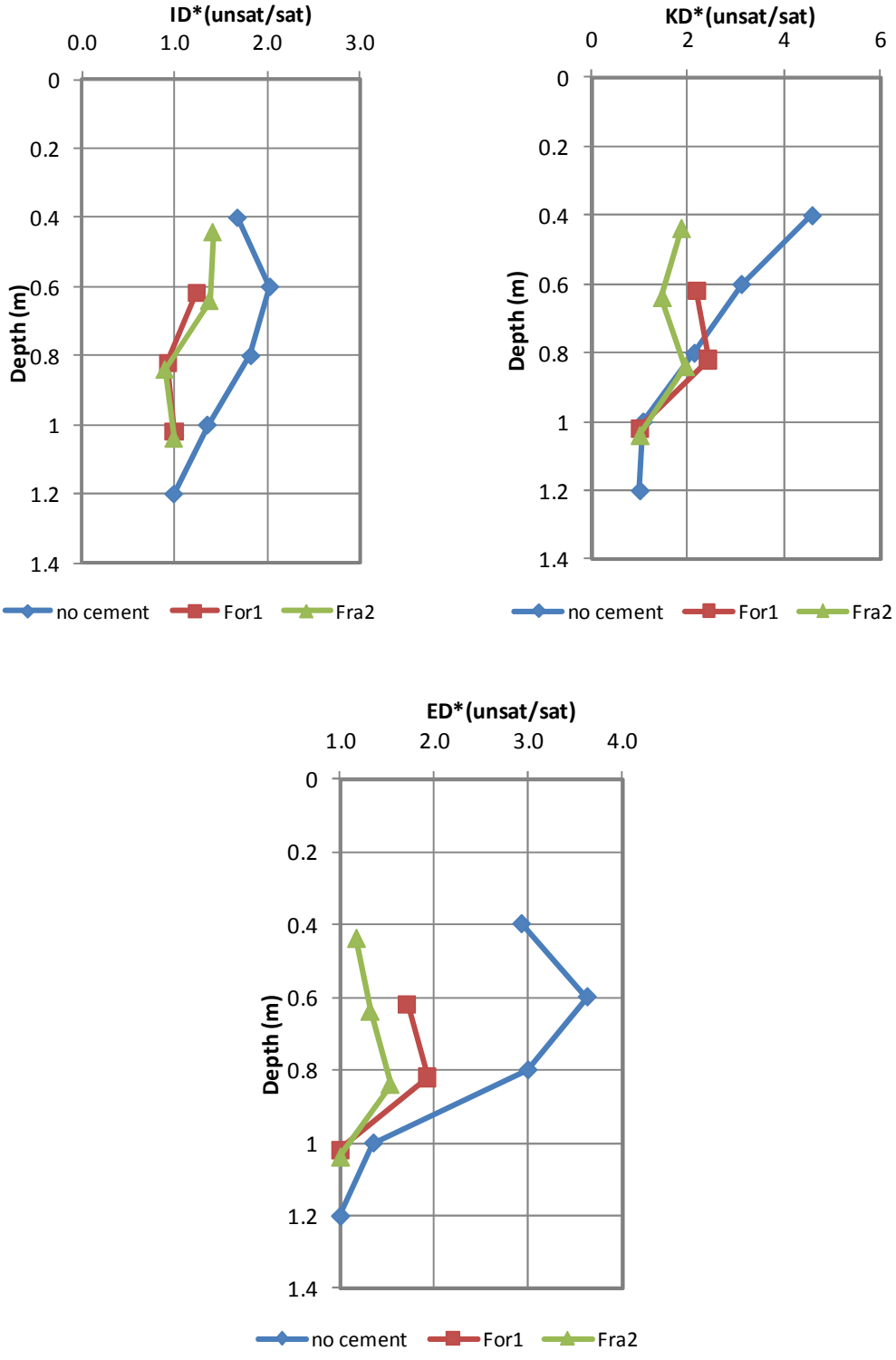


Figure 10.43 - I_D*, K_D* and E_D* normalized parameters obtained in pushed conditions.

In this figure, I_D values reveals independency towards saturation levels in cemented soils, due to the low relative influence of suction factor when compared to cementation, while in non-cemented samples suction plays a fundamental role in the magnitude of the parameter. On the other hand, the remaining intermediate parameters seem to be

more affected by suction as cementation level decreases, following the behaviour observed in the case of P_1, already discussed above in this section. All these normalized parameters and also normalized compressive strength (q_u*) were plotted against cementation level (represented by q_t), as shown in Figure 10.44, revealing similar logarithmic trends observed in all situations. Accepting that observed differences are mainly due to suction, data leaves no doubt about its decreasing influence with increasing cement content, which has a relevant consequence on studies on cemented materials (usually analyzed in diverse moisture conditions, both in-situ and in laboratory), where suction can influence the respective analysis, but fortunately with no impact in main engineering properties.

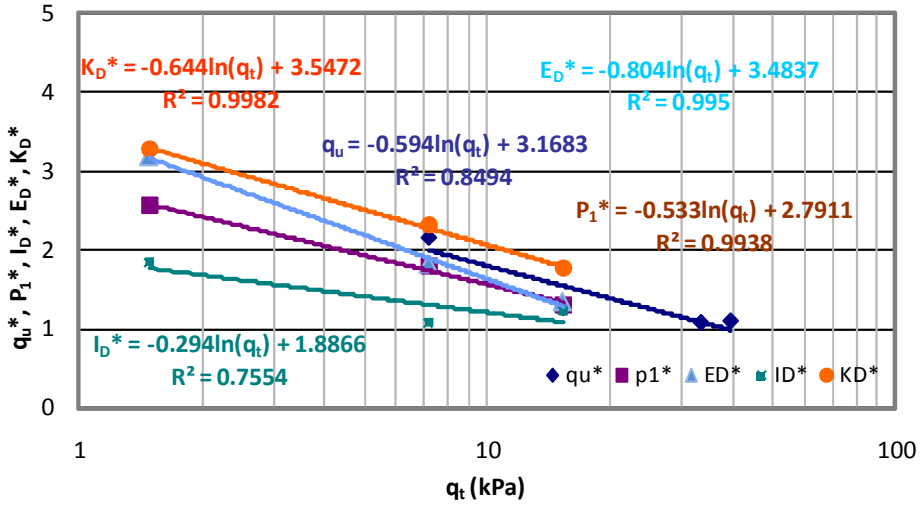


Figure 10.44 - Normalized parameters as function of tensile strength.

10.5. Deriving geotechnical parameters

The deduction of geotechnical parameters related to strength and stiffness properties presented in the following sections, will be performed only for pushed-in conditions, since the established correlations refer only to this situation and in pre-installed conditions, K_D and OCR parameters cannot be interpreted as previously discussed.

10.5.1. Strength

The main purpose of the current research was established to calibrate the deduced correlations by means of triaxial testing results, obtained for “undisturbed” natural soil samples. Effects of sampling and space variability have a major influence generating

conservative correlations, particularly in the case of lightly and sensitive cemented material. Figure 10.45, shows the evolution with depth of corrected angle of shearing resistance determined by Cruz et al. (2006) proposal and the respective normalized parameter (ϕ^*) in relation to saturated results.

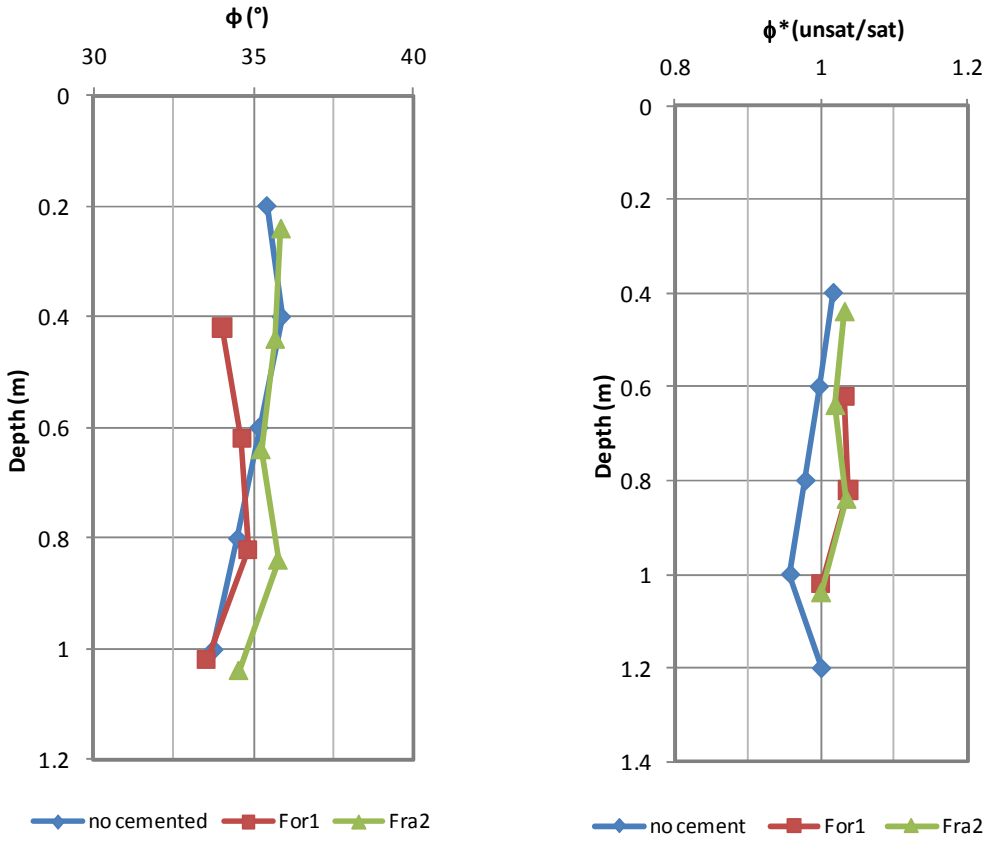


Figure 10.45 - Angle of shearing resistance results.

The results obtained under saturated conditions seem to be independent of cementation level, ranging from 34.5º to 36.2º, which are higher than 33º obtained reference triaxial testing value. These higher values show that correction factor is insufficient, which may be related to the expected conservative evaluation of cohesion intercept from which correction factors are calculated. Above water level, there is a tendency to the parameter decrease with depth and to be consistently higher in 1 - 2º. If it is accepted that shear resistance is homogeneous in the whole sample, these differences might be related to the influence of suction on respective determination. Once again, DMT seem to give positive answers to suction effects.

When OCR correlation proposed by Cruz et al. (2004, 2006) is used to derive cohesion, its evolution with depth reveals a general decrease of the parameter, reaching the lower value in the saturated measurements, as presented in Figure 10.46.

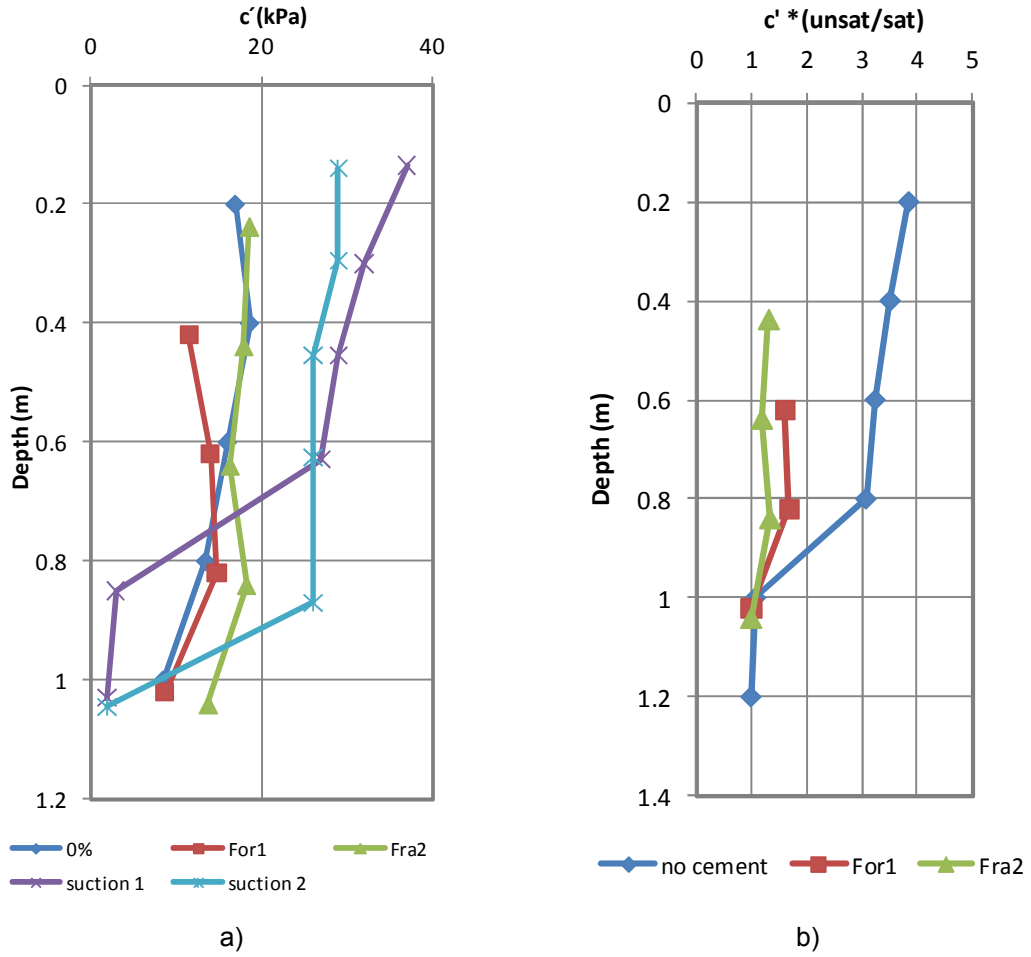


Figure 10.46 - c' deduced by DMT: a) CemSoil; b) normalized c'*.

These results strongly sustain DMT's adequacy not only to deduce cohesion but also suction effects, since the earlier is expected to be uniform in the whole penetrated soil. In fact, there is a clear increase of DMT derived cohesive intercept with the cementation level, showing a marked difference between results of non-cemented and cemented samples, with the latter at least 3 times higher. Furthermore, DMT's sensitivity to detect suction is confirmed either by non-cemented sample results in unsaturated conditions (considering that in this case the results should reflect suction alone) and by the evolution of the normalized parameter. The data reveals an obvious drop in this influence when cementation bonding increases, meaning that test results might reflect both suction and cohesion intercept.

The correlations used to derive effective cohesion intercept were established with base in careful triaxial testing programs executed on residual soil (naturally cemented) "undisturbed" samples (Cruz et al., 2004b; Cruz & Viana da Fonseca, 2006a). However, as stated in these previous works, the obtained results were affected in an unknown extent by sampling disturbance and space variability, and therefore the reference values used to settle the correlations may be deviated from "in-situ" real conditions. Using artificially cemented soils, it was possible to avoid these effects, since triaxial and CemSoil samples were prepared in the same conditions and microfabric differences (usually observed between naturally and artificially cemented soils) can also be considered irrelevant in the present case, thus creating almost ideal conditions comparing purposes. Being so, all the important influence factors were closely controlled, and so the experience can be seen as appropriate for calibration of the empirical correlations proposed by Cruz et al. (2004b) and Cruz & Viana da Fonseca (2006a).

Since DMT seems to detect cohesion intercept due to interparticle cementation and suction capillarity forces, it is important to find some references within the experience to evaluate shear strength suction contribution, once the reference for cohesion naturally arises from triaxial testing. In this context, departing from measured suctions, already presented in this chapter, it is possible to evaluate its contribution to shear strength, throughout the following term in the Fredlund et al. (1978) expression:

$$(u_a-u_w) \tan \phi^b \qquad (10.1)$$

being u_a, the atmospheric pressure, u_w the pore pressure and ϕ^b the index ratio that will vary with suction (similar to the concept of angle of shearing).

The term (u_a-u_w) corresponds to the measured suction on tensiometers, while for ϕ^b, a 13.9º reference value was obtained by Topa Gomes (2009) in Porto Granites (W_4 to W_5), which was assumed to be a reasonable approach in this analysis. Considering the homogeneity of the triaxial and CemSoil box samples, triaxial cohesion intercept can be assumed as representative of the latter in the whole sample. Being so, the higher results obtained above the water level should somehow reflect the suction. If that is accepted, the sum of results of suction contribution and triaxial cohesion gives a global cohesive component (c'_g) tested by DMT. Writing these results as function of vOCR, as proposed by Cruz et al. (2004b) and Cruz & Viana da Fonseca (2006a), a correlation

for cohesion or cohesion and suction (when the latter is present), can be outlined. In Figure 10.47 the overall cohesive intercept (c'_g), is plotted against vOCR, revealing different evolution rates as function of cement content.

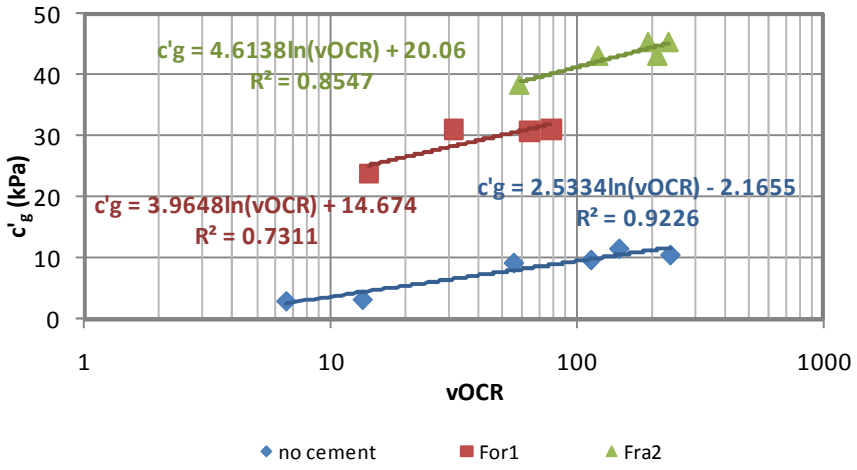


Figure 10.47 - Correlation of global cohesion intercept (c'_g) as function of OCR for no cemented and cemented mixtures.

In Figure 10.48, previous and present global correlations are presented. The correlation proposed by Cruz et al. (2004b) was based on a narrower band of vOCR values and the best fitting considered function was a straight line, while in the present case is better represented by a logarithmic function.

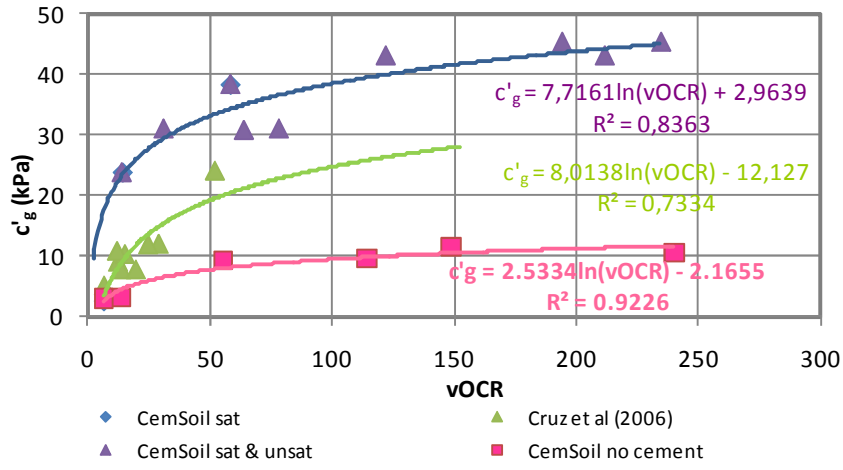


Figure 10.48 - Correlations of global cohesion intercept (c'_g) as function of vOCR.

Considering this new approach, an alteration of the earlier proposal to the same function type was introduced, revealing an obvious parallelism between both lines and suggesting that the effect of a specific sampling process is a reduction of cohesion intercept, whose extent may be dependent of sampling equipments and procedures. In the present study, the results were obtained by statically pushed-in 70mm Shelby tubes.

As stated above, to obtain suction contribution in shear strength, ϕ^b had to be assumed, and so it is important to analyse its influence in final results. A variation of 5º around the reference value was found to be large enough, although references on the subject are not abundant. Figure 10.49 represents the main correlation obtained for ϕ^b equal to14º (Equation 10.2), placed within a lower and upper bounds corresponding to ϕ^b of 10 and 20º, respectively.

$$c'_g = 7.716 \log (OCR) + 2.96 \qquad (10.2)$$

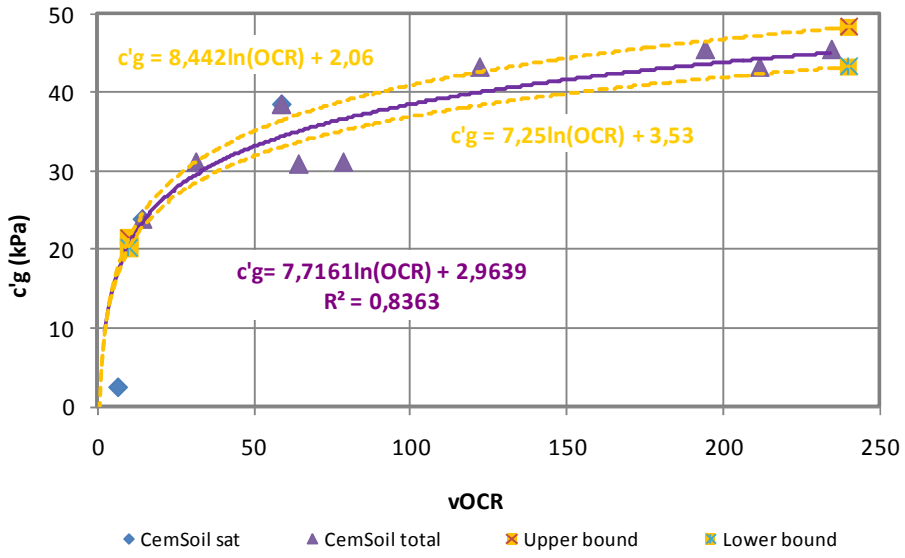
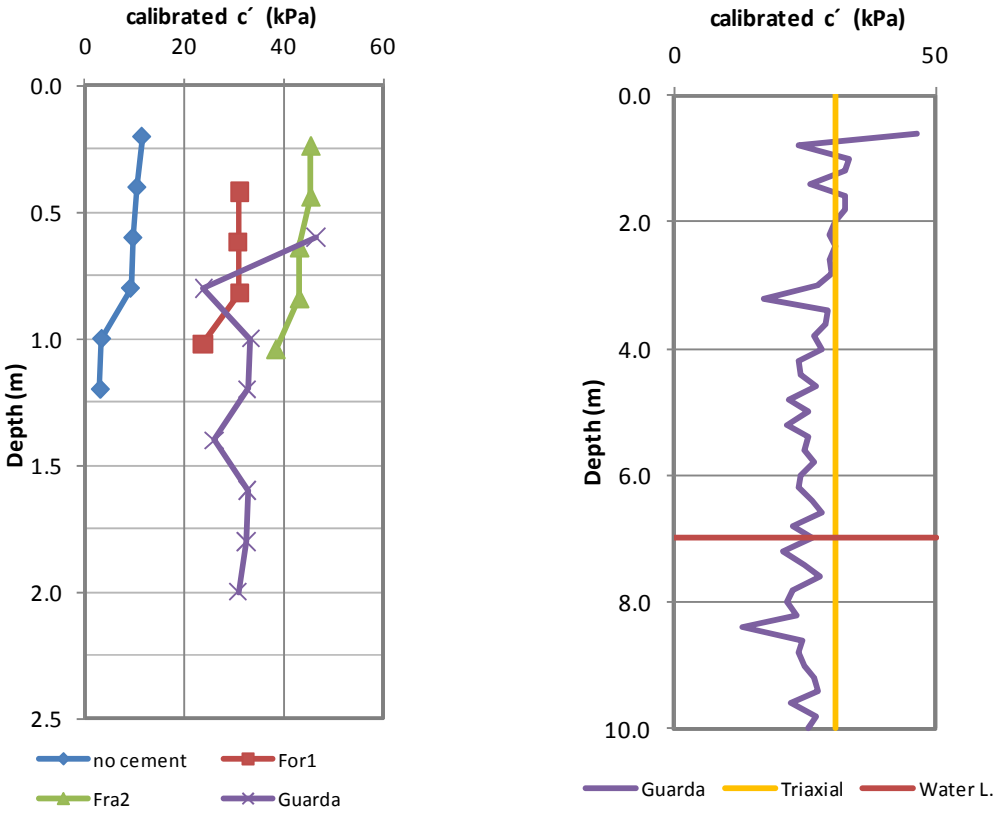


Figure 10.49 - Upper and lower expected bounds for overall cohesive intercept (c'_g) correlation.

As it can be seen the variation is not significant, and the mean value of 15º should be a reasonable approach, when the ϕ^b is not available.

The evolution of global cohesion intercept, c'_g, derived from direct application of Equation 10.2 to the present experimental data and to in-situ Guarda DMT data, is

presented in Figure 10.50, revealing the same trends observed in all other analyzed parameters. Moreover, the whole in-situ profile deduced this way shows a general decrease of overall cohesive intercept until the water level is reached. Afterwards, results tend to be fairly constant.



a) b)

Figure 10.50 - Overall cohesive intercept (c'_g) results in: a) Cemsoil; b) In-situ.

These observations confirm the good efficiency of DMT to evaluate the two components of strength generated by suction and interparticle bonding. The differences observed with triaxial data reference value are considered acceptable for the purpose of cohesion reduction, especially because they are on the safe side.

Another interesting approach is to find out the possibility of using P_1 parameter directly in the evaluation of cohesion intercept since it exhibits good correlations with tensile, compressive and deviatoric stresses, as shown in Figure 10.51. However, OCR has the great advantage of including I_D in calculations, which might be important for settling

correlations in cemented soils with other origins, especially those with higher fine content, where deviations to the trends identified in the present work shall be expected.

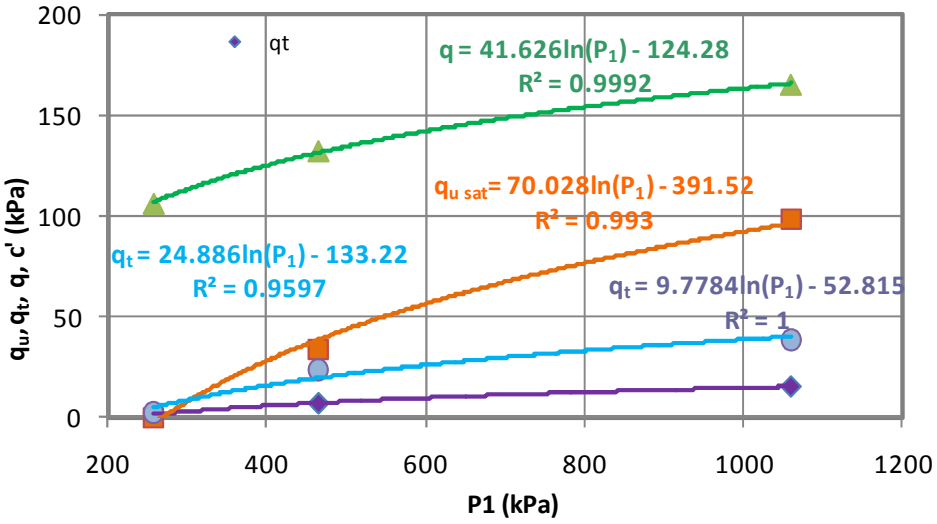


Figure 10.51 - Evolution of uniaxial compression, triaxial deviatoric and tensile strength with P_1 pressure.

As it was already explained, the proposal for correcting angle of shearing resistance (Cruz & Viana da Fonseca, 2006a) when a sedimentary approach is used (Baldi, 1986), was settled using cohesive intercept value derived from the discussed cohesive correlation. The re-adjustment of the previous data and present results generates the new trend for correcting angle of shearing resistance, presented in Figure 10.52.

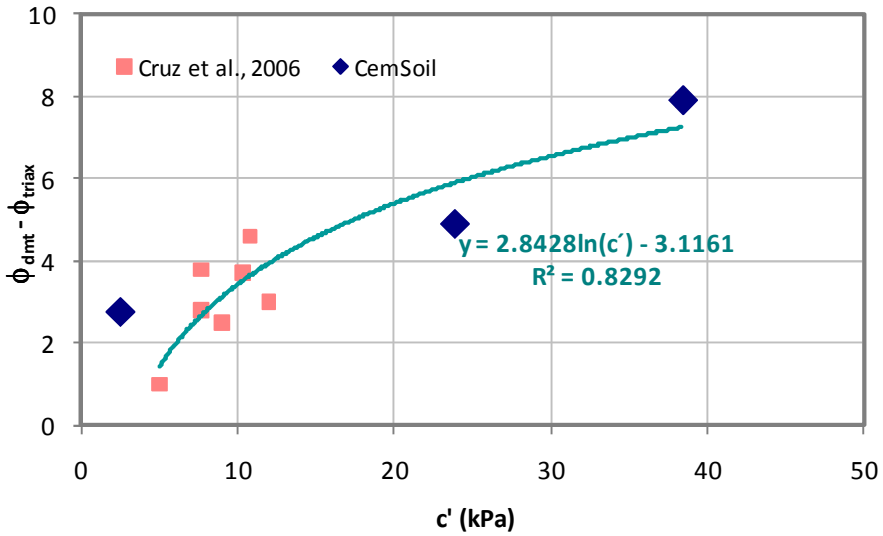


Figure 10.52 - Correlation to correct angle of shearing resistance.

Using this new correction factor, the CemSoil box pushed-in and in-situ obtained results are compared with the respective triaxial testing result, revealing adequate representation of real situation. Figure 10.52 shows that CemSoil box saturated results converge for triaxial results, while in-situ data slightly decrease with depth, due to suction effects. Saturated values converge to triaxial data, on the conservative side.

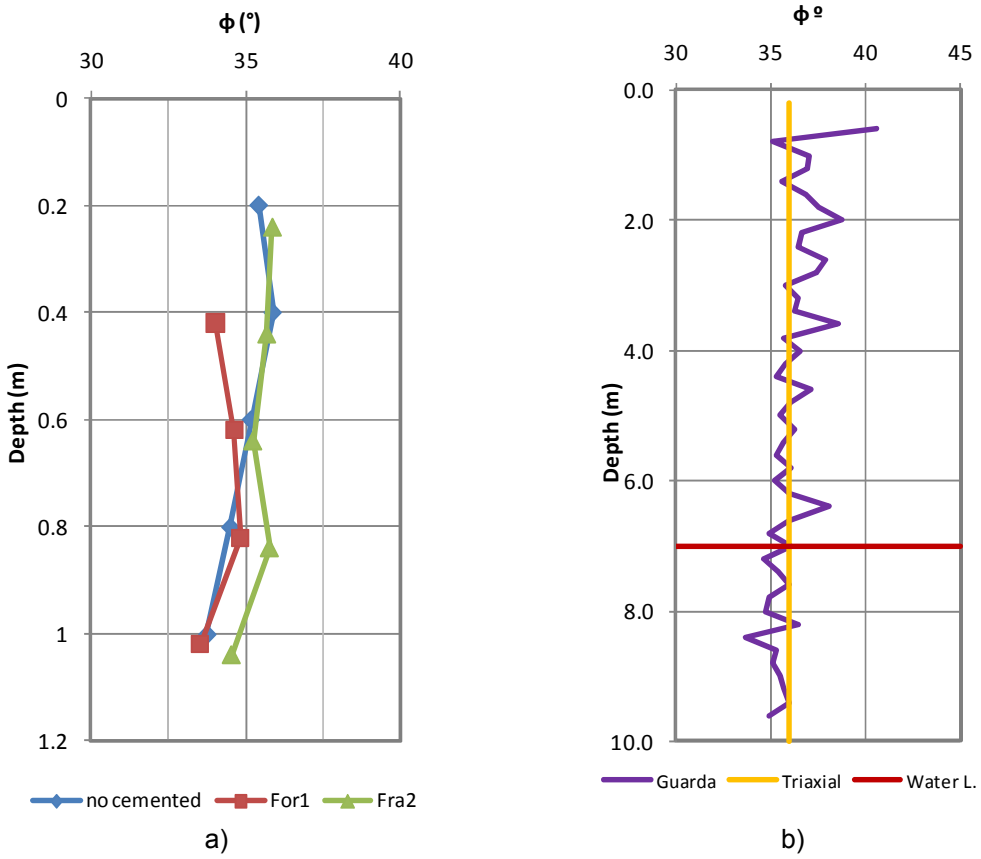


Figure 10.53 - Triaxial and deduced angle of shearing resistance results in: a) Cemsoil; b) In-situ.

10.5.2. Stiffness parameters

10.5.2.1. Deriving geotechnical parameters

One of the most important features of DMT is its efficiency deducing stiffness moduli, based in the measurement of pressure-displacement answer, as well as the possibility of assuming an approach for its interpretation. The reference parameters used in stiffness evaluation are the Constrained modulus as defined by Marchetti (1980) or the Young modulus deduced from the former through Elastic Theory considerations, as well as G_0 deduced from triaxial testing results (Viana da Fonseca, 1996; Viana da

Fonseca et al, 1998, 2008) or, more recently, from Cross-Hole tests (Cruz & Viana da Fonseca, 2006a).

10.5.2.2. Calibration of correlations using triaxial data

For calibration of correlations using laboratory data, it is important to compare DMT results with those deduced from triaxial testing for the same conditions of saturation and confining stresses (25 kPa). In this context, E_D was taken as the reference DMT parameter to compare with triaxial deduced moduli, namely the initial tangent modulus (E_i) and secant moduli ($E_{s0.1\%}$ and E_{s50}). As triaxial tests were performed in saturated conditions, comparisons were made with pushed-in saturated results. Figure 10.54 presents the evolution of the parameter with depth as well as its proximity with reference triaxial deduced moduli, revealing that DMT parameter is more or less positioned between $E_{s0.1\%}$ and E_{s50}, far from initial tangent modulus (E_i). These trends are also confirmed by the correlations with the reference moduli normalized or not to the mean effective stress (p'_i), as presented in Figure 10.55 and 10.56 and The projection of triaxial values against E_D obtained both in pushed-in and pre-installed conditions (Figure 10.55) reveal that the trends are very close and parallel, with the best fitting curves following exponential functions. In non cemented soils the lower values of E_D are obtained in pre-installed conditions, probably due to the influence of densification resulting from penetration. On the other hand, in cemented soils pre-installed conditions preserve the whole cementation structure and thus E_D is supposed to be higher.

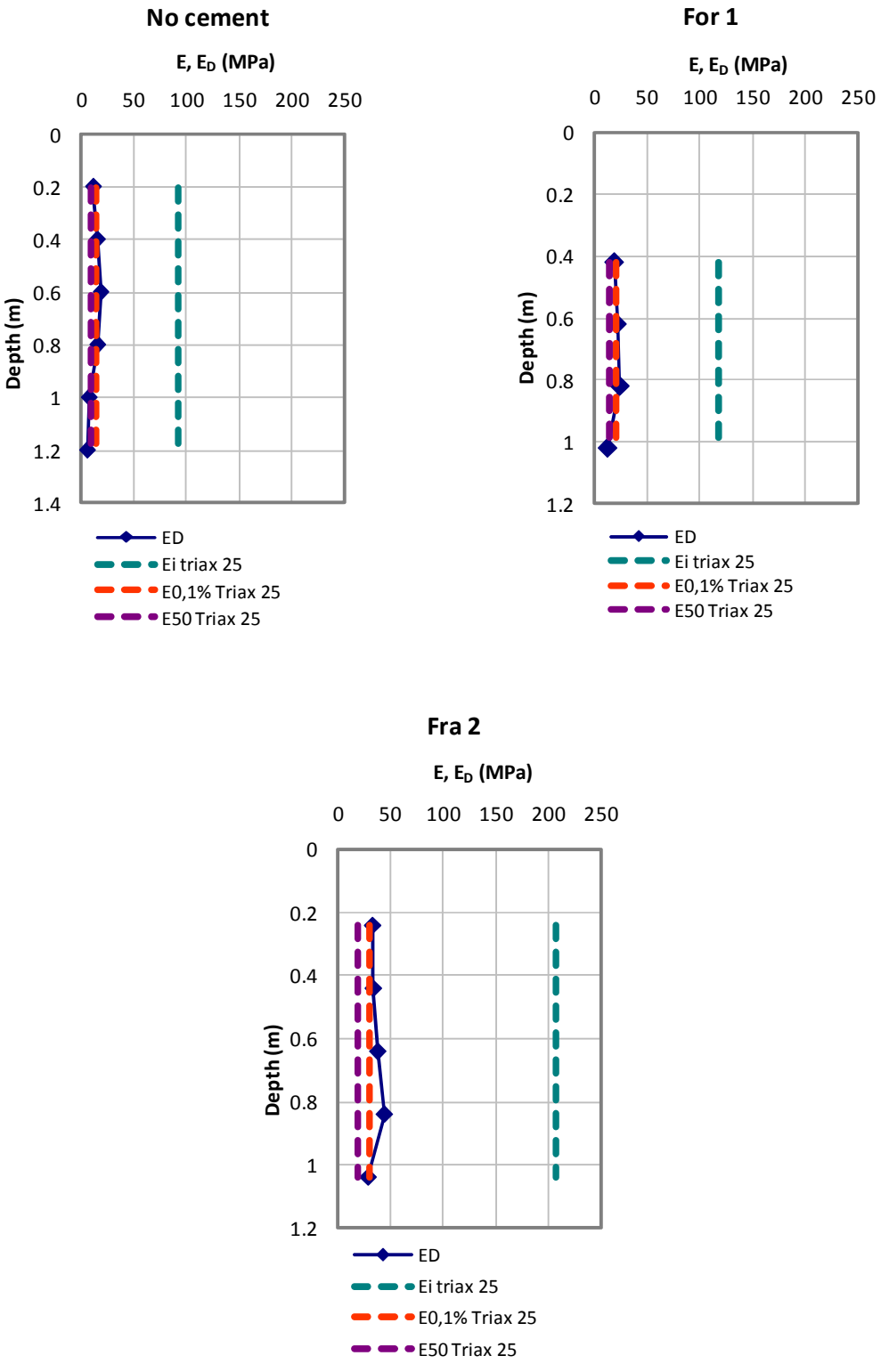


Figure 10.54 - Comparison of E_D and triaxial reference moduli.

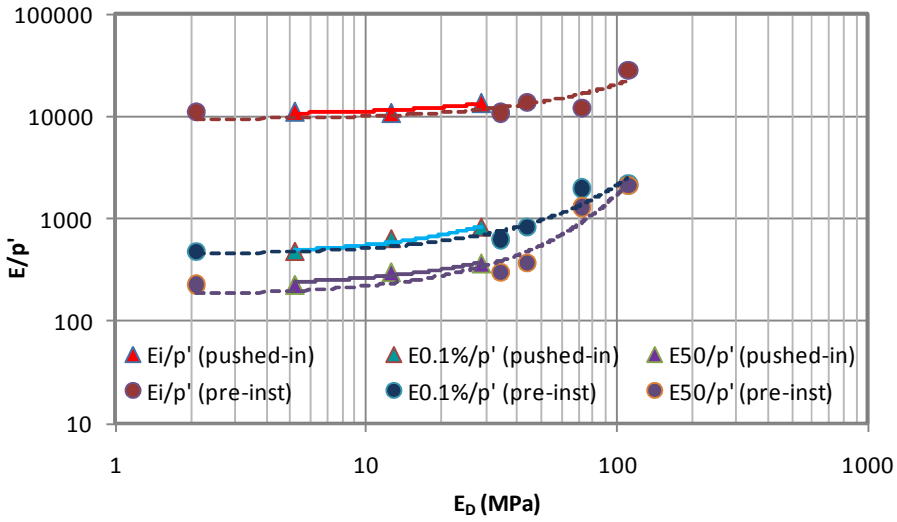


Figure 10.55 - Comparison of E_D and normalized triaxial reference moduli.

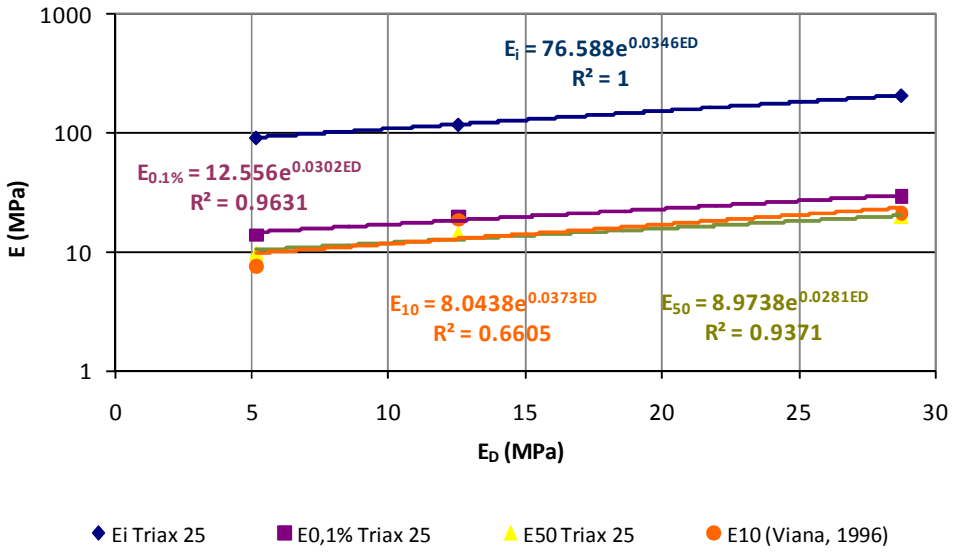


Figure 10.56 - Comparison of initial tangent and secant deformability moduli and E_D

Figures 10.57 and 10.58 represent the ratios E/E_D as function of a normalized parameter, P_{0N}, as proposed by Viana da Fonseca (1996) and already presented in Chapter 7. Although data is scarce, it seems to confirm the general previous observations, showing an evident common trend as well as the same gap between secant and tangent modulus.

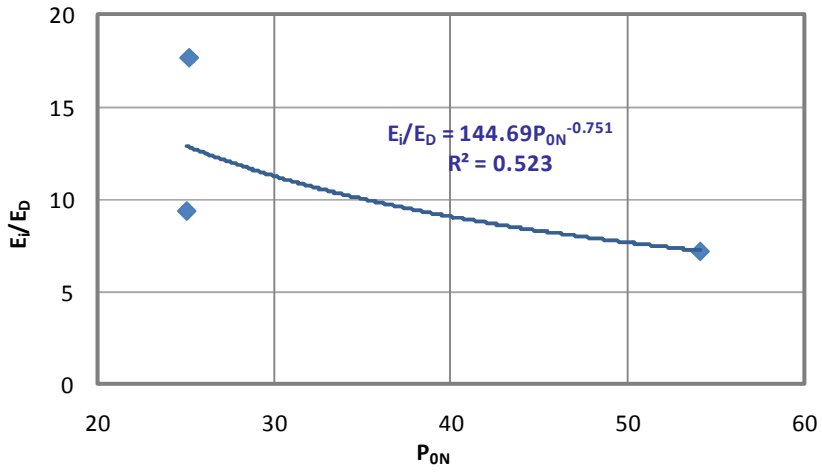


Figure 10.57 - Variation of ratio E_i/E_D as function of P_{0N} normalized parameter.

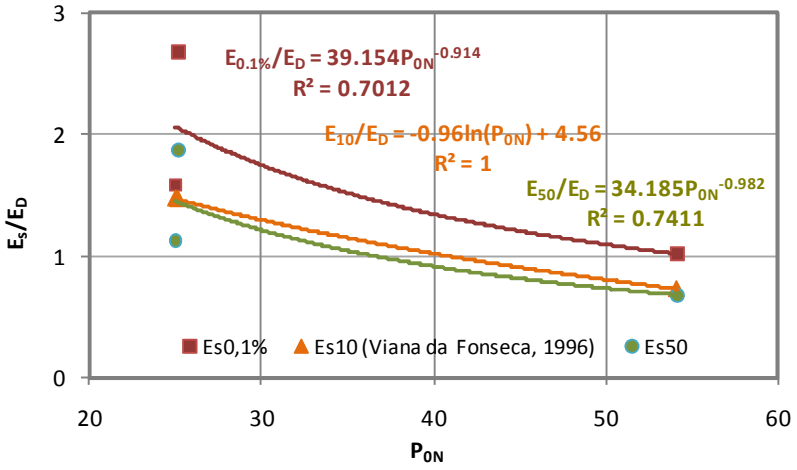


Figure 10.58 - Variation of ratio E/E_D as function of P_{0N} normalized parameter.

Finally, constrained modulus was compared with in-situ Guarda results, shown in Figure 10.59), which also presents CemSoil box normalized parameter (M*). CemSoil and in-situ results follow the general observed patterns with the other studied parameters, being the in-situ results situated between For1 and Fra2 samples. Normalized M* also follows previous trends, revealing that influence of suction is high for the low cementation level. In fact, an increasing cementation induces increasing stiffness, which reduces the suction influence in final results.

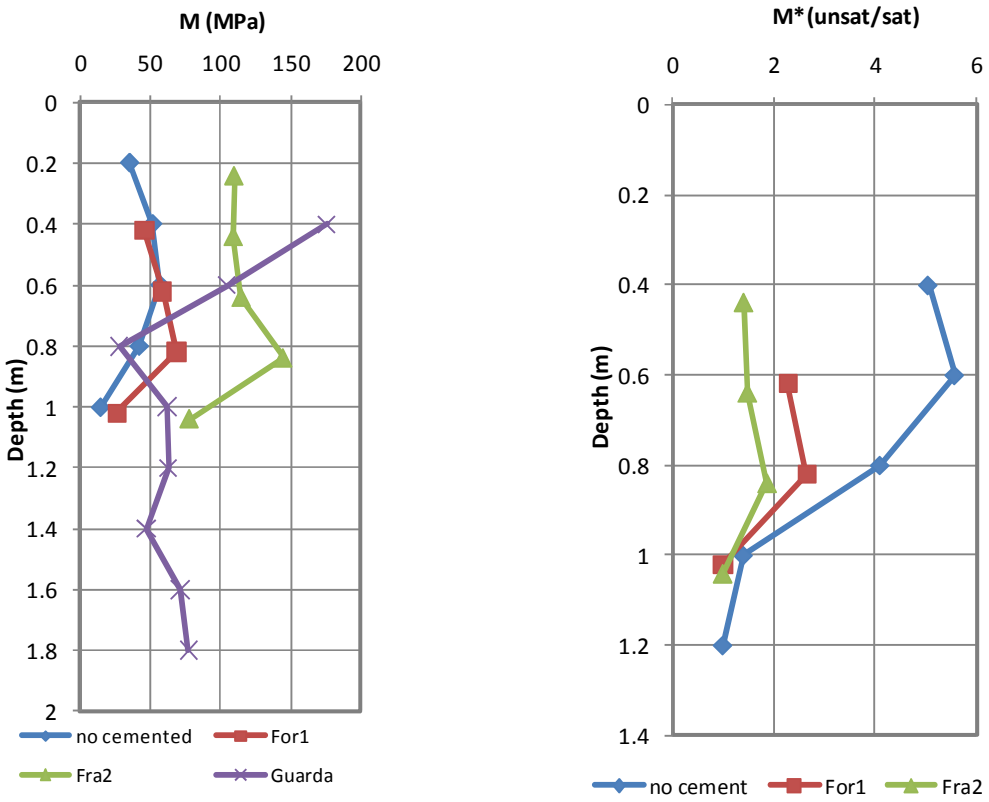


Figure 10.59 - Constrained Modulus: a) CemSoil and Guarda in-situ results; b) Normalized parameter, M*

Another important detail that ought to be dealt from the present data is the attempt to evaluate the level of strain corresponding to DMT stiffness measurements. In this context, E_D results related to both pre-installed and pushed-in conditions were positioned in E_{sec} versus axial strain plots obtained in the corresponding triaxial tests (Figure 10.60 and Figure 10.61, respectively), while E_{DMT} derived through constrained modulus (M) applying Elasticity Theory (considering a Poisson's ratio equal to 0.3) is represented in Figures 10.62 and 10.63. A summary of the axial strains related to each situation is presented in Table 10.3.

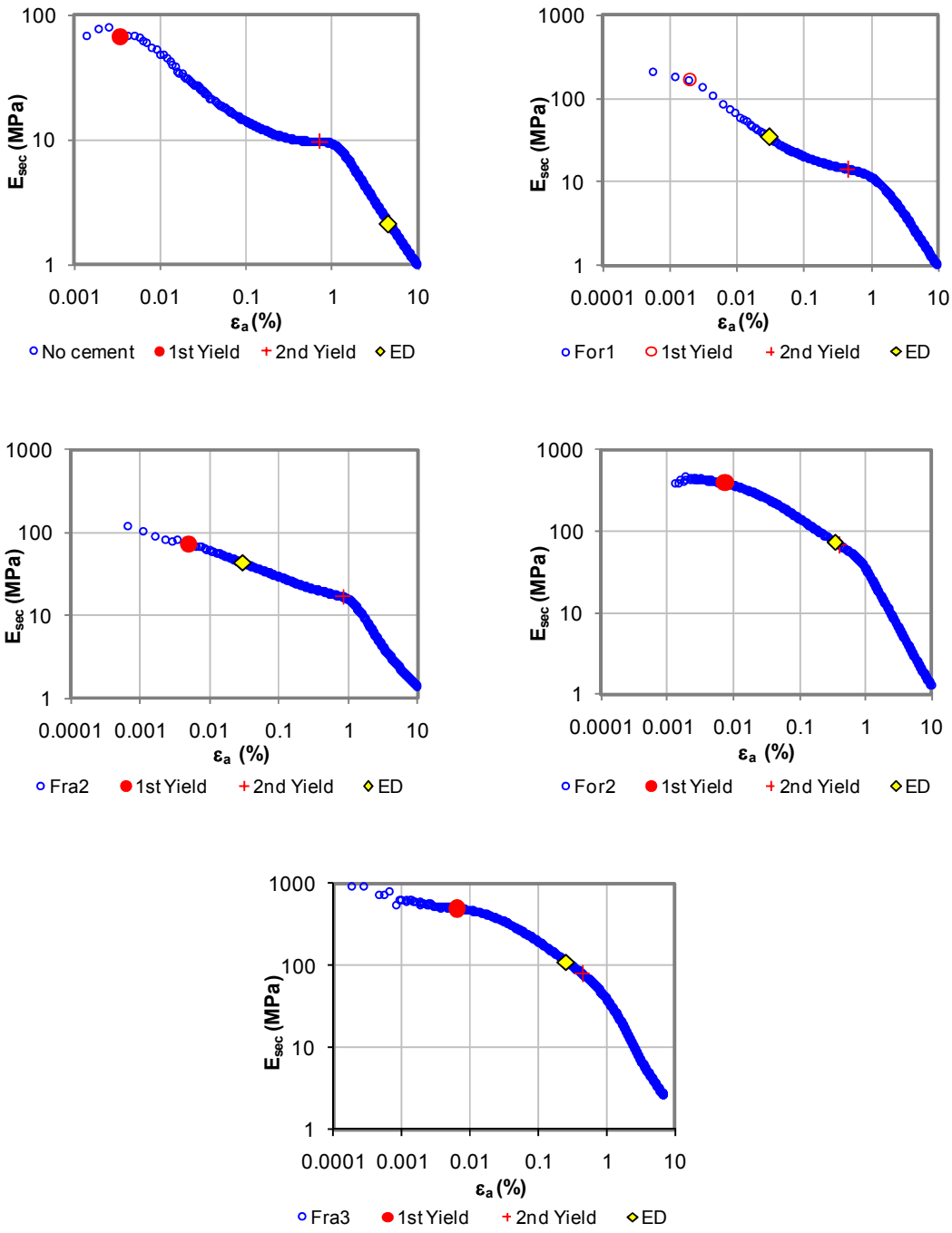


Figure 10.60 - E_D location in E_{sec} vs. axial strain (pre-installed conditions.

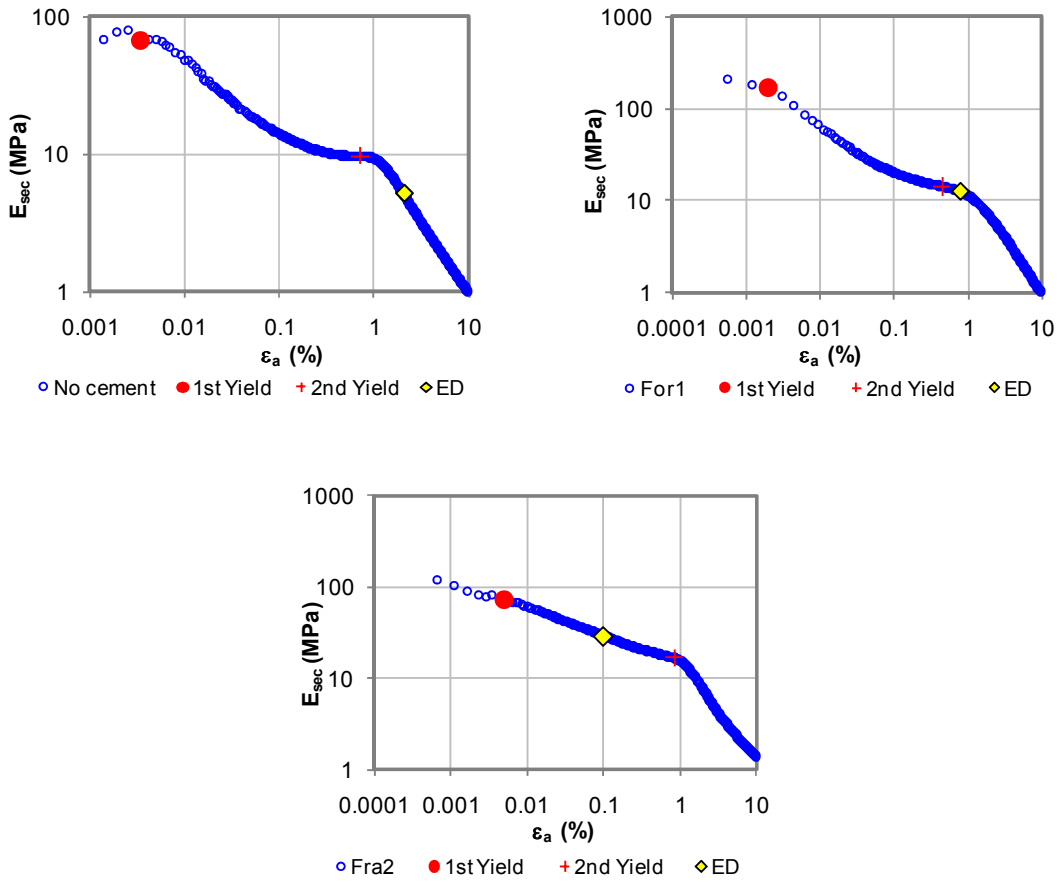


Figure 10.61 - E_D location in E_{sec} vs. axial strain (pushed-in conditions).

Table 10.3 - Summary of axial strains related to E_D and E_{DMT}.

Parameter	Conditions	Non-cemented	Cemented
E_D	Pre-installed saturated	4.5×10^{-2}	$10^{-4} – 3.5 \times 10^{-3}$
	Pushed-in saturated	2.1×10^{-2}	$10^{-3} – 10^{-2}$
E_{DMT}	Pre-installed saturated	7.0×10^{-2}	$10^{-4} – 5.0 \times 10^{-3}$
	Pushed-in saturated	1.4×10^{-2}	$10^{-4} – 10^{-3}$

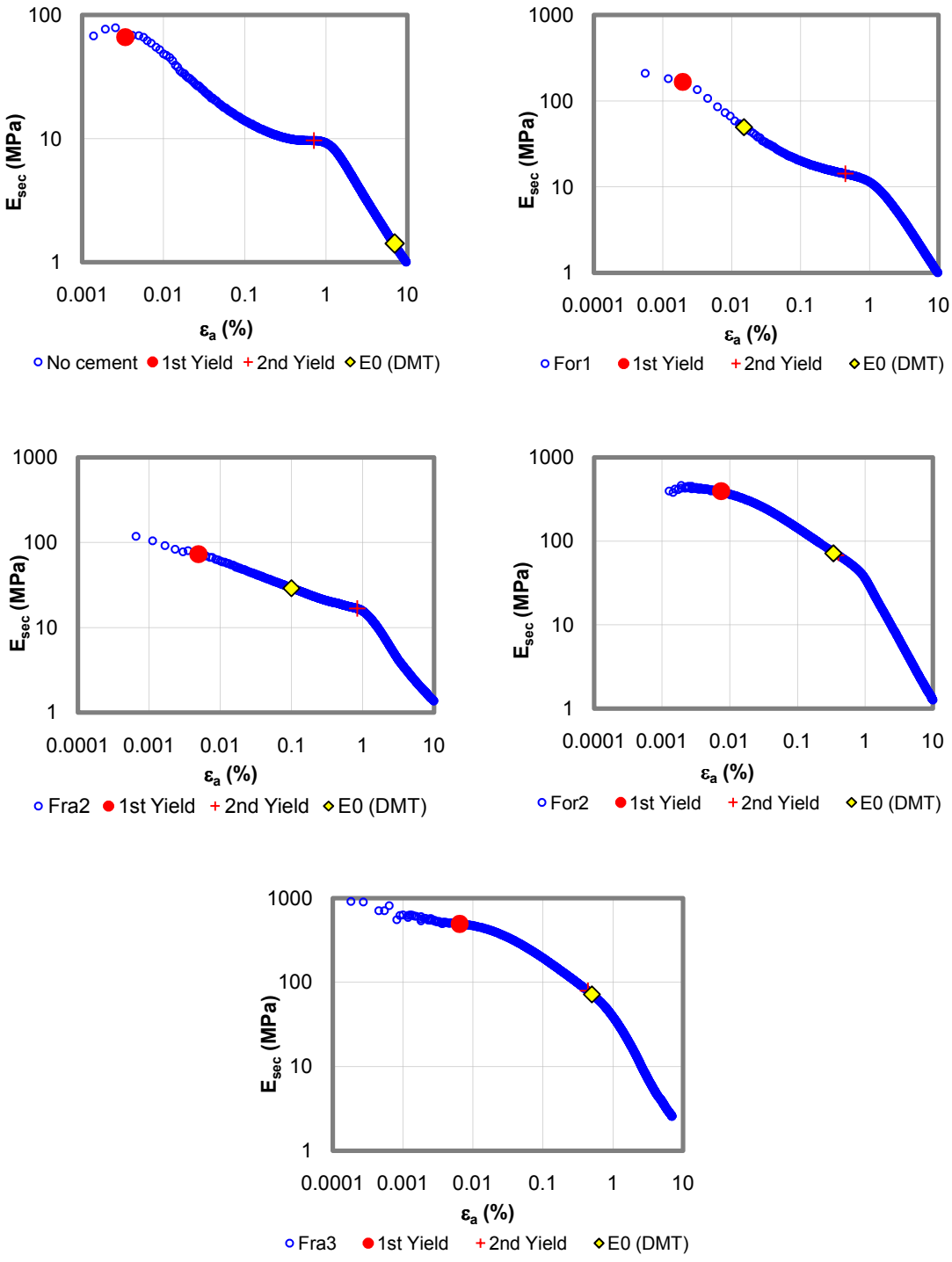


Figure 10.62 - E_{DMT} location in E_{sec} vs. axial strain (pre-installed conditions).

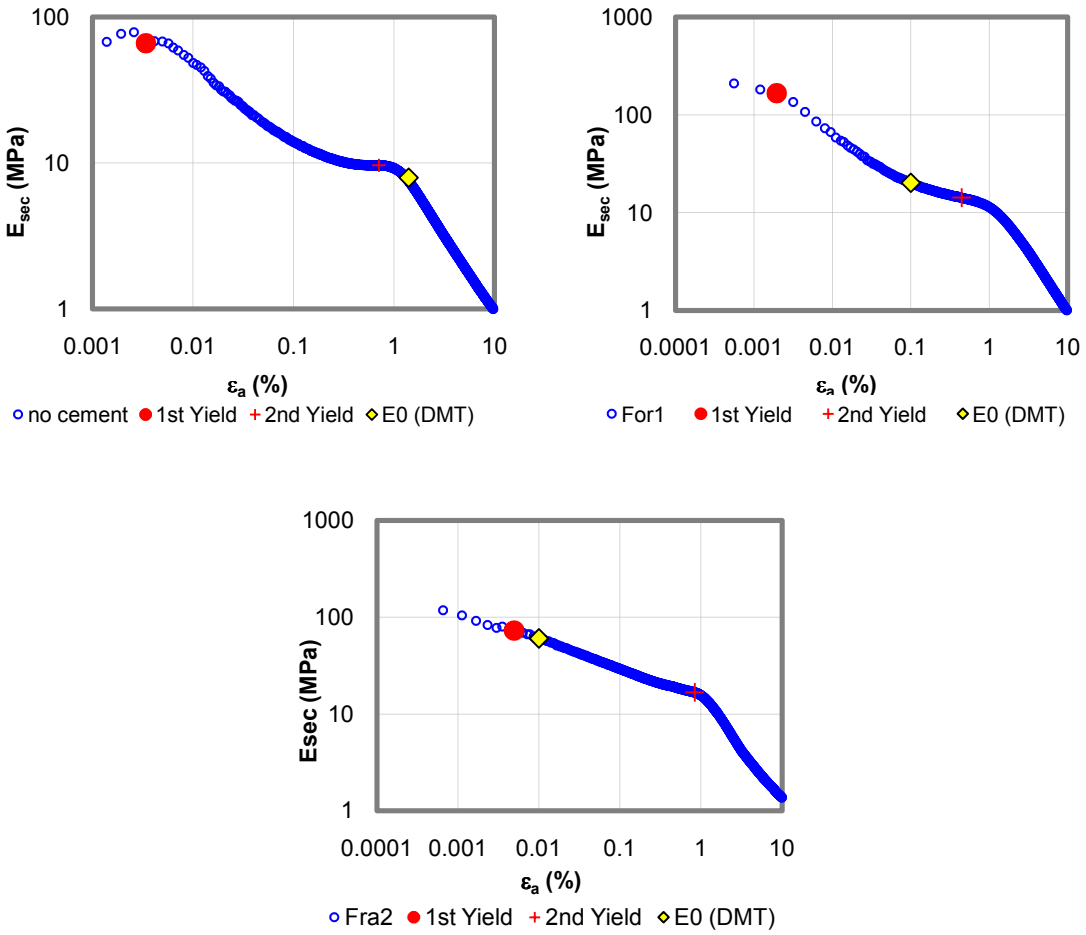


Figure 10.63 - E_{DMT} location in E_{sec} vs. axial strain (pushed-in conditions).

The presented data highlights some important aspects summarized below:

a) In non cemented soils, strain level associated to E_D and E_{DMT} lies in the intervals found in bibliography (10^{-2}), while in cemented soils the global results seem to fit within an interval with a lower order of strain magnitude (10^{-2} to 10^{-4});

b) In cemented mixtures, generally E_D and E_{DMT} are within 1st and 2nd yield (as defined by Malandraki & Toll, 2000) while in non-cemented soils they are always situated at higher axial strains than the 2nd yield;

c) Comparing the influence of installation conditions, the results of dilatometer modulus follows an expected trend with pre-installed situations corresponding to lower levels of strain, which is obviously expected due to the skeleton preservation resulting from the special condition of pre-installed assemblage;

d) Derived E_{DMT} results follow a opposite trend with the lower level of strain corresponding to pushed-in data; this situation might be related to the

empirical correction factors applied to E_D (Marchtetti, 1980) in order to correct penetration influence among other factors, thus not suitable to be applied to the pre-installed conditions.

e) In cemented mixtures under pushed-in conditions, E_{DMT} associated strain levels (which are the significative ones in day-to-day practice), are within 10^{-2} to 10^{-3}.

a)

10.5.2.3. Calibration of stiffness correlations using seismic wave data

Correlations based in triaxial testing depend very much in sample quality and so differences between correlations established from naturally and artificially cemented soils are expected. However, correlations based in Cross-Hole determinations, such as those proposed by Cruz & Viana da Fonseca (2006a), are supposed to be convergent, since the same measurement reference (shear wave velocities) was used in this framework. Global obtained results of shear modulus (G_0) confirm these expectations, as it can be observed in Figures 10.64 to 10.66, which represent the following situations:

a) G_0 obtained from DMT measurements (Cruz & Viana da Fonseca, 2006) and from Cross-hole tests performed in-situ in the same location where the soil for this experience was obtained (Figure 10.63);
b) G_0 obtained from DMT tests performed in CemSoil box in pushed-in conditions (Cruz & Viana da Fonseca, 2006), represented in Figure 10.64;
c) G_0 obtained from the seismic measurements taken during CemSoil box experiment (Figure 10.65); in this case, it should be remembered that the upper level of measurements correspond to non cemented soils, except for Fra3 sample, where cementation was applied to all layers;
d) CemSoil seismic data also shows that for lower levels of cementation, suction seems to control the magnitude of moduli (geophones at mid-level) loosing its influence as cementation increases; in saturated conditions (lower geophones), there is an obvious increase of magnitude with cementation.

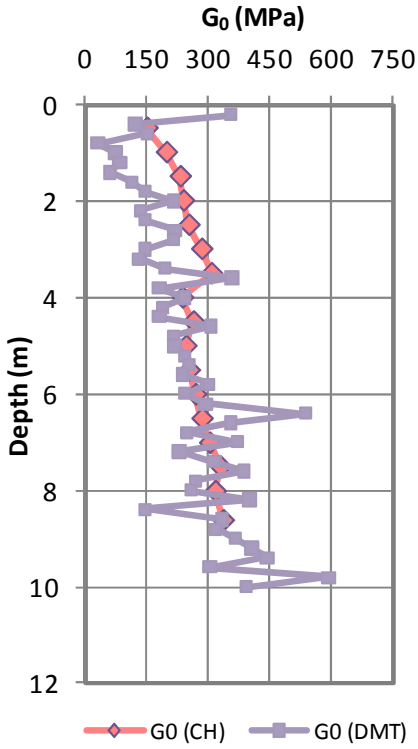


Figure 10.64 - G_0 deduced from DMT (Cruz & Viana da Fonseca, 2006a) and from Cross-hole tests, in Guarda Residual soils.

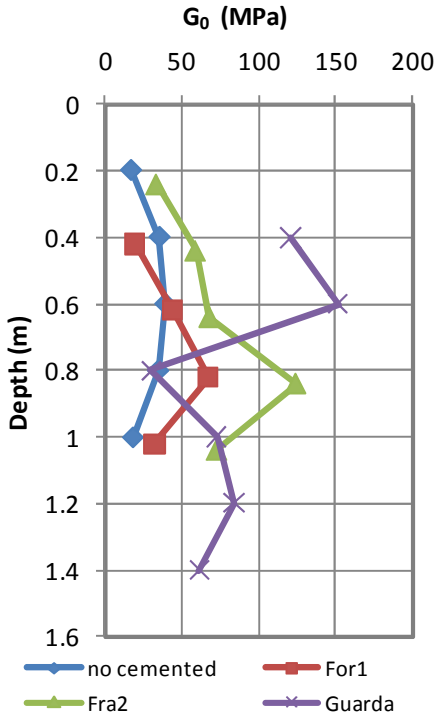


Figure 10.65 - G_0 deduced from DMT tests performed in CemSoil box (Cruz & Viana da Fonseca, 2006a).

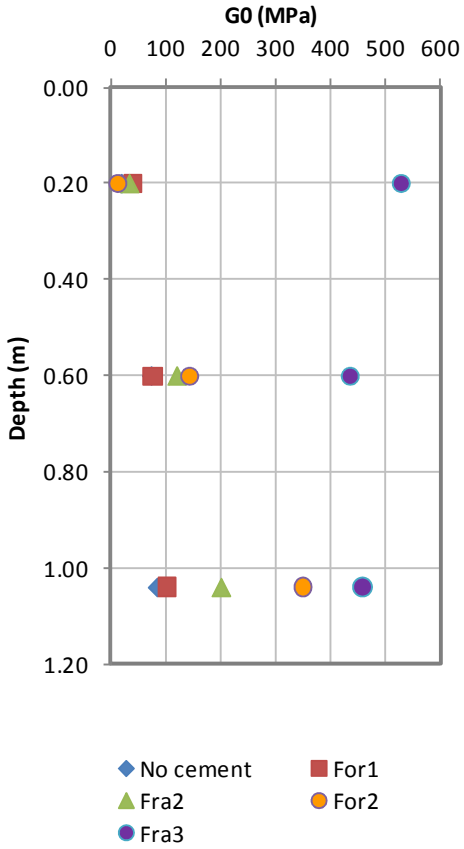


Figure 10.66 - G_0 deduced from seismic measurements within CemSoil box.

In Figure 10.67 the whole package of results obtained both in sedimentary and residual portuguese soils is presented, showing the convergence of the curves as I_D increases, overlapping for values around 5, which seems logical since for that values the percentage of fine content is too small to display a cohesive factor. In fact, bonding structures imply the presence of a cementation agent, which is represented by the fine content. Thus, when fine content is not available cementation structures shouldn't be expected. In the same figure a first attempt to draw a border line between residual and sedimentary soils is also presented.

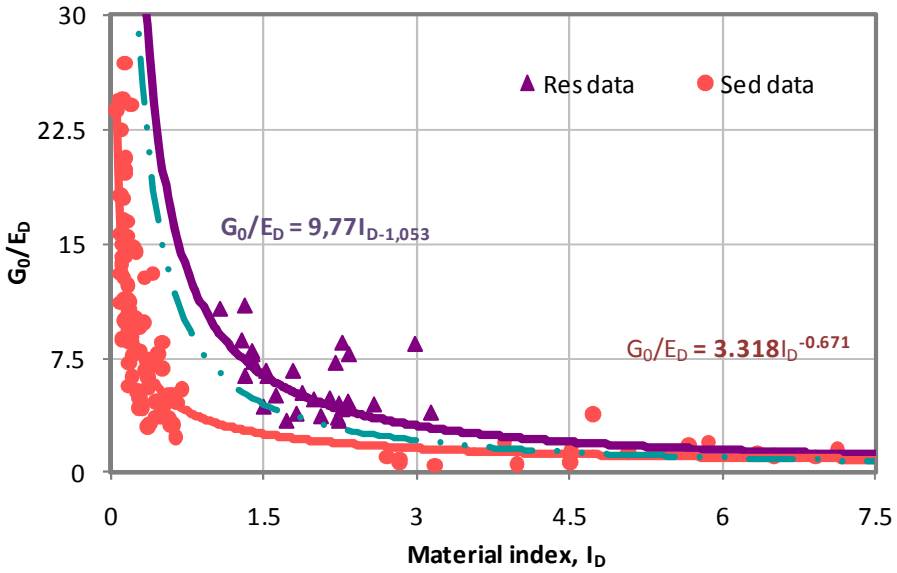


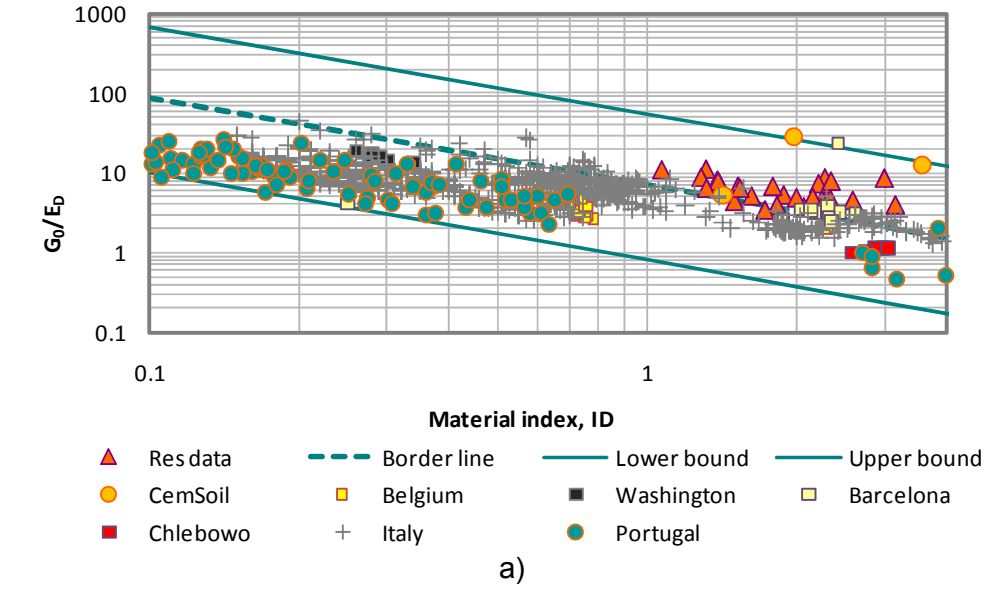
Figure 10.67 - Results of G_0 – DMT correlations in sedimentary and residual soils.

However, the representation of G_0/E_D versus I_D in a bi-logarithmic scale seems to be more appropriate to deal with data. Therefore, lower and upper bounds of this ratio related to non-cemented and cemented soils could be defined, as presented in Figure 10.68. The global considered data, included the sedimentary data obtained by Marchetti (2008, courtesy of Prof. Marchetti) already mentioned in Chapter 5. Results of shear modulus derived in the context of the present experimental work (pushed-in conditions) were used to calibrate both the upper limit and the border line. The respective bounds are represented by the following equations:

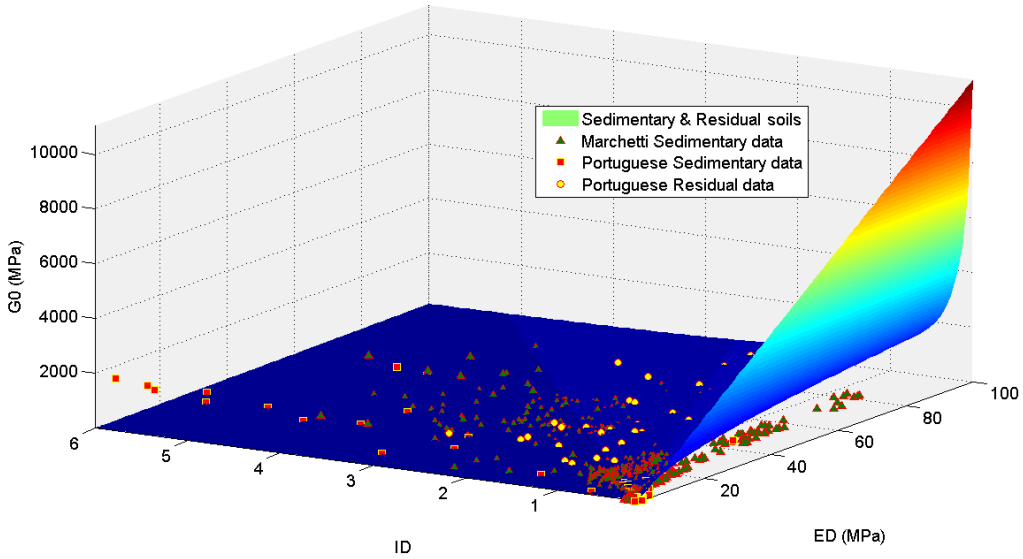
Lower sedimentary bound: $G_0/E_D = 0.8\ I_D^{-1.1}$ (10.3)

Upper sedimentary/lower residual bound: $G_0/E_D = 7.0\ I_D^{-1.1}$ (10.4)

Upper residual bound: $G_0/E_D = 55.0\ I_D^{-1.1}$ (10.5)



a)



b)

Figure 10.68 - Results of G_0 (DMT) correlations in sedimentary and residual soils, plotted in a log – log scale: a) 2D Plot; b) 3D plot

On the other hand, the plot G_0/M_{DMT} versus K_D of both residual and global sedimentary data (Figure 10.69) reveals that the former clearly assume higher rates for soils within the same granulometric range (I_D higher than 1.2), which is also confirmed by CemSoil pushed-in data. Following the same procceeding used with R_G vs I_D, G_0/M_{DMT} vs. K_D plot was also established, aiming the differentiation of cemented and non-cemented soils (Figure 10.70). The equations defining the areas of influence of both situations are presented below:

a) Lower sedimentary bound: $G_0/M_{DMT} = 1.0\ K_D^{\ 0.691}$

b) Upper sedimentary/lower residual bound: $G_0/M_{DMT} = 6.5\ K_D^{\ 0.691}$

c) Upper residual bound: $G_0/M_{DMT} = 33.0\ K_D^{\ 0.691}$

As a consequence of these data analysis, it becomes clear that both [G_0/E_D vs. I_D] and [G_0/M_{DMT} vs. K_D] can be used to detect the presence of cementation. Even though they can be used separately, it is suggested their combined use to have a redundant classification with the required input data coming from similar test origins same.

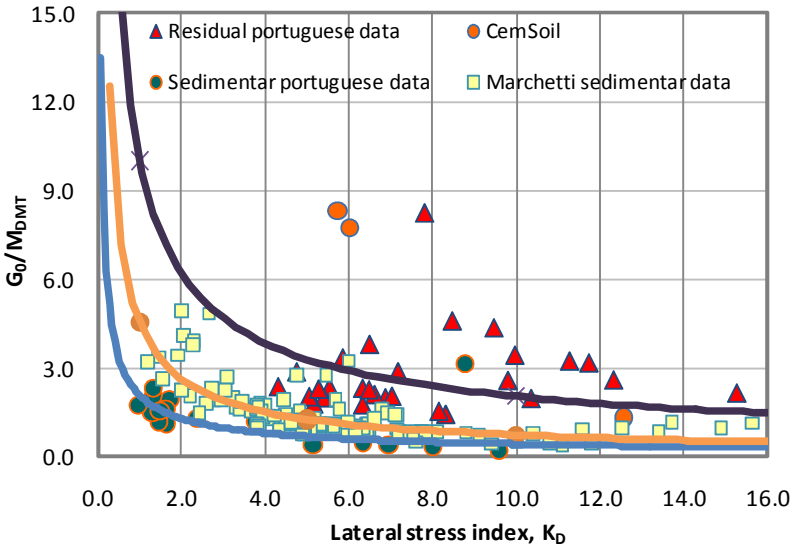


Figure 10.69 - Residual and sedimentary sand data in G_0/M_{DMT} vs. K_D space.

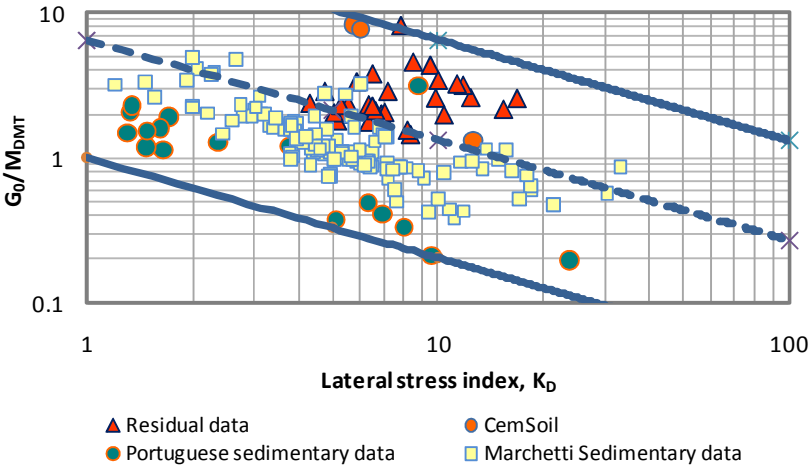


Figure 10.70 - Upper and lower bounds for residual and sedimentary sandy soils, in G_0/M_{DMT} vs. K_D plot.

It is better to bring light with a candle
Than damn the darkness
(Confucius)

PARTE D – THE MODEL

Chapter 11
The Characterization Model.

11. THE CHARACTERIZATION MODEL

11.1. Introduction

The work presented herein, together with the previous related research has revealed the usefulness and adequacy of Marchetti Flat Dilatometer test to characterize granitic residual soils, bringing obvious expectations to the enlargement of this methodology to other difficult geomaterials, such as residual soils of different nature, other intermediate geomaterials (IGM), cohesive-frictional materials, partially saturated soils and mixed granular materials characterization.

The final goal of the research aimed the establishment of a practical characterization set of procedures that could be easily applied to engineering practice in residual soils, in order to contribute to a better geotechnical parameterization and, as a consequence, to increase efficiency level in practical engineering design.

Residual soils show specific mechanical behaviour different from those established for sedimentary transported soils, mainly due to the following characteristics:

a) Presence of a cemented matrix that plays an important role on strength and stiffness behaviour, especially at shallow depths (low confining stresses);
b) Presence of an interparticle bonding that generates a cohesive-frictional material expressed in a Mohr-Coulomb strength criterion with a cohesion intercept and an angle of shearing resistance that cannot be deduced by the common sedimentary correlations developed for such soils;
c) High stiffness, especially at small strain levels, due to the presence of cementation;
d) Water levels at significant depth are frequent in residual profiles, generating suction phenomena with significant influence in strength and stiffness properties; in Porto region, as in many other residual environments, it is rather common to observe vertical excavations in these materials, as a consequence of both interparticle bonding and suction.

11.2. In-situ Test Selection

The suitability of a specific geotechnical survey is dependent on several issues such as installation needs, time of performance, cost-effectiveness and adequacy of results to design needs. Residual soil profiles are usually erratic, frequently showing hard horizons and/or boulders included and dispersed in a weathered to decomposed rock mass. The usual practice, in Portugal as in many other regions, is to use dynamic probing (SPT or DPSH) as the main source of geotechnical information, from which the limitation of derived parameters is rather inadequate to take advantage of modern numerical tools available for design. However, by combining other more comprehensive and powerfull testing techniques, such as PMT, DMT and CPTu tests and also, when it is possible, geophysical surveys specifically for the evaluation of shear wave velocities (SDMT or SCPTu are excellent means for that), it is possible to access good quality information for the whole range of intermediate granitic geomaterials (W_4 to loose soil) with no extra-cost.

In that sense, both CPTu and DMT are very easy to perform and cost saving tests with very reproducible and trustable data, but with an important limitation related to the thrust capacity needed for penetration. However, with adequate equipment and a load frame centered in a heavy truck or penetration rig, capacity can grow up to levels of 60 blows of N_{SPT}, which is perfectly suited to penetrate the main residual horizons of Portuguese granites, as discussed in Chapters 6 and 7. From the time and cost points of view, DMT and CPTu are clearly faster to perform and cheaper than classical campaigns based on borehole and SPT profiles. The usual rates show that both tests are of similar cost and become cheaper than a borehole and respective SPT tests to a depth range of 10-15m. The same 15m take 1-2 hours to perform, while borehole will take easily 3 times more.

DMT on its own, shows another interesting possibility of being driven maintaining a certain level of accuracy (obviously lower than in pushed-in conditions), which is particularly useful in the residual profiles where stiffer bodies are present within residual masses. The research performed in Porto Granitic Formation within the present framework have shown that a N_{20} (DMT) blow count can be compared with N_{SPT} and N_{20} (DPSH), providing the same kind of information of dynamic tools, represented by a blow count to penetrate a standardized element. Thus, besides the membrane expansion results, an extra control parameter is obtained, which offers a possibility of easily cross correlate test results with SPT or DPSH profiles, in combined campaigns. Even though DMT parameters are affected by driving disturbance, a

general pattern can be followed and controlled, providing data of better quality and versatility than the obtained from classical dynamic penetration tests.

On the other hand, no matter the respective level of independency, the similar modes of penetration allow easy combination of CPTu and DMT and respective test parameters, which can provide extra possibilities to derive geotechnical parameters not assessed by each test on their own. In the present research, it was only possible to perform one type of test and DMT was selected due to its higher versatility in results, but further investigation in this research topic, using a new chamber with combined SDMT, SCPTu and also geophysical survey, is being prepared in MOTA-ENGIL laboratories.

11.3. Procedure

11.3.1. Loose to Compact Soils

Since simplicity, reproducibility, reduced time-consuming, cost effectiveness and simple combination of test parameters with boreholes logging and/or other in-situ test results are guaranteed, a constitutive geotechnical model based on site investigation has good possibilities of success for engineering purposes. Thus, a proposal for a residual soil characterization protocol has been outlined from the present research, described in the following guidelines:

a) Selection of an adequate array of vertical profiling points, adequate to each specific situation; national or international recommendations followed in common practice are usually suited;
b) When the local weathering evolution shows loose to compact soils through depth (as it is frequent in Porto and Guarda granites) a number of boreholes are selected and replaced by combined DMT and CPTu tests; author´s experience reveals that the replacement of half (in campaigns with a minimum of 8 profiling points) is usually adequate, with no special losses of information arising from the abdicated boreholes; in fact, DMT and CPTu provide stratigraphy information (generally with even higher precision in thin layers or interbedded strata), making it very easy to replace a couple of boreholes by DMT and CPTu tests with no extra charge and a lot of useful and trustable information for design (Cruz et al., 2004c);

c) DMT or combined DMT and CPTu tests should be located with criteria that assume a homogeneous distribution of tests and boreholes to facilitate cross combination of results, as shown in Figure 11.1; other variations better suited for local conditions are obviously possible;
d) Geophysical surveys with emphasis to the determination of seismic wave velocities should be introduced in routine characterization campaigns, which can be achieved by means of SDMT or SCPTu techniques, with no significative extra-cost;
e) Recent research carried out in MOTA-ENGIL (Rodrigues et al., 2010), showed that seismic measurements taken during penetration or extraction of testing equipments produce similar results; since this procedure reduces both the time of execution and the pore pressure variation at seismic measurement depths a suggestion is made to perform them during extraction;
f) Seismic devices with two measurement points are preferable, since it reduces substantially the errors related to time arrival determinations; when this is not possible, adequate data analysis should be performed by skilled specialized personel in seismic analysis;
g) Careful measurements of stabilized water levels should be guaranteed;
h) Field suction measurements would be very useful, although it is not a fundamental need;

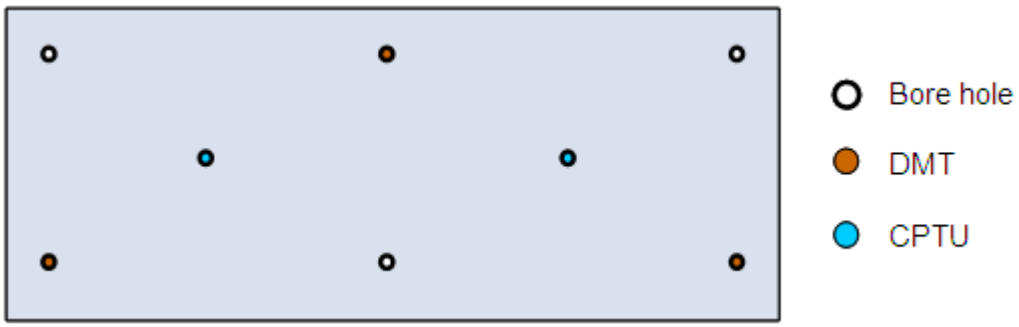


Figure 11.1 Example of a characterization protocol for residual soils

11.3.2. (W_5 to W_4) IGM and rock materials

In the cases where highly compacted soils or W_5 to W_4 rock massifs (N_{SPT} > 60) are the purpose of a specific site investigation (specially when high depths are involved) static pushing becomes unfeasible or extremely difficult, frequently recouring to intermediate pre-boring. In such case, PMT testing can be used as a complementar characterization

technique, by performing one or two pairs of PMT and DMT profiles within the same depth range for calibration purposes, followed by extra PMTs at the stiffer horizons where it was impossible to penetrate for DMT and/or CPTu testing. Careful parametric selection to cross correlate data from DMT and PMT is required, which in fact it is not difficult to find (e.g. Viana da Fonseca, 1996; Viana da Fonseca et al., 2001; Vieira de Sousa et al., 2003). Some suggestions can be presented such as E_{PMT} vs. E_D (or M), P_f vs. P_1 (or K_D) and the respective lift-off pressures (P_0). Of course the introduction of PMT has an extra cost, since 7 or 8 PMT tests (assuming a profile of 15m) will be more expensive than one DMT, CPTu or the complete profile of SPTs. However, if the tests are performed in pre-settled borehole vertical profiles, then the extra cost can be partially reduced. If more detailed mapping is required, especially to define horizontal variability often found in residual profiles, routine geophysical surveys such as seismic tests, performed in testing lines placed between vertical profiles (boreholes, DMT, CPTu or PMT tests) is suggested. Cross-hole or surface seismic testing should be appropriate in situations represented by mixed rock and soil horizons within depth of investigation. When no local experience is available, triaxial testing should be seen as a main reference for calibration purposes.

Once true rock massifs (W_3 or lower weathering degrees) are reached, in-situ soil testing is no longer suitable, and the best approach to assess strength and stiffness properties is based in rock mechanics methodologies, such as the evaluation of drilling parameters and laboratory testing on rock samples/cores, allowing for the application of RMR (Rock Mass Rating) or GSI (Geological Stress Index) classifications. In fact, these indexes are determined taking into account both rock matrix strength and joint conditions, which are the main features that influences global mechanical behaviour of rock massifs. The most common required parameters are the unit weight, uniaxial compression (or point load testing) of rock matrix, tilt testing, RQD (Rock Quality Designation) and JRC (Joint Roughness Coefficient) profiles, as well as spacing, width and weathering of joints. To assess these characteristics, rotary drilling with core recovering is required both to obtain samples for laboratorial testing and to characterize geometric characteristics of joint systems.

11.4. Deriving Geotechnical Data

To be efficient, a protocol for geotechnical characterization between diverse in-situ tests, have to provide geotechnical or other specific parameters suited for design applications. Intensive research work is required to calibrate proper correlations valid

for residual soils, since the available sedimentary correlations are not applicable and there aren´t many global frameworks dedicated to the above mentioned tests.

Due to budget restrictions, in the course of the present experiment it was only possible to study one test, and so DMT was selected for being a base for the present protocol. This option was made due to its higher parametrical versatility and recognized independency. To establish the respective application conditions and correlations for this residual soil DMT based (or combined DMT and CPTu) characterization model, a wide variety of independent data was gathered, resulting from careful combined in-situ and laboratory testing programs, performed in Porto and Guarda granitic formations with high accuracy, controlled procedures and well calibrated equipments in four well referenced granitic residual soil experimental sites (CICCOPN, CEFEUP/ISC2, IPG's and Hospital de Matosinhos), in three other sites not so well known, but with same data quality level and variety (Casa da Música Metro Station, Cunha Junior and Arvore sites) and in a calibration specific laboratory controlled experiment on a high dimension box (which can be associated to a large block sample). Furthermore, these results were interpreted having the background of an important data base related with Porto Geotechnical Map (COBA, 2003) as well as other campaigns within the same geological environment performed by the author in the surrounding areas of Porto city. The overall data analysis generated a lot of different possibilities for cross-correlating results from different origins, revealing high convergence of data interpretations and thus giving credibility to the final deduced trends. As a consequence, reliable correlations between DMT results and several mechanical parameters were established for residual soils of Porto and Guarda Granite Formations, which can also be seen as a base for being applied to other bonded soils, after adequate calibration. The applicability of DMT to test the present granitic residual soils can be seen through the conclusions arising from this whole research work, summarized as follows:

a) Soil identification and unit weight of tested soils are well determined by I_D and I_D+ E_D parameters, respectively; I_D is a versatile numerical parameter that reflects well the type of soil, easily cross-correlated with borehole information or CPTu classifications and offering a possibility of being introduced in mathematical frameworks (easily implemented for arithmetic calculations) to develop correlations valid for all type of soils;
b) From strength point of view, cohesion intercept and angles of shearing resistance can be adequately derived and corrected using the OCR parameter (Marchetti & Crapps, 1981) determined by DMT;

c) M/qt resulting from combined DMT and CPTu tests constitutes another possibility for the same evaluation, although specific correlations are needed since the existing ones (Cruz et al., 2004b, 2006b) are probably conservative due to the effects of sampling and microfabric effects present in calibration procedures;

d) Stiffness can be adequately represented either by constrained modulus (M) or Young modulus (E) derived from simple Elasticity Theory relations (E=0.8M, when Poisson coefficient is taken equal to 0.3), as well as by small strain shear modulus (G_0) when SDMT is used;

e) For the indexation of the dilatometer modulus to typical strain, the calibration experiment showed that E_D calculated results correspond to triaxial secant young modulus determined within 10^{-3} to 10^{-4} of axial strain;

f) G_0 seems to be adequately derived from E_D and I_D intermediate parameters, departing from a single expression valid for all type of soils; moreover, results in sedimentary soils reveal that K_D can also be introduced in G_0 deriving formulae; the available collected data in residual soils represent a very narrow band of K_D values and thus a correlation including the parameter in residual soils couldn´t be settled; however, a starting point was established for this purpose by assuming the best fitting functions obtained for sedimentary soils as reference planes

g) Based in the referred G_0 correlation a general plot to evaluate whether cementation conditionate the engineering behaviour was also possible to be outlined;

h) Suction effects on strength and stiffness seem to be adequately represented by DMT testing, which may be significant in partially saturated zones; the methodology developped for a global cohesion intercept evaluation integrates the suction component, whenever it is present;

i) To deduce suction values, the result obtained below water table, where suction is not presented is used as reference, which is then subtract to the global results obtained above the water level; the calculated differences are due to suction effects represented by the second term of Fredlund et al. (1978) strength criteria (with suction, $u_a - u_w$, multiplied by the tangent of angle of shearing resistance due to suction, ϕ_b); if ϕ_b is not available a reasonable value of 15º can be considered in granites, since it has been proven that a variation of $\pm$5º on the referred parameter doesn´t introduce significative deviation;

j) As for in-situ state of stress of residual soils, namely K_0 parameter, the present experience could not be used for the respective parameter calibration, but the proposal (Viana da Fonseca, 1996; Cruz et al., 1997) valid for Porto and Guarda granitic residual soils (N_{SPT} < 50) and based in combined CPTu and DMT testing, seems to give adequate answers taking the local experience into account.

In Table 11.1 the correlations calibrated by the present experimental work are presented, showing adequacy in Guarda and Porto Granite Formations characterization, and can constitute a reference base for developing specific correlations related to residual soils of different nature or other difficult geomaterials.

Table 11.1 – Correlations for deriving geotechnical parameters in Porto Granite Formation

Parameter	Equation	Reference	Remarks
Stratigraphy	Material Index, I_D	Marchetti, 1980	Accurate when pushed in. The division in silty sand/sandy silt soils reflects real grain size distribution
At rest stress state, K0	$K_0 = C_1 + C_2 . KD + C_3 . q_c/\sigma'_v$ C1 = 0.376, C3 = -0.00172	Baldi, 1988	Granitic residual data obtained by this methodology converges well with reference work in Porto Formation. (SBPT data)
	$C_2 = 0.095 * [(q_c/\sigma'_v) / K_D] / 33$	Viana da Fonseca, 1996	
Global cohesion intercept, c'g	$c'_g = 7.716 \ln (OCR) + 3.53$	Cruz, 2010	Includes suction effects, above phreatic level. M/qt should provide similar accuracy (combined DMT+CPTU might be an useful tool for suction evaluation)
Effective angle of shering resistance, ϕ'	$\phi'_{corr} = \phi'_{DMT} - 2.48 \ln (c'_g) - 3.12$ ϕ'_{DMT} obtained by Marchetti (1997) correlation	Cruz, 2010	Correction of Effects of suction, which are present together with effective components, above phreatic level
Service stiffness, E, M	E = 0,8 M M calculated by Marchetti (1980) correlation	Marchetti, 1980	Corresponds to strain levels ranging from 10-3 to 10-4 in reference to conventional axial strain
Dynamic stiffness, G0	$G_0/E_D = 9.771 I_D - 1.053$	Cruz & Viana da Fonseca,, 2006, Cruz, 2010	Correlation calibrated by seismic CH data and confirmed by the present research results

Accepting our ignorance is an act of wisdom
Ignoring it, is to live in illusion
(Lao Tsé)

Chapter 12
Final Considerations.

12. FINAL CONSIDERATIONS

The framework presented herein provided valuable and trustable information both in residual soil behaviour and its characterization by means of in-situ and laboratorial testing, allowing to establish a reference characterization protocol valid for granitic soils. This model can also be seen as a reference base to other bonded soils behaviour research, after adequate calibration works. An option was made to use a specific in-situ test and to study and to calibrate its results with an exhaustive experimental program. DMT was selected due to its high parametrical versatility, recognized independency towards operational procedures and the local extensive acumulated experience in granitic geological environments. However, some other tests could be pointed out to be tried in combination with DMT (multi-test technique), namely CPTu and PMT, with special emphasis to the former.

To establish application conditions and correlations for the proposed residual soil characterization model, a wide variety of independent data was gathered from careful combined in-situ and laboratory testing programs, performed in Porto and Guarda Granitic Formations with high accuracy and quality controlled devices. The global data set was obtained in:

a) Four well referenced granitic residual soil experimental sites - CICCOPN, CEFEUP/ISC2, IPG's and Hospital de Matosinhos (Viana da Fonseca, 1996),
b) Three other sites not so well known, but with same level of data quality and variety (Hospital de Matosinhos, Casa da Música Metro Station, Cunha Junior and Arvore sites)
c) Data from Porto Geotechnical Map (COBA, 2003) and geotechnical campaigns performed by the author within the area of research or in its neighborhood, constituting a good background to interpretation and calibration of data.
d) Physical modeling in laboratory controlled conditions, by using a calibration apparatus with significant dimension (big block sample).

The overall data analysis generated a lot of different possibilities of cross-correlating results from different origins, revealing high convergence of data interpretations and thus giving credibility to the final conclusive proposals. As a consequence, important contributions for the knowledge of these granitic residual soil geomechanical behaviour

and reliable correlations between DMT results and several mechanical parameters were outlined.

In the first place, field data resulting from Porto Geotechnical Map, calibrated by the high quality experimental sites allowed establishing global trends of variation and classification for engineering proposes. This is expected to be very practical in data interpretation, as summarized in what follows:

a) There is a continuous evolution of mechanical behaviour throughout the entire weathering profile, from W_1 massif to the highly weathered local spots represented by soils where clay matrix controls mechanical behaviour;
b) In the physical characterization context, void ratio and porosity increases with weathering degree, confirmed by decreasing of total, saturated and dry unit weights; in-situ permeability and solids unit weight remains fairly stable, despite the weathering degree;
c) Strength of the studied soils is represented by a cohesive intercept due to interparticle bonding and a angle of shearing resistance related to microfabric and density, being both affected by suction (although the implications in cohesion prevail) arising from its common unsaturated condition;
d) The global strength evolution with weathering reveals that cohesion intercept is the most sensitive parameter on strength degradation, revealing a smooth variation between W_1 to W_4, a steep drop from the latter to W_5, and following again with smooth variation in the regional soils horizons;
e) Stiffness evolution (in static conditions) follows patterns identical to the observed for strength evolution;
f) Strength and stiffness evolutions can be represented by the most common in-situ testing parameters, and thus some indexation can be settled;
g) Since available data covers all the weathering levels, it was possible to introduce an improvement to Group A of Wesley Classification (herein designated *Modified Wesley Classification*); considering mechanical behaviour, sub-divisions of Group A were proposed, following the author´s suggestion for specific classification;
h) A specific ratio (CF ratio or clay/fine ratio) between clay fraction and fine content percentages was also suggested, as a possible mean to index engineering properties to highly weathered soils.

On the other hand, previous research with the test in residual soils was assembled, compared with sedimentary experience and discussed, allowing for the following conclusions that were the base to establish a specific calibration program:

a) Both CPTu and DMT tests give important information about stratigraphy profile, easily integrated within borehole information, showing higher capacity for detecting thin layers when compared with borehole information;
b) The definition of soil type is achieved through a quantitative value (I_D and I_c for DMT and CPTu, respectively), that constitutes an important mean to numerical data treatment and to interpret mechanical behaviour of difficult soils such as intermediate (mixed) soils or residual soils;
c) Unit weight can also be derived by both tests individually, with fair accuracy identical to laboratorial results and obviously higher than the usually "estimated" value;
d) Global data has shown very consistent patterns, reproducibility and convergence to the trends observed in other in-situ test results;
e) The combination of some or all intermediate DMT parameters can simultaneously represent the influence of type of soil, stiffness, density and pore-pressure increment potential, which is decisive in correlation quality;
f) K_D can be used to derive the at rest stress of state, being obtained from a lift-off horizontal pressure; its calculation is made with good approximation by combining CPTu and DMT data, both in sedimentary and residual soils;
g) K_D profile is close to the pattern of OCR, hereby designated virtual overconsolidation ratio, vOCR; therefore, it gives valuable information on the stress history of clays and density of sands, as well as in residual soil cementation strength contribution;
h) From the strength point of view, DMT alone (through vOCR) or combined with CPTu (M/q_t) can provide numerical information related to cementated strength (with a sign in cohesion intercept) and adequately correct angle of shearing resistances when these are derived from sedimentary correlations; however, the reference values (triaxial testing) used in the establishment of respective correlations were expect to deviate from reality, at least due to sampling processes;
i) It is possible to deduce high quality stiffness parameter data from DMT, such as constrained, Young and maximum shear modulus; evaluation of stiffness properties is supported by Theory of Elasticity and numerical values are obtained by a high resolution measurement system; in CPTu case, stiffness

can only be directly derived when seismic device is available, since the test doesn´t allow for displacement/strain measurements;

j) When using combined DMT and CPTu, the number of basic test parameters (4 mechanical + 2 related with pore pressure) allows a wider sort of combinations, which might be useful quantifying some other peculiar properties of residual (or other) soils, such as suction in unsaturated soils.

The above considerations allowed outlining an experimental program, which aimed to the calibration of correlations to derive strength and stiffness parameters and also to study some possible efficiency in suction analysis. This program was based in a global laboratorial testing program performed in artificially cemented soils resulting of remoulding Guarda granite saprolites. The same soil-cement mixtures were later composed to create a big block (BB) sample confined in a large chamber where pre-installed and pushed-in DMT tests were performed. Laboratorial testing aimed to the calibration of DMT measurements and also to contribute to a better understanding of cemented soils mechanical behaviour.

In the context of residual soils mechanical behaviour, the present research was settled aiming to the knowledge of this soil, establishing an adequate calibration of the instrumented block samples. However, during the experimental program execution, as a consequence of a permanent interaction with obtained results, some complementary testing was settled to take the best profit from experimental data and thus, some interesting conclusions were achieved, as described below:

a) Uniaxial compression and tensile strengths represent well the level of cementation and both can be used as index parameters to qualify geomechanical properties in accordance to cement percentage in the soil-cement mixtures;
b) Destructured soil envelope in q:p’ space is represented by a straight line, while the presence of cement gives rise to a curved strength envelope that converges to the destructured soil envelope, at high confining stresses;
c) Stress-strain curves showed that the presence of cement generates the development of a peak deviatoric failure stress, which is as high as cementation level increases and with decreasing correspondent strain levels;
d) Strains related to peak deviatoric stresses are not coincident with maximum dilatancy;
e) It is possible to index different behaviours at low and high confining stresses;

f) Critical state analysis in artificial soils revealed that it is possible to define a single critical state line in q:p' space, but it was not possible to define it clearly in the void ratio versus mean effective stress diagram (n:lnp'); for each particular cement content it was possible to observe a convergence line drawn by the results of the same set of samples (no matter the applied confining stresses); however, different cementation levels generate different lines in n:lnp' space, suggesting that they don´t represent a unique soil type; critical state points align in a very narrow band around the defined critical state lines for each cement content, which are as steep as cement content increases; non-cemented samples constitute a lower bound of the whole situation;
g) Natural soil results indicate a band where critical state points fall into, suggesting the development of shear banding (strain localization);
h) From stiffness point of view, cemented soil data reveals the existence of more than one yield point, confirming conclusions commonly found in literature; Malandraki & Toll (2000) proposed methodology seem to be appropriate for their identifications.

Calibration experimental program was based in Big Block (BB) samples prepared in a large chamber where pre-installed and pushed-in DMT tests were performed, providing the following conclusions:

a) Penetration of the blade generates different disturbance paths in non-cemented or cemented soils; in the case of non-cemented soils it is observed that basic parameters are higher in the case of pushed-in tests revealing the expected effect of densification around the measurement system; in the cemented soil mixtures, the same insertion procedure reduces their values by local destructuration;
b) Pushed-in DMT results confirmed its efficiency evaluating soil type and unit weight;
c) DMT basic and intermediate parameters are sensitive to the variations of strength and stiffness behaviours due to cementation and suction;
d) Local experience on in-situ state of stress of residual soils, namely K_0 parameter, suggests that Baldi's (1988) sedimentary approach based in combined CPTu and DMT testing can be used in residual soils, if a correction factor is applied (Viana da Fonseca, 1996; Cruz et al., 1997);

e) Calibrated correlations were developed to derive a global cohesive intercept (c'_g), generated by both cementation and suction effects, from DMT's virtual overconsolidation ratio, vOCR (Marchetti & Crapps, 1981); a special procedure to separate cementation and suction contributions was also defined;
f) Angles of shearing resistance can be derived from its sedimentary approach (Marchetti, 1997), but a correction factor based in the magnitude of c'_g (or in OCR) ought to be applied;
g) Stiffness can be adequately represented either by constrained modulus (M), Young modulus (E) or small strain shear modulus (G_0); M and E are directly related by Elasticity Theory, by means of Poisson's ratio;
h) The calibration experiment on the large chamber showed that E_{DMT} calculated results correspond to triaxial secant modulus determined within 10^{-3} to 10^{-4} of axial strain, which is a similar strain level range of that observed in sedimentary soils;
i) A previous proposed correlation to derive G_0 (Cruz & Viana da Fonseca, 2006a) based in E_D and I_D intermediate parameters proved to be correct, mostly due to the fact that the calibration reference was sustained by shear wave velocities determined by high quality Cross-Hole tests; a general plot based in the referred correlation to evaluate whether cementation is or is not present was also outlined;
j) On the other hand, advanced mathematical analysis were made, both in sedimentary and residual soils, aiming to establish a correlation of maximum shear modulus as function of DMT intermediate parameters, E_D, I_D and K_D; in the case of sedimentary data robust correlations were obtained due to the possibility of using Prof. Marchetti's data obtained in a wide range of different environments (courtesy of Prof. Marchetti), together with Portuguese data; these correlations were then used as reference to apply in residual soil data analysis, aiming to establish a departing point for further research in residual soils from other geologic nature and/or locations.

Given the success of the experience a specific model for characterization of residual soils was possible to be established. This turns to be more like a protocol that can be described as follows:

a) In medium compact to compact soils, departing from the usual distribution of vertical profiles used in common geotechnical surveys, a number of

boreholes are selected to be substituted by DMT or combined DMT and CPTu tests; sustainable correlations for deriving soil stratigraphy, unit weight, K_0 (combined CPTu and DMT tests), cohesive intercept, angle of shearing resistance, constrained, Young and small strain shear modulus, established in the course of so many years of studies, are now available for common practice;

b) In stiffer soils, such as W_5 to W_4 rock massifs, driven DMT, PMT or SPT/DPSH tests can be used, after calibration of the respective parameters by pushed-in DMT's, in the soils where both can be performed;
c) For lower weathering degrees, rock mechanic concepts should be applied.

In the context of suggestions for further investigation, the application of this residual soil characterization model to frictional-cohesive materials other than Portuguese granites is an obvious path to follow, given the success of the present experiment. The correlations settled for granites presented herein, could be used as a departure reference and the use of I_D is suggested as a basic control variable, since it is a numerical representation of grain size variations. In the author point of view, it is probable that I_D parameter could represent an important correction to be applied, when dealing with other residual soils, at least for granular (silt and sandy soils). This might provide the possibility of developing representative correlations valid for wider soil type ranges, thus further research on other types of residual soils from schists, limestone, as well as mature or lateritic horizons is suggested. Moreover, the efficiency of DMT in detecting variations generated by thin layers of lower strength, through variations either in strength (M or K_D) or soil classification parameter (I_D), can be an important tool to explore massif local anisotropy such as old joints that gave birth to kaolinized alignments.

Furthermore, similar experience should be implemented combining CPTu and DMT testing, to recalibrate current correlations for cohesion intercept (M/qt) proposed by Cruz et al. (2004b) and Cruz & Viana da Fonseca (2006a) and also at rest stress coefficient (K_0) using the correction applied to Baldi´s (1988) sedimentary approach proposed by Viana da Fonseca (1996). This testing combination should also be studied to derive suction, since it provides extra parameter combination with possible capacity to discern the three contributions for the overall strength (suction, effective cohesion and friction). In this context, it could also be useful to study possibilities of incorporating tensiometers in DMT apparatus, since the dimensions are adequate to be used in modern equipments.

On the other hand, combination of both PMT + DMT and driven + pushed-in DMT tests are also suggested as interesting further research lines, since they can provide important means for testing strata where current DMT cannot penetrate, and so to develop a sustainable pair of tests that can provide numerical information on a complete weathering profile, from loose lateritic or saprolitic soil to highly weathered (W_4) massif.

As stated above, the present research work was settled with the main goal centered in the development of an in-situ testing model adequate to residual soils. However, the final laboratorial results allowed for some additional research programs on residual soil mechanical behaviour, especially related to the application of Critical State Soil Mechanics of these soils. In fact, obtained results suggests that the increase in cementation content creates a different soil and that it seems possible to define a pattern of critical state lines with cementated particles. On the other hand, differences between natural and artificial soils seem to reveal quite different behaviours, with the former developing localization (shear banding) while the latter seem to converge to a unique line in specific volume versus logarithmic mean effective stress. To clarify that, an extensive laboratorial program is suggested, based in undrained and drained (σ_3, σ_1 and p' constant) triaxial tests, developed together with "before and after" identification and physical characterization.

REFERENCES

Aas, G., Lacasse, S., Lunne, T., Hoeg, K. (1986). “Use of in-situ tests for foundation in clay”. Proc. ASCE Specialty Conference In-situ’ 86. Blacksburg, USA.

Almeida, F., Hermosilha, H., Carvalho, J.M., Viana da Fonseca, A., Moura, R. (2004). “ISC'2 experimental site investigation and characterization - Part II: From SH waves high resolution shallow reflection“. Viana da Fonseca and Mayne (Eds). Vol.1, pp. 419-426. Millpress, Rotterdam.

Alonso, E.E., Gens, A. & Josa, A. (1990). “A constitutive model for partially saturated soils”. Géotechnique, Vol. 40, Nº 3, pp. 405-430.

Amar, S., Gambin, M., Clark, S. (1991). “Application of pressuremeter test results to foundation design in Europe”. Société International Mec de Sol e Travaux de Fondation. ICSMFE, Balkema.

ASTM D1194-72 (Re-approved in 1987). Standard Test Method for Bearing Capacity of Soil for Static Load and Spread Footings. American Society for Testing Materials.

ASTM subcommittee D 18.02.10 (1986). Suggested Method for Performing the Flat Dilatometer Test. ASTM Geotech. Testing Journal, Vol. 9, nº 2, 93 – 101.

ASTM D 2487 (1998). Classification of soil for engineering purposes. American Society for Testing Materials.

Auld, B. (1977). “Cross-hole and Down-Hole vs by Mechanical Impulse”. J. of Geotech. Eng. Division, ASCE, 103 (GT12), 1381-1398.

Baguelin, F., Jézéquel, J.F., Shields, D.H. (1978). “The pressuremeter and foundation engineering”. Trans Tech publications.

Baldi, G., Bellotti, R., Ghionna, V., Jamiolkowski, M., Marchetti, S., Pasqualini, E. (1986a). “Flat dilatometer tests in calibration chambers”. Proc. of IV conference in use of In-situ tests: 431-446. Blacksburg, Virginia, ASCE

Baldi, G., Bellotti, R., Ghionna, V.N., Jamiolkowski, M. & Pasqualini, E. (1986b). “Interpretation of CPT's and CPTU's. II Part: Drained penetration on sands”. Proc. IV International Geotechnical Seminar on Field Instrumentation of Soil and In-situ Measurements, pp. 143-156. Nayang Technical Institute, Singapore.

Baldi, G., Bellotti, R., Ghionna N., Jamiolkowski, M. (1988). "Stiffness of Sands from CPT, SPT and DMT - a Critical Review". Penetration Testing. Institution of Civil Engineers, British Geotechnical Conference. Birmingham.

Baldi, G., Bellotti, R., Ghionna, V.N., Jamiolkowski, M. & Lo Presti, D.C.F. (1989). "Modulus of sands from CPT's and DMT's". 12th ICSMFE, Rio de Janeiro, Vol.1.

Baldi, G., Bellotti, R., Ghionna, V.N. & Jamiolkowski, M. (1991). "Settlement of shallow foundations on granular soils". J. Geotech. Engrg., ASCE, 117(1), pp 72-175.

Baligh, M. M. & Scott, D. (1975). "Quasi static deep penetration in clays". J. Geotechnical. Eng. Div. ASCE. 101, GT11, 1119-1133.

Baligh, M. (1985). "Strain path method". J. Geotech. Eng. Division, ASCE, 111 (GT9), pp 1108-1136.

Barros, J.M.C.; Pinto, C.S. (1997). "Estimation of maximum shear modulus of Brazilian tropical soils from Standard Penetration Test". Proc. 14th ICSMFE, Hamburg, Vol. 1, pp. 29-30.

Barros, J.M.C. (1997). "Módulo de cisalhamento dinâmico de solos tropicais". Tese de Doutoramento em Engenharia, Escola Politécnica da Universidade de São Paulo, Brasil.

Barton, N. R., Choubey, V. (1977). "The shear stregth of rock joints in theory and practice". Rock Mechanics, 19, 1, pp 1-54.

Battaglio, M.; Jamiolkowski, M.; Lancellotta, R.; Maniscalco, R. (1981). "Piezometer probe test in cohesive deposits". ASCE Geotech. Div. Symposium on Cone Penetrometer Testing and Experience. St. Louis, USA.

Baynes, F.J.; Dearman, W.R. (1978). "The relationship between the microfabric and the engineering properties of weathered granite". Bull. IAEG, 18, pp. 191-197.

Been, K.; Jefferies, M. G. (1985). "A state parameter for sands". Géotechnique 35, Nº 2, pp. 99-112.

Been, K.; Jefferies, M. G.; Crooks, J.H.A.; Rothenburg, L. (1987). "The cone penetration tests in sands: Part II General inference of state". Géotechnique 37, Nº 3, pp. 285-299.

Been, K.; Jefferies, M.G.; Hachey, J. (1991). “The critical state of sands”. Géotechnique 41, Nº 3, pp. 365-381.

Begemann, H. (1965). “The friction jacked cone as an aid in determining soil profile”. Proc. 6th Int. Conf. on Soil Mechnaics and Foundation Engineering. Montreal, Vol I, pp 17 – 20.

Begonha, A. J.,1989. “Alteração das rochas graníticas do Norte e Centro de Portugal. Uma contribuição”. MSc Thesis presented to Universidade Nova de Lisboa (in Portuguese).

Biarez, J.; Gambin, M.; Gomes Correia, A.; Flavigny, E.; Branque, D. (1998). “Using pressuremeter to obtain parameters to elastic-plastic models for sands”. Proc. 1st Int. Conf. on Site Characterization ISC’98 Atlanta, USA. E^{ds} Robertson & Mayne, Vol. 2, pp. 747-752.

Bieniawaski, Z. T. (1984). “Rock mechanic design in mining and tunneling”. Ed. Balkema

Bieniawski, Z.T. (1978). “Determining rock mass deformability: experience from case histories”. Int. Journal on Rock Mechanics and Mining Science, Vol 15, pp 237-248.

Bjerrum, L. (1972). “Embankments on soft ground”. ASCE special Conference on Purdue University, Indiana, USA.

Blight, G.E. (1997). “Mechanics of residual soils”. Balkema, Rotterdam.

Borden, R., Aziz, C., Lowder, W., Khosla, N. (1986). “Evaluation of pavement subgrade support characteristics by dilatometer test”. Proc. 64th Annual Meeting of the Transp. Res. Board. TR record 1022.

Bowles, J.E., (1988). “Foundation analysis and design”. 4th edition. The McGraw-Hill Companies, International Editions.

Brady, B. H.; Brown, E.T. (1985). “Rock mechanics for underground mining”. George Allen and Unwin, London.

Branco, J.J. (2008). “Caracterização de maciços rochosos. Resistência ao corte de diaclases”. MSc Thesis presented to GeoScience Dept. of University of Aveiro. (in Portuguese)

Bressani, L.A. (1990). “Experimental properties of bonded soils”. PhD thesis presented to University of London, London, U.K.

Burland, J.B. (1991). “Small is beautiful – the stiffness of soils at small strains”. Nineth Laurits Bjerrum Memorial Lecture. Canadian Geotechnical Journal, 26, pp 499-516.

Briaud, J.L., Miran, J. (1992). “The flat dilatometer test”. Report nº FHWA-SA-91-044. Federal Highway Administration. Washington D.C.

Brooker, E.W. & Ireland, H.O. (1965). “Earth pressures at rest related to stress history”. Can. Geot. Journal, Vol. 2, nº1, pp 1-15.

British Standards Institution (1999). “Code of practice for site investigations”. BS 5930. London.

Campanella, R. (1983). “Current research and development of the flat dilatometer”. 1st Int. Conf. On the Flat Dilatometer. Edmonton, Alberta.

Campanella, D.; Robertson, P., Gillespie, D.; Grieg, J. (1985). “Recent developments in in-situ testing of soils”. Proc. 11th Int. Conf. on Soil Mechanics and Foundation Engineering.. S. Francisco, USA. Balkema.

Campanella, R.G., Robertson P.K. (1991). “Use and interpretation of a research dilatometer”. Canadianan Geot. Journal: 28, 113-126.

Carvalho, J.M.; Viana da Fonseca, A.; Almeida, F.; Hermosilha, H. (2004). “ISC'2 experimental site invest.and characterization - Part I: Conventional and tomographic P and S waves refraction seismics vs. electrical resistivity”. Geotechnical & Geophysical Site Characterizaton. Viana da Fonseca and Mayne (Eds). Vol.1, pp. 433-442. Millpress, Rotterdam.

Castro, G. (1969). “Liquefaction of sand”. PhD thesis presented to Division of Engineering and Apllied Physics, Harvard University.

Cavalcante, E. H. (2002). ”Investigação teórico experimental sobre o SPT”. Tese de Doutorado, COPPE, UFRJ, Rio de Janeiro, Brazil.

Cavalcante, E. H.; Danzinger, F.A.B.; Danzinger, B.R.; Bezerra, R.L. (2002).”Medida de Energia do SPT: instrumentação para registos de força e de velocidade nas hastes”. XII COBRAMSEG – ICLBG – III SBMR, Vol.1, pp.97 – 106.

Cavallaro, A., Lo Presti, D.C.F., Maugeri, M. & Pallara, O. (1999). “Caratteristiche di deformabilità dei terreni da prove dilatometriche: analisi critica delle correlazioni esistenti”. Proc. XX Italian Geotech. Conf. CNG, Parma: 47-53. Bologna. (in Italian)

Cestare, F. (1990). “Prove Geotecniche in Sito”. 2nd edition. Geograph, Segrate. (in Italian)

Chandler R. J.; Gutierrez C. I. (1986). “The filter paper method of suction measurement”. *Géotechnique*, 36, pp. 265–268.

Chiossi, N.J. (1979) ‘’Geologia Aplicada à Engenharia’’- 2 edição. Grémio Politécnico, São Paulo.

Clayton, C.; Matthews, M.; Simons, N. (1995). “Site investigation”. 2nd Edition. Blackwell Science, Oxford.

Clayton, C., Heymann, G. (2001). “Stiffness of geomaterials at very small strains”. Geotechnique 51(3), 245-255.

Clough, G.W.; Sitar, N.; Bachus, R.C.; Rad, N.S. (1981). “Cemented sands under static loading”. J. Geot. Eng. Div., Vol. 107, GT6, pp. 799-817. ASCE, New York.

Coduto, D. (1999). “Foundation design: principles and practices”. 2nd Edition. Prentice Hall.

Cole, W.F. e Sandy, M.J. (1980). “A proposed secondary mineral rating for basalt road aggregate durability”. Australian Road Research, nº 10 (3), pp. 27-37.

COBA (2003). Carta Geotécnica do Porto. Trabalho liderado pela COBA com a colaboração da Faculdade de Ciências da Universidade do Porto. Câmara Municipal do Porto (in Portuguese).

Consoli, N.C.; Schnaid, F.; Milititsky, J. (1998). “Interpretation of plate load tests on residual soil site”. J. Geot. Geoenv. Eng., Vol. 124, Nº 9, pp. 857-867. ASCE, New York.

Consoli, N.; Caberlon, R. C; Floss, M. F.; Festugato, L. (2010). “Parameters controlling tensile and compressive strength of artificially cemented sand”. Journal of Geotechnical and Geoenvironmental Engineering, ASCE (to be published).

Consoli, N. C., Foppa, D., Festugato, L. and Heineck, K. S. (2007). “Key parameters for strength control of artificially cemented soil”. Journal of Geotechnical and Geoenvironmental Engineering, ASCE, 133(2), 197-205.

Consoli, N.C., Prietto, P.D.M., Carraro, J.A.H. and Heineck K.S. (2001). “Behavior of compacted soil-fly ash-carbide lime-fly ash mixtures”. Journal of Geotechnical and Geoenvironmental Engineering, ASCE, 127, 774-782.

Coon, R.F. Merrit, A.H. (1970). “Predicting in-situ modulus of deformation using rock quality indices”. Special Technical Publication, ASCE, 477, pp. 154 – 173.

Coop, M.R.; Atkinson, J.H. (1993). “The mechanics of cemented carbonate sands”. Géotechnique 43, Nº 1, pp. 53-67.

Costa Filho, L.M.; Vargas Jr., E.A. (1985). “Hydraulic properties. Mechanical and hydraulic properties of tropical lateritic and saprolitic soils”. Progress Report of the ISSMFE Technical Committee (1985), pp. 67-84. ABMS, Brasília, Brazil.

Cotecchia, F. and Chandler, R.J. (1997). “The influence of structure on the pre-failure behaviour of a natural clay”. Géotechnique, 47, No.3, 523-544.

County Roads Board, Victoria (1982). “Test method CRB 373.01. Secondary mineral content using a petrological microscope”. Manual of testing procedures, Vol. III. Victoria, Australia, pp. 1-6.

Coutinho, R. Q., Costa, F. Q. & Souza Neto, J. B. (1997). “Geotechnical characterization & slope in residual soil in Pernambuco, Brasil”. Proc. II PSL – 2nd Pan-American Symposium on Landslides / II COBRAE – 2nd Brazilian Conference on Slope Stability, ABMS, Rio de Janeiro, Vol.1, pp. 287-298.

Coutinho, R.Q.; Souza Neto, J.B.; Barros, M.L.S.C.; Lima, E.S.; Carvalho, H.A. (1998). “Geotechnical characterization of a young residual soil/gneissic rock of a slope in Pernambuco, Brazil”. Proc. Sec. Int. Symp. on Hard Soils–Soft Rocks, Eds. Evangelista & Picarelli, Balkema, Vol. I, pp. 115-210. Naples, Italy.

Cruz, N. (1995a). “A avaliação da coesão não drenada pelo dilatómetro de Marchetti”. 5º Congresso Nacional de Geotecnia, Coimbra. (in Portuguese)

Cruz, N.(1995b). “A avaliação de parâmetros geotécnicos pelo dilatómetro de Marchetti”. MSc thesis presented to Faculty of Science and Technology of University of Coimbra. (in Portuguese)

Cruz, N. Viana da Fonseca, A. (1997a). “A caracterização de solos residuais de granito do Norte de Portugal”. Uma Contribuição. 6º Congresso Nacional de Geotecnia, Lisboa. (in Portuguese).

Cruz, N., Viana, A., Coelho, P., Lemos, J. (1997b). “Evaluation of geotechnical parameters by DMT in Portuguese soils”. XIV Int. Conf. on Soil Mechanics and Foundation Engineering, pp 77-80. Hambourg, Germany

Cruz, N., Almeida e Sousa, J., Aguiar, A. (2000). “Ensaios com Screw Plate. Uma experiência em solos residuais”. VII Congresso Nacional de Geotecnia, pp 123-132. (in Portuguese).

Cruz, N.; Viana da Fonseca, A. (2004a). “Caracterização de maciços terrosos a partir da utilização conjunta dos Ensaios DMT e CPT(u)“. 9º Congresso Nacional de Geotecnia. Aveiro. (in Portuguese).

Cruz, N., Viana da Fonseca, A., Neves, E. (2004b). “Evaluation of effective cohesive intercept on residual soils by DMT data”. Geotechnical and Geophysical Site Characterization. Proc. 2nd Int. Site Characterization - ISC’2, Porto, Portugal, Sept. 2004. Millpress, Rotterdam

Cruz, N., Figueiredo, S. & Viana da Fonseca, A. (2004c). “Deriving geotechnical parameters of residual soils from granite by interpreting DMT+CPTU tests”. Geotechnical and Geophysical Site Characterization. Proc. 2nd Int. Site Characterization - ISC’2, Porto, Portugal, Sept. 2004. Millpress, Rotterdam, pp. 1799-1803

Cruz, N., & Viana da Fonseca, A. (2006a). “Portuguese experience in residual soil characterization by DMT tests”. Proc. 2nd International Flat Dilatometer Conference, Washington D.C.

Cruz, N. Viana da Fonseca, A. (2006b) “Characterization of stiff residual soils by dynamically push-in DMT”. International Conference on Site Characterization and Design of Earth Structures, GEOSHANGAI. Shangai, Junho de 2006. ASCE Geotechnical Special Publication nº 149, pp. 261 – 268.

Cruz, N., Devincenzi, M. & Viana da Fonseca, A. (2006a). “DMT experience in Iberian transported soils”. Proc. 2nd International Flat Dilatometer Conference, Washington, D.C., pp. 198-204.

Cruz, N.; Viana da Fonseca, A.; Santos, J. (2006b). “Compaction control and stiffness evaluation of earthfills, by DMT”. Geotechnical Luso-Brazilian Conference. Curitiba, Brasil.

Cruz, N.; Caspurro, I.; Guimarães, S.; Cunha Gomes, C.; Viana da Fonseca, A. (2008a). "Field characterization of problematic earthfills by DMT. A case history." 3rd International Conference on Site Characterization. Taipé, Taiwan.

Cruz, N.; Mateus, C.; Cruz, M.; Cruz, I.; Rodrigues, C. (2008b). “Determinação dos erros de medição associados a ensaios “In-situ”. O caso do Ensaio DMT”. XI Congresso Nacional de Geotecnia. Coimbra. (in Portuguese)

Cruz, N.; Tareco, H; Rocha, R.; Andrade, R.; Cruz, J. (2008c). “Caracterização mecânica de maciços rochosos com base na combinação de prospecção mecânica e geofísica”. IV Congresso Luso-Brasileiro de Geotecnia. Coimbra. (in Portuguese)

Cruz, N.; Tareco, H; Gonçalves, F.; Vieira Simões, E.; Hipólito, A. (2008d). “Caracterização de maciços cársicos com base em prospecção com Georadar. Um caso prático”. XI Congresso Nacional de Geotecnia. Coimbra. (in Portuguese)

Cruz, N.; Mateus, C.; Cruz, M. (2009). “Determinação dos erros de medição associados a ensaios “in-situ”. O caso do ensaio DMT”. Congreso de Métodos Numéricos en Ingenieria 2009. Barcelona, España. (in Portuguese)

Cuccovillo, T.; Coop, M.R. (1993). “The influence of bond strength on the mechanics of carbonate soft rocks”. Proc. Int. Symp. ‘Geotechnical Engineering of Hard Soils – Soft Rocks’, Eds. Anagnostopoulos et al., Balkema, Athenas, Vol. 1, pp. 447-455.

Cuccovillo, T.; Coop, M.R. (1997a). “The measurement of the local axial strains in triaxial tests using LVDTs”. Géotechnique 47, Nº 1, pp. 167-171.

Cuccovillo, T.; Coop, M.R. (1997b). “Yielding and pre-failure behaviour of structured sands”. Géotechnique 47, Nº 3, pp. 491-508.

Cuccovillo, T.; Coop, M.R. (1999). “On the mechanics of structured sands”. Géotechnique 49, Nº 6, pp. 741-760.

Cui, Y. J. & Delage, P. (1996). “Yielding and Behaviour of an Unsaturated Compacted Silt”. Géotechnique, 46, N. 2, pp. 291–311.

Dahlquist, G., Björck, Å. (1974). “Numerical methods”. Translated by Anderson. George Forsythe, Editor.

Davidson, J.; Boghrat, A (1983). “The flat dilatometer testing in Florida”. Proc. Int. Symposium on In-situ Testing of Soils and Rocks, Vol II, Paris.

Dearman, W.R. (1974). “Weathering classification in the characterisation of rock for engineering purposes in British practice”. Bull. Int. Assoc. Eng. Geol., Nº 9, pp. 33-42.

Dearman, W.R. (1976). “Weathering classification in the characterisation of rock: a revision”. Bull. Int. Assoc. Eng. Geol., Nº 13, pp. 123-127.

Décourt, L. (1989). “The standard penetration test state-of-the art report”. Proceeding 12th International Conference on Soil Mechanics and Foundation Engineering, Rio de Janeiro, Brazil. Vol. 4, A.A. Balkema Rotterdam.

Deere, D.U., (1964). “Technical description of rock cores for engineering purposes”. Rock Mechanics and Engineering Geology, Vol. 1, Nº.1, 17-22.

Deere, D.U., Miller, R.P., (1966). “Engineering classification index properties for intact rock”. Technical Report Nº AFNL-TR-65-116 Air Force Weapons Laboratory. New Mexico.

Deere, D.U.; Patton, F.D. (1971). “Slope stability in residual soils”. Proc. 4th PanAmerican Conf. Soil Mechanics and Foundation Engineering, San Juan, Porto Rico, Vol. 1, pp. 87-170.

Deere, D.U., Deere, D.W. (1988). “The RQD index practice”. Proc. Symp. Rock Classif. Eng. Purp., ASTM, Special Technical Publication 984, pp. 91-101, Philadelphia.

Devincenzi, M.; Powell, J.J.M.; Cruz, N. (2004). “Theme 1 – Mechanical in-situ testing methods”. General Report. 2nd International Conference on Site Characterization, ISC’2. Porto, Portugal. Vol. 1, pp. 253 – 263.

Devincenzi, M.; Powell, J.J.M.; Cruz, N.; Toledo, M. (2007). “Actualidad en el uso de los ensayos geotécnicos in situ”. Ingenieria Civil, 145/2007, pp. 27-40.

Diaz-Rodriguez, J.A.; Leroueil, S.; Alleman, J.D. (1992). “Yielding of Mexico City clay and other natural clays”. J. Geotechnical Engineering Div., ASCE, Vol 118(7), pp. 981-985.

Douglas, B.; Olsen, R. (1981). “Soil Classification using the electrical cone penetrometer”. ASCE Geotech. Div. Symposium on Cone Penetrometer Testing and Experience. St. Louis, USA.

Durgunoglu, H., Mitchell, J. (1975). “Static penetration resistance of soils”. Proc. of ASCE Specialty Conference on In-situ Measurements of Soil Properties, pp. 151-189. Raleigh, North Carolina, USA.

Escario, V.; Juca (1989). “Shear strength and deformation of partly saturated soils”. 12th International Conference on Soil Mechanics and Foundation Engineering, Rio de Janeiro.

Escario, V.; Juca (1989). “Shear strength and deformation of partly saturated soils”. 12th International Conference on Soil Mechanics and Foundation Engineering, Rio de Janeiro.

Eslami, A.; Fellenius, B.H. (1997). “Pile Capacity by Direct CPT and CPTu Methods Applied to 102 Case Histories”. Canadian Geotechnical Journal, Vol. 34, pp. 886-904.

Eurocode 7 (2004). “Geotechnical design”. Final Draft, ENV 1997-1, 1997-2, 1997-3. European Committee For Standardization, Brussels

Fabius, M. (1985). “Experience with dilatometer in routine geotechnical design”. Proc. 38th Canadian Geotechical Conference. Edmonton, pp. 163-169.

Fahey, M. (1998). “Deformation and in situ stress measurement”. Proc. 1st Int. Conf. on Site Characterization ISC’98 Atlanta, USA. E^{ds} Robertson & Mayne, Vol. 1, pp. 49-68.

Fahey, M. (2001a). Soil stiffness values for foundation settlement analysis. Proc. 2nd Int. Conf. on Pre-failure Deformation Characteristics of Geomaterials, Torino, Italy, Vol. 2, 1325-1332, Balkema, Lisse.

Fahey, M. (2001b). “Measuring soil stiffness for settlement prediction”. Proc. 15th Int. Conf. on Soil Mechanics and Geotechnical Engineering. Istambul, Turkey. Balkema.

Fahey, M. Randolph, M.F. (1984). “Effect of disturbance on parameters derived from self-boring pressuremeter tests in sands”. Geotechnique, 34 (1), pp. 81-97.

Fahey, M.; Carter, J. P. (1993). “A finite element study of the pressuremeter test in sand using a non-linear elastic plastic model”. Canadian Geotechnical Journal, 30, pp. 348–362

Fahey, M., Lehane, B. & Stewart, D.P. (2003). “Soil stiffness for shallow foundation design in the Perth CBD”. Australian Geomechanics, 38(3), pp. 61–89.

Fahey, M., Schneider, J. M. & Lehane, B. (2007). “Self boring pressuremeter testing in Spearwood dune sand”. Australian Geomechanics.

Ferreira, C. (2003). “Implementation and application of piezo-electric transducers for the determination of seismic wave velocities in soil specimens. Assessment of sampling quality in residual soil”. MSc thesis presented to University of Porto (in Portuguese).

Ferreira, C. (2009). “Seismic wave velocities applied to the definition of state parameters and dynamic properties of residual soils”. PhD thesis presented to University of Porto.

Finno, R. J.(1993) "Analytical Interpretation of Dilatometer Penetration Trough Saturated Cohesive Soils". Geotechnique 43, No 2, pp. 241 - 254.

Fookes, P.G.; Dearman, W.R.; Franklin, J.A. (1971). “Some engineering aspects of rock weathering with field examples from Dartmoor and elsewhere”. Quarterly Journal of Enginnering Geology, vol. 4, pp. 139-185.

Fookes, P.G.; Gourley, C.S.; Ohikere, C. (1988). “Rock weathering in engineering time”. Quarterly Journal of Engineering Geology, Vol. 21, pp. 33-57.

Fourie, A.B.; Papageorgio, G. (2001). “Defining an appropriate steady state line for Merriespruit gold tailings”. Canadian Geotechnical Journal, 38, 4, pp. 695 – 706.

Fredlund, D.G. (1979). “Appropriate concepts and technology for unsaturated soil”. Canadian Geotechnical Journal, v. 15, pp. 313-321.

Fredlund, D.G. (2006). “Unsaturated soil mechanics in engineering practice”. J. Geotechnical and Geoenvironmental Engr., ASCE, Vol.132, Nº3, pp.286-321.

Fredlund, D.G.; Morgenstern, N.R.; Widger, R.A. (1978). “The shear strength of unsaturated soils”. Canadian Geotechnical Journal, 15.

Fredlund, D.G.; Rahardjo, H. (1993). “Soil mechanics for unsaturated soils”. John Wiley & Sons.

Fredlund, D. G.; Xing, A. (1994). “Equations for the soil-water characteristic curve”. Canadian Geotechnical Journal. 31:3. p. 12.

Fredlund, M. D.; Fredlund, D. G.; Wilson, G. W. (1997). “Estimation of unsaturated soil properties using a knowledge-based system”. Philadelphia, Pennsylvania, ASCE.

Futai, M.M., Almeida, M.S.S. & Lacerda, W.A. 2007. “The laboratory behaviour of a residual tropical soil”. Characterisation and Engineering Properties of Natural Soils – Tan, Phoon, Hight & Leroueil (eds) Taylor & Francis, London, Vol. 4, pp. 2477-2505.

Futai, M.M.; Almeida, M.S.S; Lacerda, W.A. 2004. “Yield, strength and critical state conditions of a tropical saturated soil”. J. Geotech. Geoenviron. Engng 130, nº 11, pp.1169-1179.

Futai, M. M.; Ito, W. H. (2008). “Estudo da resistência de solos não saturados com medida directa de sucção”. XI Congresso Nacional de Geotecnia, Coimbra, Portugal. (in Portuguese)

Gabriel, K. (2001). “What´s on the Agenda?”. Ground Engineering, 34 (7), pp. 22-23.

Gens, A.; Nova, R. (1993). “Conceptual bases for a constitutive model for bonded soils and weak rocks”. Proc. Int. Symp. Geotechnical Engineering of Hard Soils – Soft Rocks. Athens. pp. 553-560.

Geological Society of London (1970). “The logging of rock cores for engineering purposes”. Report by the Gelological Society Engineering Group Working Party. . Q. J. Eng. Geol. 3, pp. 1-24.

Geological Society of London (1972). “The preparation of maps and plans in terms of engineering geology”. Report by the Gelological Society Engineering Group Working Party. . Q. J. Eng. Geol. 5, pp 29 - 381.

Geological Society of London (1977). “The Description of Rock Masses for Engineering Purposes”. Report by the Gelological Society Engineering Group Working Party. Q. J. Eng. Geol. 10(4), pp 335-388.

Geological Society of London (1995). “The description and classification of weathered rocks for engineering purposes”. Report by the Gelological Society Engineering Group Working Party. . Q. J. Eng. Geol. 28, pp. 207-242.

Goodmann, R.E. (1989). “Introduction to rock mechanics”. J. Wiley & Sons, New York.

Grainger, P., McCann, D., Gallois, R. (1973). “The application of seismic refraction technique to the Study of the fracturing of the Middle Chalk at Mundford”. Geotechnique, 23(2), pp. 219-232.

Graham, J.; Noonan, M.L.; Lew; K.V. (1983). “Yield states and stress-strain relationships in a natural plastic clay”. Canadian Geotechnical Journal, Vol. 20 (3), pp. 502-516.

Gravesen, S. (1960). “Elastic semi-infinite medium bounded by a rigid wall with a circular hole”. Laboratoriet for Bygninsteknik, Danmarks Tekniske Hojskole, Meddelelse No. 10, Copenhagen.

Hardin, B.O. & Richart, F.E., Jr. (1963). “Elastic wave velocities in granular soils”. Journal of Soil Mechanics and Foundation Division, ASCE, 89 (SM1), 33-65.

Hardin, B.O., Drnevich, V.P. (1972). “Shear modulus and damping in soils: design equations and curves”. Journal of the Soil Mechanics and Foundations Division, ASCE, Vol. 98, No. 7, pp. 667-692.

Hardin, B.O. & Blandford, G.E. (1989). “Elasticity of particulate materials”. J. Geot. Eng. Div., Vol. 115, GT6, pp. 788-805. ASCE, New York.

Hatanaka, M., & Uchida, A. (1996). “Empirical Correlation Between Penetration Resistance and Internal Angle of shearing resistance of Sandy Soils”. Soils and Foundations, Vol. 36, No. 4, pp. 1-9.

Hight, D.W. (1995). “Moderator’s report on session 3: drilling, boring, sampling and description”. Proc. of Int. Conf. ‘Advances in site investigation practice’. pp. 337-360. Inst. of Civil Engineers, London.

Hight, D.W. (2000). “Sampling methods: evaluation of disturbance and new practical techniques for high quality sampling in soils”. Keynote Lecture - Proc. 7º Cong. Nac. de Geotecnia, FEUP, Porto.

Ho, D.Y.F; Fredlund, D.G. (1982). “Strain rates for unsaturated soil shear strength testing”. 7th Southeast Asian Geotechnical Conference, Hong Kong.

Hoek, E., Bray J.W. (1981). “Rock slope engineering”. Revised 3th Edition. Reprinted 2001 by Spon Press for the Institute of Mining and Metallurgy, London.

Hoek, E., Brown E.T. (1980). “Underground excavation in rock”. Institute of Mining and Metallurgy, London.

Hoek, E. (1994). “Strength of rocks and rock masses”. ISRM New Journal 2(2), pp. 4-16.

Hoek, E.; Brown, E. T. (1997). “Practical estimates of rock mass strength”. Int. Journal of Rock Mechanics and Mining Sciences.

Hoek, E., Kaiser, P.K., Bawden, W.F. (1995). “Support of underground excavations in hard rock”. Ed, A. A. Balkema, Rotterdam/Brookfield.

Houlsby, G.T.; Withers, N.J. (1988). “Analysis of the cone penetration test in clays”. Geotechnique, 38(4), pp. 575-587.

Hryciw, R.D. (1990). “Small-strain-shear modulus of soil by dilatometer”. Journal of Geotechnical Eng. ASCE, Vol 116, Nº11, pp.1700-1716.

Huang, A.B. (1989). “Strain path analysis for arbitrary three-dimensional penetrometers”. Int. Journal for Numerical and Analytical Methods in Geomechanics, 13, nº5, pp 551-564.

Hvorslev, M.S., (1951). “Time lag and soil permeability in groudwater measurements”. U.S. Corps of Engineers Waterways Experiment Station, Bulletin Nº 36.

Imai, T. & Tonouchi, K. (1982). “Correlation of N value with S-wave velocity”. Proc. 2nd European Symposium on Penetration Testing, pp. 67-72. Amsterdam.

Irfan, T.Y. (1996). “Mineralogy, fabric properties and classification of weathered granites in Hong Kong”. Quarterly Journal of Engineering Geology, Vol. 29, pp. 5-35.

Irfan, T.Y.; Dearman, W.R. (1978). “The engineering petrography of a weathered granite in Cornwall, England”. Quarterly Journal of Engineering Geology, Vol. 11, pp. 233-244.

Ishihara, K. (2001). “Estimate of relative density from in-situ penetration tests”. Proc. Int. Conf. on Insitu Measurement of Soil Properties and Case Histories, Bali, pp 17-26.

ISO/CEN (2001). “Geotechnical Engineering – identification and description of rock”. International standard 14689-2

ISRM (1981). “Rock characterization testing monitoring”. ISRM Suggested methods. Edition ET Brown.

Islam, M.K. (1999). “Modelling the behaviour of cemented carbonate soils”. PhD Thesis presented to University of Sydney.

Jaky, J. (1944). “The coefficient of earth pressure at rest”. Journal of the Society of Hungarian Architects and Engineers, pp. 355-358.

Jamiolkowski, B.M., Ladd, C.C. & Jermaine, J.T., Lancelota, R. (1985). “New developments in field and laboratory testing of soils”. Theme lecture, Session II, XI ISCMFE., Vol 1, S. Francisco, CA 1985, pp. 57-153.

Jamiolkowski, M.; Ghinna, V.; Lancellotta, R.; Pasqualini, E. (1988). “New correlations of penetration tests for design practice”. Proc. of Int. Symposium on Penetration Testing, ISOPT-1, Vol 1, 263 – 296. Orlando (USA). Balkema.

Jamiolkowski, M. & Robertson, P.K. (1988). “Future trends for penetration testing”. Closing Address. 'Penetration Testing in United Kingdom' Geotechnical Conference. pp.321-342 British Institution of Civil Engineers. Thomas Telford, London.

Jamiolkowski, M., Lancellotta, R. & Lo Presti, D.C.F. 1995. “Remarks on the stiffness at small strains of six Italian clays”. Keynote Lecture 3, Proc. Int. Symp. on Pre-Failure Deformation Charact. of Geomaterials, Sapporo, Vol. 2: 817-836.

Janbu, N. (1963). “Settlement calculations based on the tangent modulus concept”. Bulletin Nº 2, Soil Mechanics. NTH, Trondheim.

Janbu, N.; Senneset, K. (1974). “Effective stress interpretation of in-situ static penetration tests”. Proc. of European Symposium on Penetration Testing, ESOPT, pp. 181 – 193. Stockholm, Sweden.

Jardine, R., Potts, D., Fourie, A., Burland, B. (1986). “Studies of the influence of non-linear stress-strain characteristics in soil structure inter-action”. Geotechnique, 36(3), 377-396.

Jardine, R.J.; Fourie, A.; Maswoswe, J.; Burland, J.B. (1991) “Field and laboratory measurements of soil stiffness”. Proc. X ECSMFE, Firenze, Vol. 1, pp. 511-514. A.A. Balkema, Rotterdam.

Jardine (1992). “Non linear stiffness parameters from undrained pressuremeter tests” Canadian Geot. J., 29, pp. 436-447.

Jardine, R.J. and Shibuya, S. (2005). “TC29 workshop: Laboratory tests. Report”. Proceedings of the 16th International Conference on Soil Mechanics and Geotechnical Engineering, Osaka. Vol.5, pp. 3275-3276.

Jendeby, L. (1992). “Deep Compaction by Vibrowing”. Nordic Geotech. Meeting, Vol. 1, pp. 19 – 24.

Jefferies, M.G.; Davies, M.P. (1993). “Use of CPTu to estimate equivalent SPT N_{60}”. Geotechnical Testing Journal, 16(4). pp. 458-468.

Johnson, R.B.; De Graff,, J.V. 1988). “Principles of engineering geology”. John Wiley and Sons.

Karlsrud, K., Lunne, T., Brattlien, K. (1996). “Improved CPTu correlations based on block samples”. Proc. Nordic Geotechnical Conference, Vol 1, pp. 195-201. Reykjavic, Iceland.

Kenney, T.C., Moum, J., and Berre, T. (1967). “An experimental study of the bonds in a natural clay”. Proc. Geotech. Conf. on Shear Strength Prop. of Natural Soils and Rocks, Oslo, v.1, p.65.

Kjekstad, O.; Lunne, T.; Clausen, C. (1978). “Comparison between in-situ cone resistance and laboratory strength for overconsolidated North Sea clays”. Marine Geotechnology, 3(1), pp. 23-36.

Konrad, J.; Law, K. (1987). “Undrained shear strength from Piezocone tests”. Canadian Geotechnical Journal, 24, pp. 392 – 405.

Kulhawy, F., Mayne, P. (1990). “Manual on estimating soil properties for foundation design”. Electric Power Research Institute, EPRI.

Kruskall, W. H., Wallis, W., A. (1952). “Use of ranks in one-criterion variance analysis”. Journal of the American Statistical Association, 47 (260), pp. 583–621.

Lacasse, S. & Lunne, T. (1988). “Calibration of dilatometer correlations”. 'Penetration Testing - 1988', Proc. ISOPT-1, Orlando, Vol. 1, pp. 537-548. Ed. De Ruiter. A.A. Balkema, Rotterdam.

Ladanyi, B. (1963). “Expansion of cavity in a saturated clay medium”. J. of Soil Mechanics and Foundations Division, ASCE, 89, nº SM4, pp. 127-161.

Ladd, C.C. e Lambe, T. W. (1963). “The strength of undistubed clay determined from undrained tests”. Symposium on laboratory shear testing of soils, ASTM, STP 361, pp. 342-371.

Lade, P.V.; Nelson, R.B.; Ito, Y.M. (1987). “Non associated flow on stability of granular materials”. Journal of Engineering Mechanics, Vol. 113, pp. 1032-1318. ASCE, New York.

Ladd, C.C.; Foot, R. (1974). “New design procedure for stability of soft clays”. J. Geot. Eng. Div., Vol. 100, nº 7, pp. 763-786. ASCE, New York.

Lade, P.V.; Overton, D.D. (1989). “Cementation effects in frictional materials”. J. Geot. Eng., Vol. 115, Nº 10, pp. 1373-1387. ASCE, New York.

Ladd, C.C., Foot, R. Ishiara, K.; Poulos, H.G.; Schlosser, F. (1977). “Stress deformation and strength characteristics”. Proc. 9th Int. Confrence on Soil Mechanics and Foundation Engineering, Vol. 2, State-of-the-Art-Paper, Tokyo, pp. 421 – 494.

Lafayette, K. P. V. 2006. “Geologic and Geotechnical Study of Erosives Processes in Slopes at the Metropolitan Park Armando de Holanda Cavalcanti – Cabo de Santo Agostinho/PE”. PhD Thesis presented to Federal University of Pernambuco. (in Portuguese).

Lagioia, R. and Nova, R. (1995) “An experimental and theoretical study of the behaviour of a calcarenite in triaxial compression.” Géotechnique. 45, pp. 633-648.

La Rochelle, P., Zebdi, P., Leroueil, S., Tavenas, F., Virely, D. (1988). “Piezocone Tests in Sensitive Clays of eastern Canada”. Proc. of Int. Symposium on Penetration Testing, ISOPT-I, Vol. 2, pp. 831 – 841. Orlando (USA). Balkema.

Lee, I.K.; Coop, M.R. (1995). “The intrinsic behaviour of a decomposed granite soil”. Géotechnique 45, Nº 1, pp. 117-130.

Leroueil, S. (1997). “Critical state soil mechanics and the behaviour of real soils”. Proc. Conference on Recent Developments in Soil and Pavement Mechanics. Rio de Janeiro, pp. 41-80.

Leroueil, S. (2001). “Some fundamental aspects of soft clay behaviour and practical implications”. Proc. 3rd Int. Conf. on Soft Soil Engineering, pp. 37-53. Hong Kong, China. Balkema.

Leroueil, S & Vaughan, P.R. (1990). “The general and congruent effects of structure in natural clays and weak rocks”. Géotechnique, Vol 40, nº 3, pp. 467- 488.

Leroueil, S. & Barbosa, P. S. A. (2000). “Combined effect of fabric, bonding and partial saturation on yielding of soils”. Proc. Asian Conf. on Unsaturated Soils, Singapore, pp. 527–532.

Leroueil, S. & Hight, D.W. (2003). “Behaviour and properties of natural and soft rocks”. Characterization and Engineering Properties of Natural Soils. Eds. Tan et al. Vol.1, pp.29-254. Swets & Zeitlinger, Lisse.

Little, A.L.(1969). “The engineering classification of residual tropical soils”. Proc. Special Session, VII Int. Conf on. Soil Mechanics and Foundation Engineering, Vol. 1, pp. 1-10. Mexico City.

Liu, M.D. and Carter, J.P. (2002) “A structured cam clay model.” Canadian Geotechnical Journal. 39(6), pp. 1313-1332.

Long, M. (2001). The influence of plasticity on sample disturbance in soft clays. International conference on in-situ measurements of soil properties and case histories, Bali, pp. 385-389.

Lopes, M. (2009). ”Avaliação da eficácia energética no ensaio SPT”. MSc Thesis presented to GeoScience Dept. of University of Aveiro. (in Portuguese)

Lo Presti, D.C.F.; Pallara, O.; Cavallaro; Lancellotta, R.; Armandi, A..; Maniscalco, R. (1993). “Monotonic and cyclic loading behavior of two sands at small strains”. ASTM Geotechnical Testing Journal, 16(4), pp. 409-424.

Lo Presti, D.C.F.; Jamiolkowski, M. Pallara, O.; Cavallaro, A.; Pedroni, S. (1997). “Shear modulus and damping of soils. Geotechnique, 47(3), pp. 603-617.

Luke, K. (1995). “The use of c_u from danish triaxial tests to calculate cone factor”. Proc. of Int. Symposium on Cone Testing, CPT’ 95, Vol. 2, pp. 219 – 214. Linkoping, Sweden.

Lumb, P. (1962). “The properties of decomposed granite”. Géotechnique. Vol.12, No. 3, pp. 226-243. London.

Lunne, T.; Kleven, A. (1981). “Role of CPT in North sea foundation engineering”. ASCE National Convention – Cone Penetration Testing and Materials, pp. 76 – 107. St Louis, USA.

Lunne, T. Christophersen, H. (1983). “Interpretation of piezocone data for offshore sands”. Proc. of the Offshore Technology Conference, Paper nº 4464. Richardson, Texas, USA.

Lunne, T. Christophersen, H., Tjelta, T. (1985). “Engineering use of piezocone data in North Sea Clays”. Proc. 11th Int. Conf. on Soil Mechanics and Foundation Engineering, Vol. 2, pp. 907 - 912. S. Francisco, USA.

Lunne, T., Lacasse, S. & Rad, N.S. (1989). “State of the art report on in-situ testing of soils”. Proc. XII ICSMFE, Rio de Janeiro, 4, pp. 2339-2403.

Lunne, T.; Robertson, P.; Powell, J. (1997). “Cone penetration testing in geotechnical practice”. E & FN Spon.

Lunne, T; Berre, T; Strandvik, S. (1997). “Sample disturbance effects in soft low plastic Norwegian clay”. Proc. Conf. on Recent Developments in Soil and Pavement Mechanics, pp. 81-92. Rio de Janeiro, Brasil.

Lutenegger, A. (1988). “Current status of the Marchetti dilatometer test”. General Proc. of Int. Symposium on Penetration Testing, ISOPT-I, Vol. 1, 137 – 155. Orlando (USA). Balkema, Rotterdam.

Lutenegger, A.J.; Timian, D.A. (1986). Flat plate penetrometer test in Marine Clays. 39th Canadian Geotechnical Conference. Ottawa, pp.301-309.

Lutenegger, A. J., Kabir, M. G. (1988). “Dilatometer C-reading to help determine stratigraphy”. Proc. ISoPT-1, Orlando, FL, Vol. 1, pp. 549-554.

Maâtouk, A.; Leroueil, S. & La Rochelle, P. (1995). “Yielding and critical state of a collapsible unsaturated silty soil”. Géotechnique, 45, no 3, pp. 465–477.

Maccarini, M.M. (1987). “Laboratory studies of a weakly bonded artificial soil”. Ph.D. Thesis, University of London, London, U.K.

Machado, S. L. & Vilar, O. M. (2003). “Geotechnical characteristics of an unsaturated soil deposit at São Carlos, Brazil”. Characterization and Engineering Properties of Natural Soils – Tan et al. (eds.), Swets & Zeitlinger, Lisse.

Malandraki, V.; Toll, D.G. (1994). “Yielding of a weakly bonded artificial soil”. Proc. Int. Symp. on Pre-failure Deformation Characteristics of Geomaterials. Hokkaido, Japan. E^{ds} Shibuya, Mitachi & Miura, Vol. 1, pp. 315-320.

Malandraki, V.; Toll, D. (2000). “Drained probing triaxial tests on a weakly bonded artificial soil”. Géotechnique, Vol. 50, Nº 2, pp. 141-151.

Mántaras, F.M.; Schnaid, F. (2002). “Cylindrical cavity expansion in dilatant cohesive-frictional materials”. Géotechnique, Vol. 52, Nº 5, pp. 337-348.

Marchetti, S. (1980). “In-situ tests by flat dilatometer”. J. Geotechnical. Eng. Div. ASCE, 106, GT3, pp. 299-321.

Marchetti, S. (1985). "On the field determination of Ko in sand". XI Int. Conference on Soil Mechanics and Foundation Engineering, Vol 5. S. Francisco.

Marchetti, S. (1988). “On the field determination of K_0 in sand. Report and discussions on the sessions”. Session Nº 2A. Proc. XI Int. Conference on Soil Mechanics and Foundation Engineering, San Francisco, Vol 5, pp. 2667-2672. A.A. Balkema, Rotterdam.

Marchetti, S. (1997). The flat dilatometer design applications. III Geotechnical Engineering Conference, Cairo University.

Marchetti, S. (1999). ‘’The flat dilatometer and its applications to geotecnhical design’’ Japanese geotechinal society International seminar. Tokyo.

Marchetti, S. & Crapps,D.K. (1981). “Flat dilatometer manual”. Internal report of GPE Inc., distributed to purchasers of DMT equipment.

Marchetti S., Monaco P., Totani G. & Calabrese M. (2001). “The flat dilatometer test (DMT) in soil investigations”. Report of the ISSMGE Technical Committee 16. Int Conf. On In-situ Measurement of Soil Properties, Bali, Indonesia. Document also available in Proc. 2nd International Flat Dilatometer Conference, Washington D.C. (2006).

Marchetti S., Monaco P., Totani G. & Calabrese M. (2006). “Comparison of moduli determined by DMT backfigured from local measurements under a 40m diameter test

load in Venice area“.Proc. 2nd International Flat Dilatometer Conference, Washington, D.C. pp. 220-231.

Marchetti, S., Monaco, P., Totani, G. & Marchetti, D. (2008). “In -situ tests by seismic dilatometer (SDMT)”. In J.E. Laier, D.K. Crapps & M.H. Hussein (eds), From Research to Practice in Geotechnical Engineering, ASCE Geotech. Spec. Publ. No. 180 (honoring Dr. John H. Schmertmann), pp. 292-311.

Martins, F.B.; Bica, A.V.D.; Bressani, L.A.; Coop, M.R. (2002). “Interacção das componentes porosidade e cimentação no comportamento mecânico de um solo arenoso”. XII COBRAMSEG – I CLBG – III SBMR, Vol. 2, pp. 657-669.

Massarch, K.; Broms, B. (1981). “Pile Driving in Clay Slopes”. Proc. 10th Int. Conf. on Soil Mechanics and Foundation Engineering. Stockholm. Balkema.

Mateus, C. (2008), ‘’Determinação dos erros de medição associados ao ensaio DMT’’ MSc Thesis presented to GeoScience Dept. of University of Aveiro. (in Portuguese)

Mateus, C.; Cruz, N.; Vieira, P., Cruz, M. Machado, L. (2010). “Determination of measurement errors related to in-situ testing. The DMT, PMT, CPTu Cases”. XII Congresso Nacional de Geotecnia. Guimarães. (in Portuguese)

Matos Fernandes, M. (2006). “Mecânica dos solos. Conceitos e princípios fundamentais”. 2ªedição. (in Portuguese)

Matthews, K. (1993). “Mass compressibility of fractured chalk”. PhD Thesis. Dept. of Civil Engineering of Universiy of Surrey.

Matthews, M., Hope, V., Clayton, C. (1996). “The use of surface waves in the determination of ground stiffness profiles”. Proc. Inst. Civ. Eng. Geotech. Eng, 119, pp. 84-95.

Mayne, P. (2001). “Ground property characterization by in-situ tests”. Proc. 15th Int. Conf. on Soil Mechanics and Geotechnical Engineering. Balkema, Istambul.

Mayne, P. W. (2006). “Interrelationships of DMT and CPT in soft clays”. Proc. 2nd Int. Conf. on Flat Dilatometer. Washington, DC. pp. 231-236.

Mayne, P.W. (2007). “Synthesis on cone penetration testing: state-of-practice”. NCHRP Project 20-05, task 37-14. Transportation Research Board. National Academies Press, Washington D.C.

Mayne, P.; Kulhawy, F. (1982). “K0 - OCR relationship in soils”. J. Geot. Eng. Div., Vol. 108, GT6, pp. 851-872. ASCE, New York.

Mayne, P.; Stewart, H. (1988). “Pore-pressure behaviour of K_0-consolidated clays”. J. Geotechnical. Eng. Div. ASCE, 1341-1346.

Mayne, P.W.; Martin, G.K. (1998). “Commentary on Marchetti flat dilatometer correlations in soils”. Geotechnical Testing Journal, 21(3), pp. 222 – 239.

Mayne, P.W.; Bachus, R.C. (1989). “Penetration pore pressures in clay by CPTu, DMT and SBPT”. Proc. XII ICSMFE, Rio de Janeiro, pp 291-294.

Mayne, P.; Rix, J. (1993). “G_{max}-q(c) relationships for clays”. Geotechnical Testing Journal, ASTM, 16(1), pp. 54-60.

Mayne, P.W., Schneider, J.A. & Martin, G.K. (1999). “Small and large strain soil properties from seismic flat dilatometer tests”. Proc. 2nd Int. Symp. on Pre-Failure Deformation Characteristics of Geomaterials, Torino, 1, pp. 419-427.

Mayne, P.W., Christopher, B.R. & DeJong, J. (2001). “Manual on subsurface investigations”. National Highway Institute. Publication No. FHWA NHI-01-031. Federal Highway Administration, Washington, DC. Geotechnical Site Characterization

Mayne, P.W. & Brown, D.A. (2003). “Site characterization of Piedmont residuum of North America”. Characterization and Engineering Properties of Natural Soils, Vol. 2, pp.1323-1339. Swets & Zeitlinger, Lisse.

Mayne, P.W.; Liao, T. (2004). “CPT-DMT interrelationships in Piedmont residuum”. Proc. 2nd Int. Conf. on Geotechnical and Geophysical Site Characterization, ISC’2. Porto. pp. 345-350.

McCann, D., Jackson, P., Green, A. (1986). “Application of Cross-Hole Seismic Measurements in Site Investigation Surveys”. Geophysics, 51, pp. 914-929.

Ménard, L. (1957). “An apparatus for measuring the strength of soils in place”. PhD thesis presented to University of Illinois.

Ménard, L. (1975) ‘’The Ménard Pressuremeter, Interpretation and application of pressuremeter test results to Foundation Design’’. Sols Soils.

Menzies, B. (1986). “An approximate correction for the influence of strength anisotropy on conventional shear measurements used to predict bearing capacity”. Geotechnique, Vol. VI.

Mesri (1975). “New design procedure for stability of soft clays”. ASCE Journal of Geot. Engrg. Div. Vol. 108, pp. 851-872.

Mesri, G., Abdel Ghaffar, E. M. (1993). “Cohesion intercept in effective stress-stability analysis”. J. Geotechnical. Eng. Div. ASCE, pp..1229 – 1249.

Mitchell, J., Gardner, W. (1975). “In-situ measurements of volume change characteristics”. Proc. of ASCE Specialty Conf. on In-situ Measurement of Soil Properties. Raleigh, North Carolina, USA.

Molenkamp, F. (1981). “Elasto-plastic double hardening model Monot”. LGM Report CO-218595: Delft Geotechnics.

Monaco, P., Totani, G. & Calabrese, M. (2006). “DMT-predicted vs observed settlements: a review of the available experience”. Proc. 2nd Int. Conf. on the Flat Dilatometer, Washington D.C., pp. 244-252.

Monaco, P., Marchetti, S.; Totani, G.; Marchetti, D. (2009). “Interrelationship between small strain modulus G_0 and operative modulus”. International Conference on Performance-Based Design in Earthquake Geotechnical Engineering, Tokyo.

Montañez, J. E. (2002). Suction and volume changes of compacted sand-bentonite mixtures. PhD Thesis presented to Imperial College of University of London.

Mooney, M.A.; Finno, R.J. & Viggiani, M.G. (1998). “A unique critical state for sand?”. J. Geot. Geoenv. Eng., Vol. 124, Nº11, pp. 1100-1108. ASCE, New York.

Moye, D. (1955). “Engineering geology for the snowy mountains scheme”. J. Inst. Eng. Australia, 27, pp. 281-299.

Nazarian, S., Stokoe, K. (1984). “In-situ shear wave velocities from spectral analysis of surface waves”. Proc. 8th World Conf. on Earthquake Engineering.

Ng, C. W. W. & Leung, E. H. Y. (2007a). “Small-strain stiffness of granitic and volcanic saprolites in Hong Kong”. Characterization and Engineering Properties of Natural Soils. Tan, Phoon,Hight & Leroueil (eds.)Vol. 4, Taylor & Francis Group, London, pp. 2507-2538.

Ng, C. W. W. & Leung, E. H. Y. (2007b). “Determination of shear-wave velocities and shear moduli of completely decomposed tuff”. Journal of Geotechnical and Geoenvironmental Engineering, Vol. 133, No. 6, pp. 630-640. ASCE.

Odebrecht, E. (2003). “Medida de energia no ensaio SPT”. PhD thesis presented to Universidade Federal do Rio Grande do Sul, Porto Alegre. (in Portuguese)

Odebrecht, E.; Schnaid, F.; Rocha, M.M; Bernardes, G.P. (2004). “Energy measurements for standard penetration tests and the effects of length of rods”. Geotechnical and geophysiscal on site conference, Porto, pp. 351-358.

Ohsaki, Y.& Iwasaki, R. (1973). “On dynamic shear moduli and Poisson ratios of soil deposits”. Soils and Foundations, 13 (4), pp. 61-73.

Parkin, A.K.; Lunne, T. (1982). “Boundary effects in the laboratory calibration of a cone penetrometer in sand”. Proc. 2nd European Symposium on Penetration Testing, ISOPT-1, Orlando, 1, pp. 221-243. Balkema, Rotterdam.

Peck, R. (1962). “Art and science in subsurface engineering”. Geotechnique, 12, pp. 60-68.

Peck, R., Hanson, W.E., Thornburn, T.H., (1974). “Foundation engineering”. 2nd Edition, John Wiley & Sons, Inc, New York.

Poulos, S.J. (1981). “The steady state of deformation”. J. Geot. Eng. Div., Vol. 17, GT5, pp. 553-562. ASCE, New York.

Powell, J., Quaterman, R. (1988). “The interpretation of cone penetration tests in clays, with particular references to rate effects”. Proc. of Int. Symposium on Penetration Testing, ISOPT-I, Vol. 2, pp. 903 – 910. Orlando (USA). Balkema.

Powell, J.; Uglow, I. (1988). “The interpretation of the Marchetti dilatometer test in UK clays”. Proc. Penetration Testing in UK. Paper 24, pp. 121 – 125.

Powell, J.J.M. & Butcher, A.P. (2004). “Small strain stiffness assessments from in situ tests”. Proc. 2nd Int. Conf. on Site Characterization, Porto, 2: pp. 1717-1722. Rotterdam: Millpress.

Puppala, A.J., Acar, Y.B., Senneset, K. (1993). “Cone penetration in cemented sands: bearing capacity interpretation”. J. Geot. Eng. Div., Vol. 119, Nº12, pp. 1990-2001. ASCE, New York.

Puppala, A.J.; Acar, Y.B.; Tumay, M.T. (1995). “Cone penetration in very cemented sand”. J. Geot. Eng., Vol. 121, Nº 8, pp. 589-600. ASCE, New York.

Puppala, A.J.; Arslan, S.; Tumay, M.T.; Acar, Y.B. (1998). “Cone penetration testing in cemented soils: Comparisons between field and laboratory chamber test results”. ”Proc. 1st Int. Conf. on Site Characterization ISC’98 Atlanta, USA. Eds Robertson & Mayne, Vol. 2, pp. 1139-1145.

Rad, N., Lunne, T. (1988). “Direct correlations between piezocone test results and undrained shear strength of clay”. Proc. of Int. Symposium on Penetration Testing, ISOPT-I, Vol. 2, 911 – 917. Orlando (USA). Balkema.

Randolph, M.; Wroth, C. (1979). “An analytical solution for the consolidation around a driven pile”. Proc. Int. Journal for Numerical and Analytical Methods in Geomechanics, 3(3), pp. 217-229.

Reiche, P. (1943). “Graphic representation of chemical weathering”. Jour. Sed. Petrol., 13, pp. 53-68.

Ricceri, G., Simonini, P. & Cola, S. (2001). “Calibration of DMT for Venice soils”. Proc. Int. Conf. on In Situ Measurement of Soil Properties and Case Histories, Bali, pp. 193-199.

Ridley, A.M. (1993). “The measurement of soil moisture suction”. PhD Thesis presented to University of London.

Ridley, A.M.; Wray, W.K. (1995). “Suction measurement: a review of current theory and practices”. Balkema, Rotterdam.

Rios Silva, S. (2007). “Modelling of a supported excavation in an access trench to the Casa da Música station in “Metro do Porto”. MSc thesis presented to University of Porto. (in Portuguese).

Rix, G.J. & Stokoe, K.H. (1992). “Correlations of initial tangent modulus and cone resistance”. Proc. Int. Symp. Calibration Chamber Testing. Potsdam, New York, pp. 351-362. Elsevier.

Robertson, P.K., Campanella, R.G., (1983). “Guidelines for geotechnical design using CPT and CPTU data”. Report Nº FHWA-PA-87-014-84-24. Vol. II, Federal Highway Administration, Washington, D.C.

Robertson, P., Campanella, R. (1983). “Interpretation of cone penetrometer test: Part I – Sand”. Canadian Geotech. J., 20, nº 4, pp. 718 – 745.

Robertson, P., Campanella, D.; Gillespie, D.; Grieg, J. (1986). “Use of Piezometer Cone Data”. Proc. of ASCE Specialty Conference In-situ’ 86. Blacksburg, USA.

Robertson, P. (1990). “Soil classification using the cone penetrometer test”. Canadian Geotechnical J., 27, pp. 151 – 158.

Robertson, P.K., (1991). “Estimation of foundation settlements in sand from CPT”. ASCE Geotechnical Engineering Congress, Boulder.

Robertson, P.K. (2009). “CPT-DMT correlations”. Journal of Geotechnical and Geoenvironmental Engineering, ASCE, pp. 1762-1772.

Rocha, M. (1981). “Mecânica das rochas”. Published by LNEC, Portugal. (in Portuguese)

Rocha, M.; Lopes, J.; Silva (1966). “A new technique for applying the method of Flat-Jack in the determination of stress inside rock masses”. 1st Congress of Int. Society of Rock Mechanics. Lisboa.

Rocha, M.; Silveira, A.; Grossmann, N.; Oliveira, E. (1969). “Determination of the deformability of rock masses along boreholes”. LNEC, Memoria nº 339, Lisboa.

Rocha, M.; Silveira, A.; Rodrigues, F.; Silvério, A.; Ferreira, A. (1970). “Characterization of the deformability of rock masses by dilatometer tests”. LNEC, Memoria nº 360, Lisboa.

Rocha Filho, P.; Antunes, F.S.; Falcão, M.F.G. (1985). “Qualitative influence of the weathering degree upon the mechanical properties of an young gneiss residual soil”. 1st Int. Conf. on Geomechanics in Tropical Lateritic and Saprolitic Soils. Vol. 1, pp. 281-294. Brasilia, Brasil.

Rocha, R.; Rodrigues, C.; Cruz, N.; Saraiva Cruz, J. (2010). “Comparing Cross-Hole, Down-Hole and Up-Hole results in volcanic massifs”. XII Congresso Nacional de Geotecnia. Guimarães. (in Portuguese)

Rodrigues, C. (2003). “Caracterização geotécnica e estudo do comportamento geomecânico de um saprólito granítico da Guarda”. PhD Thesis, University of Coimbra. (in Portuguese)

Rodrigues, C.M.G.; Antão, A.M. (1997). “Distinção quantitativa de diferentes graus de alteração em rochas graníticas, utilizando ensaios expeditos”. 6º Cong. Nac. Geotecnia, IST, Lisboa. Vol. 1, pp. 85-94. (in Portuguese).

Rodrigues, C.M.G.; Lemos, L.J.L (2000). “Comportamento intrínseco de um solo residual granítico”. 7º Cong. Nac. Geotecnia, FEUP, Porto. Vol. 1, pp. 229-240. (in Portuguese).

Rodrigues, C.M.G.; Lemos, L.J.L (2001). “Experiência na amostragem de saprólitos graníticos da Guarda com amostradores de tubo aberto”. Workshop – Técnicas de Amostragem em Solos e Rochas Brandas e Controlo de Qualidade. FEUP, Junho 2001. (in Portuguese).

Rodrigues, C.M.G.; Lemos, L.J.L (2002a). “Amostragem de saprólitos graníticos da Guarda com amostrador de tubo aberto; avaliação da qualidade”. 8º Cong. Nac. Geotecnia, LNEC, Lisboa. Vol. 1, pp. 15-24. (in Portuguese).

Rodrigues, C.M.G.; Lemos, L.J.L (2002b). “Características de resistência e deformabilidade de um saprólito granítico da Guarda: influência da amostragem”. XII COBRAMSEG – I CLBG – III SBMR, Vol. 1, pp. 25-34. (in Portuguese).

Rodrigues, C.M.G.; Sousa, L.M.O (2002c). “Influência da composição química e mineralógica no comportamento do saprólito granítico da Guarda”. 8º Cong. Nac. Geotecnia, LNEC, Lisboa. Vol. 1, pp. 321-330. (in Portuguese).

Rodrigues, C.M.G.; Cruz, N.; Lemos, L.J.L (2002d). “Caracterização geotécnica de um solo residual granítico; correlação paramétrica”. 8º Cong. Nac. Geotecnia, LNEC, Lisboa. Vol. 1, pp. 155-164. (in Portuguese).

Rodrigues, C.M.G., Lemos, L.J.L. (2004). “SPT, CPT and CH tests results on saprolitic granite soils from Guarda, Portugal.” Second Int.Conf.on Site Characterization – ISC’2, Porto. Ed. Viana da Fonseca & Mayne, Millpress, Rotterdam.

Rodrigues, C., Saraiva Cruz, J., Cruz, N., Paiva, F., Rocha, R., Vieira Simões, E. (2010). “Alternative methodology for execution of SCPTu tests with selection of the seimic source and test conditions”. XII Congresso Nacional de Geotecnia. Guimarães. (in Portuguese)

Rodrigues, C., Saraiva Cruz, J., Cruz, N., Silva, D., Lopes, M., Vieira Simões, E. (2010). " Evaluation of energy efficiency of SPT test. A case study". XII Congresso Nacional de Geotecnia. Guimarães. (in Portuguese).

Roque, R.; Janbu, N.; Senneset, K. (1988). "Basic interpretation procedures of flat dilatometer". Proc. of Int. Symposium on Penetration Testing, ISOPT-I, Vol. 1, pp. 577 – 587. Orlando (USA). Balkema.

Roscoe, K.H.; Schofield, A.N.; Wroth, C.P. (1958). "On the yielding of soils". Géotechnique 8, Nº 1, pp. 22-52.

Roscoe & Burland (1968). "On the generalised stress-strain behaviour of 'wet' clay". 'Engineering Plasticity". Ed. J.Heyman e F.A. Leckie. Cambridge University Press, Cambridge.

Ruxton, B.P.; Berry, L. (1957). "Weathering of granitic and associated erosional features in Hong Kong". Bull. Geological Soc. of America , Vol. 68, pp. 1623-1291.

Sabatini, P.J., Bachus, R.C., Mayne, P.W., Schneider, J.A. & Zettler, T.E. (2002). "Evaluation of soil and rock properties". Technical Manual. FHWA-IF-02-034. Federal Highway Admin., Washington.

Sandroni, S.S. (1985a). "Sampling and testing of residual soils in Brazil. Sampling and testing of residual soils – a review of International Practice". Technical Committee on Sampling and Testing of Residual Soils, ISSMFE, pp 31-51.

Sandroni, S.S. (1985b). "Stress relief effects in gneissic saprolitic soils". Proc. 1st Int. Conf. on Geomechanics in Tropical Lateritic and Saprolitic Soils, Brasilia, Vol. 3, pp. 290-295.

Santamarina, J. C. (2001). "Soil behaviour at the microscale: particle forces". Proc. Symp. Soil Behavior and Soft Ground Construction, in Honour of Charles C. Ladd – October 2001, MIT.

Santos, J. A. (1999). "Soil characterization by dynamic and cyclic torsional shear tests. Application to the study of piles under lateral static and dynamic loading". PhD thesis presented to Technical University of Lisbon, Portugal. (in Portuguese).

Saraiva Cruz, J. (2003) “Caracterização geotécnica através do ensaio CPTu”. Awarded BSc final work for the degree of Geotechnical Engineer. Instituto Superior de Engenharia do Porto (in Portuguese).

Saraiva Cruz, J. (2008) “Caracterização geotécnica de maciços terrosos com base emcampanhas multi-ensaios”. MSc Thesis, Instituto Superior de Engenharia do Porto (in Portuguese)

Schmertmann, J.H. (1978). Guidelines for cone penetration test, performance, and design. Federal Highway Administration, FHWA, Report TS-78-209, Washington.

Schmertamnn, J.H. (1983). “Revised procedure for calculating K_0 and OCR from DMTs with ID > 1,2 and which incorporates the penetration force measurement to permit calculating the plane-strain angle of shearing resistance”. 'DMT-Digest # 1', GPE Inc., Gainesville, pp. 16-18.

Schmertmann, J.H. (1986). “Dilatometer to compute Foundation Settlement”. Proc. ASCE Spec. Conf. on Use of In Situ Tests in Geotechnical Engineering In Situ '86, Virginia Tech, Blacksburg. ASCE Geotech. Spec. Publ. No. 6, pp. 303-321.

Schmertamnn, J.H. (1988). “A method for determining the angle of shearing resistance in sands from the Marchetti Dilatometer test”. Proc. ESOPT-II, Amsterdam.

Schnaid, F. (2000). “Ensaios de campo e suas aplicações à Engenharia de Fundações”. Oficina de Textos, São Paulo, Brasil.

Schnaid, F. (2005). “Geo-characterisation and properties of natural soils by in-situ tests”. Keynote Lecture. 16th ICSMGE, Osaka, (1), pp. 3-45. Millpress, Rotterdam.

Schnaid, F.; Mántaras, F.M. (1998). “Assessment of soil properties in cohesive – frictional materials with pressuremeter tests”. Proc. 1st Int. Conf. on Site Characterization ISC’98 Atlanta, USA. E^{ds} Robertson & Mayne, Vol. 2, pp. 811-816.

Schnaid, F.; Prietto, P. D. M.; Consoli, N. C. (2001). “Characterization of cemented sand behaviour in triaxial compression”. Journal of Geotechnical and Geoenvironmental Engineering, 127, 10, pp. 857-868.

Schnaid, F. & Mántaras, F.M. (2003). “Cavity expansion in cemented materials: structure degradation effects”. *Géotechnique*, 53 (9), pp. 797-807.

Schnaid, F.; Lehane, B.; Fahey, M.(2004) “In-situ test characterization of unusual geomaterial”. Geotechnical and Geophysical Site Characterization, ISC’2. Keynote Lecture. Viana da Fonseca, A. and Mayne, P.W.(eds.) Millpress, Rotterdam, pp. 49–74.

Schnaid, F. & Coutinho, R.Q. (2005). “Pressuremeter Tests in Brazil (National Report)”. International Symposium 50 Years of Pressuremeters, (2), pp. 305-318.

Schnaid, F.; Odebrecht, E; Rocha, M. M.; Bernardes, G.P (2009). “Prediction of soil properties from the concepts of energy transfer in dynamic penetration tests. Journal of Geotechnical and gGeoenvironmental Engineering, ASCE, Vol. 135, 8, pp. 1092-1100.

Schofield, A.N.; Wroth, C.P. (1968). “Critical state soil mechanics”. McGraw-Hill, London.

Skempton, A.W., (1986). “Standart penetration test procedures and effects in sands of overburden pressure, relative density, particle size, ageing and overconsolidation”. Geotechnique 36, Nº3, pp. 425-447.

Senneset, K.; Janbu, N.; Svano, G. (1982). “Strength and deformation parameters from cone penetrometer tests”. Proc. 2nd European Symposium on Penetration Testing, ESOPT-II, Vol. 2, pp. 863 – 870. Amsterdam. Balkema.

Senneset, K., Sandven, R., Lunne, T.,By, T., Amundsen, T. (1988). “Piezocone tests in silty soils”. Proc. of Int. Symposium on Penetration Testing, ISOPT-I, Vol. 2, pp. 955 – 966. Orlando (USA). Balkema..

Serafim, J.L.; Pereira, J.P. (1983). “Considerations of the geomechanical classification of Bieniawski”. Proc. Int Symp. On Eng. Geology and underground construction. Lisbon, Balkema.

Silva Cardoso, A. 1986.“Ensaios triaxiais dos solos residuais da cidade do Porto”. Geotecnia, nº 47, pp. 103-124. SPG, Lisboa

Sueoka, T. (1988). “Identification and classification of granitic residual soils using chemical weathering index”. 'Geomechanics in Tropical Soil'. Proc. Sec. Int. Conf., Singapore, Vol. 1, pp. 25-35. A.A. Balkema, Rotterdam.

Simons, N.; Menzies, B.;Matthews, M. (2002) “Geotechnical site investigation”. Thomas Telford.

Smith, P.R.; Jardine R.J.; Hight, D.W. (1992). “The yielding of Bothkennar clay”. Geotechnique, 42(2), pp. 257 – 274..

Smith, M.G.; Houlsby, G.T. (1995). “Interpretation of Marchetti’s dilatometer in clay”. Proc. 11th European Conf. on Soil Mechanics and Foundation Engineering. Copenhagen, Denmark. pp. 1247-1253.

Stroud, M.A. (1988). “The standart penetration test-its application and interpretation. Penetration Testing in U.K, Proc. Of the Geot. Conf. Inst of Civil Engineers, Birmingham, July, 1988, pp. 24-49. Thomas Telford. London

Sully, J.P. & Campanella, R.G. (1989). Correlation of maximum shear modulus with DMT test results in sand. Proc. XII ICSMFE, Rio de Janeiro, Vol. 1, pp.339-343

Tanaka, H. & Tanaka, M. (1998). “Characterization of sandy soils using CPT and DMT”. Soils and Foundations, Vol. 38, nº3, pp.55-65

Tatsuoka, F. & Shibuya, S. (1991). “Deformation characteristics of soils and rocks from field and laboratory Tests”. Keynote lecture, 9th Asian Reg.Conf. SMFE., Bangkok, Vol.2, pp.101-170. A.A. Balkema, Rotterdam; Report Inst. Ind. Science, Univ.of Tokyo.

Tavenas, F.; Leroueil, S. (1990). “Laboratory and in-situ stress-strain-time behaviour of soft clays”. Proc. Int. Symp. Geotechnical Engineering of Soft Soils. Mexico City. Vol 2.).

Terzaghi, K., Peck, R.B., 1948. “Soil mechanics in engineering practice”. 1st Edition, John Wiley & Sons, New York.

Terzaghi, K., Peck, R.B (1967). “Soil mechanics in engineering practice”. 2nd Edition, John Wiley & Sons, New York.

Toll, D.; Malandraki, V.; Ali Rahman, Z.; Galipolli, D. (2006). “Bonded soils: problematic or predictable”. Proc. 2nd International Conference on Problematic Soils, Malaysia, Dec. 2006, Singapore: CI-Premier, pp. 55-62

Topa Gomes, A. (2009). “Elliptical shafts by the sequential excavation method. The example of Metro do Porto”. PhD thesis presented to Faculdade de Engenharia da Universidade do Porto, Portugal. (in Portuguese)

Topa Gomes, A.; Viana da Fonseca, A.; Fahey, M. (2008). “Self-boring pressuremeter tests in Porto residual soil: results and numerical modeling”. Geotechnical and Geophysical Site Characterization Conference, ISC3. Taiwan.

Totani, G.; Calabrese, M.; Marchetti, S.; Monaco, P. (1997). “Use of In-situ Flat Dilatometer (DMT) for Ground Characterization in the Stability Analysis of Slopes”. Proc. XIV Int. Conf. On Soil Mechanics and Foundation Engineering, Session 1.2. Hambourg.

Vallejo, L.; Ferrer, M.; Ottuño, L.; Oteo, C. (2002). “Ingeniería geológica’’, Pearson Educación, Madrid.

Vaid, Y.P.; Chung, E.K.F.; Kuerbis, R.H. (1990). “Stress path and steady state”. Canadian Geotech. J., Vol. 27, Nº 1, pp. 1-7.

Vanapalli, S. K.; Fredlund, D. G.; Pufahi, D. E.; Clifton, A. W. (1985). “Model for prediction of shear strength with respect to soil suction”. Canadian Geotechnical Journal. 33:(1996), pp. 379-392.

Vargas, M. (1992). “Identification and classification of tropical soils”. Proc. US/Brazil Geotechnical Workshop on Applicability of Classical Soil Mechanics to Structured Soils. pp. 200 – 205. $E^{\underline{ds}}$. Lima, Nieto,Viotti e Bueno. Univ. Fed. Viçosa, Belo Horizonte, Brazil.

Vaughan, P.R. (1985). “Mechanical and hydraulic properties of tropical and saprolitic soils, particularly as related to their structure and mineral componenets”. Proc. 1st Int. Conf. on Geomechanics in Tropical Lateritic and Saprolitic Soils, Brasilia, Vol. 3, pp. 231-263.

Vaughan, P.R. (1988). “Characterizing the mechanical properties of in-situ residual soils”. Proc. 2nd Int. Conf. Geomechanics in Tropical Soils, Singapore, Vol. 2, pp. 469-487.

Vaughan, P.R.; Kwan, C.W. (1984). “Weathering, structure and in-situ stress in residual soils”. Géotechnique, Vol. 43, Nº 1, pp. 43-59.

Vaughan, P.R.; Maccarini, M.; Mokhtar, S.M. (1988). “Indexing the engineering properties of residual soils”. Quarterly Journal of Engineering Geology, Nº 21, pp. 69-84.

Vesic, A. (1972). “Expansion cavities in infinite soil mass”. Journal of Soil Mechanics and Foundation Engineering Division, ASCE, SM3.

Viana da Fonseca, A. (1988). “Caracterização Geotécnica de um Solo Residual do Granito da Região do Porto”. Dissertação apresentada à Faculdade de Engenharia da Universidade do Porto para obtenção do grau de Mestre em Estruturas de Engenharia Civil. Relatório 130/88, NGR, LNEC, Lisboa.

Viana da Fonseca, A. (1998). “Identifying the reserve of strength and stiffness characteristics due to cemented structure of a saprolitic soil from granite”. Proc. 2nd International Symposium on Hard Soils – Soft Rocks. Naples. Vol.1: pp. 361-372. Balkema, Rotterdam.

Viana da Fonseca, A. (2001). “Load Tests on residual soil and settlement prediction on shallow foundation”. J. Geotechnical and Geoenvironmental Eng., The Geo-Inst. ASCE. Vol.127, Nº10, pp.869-883. New York.

Viana da Fonseca, A. (1993). “Correlating in-situ parameters from different testing procedures in Oporto residual soil from granite”. Geotechnical Engineering of Hard Soils-Soft Rocks. Proc. Int. Symp., Vol. 1, pp. 841-848. Ed. Anagnastopoulos et al. A.A. Balkema, Rotterdam.

Viana da Fonseca, A. (1996) “Geomechanics of Porto residual soil from granite. Project criteria for direct foundations”. PhD thesis presented to Porto University. (in Portuguese)

Viana da Fonseca, A. (2003). “Characterising and deriving engineering properties of a saprolitic soil from granite, in Porto”. Characterization and Engineering Properties of Natural Soils. Vol 2. Edited by Leroueil, S., Phoon, K.K., Tan, T.S., Hight, D. W.

Viana da Fonseca, A.; Matos Fernandes, M.; Cardoso, A.S., Barreiros Martins, J. (1994). “Portuguese experience on geotechnical characterisation of residual soils from granite”. Proc. XIII ICSMFE, New Dehli, India, Janeiro, Vol. 1, pp. 377--380. A.A. Balkema, Rotterdam.

Viana da Fonseca, António; Matos Fernandes, Manuel; Cardoso, António Silva. (1997). “Interpretation of a footing load test on a saprolitic soil from granite”. Géotecqnique. 47:3, pp. 633-651.

Viana da Fonseca, A. & Cardoso, A. S. (1998). “Surface loading tests for mechanical characterisation of a saprolitic soil from granite of Porto”. Proc. XI Panamerican Conference on Soil Mechanics and Geotechnical – Foz de Iguassu, Brazil, 8-12 de Aug de 1999. 1, 403-409.

Viana da Fonseca, A.; Ferreira, C. (2001). “Gestão da qualidade de amostragem em solos residuais e em solos argilosos moles. Análise comparativa de velocidades de ondas sísmicas in-situ e em laboratório”. Workshop Técnicas de amostragem em solos e rochas brandas. FEUP, Portugal.

Viana da Fonseca, António; Almeida e Sousa, J. (2001). “At rest coefficient of earth pressure insaprolitic soils from granite. In: XIV International COnference on Soil Mechanics and Foundation Engineering, Istambul, 2001,

Viana da Fonseca, A., Vieira, F., Cruz, N. (2001). “Correlations between SPT, CPT, DP, DMT, CH and PLT Tests Results on Typical Profiles of Saprolitic Soils from Granite”. International Conference on In-situ Measurement of Soil Properties and Case Histories. Bali, Indonésia.

Viana da Fonseca, A.; Ferreira, C. (2002). “Bender elements como técnicas laboratoriais excelentes para avaliação de parâmetros geotécnicos referenciais”. 8º Congresso Nacional de Geotecnia, Vol. 1, pp.353-365. LNEC, Lisboa

Viana da Fonseca, A. & Almeida e Sousa, J. (2002). “Hyperbolic model parameters for FEM analysis of a footing load test on a residual soil from granite”. PARAM 2002: Int. Symposium on Identification and determination of soil and rock parameters for geotechnical design. Vol. 1, pp 429-443 Ed. J-P Magnan, Presses L’ENPC , Paris.

Viana da Fonseca, A., Ferreira, C. & Carvalho, J.(2004). “Tentative evaluation of K_0 from shear waves velocities determined on Down-hole (Vsvh) and Cross-hole (Vshv) tests on a residual soil”. Geotechnical and Geophysical Site Characterization, Viana da Fonseca, A.and Mayne, P.W.(eds.) Millpress, Rotterdam

Viana da Fonseca, A., Ferreira, C. & Carvalho, J.(2005a). “The use of shear wave velocities determined on Down-hole (Vsvh) and Cross-hole (Vshv) tests for the evaluation of K_0 in soils”. Solos e Rochas, Vol.28, Nº3, pp. 271-281

Viana da Fonseca, A.; Carvalho, J. M.; Ferreira, C.; Santos, J. A.; Almeida, F.; Hermosilha, H. (2005b). Combining geophysical and mechanical testing techniques for the investigation and characterization of ISC’2 residual soil profile. Proceedings of the

16th International Conference on Soil Mechanics and Geotechnical Engineering, 12-16 Setembro 2005, Osaka, Japan. Vol. 2, pp. 765-769.

Viana da Fonseca, A., Carvalho, C., Ferreira, C., Santos, J.A., Almeida, F., Pereira, E., Feliciano, J., Grade, J. & Oliveira, A.(2006). “Characterization of a profile of residual soil from granite combining geological, geophysical and mechanical testing techniques”. Geotechnical and Geological Engineering, 24, pp.1307-1348

Viana da Fonseca, A.; Silva, S.; Cruz, N. (2007). "Retro-analysis of a supported excavation on a saprolitic soil from granite in Porto for design optimisation". First Sri Lankan Geotechnical Society. International Conference on Soil and Rock Engineering. Colombo, Sri Lanka.

Viana da Fonseca, A. and Coutinho, R. Q. (2008). “Characterization of residual soils”. Keynote paper – 3rd International Conference on Site Characterization. Taiwan.

Viana da Fonseca, A.; Silva,S.; Cruz, N. (2009) "Geotechnical characterization by “in-situ” and lab tests to the back analysis of a supported excavation in Metro do Porto ". International Journal of Geotechnical and Geological Engineering.

Vieira de Sousa, J.F. (2002). “Modelação de ensaios de carga considerando a variação da rigidez dos solos em profundidade. Parametrização recorrente de ensaios complementares in-situ e em laboratório”. Dissertação apresentada à Faculdade de Engenharia da Universidade do Porto para obtenção do Grau de Mestre em Mecânica dos Solos e Engenharia Geotécnica. (in Portuguese)

Vieira, P. (2009) “Determinação dos erros de medição associados ao ensaio PMT”. MSc Thesis presented to GeoScience Dept. of University of Aveiro. (in Portuguese)

Wesley, L.D. (1988). “Engineering classification of residual soils”. 'Geomechanics in Tropical Soils'. Proc. Sec. Int. Conf., Singapore, Vol. 1, pp. 77-84. A.A. Balkema, Rotterdam.

Wesley, L.D.; Irfan, T.Y. (1997). “Mechanical of residual soils – ‘Classification of residual soils’ (chapter 2)”. Eds. Blight, Balkema/Rotterdam/Brookfield.

Whittle, A.J.; Aubeny, C.P. (1992). The effects of installation disturbance on interpretation of in situ tests in clay. Proc. Wroth Memorial Symp., Oxford, 27-29 July, pp. 742-767

Wissa, A.; Ladd, C.C.; Lambe, T.W. (1965). “Effective stress strength parameters of stabilized soils”. Proc. 6th Conf. of Soil Mechanics. ISSMFE, 1, pp. 412-416.

Yu, H.S., Carter, J.P., Booker, J.R. (1992). “Analysis of the dilatometer test in undrained clay”. PhD Thesis, Oxford University

Yu, H.S. & Houlsby, G.T. (1991). “Finite cavity expansion in dilatant soils: loading analysis”. Géotechnique 41(2), pp. 173-183.

Zhang Z. & Tumay M.T. (1999). “Statistical to fuzzy approach toward CPT soil classification”. ASCE Journal of Geotech. & Geoenvir. Engineering. Volume 125, No.3.

Zhu, F; Clark, J.; Paulin, M. (1995). “Factors affecting at-rest lateral stress in artificially cemented sands”. Canadian Geotechnical Journal, 32, pp. 195-203.